Childhood Glaucoma

A Case Based Color and Video Atlas

Shikha Gupta
Karthikeyan Mahalingam
Viney Gupta
Editors

MOREMEDIA
Springer

Childhood Glaucoma

Shikha Gupta
Karthikeyan Mahalingam
Viney Gupta
Editors

Childhood Glaucoma

A Case Based Color and Video Atlas

Springer

Editors
Shikha Gupta
Dr. Rajendra Prasad Centre for
Ophthalmic Sciences
All India Institute of Medical Sciences
New Delhi, India

Karthikeyan Mahalingam
Dr. Rajendra Prasad Centre for
Ophthalmic Sciences
All India Institute of Medical Sciences
New Delhi, India

Viney Gupta
Dr. Rajendra Prasad Centre for
Ophthalmic Sciences
All India Institute of Medical Sciences
New Delhi, India

ISBN 978-981-19-7465-6 ISBN 978-981-19-7466-3 (eBook)
https://doi.org/10.1007/978-981-19-7466-3

This Springer imprint is published by the registered company Springer Nature Singapore Pte Ltd. The registered company address is: 152 Beach Road, #21-01/04 Gateway East, Singapore 189721, Singapore

Dedicating the book to my beloved Masters, the Almighty, my parents, husband, my family, my students, and most of all, my patients, without whom this piece of work was impossible!

"The family motivated, the literature supported

The patients taught, the masters bestowed

The God blessed, to bring out the best.

Hoping to serve the world better through the knowledge's aroma,

Acquired over the years while treating kids with glaucoma."

—Shikha Gupta

I want to express my sincere gratitude to my seniors, Dr. Viney Gupta and Dr. Shikha Gupta, for providing guidance and for giving me the chance to take part in this prestigious work. I would also like to thank my juniors, colleagues, and all the authors who contributed to this book. This book is dedicated to Mr. Mahalingam K (my father), Mrs. Chitra M (my mother), Mrs. Kanagavalli M (my sister), Dr. Abirami S (my wife), and my dear daughter, Pranika, for providing me with unwavering support while I was writing it.

—Karthikeyan Mahalingam

The book is dedicated to my parents, my patients, and my colleagues.

—Viney Gupta

Foreword

Childhood glaucoma is a complex and challenging eye disorder that affects the vision and lives of young patients and their families. As we embark on this remarkable journey through the pages of this textbook, it is with great pleasure and admiration that I introduce you to a comprehensive and pioneering resource on this critical subject. *Childhood Glaucoma: A Case Based picture and Video Atlas* is a testament to the dedication and expertise of its authors, editors, and contributors, who have poured their knowledge and experience into its creation.

The editors, esteemed experts in the field of pediatric ophthalmology, have meticulously curated a wealth of information, ranging from the fundamentals of embryology and genetics that underlie childhood glaucoma to the intricate nuances of clinical evaluation and a diverse array of treatment options. Their deep understanding of this rare and complex condition has culminated in a resource that will undoubtedly serve as a beacon of knowledge for both novice learners and seasoned practitioners.

The strength of this textbook lies not only in its comprehensive coverage but also in its innovative approach. The inclusion of case studies and video materials not only adds a dynamic dimension to the learning experience but also mirrors the real-world challenges that clinicians face when managing childhood glaucoma. These cases bring the subject to life, allowing readers to witness the intricacies of diagnosis and treatment firsthand.

The chapters on embryology and genetics lay the essential groundwork for understanding the origins of childhood glaucoma. This foundational knowledge is complemented by a diverse range of chapters that delve into the various types of childhood glaucoma, offering detailed insights into the clinical presentation and management of each condition. The comprehensive section on clinical evaluation equips clinicians with the tools they need to make accurate diagnoses and develop personalized treatment plans. And, crucially, the section on treatment options provides a thorough exploration of the medical, surgical, and therapeutic interventions available to manage childhood glaucoma, ensuring that every reader has access to a broad spectrum of information to inform their clinical practice.

In an era where knowledge is the cornerstone of medical progress, *Childhood Glaucoma: A Case Based picture and Video Atlas* emerges as a beacon of enlightenment. It not only imparts knowledge but also nurtures the spirit of inquiry, encouraging healthcare professionals to explore the com-

plexities of childhood glaucoma and seek innovative solutions to enhance the lives of young patients.

I commend the editors, authors, and contributors for their unwavering commitment to advancing our understanding of childhood glaucoma. This textbook is not just a resource; it is a testament to the power of collaborative learning and the pursuit of excellence in patient care.

May this book inspire you to embark on a journey of discovery, compassion, and expertise in the realm of childhood glaucoma. It is our hope that the knowledge contained within these pages will not only inform but also transform the way we approach and manage this challenging condition.

Ken K. Nischal
Pediatric Ophthalmology and Strabismus
UPMC Children's Hospital of Pittsburgh
Pittsburgh, PA, USA

World Society of Pediatric Ophthalmology and Strabismus
Dublin, Ireland

Contents

Part VI Ancillary Investigations

Part VII Management and Rehabilitation

About the Editors and Contributors

About the Editors

Shikha Gupta, M.D. works as Associate Professor at Dr. Rajendra Prasad Centre for Ophthalmic Sciences, All India Institute of Medical Sciences (AIIMS), New Delhi. Dr. Gupta graduated in Medicine and completed her postgraduation in Ophthalmology from AIIMS, New Delhi. Subsequently, she obtained super-specialty training in Glaucoma, and other allied anterior segment specialities from Dr. Rajendra Prasad Centre for Ophthalmic Sciences, AIIMS. Dr. Gupta has coauthored over 180 peer-reviewed research papers in ophthalmology. She is the editor of *Textbook of Pterygium Management*, 2016, Jaypee Medical Publishers. She is currently conducting research on congenital glaucomas.

Dr. Gupta has received research awards and Young Investigator awards from various international and national societies like the Roche Collaborative Fellowship ARVO (2021), International Fellowship Award, AIIMS (2021), ARVO Developing Country Research fellowship (2020), World Glaucoma Congress (2015), American Academy of Ophthalmology (2010), Asia ARVO (2011), All India Ophthalmological Society (2021, 2016, 2012), best free paper in Glaucoma Society of India (2022, 2016), and the Delhi Ophthalmological Society (2014, 2012) on multiple occasions. She is working towards better clinical diagnosis and management of patients with congenital glaucomas and is an active member of Indian Pediatric Glaucoma Society.

She has been awarded with numerous intramural and extramural research grants both as primary investigator and as co-investigator.

Karthikeyan Mahalingam works as an Assistant Professor of Ophthalmology at Dr. Rajendra Prasad Centre for Ophthalmic Sciences, All India Institute of Medical Sciences (AIIMS), New Delhi. He graduated in Medicine from Thanjavur Medical College, Tamil Nadu, and completed postgraduation in Ophthalmology from AIIMS, New Delhi. Subsequently, he obtained sub-specialty training in Glaucoma, Neuro-Ophthalmology, Pediatric Ophthalmology, and Strabismus from Dr. Rajendra Prasad Centre for Ophthalmic Sciences, AIIMS. He has been awarded "Fellow of All India Collegium of Ophthalmology" (FAICO) in the subject Glaucoma by All India Ophthalmological Society (AIOS). He has coauthored over 60 peer-reviewed research papers in ophthalmology. He has written many chapters for books on ophthalmology. He is currently conducting research on glaucoma. He has received various research awards and prizes like the "Shri Janardhan Prasad Glaucoma Award" (by Dr. Rajendra Prasad Centre for Ophthalmic Sciences, AIIMS 2021), Young Researcher Award 2023 (by Institute of Scholars, India), First prize in Surfing the anterior segment (AIOS-YOSI Forum 2023, Delhi), Best paper of session in Glaucoma (at Annual conference of AIOS 2021), First prize in Glaucoma interesting cases (at Annual conference of Delhi Ophthalmological Society-DOS 2021), First prize in Glaucoma & Neuro-ophthalmology free paper (DOS 2021), Second prize in Allied Ophthalmic Sciences free paper (DOS 2021), etc. He is currently serving as an executive member of the Young Ophthalmologists Society of India.

Viney Gupta is Professor of Ophthalmology, Glaucoma Services of Dr Rajendra Prasad Centre for Ophthalmic Sciences, All India Institute of Medical Sciences, New Delhi, with special interests in congenital glaucomas, juvenile glaucomas, surgical glaucoma, and glaucoma genetics. He did Glaucoma Fellowship at Royal Victorian Eye and Ear Hospital (Australia) (2007–2008). He has more than 170 indexed publications in ophthalmology particularly glaucoma in peer-reviewed journals. He is the author of two books: one on Ocular Therapeutics and the other on Glaucoma Management as part of the initiative of the Glaucoma Society of India. He is currently spearheading Glaucoma Genetic Projects, especially genetics of juvenile open angle glaucoma. He has been awarded with special honors: AC Aggarwal Trophy for best free paper at Delhi Ophthalmological Society Meeting (2004), second prize for best poster at Annual Meeting of European Glaucoma Society, Florence, Italy (2004), best Clinical Research paper at AIIMS (2015). He also serves as the Examiner for postgraduates at the University of Malaysia. He has mentored postgraduate thesis in glaucoma of more than 50 students. Dr Gupta founded the Indian Pediatric Glaucoma Society and is currently serving as the President of the Society.

Contributors

Monika Arora Dr. Rajendra Prasad Centre for Ophthalmic Sciences, All India Institute of Medical Sciences, New Delhi, India

Niranjana Balasubramaniam Dr. Rajendra Prasad Centre for Ophthalmic Sciences, All India Institute of Medical Sciences, New Delhi, India

Abhijeet Beniwal Dr. Rajendra Prasad Centre for Ophthalmic Sciences, All India Institute of Medical Sciences, New Delhi, India

Ridhima Bhatia Department of Anaethesia and Critical Care, All India Institute of Medical Sciences, New Delhi, India

Parijat Chandra Dr Rajendra Prasad Centre for Ophthalmic Sciences, All India Institute of Medical Sciences, New Delhi, India

Tanuj Dada Glaucoma Services, Dr. Rajendra Prasad Centre for Ophthalmic Sciences, All India Institute of Medical Sciences, Delhi, India

Suneeta Dubey Dr. Shroff's Charity Eye Hospital, New Delhi, India

Pankhuri Dudani Department of Dermatology, All India Institute of Medical Sciences, New Delhi, India

Prerna Garg Dr. Shroff's Charity Eye Hospital, New Delhi, India

Amisha Gupta Dr. Rajendra Prasad Centre for Ophthalmic Sciences, All India Institute of Medical Sciences, New Delhi, India

Nayan Gupta Dr. Rajendra Prasad Centre for Ophthalmic Sciences, All India Institute of Medical Sciences, New Delhi, India

Shikha Gupta Dr. Rajendra Prasad Centre for Ophthalmic Sciences, All India Institute of Medical Sciences, New Delhi, India

Viney Gupta Dr. Rajendra Prasad Centre for Ophthalmic Sciences, All India Institute of Medical Sciences, New Delhi, India

Vivek Gupta Community Ophthalmology, Dr. Rajendra Prasad Center for Ophthalmic Sciences, All India Institute of Medical Sciences, New Delhi, India

Ananya Kaginalkar Dr. Rajendra Prasad Centre for Ophthalmic Sciences, All India Institute of Medical Sciences, New Delhi, India

Sushmita Kaushik Glaucoma Services, Advanced Eye Centre, Postgraduate Institute of Medical Education and Research, Chandigarh, India

Arif O. Khan Pediatric & Neuro-Ophthalmology, Eye Institute, Cleveland Clinic Abu Dhabi, Abu Dhabi, United Arab Emirates

Cleveland Clinic Lerner College of Medicine of Case Western Reserve University, Cleveland, OH, USA

Puneet Khanna Department of Anaethesia and Critical Care, All India Institute of Medical Sciences, New Delhi, India

Sudarshan Kumar Khokhar Dr. Rajendra Prasad Centre for Ophthalmic Sciences, All India Institute of Medical Sciences, New Delhi, India

Ram Kishore Dr. Rajendra Prasad Centre for Ophthalmic Sciences, All India Institute of Medical Sciences, New Delhi, India

Pawan Kumar Dr. Rajendra Prasad Centre for Ophthalmic Sciences, All India Institute of Medical Sciences, New Delhi, India

Saumya Kumar Dr. Rajendra Prasad Centre for Ophthalmic Sciences, All India Institute of Medical Sciences, New Delhi, India

Somya Kumari Dr. Rajendra Prasad Centre for Ophthalmic Sciences, All India Institute of Medical Sciences, New Delhi, India

Brajesh Lahri Dr. Rajendra Prasad Centre for Ophthalmic Sciences, All India Institute of Medical Sciences, New Delhi, India

Neiwete Lomi Dr. Rajendra Prasad Centre for Ophthalmic Sciences, All India Institute of Medical Sciences, New Delhi, India

Karthikeyan Mahalingam Dr. Rajendra Prasad Centre for Ophthalmic Sciences, All India Institute of Medical Sciences, New Delhi, India

Aayush Majumdar Dr. Rajendra Prasad Centre for Ophthalmic Sciences, All India Institute of Medical Sciences, New Delhi, India

Vaibhav Namdev Dr. Rajendra Prasad Centre for Ophthalmic Sciences, All India Institute of Medical Sciences, New Delhi, India

Venkatesh Nathiya Department of Ophthalmology, Dr. Rajendra Prasad Centre for Ophthalmic Sciences, All India Institute of Medical Sciences, New Delhi, India

Arnav Panigrahi Dr. Rajendra Prasad Centre for Ophthalmic Sciences, All India Institute of Medical Sciences, New Delhi, India

Nimmy Raj Dr. Rajendra Prasad Centre for Ophthalmic Sciences, All India Institute of Medical Sciences, New Delhi, India

Kumar Kartikay Rajaura Dr. Rajendra Prasad Centre for Ophthalmic Sciences, All India Institute of Medical Sciences, New Delhi, India

Deeksha Rani Dr. Rajendra Prasad Centre for Ophthalmic Sciences, All India Institute of Medical Sciences, New Delhi, India

Ananya Parampalli Ravindra Dr. Rajendra Prasad Centre for Ophthalmic Sciences, All India Institute of Medical Sciences, New Delhi, India

Rahul Sangwan Dr. Rajendra Prasad Centre for Ophthalmic Sciences, All India Institute of Medical Sciences, New Delhi, India

Harathy Selvan Moorfields Eye Hospital NHS Foundation Trust, London, UK

Seema Sen Ocular Pathology, Dr. Rajendra Prasad Centre for Ophthalmic Sciences, All India Institute of Medical Sciences, New Delhi, India

Suraj Singh Senjam Community Ophthalmology, Dr. Rajendra Prasad Center for Ophthalmic Sciences, All India Institute of Medical Sciences, New Delhi, India

Nawazish Shaikh Dr Rajendra Prasad Centre for Ophthalmic Sciences, All India Institute of Medical Sciences, New Delhi, India

Shakha Dr. Rajendra Prasad Centre for Ophthalmic Sciences, All India Institute of Medical Sciences, New Delhi, India

Navneet Sidhu Dr. Rajendra Prasad Centre for Ophthalmic Sciences, All India Institute of Medical Sciences, New Delhi, India

Abhishek Singh Dr. Rajendra Prasad Centre for Ophthalmic Sciences, All India Institute of Medical Sciences, New Delhi, India

Ashok Kumar Singh Glaucoma Services, Advanced Eye Centre, Postgraduate Institute of Medical Education and Research, Chandigarh, India

Radhika Tandon Cornea, Cataract and Refractive Services, Dr. Rajendra Prasad Centre for Ophthalmic Sciences, All India Institute of Medical Sciences, New Delhi, India

Vinit Tanwar Dr. Rajendra Prasad Centre for Ophthalmic Sciences, All India Institute of Medical Sciences, New Delhi, India

Ruchir Tewari Tewari Eye Centre, Ghaziabad, Uttar Pradesh, India

Manasi Tripathi Dr. Rajendra Prasad Centre for Ophthalmic Sciences, All India Institute of Medical Sciences, New Delhi, India

Toshit Varshney Dr. Rajendra Prasad Centre for Ophthalmic Sciences, All India Institute of Medical Sciences, New Delhi, India

Praveen Vashist Community Ophthalmology, Dr. Rajendra Prasad Center for Ophthalmic Sciences, All India Institute of Medical Sciences, New Delhi, India

Pradeep Venkatesh Dr. Rajendra Prasad Centre for Ophthalmic Sciences, All India Institute of Medical Sciences, New Delhi, India

Saurabh Verma Dr. Rajendra Prasad Centre for Ophthalmic Sciences, All India Institute of Medical Sciences, Delhi, India

Rahul P Vijayakumar Dr. Rajendra Prasad Centre for Ophthalmic Sciences, All India Institute of Medical Sciences, New Delhi, India

Antriksh Wahi Dr. Rajendra Prasad Centre for Ophthalmic Sciences, All India Institute of Medical Sciences, New Delhi, India

Part I

The Genesis of Childhood Glaucoma

1 Embryology and Pathophysiology of Childhood Glaucoma

Rahul P Vijayakumar, Nayan Gupta, and Karthikeyan Mahalingam

1.1 Embryology

In the human embryo, the development of eyes involves a complex and delicate process. Interruption in this process can lead to malformation of the eye and related structures, resulting in both functional and aesthetic deficits. Ocular development occurs from approximately the third week through the tenth week of gestation. The development of various structures of the eye (Fig. 1.1), and the embryonic formation of neural crest cells (Fig. 1.2) are described below. The formation of the optic cup is described in Fig. 1.3, its outer layer develops in to the neurosensory retina and its inner layer develops in to the retinal pigment epithelium.

Three waves of periocular mesenchymal cell migration, starting from the third week and continuing through the tenth week of gestation, give rise to the primordial corneal endothelium and Descemet's membrane in the first wave. The second wave insinuates between the developing cornea and the lens, subsequently developing into the iris stroma and the pupillary membrane, while the third wave differentiates into the corneal stroma (Fig. 1.4).

The normal development of the anterior chamber angle has been studied extensively but is not fully understood yet. Mesenchymal cells of neural crest cell origin give rise to structures in the angle of the anterior chamber that are related to the aqueous drainage. Figure 1.5 shows the histologic appearance of the anterior chamber angle during the seventh, eighth, and ninth months of gestation respectively. Seefelder and Wolfrum summarized the formation of the anterior chamber angle in 1906. Chronodynamics of normal anterior segment development are shown in Fig. 1.6.

Hypotheses related to the formation of anterior chamber angle are:

1. Atrophy or progressive resorption of a part of foetal tissue.

R. P Vijayakumar (✉) · N. Gupta · K. Mahalingam
Dr. Rajendra Prasad Centre for Ophthalmic Sciences, All India Institute of Medical Sciences, New Delhi, India

S. Gupta et al. (eds.), *Childhood Glaucoma*, https://doi.org/10.1007/978-981-19-7466-3_1

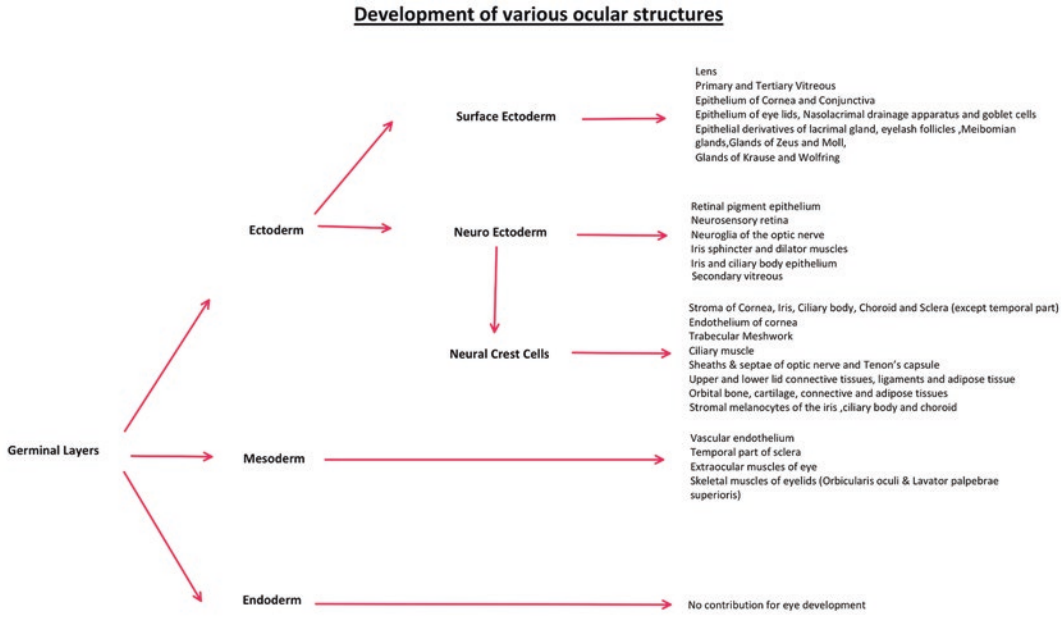

Fig. 1.1 Development of various ocular structures. At day 15 of gestational age, bilaminar embryo (ectoderm and endoderm) develops and trilaminar embryo (ectoderm, mesoderm, and endoderm) develops by day 17

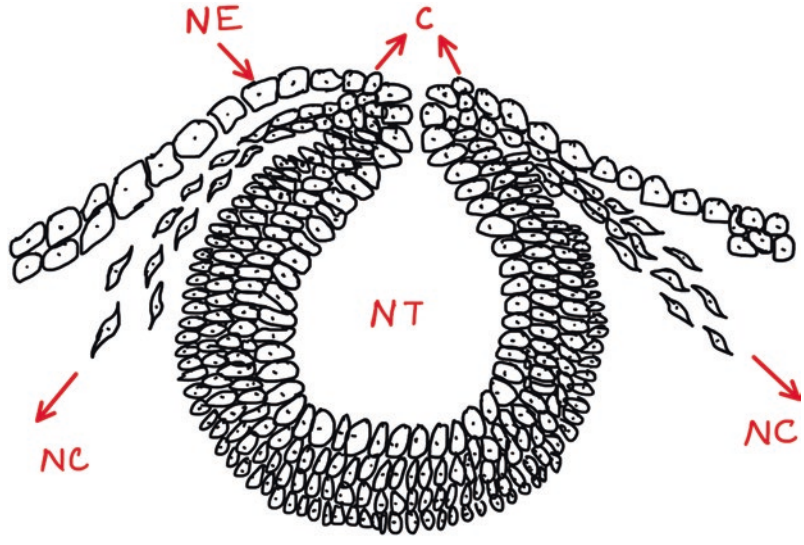

Fig. 1.2 Embryonic formation of neural crest cells (NC): These cells originate from the neuroectoderm (NE) located at the crest (C) of the neural folds, at the time when folds fuse to form the neural tube (NT). Subsequently these cells migrate beneath the ectoderm

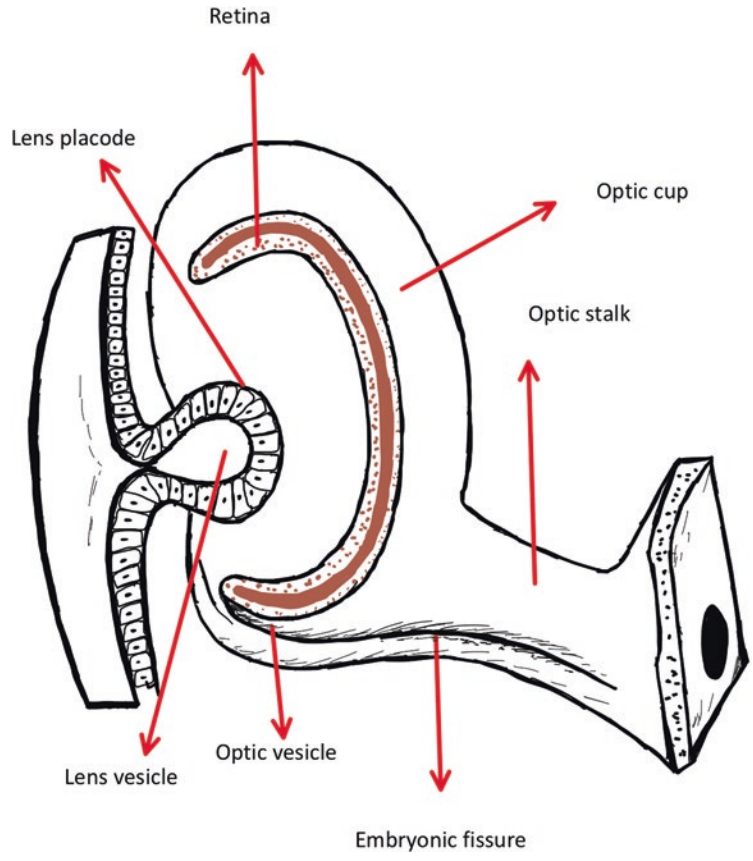

Fig. 1.3 Formation of optic cup: After the optic vesicle (day 26) extends to form the lens placode, the lens pit develops and the optic cup is formed at the end of the optic stalk. The lens pit develops into the lens vesicle (day 28) within the optic cup. The inner layer of the optic cup forms the neurosensory retina and the outer layer gives rise to retinal pigment epithelium

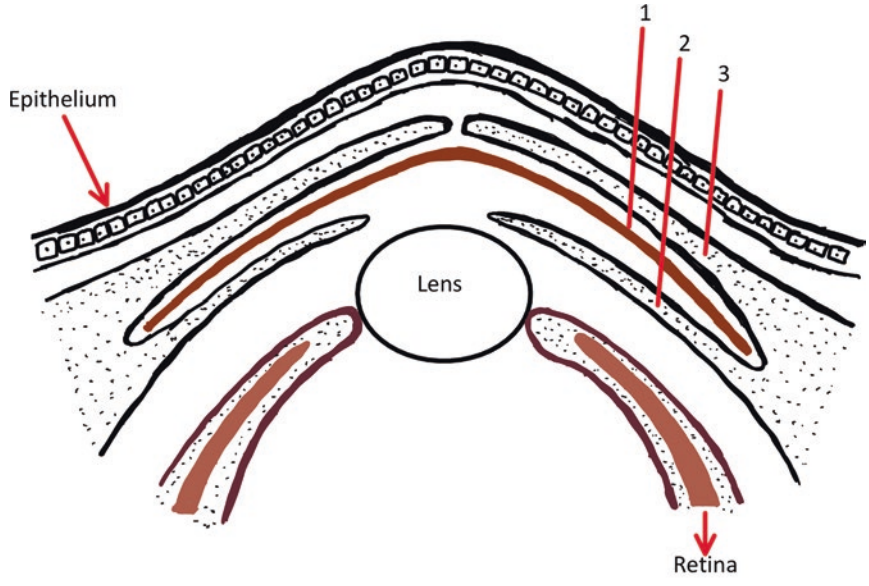

Fig. 1.4 Theory of three waves of periocular mesenchymal cell migration: First wave (1) forms the corneal endothelium, the second wave (2) forms the iris and part of the pupillary membrane, and the third wave (3) forms the keratocytes of the corneal stroma

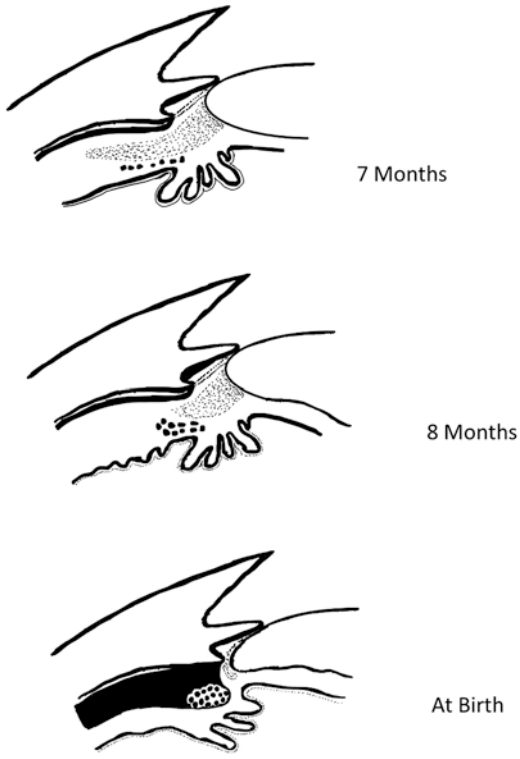

Fig. 1.5 Intrauterine development of the anterior chamber angle. Chamber angle at the seventh and eighth month: The anterior chamber just reaches the Schwalbe's line. Behind it, the mesodermal tissue has a very tight mesh (small square); it extends over the whole area from the scleral trabecular meshwork (dotted line) to the radiated muscle and the ciliary processes. In the next image (eighth month), the anterior chamber enlarges in a distal direction. The meshes of the mesodermal tissue are looser (large squares). At birth: the anterior chamber enlarges even further, and the mesodermal tissue is reduced to a thin layer that later becomes the Busacca trabecular conjunctival layer, also known as Rohen iridoscleral membrane

2. Cleavage or separation of two pre-existing layers of tissue due to differential growth rate.
3. Rarefaction: mechanical distension resulting from the growth of the anterior ocular segment.

Shield's Theory of the Development of the Anterior Chamber Angle

- Five months of gestation: The neural crest cells-derived continuous layer of endothelium creates a closed cavity of the anterior chamber, and the anterior surface of the iris inserts in front of the primordial trabecular meshwork.
- Later, this endothelial membrane disappears from the pupillary membrane, iris, and anterior chamber angle progressively, and gets incorporated into the trabecular meshwork, during the third trimester.
- The peripheral uveal tissue begins to slide posteriorly in relation to the anterior chamber angle structures.
- The trabecular meshwork development begins in the inner posterior aspect of the primordial tissue, progressing towards Schlemm's canal and Schwalbe's line.

Development of the normal angle structures comprises of bidirectional growth. Scleral spur shows an inward growth accompanied by receding uveal meshwork. As the growth progresses, there is an obliteration of the foetal uveal meshwork, leaving behind a few fine residual iris processes. When this normal developmental process comes to a halt, it results in the persistence of the foetal uveal meshwork, leading to congenital glaucoma.

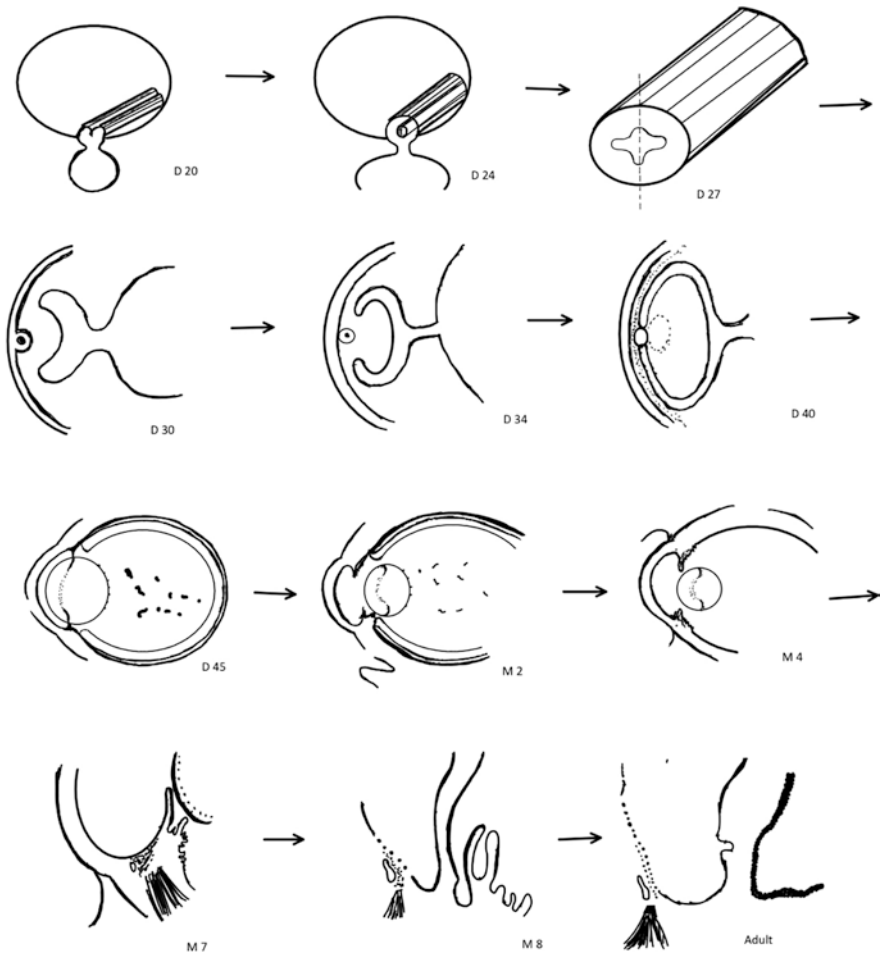

Fig. 1.6 Chronodynamics of normal anterior segment development. Day 20 (D 20): formation of neural groove; day 24 (D 24): appearance of optic pits in neural groove; day 27 (D27): crystalline placode; day 30 (D 30): crystalline vesicle joined to ectoderm; day 34 (D 34): crystalline vesicle separated from ectoderm; day 40 (D 40): paraxial mesenchyme appears around lens; day 45 (D 45): incipient anterior chamber formation; second month (M 2): crystalline vesicle separated from ectoderm, abundant endothelized angle mesodermal formation; fourth month (M 4): ciliary processes, Schlemm's canal, uveal trabecular, and corneoscleral differentiation; seventh month (M 7): fenestration of the pretrabecular endothelial (Barken) membrane; eighth month (M 8): disappearance of endothelial membrane, displacement of ciliary muscle, and resorption of mesoderm are completed. At fourth and fifth years of age: chamber angle recess formation is completed

1.2 Pathophysiology of Childhood Glaucoma

Several major theories have been put forward regarding the elevation of intraocular pressure in primary congenital glaucoma. Some of the pertinent theories include *Mann's Theory, Incomplete Cleavage Theory*, *Barkan's theory*, *Maumenee's theory*, *Kupfer's theory*, *Worst theory*, *Anderson's theory*, *Beauchamp's theory*, and *McMenamin theory*.

Barkan's theory (*1955*)

- Barkan suggested that incomplete resorption of the mesodermal cells led to membrane formation across the anterior chamber angle.
- According to Barkan and Worst, a thin membrane, later termed the Barkan's membrane, is

said to be covering the trabecular meshwork surface.
- Anderson and Maumenee were unable to prove the presence of this membrane despite extensive histologic studies with light and electron microscopy.

Anderson's Theory **(1981)**
- Figure 1.7 illustrates the process of exposing the trabecular meshwork to the anterior chamber during development.
- Anderson (through histopathology) proposed that the high insertion of the anterior uvea into the trabecular meshwork is due to a developmental arrest in the uvea's normal migration across the meshwork in the third trimester of gestation.
- He stated that in primary congenital glaucoma eyes, the iris and ciliary body have failed to recede posteriorly, and hence the posterior portion of the trabecular meshwork is overlapped by the insertion of the iris and anterior band of ciliary body.
- He also believed that the normal posterior migrations of the ciliary body and iris root are prevented by thickened trabecular beams in infantile glaucoma.

McMenamin Theory **(1991)**
McMenamin stated during development a marked increase in the extracellular matrix volume results in congenital glaucoma.

1.2.1 Angular Neurocristopathies

They are the group of diseases that involve cornea, iris, and trabecular meshwork; often associated with glaucoma. They are frequently accompanied by abnormalities of non-ocular tissues that are also derived from neural crest cells such as craniofacial and dental malformations, middle ear deafness, and malformations of the base of the skull. These diseases include Axenfeld-Rieger syndrome, Peters anomaly, and Sturge-Weber syndrome or other phakomatoses.

Axenfeld-Rieger Syndrome
In late gestation, developmental arrest of certain neural crest-derived anterior segment structures causes abnormal retention of the primordial endothelial layer on portions of the iris and anterior chamber angle. This leads to the formation of iridocorneal strands and the contraction of the tissue layer on the iris.

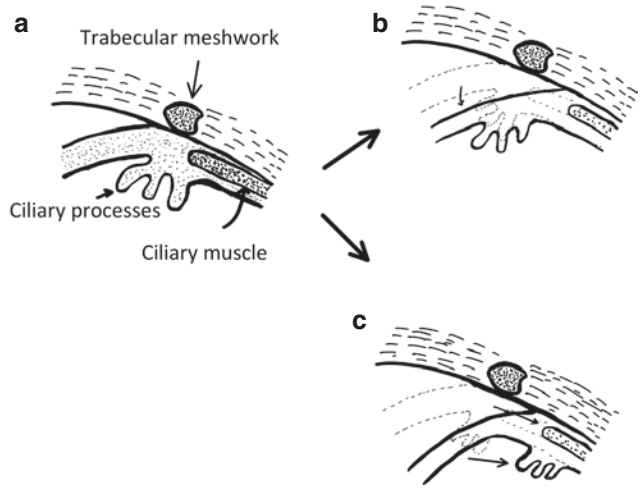

Fig. 1.7 Figure illustrates the process of exposure of trabecular meshwork to the anterior chamber during development. Early uveal tract (**a**), splitting by cleavage or atrophy of the tissue (**b**), resulting in an angle configuration in which the ciliary muscle extends into the iris and ciliary processes are situated on the posterior surface of the iris. This differential growth leads to the slippage of ciliary muscle and ciliary body posteriorly (**c**)

These disorders might be accompanied by developmental anomalies related to the pituitary gland, facial bones, and teeth as they are also derived from neural crest cells.

Peters Anomaly
Peters anomaly is characterized by abnormalities in the cornea (defects in the posterior stroma, Descemet's membrane and endothelium, extension of iris tissue strands from the iris collarette to the edge of the corneal leukoma) with or without abnormalities in the lens (cataract, central keratolenticular stalk), and the anterior chamber angle.

Incomplete migration of the neural crest-derived mesenchymal cells during early embryogenesis (first wave – central defect in endothelium and Descemet's membrane, third wave – stromal defect) could possibly lead to these abnormalities. A more severe degree of failure of mesenchymal differentiation leads to an anterior staphyloma formation.

Aniridia
Numerous mechanisms like the absence of the superficial stromal directional membrane, primary failure of the optic cup growth, and persistence of capsulo-pupillary vessels have been proposed for the causation of aniridia. In the absence of the primary pupillary membrane, the optic cup lacks a directional membrane, and hence only a rudimentary iris develops. Other abnormalities of neural crest cells are possible in this condition as well. Besides cataract and corneal abnormalities, aniridia can also be accompanied by nystagmus, amblyopia, glaucoma, as well as hypoplasia of the fovea and optic nerve.

Other Phakomatoses
Primary defects in the aqueous outflow pathway in patients with phakomatoses including Sturge–Weber syndrome and neurofibromatosis have been described. These abnormalities include the persistence of embryonic tissue in the trabecular meshwork, incomplete 'cleavage' of the iridocorneal angle, and malformation or absence of Schlemm's canal. The pathogenesis of the associated glaucoma in the absence of secondary obstruction to aqueous outflow could be attributed to the abnormalities of neural crest cells.

1.3 Conclusions

Congenital glaucoma appears to be caused by developmental anomaly of the anterior chamber angle structures which are derived from neural crest cells. Usually abnormal development is characterised by an anterior insertion of the iris and the ciliary muscle directly into trabecular meshwork, leaving behind a rudimentary scleral spur. The high insertion of the iris and ciliary body into the posterior part of the trabecular meshwork may compress the trabecular beams, along with an accumulation of abnormal extracellular matrix. There may also be basic developmental abnormalities at different levels of trabecular meshwork and Schlemm's canal. Insults during different stages at embryogenesis can cause different types of developmental glaucomas.

Suggested Reading

Allen L, Burian HM, Braley AE. A new concept of the development of the anterior chamber angle. Its relationship to developmental glaucoma and other structural anomalies. AMA Arch Ophthalmol. 1955;53:783–98.

Anderson DR. The development of the trabecular meshwork and its abnormality in primary infantile glaucoma. Trans Am Ophthalmol Soc. 1981;79:458–85.

Barkan O. Pathogenesis of congenital glaucoma. Gonioscopic and anatomic observation of the angle of the anterior chamber in the normal eye and in congenital glaucoma. Am J Ophthalmol. 1955;40:1–11.

Cibis GW, Tripathi RC, Tripathi BJ. Glaucoma in Sturge-Weber syndrome. Ophthalmology. 1984;91:1061.

Collins ET, Batten RD. Neurofibroma of the eyeball and its appendages. Trans Ophthalmol Soc. 1905;25:248.

Cook CS. Experimental models of anterior segment dysgenesis. Ophthalmic Paediatr Genet. 1989;10:33–46.

Hansson HA, Jerndal T. Scanning electron microscopic studies on the development of the iridocorneal angle in human eyes. Invest Ophthalmol. 1971;10:252–65.

Hoyt CM, Billson F. Buphthalmos in neurofibromatosis: is it an expression of giantism? J Ped Ophthalmol. 1977;14:228–34.

Kenyon KR. Mesenchymal dysgenesis in Peter's anomaly, sclerocornea and congenital endothelial dystrophy. Exp Eye Res. 1975;21:125–42.

Leib WA, Wirth WA, Geeraets WJ. Hydrophthalmos and neurofibromatosis. Confin Neurol. 1958;19:239.

Mann I. The development of the human eye. 3rd ed. Cambridge: Cambridge University Press; 1964.

Maumenee AE. Further observations on the pathogenesis of congenital glaucoma. Am J Ophthalmol. 1963;55:1163–76.

Sampaolesi R, Zarate J, Sampaolesi JR. The glaucomas: pediatric glaucomas, vol. 1. Berlin: Springer; 2009.

Schottenstein EM. Peters' anomaly. In: Ritch R, Shields MB, Krupin T, editors. The glaucomas. 2nd ed. St. Louis: Mosby; 1996. p. 887–97.

Shields MB. Axenfeld–Rieger syndrome. A theory of mechanism and distinctions from the iridocorneal endothelial syndrome. Trans Am Ophthalmol Soc. 1983a;81:736–84.

Shields MB. Axenfeld–Rieger syndrome. A theory of mechanism and distinctions from the iridocorneal endothelial syndrome. Trans Am Ophthalmol Soc. 1983b;81:736–84.

Shields MB. A common pathway for developmental glaucomas. Trans Am Ophthalmol Soc. 1987;85:222–37.

Stoilov I, Akarsu AN, Sarfarazi M. Identification of three different truncating mutations in cytochrome P4501B1 (CYP1B1) as the principal cause of primary congenital glaucoma (buphthalmos) in families linked to the GLC3A locus on chromosome 2p21. Hum Mol Genet. 1997;6:641–7.

Tripathi RC, Tripathi BJ, Cibis GW. Sturge-Weber syndrome. In: Gold DH, Weinglist TA, editors. The eye in systemic disease. Lippincott: Philadelphia; 1987.

Waring GO, Rodrigues MM, Leibson PR. Anterior chamber cleavage syndrome: a stepladder classification. Surv Ophthalmol. 1975;20:27.

Weiss JS, Ritch R. Glaucoma in the phakomatoses. In: Ritch R, Shields MB, Krupin T, editors. The glaucomas. 2nd ed. St. Louis: Mosby; 1996. p. 899–924.

Wheeler JM. Plexiform neurofibromatosis involving the choroid, ciliary body and other structures. Am J Ophthalmol. 1937;20:368.

Wiener A. A case of neurofibromatosis with buphthalmos. Arch Ophthalmol. 1925;54:481.

Worst JG. Pathogenesis and treatment of congenital glaucoma. Ophthalmologica. 1965;149:118–20. PMID: 14327829. https://doi.org/10.1159/000304741.

Worst JGF. The pathogenesis of congenital glaucoma. An embryological and goniosurgical study. Springfield: Charles C. Thomas; 1966.

2 Classification of Childhood Glaucoma

Antriksh Wahi, Aayush Majumdar, and Karthikeyan Mahalingam

Various classification systems have been proposed for childhood glaucomas.

2.1 Classification of Childhood Glaucomas

2.1.1 Based on Age of Onset

1. Neonatal or newborn onset (age 0–1 months)
2. Infantile onset (age 1–24 months)
3. Late onset or late recognized (age ≥ 24 months)

2.1.2 Based on Developmental Pattern

Developmental glaucoma: This term broadly encompasses all glaucomas resulting from abnormal development of the aqueous outflow system. This may or may not be associated with systemic anomalies.

- **Primary developmental glaucoma:** This results from maldevelopment of the aqueous outflow system.
- **Secondary developmental glaucoma**: This results from damage to aqueous outflow system due to maldevelopment of some other portion of the eye, e.g., eye with microspherophakia or dislocated lens.

2.1.3 Based on Anatomy

Hoskins–Shaffer–Hetherington proposed an **anatomical classification** that uses the extent of dysgenesis of the anterior chamber structures including involvement of trabecular meshwork, iris or cornea (Fig. 2.1).

A. Wahi (✉) · A. Majumdar · K. Mahalingam
Dr. Rajendra Prasad Centre for Ophthalmic Sciences, All India Institute of Medical Sciences, New Delhi, India

S. Gupta et al. (eds.), *Childhood Glaucoma*, https://doi.org/10.1007/978-981-19-7466-3_2

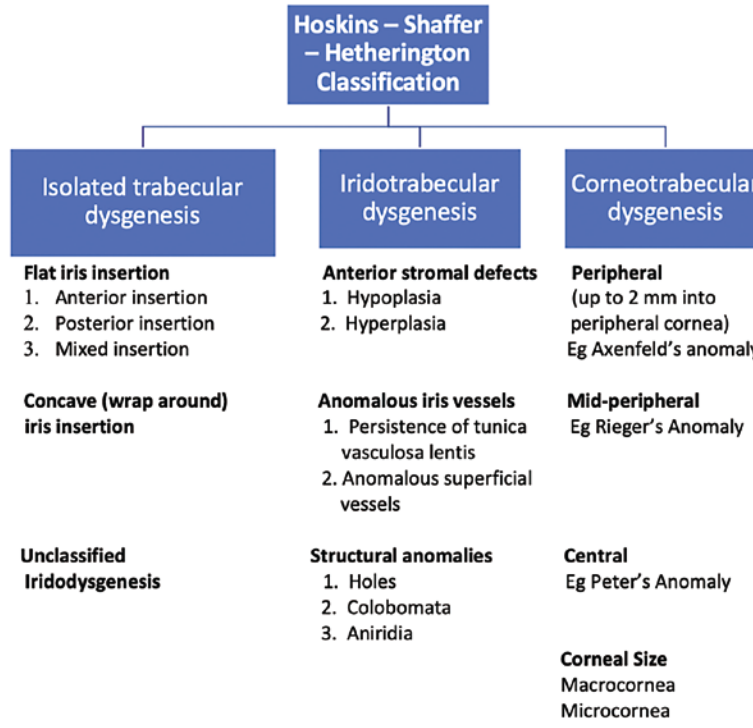

Fig. 2.1 Hoskin's anatomical classification of congenital glaucoma

2.1.4 Syndrome Classification of Congenital Glaucoma (Shaffer-Weiss, Table 2.1)

Table 2.1 The Shaffer-Weiss classification of Congenital Glaucoma

A. Primary congenital glaucoma (primary infantile glaucoma)
B. Glaucoma associated with congenital anomalies
1. Late developing primary congenital glaucoma
2. Familial hypoplasia of the iris with glaucoma
3. Developmental glaucoma with anomalous superficial iris vessels
4. Aniridia
5. Sturge-Weber syndrome
6. Neurofibromatosis
7. Marfan syndrome
8. Pierre Robin syndrome
9. Homocystinuria
10. Goniodysgenesis (iridocorneal mesodermal dysgenesis: Rieger's anomaly and syndrome, Axenfeld's anomaly, Peter's anomaly)
11. Lowe's syndrome
12. Microcornea
13. Microspherophakia
14. Rubella
15. Chromosomal abnormalities
16. Broad thumb syndrome
17. Persistent hyperplastic primary vitreous
C. Secondary glaucoma in infants
1. Retrolental fibroplasia
2. Tumors
(a) Retinoblastoma
(b) Juvenile xanthogranuloma
3. Inflammation
4. Trauma

2.1.5 Childhood Glaucoma Research Network Classification

The **Congenital Glaucoma Research Network (CGRN) classification system** is the first international consensus classification for childhood glaucoma. The CGRN proposed a classification system to classify children with glaucoma that is clinically meaningful, which helps to recognize the etiology and mechanisms that cause glaucoma in children. At the **Ninth World Glaucoma Association (WGA) Consensus (Vancouver, Canada, July 16, 2013)**, this system got recognition and has been adopted by the American Board of Ophthalmology.

Definition of Childhood

Based on national criteria: <18 years of age (USA); ≤ 16 years of age (UK, Europe, UNICEF).

***Definition of Glaucoma*: Two or More Required**

- IOP > 21 mmHg (investigator discretion if examination under anesthesia data alone due to the variable effects of anesthesia on all methods of IOP assessment)
- Optic disc cupping (neuroretinal rim narrowing): a progressive increase in cup-disc ratio (diffuse rim narrowing), cup-disc asymmetry of ≥0.2 when the optic discs are of similar size, or focal rim narrowing
- Corneal findings: Haab striae, corneal edema ,or diameter ≥ 11 mm in newborn, >12 mm in child <1 year of age, >13 mm any age

- Progressive myopia or myopic shift coupled with an increase in ocular dimensions disproportionate to the normal growth patterns
- A reproducible visual field defect that is consistent with glaucomatous optic neuropathy with no other observable reason for the visual field defect

***Definition of Glaucoma Suspect*: At Least One Required**

- IOP > 21 mmHg on two separate occasions
- Suspicious optic disc appearance for glaucoma, i.e., increased cup-disc ratio for size of optic disc
- A suspicious visual field for glaucoma
- Increased corneal diameter or axial length in setting of normal IOP

Classification Proposed by Childhood Glaucoma Research Network (CGRN) (Fig. 2.2)

The advantages of CGRN classification are manifold. It divides the childhood glaucoma into one of the seven categories. Not only this, it also allows classification for children in which the diagnosis of glaucoma may be suspected but not proven. Glaucoma suspect is diagnosed based on the presence of ocular hypertension (IOP >21 mmHg) on two separate occasions, visual field abnormalities suspicious of glaucoma, optic nerve appearance suspicious of glaucoma, or signs of ocular enlargement (e.g., increased corneal diameter or axial length) with normal IOP. Hence, its ease of use, unambiguity, and global applicability makes it the current international classification system.

2.1.5.1 Primary Childhood Glaucoma

Primary Congenital Glaucoma (PCG)

- Isolated angle anomalies (± mild congenital iris anomalies)
- Meets glaucoma definition (usually with ocular enlargement) (Fig. 2.3)
- Subcategories based on age of onset
  - Neonatal or newborn onset (0–1 month)
  - Infantile onset (> 1–24 months)
  - Late onset or late recognized (> 2 years)
- Cases with normal IOP and optic discs but typical signs of PCG (e.g., buphthalmos and Haab striae) that are not progressive may be classified as spontaneously arrested PCG.

Juvenile Open-Angle Glaucoma (JOAG)

- No ocular enlargement
- No congenital ocular anomalies or syndromes
- Open angle (normal appearance)
- Meets glaucoma definition (Age: 4-40 years)

2.1.5.2 Secondary Childhood Glaucoma

A. Glaucoma Associated with Non-acquired Ocular Anomalies

- Includes conditions of predominantly ocular anomalies present at birth which may or may not be associated with systemic signs
- Meets glaucoma definition
- List of common ocular anomalies:
  - Axenfeld-Rieger anomaly (syndrome if systemic associations)
  - Peters anomaly (syndrome if systemic associations)
  - Congenital ectropion uveae
  - Congenital iris hypoplasia
  - Aniridia
  - Persistent fetal vasculature (if glaucoma present before cataract surgery)
  - Oculodermal melanocytosis (Nevus of Ota)
  - Posterior polymorphous dystrophy
  - Microphthalmos
  - Microcornea
  - Ectopia lentis

    Simple ectopia lentis (no systemic associations)

    Ectopia lentis et pupillae

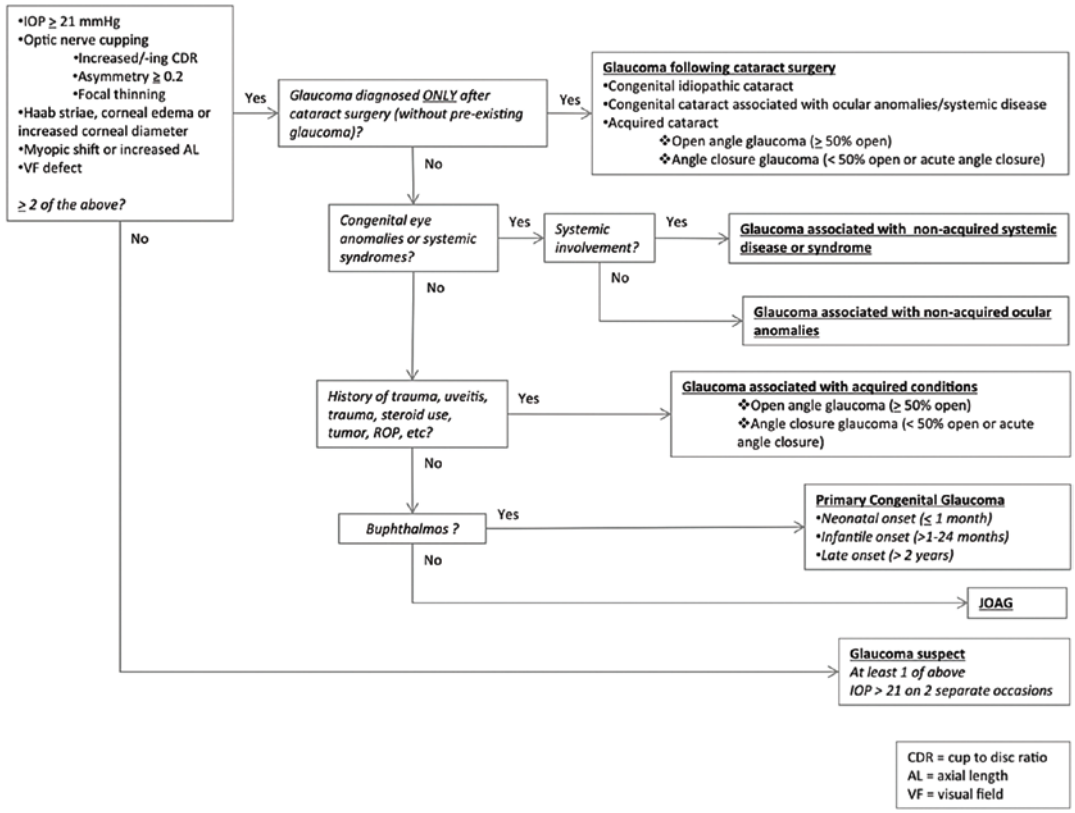

Fig. 2.2 Childhood glaucoma classification algorithm. The flow is from left to right, beginning with the required factors for the definition of glaucoma and glaucoma suspect to the final classification

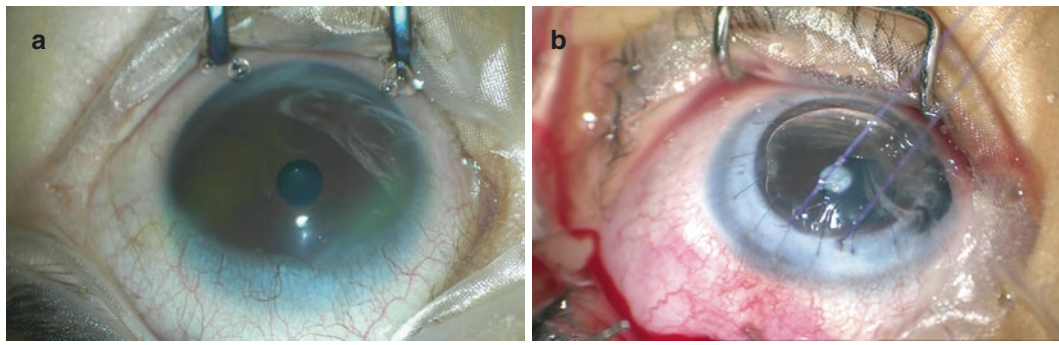

Fig. 2.3 (**a**) Clinical picture of an eye with primary congenital glaucoma showing stretched limbus. (**b**) Clinical picture of an eye with post penetrating keratoplasty glaucoma with no/minimal limbal stretching as compared to primary congenital glaucoma

B. Glaucoma Associated with Non-acquired Systemic Disease or Syndrome

- Includes conditions predominantly of systemic disease present at birth which may be associated with ocular signs
- Meets glaucoma definition
- List of common systemic syndrome or disease:
  - Chromosomal disorders such as trisomy 21 (Down syndrome)

Fig. 2.4 A case of Weill-Marchesani syndrome with short stubby hands

- Connective tissue disorders
  - Marfan syndrome
  - Weill-Marchesani syndrome (Fig. 2.4)
  - Stickler syndrome
- Metabolic disorders
  - Homocystinuria
  - Lowe syndrome
  - Mucopolysaccharidoses (Fig. 2.5)
- Phacomatoses
  - Neurofibromatosis (NF-1, NF-2)
  - Sturge-Weber syndrome (Fig. 2.6)
  - Klippel-Trenaunay-Weber syndrome
  - Rubinstein-Taybi syndrome (Fig. 2.7)
  - Waardenburg syndrome (Fig. 2.8)
  - PHACE (posterior fossa anomalies, hemangioma, arterial anomalies, cardiac anomalies, and eye anomalies) syndrome (Fig. 2.9)
- Congenital rubella

C. Glaucoma Associated with Acquired Condition

- Meets glaucoma definition after the acquired condition is recognized. An acquired condition is one that is not inherited or present at birth but which develops after birth.
- Glaucoma developing after cataract surgery is excluded from this category to highlight its frequency and differences from other conditions in the acquired condition category.
- Based on gonioscopy results:
  - Open-angle glaucoma (≥50% open)
  - Angle-closure glaucoma (<50% open or acute angle-closure)
- List of common acquired conditions:
  - Uveitis
  - Trauma (hyphema, angle recession, ectopia lentis)
  - Steroid-induced

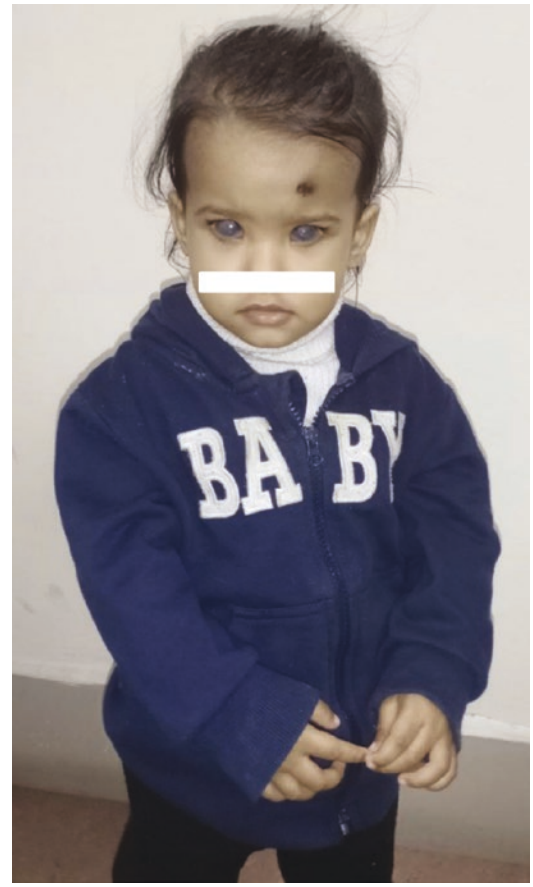

Fig. 2.5 A case of Hurler syndrome (mucopolysaccharidosis) with congenital glaucoma, corneal clouding and facial features including frontal bossing, depressed nasal bridge and fullness of cheeks

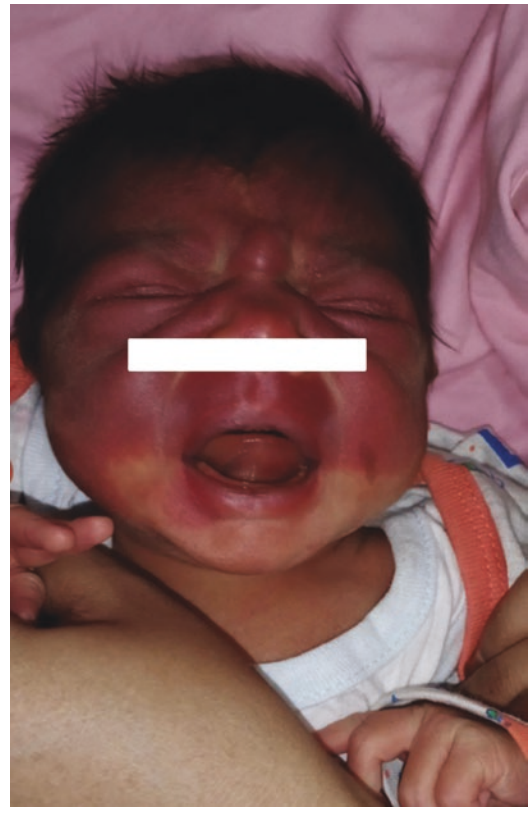

Fig. 2.6 A case of Sturge-Weber syndrome demonstrating bilateral port wine stain

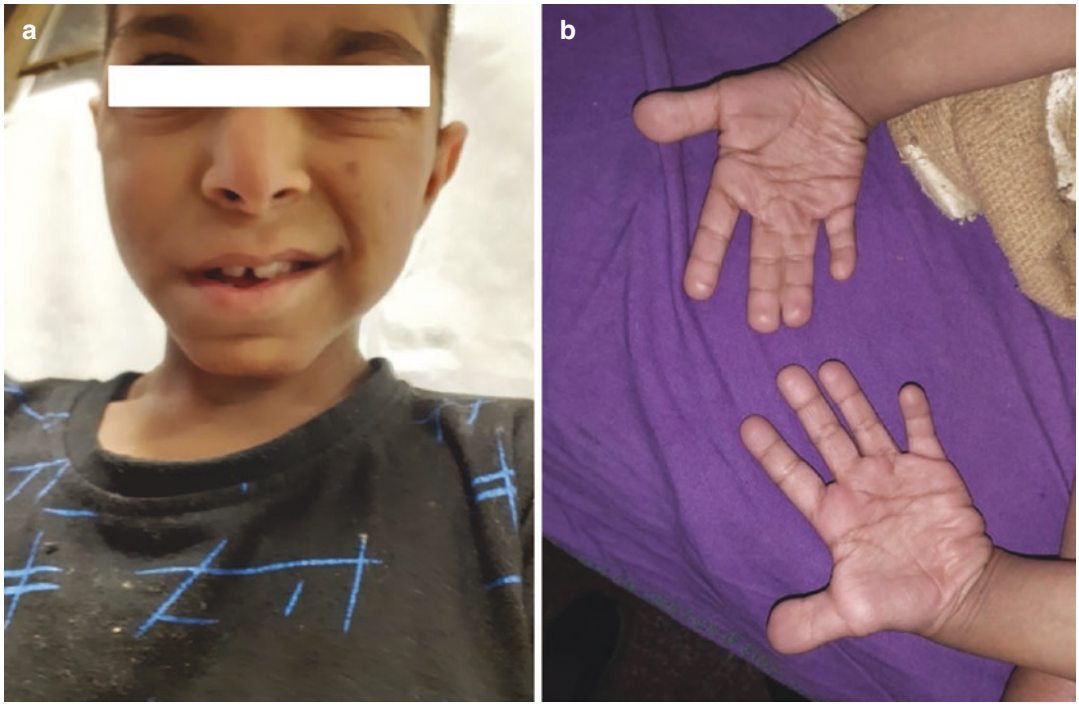

Fig. 2.7 A case of Rubinstein-Taybi syndrome with left eye glaucoma showing (**a**) beaked nose, grimacing smile and (**b**) Broad angulated thumbs

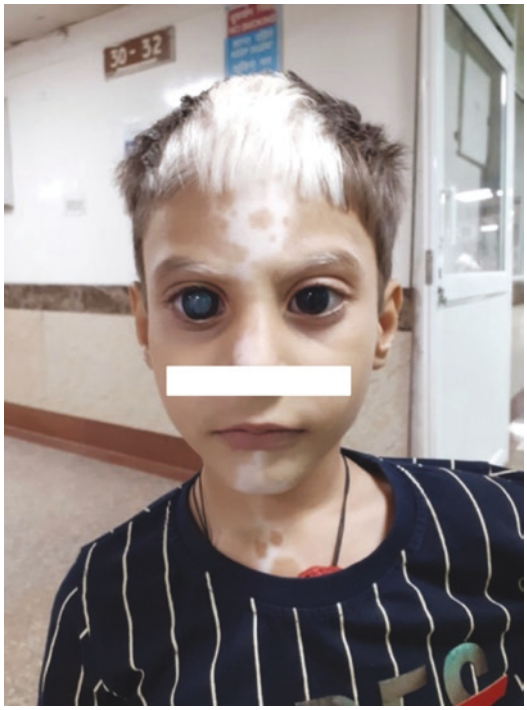

Fig. 2.8 A case of Waardenburg syndrome with right eye glaucoma and developmental cataract, depigmentation of skin, eyebrows and hair

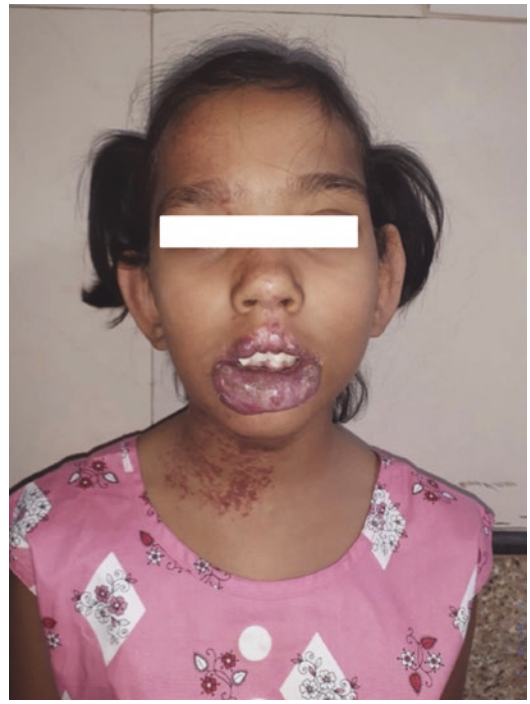

Fig. 2.9 A case of PHACE syndrome showing multiple hemangiomas on face and neck and having developmental glaucoma

- Tumors (benign/malignant, ocular/orbital), e.g., retinoblastoma, juvenile xanthogranuloma (Fig. 2.10)
- Retinopathy of prematurity (ROP)
- Post-surgery other than cataract surgery

D. Glaucoma Following Cataract Surgery

- Meets glaucoma definition after cataract surgery is performed and is subdivided into three categories based upon cataract type:
  - Congenital idiopathic cataract
  - Congenital cataract associated with ocular anomalies/systemic disease (no previous glaucoma)
  - Acquired cataract (no previous glaucoma)
- Based on gonioscopy results:
  - Open-angle glaucoma (≥50% open)
  - Angle-closure glaucoma (<50% open or acute angle closure)

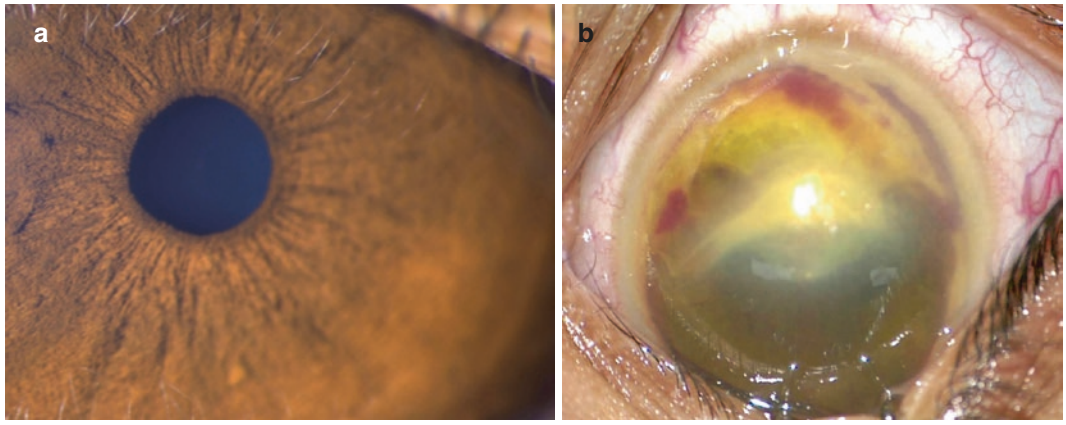

Fig. 2.10 (**a**) Clinical picture showing iris nodules in a case of juvenile xanthogranuloma. (**b**) Clinical picture showing diffuse xanthogranuloma (involving the limbus and cornea) along with hyphema

2.2 Conclusions

The classification system of childhood glaucoma has undergone considerable changes over the last few years. The advent of the Childhood Glaucoma Research Network (CGRN) has provided an objective and logical international consensus classification system that has helped us to increase our understanding of childhood glaucoma. It allows institution of consistent treatment guidelines and acquisition of data for multicenter research studies. The classification system which also addresses the prognostication and severity of the disease is the way to go in future. With increasing research and a more detailed analysis of the subject, there will certainly be more changes in the classification system in future.

Suggested Reading

Alward WLM. Axenfeld-Rieger syndrome in the age of molecular genetics. Am J Opthalmol. 2000;130(1):107–15.

Beck AD, Chang TCP, Freedman SF. Definition, classification, differential diagnosis. In: Weinreb RN, et al., editors. Childhood glaucoma: consensus series 9. Amsterdam: Kugler; 2013.

Bhatia S, Bengani H, Fish M, et al. Disruption of autoregulatory feedback by a mutation in a remote, ultraconserved PAX6 enhancer causes aniridia. Am J Hum Genet. 2013;93(6):1126–34.

Gupta V, Markan A, Somarajan BI, Sihota R, Gupta A, Gupta S, Sharma A. Phenotypic differences between familial versus non-familial Juvenile onset open angle glaucoma patients. Ophthalmic Genet. 2018;39(1):63–7.

Hoskins DH, Shaffers RN, Hetherington J. Anatomical classification of the developmental glaucomas. Arch Ophthalmol. 1984;102(9):1331–6. https://doi.org/10.1001/archopht.1984.01040031081030.

Micheal S, Siddiqui SN, Zafar SN, Iqbal A, Khan MI, den Hollander AI. Identification of novel variants in LTBP2 and PXDN using whole-exome sequencing in developmental and congenital glaucoma. PloS One. 2016;11(7):e0159259.

Ormestad M, Blixt A, Churchill A, Martinsson I, Enerback S, Carlsson P. Foxe3 haploinsufficiency in mice: a model for Peters' anomaly. Invest Ophthalmol Vis Sci. 2002;43(5):1350–7.

Reis LM, Tyler RC, Weh E, et al. Analysis of CYP1B1 in pediatric and adult glaucoma and other ocular phenotypes. Mol Vis. 2016;22:1229–38.

Shaffer R, Weiss D. Congenital and pediatric glaucomas. Saint Louis: Mosby; 1970.

Singh P, Kumar Y, Tyagi M, Kuldeep K, Das Sharma P. Childhood glaucoma: an overview. Open J Ophthalmol. 2012;2(3):71–7. https://doi.org/10.4236/ojoph.2012.23015.

Souma I, Tompson SW, Thomson BR, et al. Angiopoietin receptor TEK mutations underlie primary congenital glaucoma with variable expressivity. I Clin Invest. 2016;126(7):2575–87.

Turalba AV, Chen TC. Clinical and genetic characteristics of primary juvenile-onset open-angle glaucoma (JOAG). Semin Ophthalmol. 2008;23(1):19–25.

Weh E, Reis LM, Happ HC, et al. Whole exome sequence analysis of Peters anomaly. Hum Genet. 2014;133(12):1497–511.

Zhang X, Qin G, Chen G, et al. Variants in TRIM44 cause aniridia by impairing PAX6 expression. Hum Mutat. 2015;36(12):1164–7.

3 The Role of Genetic Testing in Childhood Glaucoma

Arif O. Khan and Antriksh Wahi

3.1 Selected Genetics of Childhood Glaucomas

3.1.1 Primary Congenital Glaucoma (PCG)

- Most cases worldwide are sporadic but **10%–40% are familial** (mostly **autosomal recessive**), often in the context of consanguinity and particularly in certain regions.
- **Three classic loci** for **PCG - GLC3A (2p22)**, **GLC3B (1p36)**, and **GLC3C (14q24.3)**.
- Genes implicated in PCG: ***CYP1B1*** **(GLC3A locus, Chr 2 p22-p21)**, ***LTBP2*** **(GLC3C locus, Chr 14q24) [questionable]**, ***MYOC*** **gene (rarely)**, and ***TEK/ANGPT1***.
- **The CYP1B1 enzyme** is in the cytochrome P450 family. Pathogenic variants in *CYP1B1* may affect the metabolism of retinol and thus might affect ocular development by affects levels of retinoic acid.
- The role of ***LTPB2*** (latent transforming growth factor beta-binding protein 2) in ocular tissues is not well defined. It is expressed in trabecular meshwork (TM) and ciliary processes. Although mutations in the gene have been reported as a rare cause of PCG, they are more often associated with primary megalocornea with zonular weakness and secondary lens-related glaucoma, a phenotype that can be mistaken as PCG.
- ***MYOC*** **or myocilin** (Chr 1q24.3-q25.2) was formally known as ***TIGR*** (trabecular meshwork-induced glucocorticoid response protein). *MYOC* is expressed in both TM and ciliary body. Mutated MYOC obstructs TM outflow with resultant increased IOP. Pathogenic variants in *CYP1B1* might interact with *MYOC* in some cases of JOAG and adult-onset POAG.
- **TEK** (tunica interna endothelial cell kinase), also known as **TIE2** (Chr 9p21), and its ligand **ANGPT1** (angiopoietin-1) represent a recently described pathway for glaucoma. TEK receptors are expressed in Schlemm's canal endothelium. Studies in mice have shown that reduced TEK signaling causes developmental defects of aqueous humor outflow structures leading to increased intraocular pressure (IOP).

A. O. Khan (✉)
Pediatric & Neuro- Ophthalmology, Eye Institute, Cleveland Clinic Abu Dhabi, Abu Dhabi, United Arab Emirates

Cleveland Clinic Lerner College of Medicine of Case Western Reserve University, Cleveland, OH, USA
e-mail: arif.khan@mssm.edu

A. Wahi
Dr. Rajendra Prasad Centre for Ophthalmic Sciences, All India Institute of Medical Sciences, New Delhi, India

S. Gupta et al. (eds.), *Childhood Glaucoma*, https://doi.org/10.1007/978-981-19-7466-3_3

3.1.2 Juvenile Open-Angle Glaucoma (JOAG)

- Represents 3.3% of all glaucoma admissions in India.
- One-third of cases are familial, often **autosomal dominant with high penetrance**. Sporadic and autosomal recessive forms are also seen.
- Nonfamilial and familial cases seem to be phenotypically similar.
- ***MYOC*** **(myocilin)** pathogenic variants are commonly associated with the phenotype.
- More than 70 identified pathogenic variants in *MYOC* contribute to increased aqueous outflow resistance (Table 3.1).
- The presence of *CYP1B1* pathogenic variants is associated with advanced visual field loss.
- Optineurin (*OPTN*) and TANK-binding kinase 1 (*TBK1*) have been associated with normal-tension JOAG.

3.1.3 Axenfeld-Rieger Syndrome (ARS)

- Typically an **autosomal dominant** pattern of inheritance
- Genetic classification
- ARS **Type 1**—pathogenic variant in ***PITX2*****; Chr 4q25**
- ARS **Type 2**—pathogenic variant in ***RIEG2*****; Chr 13q14**
- ARS **Type 3**—pathogenic variant in ***FOXC1*****; Chr 6p25**

3.1.4 Classic Aniridia (AN)

- An **autosomal dominant** inheritance in **about two-third of cases**; the remaining one-third of cases are sporadic.

Table 3.1 Risk profile for selected MYOC pathogenic variants

Risk	*MYOC* Pathogenic variant
Mild risk	Gln368STOP
Moderate risk	Thr377Met Gly252
Severe risk	Thr377Met and Gly252

- Classic aniridia is associated with pathogenic variants in ***PAX6*** **(Chr 11p13)**, which is adjacent to *WT1* (Wilms tumor predisposition gene). A deletion causing aniridia that is large enough to include *WT1* causes a predisposition to Wilms tumor of the kidney. Approximately 68% of patients with this contiguous gene syndrome will develop Wilms tumor before 3 years of age.
- Pathogenic variants in *PAX6* show almost complete penetrance with variable expressivity.
- Genetic classification.
- **AN 1**—Null mutation in ***PAX6***
- **AN 2**—Pathogenic variant in ***PAX6*** **cis-regulatory element**
- **AN 3**—Pathogenic variant in ***TRIM44*** (Chr 11p13)

3.1.5 Peters Anomaly

- **Most cases are sporadic**, although there are cases of autosomal recessive inheritance and less commonly autosomal dominant inheritance.
- Most commonly associated with pathogenic variants in ***PAX6***, ***PITX2***, ***CYP1B1***, or ***FOXC1***.

3.2 The Role of Genetic Testing in Childhood Glaucoma

When facing a child with potential glaucoma, the ophthalmologist's primary role is to make the most specific clinical diagnosis possible and facilitate medical, surgical, and amblyopia management as appropriate. In addition to the clinical exam, a good family history assessment or pedigree can be useful in making a specific diagnosis. Also potentially useful is examination of the parents, as this can reveal undiagnosed disease or signs of autosomal dominant disease, particularly for certain anterior segment dysgeneses.

Genetic testing is not typically needed for ocular management of childhood glaucoma because such management is guided by phenotype, not genotype. However, there are clinical scenarios where genetic testing is useful for children with glaucoma. These include when

1. Genetic counseling is desired and is reasonable.
2. Clinical exam suggests a potential risk for actionable extraocular disease.
3. The glaucoma is in the setting of and related to systemic disease.
4. The diagnosis is questionable (certain populations).

The term "genetic testing" encompasses different techniques (e.g., conventional sequencing, copy number variation analysis), targets (e.g., single variant, single gene, multiple genes, whole exome, whole genome), and pitfalls (e.g., variants of uncertain significance, genes of uncertain significance, incomplete penetrance, variable expressivity, mosaicism). Ophthalmologists should only consider ordering genetic testing if they are competent in genetic testing methods, indications, and interpretation or if they work with a trained individual such as a medical geneticist or genetic counselor.

3.2.1 Scenario 1: Genetic Counseling Is Desired and Is Reasonable

A newborn girl from the Arabian Gulf was born with ocular enlargement, corneal edema, and raised intraocular pressure—features of primary congenital glaucoma (Fig. 3.1a). Her older

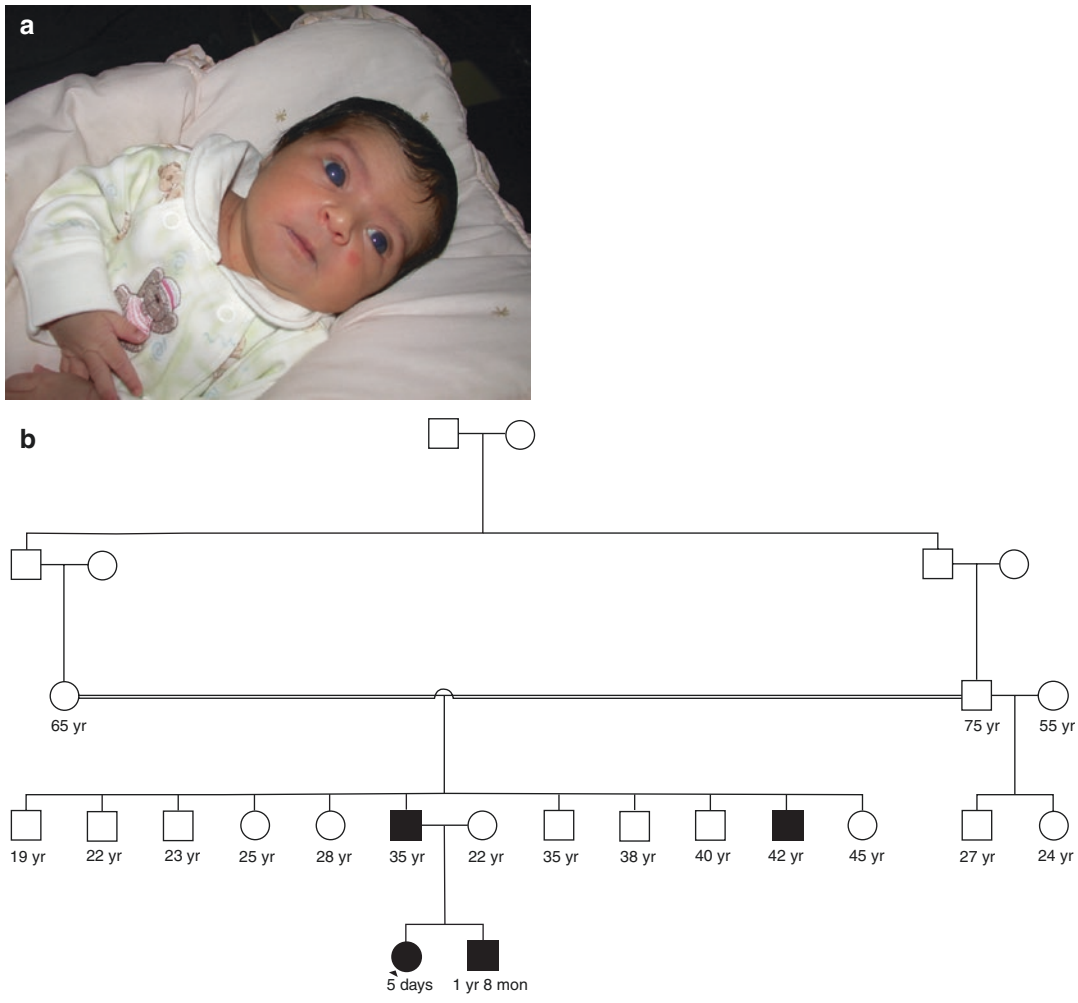

Fig. 3.1 (**a**) Corneal haze and ocular enlargement can be appreciated in this newborn with primary congenital glaucoma; (**b**) the family pedigree is shown (a simplified version, not following the convention of older individuals listed to the left)

brother also had newborn primary congenital glaucoma. The father and his brother were diagnosed with juvenile open-angle glaucoma in their 20s. The mother was unaffected. The parents were not from the same family but were from the same tribal region. This baby girl required surgical management, as did her affected relatives (Fig. 3.1b).

The parents were concerned regarding the recurrent glaucoma in their family and desired genetic counseling. This was only possible with a molecular genetic diagnosis. Given that the family was from a region of the world where biallelic *CYP1B1* pathogenic variants underlie over 90% of bilateral primary congenital glaucoma and can underlie juvenile glaucoma as well, sequencing of *CYP1B1* was performed. This uncovered homozygosity for a common *CYP1B1* pathogenic variant in the proband, her brother, and her father, explaining their disease. The unaffected mother was heterozygous for the *CYP1B1* pathogenic variant. This pattern of inheritance is known as pseudodominant (when an affected individual homozygous or compound heterozygous for pathogenic variants in a gene marries an unaffected individual heterozygous for a pathogenic variant in the same gene).

Testing for the identified specific pathogenic variant in extended family members of the proband (cascade testing) revealed relatives who were heterozygous carriers for the *CYP1B1* pathogenic variant and could then be counseled appropriately. Cascade testing also identified relatives who were homozygous for the *CYP1B1* pathogenic variant, some of whom had had undiagnosed juvenile glaucoma.

Knowledge of the underlying genetic cause for familial pediatric glaucoma can empower certain families. However, for some, knowledge of being a genetic carrier for the disease causes feelings of guilt and anxiety. Genetic counseling and education are important in alleviating these potential negative emotions. Some families consider their disease as fate and do not desire family risk assessments or preventative advice.

Learning Points

- Identification of the cause for familial congenital glaucoma can empower families and allow preventative measures. Further cascade testing can then identify other family members who are carriers, who are affected but undiagnosed, or who are not carriers.
- Genetic testing and counseling are not necessarily appropriate for all families with primary congenital glaucoma.
- Pathogenic variants are less likely to be identified in sporadic or unilateral cases of primary congenital glaucoma, particularly in regions where *CYP1B1* pathogenic variants are not prevalent.

3.2.2 Scenario 2: Clinical Exam Suggests a Potential Risk for Actionable Extraocular Disease

A newborn girl was referred as a glaucoma suspect (Fig. 3.2). Ophthalmic examination revealed bilateral peripheral keratopathy, lack of iris, anterior polar lens opacity, focal hypoplasia, and moderate cupping—the phenotype of classic aniridia. Intraocular pressures were 10 mmHg either eye. There was no history for ophthalmic disease in the family, and anterior segment examination of the parents was within normal limits. Glaucoma in classic aniridia is typically juvenile, although it can be infantile-onset. This baby girl will require regular follow-ups for the possibility of juvenile glaucoma (as well as for potential significant lens opacity and keratopathy).

Sporadic classic aniridia in a newborn is a medical indication for genetic testing. Classic aniridia is typically from a heterozygous loss-of-function pathogenic variant in the transcription factor gene *PAX6*. While familial cases are typically from intragenic pathogenic variants, sporadic cases can be from new chromosome 11p deletions. If such a new deletion encompasses not only *PAX6* but also the neighboring gene *WT1*, the *WT1* deletion confers a significant risk

for Wilms tumor of the kidney before 5 years of age. For this reason, a newborn with sporadic classic aniridia should have targeted copy number variation analysis of the *PAX6/WT1* region on chromosome 11p to uncover whether or not the child has significant risk for developing Wilms tumor. The *PAX6/WT1* contiguous gene syndrome is known as WAGR syndrome, named for its main and most common features (Wilms tumor, aniridia, genitourinary anomalies, and intellectual disability [formerly termed mental retardation]).

Fig. 3.2 Peripheral keratopathy, lack of iris, and lens opacity can be appreciated in the right eye of this newborn; the left eye (not shown) was similar

In this case, targeted analysis revealed a new 11p12–14 chromosomal deletion that included both *PAX6* and *WT1*. The child developed Wilms tumor the following year, but because of careful targeted surveillance based on the genetic diagnosis, the Wilms tumor was detected early and optimally managed.

Learning Points

Genetic testing in certain children with or at risk for childhood glaucoma can identify a risk for extraocular disease and thus lead to decreased extraocular morbidity.

3.2.3 Scenario 3: The Glaucoma Is in the Setting of and Related to Systemic Disease

A baby boy developed open-angle infantile glaucoma with buphthalmos in the setting of developmental delay and hearing impairment. Facial features were notable for arched eyebrows, broad nasal bridge, retrognathia, long philtrum, and elongated ears (Fig. 3.3a). Also notable were broad thumbs (Fig. 3.3b) and big toes. He also had hearing impairment.

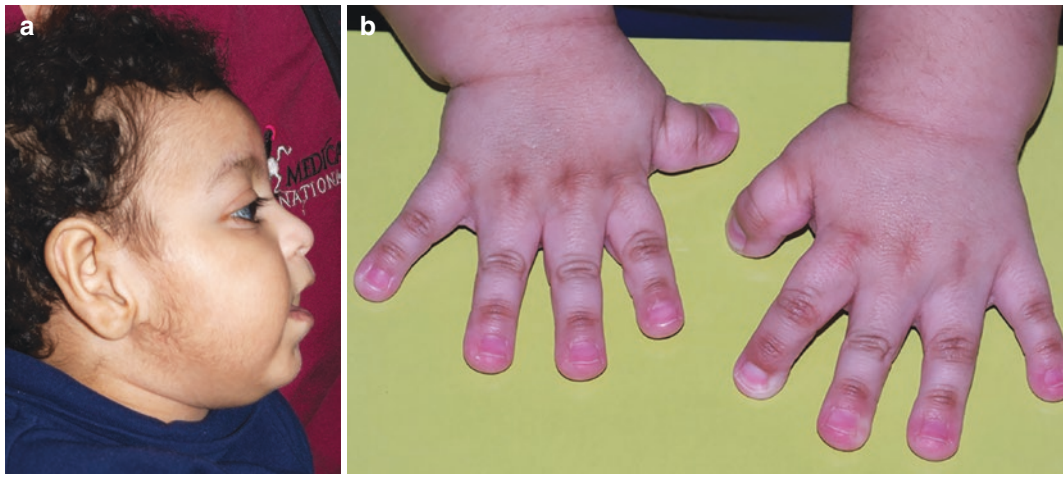

Fig. 3.3 (**a**) Arched eyebrows, retrognathia, long philtrum, and elongated low-set ears can be appreciated in side profile of this child; (**a**) Also notable were broad fingers (**b**) and toes (not shown)

Although individually rare, there are collectively many genetic multisystem syndromes that include childhood glaucoma. Any child with glaucoma in the setting of systemic disease should have an evaluation by a geneticist. In this particular case, the constellation of findings was consistent with Rubinstein-Taybi syndrome. Targeted genetic sequencing for the associated genes revealed a *CREBBP* heterozygous pathogenic variant that was not present in either parent. Obtaining a molecular result in this situation alerted the clinical team to what other issues the child was at risk for—in this case, cardiac and renal defects. In addition, the child should also undergo cancer surveillance given the risk for *CREBBP*-related malignancy.

Learning Points
Genetic testing in certain children with childhood glaucoma can identify a risk for extraocular disease and thus lead to decreased extraocular morbidity.

3.2.4 Scenario 4: The Diagnosis Is Questionable (Certain Populations)

A baby boy from the Arabian Gulf with corneal haze (Fig. 3.4) and raised measured intraocular pressure was referred for a fourth opinion. Three previous ophthalmologists had diagnosed the boy with primary congenital glaucoma and recommended urgent glaucoma surgery in both eyes. However, the pattern of haze, lack of corneal enlargement, thickness of the cornea, and hyperopic refraction through the haze were consistent with an actual diagnosis of congenital hereditary endothelial dystrophy (CHED). Unfortunately, the family was reluctant to accept the revised diagnosis in the context of three previous ophthalmologists having recommended urgent glaucoma surgery.

In general, phenotype, not genotype, guides clinical management decisions. However, in this situation, genetic testing can provide supportive evidence for the clinical impression and help the parents to accept the true diagnosis. Targeted sequencing of *SLC4A11*, the gene associated with CHED, revealed a known homozygous pathogenic variant. This confirmed the clinical diagnosis of CHED. In addition, *CYP1B1* analysis was performed for the child and was negative for pathogenic variants. Lack of *CYP1B1* pathogenic variants in a child from a region where over 90% of primary congenital glaucoma is *CYP1B1*-related supported the clinical impression of no glaucoma.

Fig. 3.4 Diffuse corneal haze can be appreciated in this newborn; note the lack of ocular enlargement

After receiving the molecular results and further discussion, the parents accepted the absence of glaucoma. He was managed appropriately as a case of CHED.

Learning Points
Ophthalmologists who care for children with glaucoma need to be aware of conditions that can mimic childhood glaucoma. Genetic testing can help support clinical impressions.

3.3 Conclusions

Several different genes are known to be associated with childhood glaucoma, and autosomal recessive cause is more common in certain areas of the world. Genetic testing is not typically required for diagnosis or management, but there are scenarios in which genetic testing has a role in childhood glaucoma. These include when a

family desire for genetic counseling and planning, a clinical exam that suggests risk for actionable extraocular disease which could be identified with genetic testing, syndromic childhood glaucoma, and, in certain populations, a questionable diagnosis. Ophthalmologists should only consider ordering genetic testing if they are competent in genetic testing methods, indications, and interpretation or if they work with a medical geneticist or genetic counselor.

Suggested Reading

Alward WLM. Axenfeld-Rieger syndrome in the age of molecular genetics. Am J Opthalmol. 2000;130(1):107–15.

Bhatia S, Bengani H, Fish M, et al. Disruption of autoregulatory feedback by a mutation in a remote, ultraconserved PAX6 enhancer causes aniridia. Am J Hum Genet. 2013;93(6):1126–34.

Franzoni A, Russo PD, Baldan F, D'Elia AV, Puppin C, Penco S, Damante G. A CGH array procedure to detect PAX6 gene structural defects. Mol Cell Probes. 2017;32:65–8.

Gupta V, Markan A, Somarajan BI, Sihota R, Gupta A, Gupta S, Sharma A. Phenotypic differences between familial versus non-familial Juvenile onset open angle glaucoma patients. Ophthalmic Genet. 2018;39(1):63–7.

Khan AO. Genetics of primary glaucoma. Curr Opin Ophthalmol. 2011;22(5):347–55.

Khan AO. A surgical approach to pediatric glaucoma. Open Ophthalmol J. 2015;9:104–12.

Khan AO, Al-Shehah A, Ghadhfan FE. High measured intraocular pressure in children with recessive congenital hereditary endothelial dystrophy. J Pediatr Ophthalmol Strabismus. 2010;47(1):29–33.

Khan AO, Aldahmesh MA, Al-Abdi L, Mohamed JY, Hashem M, Al-Ghamdi I, Alkuraya FS. Molecular characterization of newborn glaucoma including a distinct aniridic phenotype. Ophthalmic Genet. 2011a;32(3):138–42.

Khan AO, Al-Abdi L, Mohamed JY, Aldahmesh MA, Alkuraya FS. Familial juvenile glaucoma with underlying homozygous p.G61E CYP1B1 mutations. J AAPOS. 2011b;15(2):198–9.

Khan AO, Aldahmesh MA, Mohamed JY, Hijazi H, Alkuraya FS. CYP1B1 analysis of unilateral primary newborn glaucoma in Saudi children. J AAPOS. 2012;16(6):571–2.

Micheal S, Siddiqui SN, Zafar SN, Iqbal A, Khan MI, den Hollander AI. Identification of novel variants in LTBP2 and PXDN using whole-exome sequencing in developmental and congenital glaucoma. PloS One. 2016;11(7):e0159259.

Ormestad M, Blixt A, Churchill A, Martinsson I, Enerback S, Carlsson P. Foxe3 haploinsufficiency in mice: a model for Peters' anomaly. Invest Ophthalmol Vis Sci. 2002;43(5):1350–7.

Petrij F, Giles RH, Dauwerse HG, Saris JJ, Hennekam RC, Masuno M, Tommerup N, van Ommen GJ, Goodman RH, Peters DJ, et al. Rubinstein-Taybi syndrome caused by mutations in the transcriptional co-activator CBP. Nature. 1995;376(6538):348–51.

Reis LM, Tyler RC, Weh E, et al. Analysis of CYP1B1 in pediatric and adult glaucoma and other ocular phenotypes. Mol Vis. 2016;22:1229–38.

Souma I, Tompson SW, Thomson BR, et al. Angiopoietin receptor TEK mutations underlie primary congenital glaucoma with variable expressivity. I Clin Invest. 2016;126(7):2575–87.

Turalba AV, Chen TC, Taylor & Francis. Clinical and genetic characteristics of primary juvenile-onset open-angle glaucoma (JOAG). Semin Ophthalmol. 2008;23(1):19–25.

Weh E, Reis LM, Happ HC, et al. Whole exome sequence analysis of Peters' anomaly. Hum Genet. 2014;133(12):1497–511.

Zhang X, Qin G, Chen G, et al. Variants in TRIM44 cause aniridia by impairing PAX6 expression. Hum Mutat. 2015;36(12):1164–7.

Part II

Clinical Evaluation

Tonometry

4

Amisha Gupta, Pawan Kumar, and Shikha Gupta

Intraocular pressure (IOP) measurement is one of the most important investigations required for the diagnosis of disease and to monitor its severity, as well as for assessing the progression of glaucoma. This is because many patients with childhood glaucoma have hazy corneas/are uncooperative due to which the visualization and assessment of the optic nerve head is often not possible. Also, other important investigations like perimetry and optical coherence tomography cannot be performed in younger pediatric eyes.

Challenges in performing reliable pediatric tonometry (Fig. 4.1):

- Poor cooperation of young children.
- Altered corneal properties: The presence of corneal edema/opacity, altered corneal biomechanics due to stretching and variable corneal thickness: all these corneal factors hamper reliable IOP measurement.
- Need of putting the babies to sleep, offer them sedation, or need to administer general anesthesia in order to record IOP. Anaesthesia also alters IOP measurement.
- Inaccurate IOP reading due to squeezing of eyes in awake conditions.
- IOP measurement needs to be done under supine positioning in younger patients and hence slit lamp mounted tonometers used for adults can not be used in younger children.

Supplementary Information The online version contains supplementary material available at https://doi.org/10.1007/978-981-19-7466-3_4.

A. Gupta (✉) · P. Kumar · S. Gupta
Dr. Rajendra Prasad Centre for Ophthalmic Sciences, All India Institute of Medical Sciences, New Delhi, India
e-mail: shikhagupta@aiims.edu

S. Gupta et al. (eds.), *Childhood Glaucoma*, https://doi.org/10.1007/978-981-19-7466-3_4

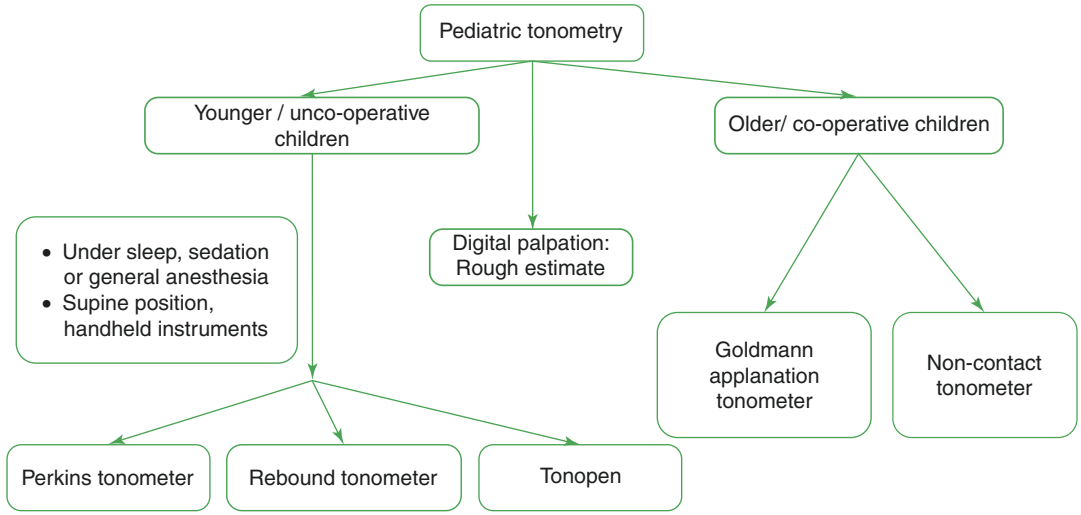

Fig. 4.1 An approach to performing pediatric tonometry

4.1 Natural Sleep/Sleep Under Sedatives

- As an outpatient procedure, tonometry in younger children can be performed in deep sleep achieved naturally with breastfeeding or through sedation (Fig. 4.2).
- The ideal stage of sedation of the child for IOP measurement may be the one with an acceptable depth of sleep with minimum effect on IOP.
- There are several sedatives available. Some of the commonly available ones are triclofos, chloral hydrate, hydroxyzine, oral midazolam, and melatonin.
- Oral triclofos is most commonly used for sedating children for IOP measurement. It is commercially available in 500 mg/5 mL concentration, and dosage is approximately 50 mg/kg or 0.5 mL/kg. Only mild side effects like nausea, vomiting, and drowsiness have been reported with the drug usage in children.
- Once the patient is in deep sleep, tonometry is performed with the patient in the supine position in the mother's lap using a handheld tonometer.

Fig. 4.2 Intraocular pressure measurement using iCare tonometer of an infant while in deep sleep aided with sedatives

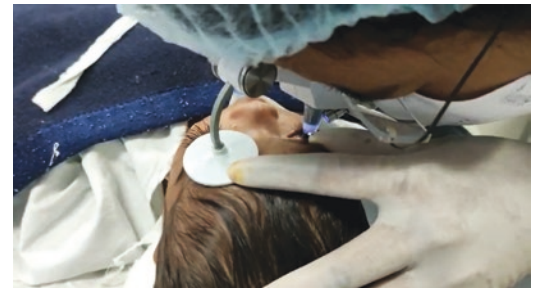

Fig. 4.3 Intraocular pressure measurement of an infant under general anesthesia using Perkins tonometer

4.2 General Anesthesia (Fig. 4.3)

- Before examining under general anesthesia (GA), fasting is required for 6 to 8 hours

depending on age. The criteria for fasting for solids/liquids is different.
- Studies have shown that the use of speculum during the procedure may increase the IOP by 4 mmHg compared to only gently lifting the eyelid. Care should be taken to use an adequately sized speculum that does not indent the globe, thereby increasing the IOP inadvertently.
- It is also important to consider the effect of general anesthesia on IOP measurements. It has been noted that general anesthesia may cause underestimation or overestimation of IOP based on the drug used.

4.3 Methods of Tonometry (Tables 4.1, 4.2)

4.3.1 Goldmann Applanation Tonometer

Goldmann Applanation Tonometry (GAT) (Figs. 4.4 and 4.5) is still considered the gold standard for measuring IOP even after the advent of several newer techniques.

4.3.1.1 Principle

GAT (Haag Streit, USA) is based on the principle of "Imbert-Fick" law. It states that the pressure (*P*) of the sphere is equal to the force (*F*) applied on its surface to flatten the given area (*A*), i.e., $P = F/A$. It uses variable force to measure the pressure of the eye by applanating a constant area with a diameter of 3.06 mm.

4.3.1.2 Procedure (Video 4.1)

- Anesthetize the eyes using local anesthesia (xylocaine 1%).
- Position the patient on the slit lamp, and ask him to look in primary gaze.
- Instill fluorescein dye in the eye.
- Insert the prism in the GAT attachment of the slit lamp so that the graduation marking "0" on the prism is aligned with the white marking on the tonometer head (Fig. 4.6).
- Turn on the cobalt blue filter.
- Rotate the GAT measurement dial at 1. Bring the prism closer to the eye till it just touches the cornea and two semicircular mires are formed.
- Align the mires using the dial so that the inner edge of the mires just touches each other (Fig. 4.7).
- Multiply the reading on the dial with 10 to get the IOP measurement in mmHg.
- Instill topical antibiotic after the procedure.

4.3.1.3 Disinfection of the Prism

GAT prism should be disinfected after each procedure by soaking in 10% bleach (sodium hypochlorite) for 5 minutes. It can also be disinfected using 70% isopropyl alcohol or 3% hydrogen peroxide. It is important to note that prism should be rinsed with sterile water and wiped dry with a clean swab after disinfection, before use.

4.3.1.4 Sources of Errors

- In high astigmatism of >4D, the IOP measurements may not be reliable. In such cases, the red line on the feeler arm is matched with the number on the prism, which corresponds to the minus axis of astigmatism.
- The IOP measurements will be falsely high or low if the cornea is thick or thin, respectively. The IOP measurements should be corrected based on the central corneal thickness of the eye in such cases.
- Improper alignment of mires.
- If the mires are too thick or thin, it will lead to overestimation or underestimation of IOP, respectively.
- Squeezing of eyes may lead to falsely high IOP.
- Pressing the prism too hard against the cornea may lead to IOP overestimation.
- GAT tends to give false readings in cases like corneal edema and corneal scarring. Despite all these, it is the gold standard for IOP measurement in older cooperative kids.

Table 4.1 Advantages and disadvantages of different tonometers

Tonometer	Advantage	Disadvantage
Goldmann Applanation Tonometer (GAT)	Most accurate Reproducible Affordable	Affected by Central Corneal Tonometry (CCT) and corneal hysteresis Requires training Needs patient's full cooperation Can be performed only in an upright position Requires topical anesthesia and fluorescein dye
Perkins Tonometer	Readings comparable to GAT Can be performed in a supine as well as upright position Hand held device Can be performed in sedated children	Not possible in very small eyes Requires skill Affected by CCT and Corneal hysteresis Requires topical anesthesia and fluorescein dye
Tonopen	Less chances of ocular infection transmission as disposable latex cap is used for each patient Portable, lightweight, quick, easy to use Can be performed in both supine and upright position Useful in edematous, scarred, or irregular corneas Useful in uncooperative patients	Significantly affected by CCT Underestimates the intra-ocular pressure (IOP) if IOP>30 mmHg Requires topical anaesthesia
Rebound tonometer	Reliable, reproducible, and rapid Easy to use Does not require anesthesia or fluorescein Can be performed in a supine or upright position No chances of infection transmssion as it uses disposable probes Calibration not required Indents a small corneal suface of 1.8 mm	Underestimates IOP >23 mmHg Slightly affected by the CCT and Corneal hysteresis
Noncontact tonometer (NCT)	Noncontact Does not require anesthesia or fluorescein Minimal risk of infection transmission Easy and rapid to use Helpful in patients sensitive to anesthesia	Influenced by corneal hysteresis and corneal thickness Overestimates IOP in thicker corneas Underestimates IOP >20 mmHg
Dynamic contour tonometry	Not affected by the CCT It has a resolution of <0.1 mmHg Wide measurement in range of 1–300 mmHg More reliable in operated LASIK (Laser-Assisted in-situ Keratomileusis) eyes	Requires more patient cooperation as IOP measurement takes 5–6 seconds Difficult in nystagmus and uncooperative patients
Trans-palpebral tonometer	Noninvasive Does not require anesthesia Does not interfere with the patient's field of vision Portable and easy to operate Can be used at home by the patient himself Shown to have better accuracy than GAT in thinned corneas after photorefractive procedures Can be used in cases like conjunctivitis, corneal erosions, sores, hypostasis, and corneal dimness	Requires skill Several studies have shown that it has lower sensitivity in measuring IOP in glaucomatous eyes

Table 4.2 Comparison of different tonometers (De Moraes CG et al 2008)

Tonometer	Handheld for younger children	Accuracy (relative to GAT)	Accuracy in irregular corneas	Accuracy in thick corneas	Corneal Contact
Goldmann applanation tonometry (GAT)	–		–	–	+
Perkins	+	Good Agreement	–	–	+
Tonopen	+	Depends on the IOP level	+	–	+
Rebound tonometer	+	Conflicting reports (good agreement or overestimates)	Little information available	–	+
Noncontact tonometer	+/– (Depends on the model)	Depends on model and IOP level	–	–	–
Dynamic contour tonometry	–	Overestimates	–	+	+
Transpalpebral tonometry	+	Poor agreement	+	+	–

Fig. 4.4 Goldmann applanation tonometer (Haag Streit, USA)

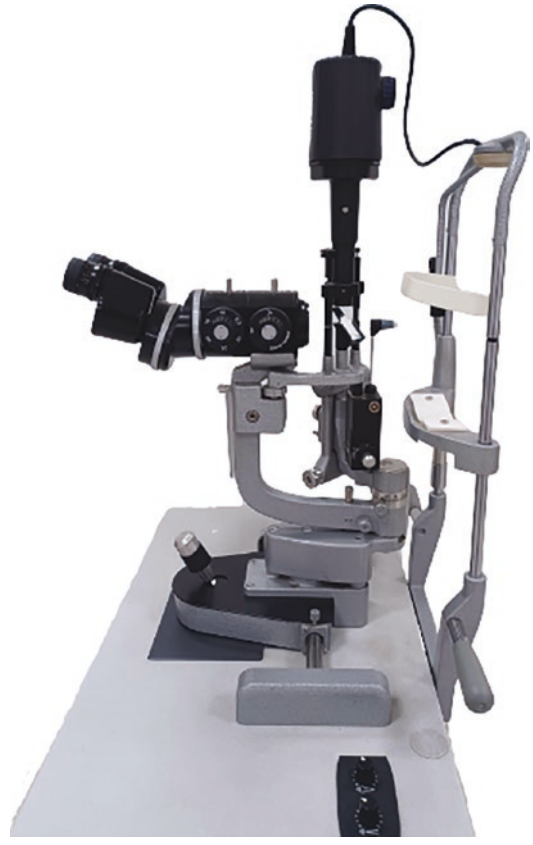

Fig. 4.5 Slit lamp-mounted Goldmann applanation tonometer (Haag Streit, USA)

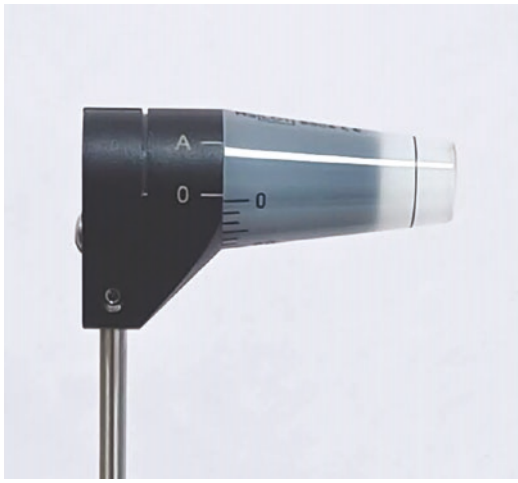

Fig. 4.6 Aligning Goldmann applanation tonometer prism with the tonometer head

Fig. 4.7 Aligning the mires in Goldmann applanation tonometry by approximating the inner edges of the two semi-circles

Fig. 4.8 Perkins tonometer (Haag Streit, USA)

4.3.2 Perkins

Perkins (Haag Streit, USA) (Fig. 4.8) is a handheld tonometer similar to GAT, measurement on which can be done in supine as well as upright position. It provides precise measurement in children even if they are less cooperative.

4.3.2.1 Principle

Same as GAT, based on 'Imbert Fick' Principle.

4.3.2.2 Procedure (Video 4.2)

- Anesthetize the patient's eye using proparacaine drops and instill fluorescein dye using the strips.
- Rotate the dial to marking 1. It will automatically turn on the cobalt blue filter.
- Fixate the patient's eye onto some target and bring Perkins close to the patient till it just

touches the central cornea and mires (same as GAT) are formed.
- Follow the procedure similar to that of GAT to measure the IOP.

4.3.2.3 Calibration (Video 4.3)
- Perkins is calibrated using a calibration disc.
- Turn on the Perkins, and position the dial on 2.
- Hold the probe facing upward, and place the calibration disc on top of the probe.
- Slightly move the dial toward marking 2.1, and this will cause the prism arm to move up if Perkins is calibrated.

4.3.3 Tonopen

Tonopen (Reichert® Technologies, NY, USA) (Fig. 4.9) is an electronic portable tonometer. It is the most widely used method of tonometry in uncooperative and young patients, as it measures the IOP in seconds.

4.3.3.1 Principle
It is a type of handheld Mackay Marg tonometer. It is based on applanation tonometry. It applanates a small region of the cornea having area of 2.36 mm^2 and diameter 1.5 mm using a plunger. The movement of the plunger is detected by a transducer which converts it to the IOP measurement.

4.3.3.2 Procedure (Video 4.4)
- Instill an anesthetic in the eye.
- In case of a cooperative patient, ask the patient to fixate in the primary position.
- Switch on the Tonopen.
- Touch the tip of the Tonopen to the center of the cornea or the clear area of the cornea ten times, taking care that the measuring tip remains perpendicular to the cornea.
- Tonopen will beep after ten readings, and the averaged reading will appear on the display.

4.3.3.3 Calibration
- Point the tip of the Tonopen straight down toward the floor.
- Press the button for approx. 15 seconds. The Tonopen will beep and display “dn.”

Fig. 4.9 Tonopen (Reichert® Technologies, NY, USA)

- Wait for approx. 15 seconds to allow Tonopen to beep again and display “UP.”

- Invert the Tonopen so that the tip points upwards.
- Wait, the Tonopen will beep again and display "Pass" if the Tonopen is calibrated or "Fail" if not calibrated.

4.3.4 Rebound Tonometer

Rebound tonometry is also the preferred method of IOP measurement in children who are not cooperative for GAT. Rebound tonometer consists of a disposable probe consisting of a small 1.8 mm diameter plastic ball mounted on a stainless steel wire (Fig. 4.10). This probe is placed in a magnetized steel shaft. iCare tonometer (iCare, Finland) is the only commercially available Rebound tonometer at present. Different models of the rebound tonometers are available in the market.

- The first commercially available rebound tonometer, iCare TA01i, was released in 2003. The tonometer was appreciated for measuring the IOP in children as it did not require any kind of anesthesia or sedation. But the main disadvantage of iCare TA01i was that it could not be used in supine position as the probe used to fall when the tonometer faced downwards.
- The updated version iCare PRO was released in 2010 to overcome this disadvantage. iCare PRO has an in-built inclination sensor that holds the probe when the tonometer is held facing downward. This allows measurement in supine position also.
- Another version of the rebound tonometer, iCare ONE, is designed for measuring the IOP at home. This tonometer can be used by the patient himself.
- iCare HOME is the upgraded version launched in 2014 with an automatic eye recognition system. The tonometer can identify the eye under examination (whether right or left) and proper tonometer positioning while taking measurements.
- The latest model iCare ic200 (Fig. 4.11), an updated version of iCare TA01i, was launched in 2016. The tonometer has better probe grasping and improved upright position sensor.

Fig. 4.10 Probe of Rebound tonometer iCare 200 iCare, Finland)

4.3.4.1 Principle

A rebound tonometer propels the probe toward the cornea by an electrical pulse generator that creates a magnetic field. After hitting the cornea, the ball decelerates. The rate of deceleration depends on the IOP of the measuring eye. If the IOP is high, the deceleration is fast, and if the IOP is low, the deceleration will be slow. To calculate the IOP, the velocity of the deceleration (rebound) after hitting the cornea is converted to a voltage that is further correlated with IOP using a proprietary algorithm.

4.3.4.2 Procedure (Video 4.5)

- Replace the probe with the new one before performing the examination.
- Ask the patient to fixate in the primary position.
- Hold the iCare tonometer so that the probe is perpendicular to the cornea at a distance of around 5 mm.
- Switch on the iCare, and press the measurement button.

Fig. 4.11 iCare model ic200 (iCare, Finland)

- It will propel the probe towards the patient and will show the mesaured IOP reading.
- Adjust the distance of the tonometer from the cornea, if the display screen shows "near" or "far" accordingly.

4.3.4.3 Calibration

iCare tonometer does not require routine calibration. It is done by the company itself.

4.3.5 Noncontact Tonometer

Noncontact tonometer (NCT) (Fig. 4.12) is the most widely used non-invasive tool for the measurement of IOP. It is very useful as a screening tool as being a non-contact device, there are minimal chances of infection transmission. It is also relatively easier to perform. NCT is primarily performed in an upright position. With the advent of new technologies, handheld NCT is also available.

4.3.5.1 Principle

NCT is based on the principle of applanation performed using air. The device emits a jet of air (air puff) and a collimated light beam. The force of

Fig. 4.12 Noncontact tonometer model Tonoref III (Nidek Co. Ltd., Japan)

the air puff increases linearly with time and flattens the cornea. Simultaneously, the collimated light beam is reflected from the central cornea and is received by the photocell present in the device. It is based on the fact that the photocell will receive maximum light when the cornea is completely flat, i.e., applanated. The force at the point when the cornea is applanated is used to calculate the IOP of the eye.

4.3.5.2 Calibration

The model eye is used to calibrate the NCT. Different companies use different types of model eyes.

4.3.5.3 Procedure (Video 4.6)

- Switch on the noncontact tonometer.
- Position the patient on the NCT station with chin on the chin-rest, and ask him to look at the fixation target positioned in the primary gaze inside the instrument with eyes wide open.
- Instruct the patient not to move or close the eye when a puff of air will touch his eyes.
- Focus the mires at the center of the cornea.
- Once the mires are focused, the NCT will automatically measure the IOP if it is on automatic mode.
- On the manual mode, press the acquisition button, when mires are focused.

4.3.6 Transpalpebral Tonometer

Transpalpebral tonometers are new-generation tonometers that measure IOP through the eyelid. It is non-invasive and can be used by the patient's parents for home IOP monitoring of the child. TGDc-01 (DevelopAll Inc., USA) is the commercially available transpalpebral tonometer. Diaton is an upgraded version of the TGDc-01. Diaton has a vertical alignment sensor and an in-built software for averaging the IOP readings.

4.3.6.1 Principle

Transpalpebral tonometer calculates the IOP by measuring the elastic reaction of the eye when an object of definite weight falls freely on the tarsal plate of the eyelid on the sclera.

4.3.6.2 Procedure

- Recline the patient to supine position and ask the patient to fixate 45° inferior to the primary position.
- Without pressing the eye, pull the upper lid so that the edge of the lid coincides with the upper limbus.
- Place the tonometer on the upper lid so that the tip of the tonometer touches the lid vertically.
- Keep holding the tonometer until it produces a short sound which indicates that the reading is taken.
- Repeat the measurements thrice, and press the button. The tonometer will display the average IOP reading.

4.3.7 Dynamic Contour Tonometer (DCT)

Dynamic contour tonometer is a digital tonometer that measures the transcorneal pressure with minimal deformation of the cornea. It measures the pulsatile ocular blood flow over a period of about 5 seconds. DCT is independent of the central corneal thickness and corneal properties. Pascal Dynamic Contour Tonometer (SMT Swiss Microtechnology AG, Switzerland) is the commercially available DCT which is a slit lamp mounted tonometer similar to GAT. In the pediatric setting, it can only be used in older children who can be seated on slit lamp.

4.3.7.1 Principle

It is based on the principle of "contour matching." The tip of the probe of DCT that touches the cornea has a concave surface of radius 10.5 mm

which matches the corneal contour. The probe tip, when comes in contact with the central cornea, takes the shape of the probe, and the pressure equilibrium is obtained on both the sides of the cornea. As the shape of the tip almost matches with that of the cornea, the tangential and bending forces no longer act within the corneal area under consideration. Assuming that in such conditions, the apex of the cornea is free from any of the abovementioned forces, the pressure on both sides of the cornea will be equal. The pressure is, hence, calculated using a piezoelectric pressure sensor. This sensor has a diameter of <0.25mm^2.

4.3.7.2 Procedure

- Anesthetize the eyes using local anesthesia (xylocaine 1%).
- Position the patient on the slit lamp, and ask him to look in primary gaze.
- Bring the slit lamp closer to the eye so that the tip of the probe touches the corneal center.
- A continuous sound will be heard. After about 4–5 seconds, OK sound will be heard which signifies that measurement has been taken.
- Retract the slit lamp.
- Instill topical antibiotic after the procedure.

4.3.8 Digital Tonometry (Palpation)

There are various instruments to measure the IOP. The main fallacy with these devices is that most of these depend on the corneal parameters, hence are not precise. In pediatric glaucoma, many children have edematous or scarred cornea, and hence, the IOP measurement with the abovementioned instruments is not very reliable, especially in the extreme range. In such scenarios, the IOP measured by such instruments may be grossly rechecked using the palpation method.

4.3.8.1 Procedure (Video 4.7)

Ask the patient to look down. Keep the index fingers of both hands on the eyeball to be examined, above the tarsal plate. Push the eyeball with the index finger of one hand, and sense the firmness of the globe with the other finger of the other hand (Fig. 4.13).

Fig. 4.13 Measuring intraocular pressure of a child by digital palpation method

4.4 Conclusions

There are several methods to measure the IOP in children. Each of the methods has certain advantages and disadvantages. The choice of the method to perform tonometry in children varies from case to case. Though difficult to perform in children, if performed accurately with an adequate tool, it really is the most important tool to follow up children with glaucoma.

Suggested Reading

Brusini P, Salvetat ML, Zeppieri M. How to measure intraocular pressure: an updated review of various tonometers. J Clin Med. 2021;10(17):3860. https://doi.org/10.3390/jcm10173860.

De Moraes CG, Prata TS, Liebmann J, Ritch R. Modalities of tonometry and their accuracy with respect to corneal thickness and irregularities. J Optom. 2008;1(2):43–9.

Epley KD, Tychsen L, Lueder G. The effect of an eyelid speculum on intraocular pressure measurement in children. Am J Ophthalmol. 2002;134(6):926–7.

Fayed MA, Chen TC. Pediatric intraocular pressure measurements: tonometers, central corneal thickness, and anesthesia. Surv Ophthalmol. 2019;64(6):810–25. Epub 2019 May 24. https://doi.org/10.1016/j.survophthal.2019.05.003.

Gao F, Liu X, Zhao Q, Pan Y. Comparison of the iCare rebound tonometer and the Goldmann applanation tonometer. Exp Ther Med. 2017;13(5):1912–6.

Gopesh T, Camp A, Unanian M, Friend J, Weinreb RN. Rapid and accurate pressure sensing device for direct measurement of intraocular pressure. Transl Vis Sci Technol. 2020;9(3):28.

Senthil S, Nakka M, Rout U, Ali H, Choudhari N, Badakere S, Garudadri C. Changes in intraocular pressures associated with inhalational and mixed anesthetic agents currently used in ophthalmic surgery. Indian J Ophthalmol. 2021;69(7):1808–14. https://doi.org/10.4103/ijo.IJO_2923_20.

Troost A, Yun SH, Specht K, Krummenauer F, Schwenn O. Transpalpebral tonometry: reliability and comparison with Goldmann applanation tonometry and palpation in healthy volunteers. Br J Ophthalmol. 2005;89(3):280–3. https://doi.org/10.1136/bjo.2004.050211.

Childhood Glaucoma: Gonioscopy

5

Ananya Kaginalkar, Shikha Gupta, and Viney Gupta

Alexios Trantas first coined the word "gonioscopy," originating from the Greek words of "gonia" meaning angle and "skopein" meaning to observe while visualizing the anterior chamber angle in an eye with keratoglobus.

The basis of gonioscopy lies in the optical principle of total internal reflection which precludes the direct visualization of the anterior chamber angle in healthy eyes. The critical angle for the air cornea interface is approximately 46° (i.e., when the angle of incidence (i) = 46°, the angle of refraction (r) = 90°.

Principle of Gonioscopy When light rays coming from the anterior chamber exceed the critical angle (i.e., angle of incidence (**i**) > 46°), the light rays undergo total internal reflection and are therefore reflected back into the anterior chamber making an angle of refraction (**r**) thereby precluding the visualization of the anterior chamber angle (Fig. 5.1).

This problem is circumvented by using goniolens or gonioprism to eliminate the air-cornea interface. Light rays from the anterior chamber angle thus enter the contact lens and pass through the contact lens air interface and can therefore be visualized.

Gonioscopy on the pediatric eyes requires special consideration as a considerable number of examinations are done under general anesthe-

Fig. 5.1 Total internal reflection

Supplementary Information The online version contains supplementary material available at https://doi.org/10.1007/978-981-19-7466-3_5.

A. Kaginalkar (✉) · S. Gupta · V. Gupta
Dr. Rajendra Prasad Centre for Ophthalmic Sciences, All India Institute of Medical Sciences, New Delhi, India
e-mail: shikhagupta@aiims.edu

S. Gupta et al. (eds.), *Childhood Glaucoma*, https://doi.org/10.1007/978-981-19-7466-3_5

sia, requiring special techniques and lenses to carry out the gonioscopic evaluation.

Gonioscopy can be performed utilizing one of the following two optical principles:

(a) Direct gonioscopy
(b) Indirect gonioscopy

5.1 Direct Gonioscopy

Direct gonioscopy involves direct visualization of the angle utilizing a **goniolens** and a handheld biomicroscope with a separate light source such as the Barkan focal illuminator or an operating microscope.

5.1.1 Principle of Direct Gonioscopy

A steep convex lens (goniolens) is used which has an anterior curvature such that light rays incident on this surface with an angle of incidence (**i**) from the anterior chamber angle are refracted at the contact lens air interface closer to the perpendicular axis making an angle of refraction (**r**) which allows for an erect view of the anterior chamber angle (Fig. 5.2).

This method is most commonly utilized while evaluating the anterior chamber angle in the setting of sedation/general anesthesia for ease of examination as it provides an erect view of the angle and also proves to be of assistance while carrying out surgical procedures. Hence its utility is most pronounced in the setting just before the surgery and especially in eyes with neonatal/infantile glaucoma to confirm diagnosis and as a prerequisite before angle surgery to rule out adhesions in the angle. The use of this method is particularly useful in angle surgeries that require intraoperative direct gonioscopy in order to visualize the anterior chamber angle and carry out various angle-based procedures.

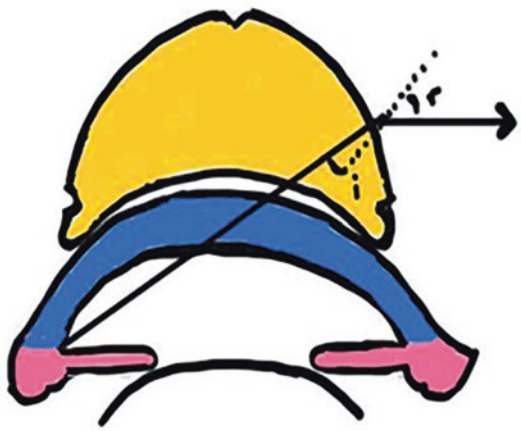

Fig. 5.2 Principle of direct gonioscopy

5.1.2 Lenses

Commonly used goniolenses to evaluate the angle in pediatric populations are enumerated below:

1. *Koeppe Lens:* This is a prototype diagnostic goniolens, which is made of barium crown glass or plastic and is available in different diameters (16–22.5 mm) with different posterior radii of curvature. The power of the lens is +50 D. Koeppe lens has a magnification of 1.5× which in combination with 16x of the oculars yields a total magnification of 24×. Fundoscopy can also be performed through these lenses using a direct ophthalmoscope and a high-plus power lens. These lenses, however, are not provided with a handle (Fig. 5.3a, b).
2. *Swan Jacob Lens:* This is a surgical goniolens that can be used in all pediatric patients. This lens is provided with an anodized aluminum handle which facilitates easy manipulation for angle visualization during surgery. It provides an image magnification of 1.20× and has a contact diameter of 9 mm in Volk surgical goniolenses (Volk Optical Inc., Mentor, OH, USA) and 9.5 mm in Ocular lenses (Ocular Instruments, WA, USA), respectively. It is particularly useful while performing goniotomy, goniosynechialysis, ab interno trabeculotomy, and microinvasive glaucoma surgeries (Fig. 5.3c).
3. *Richardson Shaffer Lens:* This lens is used for infants and is a smaller Koeppe lens.

4. *Layden Lens:* This lens is used in premature infants and has a diameter of 10.5 and 11.5 mm (Fig. 5.3d).
5. *Hoskins Barkan Lens:* It is a prototype surgical lens and does not have an attached rod. The infant lens (Ocular Instruments, WA, USA) is oval and conical in shape with a 10 mm diameter. The premature infant lens has the same shape and design except the dimensions are 1 mm smaller, i.e., 9 mm lens is used for premature infant surgery. These lenses provide a magnification of 1.30× and are designed for transverse goniotomy surgeries with loupes or an operating microscope but can also be used as a diagnostic lens (Fig. 5.3e).
6. *Thorpe Surgical Gonioscopic Lens*: This lens has a dome-shaped design with an attached rod. It is mainly used in angle-based surgical procedures.
7. *Ritch Panoramic Gonioprism:* This lens has a unique design that leaves half the cornea closest to the surgeon exposed for the use of instruments, incisions, and corneal retraction sutures. The lens provides a 160° direct view of the angle.180° visualization of the anterior chamber angle is possible with minimal rotation of this lens.
8. *Ahmed DVX Surgical Gonio Lens:* Ahmed Direct View Extreme wide field lens (Ocular Instruments, WA, USA) is the latest surgical gonioscope. It has the widest double mirror field of view, and therefore the angle can be visualized without rotation of the handle. It provides an upright direct viewing, and hence angle can be visualized without tilting the microscope or the eye of the patient (Fig. 5.3f).
9. *Mori Upright Surgical Goniolens:* This surgical goniolens (Ocular Instruments, WA, USA) has a two-mirror design that redirects the oblique gonioscopic images to form a coaxial image enabling the surgeon to have a 360-degree view of the anterior chamber. The central view is to observe the instruments as they pass the anterior chamber. It is directly handheld and has a contact diameter of 11.5 mm with a magnification of 0.80× and a static field of view of 110°.

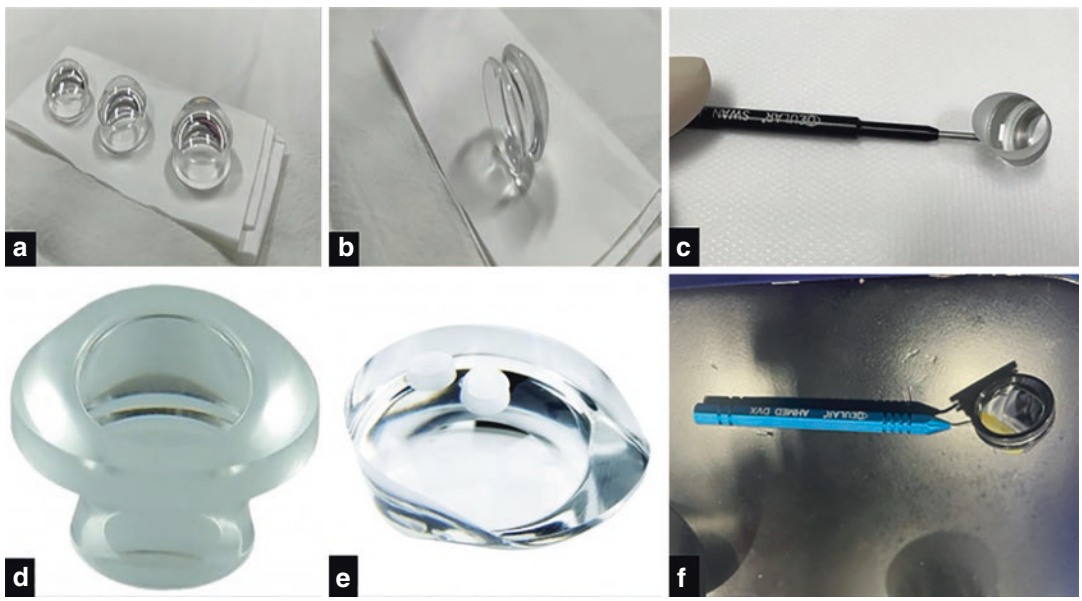

Fig. 5.3 Koeppe lenses with diameters of 16, 18, and 20 mm, respectively (**a**) and cross-sectional view of Koeppe lens (**b**), Swan Jacob surgical goniolens (Ocular) (**c**), Layden lens (Ocular Instruments, WA, USA) (**d**), Hoskins-Barkan lens (Ocular Instruments, WA, USA) (**e**), and Ocular Ahmed DVx lens (**f**)

Sterilization of goniolenses: Most of the lenses used in direct gonioscopy are sterilized with ethylene oxide gas, while some glass lenses can be autoclaved.

5.1.3 Procedure of Direct Gonioscopy (Video 5.1)

Positioning: Head of the patient is tilted 30–45° away from the surgeon while the microscope is tilted by the same angle towards the surgeon sitting temporally (Fig. 5.4a, b).

Procedure: A clean and sterile goniolens is placed on the eye of the patient lying in the supine position using a viscoelastic substance as an optical coupler (Fig. 5.4c). The lens is then rotated using the handle in the direction of the angle to be visualized while still maintaining contact with the ocular surface, without applying undue pressure. This enables the examiner to obtain a 360-degree view of the angle while shifting positions and can be used to perform goniotomy/goniosynechialysis procedures (Fig. 5.4d).

RetCam Gonioscopy: RetCam known as EyeCam (Clarity Medical System, Pleasanton, CA, USA) essentially used for pediatric fundus evaluation can be used for pediatric direct gonioscopy and allows for goniophotographic documentation of angle structures, with the inclusion of a 130-degree lens (Fig. 5.5a, b). The hardware consists of a handheld digital video camera con-

Fig. 5.4 Direct gonioscopy procedure: Head tilt of the patient 30–45° away from the surgeon (**a**), microscope tilt of 30–45° toward the surgeon sitting temporally (**b**), Swan Jacob lens placed on the cornea using methylcellulose as a coupling agent (**c**) and direct angle visualization via the goniolens (**d**)

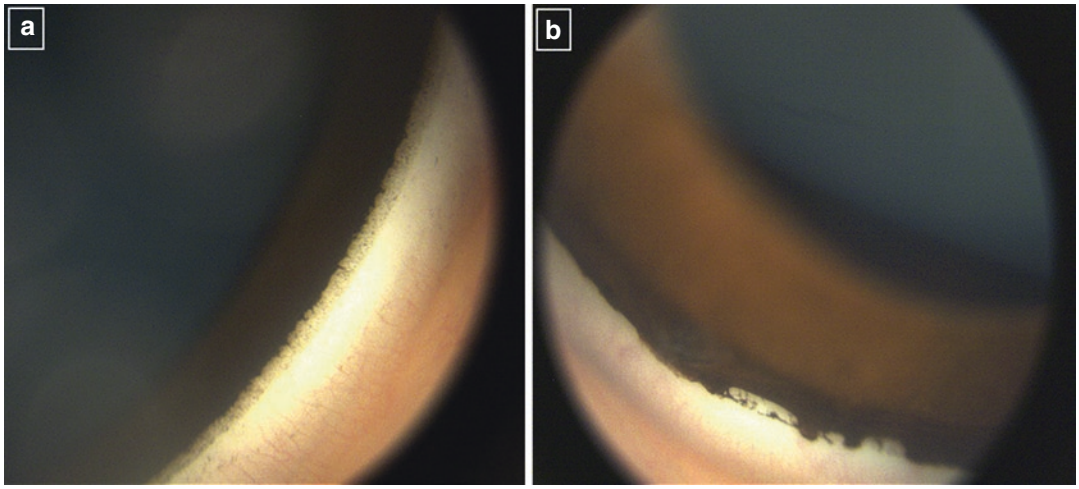

Fig. 5.5 RetCam gonioscopy showing anterior insertion of iris (**a**) and wraparound iris configuration (**b**)

nected fiber optically to a light-emitting control unit and computer assembly. The anterior chamber angle is visualized after application of a coupling agent by placing the 130-degree lens close to the limbus, opposite to the angle to be viewed. However, major limiting factors of this diagnostic modality are the cost of the equipment (USD 125,000 in India), bulky and stationary design of the machine, and limited availability in routine examination rooms and operation theaters.

Additional techniques to visualize anterior chamber angle structures intraoperatively: In certain situations like hazy cornea (excluding severe corneal haze) or featureless angle, we can use indocyanine green dye (ICG) and external jugular vein compression technique to identify angle structures intraoperatively. Intracameral administration of 0.2% ICG dye aids in accurate identification of the trabecular meshwork by imparting a bright green hue to it, thereby differentiating it from other angle structures and allowing precise identification and cannulation of Sclemm's canal (SC) in surgical procedures such as gonioscopic-assisted transluminal trabeculotomy (GATT). In featureless angles, wherein it is difficult to identify angle structures, external jugular vein compression results in engorgement of the SC visualized as a circumferential tangential red streak, thereby aiding in identification of SC increasing the success of surgical procedures such as GATT.

5.2 Indirect Gonioscopy

In older children cooperative for slit lamp examination, indirect gonioscopy can be carried out using **gonioprisms**.

5.2.1 Principle

In indirect gonioscopy, light rays from the anterior chamber angle are reflected by a mirror in the contact lens (gonioprism) and leave the lens at nearly right angle to the contact lens-air interface providing a view of the angle 180 degrees opposite to the mirror visualized (e.g., superior angle is visualized in the inferior mirror) (Fig. 5.6).

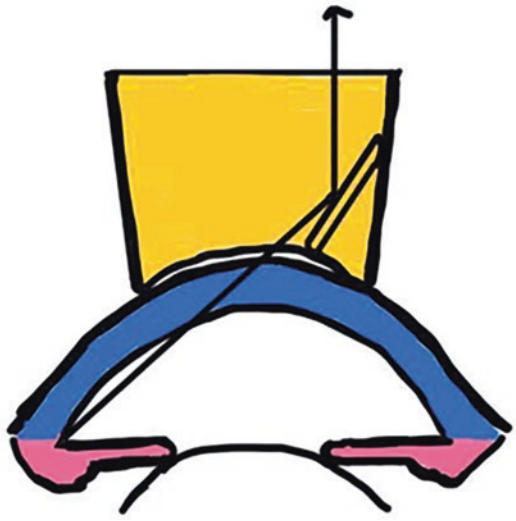

Fig. 5.6 Principle of indirect gonioscopy

5.2.2 Lenses

Gonioprisms are used for indirect gonioscopy in conjunction with a slit lamp.

Following lenses can be utilized for indirect gonioscopy in older children (Figs. 5.7 and 5.8):

Gonioprisms requiring coupling agents	Gonioprisms not requiring coupling agents
Goldmann single mirror	Zeiss four mirror
Goldmann two mirror	Posner four mirror
Goldmann three mirror	Sussman four mirror
Allen-Thorpe gonioprism	Volk six mirror

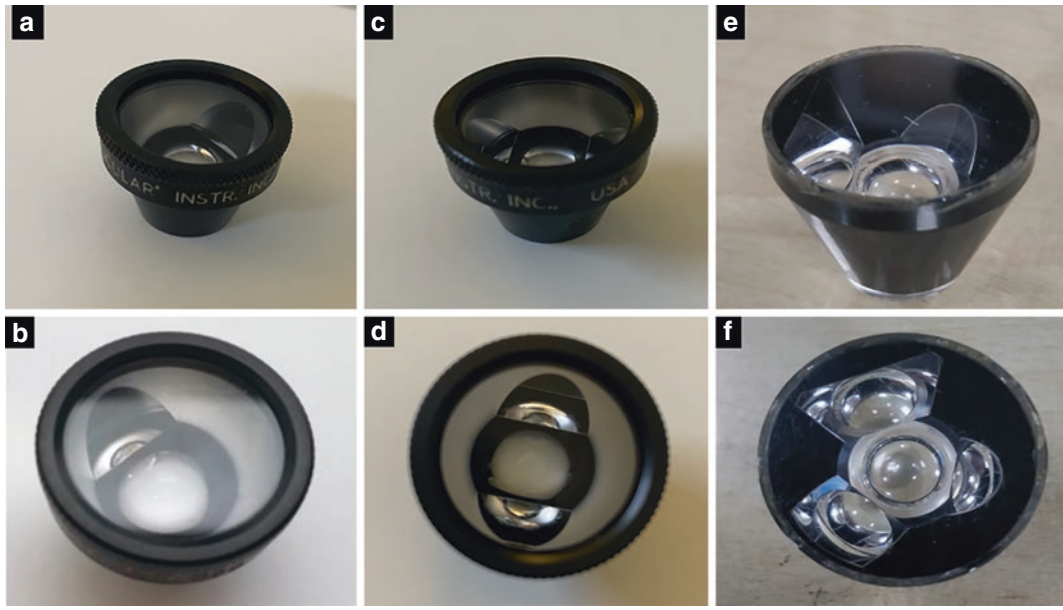

Fig. 5.7 Gonioprisms requiring coupling agents: Goldmann single-mirror lens (**a**, **b**), Goldmann two-mirror lens (**c**, **d**) and Goldmann three-mirror lens (**e**, **f**)

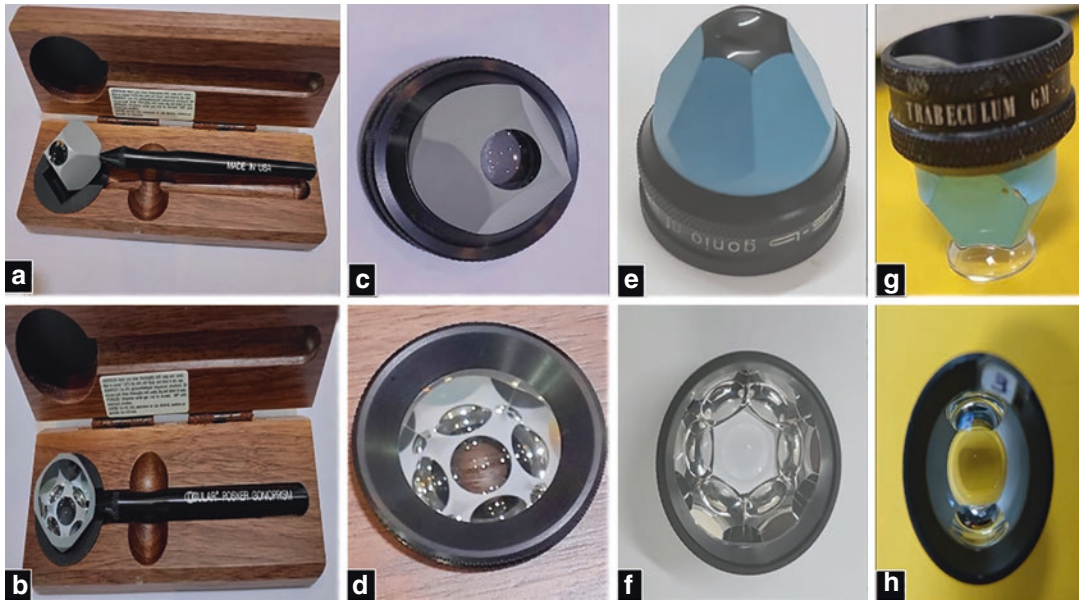

Fig. 5.8 (1) Gonioprisms not requiring coupling agents: Posner four mirror (**a**, **b**), Sussman four mirror (**c**, **d**), and Volk six-mirror goniolens (**e**, **f**) (2) trabeculum goniolens (**g**, **h**)

5.2.3 Procedure of Indirect Gonioscopy (Video 5.2)

Procedure: The goniolens surface is cleaned and disinfected with an alcohol sponge/2% glutaraldehyde or dilute (1:10) household bleach. The lens is then rinsed off with water and dried. A fluid bridge of artificial tears or viscoelastic gel may or may not be used depending upon the type of gonioprism used (Fig. 5.9a, b). After applying a topical anesthetic in the lower fornicial cul-de-sac, the patient is positioned at the slit lamp. The lateral canthus of the patient should be aligned with the canthal marker of the slit lamp. The illumination arm of the slit lamp is placed 15–30° from the observation arm, and the magnification is kept at 10×. The gonioprism is then placed against the cornea of the patient while asking him/her to look in the downward direction and parting the eyelids of the patient with the other hand (Fig. 5.9c). The angle is viewed "indirectly" through a mirror placed 180 degrees opposite from the quadrant being viewed. 1*1 mm narrow slit beam (2 or 3 mm slit beam can be used as well) is made with focal illumination (Fig. 5.9d), and the corneal wedge is identified. Light should not be allowed to enter the pupil to avoid constriction. The lines of the corneal wedge intersect at Schwalbe's line which is used as the landmark for identifying the anterior chamber angle structures. The magnification is then increased to 16 or 25× to visualize the rest of the angle structures. The lens is then rotated to allow visualization of all 360° of the angle, or the quadrants are studied with the four mirrors. The lens is then removed by asking the patient to look nasally and squeezing his/her lids forcefully. Pressure is applied to nudge the lens on the temporal side to introduce air, and the lens is removed. A topical antibiotic drop should be used after the procedure.

These lenses cannot be used in surgical procedures such as goniotomy and are only suitable for slit lamp-based diagnostic evaluations.

Thus, indirect gonioscopy can be carried out in cooperative young children and adolescents for diagnostic purposes.

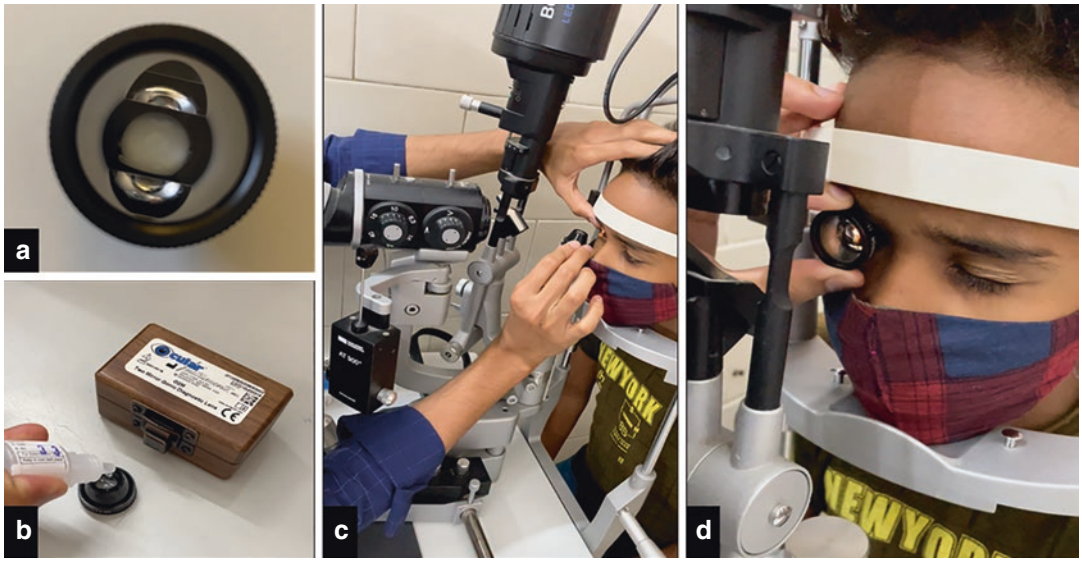

Fig. 5.9 Indirect gonioscopy procedure. Goldmann two-mirror gonioprism (**a**), coupling fluid is placed on the gonioprism (**b**), patient positioned on the slit lamp with lateral canthus at level of canthal marker (**c**). 1*1 mm narrow beam of light focused on the angle to be visualized (**d**)

5.3 Case-Based Examples

Case 5.1
Unilateral primary congenital glaucoma (PCG) undergoing trabeculotomy with trabeculectomy in the right eye.

Learning Points

- The trabecular meshwork is nonpigmented and smooth in infants but becomes coarser and more pigmented with advancing age as flow through the trabecular meshwork is through the posterior portion. The normal angle recess forms following birth during the first 6–12 months of life, and the ciliary body is seen subsequently as posterior iris recession commences, as a distinct band anterior to iris insertion. In a normal newborn, a flat insertion of the iris into the angle wall posterior to the scleral spur is most often present.
- Gonioscopic findings in PCG may consist of one of the following:
  - Open angle with high iris root insertion either at or anterior to scleral spur with altered translucency of the angle (historically thought to be Barkan's membrane) rendering indistinct ciliary body band (key distinguishing feature from a normal angle), trabecular meshwork, and scleral spur (Fig. 5.10).
  - Concave iris or "wraparound" iris is seen in PCG and occurs as a form of isolated tra-

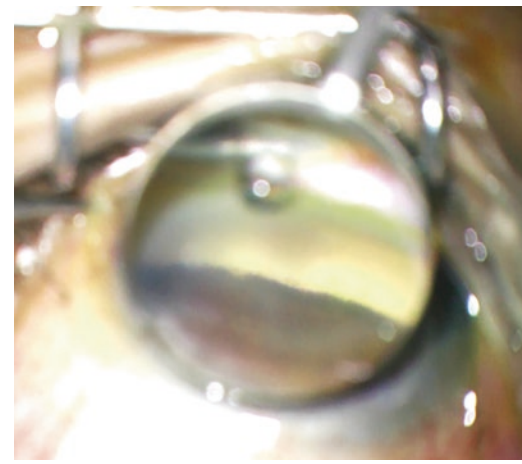

Fig. 5.10 Gonioscopy is done using Swan Jacob lens showing anterior iris insertion onto the posterior trabecular meshwork with rest of the angle appearing featureless

beculodysgenesis wherein the plane of the iris is posterior to scleral spur, but the anterior stroma sweeps upward over the trabecular meshwork obscuring the scleral spur and inserts just posterior to Schwalbe's line (Fig. 5.11). This conformation is recognized most easily in brown irides and is seen less commonly than the flat iris insertion.
- Multiple filiform iris processes can be seen in eyes with PCG.
- *Featureless angle*.
- *Lister's morning mist:* Scalloped border of iris pigment epithelium and trabecular meshwork itself appears through translucent peripheral iris stroma as if viewed through the morning mist.
- *Loch Ness Monster phenomenon*: Although the angle is avascular, loops of vessels from the major arterial arcade may be seen above the iris root.

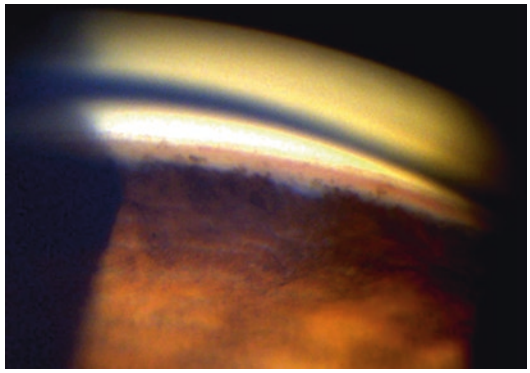

Fig. 5.11 Anterior iris insertion with wraparound configuration

Case 5.2

A case of juvenile onset open-angle glaucoma (JOAG) demonstrating a high insertion of the iris into the posterior trabecular meshwork with many prominent iris processes.

Learning Points

- Gonioscopic features of JOAG consist of:
  - High iris insertion with the root of iris inserted onto the trabecular meshwork, anterior to the ciliary body
  - Thick trabecular band with lack of pigmentation and differentiation from the scleral spur appearing as a featureless angle with a ground-glass appearance (Fig. 5.12a)
  - Prominent anomalous multiple iris processes extending onto trabecular meshwork in at least two quadrants (180°). They may be present alone or in association with a high iris insertion (Fig. 5.12b)
- High insertion of the iris is the most common form of goniodysgenesis observed.
- Two-thirds of JOAG patients present with developmental anomalies of angle, while one-third may have normal appearing angles.

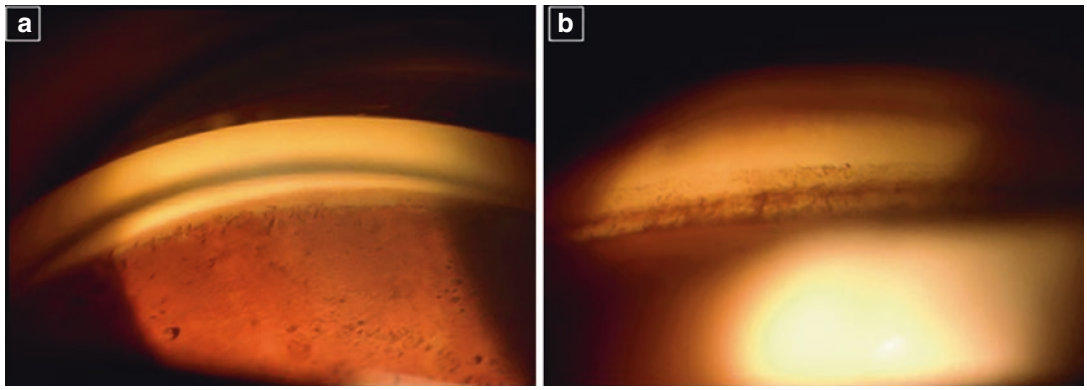

Fig. 5.12 Angle characteristics seen in JOAG: Featureless angle in JOAG (**a**), multiple iris processes extending onto trabecular meshwork (**b**)

Case 5.3
A case of Axenfeld Rieger (AR) anomaly with glaucoma, planned for trabeculectomy.

Learning Points
- Salient gonioscopic features in AR syndrome are:
  - Tissue strands ranging from threadlike to broadband like in size, bridge the anterior chamber angle from the peripheral iris to the prominent ridge, extending for a clock hour or more of the circumference, characteristically called as high peripheral anterior synechiae (PAS). The color and texture of these strands are similar to the adjacent iris (Fig. 5.13).
  - Prominent Schwalbe line with variable anterior displacement known as posterior embryotoxon. It may be incomplete, limited to the temporal quadrant, or maybe seen as a complete 360 degrees prominent ridge (Fig. 5.14).
  - Peripheral iris changes in the form of iris hypoplasia, atrophy, or hole formation may also be visible.

Case 5.4
A child diagnosed with Sturge-Weber syndrome (SWS) presenting with a port wine stain and history of seizures.

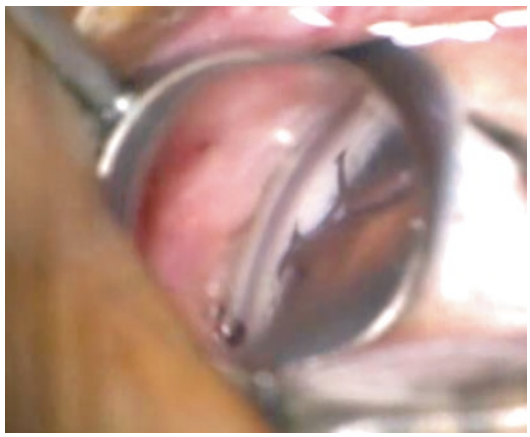

Fig. 5.13 Gonioscopy is done using Swan Jacob lens showing iridocorneal adhesions inserting onto and even beyond the Schwalbe's line confirming the diagnosis of Axenfeld-Rieger syndrome (ARS)

The differential diagnosis for open-angle glaucoma with blood in Schlemm's canal is:

- Causes of elevated episcleral venous pressure such as carotid-cavernous fistulas and orbital varices.
- Conditions obstructing venous flow such as thyroid-associated ophthalmopathy, superior vena cava syndrome, cavernous sinus thrombosis, and orbital amyloidosis.
- Blood in Schlemm's canal may also appear in gonioscopy due to excessive pressure applied by the goniolens. It may also normally be seen post phacoemulsification intraoperatively due to excessive fluid filtration effected through the angle.

Learning Points
- Glaucoma in SWS shows a bimodal peak of age:
  - *Early-onset (congenital form)*: In these patients, gonioscopy reveals abnormal angles with a poorly developed scleral spur and anteriorly displaced iris root.
  - *Late-onset*: These patients often have normal-appearing angles. The mechanism in these cases is attributed to elevated episcleral venous pressure that occurs due to small arteriovenous fistulas in the episcleral vessels.
- Open angle and blood in the Schlemm's canal are seen in SWS cases on gonioscopy but are not pathognomonic (Fig. 5.15).
- Gonioscopy may also show angle closure secondary to choroidal effusion or suprachoroi-

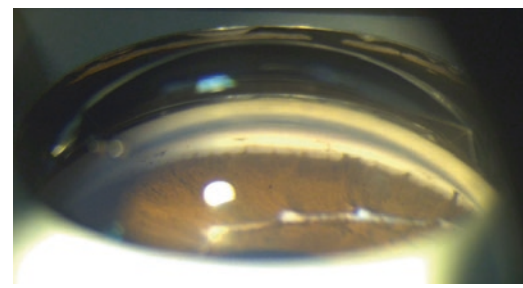

Fig. 5.14 Gonioscopic appearance of detached posterior embryotoxon with peripheral anterior synechiae seen in a case of ARS

dal hemorrhage caused due to anterior displacement of lens iris diaphragm. Neovascularization of the angle may also be seen secondary to ischemia.

Goniophotographic examples of a few more disease pathologies (Figs. 5.16, 5.17, and 5.18).

Approach to gonioscopy in pediatric population (Fig. 5.19).

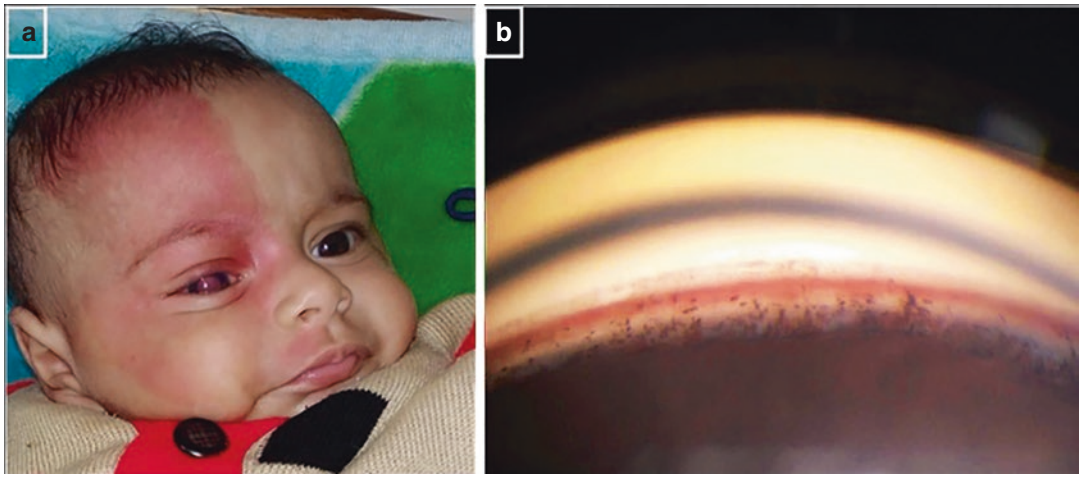

Fig. 5.15 Port wine stain in Sturge-Weber syndrome (**a**), gonioscopy demonstrating an open angle and blood in Schlemm's canal (**b**)

Fig. 5.16 Gonioscopic appearance of rudimentary iris stump and ciliary processes in a case of Aniridia

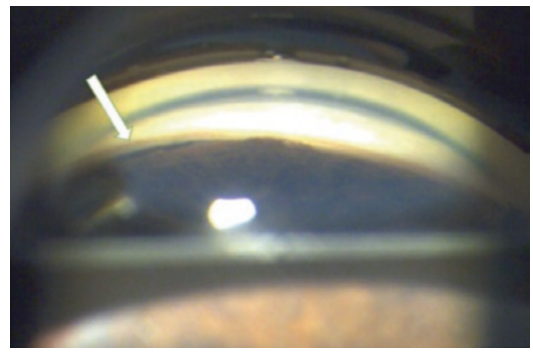

Fig. 5.17 Gonioscopy demonstrating the presence of a cyclodialysis cleft (white arrow) in a case with persistent hypotony

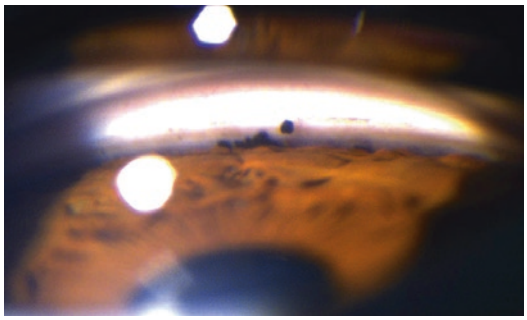

Fig. 5.18 Gonioscopy demonstrating the presence of a pigmented angle in a patient of oculodermal melanocytosis (Nevus of Ota)

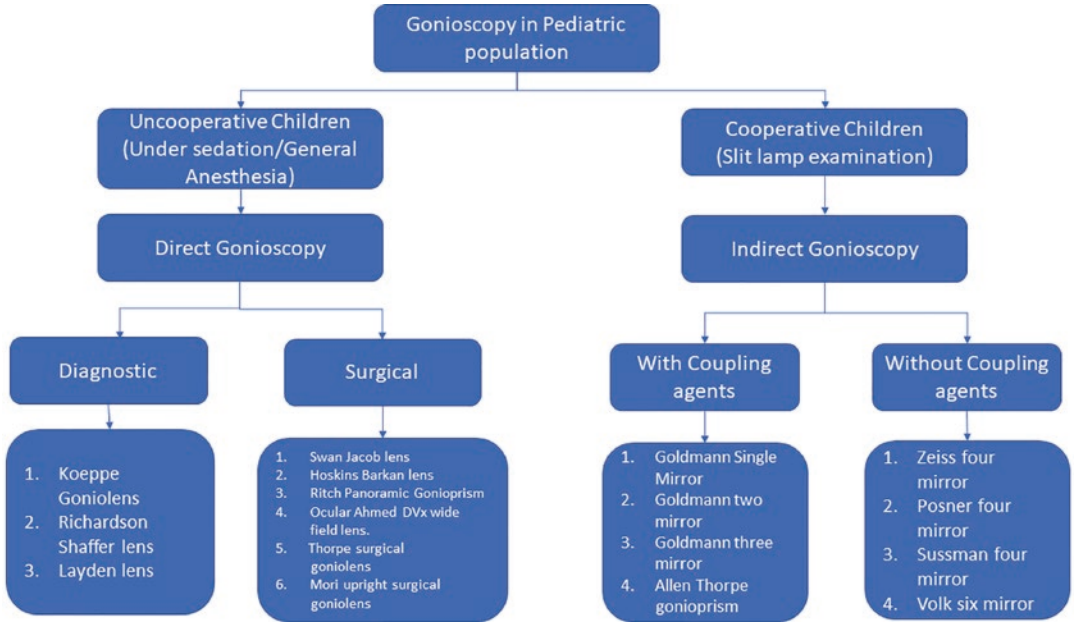

Fig. 5.19 Approach to Gonioscopy in pediatric population

5.4 Conclusions

Paediatric gonioscopy can be challenging, requiring careful selection of gonioscopy techniques for both diagnostic and surgical uses. Selection of the appropriate goniolens can aid surgical procedures with no/ minimal manipulation of the lens for visualisation. Special techniques like ICG dye injection/ external jugular vein compression can help enhance angle visualisation especially in eyes with featureless angles. Indirect gonioscopy can be carried out in an out patient setting for cooperative children and adolescents thus helping in accurate clinical diagnosis of angle disorders.

Suggested Reading

Allingham RR, Damji KF, Shields MB, editors. Shields textbook of glaucoma. 6th ed. Philadelphia: Wolters Kluwer Health/Lippincott Williams & Wilkins; 2011. p. 610.

Alward WLM. Color atlas of gonioscopy. San Francisco, CA: Foundation of the American Academy of Ophthalmology; 2001. p. 128.

Azad R, Chandra P, Chandra A, Gupta A, Gupta V, Sihota R. Comparative evaluation of RetCam vs. gonioscopy images in congenital glaucoma. Indian J Ophthalmol. 2014;62(2):163.

Chandrakanth P, Ravichandran R, Nischal N, Subhashini M. Trash to treasure Retcam. Indian J Ophthalmol. 2019;67(4):541.

Gupta V, Srivastava RM, Rao A, Mittal M, Fingert J. Clinical correlates to the goniodysgensis among juvenile-onset primary open-angle glaucoma patients. Graefes Arch Clin Exp Ophthalmol. 2013;251(6):1571–6.

Gupta S, Panigrahi A, Mahalingam K, Kumari S, Gupta V. External jugular vein compression aided gonioscopy assisted transluminal trabeculotomy in eyes with congenital glaucoma. J Glaucoma. 2022;31(7):e43–5.

Lambiase A, Mantelli F, Bruscolini A, La Cava M, Abdolrahimzadeh S. Ocular manifestations of Sturge-Weber syndrome: pathogenesis, diagnosis, and management. Clin Ophthalmol. 2016;10:871.

Morales J, Al Shahwan S, Al Odhayb S, Al Jadaan I, Edward DP. Current surgical options for the management of pediatric glaucoma. J Ophthalmol. 2013;2013:1–16.

Panigrahi A, Huang AS, Arora M, Kumari S, Mahalingam K, Gupta V, et al. Indocyanine Green Aided Schlemm's Canal Identification during gonioscopic assisted transluminal trabeculotomy. J Glaucoma. 2022;31:e69. https://journals.lww.com/10.1097/IJG.0000000000002047.

Sinha A, Mohan S, Gupta V, Sihota R. Gonioscopy. DOS Times. 2005;10:322–8.

Vinekar A, Rao SV, Murthy S, Jayadev C, Dogra MR, Verma A, et al. A novel, low-cost, wide-field, infant retinal camera, "Neo": technical and safety report for the use on premature infants. Transl Vis Sci Technol. 2019;8(2):2.

6 Fundus Evaluation in Childhood Glaucoma

Abhishek Singh, Karthikeyan Mahalingam, and Shikha Gupta

The comprehensive ophthalmic assessment is incomplete without fundoscopy, especially without a stereoscopic view of the optic nerve head (ONH), where the initial changes of glaucomatous damage appear, aiding in early diagnosis and management in children.

Problems with disc interpretation in children are:

- Wide morphological disparities of normal ONH in children of growing age (Fig. 6.1)
- Optic nerve tilting in eyes of congenital glaucoma with acquired myopia
- Optic disc reversal following IOP lowering surgeries
- Inter-observer variability

Devices that objectively measure retinal nerve fiber layer (RNFL) and ONH parameters in glaucoma have been developed, which apart from capturing fundus, evaluate the structural deterioration and allow temporal monitoring of disease. Confocal scanning laser ophthalmoscopy (Heidelberg Retinal Tomography, HRT), scanning laser polarimetry (GDx), optical coherence tomography (OCT), and scanning retinal thickness analyzer are some examples. Recent attention has been directed to OCT angiography and macular thickness for early detection of glaucoma. Adaptive optics enables the visualization of three-dimensional individual microstructures in vivo. However, the use of these modern devices requires patient collaboration and is more suited for research purposes at present.

Clinical fundus examination is imperative in childhood glaucoma screening although corneal clarity, pupillary dilation, and cooperation of the child are indispensable. It remains the clinical gold standard for analyzing ONH and RNFL in glaucoma, despite newer improved computer-based modalities. Red-free photographs help in visualization of the RNFL defects in the best possible way (Fig. 6.2).

Different techniques for fundus evaluation in children with different age groups is summarised in the flowchart (Fig. 6.3). Various methods of fundoscopy available in children are:

- Performing dilated ophthalmoscopy in photophobic children of congenital glaucoma demands deft expertise. Decreasing light intensity and distracting the children using colorful toys or smartphone applications can be helpful (Fig. 6.4a).
- In uncooperative kids, one or two assistants should help to hold the kid still (infants may be wrapped in the cloth), then fundus is examined utilizing a 28- or 30-diopter lens with an indirect ophthalmoscope, or using a 90-D lens with a portable slit lamp (can give magnified view) holding the eyelids apart using the wire speculum. Peripheral screening of the retina is

A. Singh (✉) · K. Mahalingam · S. Gupta
Dr. Rajendra Prasad Centre for Ophthalmic Sciences, All India Institute of Medical Sciences, New Delhi, India

S. Gupta et al. (eds.), *Childhood Glaucoma*, https://doi.org/10.1007/978-981-19-7466-3_6

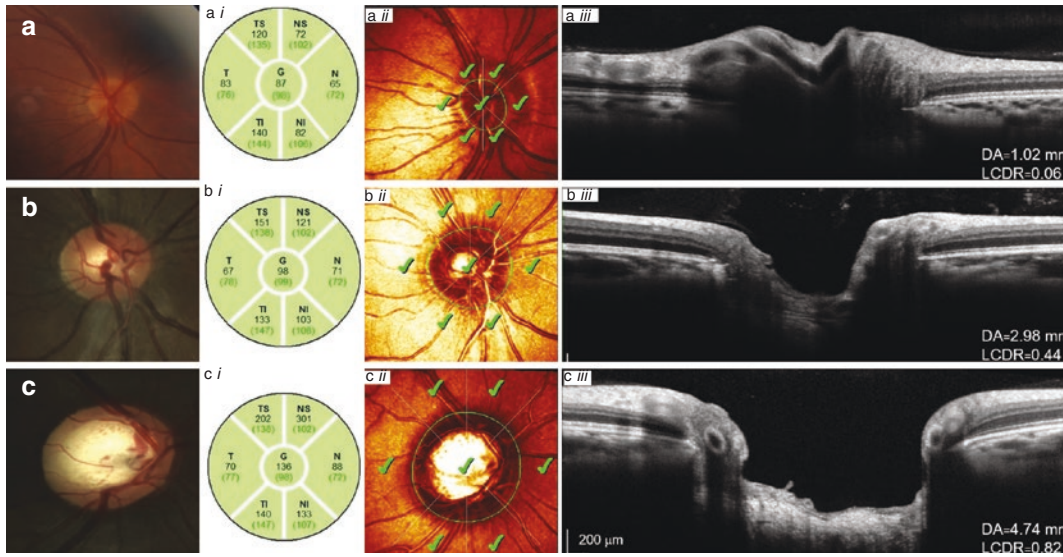

Fig. 6.1 (**a**) A microdisc, (**b**) an average-sized disc, and (**c**) a megalopapilla with peripapillary retinal nerve fiber layer (RNFL) optical coherence tomography (OCT) (*i*), Heidelberg Retinal Tomography (HRT) scan (*ii*), and enhanced depth imaging (*iii*). The number of retinal ganglion cell axons passing through the optic nerve is similar irrespective of the size of disc, so despite being non-glaucomatous, a larger disc (megalopapilla) will have larger cup disc ratio compared to smaller disc

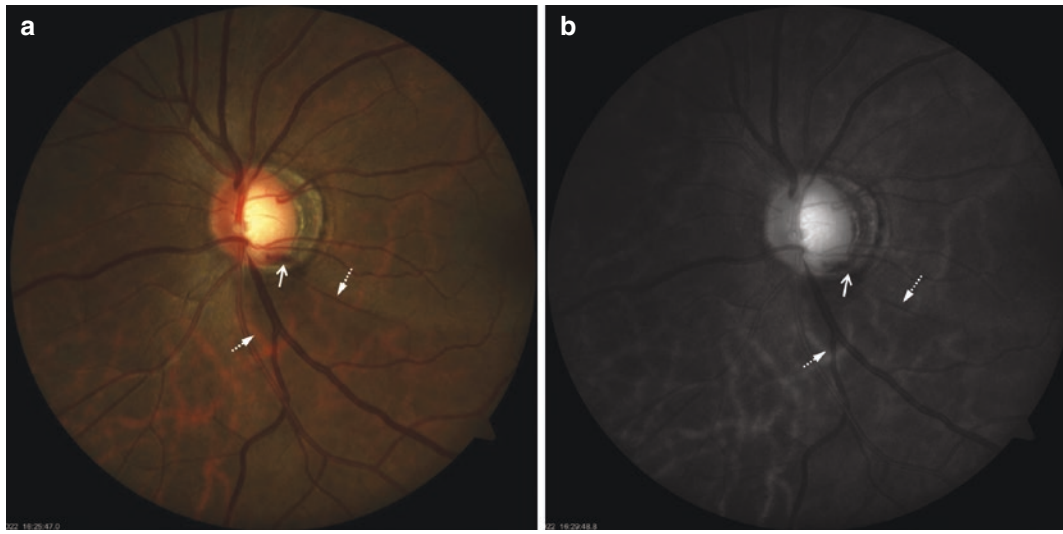

Fig. 6.2 (**a**) Color and (**b**) red-free photograph of 16-year-old patient with juvenile low-tension glaucoma, showing optic disc hemorrhage (a common finding due to inadequate intraocular pressure (IOP) control, high IOP fluctuations, or ischemic etiology) and retinal nerve fibre layer defect

essential to rule out peripheral retinal degenerations in greatly stretched eyes using Flynn scleral depressor (Fig. 6.4b, c). An examination under anesthesia/sedation might be needed in extremely unco-operative kids for fundus examination.

- Direct fundoscopy can also be performed through a modified Koeppe lens or with direct

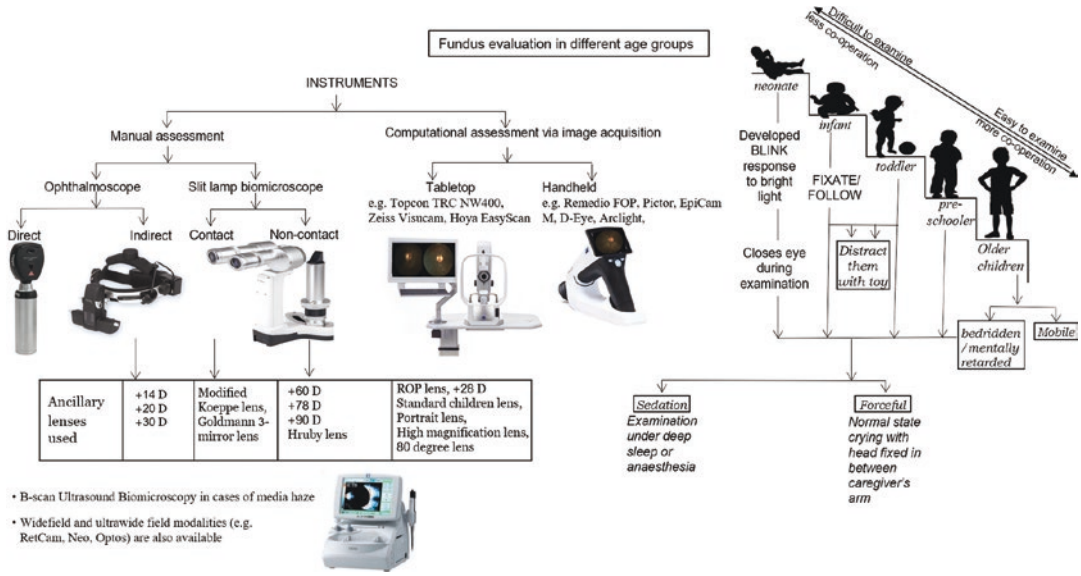

Fig. 6.3 Flowchart: Fundus evaluation in different age groups

Fig. 6.4 (**a**) Distracting the child by a cartoon while performing indirect ophthalmoscopic examination, (**b**) examining fundus with the use of wire speculum and a 20 D lens during examination under anesthesia (EUA), (**c**) scleral indentation indirect ophthalmoscopy to look at retinal periphery, (**d**) direct ophthalmoscopy during sedation in caregiver's arms, (**e**) fundus visualization in a toddler using portable handheld fundus camera, (**f**) RetCam used for fundus examination in infant, and (**g**) fundus imaging in a young child old and cooperative enough to fixate

ophthalmoscopes in the undilated pupil (with or without sedation/anesthesia) (Fig. 6.4d). Direct ophthalmoscope gives a magnified view of optic disc but lacks stereopsis (as compared to indirect ophthalmoscopy or 90-D lens/slit lamp biomicroscopy). However, the use of direct ophthalmoscope is limited in higher degrees of astigmatism and ametropia, as it may fallaciously elongate the disc in the meridian of greatest refraction.

- Fundus imaging using fundus camera (e.g., Zeiss Visucam, Clarity RetCam™, 3nethra

Neo, Nikon Optos® UWF™, Remedio FOP, etc.) is beneficial in documenting subtle changes over time and is free from interobserver variations in documenting cup-to-disc ratios (Fig. 6.4e–g). Fundus imaging is better tolerated than indirect binocular ophthalmoscopy in photophobic children allowing nonmydriatic imaging with a dimmer flashlight in a faster and more comfortable manner.

- Different instruments provide fundus images with specific magnification and field of view when kept at a particular working distance. This must be kept in mind while interpreting imaging across different modalities.
- Opaque eyes with hazy media require ultrasonography (USG) where the measured cup diameter reflects an approximate estimate of cup disc ratio (CDR), through the relationship: $y = 1.64x + 0.03$ (where y and x stand for USG cup diameter the clinical CDR, respectively). USG can be useful to detect cupping if the CDR is greater than 0.5:1 and sensitivity increases as the CDR increases.

The fundus in healthy newborns is comparatively less pigmented than in adults, causing conspicuous choroidal vasculature with pink ONH and a small physiological cup, though slight pale to grayish fundus can also be seen depending on the amount of melanin pigment. Glaucomatous cupping in young children is more marked by the effect of IOP than in adults, with concentric enlargement of the cup, presumably caused by lack of connective tissue at the level of lamina cribrosa. Vertical bipolar loss of neuroretinal rim tissue is observed in older glaucomatous children akin to adults, due to morphometric gradient of thick axonal distribution over larger lamina cribrosa pores with least interpore connective tissue at superior and inferior sectors.

6.1 Case Examples

Case 6.1

A 4-year-old girl with bilateral primary congenital glaucoma of infantile origin with buphthalmos status post trabeculectomy in both eyes, presented with leucomatous corneal opacity in the right eye (RE) and clear cornea with Haab's stria in the left eye (LE). Her RE fundus was examined using B-scan ultrasonography and LE using handheld fundus photography to look for ONH and posterior segment pathology (Fig. 6.5).

Learning Points

- Clinically assessed disc ratios of 0.6:1,0.7:1, 0.8:1, 0.9:1 to total cupping correspond to USG cup measures of 1.02 ± 0.11 mm, 1.23 ± 0.14 mm, 1.35 ± 0.072 mm, 1.45 ± 0.084 mm, 1.75 ± 0.15 mm, respectively, in adults.
- A prominent white sheen in the fundus due to reflection from the internal limiting membrane is a normal finding observed in children, which loses opalescence as children progress

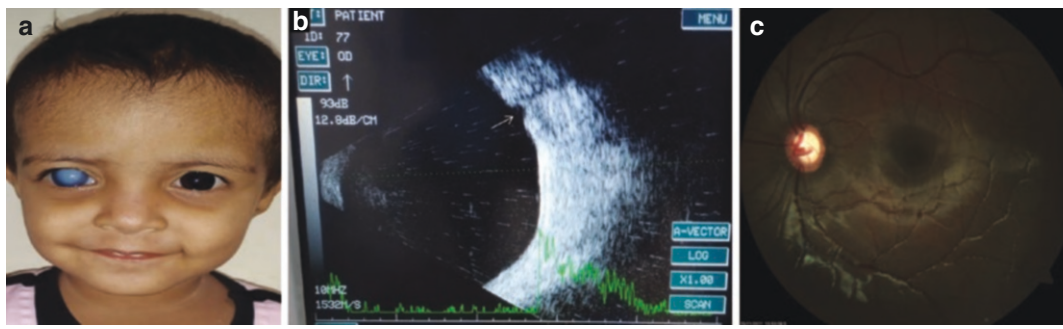

Fig. 6.5 (**a**) Clinical picture of a girl with bilateral primary congenital glaucoma; (**b**) B-scan ultrasound image of right eye showing advanced cupping and (**c**) fundus photograph of left eye with superior and inferior neuroretinal rim thinning, showing concentric cup enlargement

to adulthood (Figs. 6.5c and 6.6a). The above finding is not to be confused with gray-whitish patches of the retinal nerve fiber with frayed bordered myelin sheath found in 1% of the population (Fig. 6.6b).

- Glaucoma diagnosis is possibly difficult in highly myopic eyes due to deformed papillary and peripapillary structures in response to axial elongation of eyeball, spuriously mimicking glaucomatous optic deformation. Moreover, there are vast variations in myopic ONH in terms of size, tilt, torsion, and atrophy (Fig. 6.7).
- Glaucomatous optic neuropathy should be differentiated from congenital disc anomalies (Fig. 6.8.)
- A careful peripheral fundus examination is essential to rule out any associated retinal or systemic condition, viz., choroidal hemangioma leading to subretinal hemorrhage or exu-

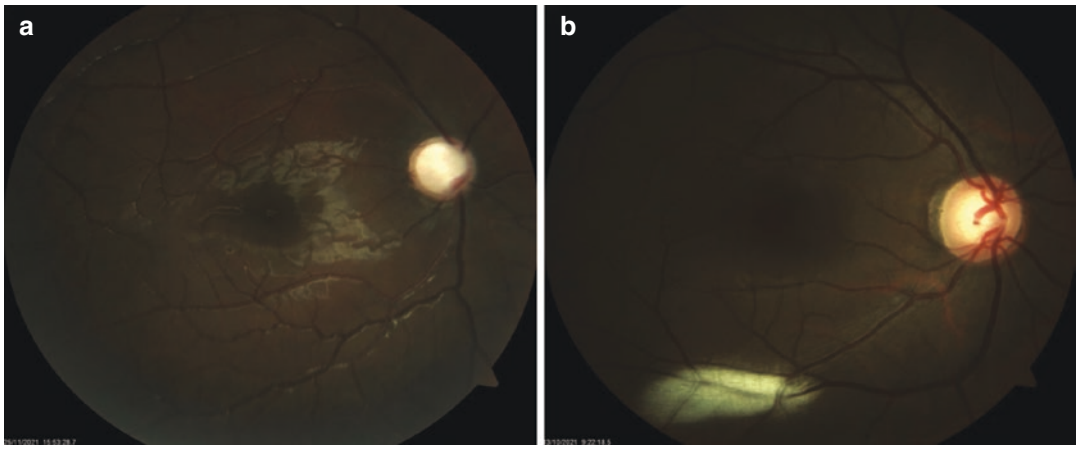

Fig. 6.6 Right eye fundus images in (**a**) a 3-year-old child with concentric cupping, see the discernible white sheen near the macula, (**b**) myelinated nerve fibers inferior to disc at 6–7 clock hours

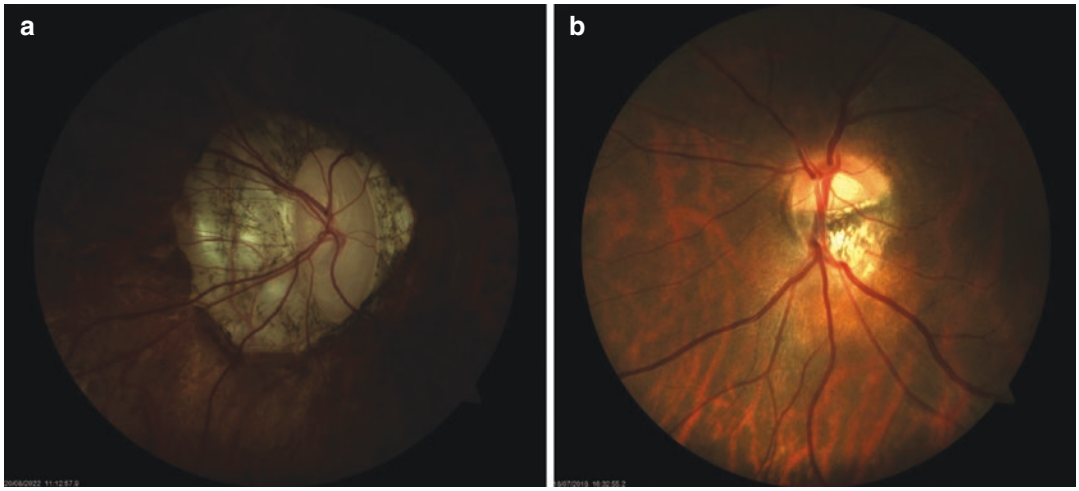

Fig. 6.7 (**a**) A large myopic optic nerve head (ONH) in Ehlers-Danlos syndrome with associated glaucoma. The disc is tilted, pale, with large areas of peripapillary atrophy and associated retinal thinning making it difficult to assess for glaucomatous damage and progression, (**b**) a small tilted and distorted ONH with inferior crescent in a myopic child with congenital tilted disc syndrome

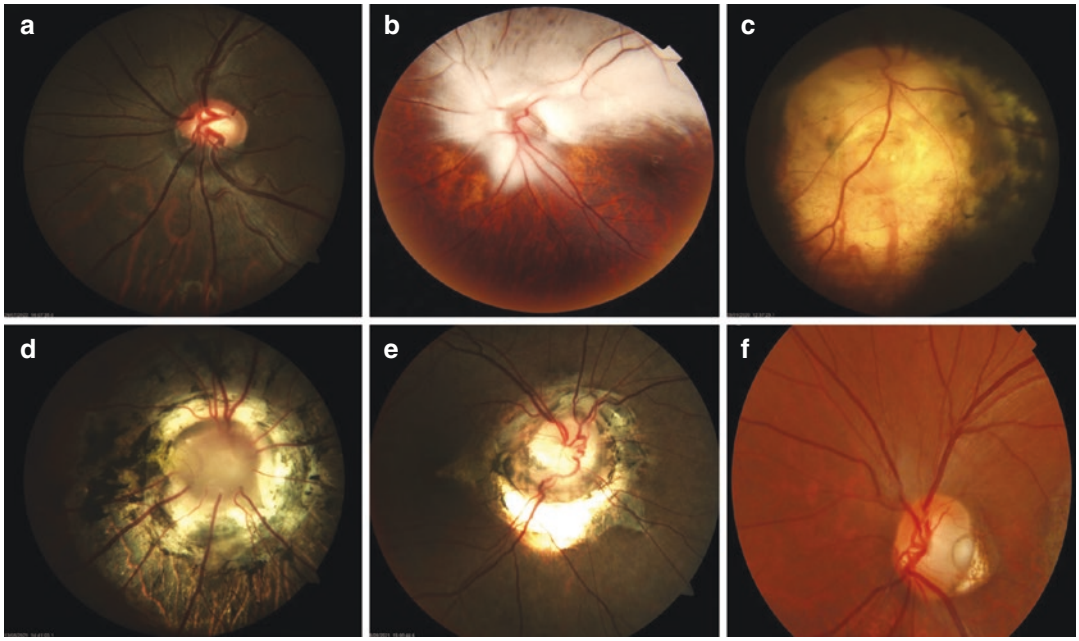

Fig. 6.8 Congenital disc anomalies mimicing glaucoma: (**a**) Optic disc hypoplasia (double ring sign), (**b**) myelinated nerve fibers extending in superior half of fundus, (**c**) optic disc coloboma, (**d**) morning glory anomaly, (**e**) peripapillary staphyloma, and (**f**) optic disc pit

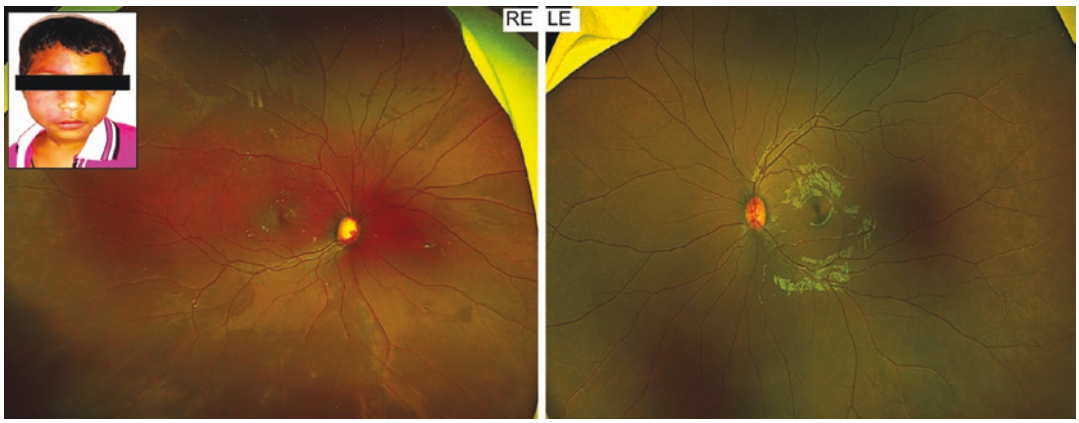

Fig. 6.9 "Tomato ketchup" or "tomato catsup" appearance of right fundus due to circumscribed choroidal hemangioma compared with the fellow left eye. Note advanced glaucomatous cupping in RE compared to a healthy disc in LE. About 40% of the total affected patients develop choroidal hemangioma, due to thick posterior vasculature

dative retinal detachment (RD) in Sturge-Weber syndrome (Fig. 6.9), foveal hypoplasia in aniridia (Fig. 6.10), pigmentary retinopathy in congenital rubella syndrome, etc.

- The subsequent observation of papillary and retinal vasculature is required in young children post successful IOP control. Young children are more prone to vessel dilation, and generally, vessels return to their normal appearance. Significant blood vessel dilation can mimic congenital vascular diseases or aneurysms, but they return to normal morphology once hypotony is corrected post-

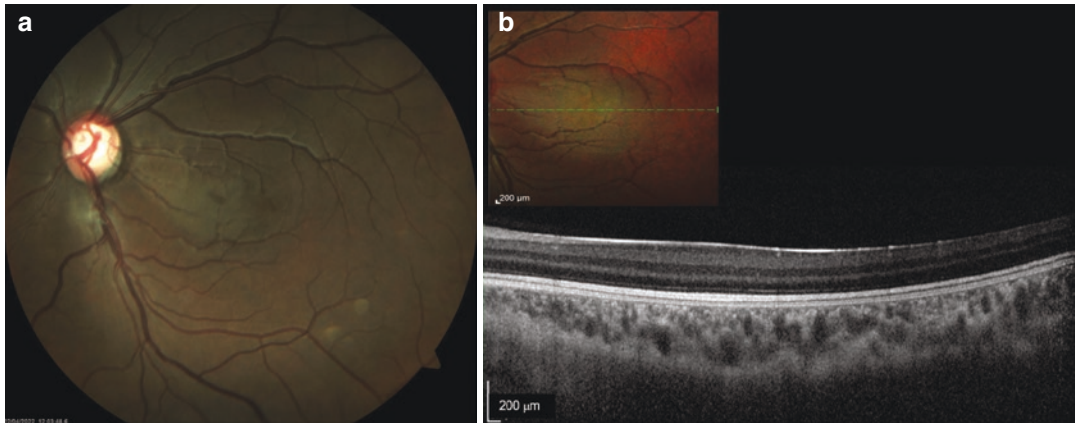

Fig. 6.10 (**a**) Absence of foveal avascular zone in left eye with vessels almost reaching up to the foveal center, depicting foveal hypoplasia in a child with congenital aniridic glaucoma, (**b**) absence of the foveal pit on LE OCT macular scan

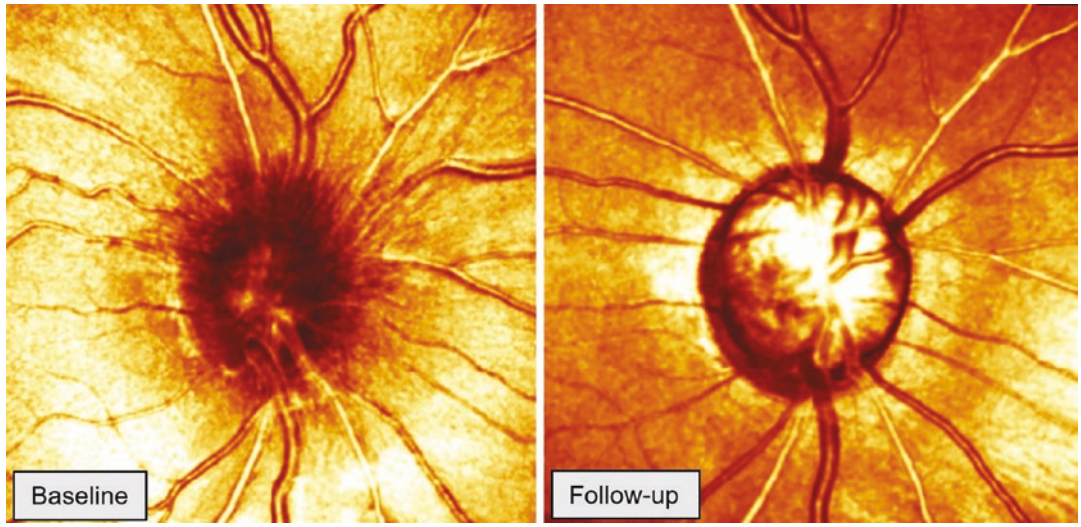

Fig. 6.11 Baseline and final follow up disc images from Heidelberg Retinal Tomography (HRT3) of a unilateral glaucoma patient who was lost to follow-up after glaucoma filtering surgery LE. He had returned to the clinic after a decade with advanced glaucomatous cupping in the fellow eye (RE). The HRT image below shows absence of cupping in the RE at baseline and advanced glaucomatous cupping at follow up

filtering surgery. The incidence of hemorrhages and vein occlusion due to elevated IOP is unlikely in newborns.

- Even after initial successful surgical intervention, the surgery may fail at any stage. It is also observed that glaucoma may develop in fellow eyes in some unilateral cases. Therefore, the disease mandates lifelong follow-up of the patient (Fig. 6.11).

Case 6.2

A young boy with unilateral advanced juvenile open-angle glaucoma was diagnosed and operated upon for glaucoma filtering surgery at the age of 10 years. He was regularly following up since 5 years of age. His IOP was successfully controlled to 10 mmHg in the present visit, with IOP fluctuations of 3.7 ± 2.1 mmHg. On comparing his current fundus photograph with

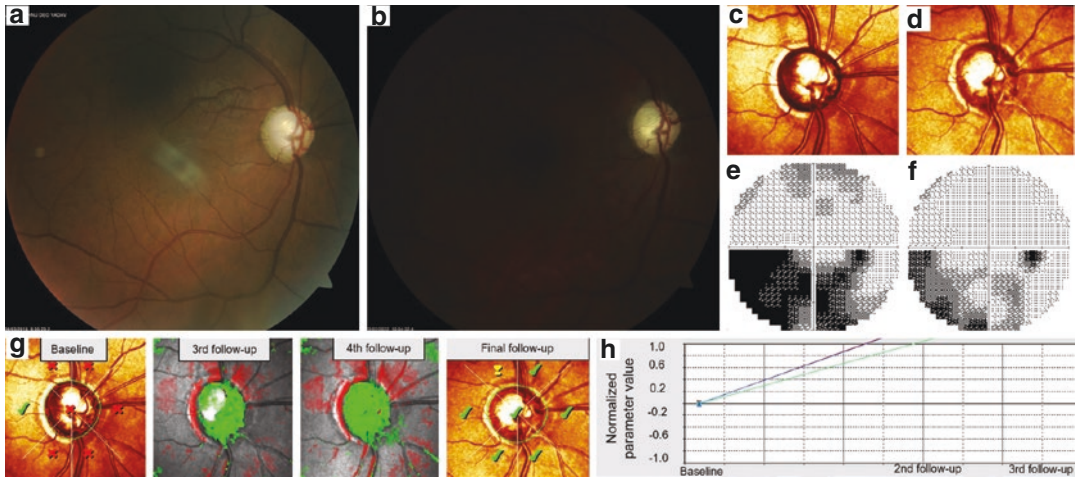

Fig. 6.12 Baseline (**a**) and final follow-up (**b**) fundus photograph RE showing reversal of cupping in **b**. Disc images from Heidelberg Retinal Tomography (HRT_3) show a decrease in linear cup/disc ratio from 0.90 (**c**) to 0.68 (**d**). Grayscale from baseline visual field (**e**) and final visual field (**f**) represent an improvement in visual field. Functional vision improvement also corroborates with structural recovery as seen on topographic change analysis (**g**). Parametric change chart depicting the significant change in cup volume over time (**h**)

the baseline, it was found that his optic disc cupping had reversed from initial presentation. The optic cup volume at the first and the last visits was 1.03 mm^3 and 0.41 mm^3, respectively. There was an improvement in the visual fields noted from perimetry records, the baseline mean deviation was −17.61 dB, and the final mean deviation was −8.32 dB. The visual field index increased from 62% to 82% (Fig. 6.12a-h).

Learning Points

- Acute optic disc cupping in newborns: There is a flexible scleral canal enlargement concurrent with the generalized stretching of the globe following rise in IOP. Early normalization of IOP before the onset of neuronal atrophy reduces stress at cribriform plate, with consequent expansion of neuroretinal rim fibers attributed to disc reversal. Regeneration of damaged retinal ganglion tissue or astroglial proliferation occurs less often.
- Reversal of cupping can rarely be observed in older children or even adults with or without improvement of visual fields, after sustained IOP control.
- A long learning curve to obtain reliable perimetry should not be mistaken for improved visual function in children. HRT parameter "cup volume" can be considered for disc reversal, if a decrease of more than 5% of initial cup volume is observed.
- Prolonged hypotony after glaucoma filtering surgery can lead to vision loss. Fundus changes in hypotony include optic nerve head edema (altered translaminar pressure gradient causes anterior bowing of lamina cribrosa, which in turn restricts axoplasmic flow and leads to disc swelling in acute phase), chorioretinal folds and vascular tortuosity (Fig. 6.13).

Case 6.3

A 17-year-old girl who had undergone trabeculectomy with mitomycin-C (MMC) as adjunct in her both eyes for neonatal glaucoma at 3 months of age presented with the complaints of sudden diminution of vision, with floaters and flashes in her left eye. Her visual acuity was RE 6/60 and LE finger counting close to face. Her IOP were 16 and 4 mmHg in RE and LE, respectively. Both eyes had filtering bleb in the superonasal quadrant and there was no leak on Seidel test. Her fundus evaluation revealed myopic tessellated fundus in RE with lattice degeneration in the periphery of superior retina (Fig. 6.14) and rhegmatogenous

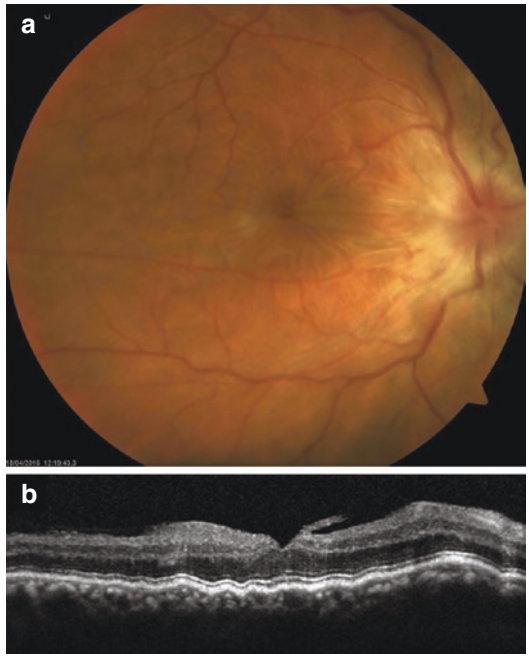

Fig. 6.13 (**a**) Changes in the fundus in hypotony maculopathy, showing disc swelling and edema, retinal and macular folds, and engorged retinal veins. (**b**) OCT showing wrinkling of chorioretinal layers

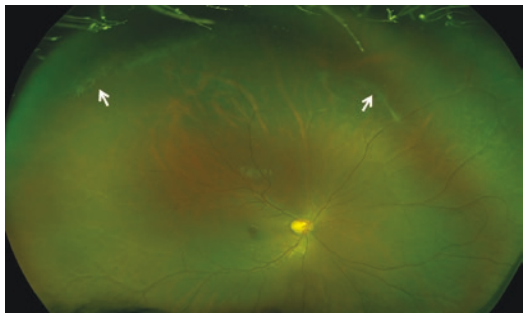

Fig. 6.14 Fundus picture of right eye showing lattice degeneration (white arrows) at superonasal retina

retinal detachment (RD) involving inferior retina in LE along with advanced glaucomatous optic neuropathy (Fig. 6.15). The patient was advised laser delimitation of lattices in RE and vitreoretinal surgery was performed along with silicone oil tamponade in LE.

Learning Points

- The prevalence of pathological peripheral retinal degenerations in high myopic buphthalmic eyes is 15%, necessitating vigorous regular screening for peripheral retinal abnormalities, especially those with axial length ≥26 mm.
- Eyes with high myopia and high preoperative IOP are more prone to develop postoperative choroidal detachment, exudative RD, or suprachoroidal hemorrhage if IOP is lowered suddenly to very low levels. Hence controlled IOP lowering should be performed intraoperatively, and preferably an anterior chamber maintainer should be placed to prevent sudden intraoperative hypotony (Fig. 6.16).
- Traumatic rhegmatogenous RD accompanied by release of damaged photoreceptors, obstructing the aqueous outflow, may cause high IOP sometimes (Schwartz-Matsuo syndrome).
- A sudden drop in chronic uncontrolled IOP following surgical intervention can cause early or late onset suprachoroidal hemorrhage and exudative RD.

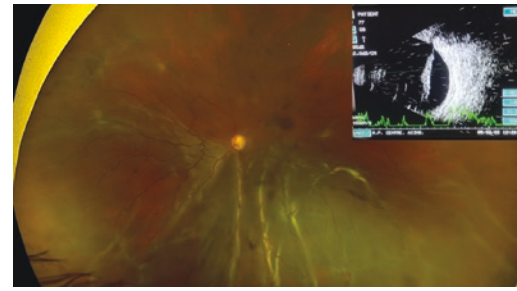

Fig. 6.15 Fundus picture of left eye showing 0.9:1 cup-to-disc ratio with inferior rhegmatogenous retinal detachment, the same observed on B-scan USG, a thick membranous detachment from the inferior margin of optic nerve head showing a high amplitude peak at 77dB gain on A-scan

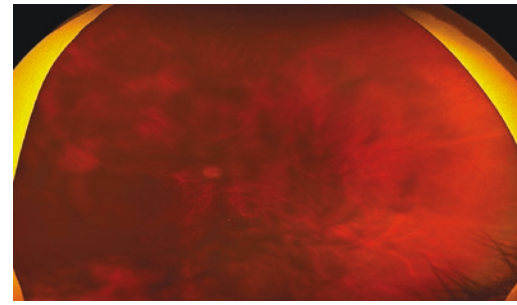

Fig. 6.16 Fundus picture showing choroidal detachment with vitreous hemorrhage due to sustained hypotony

- Parents need to be aware apropos of the signs of postoperative complications, aiding in early detection with prompt treatment.

6.2 Conclusions

Fundus evaluation is challenging in children with glaucoma, mainly due to their unco-operative nature and sometimes, corneal haze caused by high IOP. Stereoscopic fundus evaluation through 90-D lens/slit lamp biomicroscopy gives a better assessment of cup–disc ratio. Image acquisition techniques have the advantage of documenting subtle changes over time and are usually free from inter-observer variations.

Suggested Reading

Agarwal K, Vinekar A, Chandra P, Padhi TR, Nayak S, Jayanna S, Panchal B, Jalali S, Das T. Imaging the pediatric retina: an overview. Indian J Ophthalmol. 2021;69(4):812–23. PMID: 33727440; PMCID: PMC8012979. https://doi.org/10.4103/ijo.IJO_1917_20.

Gupta S, Gogia V, Jose C, Chanana B, Bypareddy R, Kapoor KS, Gupta V. Peripheral retinal degenerations and rhegmatogenous detachment in primary congenital glaucoma. Retina. 2016;36(1):188–91. https://doi.org/10.1097/IAE.0000000000000688.

Harju M, Saari J, Kurvinen L, Vesti E. Reversal of optic disc cupping in glaucoma. Br J Ophthalmol. 2008;92(7):901–5. https://doi.org/10.1136/bjo.2007.135350.

Pujari A, Swamy DR, Selvan H, Agarwal D, Sihota R, Gupta S, Gupta N, Dada T. Clinical, ultrasonographic and optical coherence tomography correlation of optic nerve head cupping in glaucoma patients. Indian J Ophthalmol. 2019;67(10):1663–6. PMID: 31546504; PMCID: PMC6786225. https://doi.org/10.4103/ijo.IJO_24_19.

Quinn N, Csincsik L, Flynn E, Curcio CA, Kiss S, Sadda SR, Hogg R, Peto T, Lengyel I. The clinical relevance of visualising the peripheral retina. Prog Retin Eye Res. 2019;68:83–109. Epub 2018 Oct 10.

Salmon F, J. Kanski's clinical ophthalmology. 9th ed. Amsterdam: Elsevier; 2019.

Tan NYQ, Sng CCA, Jonas JB, Wong TY, Jansonius NM, Ang M. Glaucoma in myopia: diagnostic dilemmas. Br J Ophthalmol. 2019;103(10):1347–55. Epub 2019 Apr 30. https://doi.org/10.1136/bjophthalmol-2018-313,530.

Varshney T, Parthasarathy DR, Gupta V. Artificial intelligence integrated smartphone fundus camera for screening the glaucomatous optic disc. Indian J Ophthalmol. 2021;69(12):3787–9. PMID: 34827055; PMCID: PMC8837288. https://doi.org/10.4103/ijo.IJO_1831_21.

Pediatric Perimetry

7

Kumar Kartikay Rajaura, Abhishek Singh, and Viney Gupta

7.1 Introduction

The term "perimetry" is derived from the Latin word "*perimetros*" which depicts the functional measurement of visual fields. It is an essential procedure in the diagnosis and management of glaucoma. The first clinical attempt at a quantitative visual fields was made in 1856 by Albrecht von Graefe. Thenceforth, it had evolved through various measuring modalities, e.g., Bjerrum tangent screen, Lister's Arc perimeter, and Goldmann perimeter, to its present state of quick repeatable automated perimeters, viz., Humphrey Field Analyzer (HFA), Octopus, Oculus, Kowa, etc. More accessible and portable units like Melbourne Rapid Fields (MRF), Virtual Reality Perimeter, etc., popular for their ease, comfort, and in-office testing, are on the verge of advancements. In general, bowl perimeters can be more intimidating for children compared to flat screens, since they need to keep their chins steady inside the bowl for a long time.

7.1.1 Perimetry in Children

Performing a reliable perimetric test in children is a challenging task, involving a longer learning curve (Table 7.1). The most challenging requirement from a child's perspective is to maintain fixation on a central target, requiring a conscious effort to the presented stimulus. Children overall have a reduced ability to understand the task and maintain concentration and, hence, are more likely to provide inappropriate responses as evidenced by the higher rates of false-positives as well as fixation losses.

Visual field defects in children are generally detected in late adolescence resulting in a delay in management. Hence it becomes necessary to aim at early detection of VF loss and provide early rehabilitation. Standard automated perimetry (SAP) is considered the gold standard for assessing glaucomatous visual functions and progressive damage. MRF (Glance Opticals, Australia), an iPad tablet-based tangent perimetry, shows similar potential comparable to the HFA (Table 7.2).

HFA (Carl Zeiss-Humphrey Systems, Dublin, California, USA) and Octopus 900(OVF, haag street, USA) are the two most used perimeters in clinical practice. Most of the perimeters use a constant background luminance at which the fovea has the highest sensitivity for photopic cone-related vision. There is minimal effect of lens color, media transparency, and pupil size at this luminance.

K. K. Rajaura (✉) · A. Singh · V. Gupta
Dr. Rajendra Prasad Centre for Ophthalmic Sciences, All India Institute of Medical Sciences, New Delhi, India

S. Gupta et al. (eds.), *Childhood Glaucoma*, https://doi.org/10.1007/978-981-19-7466-3_7

Table 7.1 Various modalities tested for pediatric perimetry

Modality	Authors/ inventors	Methodology	Limitations
Saccadic vector optokinetic perimetry	Murrey et al.	Used eye tracking to detect the natural saccadic eye response of gaze orientation toward visual field stimuli	A limited number of patients tested with no comparable measures like mean deviation and reliability parameters
Dome perimetry (Fig. 7.1a)	Satgunam et al.	A hemispherical dome with LED lights was constructed in which infants were kept in the supine position in a dark room while monitoring eye and head movement with an infrared camera	Used in infants and mentally challenged patients. It observed the gross visual fields in infants
LED TV perimetry (MathWorks, Inc., Natick, MA) (Fig. 7.1b)	Miranda et al.	LED-TV-based perimetry to play a game where software and hardware were combined to provide an enjoyable testing method to children	Limited number of patients tested, lack of parameters to assess the progression, and longer time taken to conduct perimetry (8.22 min)
Brain-computer interface (nGoggle Inc.)	Nakinishi et al.	Cell phone-based mounted display, electrode wires, a computer system with software to record electrical brain responses to visual evoked stimuli It is used for assessing the electrical brain responses associated with visual field stimulation	Complex system with multiple wiring appliances
Head-mounted perimeter (IMO) (CREWT Medical Systems, Tokyo, Japan) (Fig. 7.1c)	Matsumoto et al.	Performs visual field (VF) testing under flexible conditions that showed the mean sensitivity (MS) being comparable to mean deviation (MD) of Humphrey Field Analyzer (HFA)	High/irregular reliability parameters. Costlier and more difficult to perform in children due to apparent discomfort and distraction
Damato campimetry (Precision Vision, Villa Park, Ill) (Fig. 7.1d)	Rowe et al.	Portable device to assess the visual field, with an optimal sensitivity of 81% and a specificity of 72% based on comparison with a Humphrey 24-2 program	Studies needed to establish a close relationship with HFA and no comparison with 30-2 program
Tubigen mobile campimetry (CNPq-Brazil)	Bruckmann et al.	Mobile-based campimetry which is comparable to octopus and gives faster results	Lacks specificity, particularly in glaucomatous fields
C3 field analyzer (Alfaleus Tech., Remedio, India)	Mees et al.	Head-mounted virtual reality perimeter that evaluates the central 30° of the visual field in the exact 54 locations as HFA.	Not as reliable in identifying field deficits as in HFA
Virtual reality glasses (VRmagic, Mannheim, Germany) (Fig. 7.1f)	Tsapakis et al.	Smartphone with 6-in. display and software that implements an algorithm to test 52 points of the central 24°	Larger sample size is needed for validation
VisuALL head-mounted perimeter (macro, Jacksonville) (Fig. 7.1e)	Olleyes Inc.	Head-mounted flexible perimetry (under evaluation)	Validation needed for pediatric perimetry
Visual Field Easy (VFE) (George Kong softwares)	Marc et al.	IPad-based application used for glaucoma screening in Nepal	Lack of eye-tracking, long testing time, and high false-positive rate

Fig. 7.1 (**a**) Image showing dome-shaped perimetry in infants. (**b**) Image showing display setup of LED TV-based perimetry. (**c**) Image of a head-mounted perimeter IMO with connected display screen. (**d**) Image showing mobile-based campimetry. (**e**) Image of a head-mounted perimeter VISUALL (Bluetooth voice connectivity). (**f**) Virtual reality glasses in head-mounted mobile-based perimeter

Table 7.2 Comparison of Humphrey Field Analyzer (HFA) with iPad-based perimetry (Melbourne Rapid Fields - MRF)

	HFA	MRF
Shape	Bowl-shaped static perimetry	Tablet-based flat screen perimetry
Algorithms used	Uses SITA STANDARD/SITA FAST algorithm	Uses BYES prediction algorithm
Degree of visual fields tested	Measures 30-2, 24-2, and 10-2 degrees of visual field	Measures central 16° with central fixation (fixation target can be moved to assess peripheral field ~30 * 24°)
Clinical settings	Dark room procedure	Can be done in ambient light (outpatient department basis)
Refraction	Refractive correction by adding corrective lenses in the HFA	Can be done wearing glasses
Time required	Takes relatively longer time	Lesser time required
Repeatability	Good repeatability in children	Relatively less repeatability (although comparable to HFA)

7.2 Case Examples

Case 7.1

A 12-year-old male child with unilateral primary congenital glaucoma (left eye, LE) presented with intraocular pressure (IOP) of 12 mmHg (LE on no glaucoma medications) and vertical cup-disc ratio of 0.8:1 (LE) (Fig. 7.2). Patient was operated (trabeculectomy with trabeculotomy under 0.02% mitomycin C) at 1 month of age and achieved normalization of IOP thereafter, and was kept on regular monitoring. He underwent visual field testing on Humphrey visual field (HVF) analyzer 30-2 SITA standard (SS) protocol (Fig. 7.3), and subsequently Melbourne rapid fields (MRF) were done (Fig. 7.4). Both HVF and MRF showed high fixation losses, but reliability indices (false positives and false negatives) were better in MRF. Again HVF (24-2 SS) was repeated which then showed early visual field defects (Fig. 7.5), with good reliability albeit with relatively longer duration required.

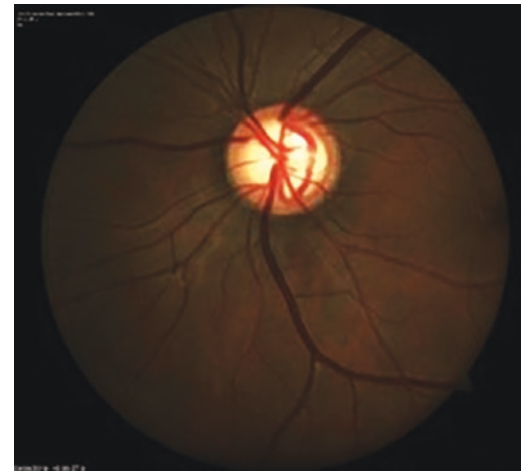

Fig. 7.2 LE fundus clinical picture of the patient having vertical cup-disc ratio of 0.8:1

Key Points

- The fourth visual field test (HFA) was taken as a baseline field test to look for any progression in the future as the previous three exams were not reliable.
- It takes a longer learning curve for children to give a reliable baseline field. Early diagnosis and intervention helped in good visual prognosis, restricting the child's field defect to mild visual field changes only, with no progression noted over the next 2 years.
- Upper limit cutoff values for reliability were taken as 25%, 35%, and 35% (in MRF) and 20%, 33%, 33%, (in HVF) for fixation loss, false positive, and false negative, respectively.

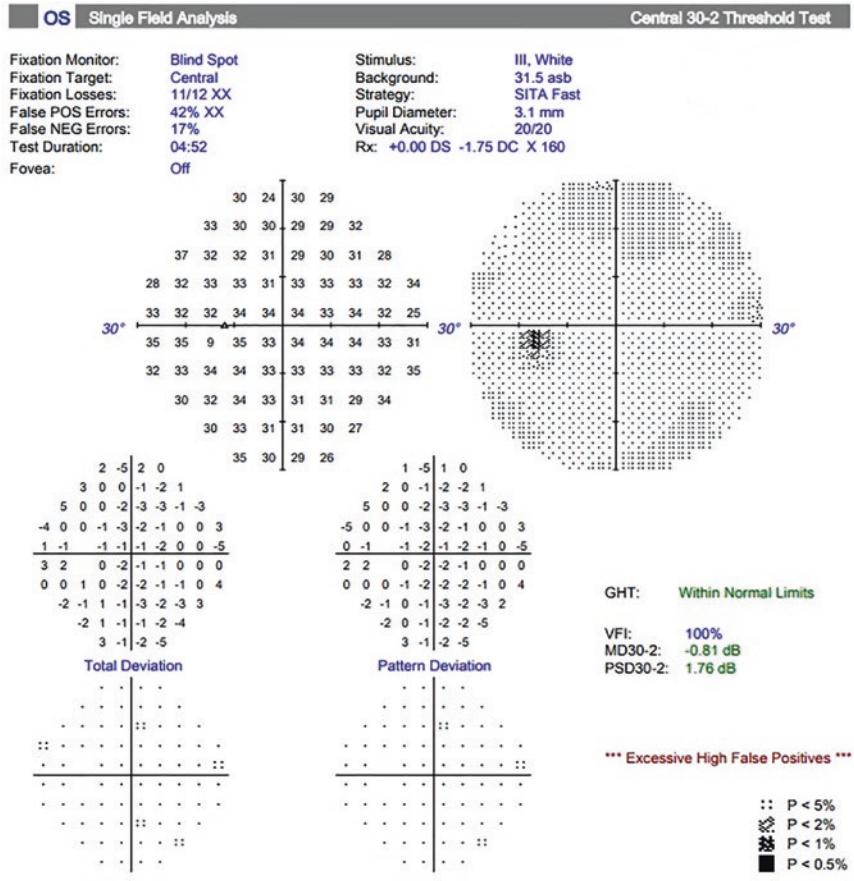

Fig. 7.3 30-2 SITA standard visual field of left eye on Humphrey field analyzer showing excessive high false-positive errors. Visual field was hence rendered to be unreliable with high percentages of fixation loss and false-positive parameters

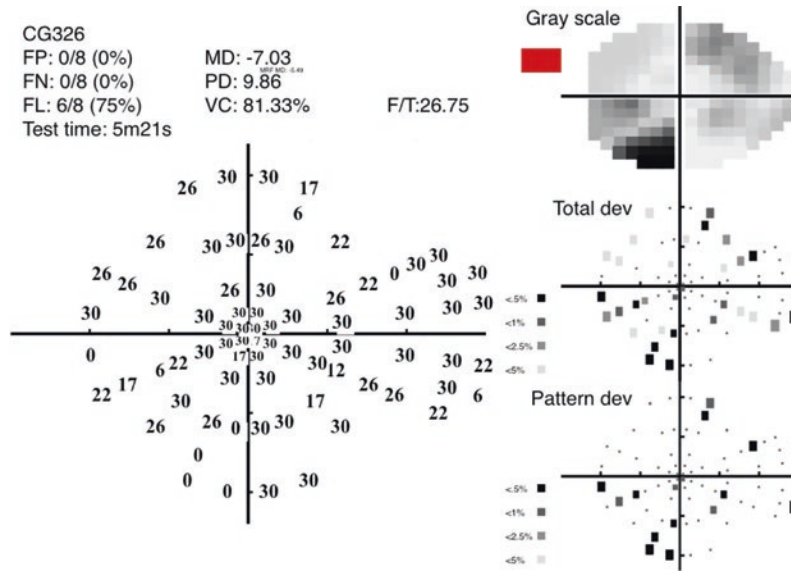

Fig. 7.4 Melbourne rapid fields (iPad-based perimetry/home-based perimetry) of left eye showing early visual field defect (showing inferior arcuate defect), performed in a significantly lesser time

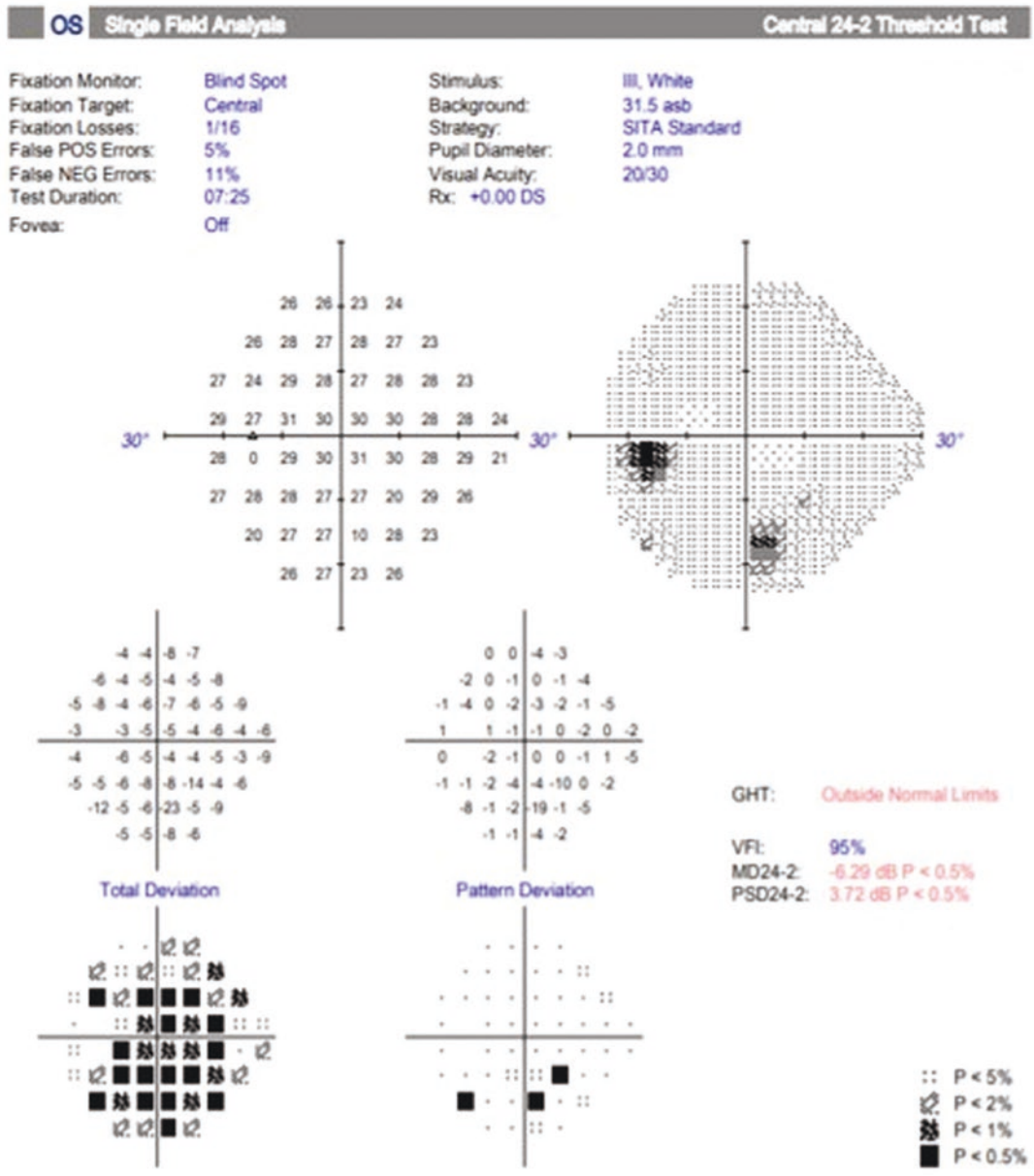

Fig. 7.5 Subsequent 24-2 SS-HVF of the same patient (left eye) showing inferior arcuate defect with reliable parameters this time. Time taken to conduct this reliable visual field was found to be significantly more than MRF

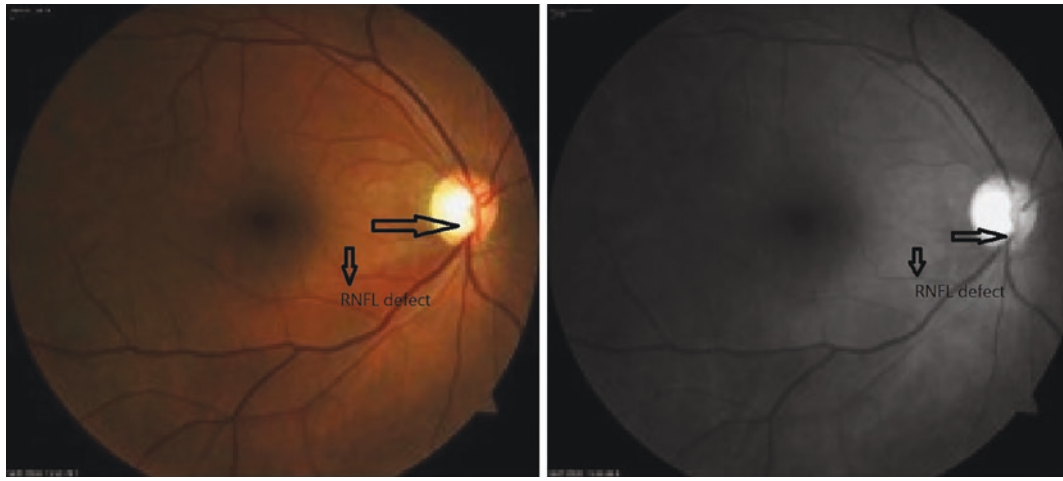

Fig. 7.6 Fundus clinical picture of right eye showing inferior notching (horizontal arrow) with corresponding retinal nerve fiber layer (RNFL) defect (vertical arrow) visualised in both colour (left image) and red-free (right image) photographs

Case 7.2

Sixteen-year boy was referred to glaucoma speciality clinic due to increased IOP (right eye, RE−28 mmHg and LE 12 mmHg). The child was a case of both eye (BE) high myopia who had undergone right eye (RE) cataract and vitreoretinal surgery (with encirclage) with silicone oil insertion at 15 years of age, which was later removed. On examination, a pale disc with approximate cupping of 0.7:1 was noted in RE with inferior notching and retinal nerve fiber layer wedge defect (Fig. 7.6). 30-2 SITA standard automated perimetry was performed which showed superior arcuate defect (Fig. 7.7) with concordant changes on MRF (Fig. 7.8) and accordingly target IOP was set to be early to mid teens. Topical medications including prostaglandin agonist, beta-blocker, and carbonic anhydrase inhibitor were administered to achieve target IOP.

Key Points

- Vitreoretinal surgery with silicone oil is known to cause an increase in IOP leading to irreversible optic nerve changes if not treated meticulously.
- IOP should always be checked while ensuring the final tie of encirclage band, estimated by looking at the disc pulsations as well by digital palpation method.
- Target IOP should be decided after assessing both disc and visual field changes.
- In cases where the disc assessment is spurious due to pallor, congenital disc anomalies, high myopia, knowing the exact perimetry can help tailor therapy.

Case 7.3

A 10-year child presented to the outpatient department at our center with visual acuity of 6/18 in both eye. Direct ophthalmoscopic examination revealed extensive peripapillary myelination of retinal nerve fiber layer (MNF) BE as well as neuroretinal rim involvement RE (Fig. 7.9). Baseline IOP measurement was recorded as 21 and 22 mmHg in RE and LE, respectively, with poor cup-disk ratio (CDR) differentiation on disc assessment. BE angles were found to be open on gonioscopy. Clinical diagnosis of peripapillary myelinated nerve fiber (MNF) was made followed by visual field examination. HVF 30-2 SS RE showed a temporal wedge defect, while LE showed superior glaucomatous arcuate defect

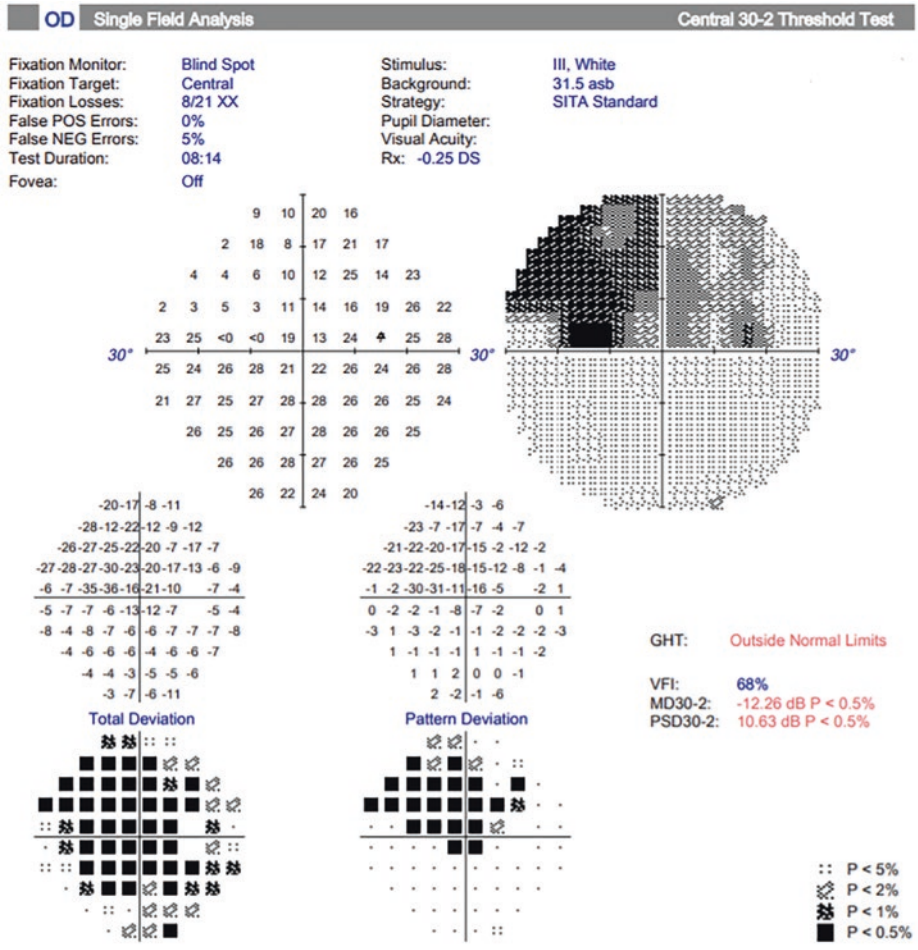

Fig. 7.7 30-2 SITA standard visual field of the patient's right eye showing superior arcuate defect

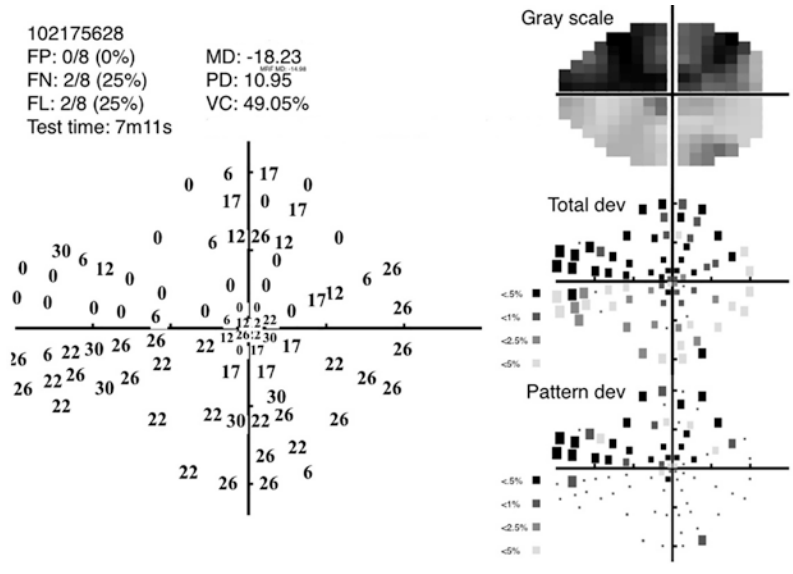

Fig. 7.8 Melbourne rapid fields (iPad perimetry/home-based perimetry) of right eye showing the reproducible superior arcuate defect

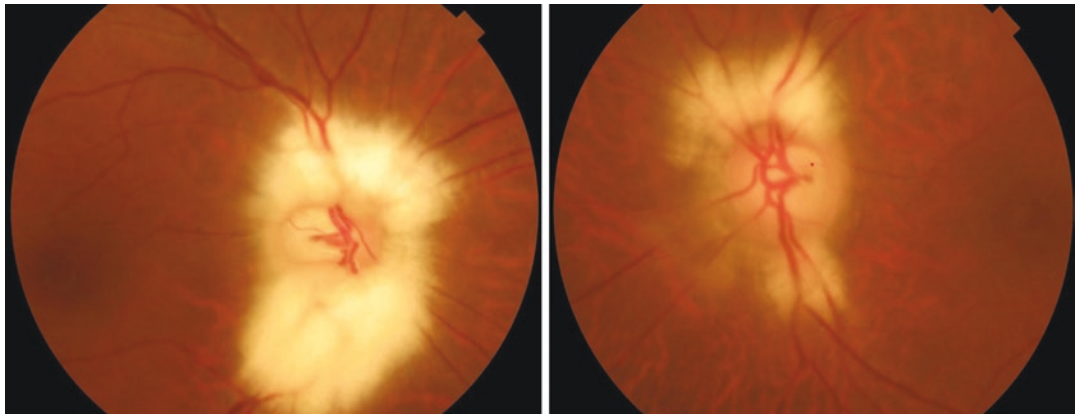

Fig. 7.9 Fundus images of right eye (left side figure) showing myelinated nerve fiber invoving the neuroretinal rim and left eye (right side figure) showing myelinated nerve fiber with suspected inferior rim notch in left eye

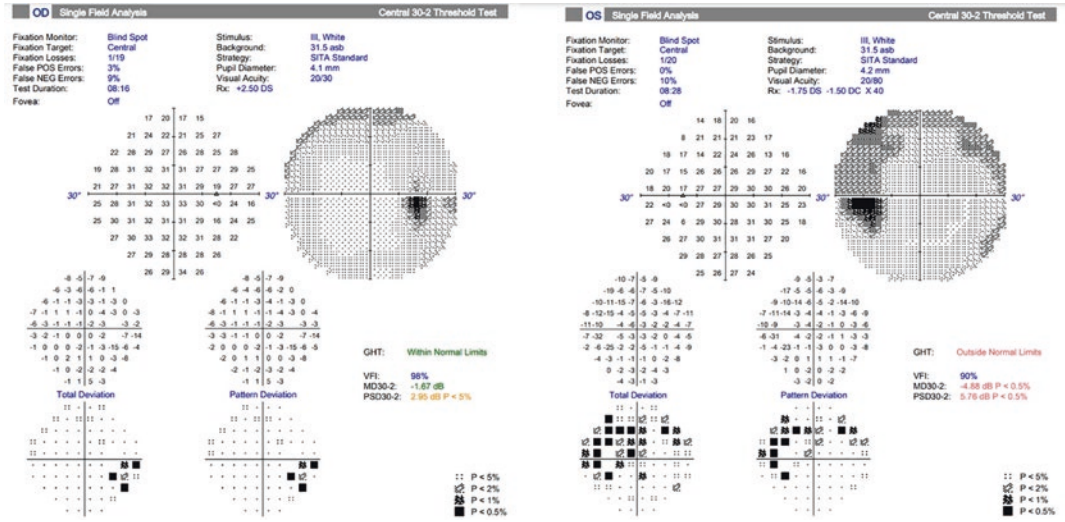

Fig. 7.10 30-2 SITA standard visual field test showing temopral wedge defect in right eye (left side figure) and superior arcuate defect in left eye (right side figure)

(Fig. 7.10) which could have been missed due to an erroneous assessment of optic nerve head.

Key Points

- It is difficult to assess glaucomatous changes if there is associated optic nerve and fundus anomalies.
- Conditions like MNF, morning glory syndrome, coloboma involving optic disc, optic nerve head staphyloma, disc drusen, tilted/torsional disc, familial exudative vitreoretinopathy, and treated or regressed retinopathy of prematurity usually result in fallacious assessment of optic nerve head.
- Such congenital anomalies should be prudently investigated by doing baseline visual field testing to diagnose associated glaucoma.
- Progression of visual field defect can confirm glaucoma in the presence of inadequate disc assessment and fallacious tonometry readings.

7.3 Progression on HFA

The Humphrey Visual Field Analyzer (HFA; Carl Zeiss Meditec, Inc., Dublin, CA) uses Glaucoma Progression Analysis (GPA) software to check progression. This specialized program assists clinicians in evaluation of serial visual fields. It identifies areas where progression may be occurring. It is available for standard (white-on-white) programs 24-2 and 30-2. It can be used with Swedish Interactive Threshold Algorithm (SITA)-Standard and SITA-Fast testing for baseline and follow-up examinations.

GPA uses pattern deviation plots to assess perimetric progression. The software compares a patient's baseline visual fields (at least two reliable ones are needed and are averaged) to each subsequent visual field. Every test location in each follow-up field is evaluated relative to the baseline.

- Change needs to be present in at least three consecutive visual fields before progression can be confirmed.
- The grayscale, absolute threshold values, total and pattern deviation probability plots, mean deviation, and pattern standard deviation indices are provided.
- Losses of fixation, false negatives, and false positives are also shown to be sure about the reliability of the two fields.
- At the bottom, it presents a mean deviation plot for all of the examinations in the series which gives the slope associated with change in the mean deviation.
- When change is initially noted on subsequent visual fields at a particular given location, an open triangle appears at that location.
- If it is present on two consecutive tests, a half-filled triangle appears.
- If a repeatable change is seen on three consecutive tests, a closed triangle appears.
- It reports "possible progression" if two consecutive fields show the same ≥3 changing from baseline.
- It reports "likely progression" if three consecutive fields show change at the same ≥3 points (Figs. 7.11–7.13).

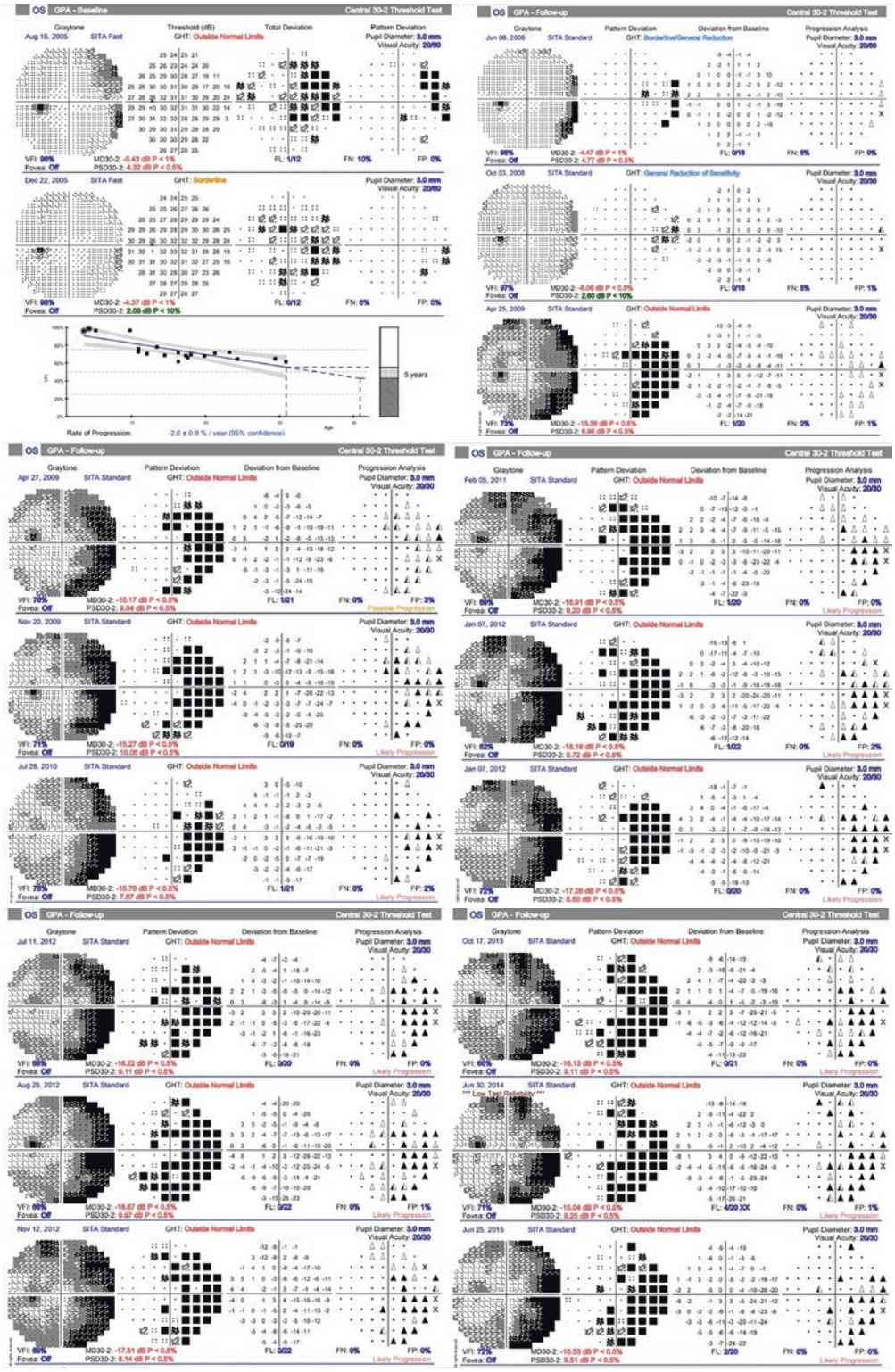

Figs. 7.11–7.13 GPA progression analysis in left eye of a 12-year child on follow-up since 2005. VFI plot shows a downward slope with a progression late of −2.6 ± 0.9%. GPA on every analysis since 2009 and onward showing "likely progression"

7.3.1 Visual Field Index Analysis

- Visual field index (VFI) is the representation of visual field function as a percentage of a normal age-adjusted visual field.
- It is based on total and pattern deviation, and so it's better than mean deviation (which is based on total deviation/affected by media haze).
- VFI Plot: Regression analysis of VFI values and 3–5-year projection.
- VFI Plot being a trend-based analysis as compared to GPA (event-based analysis) tells more accurately about the rate of progression.
- VFI Bar: A graphical depiction of the patient's remaining useful vision at the current VFI value along with a 3–5-year projection of the VFI regression line if the current trend continues.

7.4 Progression on MRF

MRF itself doesn't provide a specialized software to detect and grade progression (Fig. 7.14). Therefore, increase in mean deviation grossly explains about the probable progression of the disease and it has to be clinically correlated (with increase in cup-disk ratio) before determining the need for intervention. One has to understand the test to test variability, the magnitude of change needed to term it as clinically significant and check the reliability of tests while assessing for progression.

7.5 Prospects

A 16-year boy with BE operated trabeculectomy for steroid-induced glaucoma with panuveitis and on oral steroids with controlled IOP has been advised to assess visual fields at home using iPad-based MRF due to difficulty in following up at hospital. Progression was recorded by MRF in four subsequent fields over 1 year, and results were notified to the consulting physician by the application. Child was called up, and antiglaucoma medications were stepped up to achieve a new target IOP.

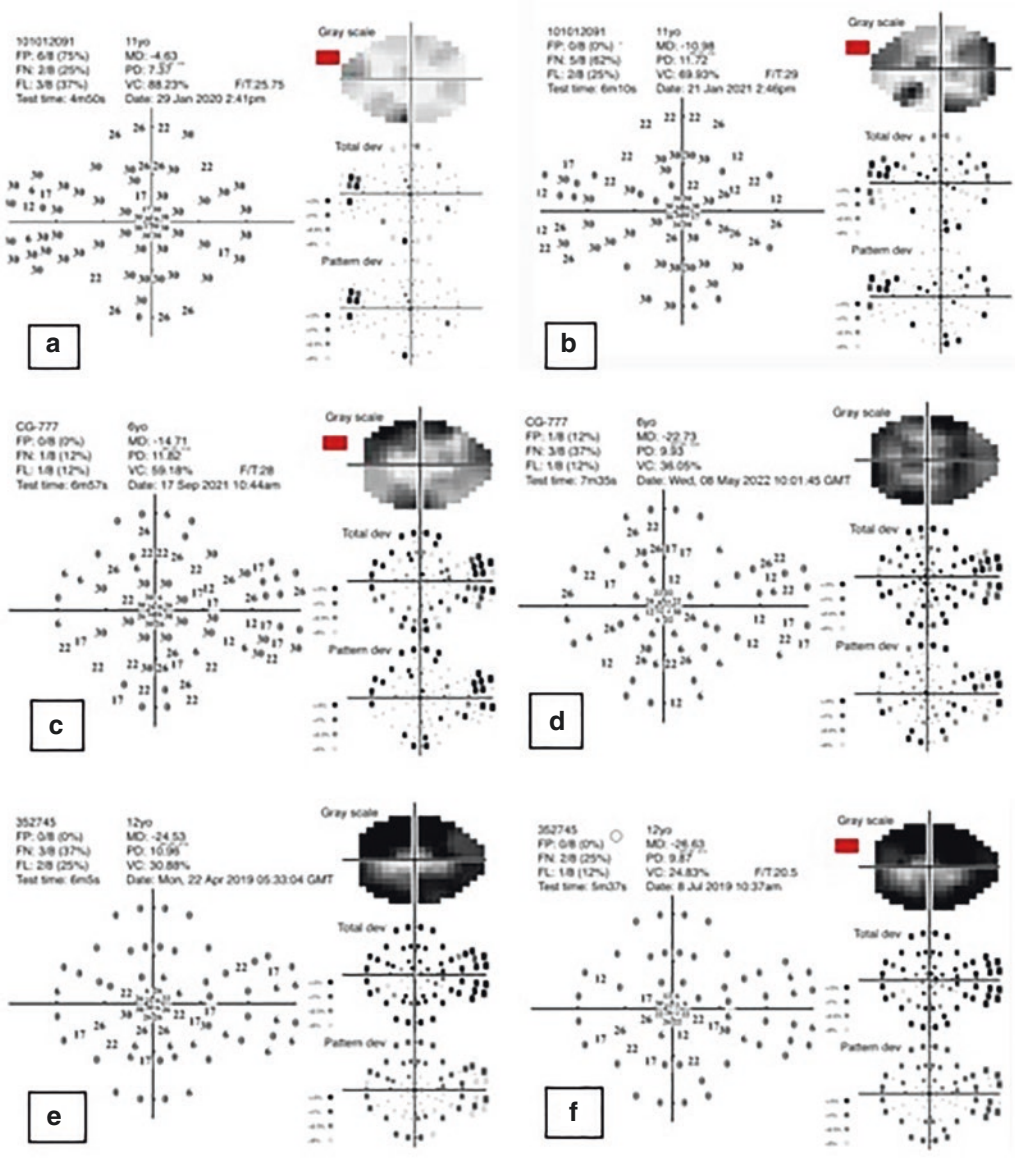

Fig. 7.14 (**a**, **b**) Shows progression in an 11-year child with increase in mean deviation of −6.35 over a year. (**c**, **d**) Shows progression in a 6-year child with increase in mean deviation of −8.02 over 8 months. (**e**, **f**) Shows progression in a 12-year child with increase in mean deviation of −2.10 dB over a period of 2 months

7.6 Conclusions

To summarize, it takes a complicated and prolonged learning curve to get a reliable visual field by standard automated perimetry particularly in the pediatric age group. Hence handheld and portable perimetric devices like iPad-based perimetry (MRF), smartphone-based perimetry, and head-mounted perimeters (IMO or VisuALL) provide an easy and reliable alternative. These provide ease of use (playful activity for children), comfortable positioning, portability, lower fixation losses, and economic advantage. Hence, these newer perimetric modalities have a great potential in the delivery of good-quality vision care for pediatric glaucoma.

Suggested Reading

Anderson DR. Perimetry with and without automation. 2nd ed. St Louis: Mosby; 1987.

Aslam TM, Rahman W, Henson D, Khaw PT. A novel paediatric game-based visual-fields assessor. Br J Ophthalmol. 2011;95(7):921–4.

Bengtsson B, Olsson J, Heijl A, Rootzen H. A new generation of algorithms for computerized threshold perimetry, SITA. Acta Ophthalmol Scand. 1997;75:368–75.

Bruckmann A, Volpe NJ, Paetzold J, Vonthein R, Schiefer U. Comparison of advanced visual field defects measured with the Tübingen Mobile Campimeter and the Octopus 101 perimeter. Eur J Ophthalmol. 2010;20(1):149–86.

Han S, Baek SH, Kim US. Comparison of three visual field tests in children: frequency doubling test, 24-2 and 30-2 SITA perimetry. Semin Ophthalmol. 2017;32(5):647–50.

Heijl A, Leske MC, Bengtsson B, et al. Measuring visual field progression in the Early Manifest Glaucoma Trial. Acta Ophthalmol Scand. 2003;81:286–93.

Johnson CA, Wall M, Thompson HS. A history of perimetry and visual field testing. Optom Vis Sci. 2011;88(1):E8–15.

Kass MA, Heuer DK, Higginbotham EJ, et al. The Ocular Hypertension Treatment Study: a randomized trial determines that topical ocular hypotensive medication delays or prevents the onset of primary open angle glaucoma. Arch Ophthalmol. 2002;120:701–13.

Kong YX, He M, Crowston JG, Vingrys AJ. A comparison of perimetric results from a tablet perimeter and Humphrey field analyzer in glaucoma patients. Transl Vis Sci Technol. 2016;5:2.

Matsumoto C, Yamao S, Nomoto H, Takada S, Okuyama S, Kimura S, et al. Visual field testing with head-mounted perimeter 'imo'. PLoS One. 2016;11(8):e0161974.

Mees L, Upadhyaya S, Kumar P, Kotawala S, Haran S, Rajasekar S, et al. Validation of a head-mounted virtual reality visual field screening device. J Glaucoma. 2020;29(2):86–91.

Miranda MA, Henson DB, Fenerty C, Biswas S, Aslam T. Development of a pediatric visual field test. Transl Vis Sci Technol. 2016;5(6):13.

Murray IC, Perperidis A, Cameron LA, McTrusty AD, Brash HM, Tatham AJ, et al. Comparison of saccadic vector optokinetic perimetry and standard automated perimetry in glaucoma. Part I: threshold values and repeatability. Transl Vis Sci Technol. 2017;6(5):3.

Nakanishi M, Wang YT, Jung TP. Detecting glaucoma with a portable brain-computer interface for objective assessment of visual function loss. JAMA Ophthalmol. 2017;135(6):550–7.

Olsen AS, Alberti M, Serup L, la Cour M, Damato B, Kolko M. Glaucoma detection with damato multifixation campimetry online. Eye (Lond). 2016;30(5):731–9.

Patel DE, Cumberland PM, Walters BC, Russell-Eggitt I, Rahi JS, OPTIC Study Group. Study of optimal perimetric testing in children (OPTIC): feasibility, reliability and repeatability of perimetry in children. PLoS One. 2015;10(6):e0130895.

Phu J, Kalloniatis M. Ability of 24-2C and 24-2 grids in identifying central visual field defects and structure-function concordance in glaucoma and suspects. Am J Ophthalmol. 2020;219:317–31.

Sample PA, Boden C, Zhang Z, et al. Unsupervised machine learning with independent component analysis to identify areas of progression in glaucomatous visual fields. Invest Ophthalmol Vis Sci. 2005;46:3684–92.

Satgunam P, Datta S, Chillakala K, Bobbili KR, Joshi D. Pediatric perimeter-a novel device to measure visual fields in infants and patients with special needs. Transl Vis Sci Technol. 2017;6(4):3.

Tahir HJ, Murray IJ, Parry NR, Aslam TM. Optimisation and assessment of three modern touch screen tablet computers for clinical vision testing. PLoS One. 2014;9:e95074.

Tsapakis S, Papaconstantinou D, Diagourtas A, Droutsas K, Andreanos K, Moschos MM, et al. Visual field examination method using virtual reality glasses compared with the Humphrey perimeter. Clin Ophthalmol. 2017;11:1431–43.

Walters BC, Rahi JS, Cumberland PM. Perimetry in children: survey of current practices in the United Kingdom and Ireland. Ophthalmic Epidemiol. 2012;19(6):358–63.

Wilscher S, Wabbels B, Lorenz B. Feasibility and outcome of automated kinetic perimetry in children. Graefes Arch Clin Exp Ophthalmol. 2010;248(10):1493–500.

Examination Under Anesthesia

8

Ridhima Bhatia, Puneet Khanna,
and Karthikeyan Mahalingam

8.1 Introduction

To reduce the degree of visual impairment in young glaucoma patients, early diagnosis and treatment are critical. Clinical examinations of children, particularly young children, are sometimes hampered by their unwillingness to cooperate, and subjective testing is frequently impossible. Therefore, serial examinations under anesthesia (EUA) are commonly used by pediatric glaucoma specialists to achieve specific assessment goals, such as establishing a baseline examination, setting an intraocular pressure (IOP) goal, initiating therapy to lower pressure, monitoring treatment effect and glaucomatous progression, and modifying the IOP goal and treatment as indicated by the patient's course. While many advances have reduced the frequency of examination under anesthesia (EUA) in the operating room, in the care of a specific child with glaucoma, the EUA remains important in providing optimal care for children with glaucoma to supplement those examination details that may not be easily obtained in the clinic.

R. Bhatia · P. Khanna (✉)
Department of Anaethesia and Critical Care, All India Institute of Medical Sciences, New Delhi, India

K. Mahalingam
Dr. Rajendra Prasad Centre for Ophthalmic Sciences, All India Institute of Medical Sciences, New Delhi, India

8.2 Pre-procedure Concerns

Childhood glaucoma usually presents within 6 months of life. As a result, examinations under anesthesia often begin in the neonatal period and continue until the child becomes cooperative, which is usually around the age of 4–5 years.

Often the childhood glaucoma is typically sporadic, but certain childhood glaucomas are linked to systemic illnesses or syndromes. Therefore, while the majority of children undergoing EUA are otherwise healthy, day-case patients, special caution should be exercised when approaching syndromic babies. The majority of these syndromes are linked to difficult airway or developmental disabilities. In addition, cardiac connections are not rare. Table 8.1 summarizes various disorders related to glaucoma and anesthetic problems often encountered during administration of anesthesia.

The American Society of Anesthesiologists recommended fasting guidelines should be followed before the procedure, that is, 2 h for clear liquid, 4 h for breast milk, 6 h for topical feed/rice-based cereal, and 8 h for solids. In children undergoing ophthalmic examination under general anesthesia, increased preoperative fasting time may be a risk factor for postoperative emergence delirium and, hence, must be avoided. Besides, multiple exposures of general anesthesia at an early stage of life are a risk factor for

S. Gupta et al. (eds.), *Childhood Glaucoma*, https://doi.org/10.1007/978-981-19-7466-3_8

Table 8.1 Syndromes associated with childhood glaucoma and associated anesthesia concerns

Syndrome	Features	Anesthesia concerns
• Peters plus syndrome	• Developmental delay	• Difficult airway
	• Cleft lip, cleft palate	• Neurocognitive impairment exaggerated by inhalational agent
• Axenfeld-Rieger syndrome (anterior segment dysgenesis)	• Dysmorphic features	• Difficult airway
	• Dental anomalies	• Risk of intraoperative cardiac event
	• Sensorineural hearing loss	
	• Cardiac malformations	
	• Endocrine and orthopedic abnormalities	
• Lowe Syndrome	• Congenital hypotonia	• Neurocognitive impairment exaggerated by inhalational agent
	• Delayed development	
	• Proximal renal tubular dysfunction (renal Fanconi type)	
	• Progressive chronic renal failure and End Stage Renal Disease after age 10–20 years	
• Neurofibromatosis Type 1	• Multiple café au lait spots	• Neurocognitive impairment exaggerated by inhalational agent
	• Axillary and inguinal freckling, cutaneous neurofibromas	
	• Learning disabilities in ≥50% of individuals	
• Stickler Syndrome (hereditary progressive arthro-ophthalmopathy)	• Prominent eyes, a small nose with a scooped-out facial appearance, a receding chin	• Difficult airway
	• Cleft palate	
	• Hearing and joint problems	
• Sturge-Weber syndrome	• Encephalotrigeminal angiomatosis with associated facial port-wine stain	• Neurocognitive impairment exaggerated by inhalational agent
	• Cerebral calcifications	• Perioperative seizure
	• Seizures	
	• Developmental delay	

developing attention deficit hyperactive disorder in later ages. Alternatively, the examination can be performed under sedation in the presence of anesthesiologists using various drugs like ketamine and/or dexmedetomidine.

8.3 Intraoperative Management

Normally, ophthalmic examination under anesthesia takes around 7–15 minutes. Because most of these children will require repeated EUA, it is best to handle them gently. This can usually be accomplished satisfactorily using an inhalation technique and a laryngeal mask airway (LMA) (Figs. 8.1, 8.2, and 8.3). Intubation should be avoided as it can result in a fallacious increase in IOP. Furthermore, various anesthetic agents can alter IOP, depending upon the duration and depth of anesthesia, and thus, affecting the accurate measurement and further treatment.

Desflurane and sevoflurane are the most common halogenated agents used in practice. Although desflurane is less preferred by pediatric anesthesiologists compared to sevoflurane due to its irritating effect, both desflurane and sevoflurane are known to decrease IOP. In children aged 3–16 years old, Sahin and colleagues demonstrated a statistically significant decrease in IOP from 10.57 and 10.25 mmHg to 7.90 (25%) and

Fig. 8.1 Difficult airway secured with laryngeal mask airway

Fig. 8.2 Child undergoing examination under anesthesia with laryngeal mask airway in situ

Fig. 8.3 Picture depicting pediatric circuit, mask, laryngoscope, endotracheal tube, and laryngeal mask airway

6.97 mmHg (32%), at 2 min, in the desflurane and sevoflurane groups, respectively.

Ketamine is a dissociative anesthetic that has been used during EUA to acquire IOP readings. However, the potential impact of ketamine on IOP has been debated. Halstead et al. reported no significant change in IOP up to 10 minutes after intravenous ketamine injection. Similarly, Drayna et al. found no difference between baseline IOP and up to 30 minutes after intravenous ketamine administration. On the other hand, Wadia et al. reported a median increase of 3 mmHg in IOP up to 30 minutes after intravenous ketamine. When compared to sevoflurane, IOP measured after ketamine sedation is more likely to represent the awake IOP.

Intranasal (IN) dexmedetomidine has recently become popular for pediatric ophthalmic procedure sedation. Dexmedetomidine is a highly selective α2-adrenergic receptor agonist with combined sedative, anxiolytic, and mild analgesic effects. In children aged 6 months to 3 years, dexmedetomidine at a dose of 3 μg/kg has been used safely and efficiently for noninvasive procedures. In another study by Dhingra et al., the dose of 3.5 μg/kg was more successful for postoperative follow-up examinations of pediatric glaucoma patients. However, the data determining the effect of IN dexmedetomidine on IOP in children is still limited. Table 8.2 summarizes the effect of various factors in anesthesia on IOP.

Table 8.2 Table summarizing the effect of various factors used during anesthesia on intraocular pressure

S. no.	Factor	Effect on intraocular pressure (IOP)
1	Blood pressure (BP)	Increase in BP causes increase in IOP
2	Hypercapnia	Decreases IOP due to increased venous dilatation and increased aqueous outflow
3	Hypoxia	Decreases IOP
4	Inhalational agents	Decrease IOP
5	Propofol/thiopentone	Sharp decrease in IOP
6	Ketamine	Either no effect or increase in IOP
7	Midazolam	No effect or decrease in IOP
8	Dexmedetomidine	Not evaluated
9	Succinylcholine	Increases IOP
10	Non-depolarizing muscle relaxants	Not evaluated
11	Facemask	Interferes with IOP measurement
12	Intubation	Increases IOP
13	Laryngeal Mask Airway	No significant change

Table 8.3 Parameters that ought be noted during EUA (Fig. 8.4)

Parameter	Right eye	Left eye
Cornea:		
• Clarity/scar/Haab's striae		
• Diameter		
• Central corneal thickness		
Bleb grading		
Anterior chamber details		
• Iris/pupil		
• Angle		
• Lens status		
Fundus		
IOP in mmHg		
USG for posterior segment examination (if media haze)		
Axial length in mm		
UBM/ASOCT findings		
Refraction		

USG ultrasonography, *UBM* ultrasound biomicroscopy, *ASOCT* anterior segment optical coherence tomography, *IOP* intraocular pressure

8.4 Order of Examination During EUA (Table 8.3)

- IOP should be measured as soon as possible after the patient is anesthetized, so that the effect of anesthetic agent in IOP measurement is minimized. Perkin's is the gold-standard portable tonometer requiring fluorescein dye for staining, if possible, the use of dye should be avoided or it should be washed thoroughly as it interferes with further examination. The use of eye speculum can falsely show high IOP (up to 4 mmHg).
- Corneal diameters, clarity, the presence of Haab's striae/opacity, should be noted.
- Anterior chamber details can be seen by:
  - Operating microscope, direct gonioscopy
  - Portable slit lamp biomicroscopy
  - Intraoperative optical coherence tomography (iOCT)/FLEX OCT/ultrasound biomicroscopy (useful in case of the opaque

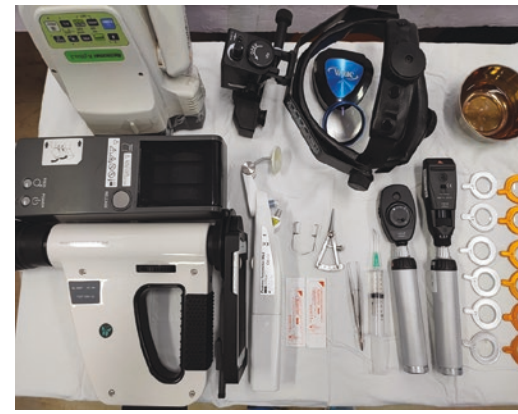

Fig. 8.4 Picture showing ophthalmic instruments that may be necessary while performing examination under anesthesia. Auto ref/keratometer (Retinomax K-plus 3, Tokyo, Japan), indirect ophthalmoscope (Appasamy associates, Chennai, India), 20D lens, sterile bowl, refraction set (lenses), streak retinoscope, direct ophthalmoscope (Heine, Herrsching, Germany), saline, globe holding forceps, Castroviejo calliper, wire speculum, fluorescein strips, Perkins tonometry, hand-held fundus camera (Remidio's Fundus on phone, NM-10, Bengaluru, India)

cornea and to measure central corneal thickness)
- Refraction using a streak retinoscopy or autorefractometry.
- Fundus examination with direct or indirect ophthalmoscopy, handheld fundus photography.
- Ultrasound B scan for posterior segment examination in case of media opacity and A scan to measure axial length.
- If a patient has been previously operated on, bleb status, suture removal (if needed), and bleb needling (in case of encysted bleb) can be done.

8.5 Post-operative Management

The child should be observed in the post-anesthesia care unit (PACU) for post-operative nausea and vomiting and discharged after discharge criteria are met.

8.6 Follow-Up

- In uncomplicated cases, EUA needs to be repeated postoperatively at 4–6 weeks, then at every 3–6 months for the first 2 years, and every year till the child is old enough for examination without anesthesia.
- Frequency of EUA should be tailored according to the severity of glaucoma and need. EUA might be needed at 2–4 weeks if releasable sutures were used or even earlier, if post-operative shallowing of the anterior chamber occurs or any interventions like bleb needling for high IOP is planned.
- As repeated EUAs are harmful to children, we should try to reduce their frequency. Recent advances in measuring IOP and corneal diameters have reduced the frequency of EUA.
  - IOP measurement with devices such as, iCare rebound tonometer (iCare Finland Oy, Vantaa, Finland) can be performed when the child is sleeping or even awake (in cooperative child) without the need of even topical anesthesia. Tonopen can be used to measure IOP in children while sleeping, needs topical anesthesia.
  - Corneal diameter can be measured with U-tool (novel method) in 80% of children without the need for sedation or anesthesia (Fig. 8.5).

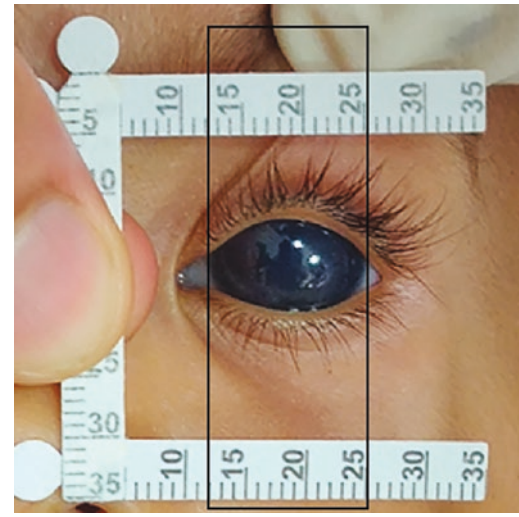

Fig. 8.5 Corneal diameter measured using novel U-tool. (Bafna et al 2022)

8.7 Case Scenarios

Case 8.1
6-month-old male with no other comorbidities posted for examination under anesthesia.

It generally takes 10–15 min for the procedure. Owing to small age of the patient and increase risk of apnea in this age groups, it is important to secure the airway during the entire procedure. Thus, general anesthesia with LMA is preferred in younger kids.

Case 8.2
5-year-old female with Down's syndrome and normal airway on examination posted for suture removal.

Depending upon the number of sutures and expertise of the ophthalmologist, the procedure usually takes 1–4 min. Also, it is comparatively easier to secure intravenous lines in children of

this age group. As a result, this can be easily done under sedation using ketamine. Dexmedetomidine is avoided as patients with Down's syndrome are more prone to bradycardia.

8.8 Conclusions

- A comprehensive pre-anesthetic checkup is important before any procedure under anesthesia.
- The plan of anesthesia depends mainly upon the patient profile, duration of the procedure, and expertise of the anesthesiologist and ophthalmologists.
- It is preferred to secure airway in case of anticipated difficult airway, difficult intravenous access, and/or syndromic babies.
- Postoperative monitoring should be done in the PACU.

Suggested Reading

Bafna RK, Mahalingam K, Rakheja V, et al. Validating the use of U-tool as a novel method for measuring the corneal diameter in infants screened for congenital glaucoma. Indian J Ophthalmol. 2022;70(1):143–6. https://doi.org/10.4103/ijo.IJO_930_21.

Behrle N, Birisci E, Anderson J, Schroeder S, Dalabih A. Intranasal dexmedetomidine as a sedative for pediatric procedural sedation. J Pediatr Pharmacol Ther. 2017;22(1):4–8.

Blumberg D, Congdon N, Jampel H, Gilbert D, Elliott R, Rivers R, Munoz B, Quigley H. The effects of sevoflurane and ketamine on intraocular pressure in children during examination under anesthesia. Am J Ophthalmol. 2007;143(3):494–9.

Dhingra D, Ghai B, Sabharwal P, Saini V, Snehi S, Kaur M, Pandav SS, Kaushik S. Evaluation of intranasal dexmedetomidine as a procedural sedative for ophthalmic examination of children with glaucoma. J Glaucoma. 2020;29(11):1043–9.

Drayna PC, Estrada C, Wang W, Saville BR, Arnold DH. Ketamine sedation is not associated with clinically meaningful elevation of intraocular pressure. Am J Emerg Med. 2012;30(7):1215–8.

Halstead SM, Deakyne SJ, Bajaj L, Enzenauer R, Roosevelt GE. The effect of ketamine on intraocular pressure in pediatric patients during procedural sedation. Acad Emerg Med. 2012;19(10):1145–50.

Khanna P, Saini K, Sinha R, Nisa N, Kumar S, Maitra S. Correlation between duration of preoperative fasting and emergence delirium in pediatric patients undergoing ophthalmic examination under anesthesia: a prospective observational study. Pediatr Anesthes. 2018;28(6):547–51.

Şahin A, Tüfek A, Cingü AK, Çaça I, Tokgöz O, Balsak S. The effect of I-gel™ airway on intraocular pressure in pediatric patients who received sevoflurane or desflurane during strabismus surgery. Pediatr Anesth. 2012;22(8):772–5.

Sprung J, Flick RP, Katusic SK, Colligan RC, Barbaresi WJ, Bojanić K, Welch TL, Olson MD, Hanson AC, Schroeder DR, Wilder RT. Attention-deficit/hyperactivity disorder after early exposure to procedures requiring general anesthesia. Mayo Clin Proc. 2012;87(2):120–9.

Thanapaisal S, Oatts J, Zhao J, et al. Effect of general anaesthesia on intraocular pressure in paediatric patients: a systematic review. Eye (Lond). 2021;35(4):1205–12. https://doi.org/10.1038/s41433-020-1093-8.

Wadia S, Bhola R, Lorenz D, Padmanabhan P, Gross J, Stevenson M. Ketamine and intraocular pressure in children. Ann Emerg Med. 2014;64(4):385–8.

Part III

Primary Childhood Glaucoma

Primary Congenital Glaucoma

9

Karthikeyan Mahalingam and Shikha Gupta

The term primary congenital glaucoma (PCG) was first described by Hippocrates (460–377 BC), while Berger first linked the elevated intraocular pressure (IOP) to enlargement of the globe. Buphthalmos is the visible enlargement of the globe at birth or soon after birth due to congenital glaucoma. PCG is developmental glaucoma occurring due to an obstruction in aqueous outflow as a result of abnormal development of the trabecular meshwork and anterior chamber angle (pathophysiology is explained in Chap. 1). The anatomical classification of developmental glaucoma is mentioned in Chap. 2, where PCG is essentially labeled as glaucomas with isolated trabeculodysgenesis. PCG can be sporadic or inherited in an autosomal recessive pattern. Some of the genetic associations include mutations in known genes like *CYP1B1*, *LTBP2*, *TEK*, *MYOC*, *GPATCH*, *PLOD2*, and *PRSS56*. Based on the presentation, it is further classified into neonatal PCG (<1 month), infantile PCG (>1 month to 24 months), or late-onset PCG (>24 months). Table 9.1 lists classification for PCG based on disease severity (Gupta V et al 2022).

Table 9.1 Severity staging for primary congenital glaucoma (PCG). *Each parameter is worth 1 point. A case is severe if total score is ≥4.

Parameters*	Non-severe PCG	Severe PCG
Age of onset	Infantile	Neonatal
Corneal diameter (in mm)	<13	≥13
Axial length (in mm)	<24	≥24
Corneal haze	Clear cornea or anterior segment structures can be made out despite the haze	Total (no anterior segment structures visible)
Corneal haze after IOP lowering	Reduced	Persisting
Surgeries required for IOP control	≤2	>2

9.1 Case Examples

Case 9.1

A 6-day-old male child presented with an enlarged eyeball and hazy enlarged cornea of both eyes (Fig. 9.1) since birth. Parents also complained that the child had photophobia and watering.

Supplementary Information The online version contains supplementary material available at https://doi.org/10.1007/978-981-19-7466-3_9.

K. Mahalingam · S. Gupta (✉)
Dr. Rajendra Prasad Centre for Ophthalmic Sciences, All India Institute of Medical Sciences, New Delhi, India
e-mail: shikhagupta@aiims.edu

S. Gupta et al. (eds.), *Childhood Glaucoma*, https://doi.org/10.1007/978-981-19-7466-3_9

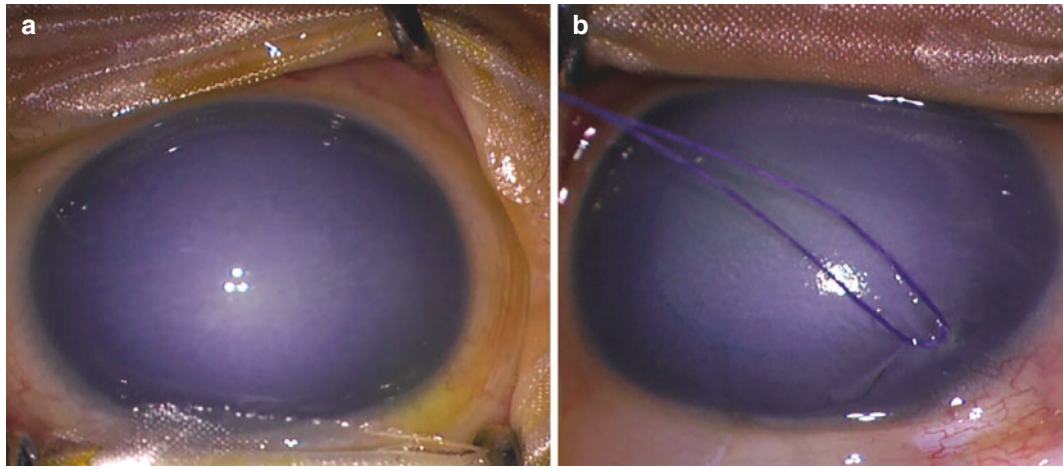

Fig. 9.1 Clinical picture of right eye (RE) (**a**) and left eye (LE) (**b**) of neonatal PCG showing enlarged corneal diameter, stretched limbus, and central corneal haze with peripheral clearing

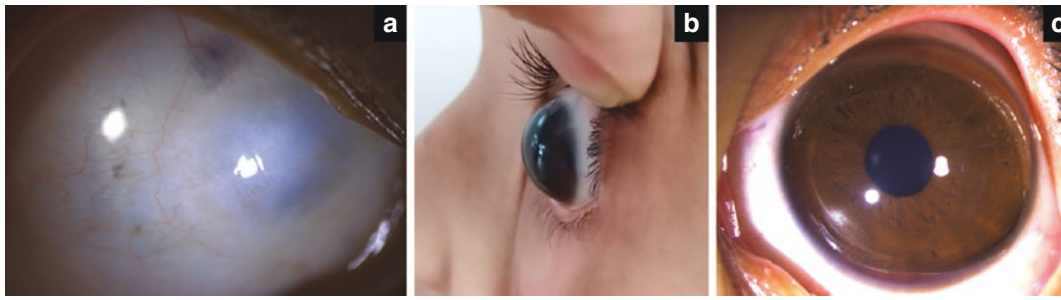

Fig. 9.2 Differentials of primary congenital glaucoma: (**a**) clinical picture of sclerocornea showing a small opacified cornea with no definitive boundary between sclera and cornea, (**b**, **c**) clinical picture of keratoglobus showing globular protrusion of cornea from limbus to limbus

Examination: The child had enlarged corneal diameter, stretched limbus, and central corneal haze with peripheral clearing (Fig. 9.1a, b), and IOP (measured while sleeping) was 28 mmHg in the right eye (RE) and 32 mmHg in the left eye (LE). Central corneal thickness was 850 μm (RE) and 910 μm (LE). No other systemic comorbidities were present.

Diagnosis: The patient was diagnosed with both eye neonatal PCG.

Differential diagnosis:

- Congenital hereditary endothelial dystrophy: Bilateral symmetric diffuse corneal opacification varying from a blue-gray ground-glass appearance to total corneal opacification (involving peripheral cornea unlike in PCG), without megalocornea. However rarely CHED and congenital glaucoma may coexist.
- Other conditions with corneal opacity/edema: Sclerocornea (Fig. 9.2a), obstetric trauma causing tears in Descemet's membrane, ulcers, metabolic diseases, and other corneal dystrophies – look for high IOP and megalocornea.
- Nasolacrimal duct obstruction: Only epiphora will be present, the absence of corneal involvement as well as photophobia.
- Axial myopia, megalocornea, and keratoglobus (Fig. 9.2b,c): Only enlargement of the eye (axial myopia)/cornea alone in megalo-

cornea or globular protrusion of corneal (keratoglobus) with no limbal stretching and presence of clear cornea and normal IOP.
- Proptosis (Video 9.1) due to any intraorbital mass lesion: There will be only outward protrusion of eye and imaging (ultrasonography, computed tomography or magnetic resonance imaging) would help to find the mass lesion/confirm the diagnosis.

Treatment: Initially started on BE betaxolol bd, pilocarpine 2% TDS, and oral acetozolamide 250 mg (1/8) tablet TDS.

It was followed up with both eyes combined trabeculectomy with trabeculotomy (CTT) augmented with mitomycin C 0.04% under general anesthesia.

Learning Points
- The classic triad for symptoms of PCG includes epiphora (Fig. 9.3), photophobia, and blepharospasm.
- Neonatal PCG presents within the first month of birth. It has a worse prognosis than infantile PCG. Angle surgeries are less effective in severe PCG with corneal haze and enlarged eye compared to non-severe PCG.
- Brimonidine is contraindicated in children less than 2 years of age due to the risk of central nervous system depression. It is better to avoid till 6 years of age, in children with cognitive impairment and children with weight <15 kg.

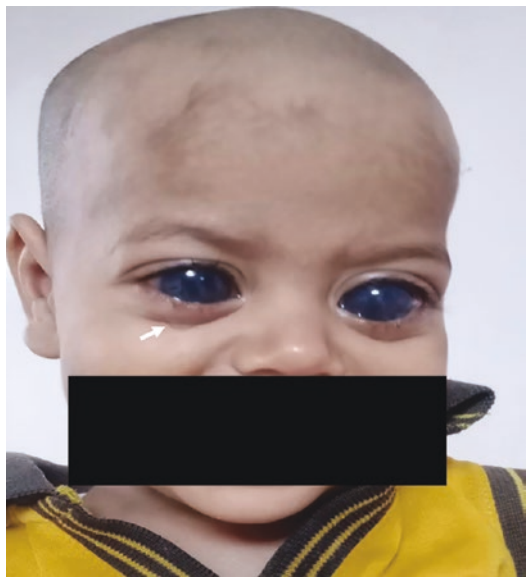

Fig. 9.3 Clinical picture of a child with primary congenital glaucoma having epiphora (white arrow) due to corneal involvement caused by uncontrolled intraocular pressure in both eyes

Case 9.2

A 10-month-old female child presented with an enlarged eyeball and whitish localized opacity of the cornea in the LE.

Examination: The patient had enlarged cornea, stretched limbus, and Haab's striae in LE (Fig. 9.4a), while RE appeared normal. IOPs were RE 10 mmHg and LE 24 mmHg. Central corneal thickness: RE 522 μm and LE 682 μm. Axial lengths (AL) were RE 21 mmHg and LE 23 mmHg.

Diagnosis: Unilateral non-severe PCG associated with focal corneal edema due to Haab's striae (LE).

The differential diagnosis for unilateral PCG:

- Retinoblastoma (Fig. 9.5): Look for leucokoria. As a result, distant direct ophthalmoscopy showing a good glow is a necessary requisite before labeling a child with unilateral buphthalmos as primary congenital glaucoma. Fundus examination with indirect ophthalmoscopy or ultrasonography (in case of media haze) to look for mass with calcification confirms the diagnosis.
- Traumatic glaucoma: Rule out the history of trauma.
- Persistent fetal vasculature (PFV) with glaucoma: Initially affected eye may be smaller at birth which when affected with glaucoma too can undergo corneal stretching and increase in AL secondary to increased IOP.
- Other differential diagnoses: congenital anomalies and unilateral microphthalmos with secondary glaucoma.

Examination under anesthesia (EUA): In LE, crescentic opacification corresponding to Haab's striae was seen, intraoperative OCT (iOCT) shows scans which show horizontal and vertical

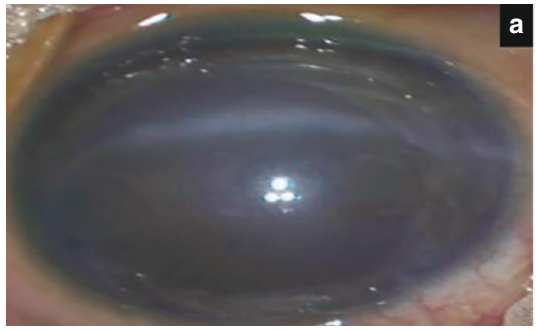

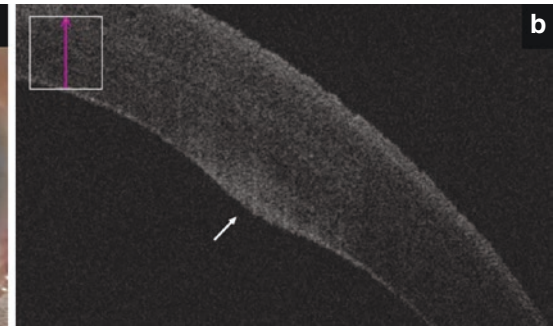

Fig. 9.4 (**a**) Clinical picture of an unilateral primary congenital glaucoma showing Haab's striae (**b**) microscope-integrated intraoperative OCT picture (iOCT machine) (rescan 700 microscope-mounted OCT system, Carl Zeiss Meditec Jena, Germany) showing the morphological appearance of Haab's striae, note the posterior intracameral bulge with posterior corneal hyper-reflectivity at the site of Haab's striae

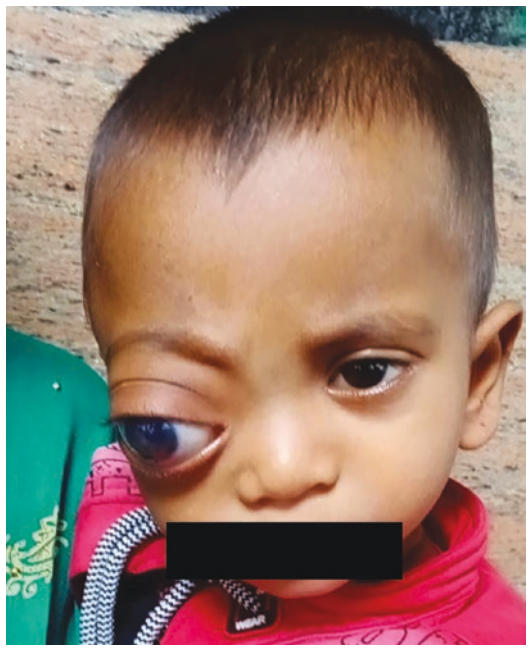

Fig. 9.5 Clinical picture of a patient with right eye retinoblastoma showing enlargement and protrusion of the eye

cross-sections across the Haab's striae (Fig. 9.4b). Fundus: RE cup-disk ratio (CDR) 0.2:1, healthy neuro-retinal rim, LE good glow was present CDR 0.7:1, and circumferential thinning of the neuroretinal rim.

Treatment: LE microvitreoretinal blade assisted 200° goniotomy through two side ports was performed under Healon (Abbott Medical Optics, Santa Ana, California) cover under general anesthesia.

During follow-up at 5 years, the RE showed IOP of 24 and 28 mmHg on 2 consecutive follow-ups. CRD remained 0.2:1. She was started on betaxolol drops for control of IOP.

Learning Points

- PCG is usually bilateral (70–95%), and unilateral presentation is uncommon (Figs. 9.6 and 9.7). Fellow eyes of unilateral PCG may not have subtle angle dysgenesis, manifesting later in life, so they should be monitored for IOP rise on every follow-up. Development of ocular hypertension (like in this case) or glaucomatous optic neuropathy calls for treatment.
- Refraction and amblyopia therapy must not be missed while following up congenital glaucoma patients, especially if unilateral.

Case 9.3

A case of a 6-year-old male patient with bilateral PCG. He had a history of both eyes operated trabeculotomy with trabeculectomy augmented with mitomycin C at 1.5 years of age.

Examination: BE best-corrected visual acuity 6/12 (power of glasses: RE −4.75DS/−2DC, LE −4.25DS/−1DC). BE showed Haab's striae (Fig. 9.8a–d) involving central cornea. AS OCT of BE angle showed anterior iris insertion and hyper-reflective membrane causing angle

Fig. 9.6 Clinical picture of a child with bilateral primary congenital glaucoma showing enlarged eyes, stretched limbus and diffuse corneal haze in both eyes

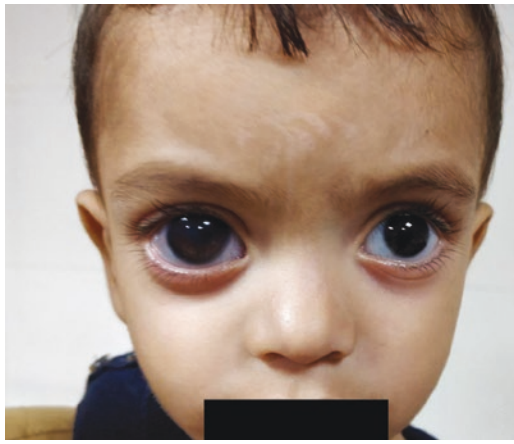

Fig. 9.7 Clinical picture of a child with (unilateral) right eye primary congenital glaucoma. Note the enlargement of eye and stretching of limbus in right eye compared to left eye

dysgenesis (Fig. 9.8e). Current IOPs were RE: 10 mmHg and LE 12 mmHg.

Management: The patient was advised to use refractive glasses and undergo lifelong follow-up.

Learning Points

- The anterior chamber angle in PCG usually shows anterior iris insertion, hyper-reflective membrane over angle, and the absence of identifiable Schlemm's canal. The angle is wide open with prominent angle dysgenesis. Iris configuration may range from flat, concave to wraparound iris configuration.
- Causes of decreased vision in PCG: Corneal scarring from Haab's striae, corneal decompensation or associated irreversible corneal opacity, a refractive error such as myopia (axial elongation) or myopic astigmatism [corneal stretching, Haab's striae (Fig. 9.9) or bleb induced], glaucomatous optic neuropathy, and amblyopia more prominent in unilateral cases (if refractive glasses are not used).
- Parameters that need to be assessed during follow-up (by EUA until old enough for cooperation):
  - IOP
  - Bleb status
  - Corneal diameter (once enlarged, do not reverse even if IOP is controlled)
  - Corneal opacification (may clear if IOP is controlled)
  - Cup-disc ratio (may reverse if IOP is controlled)
  - Refraction
  - Peripheral retinal screening to rule out retinal degeneration or tears
  - Ultrasound A-scan: Axial length (not reversible even if IOP is controlled), B-scan if there is significant corneal opacity to look at posterior segment

Case 9.4

A 4-month-old male child presented with an enlarged eyeball in both eyes. The patient had a family history of congenital glaucoma in his elder sister. Parents gave a history of consanguineous marriage.

Pedigree chart: (Fig. 9.10)

Examination: Enlarged corneal diameters in both eyes: RE 12.5 mm and LE 12 mm. Corneal haze in both eyes (RE > LE) (Fig. 9.11). IOPs were RE 24 mmHg and LE 22 mmHg on medical treatment.

Diagnosis: BE infantile PCG

Treatment: Same as Case 9.1

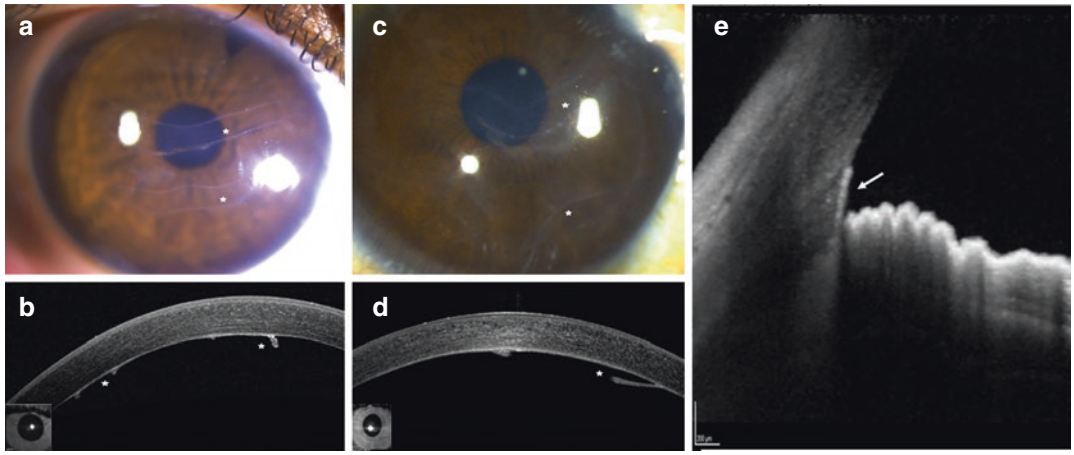

Fig. 9.8 Slit-lamp clinical picture (**a**, **c**) and AS-OCT (**b**, **d**) of bilateral primary congenital glaucoma showing Haab's striae in central and peripheral cornea (star). (**e**) Anterior segment OCT of right eye angle showing anterior iris insertion and hyper-reflective membrane over the angle (arrow), the Schlemm's canal is not visible

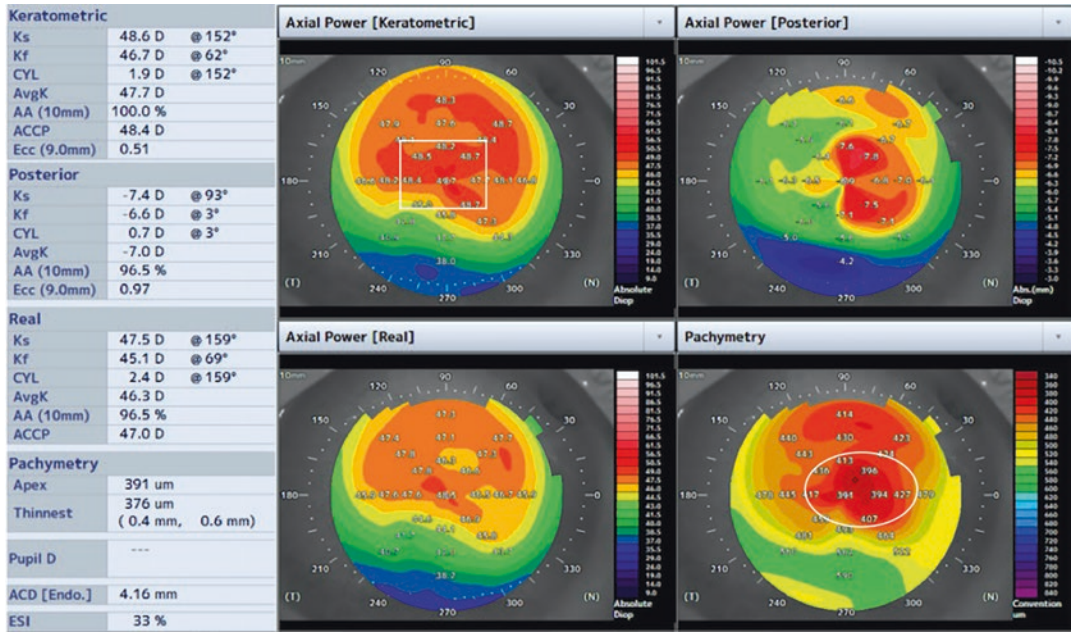

Fig. 9.9 Corneal tomography (Pentacam Comprehensive Eye Scanner- Oculus Optikgeraete GmbH; Wetzlar, Germany) in a primary congenital glaucoma with Haab's striae showing corneal astigmatism upto 7D and corneal steepening (box) and thinning (oval)

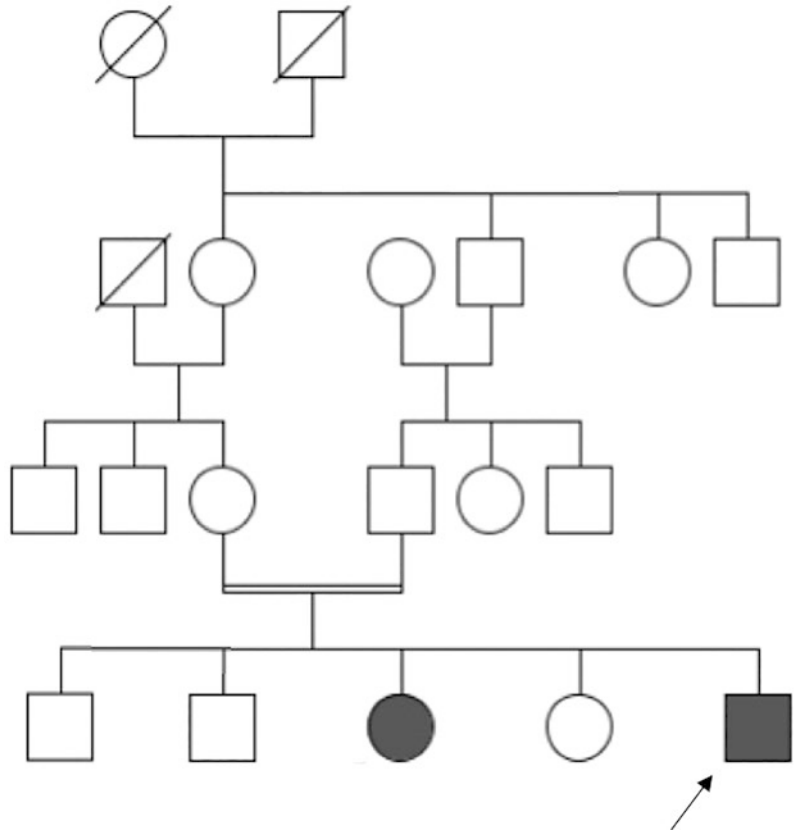

Fig. 9.10 Pedigree chart showing consanguinity and positive family history of a 4 month old child born with both eye primary congenital glaucoma (elder sister has similar disease)

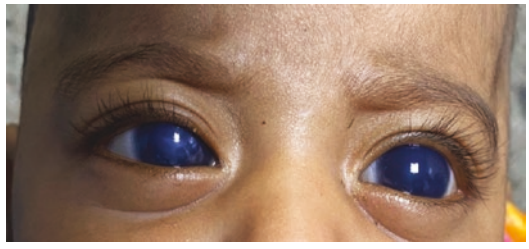

Fig. 9.11 Clinical picture of bilateral infantile primary congenital glaucoma showing enlarged eyeball and corneal haze in both eyes

Learning Points

- PCG occurs in both sporadic and familial patterns (sporadic common).
- Family history is positive in 10–40% of cases, and there is an increased incidence with consanguinity.

9.2 Management of PCG (Fig. 9.12)

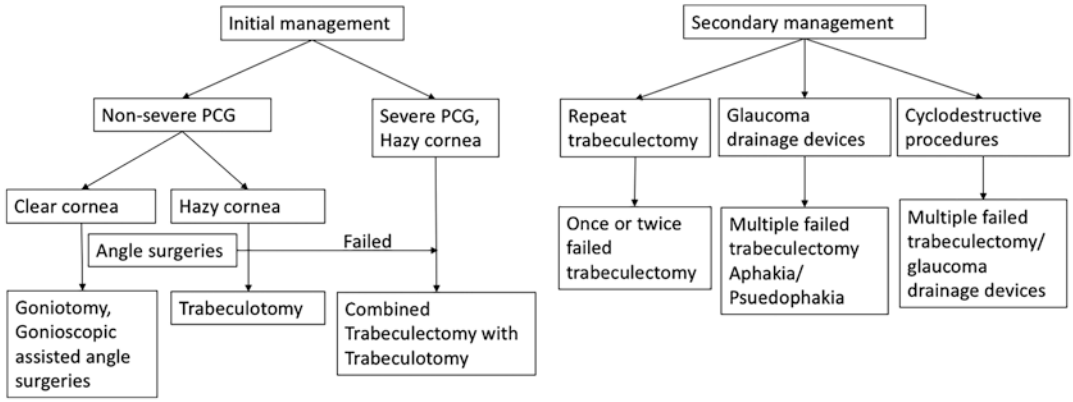

Fig. 9.12 Flow chart showing management of primary congenital glaucoma. Severe and non-severe glaucoma as proposed by the authors (Gupta V et al 2022). PCG- primary congenital glaucoma

9.3 Conclusions

Primary congenital glaucoma has varied clinical presentations (differences in age of onset, severity of signs & symptoms, and response to treatment). Most of them need surgical management for IOP control. Apart from IOP control, refraction & glass prescription (especially in unilateral cases) must be emphasised to prevent ambylopia. With constant efforts, these children grow up to live a productive social and occupational life.

Suggested Reading

Azad RV, Chandra P, Chandra A, Gupta A, Gupta V, Sihota R. Comparative evaluation of RetCam vs. gonioscopy images in congenital glaucoma. Indian J Ophthalmol. 2014;62(2):163–6. https://doi.org/10.4103/0301-4738.116487. PMID: 24008788; PMCID: PMC4005231.

Gupta V, Jha R, Srinivasan G, Dada T, Sihota R. Ultrasound biomicroscopic characteristics of the anterior segment in primary congenital glaucoma. J AAPOS. 2007;11(6):546–50. https://doi.org/10.1016/j.jaapos.2007.06.014. Epub 2007 Aug 27. PMID: 17720567.

Gupta V, Chaurasia AK, Gupta S, Gorimanipalli B, Sharma A, Gupta A. In vivo analysis of angle dysgenesis in primary congenital, juvenile, and adult-onset open angle glaucoma. Invest Ophthalmol Vis Sci. 2017;58(13):6000–5. https://doi.org/10.1167/iovs.17-22,695. PMID: 29183046.

Gupta V, Singh A, Pandya I, Sofi R, Sen S, Somarajan BI, Gupta S, Nag TC. Differences in outflow channels between two eyes of unilateral primary congenital glaucoma. Acta Ophthalmol. 2021;99(2):187–94. https://doi.org/10.1111/aos.14540. Epub 2020 Jul 23. PMID: 32701215.

Gupta V, Bhandari A, Gupta S, Singh A, Gupta A. Consanguinity and severity of primary congenital glaucoma. J AAPOS. 2022;26(3):119.e1–5. https://doi.org/10.1016/j.jaapos.2022.01.010.

Ko F, Papadopoulos M, Khaw PT. Primary congenital glaucoma. Prog Brain Res. 2015;221:177–89. https://doi.org/10.1016/bs.pbr.2015.06.005. Epub 2015 Sep 9. PMID: 26518078.

Yu Chan JY, Choy BN, Ng AL, Shum JW. Review on the management of primary congenital glaucoma. J Curr Glaucoma Pract. 2015;9(3):92–9. https://doi.org/10.5005/jp-journals-10008-1192. Epub 2016 Feb 2. PMID: 26997844; PMCID: PMC4779948.

10 Juvenile Onset Open-Angle Glaucoma

Harathy Selvan, Abhishek Singh, and Viney Gupta

Juvenile-onset open-angle glaucoma (JOAG) is a subset of primary open-angle glaucoma diagnosed between 4 and 40 years of age. It manifests widespread genotypic and phenotypic heterogeneity. Myocilin (*MYOC*) mutations are the most commonly attributed genetic cause. The classic triad of the disease includes a baseline intraocular pressure (IOP) >21 mmHg, typical glaucomatous optic neuropathy, and corroborating visual field defects. When the IOP remains elevated without supportive structural or functional damage, it is termed as juvenile ocular hypertension (JOHT). Alternately, if the baseline IOP has been ≤21 mmHg, but with corroborating structural and functional glaucomatous defects in the absence of any neurological cause, then it is termed as juvenile normal tension glaucoma (JNTG).

The pathophysiology underlying the disease is immaturity of the conventional outflow pathways. On gonioscopy, they could be appreciated as an anterior iris insertion, prominent iris processes, or a featureless angle. Depending on the age at onset, highest untreated intraocular pressure, iris features, and gonioscopy findings, the authors have identified four distinct groups of JOAG using cluster analysis (Table 10.1 and Fig. 10.1).

H. Selvan (✉)
Moorfields Eye Hospital NHS Foundation Trust, London, UK

A. Singh · V. Gupta
Dr. Rajendra Prasad Centre for Ophthalmic Sciences, All India Institute of Medical Sciences, New Delhi, India

In up to 40% of the eyes, anterior-segment optical coherence tomography reveals a hyperreflective membrane covering the trabecular meshwork (TM) and/or absent Schlemm's canal (SC). These signs could reflect the severity of dysgenesis; however, histopathological study of the angle remains the gold standard. The differential diagnosis for JOAG have been discussed in Table 10.2.

The structural and functional defects of JOAG are similar to that of adult-onset POAG. High IOP, long-term IOP fluctuations and increase in myopic refractive error are known risk factors for progression. Prompt treatment and lifelong monitoring are crucial to maintain the patient's visual functions and quality of life.

Table 10.1 JOAG clusters identified by cluster analysis

Cluster 1	Normal appearing iris and angles (Fig. 10.1a). They had the lowest baseline IOP of all clusters and age of onset later than other clusters
Cluster 2	Normal iris morphology with a featureless angle (Fig. 10.1b). They were associated with the earliest age of onset among all the clusters
Cluster 3	Normal iris morphology with either a high iris insertion or prominent iris process (Fig. 10.1c). High iris insertion eyes showed higher mean IOP than those with isolated prominent iris processes
Cluster 4	Abnormal iris features (prominent or absent crypts) and varied gonioscopic appearance (Fig. 10.1d). Those with prominent crypts and high iris insertion resembled mild forms of Axenfeld-Rieger's anomaly and manifested highest baseline untreated IOP

S. Gupta et al. (eds.), *Childhood Glaucoma*, https://doi.org/10.1007/978-981-19-7466-3_10

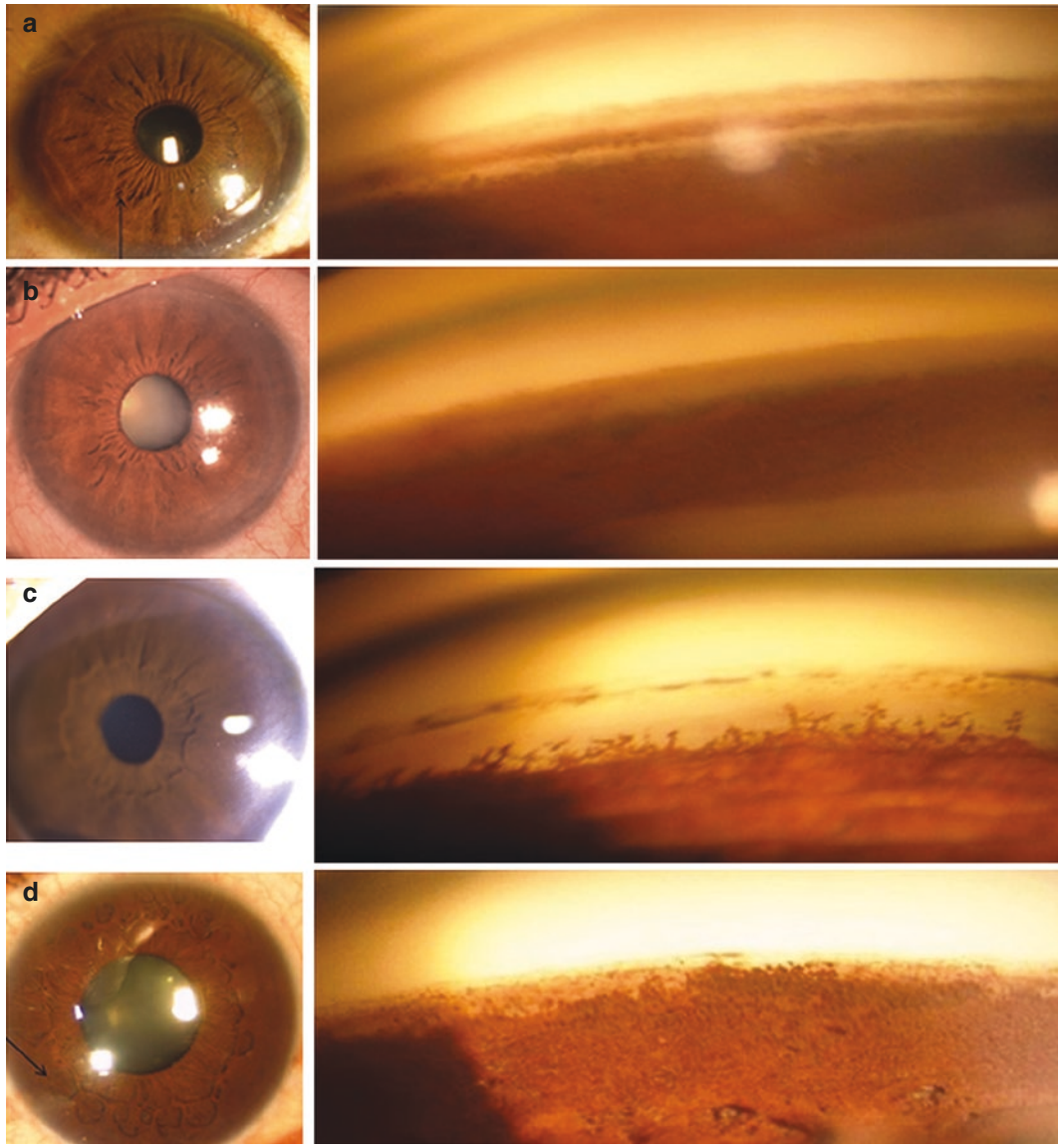

Fig. 10.1 Iris and angle features of different JOAG clusters. (**a**) Cluster 1 showing normal iris and angle morphology. (**b**) Cluster 2 showing normal iris features and a featureless angle. (**c**) Cluster 3 showing normal iris features and prominent iris processes. (**d**) Cluster 4 showing prominent iris crypts and a high iris insertion. The crypts are marked by a black arrow. (Images reproduced with permission from Birla S, Gupta D, Somarajan BI, Gupta S, Chaurasia AK, Kishan A, Gupta V. Classifying juvenile onset primary open angle glaucoma using cluster analysis. Br J Ophthalmol. 2020 Jun;104(6):827–835. doi: 10.1136/bjophthalmol-2019-314660)

Table 10.2 Differential diagnosis for juvenile open-angle glaucoma (JOAG), juvenile ocular hypertension (JOHT), and juvenile normal tension glaucoma (JNTG)

Differential diagnosis	Specific features
Juvenile open-angle glaucoma (JOAG) and juvenile ocular hypertension (JOHT)	
Steroid-induced glaucoma	A straightforward history of steroid use (topical and/or systemic), or history of seasonal allergy, chronic red eyes, skin diseases, systemic inflammatory disorders like asthma, nephrotic syndrome, and over-the-counter medication intake should raise suspicion. In most cases, intraocular pressure (IOP) tends to decrease with time when steroids are withdrawn
Pigmentary glaucoma	Immediate post-exercise blurred vision, colored halos, Krukenberg spindle, a very deep anterior chamber, Zentmayer ring, Sampaolesi line, and excessive 360° uniform angle pigmentation on gonioscopy differentiate this condition from JOAG. A concave iris configuration on ultrasound biomicroscopy (UBM) confirms the diagnosis
Uveitic glaucoma	Uveitis in remission with minimal tell-tale signs could be confused with JOAG. Remnant keratic precipitates and retrolental cells may offer a valuable clue. Chronic steroid usage may alter the picture, leading to an unsuspecting white eye with high IOP
Posner Schlossman syndrome (PSS)	Unilateral subtle uveitis with very high IOP could be misdiagnosed as JOAG. Slit-lamp examination may reveal fine keratic precipitates, 0.5 to 1+ cells, and minimal flare. Presumed due to viral etiology, PSS manifests as acute episodes with pressures being lower during remission periods
Primary angle closure glaucoma (PACG) of young	A dark-room gonioscopy aids in differentiating PACG of the young from JOAG. Peripheral anterior synechiae and blotchy pigmentation in PACG could be confused with high iris insertion and prominent iris processes, respectively
Developmental glaucoma	Mild cases of anterior segment dysgenesis may be missed in the early years due to their subtle features. Careful gonioscopy to identify a prominent Schwalbe's line (posterior embryotoxon) and developmental iridocorneal adhesions can clinch the diagnosis. In Rieger's anomaly, an altered iris pattern can also be noted
Late-onset primary congenital glaucoma (PCG)	Late-onset PCG diagnosed at >2 years of age could be confused with JOAG as both conditions can manifest varying degrees of angle dysgenesis and myopia. Corneal diameters >13 mm and the presence of Haab striae support the diagnosis of the former
Other secondary open-angle glaucomas (traumatic glaucoma, post retinal detachment surgery or intravitreal injections, uveitis)	The affected eye may manifest secondary glaucoma, while the other eye could show a steroid-induced or primary OHT
Juvenile normal tension glaucoma (JNTG)	
Intracranial space-occupying lesions	Compression of the visual pathway can result in visual field defects analogous to glaucoma, but with normal intraocular pressures
Megalopapilla	A congenitally anomalous large optic nerve head with a large cup could be confused with JNTG. However, the NRR, contour of blood vessels, and visual field reports are under normal limits in the former
Optic disc cupping secondary to prematurity	Low birth weight, fetal growth restriction, and prematurity have been associated with pseudoglaucomatous cupping. Thinning of periventricular optic radiations and/or transsynaptic degeneration of retinal ganglion cells can result in visual field defects despite normal IOP, mimicking JNTG

10.1 Case Examples

Case 10.1

A 15-year-old boy presented with complaints of colored halos in both eyes (BE). There was a family history of glaucoma in his father, diagnosed at the age of 35.

Examination: Best-corrected visual acuity (BCVA) in right eye (RE) was 6/9, left eye (LE) was 6/6 and applanation IOP in RE was 40 mmHg and LE was 32 mmHg. On gonioscopy, RE showed prominent iris processes, and LE showed high iris insertion along with prominent iris processes (Fig. 10.2). Iris pattern was normal in BE. Fundus examination showed RE myopic tessellated fundus with a pale tilted optic disc and CDR 0.9:1 with annular peripapillary atrophy. The LE showed a tilted disc with CDR 0.8:1, inferior neuroretinal rim (NRR) thinning, and a temporal crescent (Fig. 10.3). BE peripheral retinal examination and maculae were within normal limits.

Investigations: (a) Cycloplegic refraction – RE −13DS, LE −6.5 DS; (b) Ultrasound pachymetry – RE 500 μm, LE 505 μm; (c) HVF 30-2 SS – RE biarcuate scotoma, LE inferior arcuate, and central scotoma (Fig. 10.4); (d) axial length – RE 28.5 mm and LE 26.2 mm

Diagnosis: BE familial JOAG with high axial myopia RE > LE

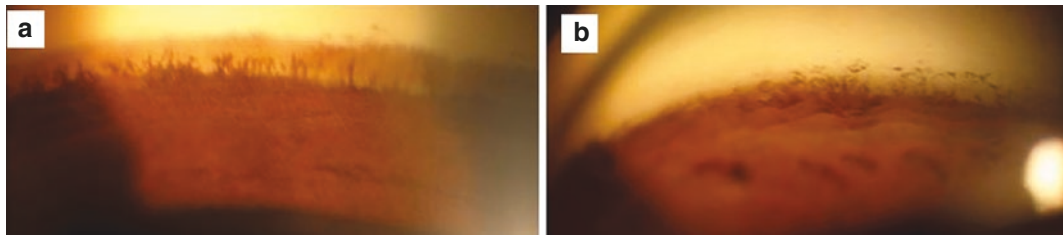

Fig. 10.2 Goniophotographs: (**a**) RE showing wide open angles with prominent iris processes. (**b**) LE showing an open angle with high iris insertion and prominent iris processes. (Reproduced with permission from Selvan H, Gupta S, Wiggs JL, Gupta V. Juvenile-onset Open-angle Glaucoma - A Clinical and Genetic Update. Surv Ophthalmol. 2021 Sep 15:S0039-6257(21)00184-3. doi: 10.1016/j.survophthal.2021.09.001)

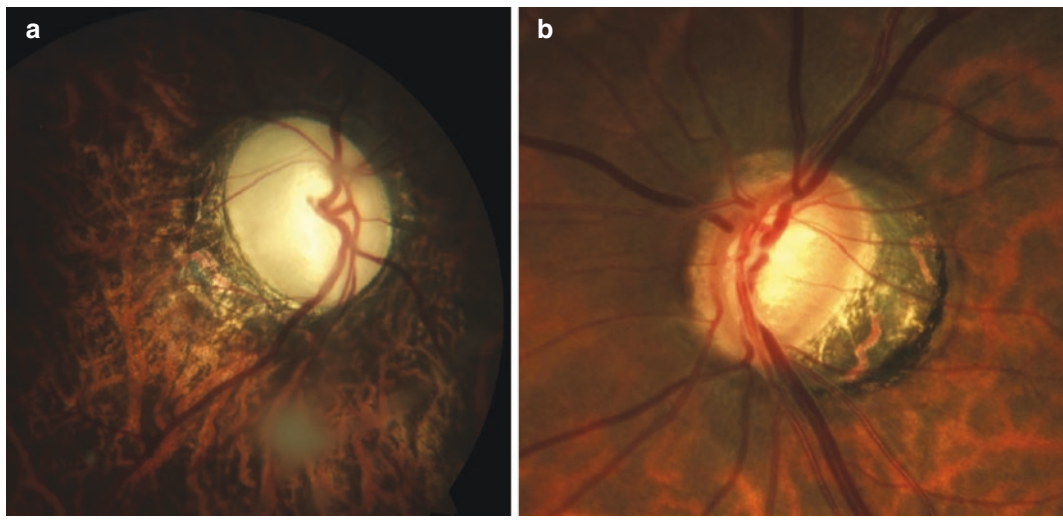

Fig. 10.3 Fundus photographs: (**a**) right eye shows myopic tessellated fundus with a pale tilted optic disc, CDR 0.9:1, and annular peripapillary atrophy. (**b**) Left eye showing a myopic tilted disc with CDR 0.8:1, inferior NRR thinning, and a temporal crescent

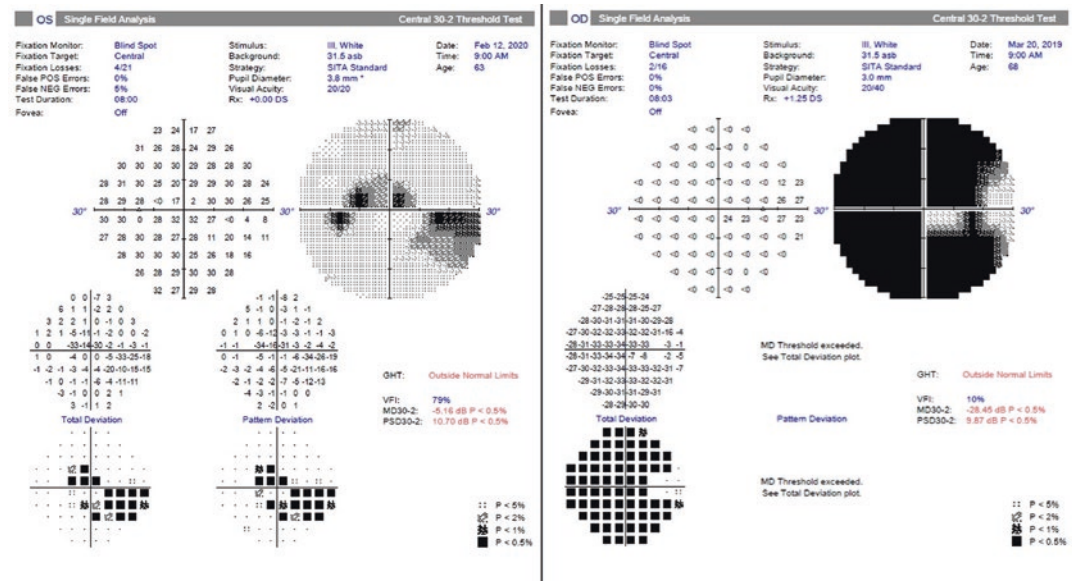

Fig. 10.4 Humphrey visual field 30-2 Sita Standard: (OS) LE showing an inferior arcuate and central scotoma, (OD) RE showing dense biarcuate scotoma with a temporal island of vision

Differential diagnosis: Table 10.2
Management:

(a) Treatment: Intravenous mannitol 20% 1 g/kg stat dose, oral acetazolamide 250 mg TDS, BE topical latanoprost HS, fixed-dose combination of brimonidine 0.2% + timolol maleate 0.5% BD followed by listing for sequential trabeculectomy with MMC.
(b) Family screening: Clinical screening of the sibling aged 20 years identified signs of JOAG in her as well (Fig. 10.5). Genetic screening of the family identified myocilin (*MYOC*) mutation.

Learning Points

- JOAG has been typically considered as an autosomal dominant disease with variable penetrance and expressivity; however, autosomal recessive and sporadic forms are also common.
- *MYOC* and *CYP1B1* are the commonly identified genes contributing to JOAG.
- Higher degrees of myopia are a risk factor for progression among JOAG patients.

Case 10.2

A 17-year-old girl presented with painless decrease of vision in LE incidentally noted a week back. There was no family history of any eye diseases.

Examination: BCVA RE was 6/6 and LE finger counting at 1 m. Applanation IOP in RE was 28 mmHg and LE was 36 mmHg. BE iris showed prominent iris crypts, and gonioscopy revealed featureless angles (Fig. 10.6). Optic disc showed glaucomatous cupping in BE, with a CDR of 0.8:1 in RE and 0.9:1 in LE, with circumferential NRR thinning BE (Fig. 10.7).

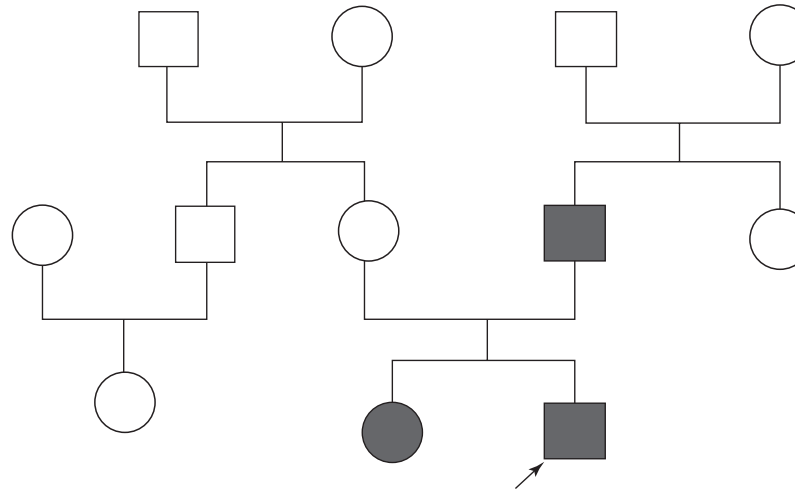

Fig. 10.5 Pedigree chart demonstrating family members affected by JOAG

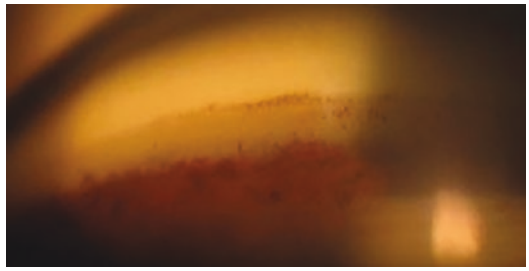

Fig. 10.6 Goniophotograph showing a featureless angle. (Reproduced with permission from Selvan H, Gupta S, Wiggs JL, Gupta V. Juvenile-onset Open-angle Glaucoma - A Clinical and Genetic Update. Surv Ophthalmol. 2021 Sep 15:S0039-6257(21)00184-3. doi: 10.1016/j.survophthal.2021.09.001)

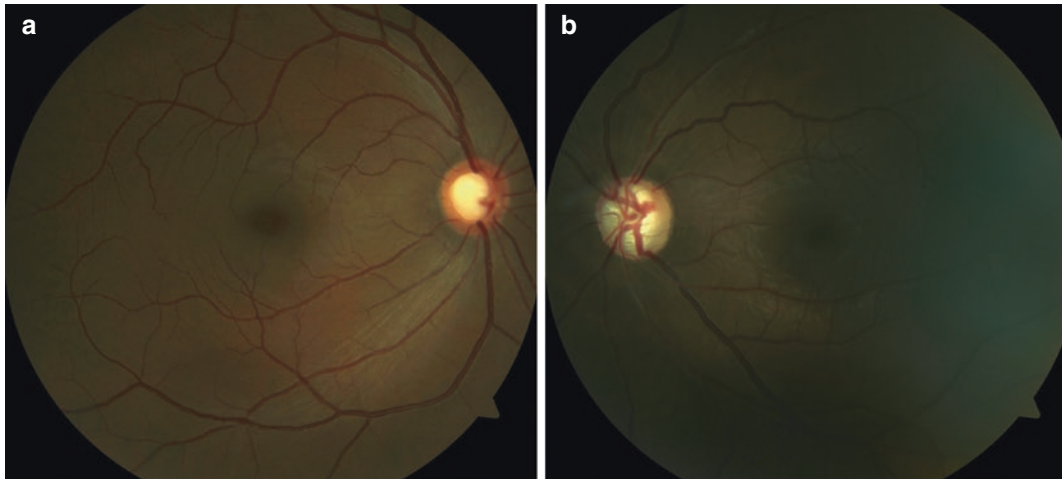

Fig. 10.7 Fundus photographs (**a**) RE showing a CDR of 0.8:1 with circumferential NRR thinning. (**b**) LE showing a CDR of 0.9:1 with circumferential NRR thinning and pallor

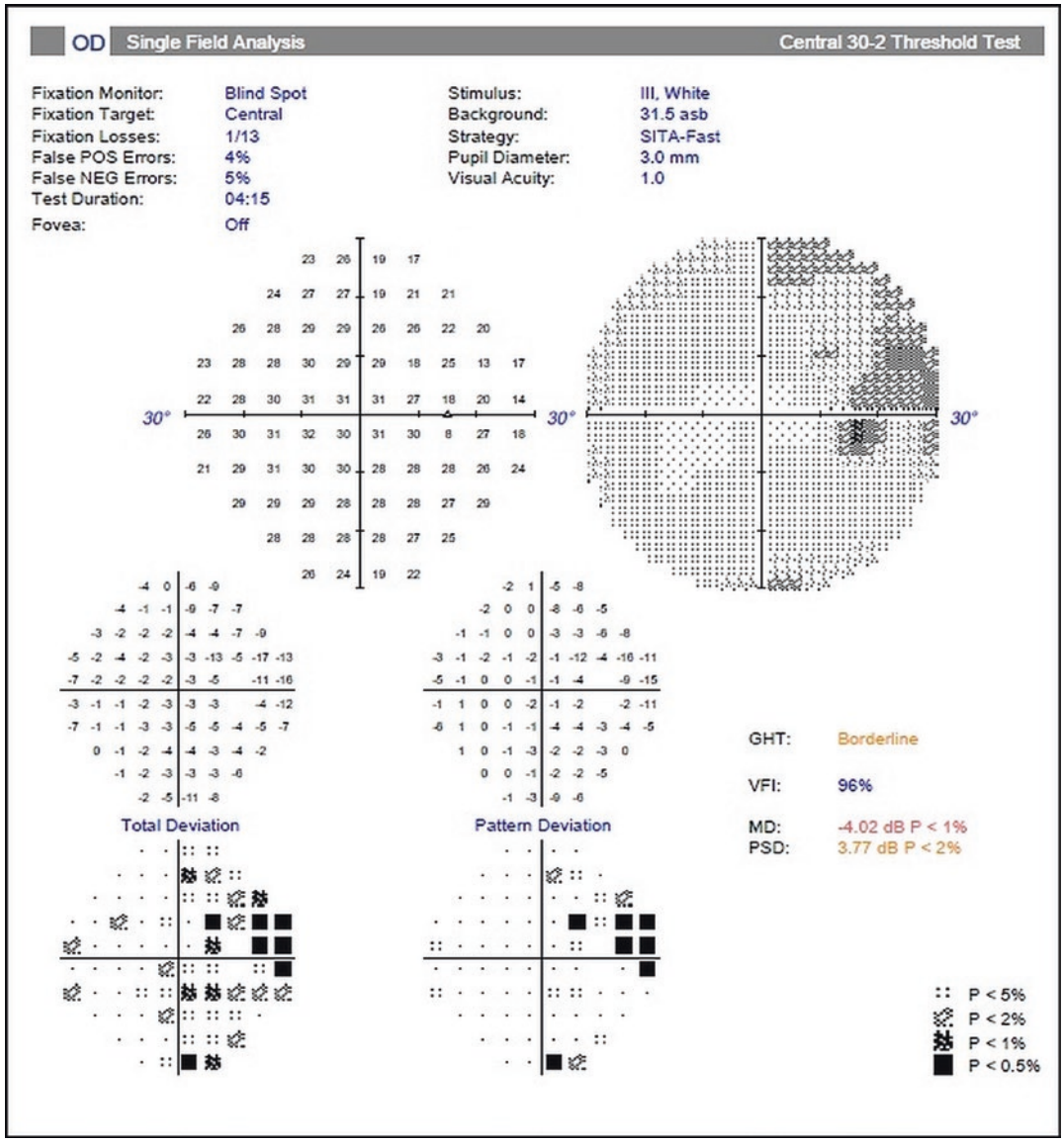

Fig. 10.8 HVF 30-2 Sita Fast of (OD) RE showing a temporal wedge defect

Investigations: (a) Ultrasound pachymetry – RE 520 μm, LE 525 μm (b) HVF 30-2; RE showed a temporal wedge defect (Fig. 10.8).

Diagnosis: BE JOAG with RE early disease, LE advanced glaucomatous optic neuropathy.

Differential diagnosis: Table 10.2

Treatment: RE microinvasive glaucoma surgery (goniotomy); LE diode laser cyclophotocoagulation

Learning Points

- JOAG could be asymmetric depending up on the severity of underlying angle dysgenesis. The true extent of dysgenesis cannot be predicted by the gonioscopic picture alone.
- The management of JOAG depends upon the age at presentation, severity of the disease, anticipated visual prognosis, and the patient's social care system.

Case 10.3

A 12-year-old girl was brought by her parents for routine yearly spectacle check. There were no visual complaints or family history of any eye diseases.

Examination: BCVA RE 6/9 and LE 6/6. Applanation IOP: RE 30 mmHg and LE 26 mmHg. The anterior segment examination was normal, with a normal patterned iris in BE. Gonioscopy showed normal open angles BE. Fundus examination however showed a CDR of 0.9:1 with NRR pallor in RE and a healthy disc with 0.6:1 in LE (Fig. 10.9).

Investigations: (a) Cycloplegic refraction: RE-3 DS/−0.5 DC at 30°, LE −2.75 DS; BE stable as compared to her previous prescription; (b) Ultrasound pachymetry – RE 575 μm, LE 580 μm; (c) RNFL OCT – RE showed global thinning, LE showed a normal study (Fig. 10.10); (d) HVF 30-2 SS – RE showed biarcuate scotoma with central tunnel vision, LE was within normal limits (Fig. 10.11); (e) ASOCT of angle – BE open angles with visible Schlemm's canal, larger in LE (Fig. 10.12).

Diagnosis: RE JOAG, LE JOHT

Differential diagnosis: Table 10.2

Treatment: RE trabeculectomy with mitomycin-c, LE selective laser trabeculoplasty

Learning Points

- JOAG is usually a bilateral disease; however, up to 25% can present with unilateral disease. Sporadic cases, especially if unilateral, may present at an advanced stage as compared to familial cases.
- In cases of unilateral JOAG, nearly 40% could show JOHT in their fellow eyes, especially in the early stages of the disease.
- Identification of Schlemm's canal on angle ASOCT is a strong predictor of response to SLT in JOAG eyes.

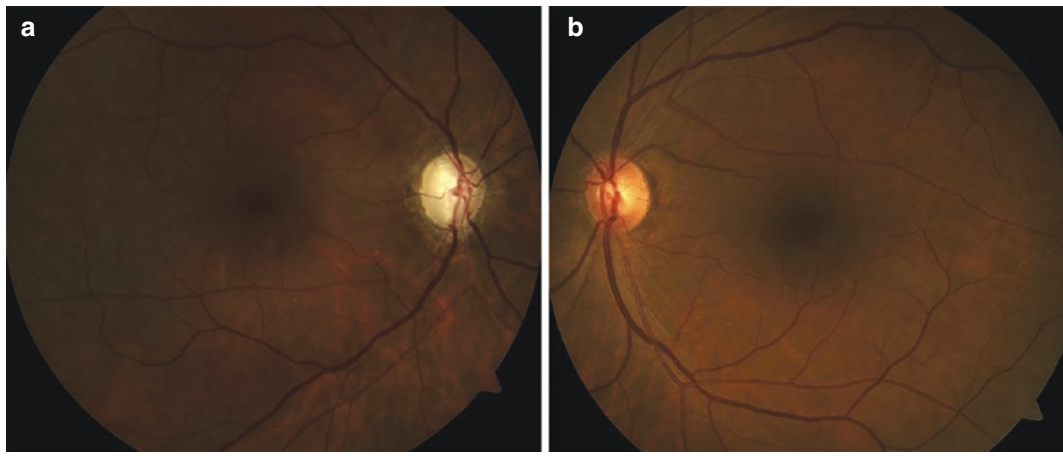

Fig. 10.9 Fundus photographs: (**a**) RE showing a CDR of 0.9:1 with circumferential NRR thinning and pallor. (**b**) LE showing a CDR of 0.6:1 with a healthy NRR

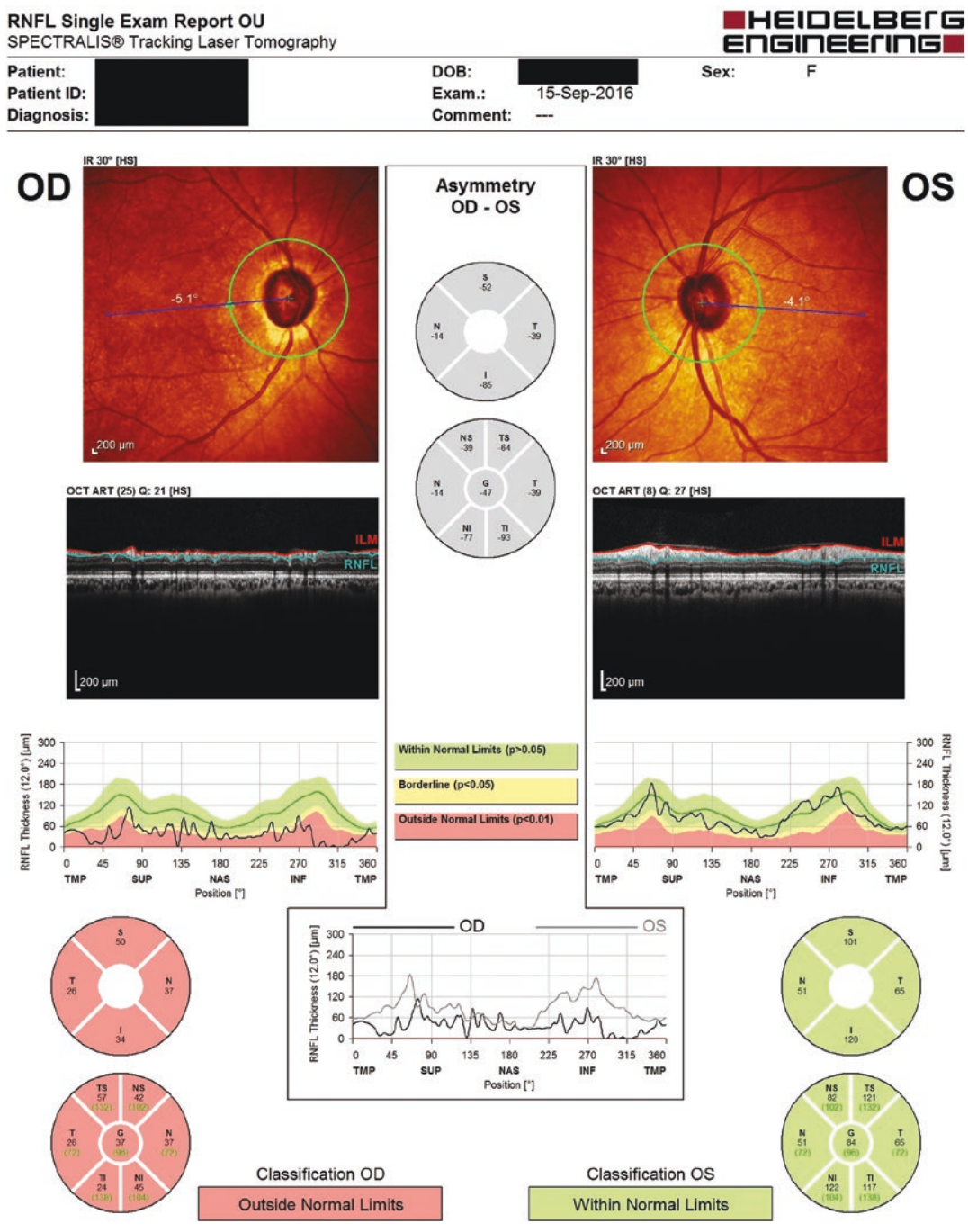

Fig. 10.10 RNFL OCT study showing OD global NRR thinning and OS normal study

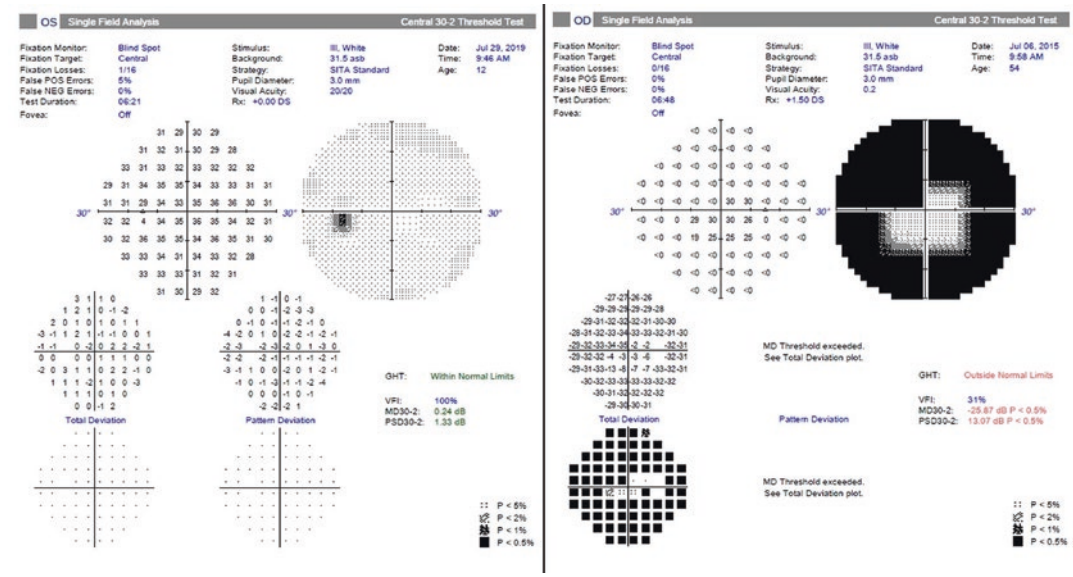

Fig. 10.11 HVF 30-2 SS: (OS) LE within normal limits, (OD) RE shows a biarcuate scotoma with central tunnel vision

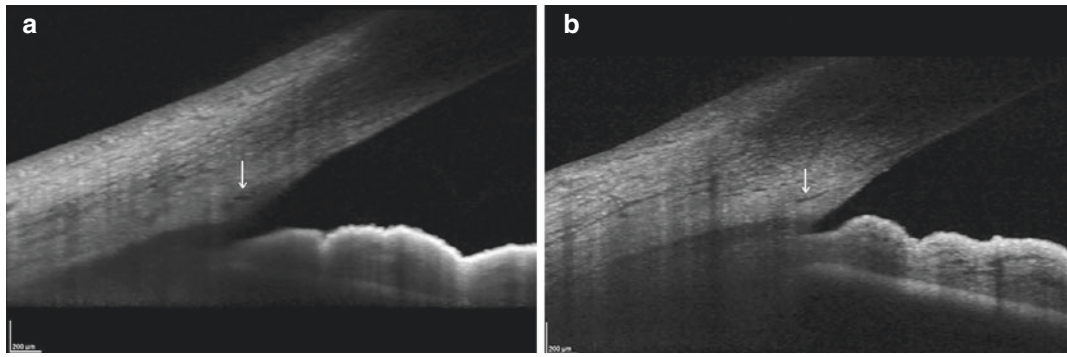

Fig. 10.12 ASOCT: (**a**) RE shows open angle with small Schlemm's canal (white arrow). (**b**) LE shows open angle with visible Schlemm's canal (white arrow)

Case 10.4

An 18-year-old female was referred to glaucoma facility from the refractive clinic for optic disc cupping. There were no ocular or systemic complaints.

Examination: BCVA with glasses 6/6 BE, Goldmann IOP – RE 18 mmHg, LE 16 mmHg. Anterior segment and gonioscopy was unremarkable BE. Fundus examination showed BE CDR of 0.8 with inferior NRR thinning (LE > RE); maculae were normal. RNFL defects were appreciable in both eyes (Fig. 10.13).

Investigations: (a) Diurnal variation of IOP – RE 12–18 mmHg, LE 12–20 mmHg. (b) USG pachymetry, RE 480 µm, LE 482 µm (c) RNFL OCT: significant inferotemporal thinning in both eyes. RE also showed supero-temporal thinning (Fig. 10.14). (d) HRT – BE showed corresponding thinning, and additional borderline inferonasal thinning. BE Moorfield regression analysis (MRA) was classified as "outside normal limits" (Fig. 10.15). (e) HVF 30-2 SS: RE superior arcuate scotoma + inferior large nasal step, LE central scotoma (Fig. 10.16). (f) MRI brain and orbits

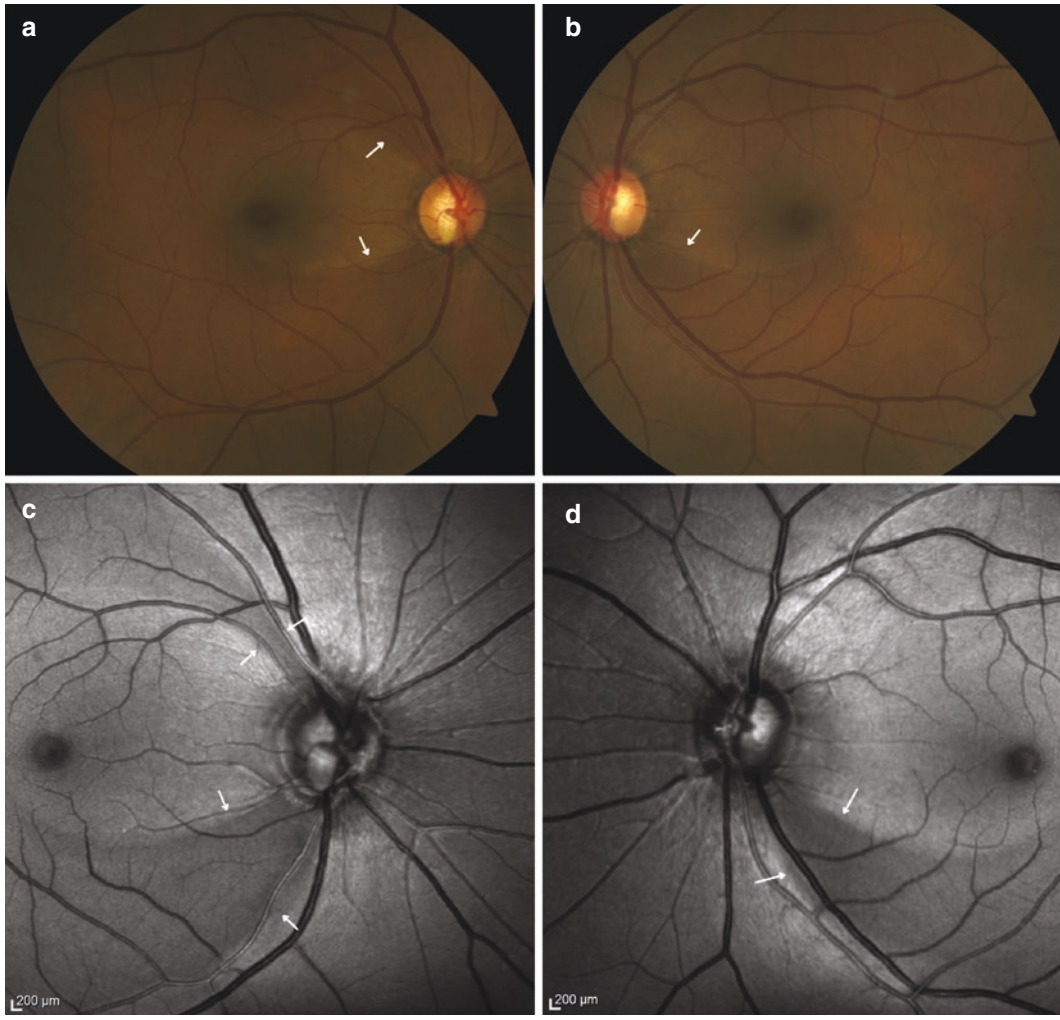

Fig. 10.13 (**a**, **b**) Color fundus photographs of RE and LE, respectively, showing a CDR of 0.8:1 with inferior NRR notching and RNFL defects (white arrows). (**c**, **d**) Corresponding green reflectance Spectralis images showing prominent RNFL defects (white arrows)

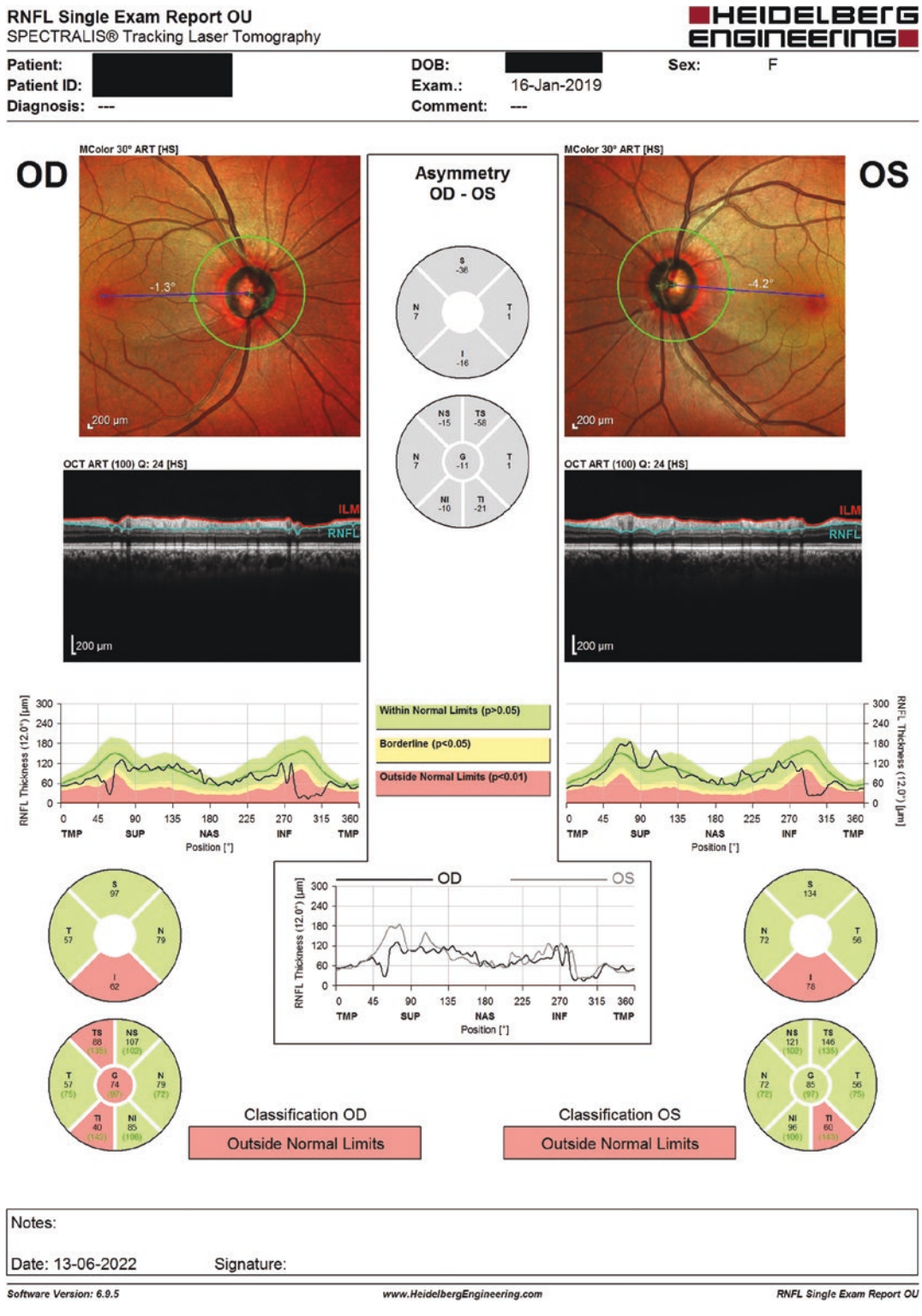

Fig. 10.14 RNFL OCT: OD and OS both show significant inferotemporal RNFL thinning. OD also shows superotemporal thinning. Both eyes have been classified as "outside normal limits"

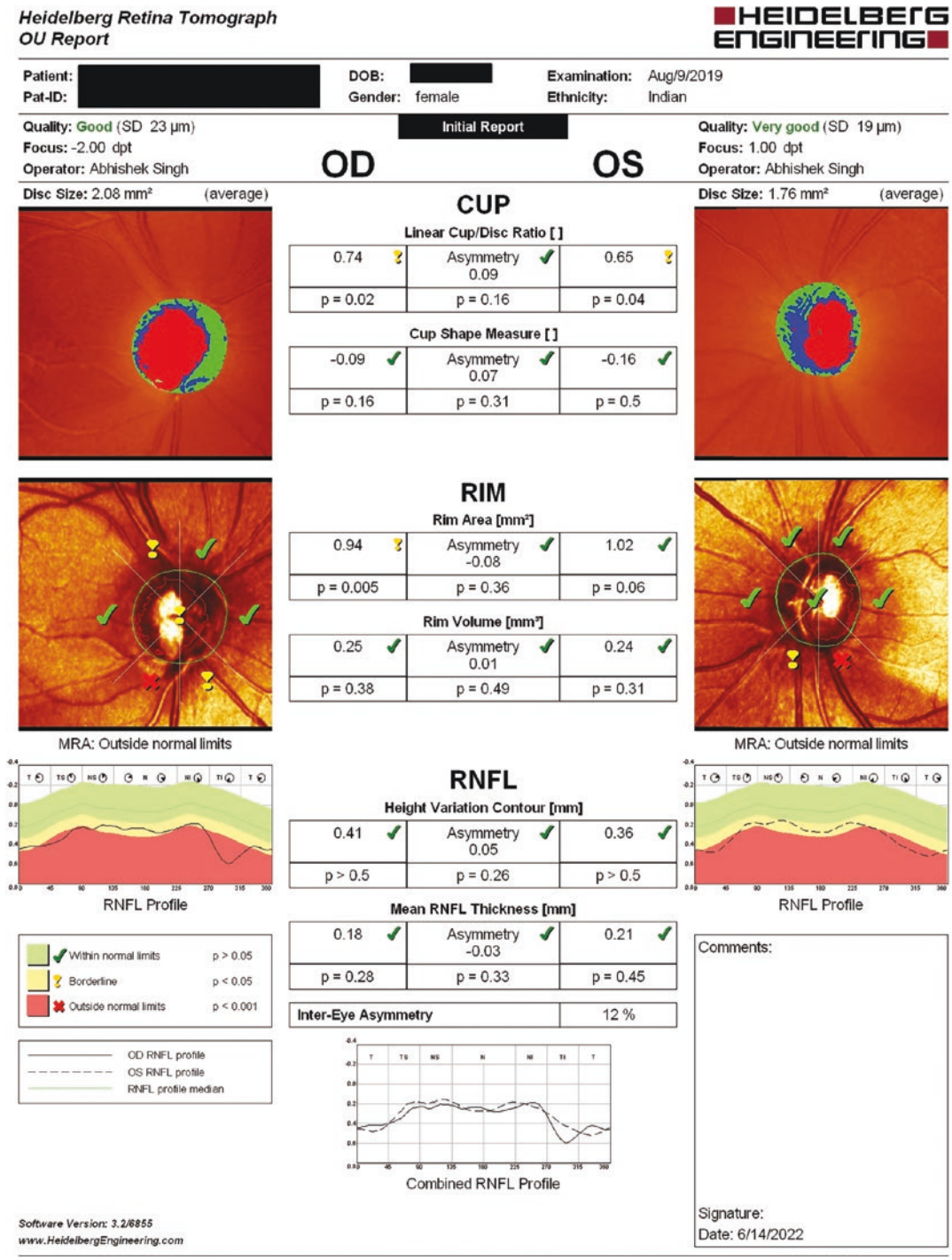

Fig. 10.15 Heidelberg Retinal Tomography report shows BE inferotemporal significant thinning and inferonasal borderline thinning. RE also shows additional superotemporal borderline thinning. Moorfield regression analysis (MRA) classifies both eyes as "outside normal limits"

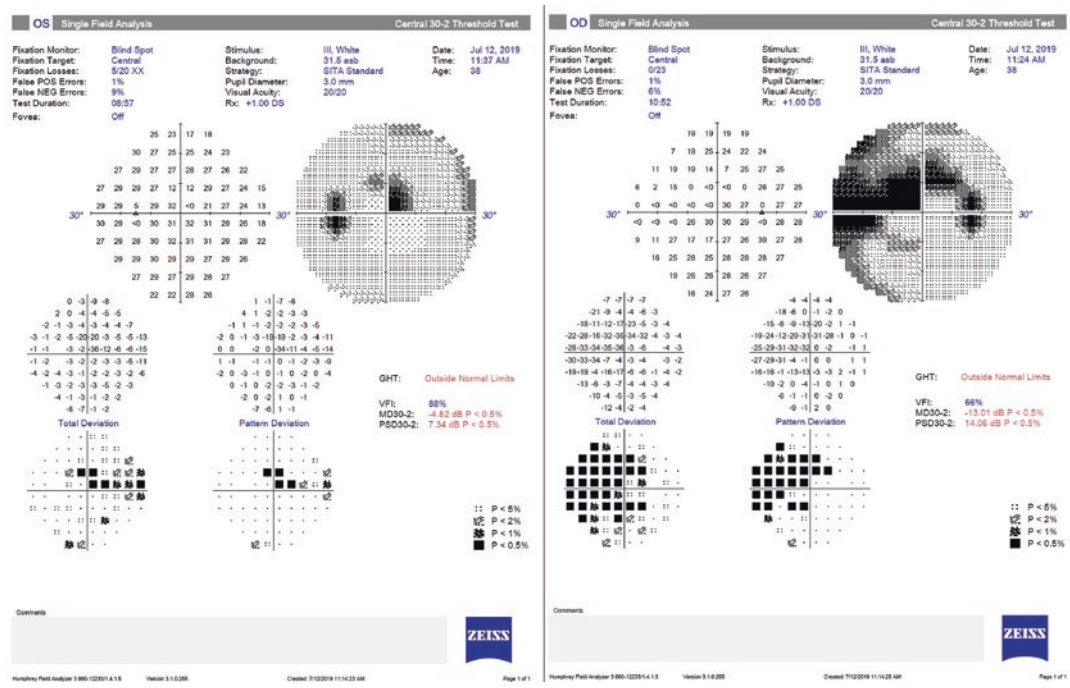

Fig. 10.16 Humphrey visual field 30-2 Sita Standard; (OS) LE shows central scotoma (OD) RE shows superior arcuate scotoma + large inferior nasal step

with contrast: bilateral visual pathways and brain study were normal.

Diagnosis: BE juvenile normal tension glaucoma (JNTG)

Differential diagnosis: Table 10.2

Treatment: The patient was started on BE latanoprost HS.

Learning Points

- JNTG is a less studied category of juvenile primary open-angle glaucomas.
- It is important to exclude other causes of VF defects by appropriate neuroimaging before labeling a patient as JNTG.
- Rho kinase inhibitors (ROCK inhibitors), the newer anti-glaucoma agents, have been shown to improve ocular blood flow and protect against retinal ganglion cells apoptosis. The neuroprotective features of this drug could possibly target the specific pathomechanisms of JNTG.

10.2 Management Strategies (Fig. 10.17)

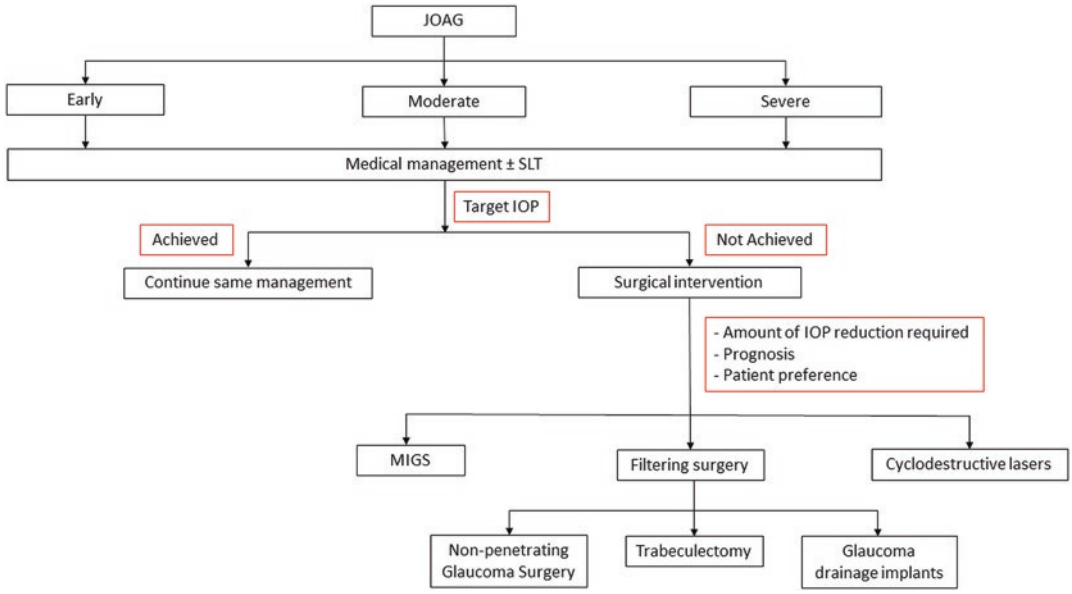

Fig. 10.17 Management strategies for JOAG. *IOP* intraocular pressure, *JOAG* juvenile open-angle glaucoma, *MIGS* microinvasive glaucoma surgery, *SLT* selective laser trabeculoplasty. Severity staging as per Hodapp-Anderson-Parisch criteria

10.3 Conclusions

JOAG is a less well-studied subset of primary glaucomas. JOHT and JNTG are even further sparsely known. They present with peculiar gonioscopic features, appearing as a continuum of primary congenital glaucomas, but their structural and functional defects are closer to adult-onset primary open-angle glaucomas. Nevertheless, they are treated with a stricter target than the latter in view of their young age. Genetic studies and counselling, life-long monitoring, and social support systems play important roles.

Suggested Reading

Birla S, Gupta D, Somarajan BI, et al. Classifying juvenile onset primary open angle glaucoma using cluster analysis. Br J Ophthalmol. 2020;104(6):827–35. https://doi.org/10.1136/bjophthalmol-2019-314,660.

Gupta V, Gupta S, Dhawan M, Sharma A, Kapoor KS, Sihota R. Extent of asymmetry and unilaterality among juvenile onset primary open angle glaucoma patients. Clin Exp Ophthalmol. 2011;39(7):633–8. https://doi.org/10.1111/j.1442-9071.2011.02522.x.

Gupta V, Somarajan BI, Gupta S, et al. The inheritance of juvenile onset primary open angle glaucoma. Clin Genet. 2017;92(2):134–42. https://doi.org/10.1111/cge.12906.

Gupta S, Singh A, Mahalingam K, et al. Myopia and glaucoma progression among patients with juvenile onset open angle glaucoma: a retrospective follow up study. Ophthalmic Physiol Opt. 2021;41(3):475–85. https://doi.org/10.1111/opo.12805.

Selvan H, Gupta S, Wiggs JL, Gupta V. Juvenile-onset open-angle glaucoma - a clinical and genetic update. Surv Ophthalmol. 2022;67(4):1099–117. https://doi.org/10.1016/j.survophthal.2021.09.001.

Turalba AV, Chen TC. Clinical and genetic characteristics of primary juvenile-onset open-angle glaucoma (JOAG). Semin Ophthalmol. 2008;23(1):19–25. https://doi.org/10.1080/08820530701745199.

Part IV

Secondary Childhood Glaucoma with Non Acquired Conditions

Axenfeld-Rieger Syndrome

11

Arnav Panigrahi, Shikha Gupta, and Viney Gupta

Axenfeld-Rieger syndrome (ARS) is a clinically and genetically heterogeneous group of developmental disorders affecting primarily the anterior segment of the eye, often leading to secondary glaucoma. It encompasses the following phenotypes:

(a) Axenfeld Anomaly (AXA): It refers to the isolated presence of a posterior embryotoxon (PE), the white line originally described by Axenfeld, with peripheral iris strands inserting onto it (peripheral anterior segment changes).
(b) Axenfeld Syndrome (AXS): It refers to the presence of AXA, along with systemic abnormalities. The systemic abnormalities include:
    - Craniofacial dysmorphism presenting as hypertelorism, maxillary hypoplasia, and a broad flat nasal bridge
    - Dental abnormalities like small (microdontia), reduced (hypodontia/oligodontia) or absent (anodontia) teeth
    - Cardiovascular abnormalities
    - Redundant periumbilical skin, resembling umbilical hernia
(c) Rieger Anomaly (RA): Originally described by Rieger, it refers to the presence of PE along with iris changes like corectopia, polycoria, iris hypoplasia, and atrophy (mid-peripheral anterior segment changes).
(d) Rieger Syndrome (RS): The presence of RA along with the systemic features typical of ARS.

The presence of PE may not be mandatory for the diagnosis of ARS as is seen in few cases (Shields 1983; Panigrahi et al. 2023). The presence of iris features typical to ARS, along with systemic anomalies, is sufficient to diagnose a case of ARS despite the absence of PE.

ARS is believed to be inherited in an autosomal dominant manner with complete penetrance and variable expressivity, although sporadic cases are very frequently encountered in authors' experience. Three genes have been implicated in its causation: *PITX2* (4q25), *FOXC1* (6p25), and an unidentified gene in the locus 13q14. Despite our current understanding, the underlying genetic defect remains unknown in almost 60% of the cases.

Glaucoma is seen in nearly half the cases of ARS, goniodysgenesis being the primary cause of glaucoma.

The main pathology in ARS seems to be a developmental arrest, late in gestation, leading to incomplete involution and subsequent contraction of the primordial endothelial cells. Retention and contraction of these cells brings about patho-

A. Panigrahi (✉) · S. Gupta · V. Gupta
Dr. Rajendra Prasad Centre for Ophthalmic Sciences, All India Institute of Medical Sciences, New Delhi, India

S. Gupta et al. (eds.), *Childhood Glaucoma*, https://doi.org/10.1007/978-981-19-7466-3_11

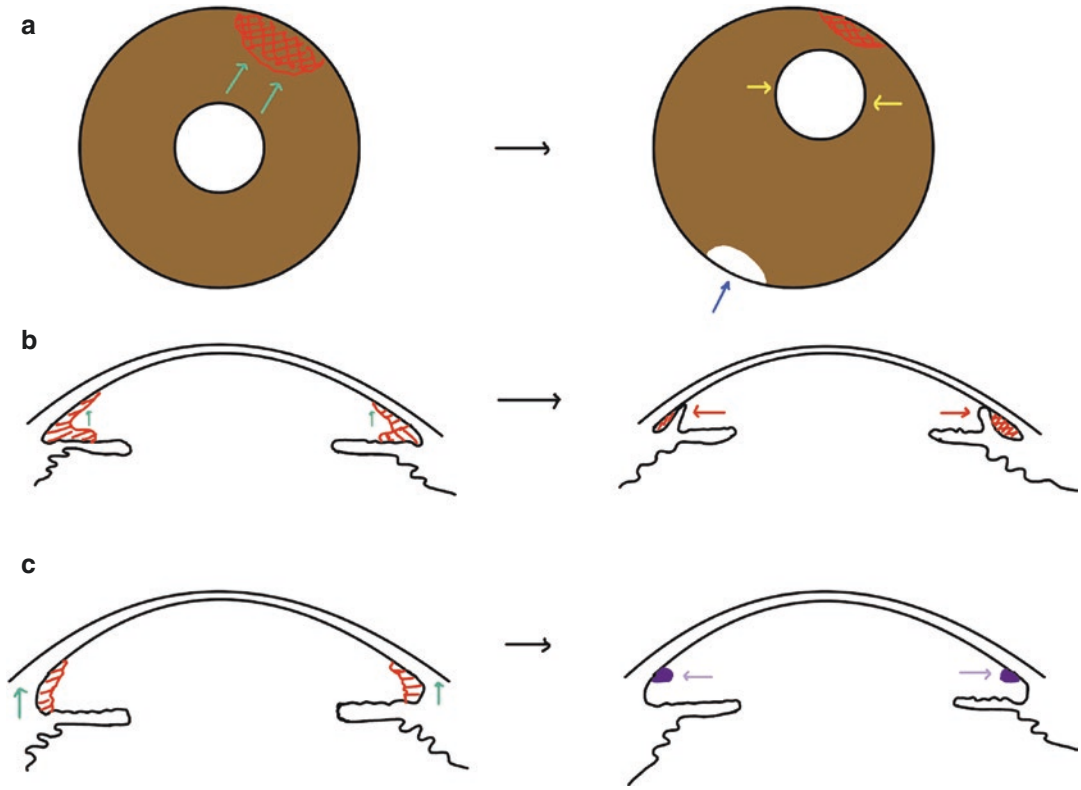

Fig. 11.1 Schematic representation of pathogenesis of ARS. Retention of primordial embryonic endothelium (red area) and its subsequent contraction (green arrows) is responsible for the clinical features of the disease. When present on iris surface (**a**), it leads to displacement of pupil (corectopia) towards the site of contraction (yellow arrows), and formation of iris holes with hypoplasia opposite to the direction of pull (blue arrow). Contraction of tissue at iridocorneal angle (**b**), when contiguous with the aberrant tissue on the iris surface, pulls the iris toward the cornea leading to formation of iridocorneal adhesions (red arrow) which typically adhere at a level higher than the Schwalbe's Line or the posterior embryotoxon. Isolated contraction of the tissue at iridocorneal angle (**c**), and its subsequent condensation, leads to anterior displacement of Schwalbe's line with formation of a thickened ridge (purple arrows), classically termed as posterior embryotoxon

logical changes responsible for the classical phenotypic features of ARS (Fig. 11.1).

The time at which the aforementioned developmental arrest occurs may vary from person to person, and the site of these primordial cells may even vary within two eyes of the same person, leading to the phenotypic heterogeneity seen in ARS.

Differentials of ARS include primary congenital glaucoma (PCG), iridocorneoendothelial (ICE) syndrome, Peter's anomaly, iris hypoplasia (IH), and congenital hereditary endothelial dystrophy (CHED), depending upon the age of onset and presentation. Differentiating ARS from these diseases is necessary for appropriate management and genetic counseling (Table 11.1).

Table 11.1 Features differentiating primary congenital glaucoma (PCG), iridocorneoendothelial (ICE) syndrome, Peter's anomaly, iris hypoplasia (IH), and congenital hereditary endothelial dystrophy (CHED) from Axenfeld-Rieger syndrome (ARS)

	PCG	Peter's	ARS	ICE	IH	CHED
Age of presentation	<2 years	At birth	Usually in childhood, may present anytime from birth to adulthood	Young adulthood	Usually early adulthood	<1 year
Laterality	Usually bilateral	Bilateral, may be asymmetric	Bilateral, usually highly asymmetric	Unilateral	Bilateral	Bilateral, symmetric
Sex predilection	None	None	None	Females	None	None
Corneal edema	Diffuse	Central	May be seen peripheral to PE; diffuse in infantile onset glaucoma	Initially peripheral, may proceed to diffuse involvement	None	Diffuse
Corneal features	Haab's striae may be seen, can lead to permanent corneal scarring	Central defect in Descemet's membrane with absent endothelium (Type 1)	Posterior embryotoxon (PE), with iris strands adherent to it, band-shaped keratopathy, microcornea and thick cornea can be appreciated	Abnormal proliferation of endothelial layer with silver/grey appearance	Normal	Marked diffuse limbus-limbus corneal clouding without limbal stretch
Iris features	Normal	Iridocorneal adhesion may be seen at the margins of the endothelial deficient zone	Corectopia, iris atrophy, iris hole formation, iris whorling, ectropion uveae and partial aniridia may coexist	Corectopia, iris atrophy, iris hole formation, ectropion uveae (essential iris atrophy), pedunculated tan iris nodules (Cogan Reece syndrome)	Hypoplastic anterior iris stroma with posterior pigment epithelium seen through it, prominent iris vessels	Normal
Gonioscopic features	Normal, high iris insertion or wraparound iris configuration may be seen	Open angles, multiple goniosynechiae may be seen	High iris processes traversing the trabecular meshwork to insert onto the PE	Multiple high peripheral anterior synechiae (PAS), abnormal membrane may be seen	High iris insertion, gonio-synechiae may be seen	Open angles

(continued)

Table 11.1 (continued)

	PCG	Peter's	ARS	ICE	IH	CHED
Mechanism of glaucoma	Dysgenesis of the trabecular meshwork	Dysgenesis of the trabecular meshwork	Dysgenesis of the trabecular meshwork, aqueous outflow obstruction by abnormal membrane or PAS, progressive angle closure	Aqueous outflow obstruction by abnormal membrane or PAS, progressive angle closure	Dysgenesis of the trabecular meshwork	Usually not associated with glaucoma. If associated, angle dysgenesis
Inheritance pattern	Sporadic (90%), autosomal recessive (AR) in familial cases	Sporadic, cases of autosomal dominant and recessive inheritance have been reported	Autosomal dominant with complete penetrance and variable expressivity	Acquired, virus mediated	Autosomal recessive	Autosomal recessive
Associated genes	*GLC3A-D*	*PAX6*, *PITX2*, *FOXC1*, *FOXE3*, *CYP1B1*, *B3GALTL*	*FOXC1*, *PITX2*, 13q14 loci (gene unidentified), *CYP1B1* (atypical ARS)	None	*PITX2*, *FOXC1*	*SLC4A11*

11.1 Case Examples

Case 11.1

History: An 11-year-old male child of BE Axenfeld anomaly (AXA) with RE neonatal onset of congenital glaucoma presented for routine examination. He had been operated at the age of 3 years with RE combined trabeculectomy plus trabeculotomy (CTT), augmented with mitomycin C 0.04% under general anaesthesia (GA).

Examination: Best-corrected visual acuity (BCVA) was finger counting close to face (FCCF) with projection of rays (PR) inaccurate in the RE and 6/6 in the LE. Intraocular pressure (IOP) was 28 and 24 mmHg in RE and LE, respectively, with RE having near total vertical cup disc ratio and LE showed a vertical cup disc ratio (CDR) of 0.3:1. Slit lamp evaluation of BE revealed the presence of posterior embryotoxon (PE) with gonioscopy revealing peripheral iris strands inserting onto this line (Fig. 11.2a–d). Systemic examination revealed the presence of hypertelorism, flattened nasal bridge, and maxillary hypoplasia, along with hypodontia with truncated crowns (Fig. 11.3a, b).

Diagnosis: The child was diagnosed with BE Axenfeld syndrome (AXS) with RE advanced glaucomatous optic neuropathy with failed CTT and LE ocular hypertension.

Treatment: The patient was started on e/d dorzolamide-timolol BD and e/d latanoprost HS in BE, with additional e/d pilocarpine TDS in the RE. His IOP were controlled on the aforementioned medications.

Learning Points

- Glaucoma in ARS is usually bilateral but can be asymmetric. These children need to be kept on long-term follow-up, since they have a high probability of developing glaucoma in the fellow eye over follow-up.
- The severity of glaucoma is not related to the disease phenotype, extent of PE, or iridocorneal adhesions, as seen in this patient. The extent of iridocorneal adhesions is smaller in the RE as compared to the LE, despite the glaucomatous damage being limited to the RE only.
- Neonatal or infantile onset glaucoma is usually misdiagnosed as PCG at first presentation due to associated corneal edema, which pre-

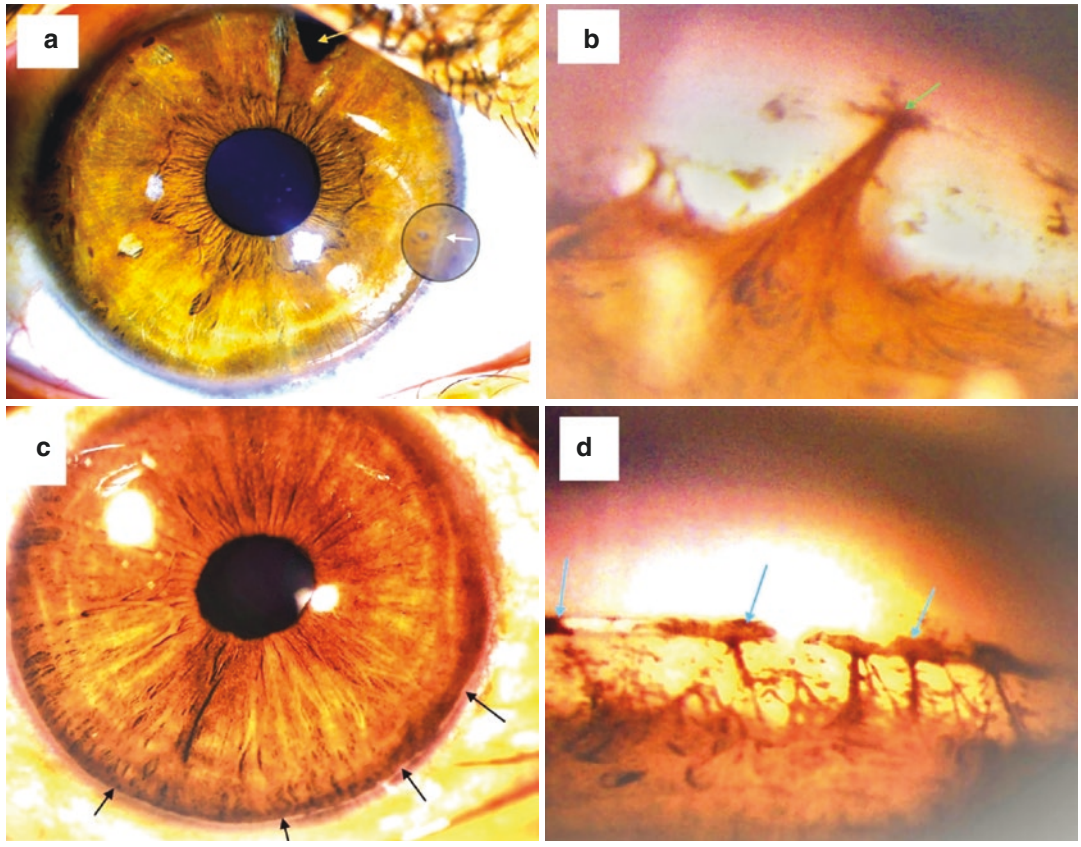

Fig. 11.2 Clinical picture of RE (**a**) reveals the presence of posterior embryotoxon nasally (black arrows; magnified inset) and surgical iridectomy superiorly (blue arrow). Gonio-photograph of the same (**b**) shows iris strands adherent to the PE. Clinical photograph of the LE (**c**) reveals the presence of a PE along the inferior 180° (black arrows). Gonioscopy revealed the corresponding presence of a prominent anteriorly displaced Schwalbe's line with iris tissue adherent to it (**d**, blue arrows)

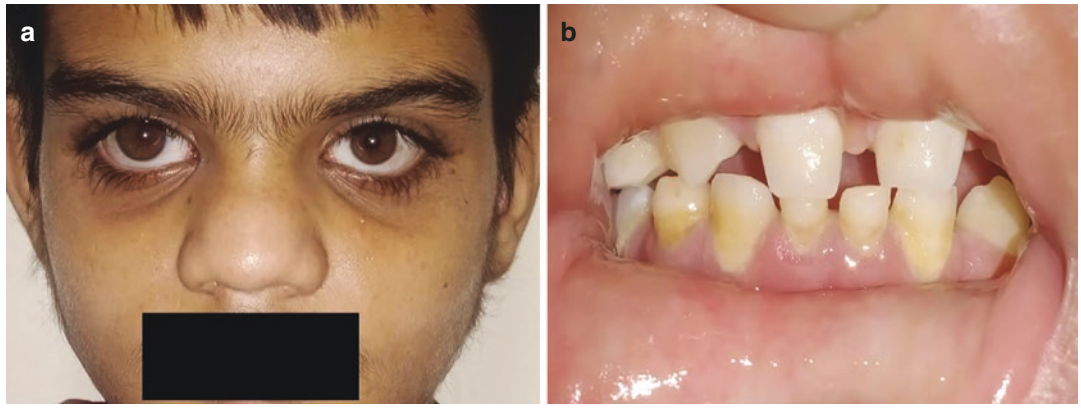

Fig. 11.3 Facial photograph of the patient (**a**) reveals the presence of a broad, depressed nasal bridge, hypertelorism, and mid facial flattening due to maxillary hypoplasia. Dental photograph (**b**) reveals reduced number of teeth (hypodontia) with the presence of broken crowns in some of them. These features are believed to be secondary to ectodermal dysplasia, the core defect responsible for the pathogenesis of ARS

vents adequate examination of corneal and iris features, despite examining under anesthesia. Correct diagnosis is usually made, when the cornea clears (post IOP reduction) sufficiently to allow anterior segment evaluation or after angle imaging on intraoperative OCT/UBM/ASOCT.

- Corneal diameter in children with PCG was found to be significantly higher than those with ARS ($p = 0.01$), in a recent study conducted by the authors (unpublished data). This could be attributed to the difference in ultrastructure of the pre-Descemet layer (PDL) within the two groups.
- CTT is safe and effective as the primary treatment modality in treatment of ARS. According to a study by Mandal et al. on Indian population, 68.2% of the patients treated with CTT had target IOP without any medication at the end of the observation period (median 66 months). The success rate of CTT in PCG at the end of 5 years is noted to be 66.2%, similar to that in ARS patients.

Case 11.2

History: An 8-year-old male was brought to the OPD at the age of 1.5 years with complaints of increased corneal diameters in BE by his parents.

Examination: Examination under anesthesia (EUA) revealed BE enlarged corneas with horizontal diameter of 14 mm and vertical diameter of 14.5 mm. IOP was controlled, being 13 and 15 mmHg, respectively. Anterior segment evaluation revealed the presence of multiple large Haab's striae, with iris changes of corectopia, polycoria, and iris hypoplasia seen in both the eyes. Posterior embryotoxon (PE) was seen in the right eye, although peripheral iridocorneal adhesions and high PAS were seen in both the eyes on gonioscopy (Fig. 11.4a–d). Posterior segment evaluation revealed BE healthy disc with a vertical CDR of 0.6:1 with a healthy neuroretinal rim (NRR) in BE. Systemic examination revealed no abnormalities.

Diagnosis: The patient was diagnosed with Rieger anomaly (RA).

Management: Despite the presence of enlarged corneal diameters and Haab's striae on presentation, IOP and optic disc were within normal limits. The patient was kept on routine follow-up to look for signs of progression. The patient showed no evidence of disease progression despite not being on any medication. He was prescribed glasses with power of 0.25D at 90° in the RE and −2.00D(s)/−1.25D(c) at 90° in the LE. Currently, the patient has a BCVA of 6/9 in the RE and 6/12 in the LE, with IOP being 12 and 14 mmHg on no medications.

Differential diagnosis (at the time of presentation):

- Primary Congenital Glaucoma (PCG): Associated with isolated trabeculodysgenesis in the absence of iris changes.
- Peter's Anomaly: These children present with a central corneal opacity, usually present at birth.
- Congenital Hereditary Endothelial Dystrophy: These children present with neonatal or infantile onset corneal edema, but the IOPs are normal and hence Haab's striae do not form.

Learning Points

- Features of buphthalmos and Haab's striae are not specific to primary congenital glaucoma but can be seen in cases with increased IOP with onset before 1 year of age. The former is due to the outward stretching force of increased IOP on an immature elastic developing globe, whereas the latter is due to the same causing rupture of a relatively inelastic Descemet membrane.
- The presence of buphthalmos and Haab's striae without any neuroretinal rim (NRR) abnormality indicates a congenital pathology with early onset transient increase in IOP, insufficient to cause NRR damage, followed by spontaneous resolution of the same. Spontaneous regression of congenital glaucoma may occur due to opening up of alternate channels for aqueous outflow.
- Reduced BCVA despite the absence of glaucomatous damage might be due to corectopia and/or the slit like pupil configuration, inducing spherical and higher order aberrations. Adequate refractive correction is required to prevent the development of amblyopia.

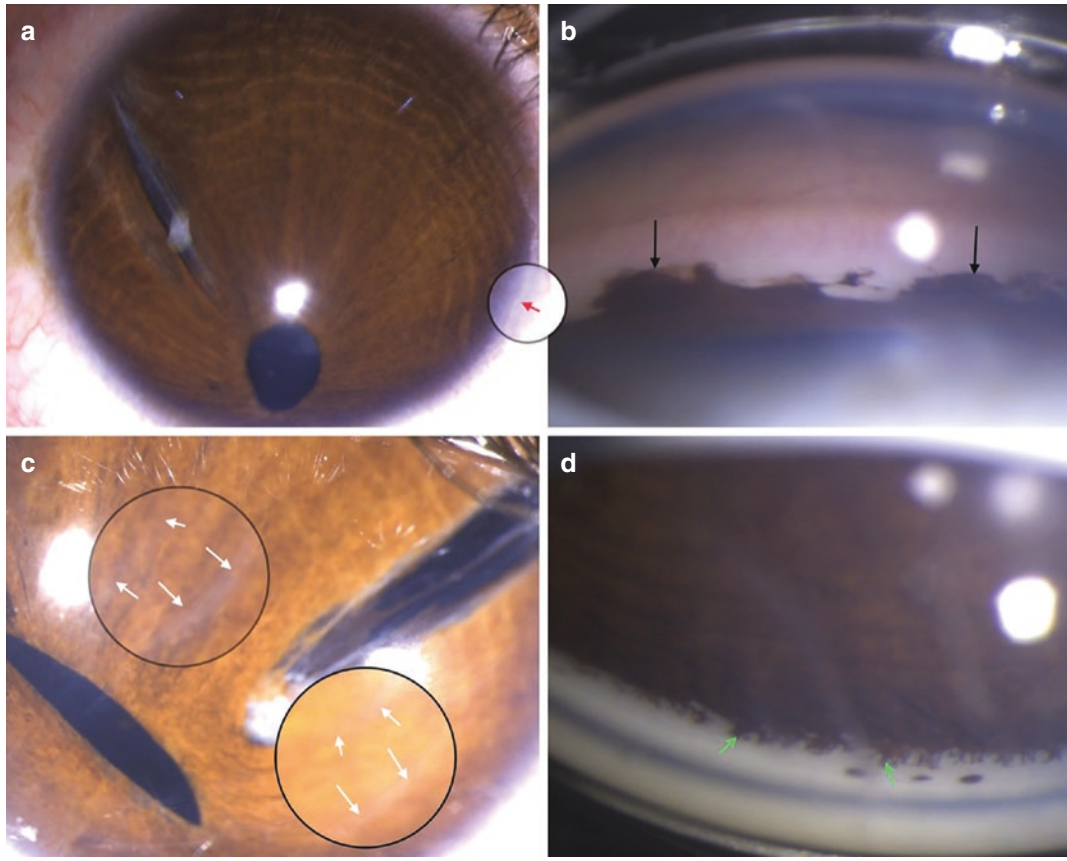

Fig. 11.4 Clinical photograph of the RE (**a**) reveals the presence of PE in the nasal quadrant (magnified inset, red arrow). Gonioscopy (**b**) shows broad-based high iridocorneal adhesions (black arrows). Multiple Haab's striae can be seen in the LE (**c**, magnified inset), indicating early onset increase in IOP and supporting the presence of increased corneal diameters. Gonioscopy of the LE (**d**) reveals the presence of fine iris processes inserting onto an anteriorly displaced Schwalbe's line (green arrows)

Optical iridectomy can also be done to improve visual quality.

- Primary iris changes with PE are diagnostic of RA.

Case 11.3

History: An 8-year-old female was brought to the OPD by her parents with the complaints of diminution of vision in BE.

Examination: Her BCVA was 6/24 in the RE and 6/12 in the LE, with the corresponding IOPs being 28 and 18 mmHg, respectively. Anterior segment evaluation revealed small corneal diameters (9.5 × 10 mm), the presence of multiple peripheral iridocorneal adhesions with associated corneal opacity (Fig. 11.5a, white arrows) in the RE with superotemporally "pulled" iris resulting in corectopia. LE shows the presence of a persistent pupillary membrane (PPM) (Fig. 11.5b, green arrow), with no obvious posterior embryotoxon or iridocorneal adhesions. Gonioscopy revealed the presence of PAS and high peripheral iridocorneal adhesions at multiple noncontiguous points in BE (Fig. 11.5c, d). Fundus evaluation revealed a vertical CDR of 0.6:1 in the RE and 0.4:1 in the LE. Systemic examination revealed the presence of orofacial features like depressed nasal bridge, hypertelorism, and maxillary hypoplasia.

Diagnosis: The patient was diagnosed with Rieger Syndrome (RS) with RE secondary glaucoma.

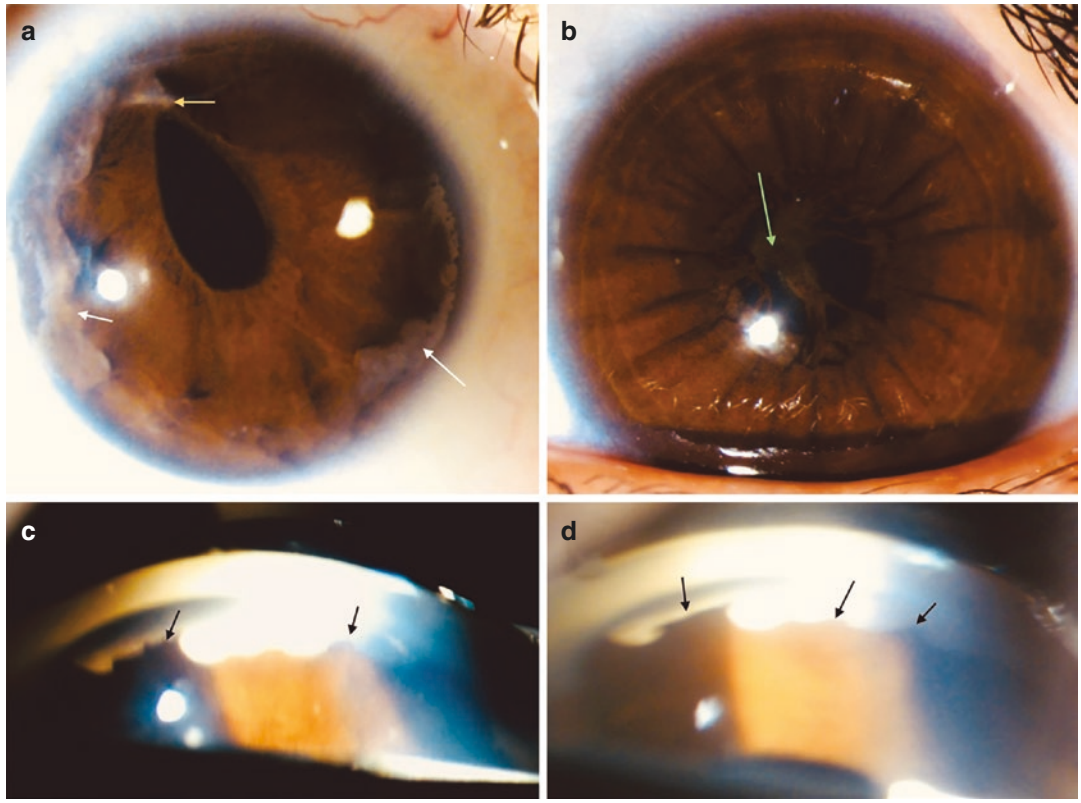

Fig. 11.5 Clinical photograph of the RE (**a**) shows multiple obvious iridocorneal adhesions (white arrows). One of the adhesions has pulled the pupillary margin superotemporally, resulting in corectopia and a keyhole-shaped pupil (yellow arrow). LE (**b**) shows no significant iridocorneal abnormality, except for the presence of a persistent pupillary membrane (PPM) (green arrow). Gonioscopy of RE (**c**) and LE (**d**) revealed the presence of high iridocorneal adhesions

Management: She was started on e/d dorzolamide-timolol BD and e/d latanoprost HS in the RE. Her IOPs were controlled on the aforementioned medications.

Learning Points

- The phenotypic heterogeneity seen in ARS is quite remarkable, as is seen in this patient with the RE showing significant iridocorneal changes, despite the similar gonioscopic findings in BE.
- PE may be a subtle finding or may be masked by high rise PAS as in this case, making its identification difficult on slit lamp examination. Gonioscopic identification high iris strands are sufficient to diagnose ARS in such cases, making it mandatory to perform gonioscopy in all patients with elevated IOP.
- Long-term follow-up is necessary to monitor the disease progression the RE and look for early signs of glaucoma in the LE.
- The presence of PPM is rare in cases of ARS.

Case 11.4

History: A 12-year-old female presented to the OPD with complaints of diminution of vision since childhood. There was no history of previous surgery. She was initially diagnosed as ICE syndrome by a local practitioner.

Examination: She had a BCVA of 6/18p (+4DS/−1DC) and 6/24 (+6DS/−1.5DC) in the RE and LE, respectively, at the time of examination, with her 30 mmHg in both eyes (BE).

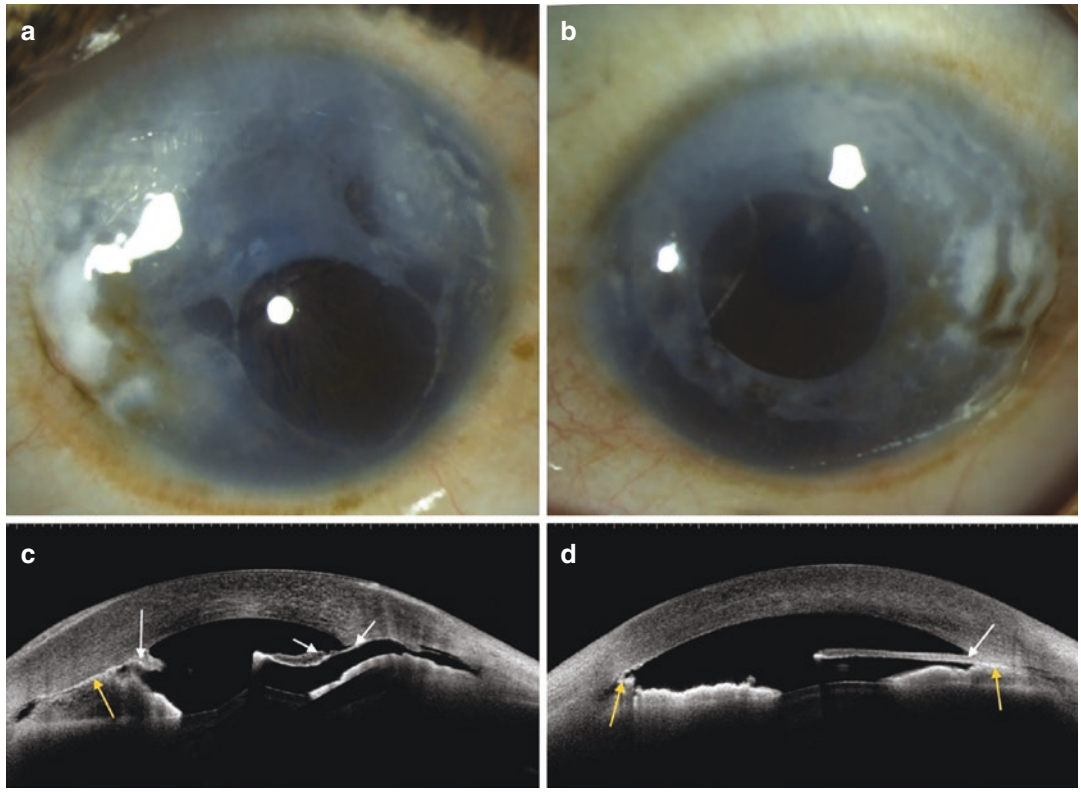

Fig. 11.6 Clinical photograph of the patient reveals corneal opacity with a gray translucent membrane on the endothelial surface, with eccentric sparing in the RE (**a**) and central sparing in the LE (**b**). ASOCT of the RE (**c**) and LE (**d**) reveals the presence of hypertrophic PE (white arrows) simulating the presence of double cornea, with high iridocorneal adhesions being evident in both of them (Reproduced with permission from Mahalingam K, Singh A, Gupta V, Gupta S. Hyperproliferative embryotoxon simulating double cornea. BMJ Case Rep. 2021;14(12):e246960. doi:10.1136/bcr-2021-246960)

Anterior segment evaluation revealed the presence of microcornea with near total corneal opacities in both the eyes, with a small circular zone of clear cornea. No significant iris changes were seen through the clear zone (Fig. 11.6a, b). Fundus evaluation revealed a CDR of 0.4:1 in the LE, although corneal opacity precluded the examination of the RE. USG B scan confirmed the absence of any significant cupping in the RE. Corneal diameters were 9.5 * 10 cm in the RE and 10 * 10.5 cm in the LE, with central corneal thickness (CCT) being 814 and 756 μm. ASOCT revealed the presence of a hyperproliferative PE (retrocorneal membrane) with increased corneal thickness. It also revealed the presence of high iridocorneal adhesions (Fig. 11.6c, d). She had facial features of hypertelorism, depressed nasal bridge, and maxillary hypoplasia (Fig. 11.7a), along with the presence of umbilical hernia (Fig. 11.7b). Similar facial features were seen in her 6-year-old brother, who was later diagnosed as ARS.

Diagnosis: The patient was diagnosed with Axenfeld-Rieger syndrome with alternative divergent squint with anisometropic amblyopia.

Differential diagnosis:

- **Operated penetrating keratoplasty with secondary glaucoma** (on gross examination): The absence of previous history of surgery and suture marks ruled out this diagnosis.
- **Iridocorneoendothelial (ICE) Syndrome**: Initially diagnosed as ICE syndrome, this remains the main differential to be considered in this patient. The features of near total corneal opacity with a glistening thickened mem-

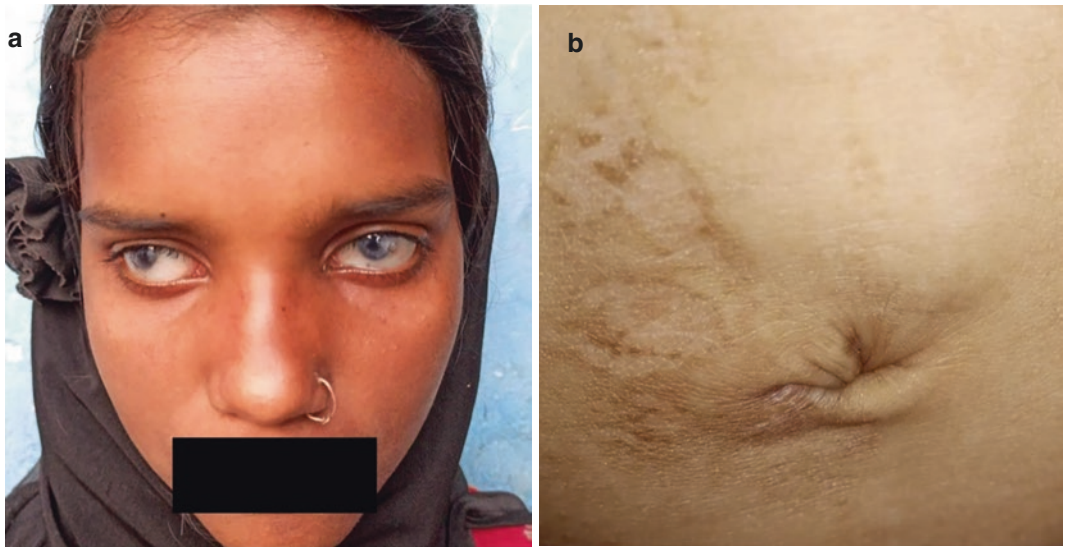

Fig. 11.7 Facial photograph of the patient (**a**) reveals the presence of depressed nasal bridge, hypertelorism, and maxillary hypoplasia. She also had umbilical hernia (**b**)

brane under the endothelium in a young girl are highly suggestive of Chandler's syndrome, a part of the ICE spectrum. Further considerations, like the age of onset in childhood, bilateral presentation, and the presence of similar features in her brother, make the diagnosis of ICE highly unlikely, tilting the diagnosis in the favor of ARS.

Management: The patient was started on e/d netarsudil HS (due to its endothelio-protective action) and brimonidine-timolol BD in BE. Currently, her IOP is 16 mmHg in BE.

Learning Points

- Although ARS is classically inherited in an autosomal dominant pattern, sporadic cases are frequently seen, as are cases in which multiple siblings are affected without the presence of the disease in the immediate preceding generation (this case). This is highly unlikely in case of autosomal dominant mode of inheritance, where the disease is present in all the generations and skipping of generation is not usually seen. The presence of a germline mutation may be responsible for such presentation, but this requires further credence on genetic testing.
- The presence of microcornea signifies an altered anatomy, with structural alterations being highly likely in adjacent structures. This makes such patients poor candidates for CTT, with DLCP being the primary surgical modality for IOP control in such cases.
- The advent of ASOCT and UBM has revolutionized the diagnosis of ARS, with these investigative modalities acting as adjunct to gonioscopy, or even as the primary modality when gonioscopy is not possible. Subtle angle anomalies can be picked up on imaging.
- There may be variable degrees of posterior embryotoxon proliferation leading to such kind of presentation.

11.2 Management Protocol

The absence of Schlemm's canal is probably responsible for the poor response to medical therapy seen in patients of ARS, as there is no channel to drain the aqueous out. It follows that angle surgeries like goniotomy and trabeculotomy are relatively ineffective in ARS, as they act by creating a patent pathway between the angle and Schlemm's canal. Filtration surgeries are the

mainstay of therapy in patients of ARS in glaucoma, as they are not dependent on the presence of a patent Schlemm's canal for the drainage of aqueous. This is the reason why most of the cases presented in this chapter were eventually taken up for trabeculectomy. Glaucoma drainage devices can be considered in cases with multiple failed trabeculectomies. Detailed management plan for patients with ARS and glaucoma is given below in Fig. 11.8.

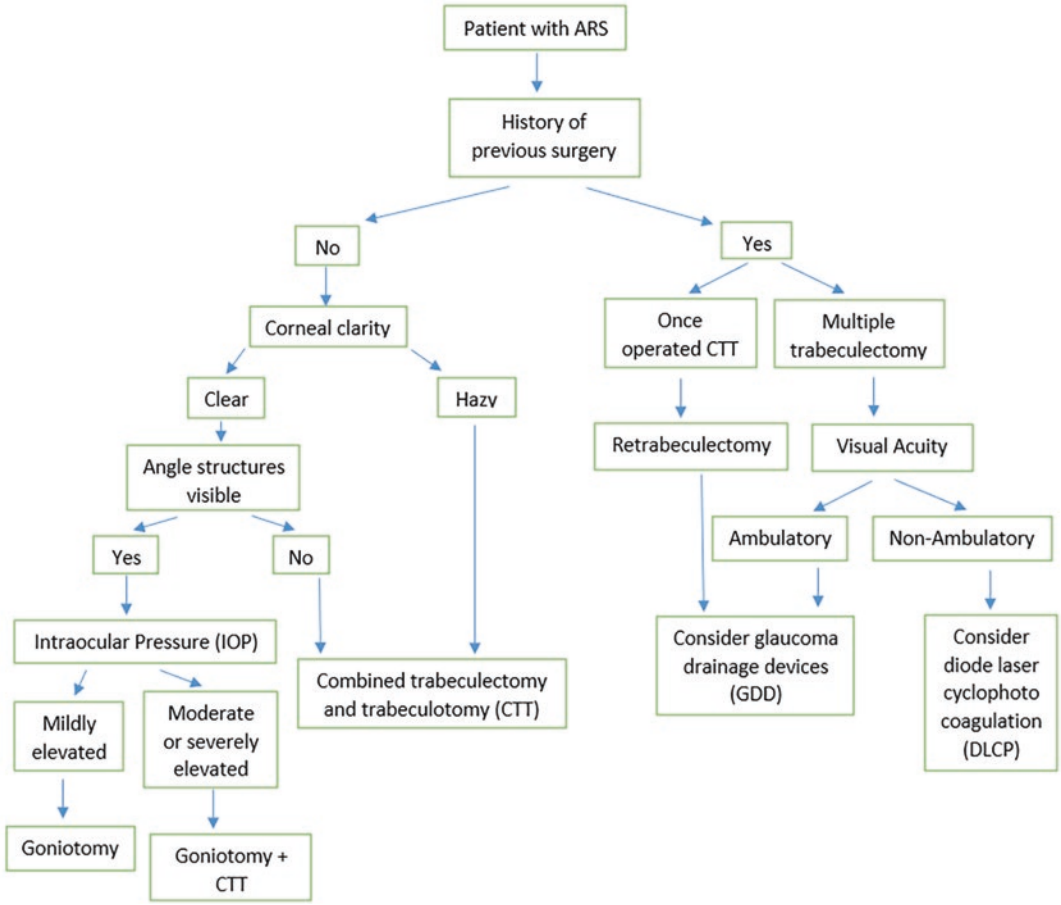

Fig. 11.8 Stepwise approach for management of Axenfeld-Rieger syndrome (ARS) with glaucoma

11.3 Conclusions

Axenfeld Rieger syndrome is a genotypical and phenotypically heterogeneous disorder, with a wide range of ocular and systemic features. Those suffering from this entity are at potential risk of going blind due to having a refractory form of glaucoma, commonly associated with this disease. Management of glaucoma associated with this disease is complicated, owing to distal Sclemm's canal dysgenesis rendering it unamenable to angle surgeries, leaving filtration surgeries and drainage implants as the only reasonable options. Awareness regarding this rare condition is equally necessary amongst general ophthalmologists and glaucoma specialists, thereby aiding in early referrals and optimal management, which can often be vision-saving.

Suggested Reading

Chang TC, Summers CG, Schimmenti LA, Grajewski AL. Axenfeld-Rieger syndrome: new perspectives. Br J Ophthalmol. 2012;96(3):318–22. https://doi.org/10.1136/bjophthalmol-2011-300801.

Hjalt TA, Semina EV. Current molecular understanding of Axenfeld-Rieger syndrome. Expert Rev Mol Med. 2005;7(25):1–17. https://doi.org/10.1017/S1462399405010082.

Mahalingam K, Singh A, Gupta V, Gupta S. Hyperproliferative embryotoxon simulating double cornea. BMJ Case Rep. 2021;14(12):e246960. https://doi.org/10.1136/bcr-2021-246960.

Mandal AK, Pehere N. Early-onset glaucoma in Axenfeld–Rieger anomaly: long-term surgical results and visual outcome. Eye. 2016;30(7):936–42. https://doi.org/10.1038/eye.2016.66.

Mandal AK, Gothwal VK, Nutheti R. Surgical outcome of primary developmental glaucoma: a single surgeon's long-term experience from a tertiary eye care centre in India. Eye. 2007;21(6):764–74. https://doi.org/10.1038/sj.eye.6702324.

Panigrahi A, Gupta S, Gupta V. Peripheral Anterior Synechiae as a Manifestation of Axenfeld-Rieger Anomaly. Ophthalmology. 2023;130(9):972. https://doi.org/10.1016/j.ophtha.2022.09.008.

Seifi M, Walter MA. Axenfeld-Rieger syndrome. Clin Genet. 2018;93(6):1123–30. https://doi.org/10.1111/cge.13148.

Shields MB. Axenfeld-Rieger syndrome: a theory of mechanism and distinctions from the iridocorneal endothelial syndrome. Trans Am Ophthalmol Soc. 1983;81:736–84.

Sim KT, Karri B, Kaye SB. Posterior embryotoxon may not be a forme fruste of Axenfeld-Rieger's syndrome. J Am Assoc Pediatr Ophthalmol Strabismus. 2004;8(5):504–6. https://doi.org/10.1016/j.jaapos.2004.06.012.

Zepeda EM, Branham K, Moroi SE, Bohnsack BL. Surgical outcomes of glaucoma associated with Axenfeld-Rieger syndrome. BMC Ophthalmol. 2020;20(1):172. https://doi.org/10.1186/s12886-020-01417-w.

Peters Anomaly with Glaucoma

12

Monika Arora, Ananya Kaginalkar, and Radhika Tandon

12.1 Introduction

Albert Peter coined the term "Peters anomaly" in 1906 to describe a rare congenital malformation of the anterior segment of the eye. It is characterized by a central corneal opacity and defects in the posterior stroma, Descemet's membrane and endothelium in the opacified area. Iris strands typically emerge from the collarette and extend to the periphery of the corneal leukoma. Although the peripheral cornea is usually clear, varying degrees of clouding may accompany the central opacification, leading to severe stimulus deprivation amblyopia. Peters anomaly is associated with a wide range of congenital ocular and systemic abnormalities and is bilateral in about 80% of patients. The incidence of Peters anomaly is 1.2 per 100,000 births. The main objective of this chapter is to explain the pathogenesis of Peters anomaly, its various types, and complications like glaucoma associated with the anomaly, along with the medical and surgical management options.

12.2 Genetics

The majority of cases are sporadic; however, it can be inherited as an autosomal dominant (AD) or recessive (AR) trait. Mutations in the *PAX6* gene, *PITX2* gene, *FOXC1* gene, and *CYP1B1* gene are responsible for the Peters anomaly. These genes play an essential role during embryogenesis.

12.3 Pathophysiology of Peters Anomaly and Associated Glaucoma

The anterior segment of the eye comprises all the structures lying in front of the anterior vitreous face which includes the ciliary body, lens, iris, and cornea. Migration, differentiation, and cells derived from the neural crest are extremely important for ocular development in general and the anterior segment in particular (Fig. 12.1). Aberrant migration or defective differentiation of neural crest cells leads to anterior segment dysgenesis (ASD). In Peters anomaly, corneal opacity occurs due to inadequate separation of the cornea from the iris and/or lens, resulting in a central or peripheral corneal opacity.

M. Arora (✉) · A. Kaginalkar · R. Tandon
Dr. Rajendra Prasad Centre for Ophthalmic Sciences, All India Institute of Medical Sciences, New Delhi, India

S. Gupta et al. (eds.), *Childhood Glaucoma*, https://doi.org/10.1007/978-981-19-7466-3_12

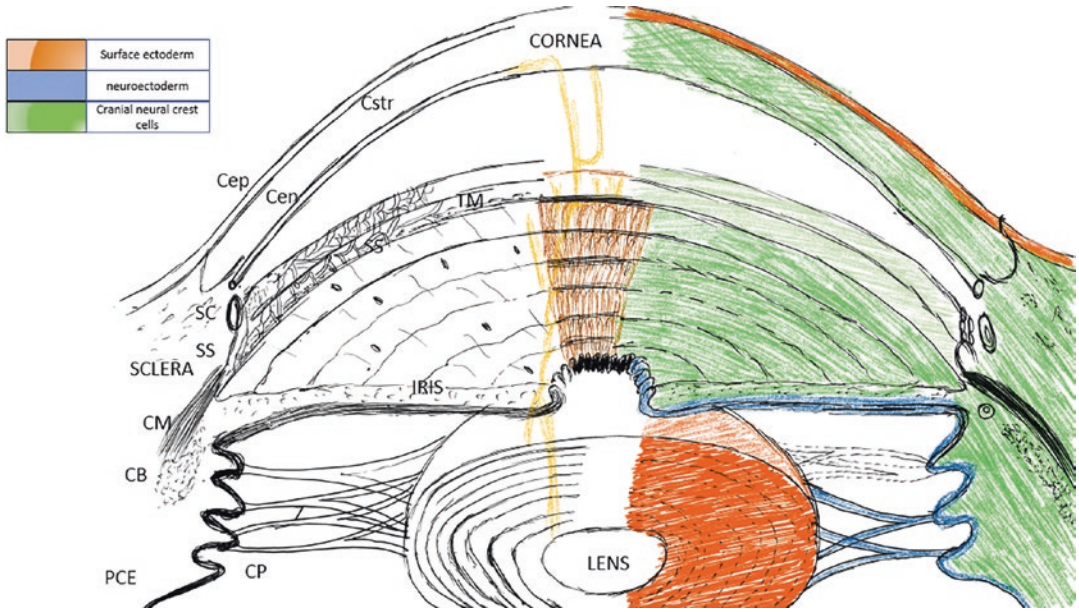

Fig. 12.1 Schematic representation of the anterior segment illustrating the anatomy and the corresponding embryological derivatives (red-surface ectoderm; blue-neuroectoderm; green-cranial neural crest cells). Cep, corneal epithelium; Cen, corneal endothelium; Cstr, corneal stroma; SL, Schwalbe's line; SS, scleral spur; CB, ciliary body; CP, ciliary process; CM, ciliary muscle; PCE, pigmented ciliary epithelium; SC, Schlemm's canal; TM, trabecular meshwork; Z, zonule/suspensory ligament of lens

The risk of developing glaucoma is estimated to be 50–70% in Peters anomaly. Glaucoma usually occurs due to either one or a combination of the following features:

1. Dysgenesis of trabecular meshwork or Schlemm's canal
2. Formation of iridocorneal and/or corneo-lenticular adhesions leading to secondary angle closure

12.4 Clinical Picture

Peters anomaly presents in a wide phenotypic spectrum. The classification is mainly based on the size and density of the corneal leukoma with posterior stroma and Descemet's membrane defect with or without iridocorneal adhesions and/or corneo-lenticular adhesions with or without cataract. The severity of the disease is determined by the size and density of the corneal opacity, corneo-lenticular adhesion, corneal staphyloma or any associated ophthalmic associations, most importantly glaucoma. The visual outcome remains guarded regardless of treatment modality.

12.5 Types of Peters Anomaly

The anatomic step-ladder classification of Peters anomaly is by far the most acceptable and simple.

1. Posterior corneal defect with leukoma: It is the simplest form. The iris, angle and lens are normal, but a defect in the posterior cornea and Descemet's membrane because of the primary failure during corneal endothelial development consequently produces an overlying corneal opacity. This opacity is usually central or oval. The affected cornea is rarely vascularized, and the peripheral cornea is usually clear (Fig. 12.2a).
2. Posterior corneal defect with leukoma and adherent iris strands: The iris strands, which usually arise from the collarette, attach to the edge of the posterior corneal defect (Fig. 12.2b).

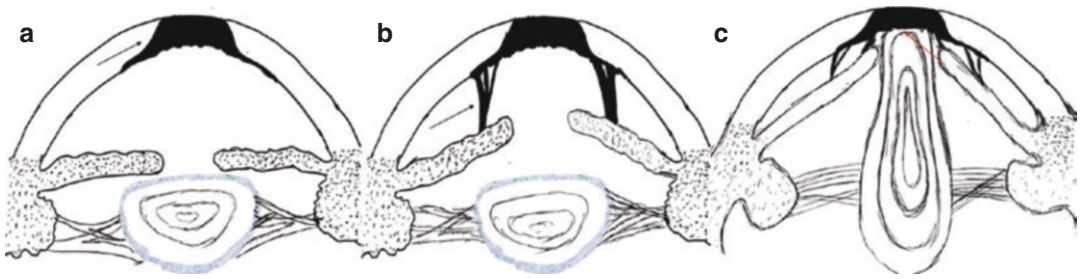

Fig. 12.2 Schematic representation of step ladder classification of Peters anomaly. (**a**) Representation of the posterior corneal defect which is known as 'von Hippel' internal corneal ulcer with central leukoma. (**b**) Representation of iris strands attached to the central corneal opacity. (**c**) Representation of corneo-lenticular touch with iris strands adhered to the central corneal opacity

3. Posterior corneal defect with leukoma, adherent iris strands, and corneo-lenticular contact with lens abnormality (Fig. 12.2c); there are five spectrums of lens abnormality: (a) lens adheres to the posterior corneal stroma with the absence of Descemet's membrane and lens capsule; (b) lens does not adhere to the cornea but only moves forward; (c) lens in place with only anterior lens capsule and cortex adherent to the posterior stroma; (d) lens is in place but has a cone-shaped alignment with posterior corneal defect; and (e) lens is in place but having anterior polar or nuclear cataract.

Another classification for Peters anomaly is based on pathogenesis, which is subdivided into type I, type II, and Peters plus syndrome. Type I Peters anomaly is categorized by central corneal opacity and iridocorneal adhesions (Fig. 12.2b). Type II Peters anomaly has a more severe phenotype with corneal opacity and lens involvement with iridocorneal touch with or without cataract (Fig. 12.2c). The Peters plus syndrome includes characteristics of either type 1 or type 2 Peters, which includes cardiac, craniofacial, skeletal, auditory, and urogenital abnormalities like cleft lip/palate, short stature, and mental retardation.

12.6 Differential Diagnosis

Congenital corneal opacities (CCOs) can be due to glaucoma, infection, trauma, developmental, metabolic, genetic or idiopathic factors, either alone or in combination.

1. **Sclerocornea**: Inheritance is sporadic. Though it is usually bilateral, but usually asymmetric. Sclerisation of the peripheral cornea or entire cornea makes limbus identification difficult. Nonprogressive in nature.
2. **Primary congenital glaucoma (PCG)**: Congenital glaucoma is the most important differential diagnosis of CCO. PCG patients have unique signs and symptoms which include epiphora, photophobia and blepharospasm which are present due to irritation that accompanies corneal oedema caused by elevated intraocular pressure (IOP) with enlarged cornea and buphthalmos. The tears in Descemet's membrane can be single or multiple and appear as elliptical, glassy, parallel ridges on the posterior cornea, either peripherally or across the visual axis.
3. **Congenital hereditary endothelial dystrophy (CHED)**: The mode of inheritance is autosomal dominant/autosomal recessive (AD/AR). The cornea is avascular, with diffuse corneal oedema ranging from a ground-glass appearance to total corneal opacity. There won't be any iridocorneal adhesion or posterior corneal defect differentiating it from Peters anomaly. High central corneal thickness (CCT) can cause IOP to be measured erroneously.
4. **Posterior polymorphous dystrophy (PPMD)**: The mode of inheritance is AD, less common than CHED occurs rarely at birth, and usually presents in two or three decades of life. Bilateral with diffuse corneal oedema which clears slowly, with normal corneal

thickness. Peripheral anterior synechiae (PAS) are characteristics feature. Nonprogressive in nature.

5. **Dermoid**: Dermoid is unilateral or bilateral, sporadic in onset. These are congenital benign tumours, classified under choristomas. The most common site is the inferotemporal limbus, containing hair follicles, sweat glands or sebaceous glands with normal IOP and CCT. Other ocular abnormalities include lid coloboma, aniridia and microphthalmos. Dermoid (one-third) cases are associated with Goldenhar syndrome.
6. **Congenital corneal ulcer**: Congenital corneal opacities caused by corneal ulcers are rarely present at birth and may be due to herpes simplex, bacterial and neurotrophic keratitis. Rubella is found in 6% of babies during the first trimester of pregnancy.
7. **Acquired traumatic breaks in the Descemet's membrane**: During delivery, injuries to the Descemet's membrane can be caused by forceps. The Descemet's membrane rupture is vertical and linear which can lead to stromal and epithelial oedema and with time corneal opacity develops.

12.7 Evaluation of Patient with Peters Anomaly

The ophthalmic evaluation includes visual acuity (Snellen when applicable) and final refraction (spherical equivalent), anterior segment examination, an IOP measurement, central corneal thickness (CCT), axial length, and a fundus examination with an indirect ophthalmoscope or ultrasonography (USG) if the fundus is invisible.

In opaque corneas, ultrasound biomicroscopy provides valuable information about the presence of iridocorneal or corneo-lenticular adhesions, as well as other lens and angle anomalies that can guide management. Anterior segment optical coherence tomography (AS-OCT) also provides high-resolution images of the anterior segment. Both of these high-resolution imaging modalities are portable and can be used during examination under anaesthesia (EUA).

12.8 Management of Glaucoma in Peters Anomaly

Conservative management: Elevated IOP without any optic nerve head (ONH) changes can be controlled medically with topical glaucoma medications.

Surgical management includes:

1. Angle surgery (ab interno or ab externo)
2. Combined trabeculectomy and trabeculotomy with mitomycin C
3. Glaucoma drainage device (GDD) placement
4. Laser cycloablation (trans-scleral or endoscopic)
   (a) Due to overlying corneal opacity, ab interno angle surgery is technically difficult and can only be performed with smaller opacities. Angle surgery has a low success rate, and the ineffectiveness of angle surgery is likely related to the closed-angle configuration. However, even with an open-angle configuration, angle surgery in the Peters anomaly may still fail because of angle dysgenesis.
   (b) Ab externo trabeculotomy can be tried, but often it is combined with trabeculectomy for better outcomes. The effectiveness of trabeculectomy is increased when augmented with MMC.
   (c) Laser cycloablation (trans-scleral or endoscopic), in which the ciliary body is treated for 180–270° with the G-probe, has long-term good results when combined with drainage devices (Table 12.1).

Table 12.1 Survival rate of different glaucoma surgeries in Peters anomaly (Dolezal et al 2019)

Type of glaucoma surgery	Survival rate % (1 year)	Survival rate %
Trabeculectomy	36	18 (2 years)
GDD	75	38 (5 years)
Laser cycloablation	78	52 (10 years)
GDD + cycloablation	100	100 (20 years)

(d) Based on the anatomy of the Peters anomaly, GDD implantation may require lensectomy, vitrectomy and posterior tube placement to prevent corneal decompensation. Posterior tube placement prevents corneal decompensation, but there is a risk of retinal detachment. This is especially true in situations with severe dysgenesis in which the pars plana may be abnormally located or even absent. As a result, the retina may insert anteriorly, sometimes even within the lens–cornea complex.

Amblyopia treatment is attempted when the media opacity is not too dense to allow for fundus examination. The medical treatment is comprised of occlusion therapy with or without pupil dilation with mydriatics.

Preoperative glaucoma can act as an independent risk factor for optical keratoplasty graft failure due to:

1. High IOP can lead to rapid endothelial decompensation.
2. Glaucoma medications can also lead to an increased risk of graft rejection and ocular surface-related failures because of increased leukocyte and fibroblast accumulation in the conjunctival and limbal area leading to an immunological reaction against the graft. So, it is necessary to control the IOP before keratoplasty.

Corneal transplantation has been shown to aggravate glaucoma by crowding anterior chamber structures and increasing the risk of angle closure. Modifications to the penetrating keratoplasty (PKP), such as oversizing the graft and creating peripheral iridectomies in each quadrant, are made to minimize the worsening of IOP. Patients with mild disease have better visual outcomes than those with severe illness. According to research, overall graft success in the Peters anomaly ranges from 50 to 70% after 1 year to 30% after 5–10 years (Dolezal KA et al 2019). Generally, IOP control is followed by corneal grafting or can be combined in one sitting with higher risks of failure.

Case 12.1

History: A 2.5-year-old female child presented with right eye (RE) corneal opacity, photophobia and watering with baseline IOP of 26 and 12 mmHg in RE and left eye (LE), respectively. RE Ultrasound (USG) examination was anechoic with increased cup-disk ratio, and the left eye fundus was normal. The patient was started on a combination of eyedrop dorzolamide (2%) and timolol (0.5%) twice a day in RE.

EUA: Central corneal opacity measuring about 2.5 mm in diameter in RE (Fig. 12.3a). AS-OCT revealed a Descemet's membrane defect known as von Hippel internal corneal ulcer (yellow arrow) with iridocorneal adhesion (red arrow) (Fig. 12.3b) with IOP RE 20 mmHg and LE 12 mmHg (Tonopen), respectively. Corneal diameter of RE 12.00 * 11.5 mm, LE 11.0 * 11.0 mm. Central corneal thickness (CCT) was RE 660 μm and LE 520 μm with ONH cupping in RE 0.9:1 and LE 0.3:1. Axial lengths in RE and LE were 22.50 and 21.50 mm, respectively. Refraction could not be done due to poor streak formation.

Diagnosis: RE type 1 Peters anomaly associated with secondary glaucoma.

Management: The patient underwent RE trabeculectomy with MMC. The patient is also planned for optical keratoplasty (PKP). On follow-up after trabeculectomy, the IOP was controlled in RE without any glaucoma medication.

Learning Points

- Glaucoma severity is unrelated to laterality or the presence of a systemic abnormality. If there is corneal opacity covering more than half of the cornea, corneal-lenticular adhesion, corneal staphyloma or an underlying ophthalmic anomaly such as microphthalmia, persistent hyperplastic primary vasculature (PHPV), aniridia or cataract, the visual prognosis is worse.
- If keratoplasty is performed immediately after glaucoma filtration surgery, glaucoma filtration surgery faces a high probability of failure due to inflammation. In such cases, limited quadrant cyclodestructive or micropulse procedure can be done as an interim procedure till

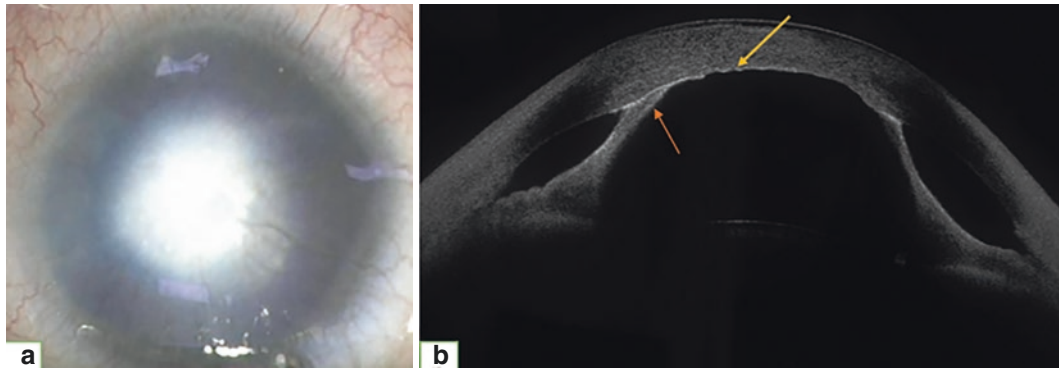

Fig. 12.3 (**a**) Intraoperative image showing central corneal leukoma measuring about 2.5 mm in diameter. (**b**) AS-OCT image of right eye representing thick cornea measuring 660 μm with a posterior cornea defect (yellow arrow) with iridocorneal adhesion (orange arrow)

keratoplasty is performed. Similarly, diode laser cyclophotocoagulation (DLCP) or micropulse can also be done in the immediate postoperative period after PKP, but the risk of graft failure due to inflammation caused by cyclodestructive procedure should be kept in mind. A GDD instillation also remains a viable approach to perform pre-PKP. Else, keratoplasty should be timed at least after 3 months of trabeculectomy.

Case 12.2

History: A 9-day-old child presented with white cornea, watering and photophobia since birth in both eyes. On examination, there was central corneal opacity with IOP of RE 28 mmHg and LE 22 mmHg on Tonopen with CCT RE 580 μm and LE 600 μm. USG of both eyes (BE) was anechoic with ONH cupping.

EUA: Central corneal opacity measured about 3.5 mm in diameter in BE (Fig. 12.4a). UBM and AS-OCT RE revealed central posterior stroma and Descemet's membrane defect (red arrow) and iridocorneal adhesion (yellow arrow) (Fig. 12.4b) with IOP RE 20 mmHg and LE 20 mmHg, respectively. Corneal diameters measured RE 12.5 mm * 11.0 mm and LE 12.0 mm * 11.0 mm. CCT was RE 580 μm and LE 600 μm with ONH cupping RE 0.9:1 and LE 0.8:1. Refraction could not be done due to poor streak formation. Axial length in RE and LE was 22.50 and 21.50 mm, respectively.

Diagnosis: Type 1 Peters anomaly associated with secondary glaucoma in both eyes.

Management: The patient was planned for RE trans-scleral DLCP due to prolonged latency on visual evoked potential response and LE trabeculectomy with MMC, as there were more than 270-degree iridocorneal adhesions in LE, making GDD tube placement difficult in the anterior chamber or in the sulcus (clear lens). On follow-up, the IOPs were controlled in BE, and the patient was operated for optical keratoplasty in BE.

Learning Points

- Many factors are responsible for poor visual outcomes in the Peters anomaly:
  - Apart from the typical anatomical defects of the Peters abnormality, these eyes have preexisting ocular anomalies also.
  - These eyes are more prone to develop graft failure, glaucoma, retinal detachment and phthisis as a result of keratoplasty.
  - These children are unlikely to adhere to optical correction and amblyopia treatment.

Finally, in many of these youngsters, a delay in keratoplasty can lead to the development of visual deprivation amblyopia.

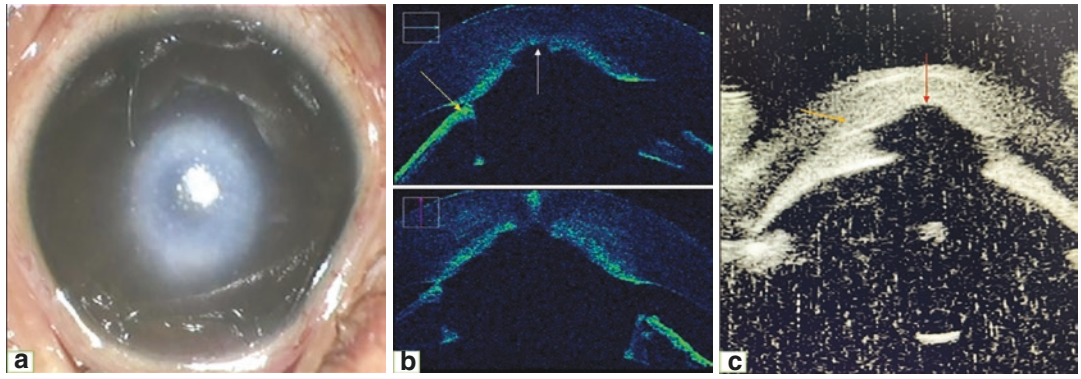

Fig. 12.4 (**a**) Image represents central corneal opacity measuring 3.5 mm in diameter. (**b**) AS-OCT image showing irido corneal adhesion (yellow arrow) and von Hippel internal corneal ulcer (white arrow). (**c**) UBM showing irido corneal adhesion with the thick cornea (yellow arrow) and von Hippel internal corneal ulcer (red arrow)

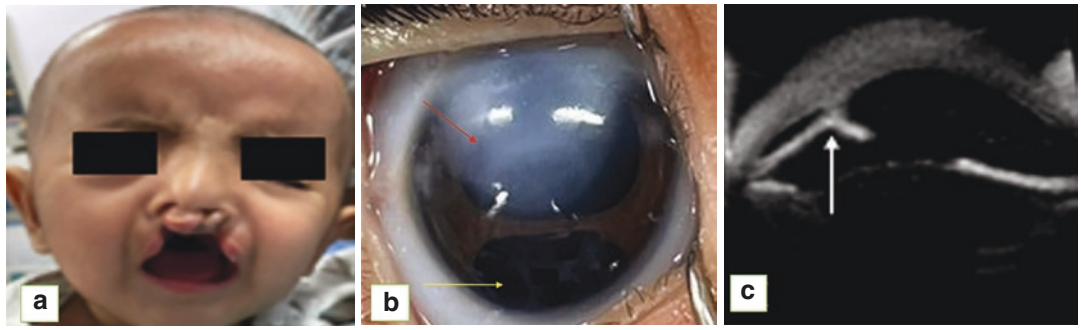

Fig. 12.5 (**a**) Systemic examination showing cleft lip and cleft palate. (**b**) Image showing superior corneal opacity measuring about 3.5 mm in diameter (red arrow) and surgical optical inferior iridectomy (yellow arrow). (**c**) AS-OCT image showing supero-temporal iridocorneal adhesion (white arrow) with the thickened central cornea

- IOP readings are profoundly affected by the CCT (e.g. thicker CCTs 'overestimate' and thinner CCTs 'underestimate' true IOP, for every 70 μm variation in CCT, there is an IOP variation of 5 mmHg), and there is a significant risk factor for developing glaucoma damage, independent of IOP corrections, with thinner CCT.

Case 12.3

History: A 5-month-old male child presented with RE whitish opacity since birth and absence of LE. On torch light examination, there was the presence of paracentral corneal opacity with IOP in RE 28 mmHg with Tonopen, and the patient was started on Iobet (0.25%) eyedrop twice a day. USG of RE was anechoic with ONH cupping. Systemic examination revealed cleft palate and cleft lip with syndactyly.

EUA: Paraxial corneal opacity measuring about 3.5 mm in diameter in RE (Fig. 12.5a) and anophthalmia in LE. UBM revealed (Fig. 12.5c) iridocorneal adhesion in the superior angle (red arrow). IOP in RE was 20 mmHg (Tonopen), with a corneal diameter of 12.5 * 11.5 mm with CCT RE 560 μm and ONH cupping of 0.7:1. Axial length in RE was 22.40 mm. Refraction could not be done due to poor streak formation.

Diagnosis: Peters plus syndrome and LE anophthalmia.

Management: Surgical optical inferior iridectomy with 6 clock hours goniotomy in inferonasal and inferotemporal angle was performed in RE. After control of IOP patient underwent optical keratoplasty.

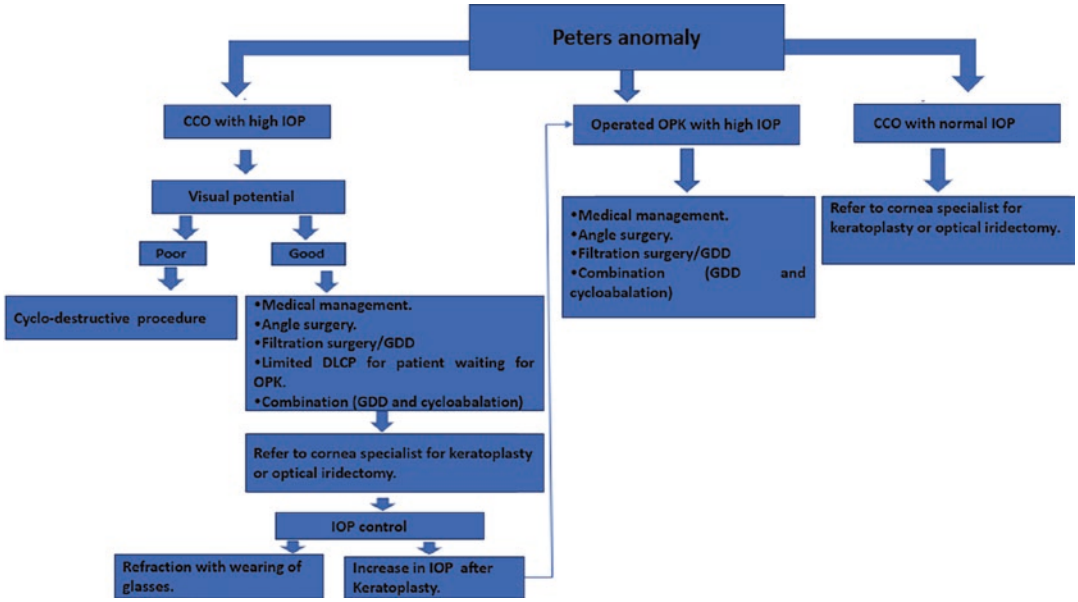

Fig. 12.6 Flow chart showing the management of Peters anomaly (*CCO* congenital corneal opacity, *IOP* intraocular pressure, *OPK* optical penetrating keratoplasty, *DLCP* diode laser cyclophotocoagulation, *GDD* glaucoma drainage device)

Learning Points

- Angle surgery has a low success rate due to closed angles and severe angle dysgenesis in Peters anomaly. However, in amenable eyes with non-severe angle dysgenesis, it can be performed as a first-line option, being lesser invasive than other IOP-lowering surgeries.
- After medical or surgical control of IOP, cycloplegic refraction should be performed. Anisometropic and strabismic amblyopia, as well as myopic astigmatism, are prominent causes of visual loss among these children, especially in unilateral cases.
- When compared to PKP, optical iridectomy is easier to perform, with a lower risk of complications like graft failure or rejection. As a result, it is preferred over PKP in some circumstances with clear peripheral cornea providing ambulatory vision.
- Vigorous amblyopia management is as important as adequate glaucoma control.

Management of eyes with Peters anomaly (Fig. 12.6)

12.9 Conclusions

Clinical picture of Peters anomaly can vary from subtle corneal opatity to significant corneal opacity with iridolenticular or corneolenticular adhesions and secondary glaucoma. In patients with Peters anomaly having significant corneal opacity and uncontrolled secondary glaucoma, the timing of glaucoma surgery or keratoplasty should be planned cautiously to increase the success rate of either procedures.

Suggested Reading

Dolezal KA, Besirli CG, Mian SI, Sugar A, Moroi SE, Bohnsack BL. Glaucoma and cornea surgery outcomes in peters anomaly. Am J Ophthalmol. 2019;208:367–75.

Elbaz U, et al. Phenotypic spectrum of Peters Anomaly: implications for management. Cornea. 2022;41(2):192–200.

Idrees F, Vaideanu D, Fraser SG, Sowden JC, Khaw PT. A review of anterior segment dysgeneses. Surv Ophthalmol. 2006;51(3):213–31.

Nischal KK. Developmental anomalies of the anterior segment and globe. In: Pediatric ophthalmology and strabismus. New York: Springer; 2003. ISBN: 978-1-4899-0511-6.

Rezende RA, Uchoa UBC, Uchoa R, Rapuano CJ, Laibson PR, Cohen EJ. Congenital corneal opacities in a cornea referral practice. Cornea. 2004;23(6):565–70.

Salik I, Gupta A, Tara A, Zaidman G, Barst S. Peters anomaly: a 5-year experience. Paediatr Anaesth. 2020;30(5):577–83.

Stahl ED. Anterior segment dysgenesis. Int Ophthalmol Clin. 2014;54(3):95–104. https://doi.org/10.1097/IIO.0000000000000031. PMID: 24879108.

Yang LL, Lambert SR, Lynn MJ, Stulting RD. Surgical management of glaucoma in infants and children with Peters' anomaly: long-term structural and functional outcome. Ophthalmology. 2004;111(1):112–7. https://doi.org/10.1016/j.ophtha.2003.02.002. PMID: 14711722.

Yang LLH, Lambert SR, Drews-Botsch C, Stulting RD. Long-term visual outcome of penetrating keratoplasty in infants and children with Peters anomaly. J AAPOS. 2009;13(2):175–80.

Yoshikawa H, Sotozono C, Ikeda Y, Mori K, Ueno M, Kinoshita S. Long-term clinical course in eyes with peters anomaly. Cornea. 2017;36(4):448–51. https://doi.org/10.1097/ICO.0000000000001161. PMID: 28207433.

13 Congenital Ectropion Uveae with Glaucoma

Vinit Tanwar, Karthikeyan Mahalingam, and Shikha Gupta

13.1 Introduction

Ectropion uveae is defined as an outward rotation of the iris pigment epithelium onto the anterior surface of the iris. It is classified into congenital and acquired variants (Table 13.1). Congenital ectropion uveae (CEU) was first described by Wicherkiewicz and Spiro; it is a rare, nonprogressive anomaly characterized by non-tractional hyperplasia/proliferation of iris pigment epithelium on the anterior surface of the iris stroma at birth. It is characteristically a unilateral condition with ipsilateral glaucoma with few reports documenting bilateral presentation. Most of the patients belong to the second decade of life, with few reports of CEU in infancy. It can also be associated with other ocular abnormalities such as blepharoptosis, and gonioscopic characteristics such as iridotrabecular dysgenesis, prominent Schwalbe's line, and iris processes.

V. Tanwar (✉) · K. Mahalingam · S. Gupta
Dr. Rajendra Prasad Centre for Ophthalmic Sciences, All India Institute of Medical Sciences, New Delhi, India

S. Gupta et al. (eds.), *Childhood Glaucoma*, https://doi.org/10.1007/978-981-19-7466-3_13

Table 13.1 Differences between acquired and congenital ectropion uveae

S. No.	Acquired ectropion uveae	Congenital ectropion uveae
1.	Common, progressive	Rare, nonprogressive
2.	Caused by the presence of tractional component due to the shrinkage of abnormal fibrovascular tissue present on the pigment epithelium	Occurs due to failure of regression of primordial endothelium, resulting in hyperplasia of iris pigment epithelium over the anterior surface of the iris
3.	Associated with inflammatory and/or ischemic pathological processes involving the anterior portion of the iris. Examples: Neovascular glaucoma or iridocorneal endothelial syndromes	Can be isolated or associated with Axenfeld-Reiger syndrome or aniridia
4.	Gonioscopy is usually associated with closed angles	Gonioscopy is usually associated with open angles with high iris insertion in isolated cases

13.2 Etiopathogenesis

Failure of regression of primordial endothelium in the anterior chamber due to the developmental arrest of neural crest tissue in utero occurs. This results in hyperplasia of iris pigment epithelium over the anterior surface of the iris. Glaucoma is a common complication and may develop at any stage from infancy to early adulthood. The proposed etiology behind the underlying elevated intraocular pressure (IOP) is the anterior insertion of the iris and trabecular meshwork dysgenesis. Usually, nonprogressive glaucoma occurs but progressive glaucoma due to angle dysgenesis has been reported too.

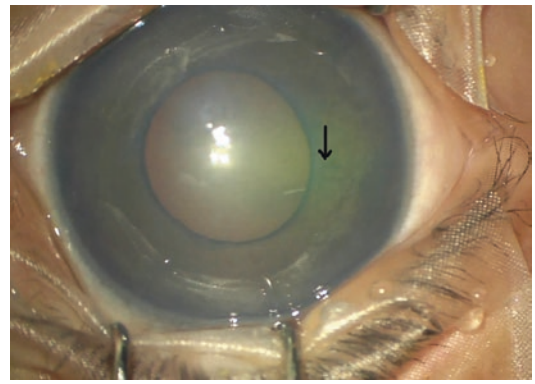

Fig. 13.1 Clinical picture of RE showing 360° congenital ectropion uveae (CEU) in a child with bilateral congenital glaucoma, increased corneal diameter and with visible iris vessels (arrow) through atrophic iris stroma

13.3 Case Examples

Case 13.1

A 3-week-old male child was referred with the triad of blepharospasm, lacrimation, and buphthalmos. There was no significant family history, and antenatal and natal history was uneventful.

On examination under anesthesia: The patient had enlarged edematous corneae with no Haab's striae in both eyes (BE). Corneal diameters in the right eye (RE) were 14 × 14 mm and the left eye (LE) were 13.5 × 14 mm. IOP measured in RE was 28 mmHg and LE 30 mmHg. BE pupils had 360° CEU with smooth, cryptless iris surface, and anomalous iris vascularization visible through atrophic iris stroma was present BE (Fig. 13.1). CCT was RE 598 μm and LE 568 μm. Axial lengths were RE 21.89 mm and LE 21.33 mm. On fundus examination: RE cup-disc ratio (CDR) 0.9:1 and LE CDR 0.7:1. The patient had no systemic abnormalities.

Diagnosis: BE neonatal glaucoma with bilateral neonatal-onset congenital ectropion uveae (N-CEU). Another example of Neonatal onset Congenital ectropion uveae (N-CEU) depicted in Fig. 13.2.

Differential diagnosis:

- **Neonatal-primary congenital glaucoma (PCG)**: Similar to N-CEU, N-PCG presents with elevated IOP and increased cup-to-disc ratio on examination, is typically bilateral (can be asymmetric), and commonly presents with the classical triad of epiphora, photophobia, and blepharospasm soon after birth. Corneal edema and buphthalmos are also common findings of PCG. It is not associated with iris changes seen in CEU like aniridia, iris hypoplasia, or ectropion uveae and offers a better prognosis than N-CEU (Table 13.2).

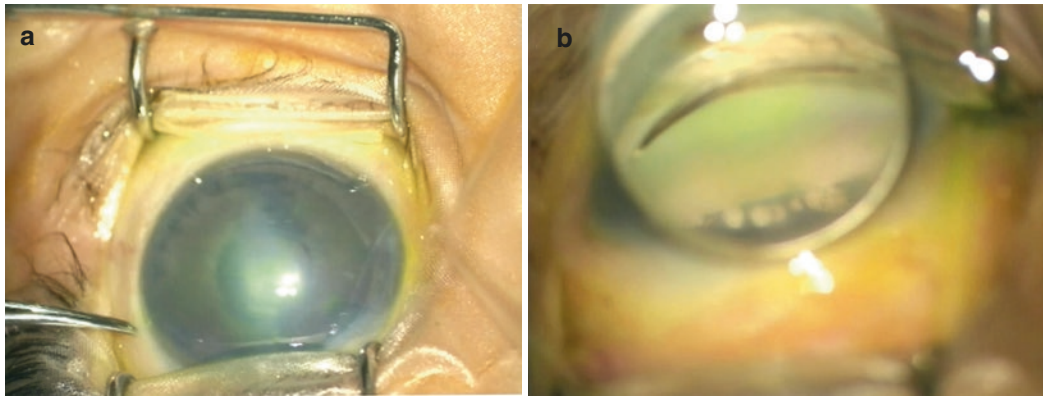

Fig. 13.2 (**a**) Neonatal-onset congenital ectropion uveae (N-CEU) intraoperative picture showing Haab's striae and iris hypoplasia. (**b**) Intraoperative gonioscopy using Swan Jacob goniolens showing angle dysgenesis, high iris insertion onto a prominent Schwalbe's line

Table 13.2 Differences between Neonatal Congenital Ectropion Uveae (CEU) and Neonatal Primary Congenital Glaucoma (PCG)

S. No.	Neonatal CEU or early onset CEU with glaucoma	Neonatal PCG
1.	Rare entity	More common than CEU
2.	Genetic associations were not known till now	Most cases are sporadic. Genetic associations include *CYP1B1*, *LTBP2*, *PLOD2*, *TEK*, *GPATCH*, and *PRSS56* (10–50% of affected in different populations)
3.	Presents as bilateral, progressive neonatal glaucoma with angle dysgenesis. Associated with thick and hazy corneas	Mostly bilateral (80%) and progressive
4.	Typically present as smooth, cryptless iris surface, iris stromal atrophy/ hypoplasia, and proliferation of iris pigment epithelium onto the anterior surface of the iris	Iris hypoplasia or ectropion absent Typically associated with isolated trabeculodysgenesis
5.	Less favorable prognosis than neonatal PCG	Neonatal PCG has a worse prognosis than later-onset PCG, but the prognosis is better than N-CEU

- **Axenfeld-Reiger syndrome (ARS)**: Both are associated with arrest in neural crest development with resulting anterior segment abnormalities. ARS is bilateral and has an autosomal dominant inheritance pattern and is typically associated with other ocular findings such as posterior embryotoxon, iris atrophy, corectopia, or polycoria. Facial abnormalities, such as maxillary hypoplasia or dental defects, may also be found in ARS as opposed to CEU. Sometimes the two conditions may overlap.
- **Iridocorneal endothelial syndrome (ICE)**: This is a unilateral condition, unlike N-CEU. Unlike CEU, ICE commonly occurs in middle-aged female adults. In ICE, corneal (edema) or iris involvement (polycoria, corectopia, ectropion uveae, and nodules) can be present. Pathognomonic of ICE is high peripheral anterior synechiae (PAS) above Schwalbe's line, whereas, in CEU, iris insertion usually does not extend above Schwalbe's line (Fig. 13.3).
- **Aniridia**: Neonatal onset Congenital ectropion uveae (N-CEU) is also sometimes associated with partial aniridia which is believed to be the closest phenotype of N-CEU.

Management: The patient was started on BE brinzolamide 1% BD, betaxolol 0.25% BD, pilocarpine 2% BD, oral acetozolamide 250 mg (1/8) tablet TDS, and planned for BE combined trabeculotomy-trabeculectomy with mitomycin C under general anesthesia.

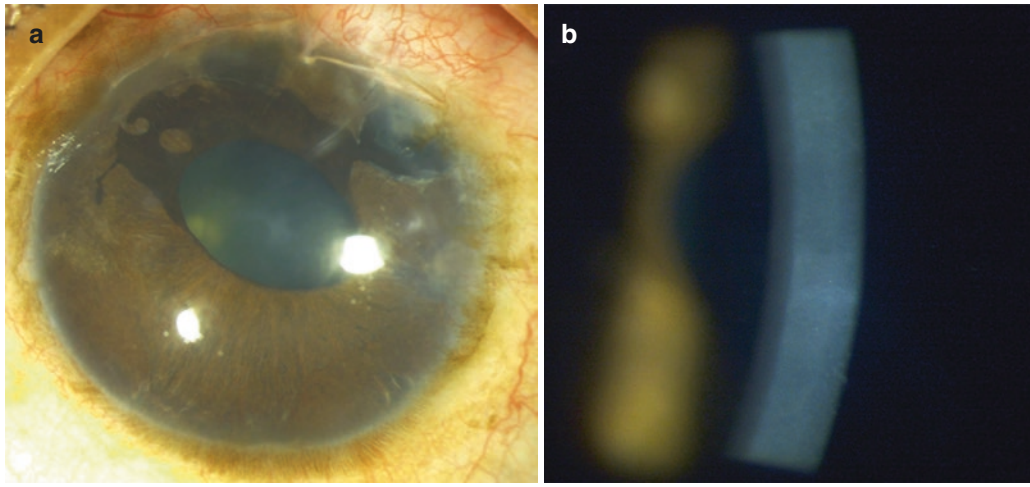

Fig. 13.3 (**a**) Clinical picture of Iridocorneal endothelial syndrome (ICE) showing ectropion uveae, corectopia and area of iris atrophy. (**b**) Hammered Silver appearance of endothelium in ICE syndrome

Case 13.2

A 7-year-old boy presented with loss of vision in both eyes (BE) since early childhood. His best-corrected visual acuity at presentation was 6/12 in the right eye (RE) and 6/24p in the left eye (LE). In RE and LE, IOP was 22 mmHg and 28 mmHg, respectively. Corneal diameters were 12 mm in both eyes. Anterior segment examination of RE showed an oblique band of hypoplastic iris tissue with exposed bare posterior pigmented epithelium and inferotemporal corectopia and polycoria and 3 clock hours of ectropion uveae in the superior temporal part of the pupil. LE showed iris stromal hypoplasia, multiple atrophic patches, 360° ectropion uveae, corectopia and polycoria, partial loss of pupillary ruff, and prominent posterior embryotoxon in the inferior part (Fig. 13.4). Gonioscopy BE revealed posterior embryotoxon with attached iris strands and peripheral anterior synechiae. The fundus showed a vertical CDR of 0.7:1 in RE and 0.9:1 in LE. The systemic evaluation revealed maxillary hypoplasia, broad nasal bridge, oligodontia, microdontia, and an operated atrial septal defect.

Diagnosis: Bilateral Axenfeld-Rieger syndrome (ARS) with CEU with glaucoma – an overlap variant (two other examples of similar overlap syndrome of ARS with CEU are depicted in Figs 13.5 and 13.6).

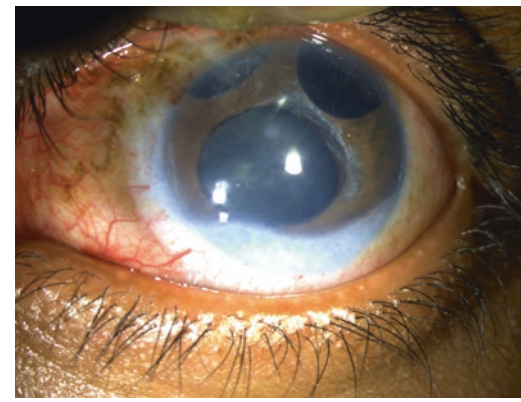

Fig. 13.4 Clinical picture of LE showing multiple iris atrophic patches, 360° ectropion uveae, corectopia and polycoria, partial loss of pupillary ruff, and prominent posterior embryotoxon in the inferior part. The patient has undergone glaucoma drainage device implantation in the superonasal quadrant, the tube is visible in the anterior chamber

Differential diagnosis:

- **ICE (Iridocorneal Endothelial) Syndrome:** This is unilateral in nature, has accompanying corneal endothelial changes, manifests in middle age, has female predominance, and lacks systemic abnormalities unlike seen in overlap cases of ARS with CEU.
- **Peter's Anomaly:** It is characterized by a central corneal opacity associated with an absence of Descemet's membrane and endothelial lay-

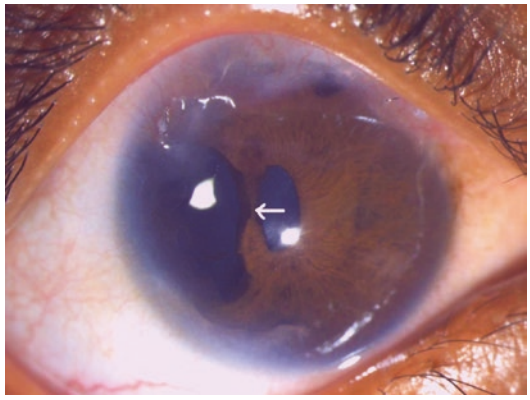

Fig. 13.5 Patient of Axenfeld-Rieger syndrome (ARS) with polycoria, peripheral iridocorneal adhesions and ectropion uveae (arrow)

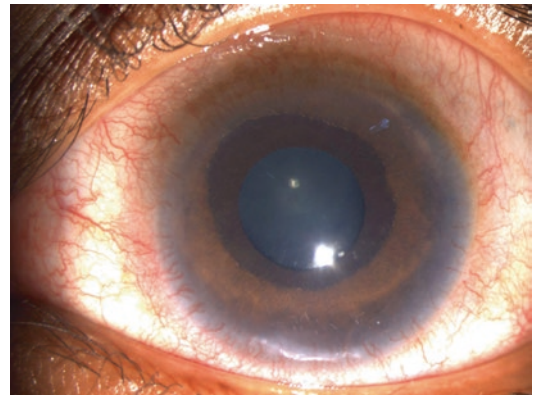

Fig. 13.7 Clinical picture of LE showed 360° ectropion uveae with crytpless iris surface in a child with late onset unilateral glaucoma

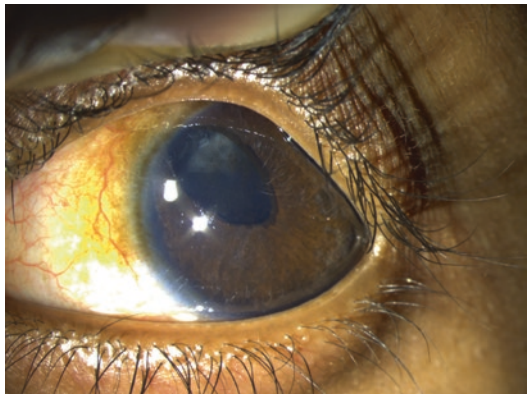

Fig. 13.6 Patient of Axenfeld-Rieger syndrome (having posteror embryotoxon on goniosocpy) with ectropion uveae, peripheral iris stromal atrophy with corectopia

ers as well as varying degrees of iridocorneal adhesions arising from the border of the corneal opacity.

- **Aniridia:** A bilateral heterogeneous condition with variable appearance of the iris from a rudimentary stump to mild iris atrophy (partial aniridia). It is characterized by the presence of foveal hypoplasia and iris hypoplasia and sometimes may be associated with ectropion, also simulating CEU.

Treatment: Initially started on BE timolol 0.25% bd, Dorzox 2% TDS, oral acetozolamide 250 mg (1/8) tablet TDS. It was followed up with LE combined trabeculectomy augmented with mitomycin C 0.04% for 2 min under general anesthesia.

Learning Points

- CEU can present as an impure form when it coexists with other ocular anomalies like Axenfeld-Rieger syndrome (ARS) or aniridia.
- CEU is a refractory form of glaucoma, when co-associated with other variants can impart a poorer prognosis for IOP control.
- All patients with such ocular features should be thoroughly examined to look for other subtle signs like partial ectropion, iris hypoplasia, corectopia, or aniridia.

Case 13.3

A 17-year-old boy presented with a history of headache and epiphora in the LE for the past 6 months. There was no history of trauma, previous episodes, prior surgery, or drug intake. On examination, uncorrected visual acuity was 6/6 in RE and 6/60 in LE. Anterior segment examination of RE is within normal limits, and in LE 360° thick velvety ectropion uveae with hypoplastic iris stroma and cryptless iris surface were present (Fig. 13.7). The IOP was 16 mmHg RE and 36 mmHg LE. Central corneal thickness was 518 μm RE and 568 μm LE. Gonioscopy RE showed open angles, while LE revealed anterior iris insertion onto the anterior nonpigmented trabecular meshwork. Fundus evaluation revealed a CDR of 0.3:1 in RE and 0.8:1 in LE with vertical elongation.

There were café-au-lait spots on several areas of the skin, especially on the trunk and back (Fig. 13.8). X-ray orbit and brain were normal.

Diagnosis: Neurofibromatosis with LE late-onset CEU with secondary glaucoma.

Treatment: Initially topical timolol 0.5% BD, latanoprost 0.05% HS, and dorzolamide 2% TDS, along with oral acetazolamide, were started. After a month, IOP was 28 mmHg. The patient was then subjected to trabeculectomy surgery with 0.02% mitomycin for 3 min under LA. IOP in LE was 12 mmHg at 1-month follow-up with well-filtering bleb.

Learning Points

- Though late-onset unilateral CEU (Table 13.3) is a nonprogressive disease, the occurrence of glaucoma is usually progressive, can occur at any age, and is associated with a poor prognosis.
- Filtering surgery is often required to control IOP.
- Neurofibromatosis is the most commonly associated systemic abnormality with unilateral CEU, while other disorders like Prader–Willi syndrome, Rieger anomaly, and facial hemihypertrophy have been described occasionally.

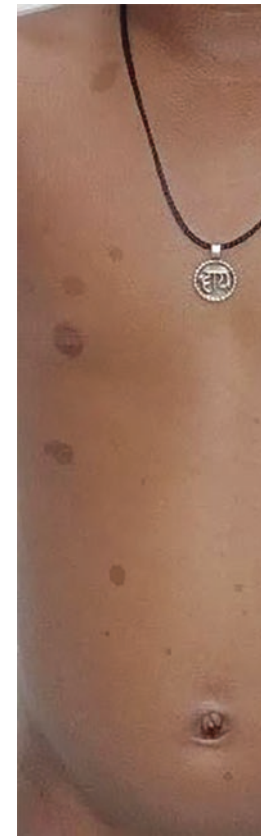

Fig. 13.8 Multiple Café-au-lait spots on the chest and abdomen in a child with neurofibromatosis, simulating the appearance of milk with coffee as the color is variegated from light to dark brown

Table 13.3 Differences between ususally seen clinical manifestations of neonatal and late-onset Congenital Ectropion Uveae (CEU)

S. No.	Neonatal CEU or early-onset CEU with glaucoma	Late-onset CEU with glaucoma
1.	Bilateral presentation in a neonate	Characteristically unilateral condition in older children or young adults
2.	Blepharoptosis is absent	Sometimes associated with blepharoptosis and spindle neurofibromas
3.	Associated with a severe form of glaucoma with varying degrees of iris hypoplasia	Less severe glaucoma than N-CEU, presents late
4.	Worse prognosis as compared to late-onset CEU with glaucoma.	Though the prognosis is poor, its better than early-onset CEU with glaucoma

13.4 Conclusions

Congenital Ectropion Uveae (CEU), is a rare, non-progressive anomaly which is observed at birth, and which often presents unilaterally with ipsilateral glaucoma. It is important to differentiate between CEU and other entities such as primary congenital glaucoma, iridocorneal endothelial syndrome, aniridia, and Axenfeld-Reiger syndrome as they have different management strategies. Accurate diagnosis and appropriate and timely management can prevent vision loss and improve the patient's quality of life.

Suggested Reading

Dowling JL, Albert DM, Nelson LB, Walton DS. Primary glaucoma associated with iridotrabecular dysgenesis and ectropion uveae. Ophthalmology. 1985a;92(7):912–21.

Dowling JL, Albert DM, Nelson LB, Walton DS. Primary glaucoma associated with iridotrabecular dysgenesis and ectropion uveae. Ophthalmology. 1985b;92:912–21.

Duke-Elder S. System of ophthalmology. Vol. III, Part 2: Congenial deformities. London: Henry Kimpton; 1963. p. 599.

Hertzberg R. Congenital ectropion uveae and glaucoma. Austr N Z J Ophthalmol. 1985;13:45–8.

Kaushik S, Dhingra D, Vibha B, Saini A, Gupta G, Snehi S, Singh N, Thattaruthody F, Pandav SS. Neonatal-onset congenital ectropion uveae: a distinct phenotype of newborn glaucoma. Am J Ophthalmol. 2020;223:83.

Khan AO, Aldahmesh MA, Al-Abdi L, Mohamed JY, Hashem M, Al-Ghamdi I, Alkuraya FS. Molecular characterization of newborn glaucoma including a distinct aniridic phenotype. Ophthalmic Genet. 2011;32:138–42.

Mandal AK. Late-onset unilateral primary developmental glaucoma associated with iridotrabecular dysgenesis, congenital ectropion uveae and thickened corneal nerves: a new neural crest syndrome. Ophthalmic Surg Lasers. 1999;30(7):567–70.

Politi F, Sachs R, Barishak R. Neurofibromatosis and congenital glaucoma: a case report. Ophthalmologica. 1977;176:155–9.

Ritch R, Forges M, Hetherington J, Harrison R, Podos SM. Congenital ectropion uveae with glaucoma. Ophthalmology. 1984;91:326–31.

Roth H, Shaffer RN. Neurofibromatosis and glaucoma. In: Bellows JG, editor. Contemporary ophthalmology: honoring Sir Stewart Duke-Elder. Baltimore, MD: Williams & Wilkins; 1972. p. 180–9.

Sethi HS, Pal N, Dada T. Bilateral juvenile glaucoma with iridotrabecular dysgenesis, congenital ectropion uveae, and thickened corneal nerves. Eye. 2005;19(12):1347–9.

Spiro G. Ein Fall von ectropion uveae congenitum. Centralbi Prakt Augerheikd. 1896;20:310–1.

Wicherkiewicz B. Beitrag zur Kenntniss des Ectropion Uveae congenitum. Albrecht Von Graefes Arch Ophthalmol. 1891;37:204–27.

Wilson ME. Congenital iris ectropion and a new classification for anterior segment dysgenesis. J Pediatr Ophthalmol Strabismus. 1990;27(1):48–55.

Wolter JR, Butler RG. Pigment spots of the iris and ectropion uveae with glaucoma in neurofibromatosis. Am J Ophthalmol. 1963;56:964–73.

Aniridia with Glaucoma

14

Brajesh Lahri, Karthikeyan Mahalingam, and Shikha Gupta

14.1 Introduction

Aniridia is a rare, congenital, inherited bilateral disorder affecting a wide range of structures of the eye. The incidence of aniridia varies from 1/64,000 to 1/96,000 among various study populations. No racial or sexual differences are recognized. It is a complex embryologic malformation that involves the iris, trabecular meshwork, and cornea. The term aniridia is a misnomer, as a small remnant of iris tissue may be found in most affected eyes. The most common mode of inheritance of aniridia is autosomal dominant. Aniridia is caused due to genetic haploinsufficiency expression of the PAX6 gene located on chromosome 11p13. The incidence of glaucoma in patients affected with aniridia is very high, with studies showing incidence up to 50%.

14.2 Clinical Features

- *Iris*: Hypoplasia of the iris is the hallmark feature of aniridia. The appearance of the iris may range from relatively normal with only mild hypoplasia noticeable on detailed examination to a small stump of iris tissue being present. The hypoplastic remnant of the iris can be visible on slit lamp examination, but sometimes it can be visualized only after performing the gonioscopic examination. When the abnormality of the iris is very subtle, fluorescein angiography can be helpful to demonstrate collarettes and blood vessels of the iris.
- *Cornea*: Limbal stem cell deficiency (LSCD) and keratopathy are the most common associations seen in aniridia. LSCD leads to conjunctivalization of the cornea, clinically appreciated as circumferential pannus formation and corneal opacification, which proceeds in a centripetal pattern. The ultimate end result is the development of total leucomatous corneal opacity. Optical penetrating keratoplasty (OPK) is used for the management of such patients. The rates of graft failure are higher in patients with aniridia due to preexisting limbal stem cell deficiency (LSCD) and also due to the high incidence of secondary glaucoma in these patients. Keratoprosthetic devices are another potential remedial option for advanced keratopathy in aniridia.
- *Lens*: Aniridia is often associated with abnormalities of the lens. One of the most important factors affecting the visual acuity of the patient is cataract formation. Apart from cataracts, other abnormalities associated with aniridia are congenital aphakia, varying degrees of subluxation, and lens resorption.

B. Lahri (✉) · K. Mahalingam · S. Gupta
Dr. Rajendra Prasad Centre for Ophthalmic Sciences, All India Institute of Medical Sciences, New Delhi, India
e-mail: shikhagupta@aiims.edu

S. Gupta et al. (eds.), *Childhood Glaucoma*, https://doi.org/10.1007/978-981-19-7466-3_14

- *Glaucoma*: Glaucoma occurs in almost 20–55% of children suffering from aniridia. Anterior segment dysgenesis leading to trabecular dysgenesis and impaired development of Schlemm's canal has been described as causes of glaucoma in aniridia patients, presenting in infancy or early childhood. The mechanism of glaucoma for that developing glaucoma later in life is the rotation of the rudimentary iris stump leading to synechial occlusion of angle and blockage of aqueous outflow.
- *Posterior Segment*: Patients suffering from aniridia also show foveal abnormalities, foveal hypoplasia being the commonest, affecting 40–50% of the patients. Foveal hypoplasia further leads to poor visual acuity and poor development of fixation response of affected eyes, leading to nystagmus.

14.3 Pathophysiology of Glaucoma in Aniridia: Fig. 14.1 (Table 14.1)

14.3.1 Differential Diagnosis

- **Peter's Anomaly:** Central corneal opacity of variable severity and an underlying defect of the posterior stroma, Descemet's membrane, and endothelium. There can be coexisting iridocorneal or iridio-corneo-lenticular adhesions.
- **Ectopia Lentis:** Dislocation of the lens not associated with iris defects.
- **Iris Coloboma:** There is a localized absence of the iris and a keyhole-shaped deformity of the pupil; the remaining iris is normal. Iris colobomas are not usually associated with decreased visual acuity and nystagmus.

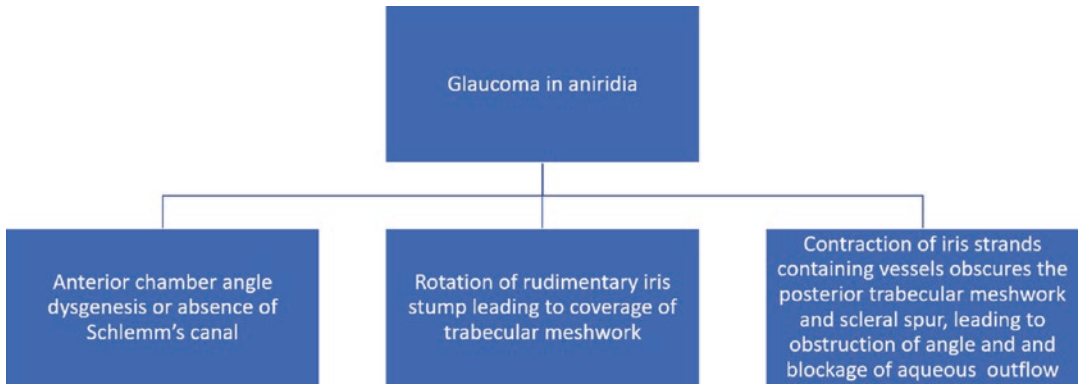

Fig. 14.1 Flowchart explaining the pathophysiology of glaucoma associated with aniridia

Table 14.1 Summary of the different syndromic associations with Aniridia along with their genetic relationship

Syndrome	Clinical features	Chromosomes involved	Genes involved	Inheritance	Type of mutation
1. WAGR Syndrome	*W*ilms tumor, *a*niridia, *g*enitourinary anomalies, and mental *r*etardation	11p13	PAX-6, WT-1	Sporadic	Cytogenetic deletions and submicroscopic deletions
2. Miller syndrome	Wilms tumor, aniridia	11p13	PAX-6	Sporadic	Exonal Deletions
3. Isolated aniridia	Aniridia	11p13	PAX-6, TRIM 44	Inherited (autosomal dominant)	Alteration of gene sequences, exon deletions
4. Gillespie syndrome	Aniridia, intellectual disability, cerebellar ataxia	3p26	ITPR-1	Inherited (autosomal recessive)	Nonsense mutation

- **Oculocutaneous Albinism:** Diffuse iris transillumination, hypopigmented fundus, and associated hypopigmentation of hairs and skin.

14.4 Case Examples

Case 14.1

History: A 15-year-old female presented with complaints of diminished vision in both eyes (BE), photophobia, and watering noticed over the last 5 years. There was no family history of a similar illness. The child was diagnosed with sporadic aniridia. An ultrasound examination of the abdomen was done, and no intra-abdominal mass was detected.

Examination: The patient's best-corrected visual acuity (BCVA) was 6/24 in the right eye (RE) and 6/36 in the left eye (LE); intraocular pressure (IOP) was 16 mmHg and 28 mmHg RE and LE, respectively. Anterior segment evaluation revealed normal corneal diameters (11.5 × 11 mm), the absence of iris on slit lamp examination, with visible zonules 360° (Fig. 14.2a, b) in BE. Gonioscopy revealed the presence of rudimentary iris stumps with closed angles in both eyes (Fig. 14.2c, d). Disc evaluation revealed a cup-disc ratio of 0.5:1 RE and 0.8:1 LE, and a dull foveal reflex was seen in both eyes.

Diagnosis: The patient was diagnosed with BE aniridia with LE secondary glaucoma.

Management: The patient was initially started on topical glaucoma medications i.e. **Timolol, Dorzolamide**, and **Pilocarpine**, but the IOP was not controlled. Subsequently, she underwent LE Ahmed glaucoma valve (AGV) Implantation and the IOP was controlled after the surgery.

Learning Points

- Patients with aniridia frequently present with poor visual acuity, which can be attributed to

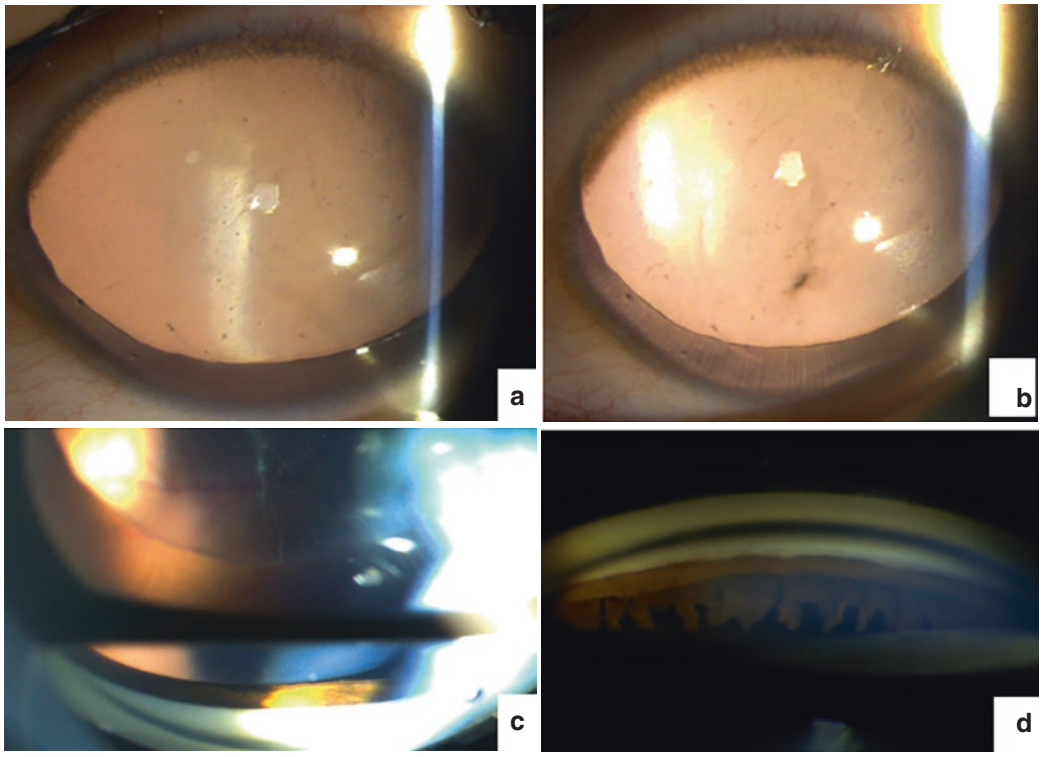

Fig. 14.2 Clinical picture (**a**) of the right eye showing the absence of the iris. (**b**) shows the absence of iris and visible zonules in left eye (**c**) Gonioscopy of right eye showing visible zonules and iris stump at low magnification (**d**) high magnification gonioscopy view of left eye showing high iris insertion leading to angle closure, residual iris stump along with visible ciliary processes

foveal hypoplasia, astigmatism, and rarely optic nerve hypoplasia.
- Glaucoma seen in patients with aniridia is often refractory to medical therapy, and surgical intervention is frequently required.
- Goniotomy has been found to be effective in a prophylactic role when angles are open and the patient hasn't developed glaucoma or in early stages of glaucoma. In patients with advanced stages of aniridic glaucoma with closed angles, goniotomy is not effective and has a limited role, due to widespread angle dysgenesis.
- Trabeculotomy, trabeculectomy, and glaucoma drainage devices like AGV are treatment options available for aniridic glaucoma with angle closure and severe angle dysgenesis.
- Existing literature shows success rates of trabeculectomy (IOP <21 mmHg) at 5 years to range from 45% to 83% at 5 years. The success rates of AGV implant vary from 85% to 100% at 2 years as reported by previous studies.
- Long-term results of surgical interventions in aniridic glaucoma are not satisfactory, and a high failure rate is seen. A higher risk of developing fibrosis after surgical procedures is reported as a cause of increased failure rate of trabeculectomies and glaucoma drainage device surgeries.
- A thorough systemic examination is essential in cases of aniridia. Wilms tumor should be ruled out in cases with sporadic aniridia.

Case 14.2

History: A 15-year-old male presented with complaints of diminished vision in both eyes for the last 6 months. The patient was diagnosed with both eye aniridia with secondary glaucoma 5 years back and underwent both eye trabeculectomy with MMC.

Examination: The patient's BCVA was 6/60 in the RE and 4/60 in the LE; IOP was 34 and 32 mmHg in RE and LE. The central corneal thickness (CCT) was RE 600 μm and LE 610 μm. Anterior segment evaluation revealed an absence of iris on slit lamp examination, with visible zonules 360° in both eyes (Fig. 14.3a). Gonioscopy revealed the presence of rudimentary iris stumps with open angles in both eyes. Disc evaluation revealed a cup-disc ratio of 0.8:1 RE and 0.9:1 LE. The child also showed an avascular flat bleb in both eyes.

Diagnosis: BE aniridia with secondary glaucoma with operated failed trabeculectomy with an anterior subluxated lens in RE.

Management: The patient first underwent LE Ahmed glaucoma valve (AGV) implantation followed by RE AGV implantation surgery along

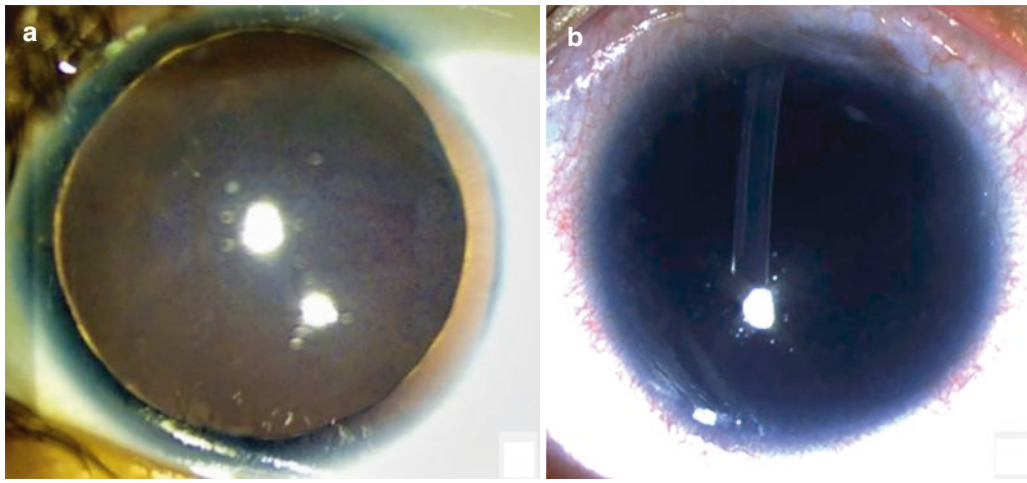

Fig. 14.3 Clinical picture (**a**) of the right eye of an aniridia patient with anterior subluxation of lens and secondary glaucoma. Right eye image (**b**) showing postoperative image after lens aspiration (aphakia) and Ahmed glaucoma valve (AGV) implantation with a tube visible in the anterior chamber

with lens aspiration (Fig. 14.3b). Post-surgery, after 1 week, BCVA was 6/60 RE and 6/36 LE. The patient's IOP was 12 mmHg in RE and 10 mmHg in LE, respectively.

Learning Points

- In view of the high rates of failure of trabeculectomy in aniridia patients, glaucoma drainage devices (GDDs) like Ahmed glaucoma valve (AGV), and Baerveldt implant can be used for IOP control.
- In view of thick CCT, the patient should be kept on frequent follow-ups to elicit any rise in IOP or disc change suggestive of glaucoma progression.

Case 14.3

History: The parents of a 1-year-old female complained of excessive watering from both eyes of the child and photophobia.

Examination: The patient's visual acuity was followability of light in both eyes. IOP was 24 and 22 mmHg in the right eye and left eye. Examination under anesthesia revealed corneal edema, absence of iris, clear lens, with visible zonules 360° in both eyes, with the presence of rudimentary iris stump in both eyes. Posterior segment evaluation revealed a cup-disc ratio of 0.8:1 RE and 0.9:1 LE.

Diagnosis: BE aniridia with infantile glaucoma.

Management: The patient underwent BE trabeculectomy under GA (Fig. 14.4a).

Intraoperatively surgery in right eye was uneventful, while in the left eye intraoperatively, anterior chamber shallowing was noted which was accompanied by suprachoroidal hemorrhage as evidenced by the change in color of fundal glow from bright orange (Fig. 14.4b) to dull red color (Fig. 14.4c). Postoperatively, the patient was found to have increased IOP, and dull fundal glow, both eyes. Ultrasound examination revealed suprachoroidal hemorrhage (Fig. 14.4d). The patient underwent drainage for suprachoroid hemorrhage in BE, and IOP was controlled.

Learning Points

- The incidence of suprachoroidal hemorrhage after trabeculectomy has been reported to be between 0.7% and 3% and is even higher in the case of patients with aniridia.
- Patients with aniridia are at higher risk of developing complications like choroidal detachment, retinal detachment, suprachoroidal hemorrhage, and vitreous hemorrhage, and rarely hypotonic maculopathy can also be seen. This is attributed to poor lens vitreous interface and lesser resistance of the vitreous to prolapse anteriorly. The risk of these complications can be reduced by allowing minimum fluctuations in anterior chamber depth intraoperatively by either using viscoelastic substances or anterior chamber maintainer with balanced salt solution.
- Aniridia is associated with poor long-term outcomes of filtering procedures like trabeculectomy, which has been attributed to higher rates of fibrosis in eyes with aniridia.

Case 14.4

History: A 12-year-old male presented with complaints of diminished vision in both eyes, left more than right for the last 4 years. The patient was diagnosed with LE cataract 2 years back and underwent LE cataract surgery with posterior chamber (intraocular lens) IOL implantation. The patient had a good gain of vision following surgery and vision remained good till the next 1 year. He started having painless, progressive, diminution of vision in the last 1 year. The patient also complained of intermittent episodes of eye pain.

Examination: The patient's BCVA was 6/24 in the RE and perception of light, with an inaccurate projection of light in the LE; IOP was 38 and 6 mmHg in the RE and LE. Anterior segment evaluation revealed the absence of the iris. The cornea showed poor ocular surface, superficial neovascularization, and diffuse haze, suggestive of aniridic keratopathy with pannus. The examination also revealed the posterior chamber

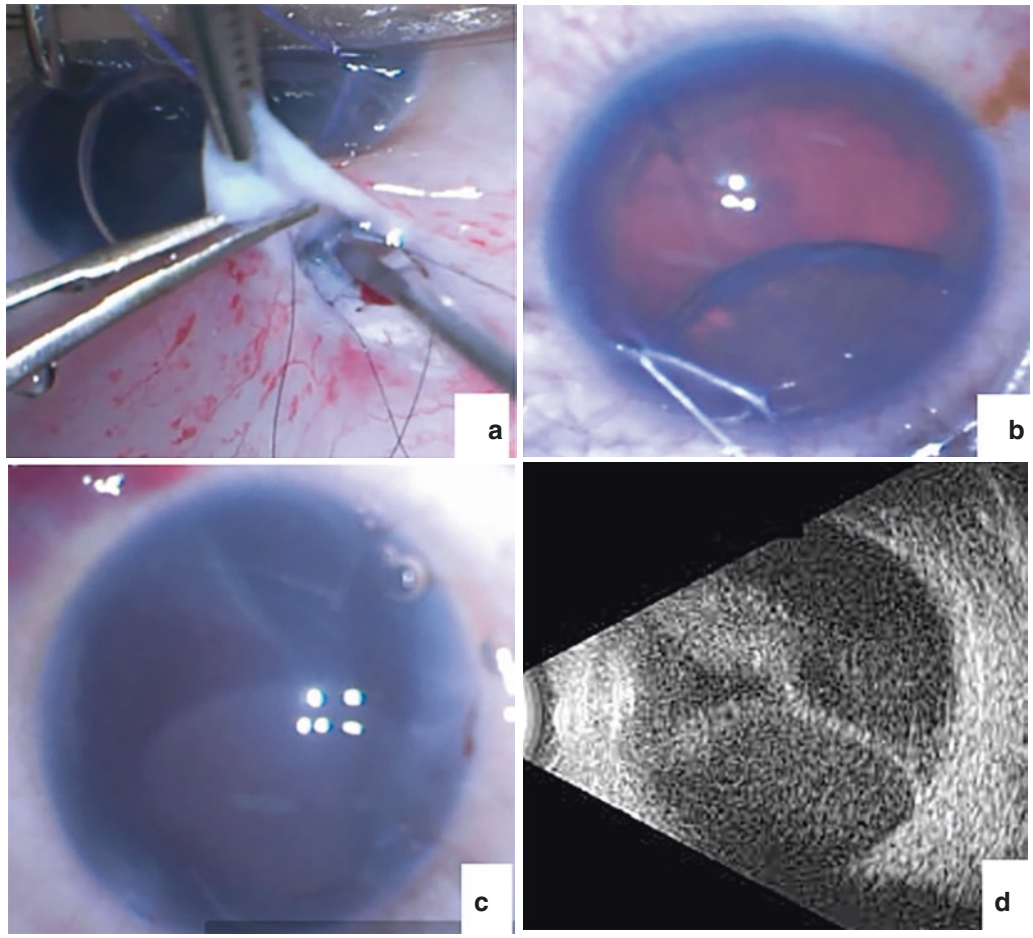

Fig. 14.4 Clinical picture (**a**) of the left eye of an aniridia patient undergoing trabeculectomy. Left eye image (**b**) shows the intraoperative normal orange fundal glow. Image (**c**) shows a dull red fundal glow suggestive of intraoperative suprachoroidal hemorrhage. Clinical picture (**d**) shows the presence of suprachoroidal hemorrhage (kissing choroidal domes with intra-dome echoes suggestive of haemorrhage) on a B-Scan ultrasound examination of the left eye

IOL in situ and the presence of a membranous structure in the anterior chamber, surrounding the IOL leading to nasal decentration of IOL (Fig. 14.5). LE revealed shrinkage of the eyeball with ill-defined structures of the eye. Gonioscopy revealed the presence of rudimentary iris stumps with open angles. Disc evaluation revealed a cup-disc ratio of 0.8:1 in RE, and no glow was present in LE.

Diagnosis: BE aniridia with RE secondary glaucoma with RE pseudophakia with RE aniridia fibrosis syndrome (AFS) with decentered IOL with LE phthisis bulbi secondary to AFS.

Management: The patient was initially started on topical glaucoma medications, i.e., **timolol, dorzolamide, brimonidine, and travoprost, but the IOP was not controlled**. Subsequently, patient underwent RE trabeculectomy with 0.04% mitomycin C application for 2 min, and the IOP was controlled after the surgery. The patient also underwent a membranectomy at the time of surgery following which IOL centration got corrected. The postoperative vision after 1 week was RE 6/12, LE perception of light with an inaccurate projection of light, and IOP of RE was 16 mmHg after surgery.

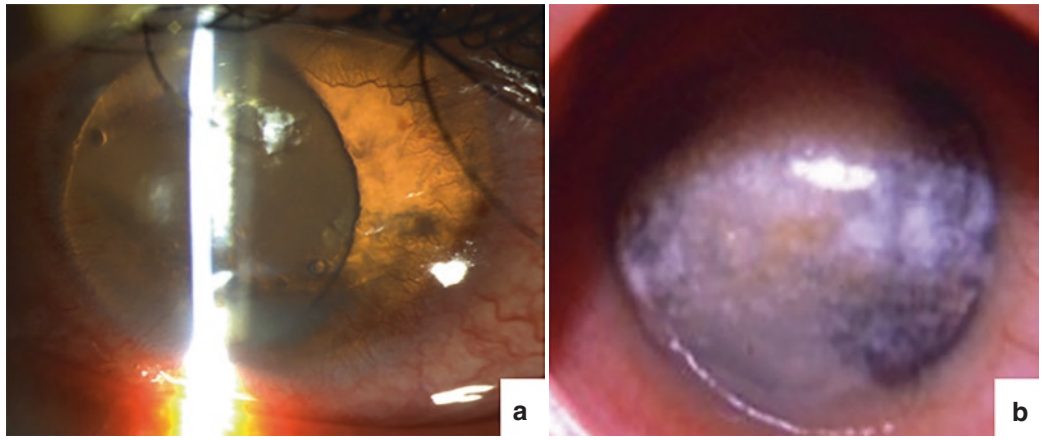

Fig. 14.5 Clinical picture (**a**) showing the right eye of a patient with aniridia with superior pannus, revealing a fibrous membrane in the anterior chamber along with decentration of the intraocular lens (**b**) showing the left eye of the same patient having phthisis bulbi secondary to aniridia fibrosis syndrome

Learning Points

- Aniridia fibrosis syndrome (AFS) is a rare complication described after any intraocular surgery in the eye, most commonly after the implantation of an intraocular lens following the removal of a cataractous lens. The risk factors for aniridic fibrosis syndrome are not clearly understood, and the exact incidence is not known.
- It is characterized by a progressive fibrotic membrane of the anterior chamber that develops after ophthalmic surgery.
- The membrane in aniridia fibrosis syndrome (AFS) has been shown to originate from rudimentary iris stumps. It is first noticeable on the posterior surface of IOL, and later as it grows, it leads to the decentration of the IOL, as evident in our case (Fig. 14.5a). It can also lead to tilting of the IOL and in very severe cases can cause IOL-corneal touch.
- Aniridia fibrosis syndrome can lead to other complications like IOL decentration, IOL entrapment, corneal decompensation, membrane formation over keratoprosthesis devices, retinal detachment, and rarely phthisis bulbi as seen in our case (Fig. 14.5b).

14.5 Conclusions

In all patients with aniridia, glaucoma screening is of paramount importance. Management of glaucoma in aniridia is challenging due to poor response to medical therapy and several vision-threatening complications which are associated with glaucoma surgery. Early management and follow-up are the key factors to preserve maximum vision in these children. Adequate perioperative measures should be taken to decrease the risk of complications.

Suggested Reading

Arroyave P, et al. Use of glaucoma drainage devices in the management of glaucoma associated with aniridia. Am J Ophthalmol. 2003;135:155. https://pubmed.ncbi.nlm.nih.gov/12566018/. Accessed 6 Feb 2023

Brauner SC, Walton DS, Chen TC. Aniridia. Int Ophthalmol Clin. 2008;48(2):79–85. https://doi.org/10.1097/IIO.0b013e318169314b.

Chen TC, Walton DS. Goniosurgery for prevention of aniridic glaucoma. Arch Ophthalmol. 1999;117(9):1144–8. https://doi.org/10.1001/archopht.117.9.1144.

Hingorani M, et al. Aniridia. Eur J Hum Genet. 2012;20:1011. https://pubmed.ncbi.nlm.nih.gov/22692063/. Accessed 6 Feb 2023.

Jain A, et al. Aniridic glaucoma: long-term visual outcomes and phenotypic associations. J Glaucoma. 2015;24:539. https://pubmed.ncbi.nlm.nih.gov/24618569/. Accessed 6 Feb 2023.

Landsend ECS, Lagali N, Utheim TP. Congenital aniridia - a comprehensive review of clinical features and therapeutic approaches. Surv Ophthalmol. 2021;66(6):1031–50. https://doi.org/10.1016/j.survophthal.2021.02.011.

Lee HJ, Colby KA. A review of the clinical and genetic aspects of aniridia. Semin Ophthalmol. 2013;28(5–6):306–12. https://doi.org/10.3109/08820538.2013.825293.

Midha N, et al. Systemic associations of childhood glaucoma: a review. J Pediatr Ophthalmol Strabismus. 2018;55:397. https://pubmed.ncbi.nlm.nih.gov/30452766/. Accessed 6 Feb 2023.

Tsai JH, Freeman JM, Chan CC, et al. A progressive anterior fibrosis syndrome in patients with postsurgical congenital aniridia. Am J Ophthalmol. 2005;140(6):1075–9. https://doi.org/10.1016/j.ajo.2005.07.035.

Lens-Associated Glaucomas

15

Abhijeet Beniwal, Karthikeyan Mahalingam, and Shikha Gupta

15.1 Introduction

Lens-induced secondary glaucomas can be broadly divided into open-angle glaucomas (phacolytic glaucoma, phaco-antigenic glaucoma, post-traumatic lens particle-induced glaucoma) or angle-closure glaucomas (phacomorphic glaucoma or phacotopic glaucoma). Phacolytic/phacomorphic glaucomas are not usually seen in the pediatric age group. Postsurgical and post-traumatic lens-induced glaucoma are discussed elsewhere. In this chapter, we will mainly discuss phacotopic glaucomas (glaucoma due to subluxation/dislocation of the lens).

15.2 Pathophysiology

Pathophysiology of glaucoma associated with subluxation/dislocation of the lens is:

- Some syndromes are associated with inherent angle dysgenesis contributing to glaucoma.
- Generalized zonulopathy, subluxation, or dislocation of lens leading to pupillary block are the most common mechanisms of acute glaucoma.
- A chronically shallow angle due to anterior lens luxation can lead to peripheral anterior synechiae (PAS) formation and subsequent angle closure glaucoma.
- In cases with post-traumatic ectopia lentis, ongoing trabeculitis or PAS due to trauma/inflammation may also contribute to the development of glaucoma.

Phacotopic glaucoma can be seen in congenital disorders like isolated ectopia lentis or with systemic associations like Marfan syndrome, homocystinuria, Weil-Marchesani syndrome, etc., or maybe acquired in cases after trauma. It can also be seen in conditions like aniridia, megalocornea, congenital glaucoma, high myopia, etc.

Incidence of glaucoma in congenital subluxation is around 50%, and the age of presentation is bizonal, i.e., in infancy and teenage. Most cases are not recognized till late, leading to permanent visual loss. Causes for vision loss other than glaucoma are untreated refractive errors (myopia, astigmatism), amblyopia, cataract, and retinal changes, these challenges add to the burden that need to be addressed for proper visual rehabilitation in these patients (Table 15.1).

Case 15.1

A 16-year-old patient presented with diminished vision in both eyes for a few years. On examination, best-corrected visual acuity (BCVA) was 6/60 in the right eye (RE) and 6/36 in the left eye (LE), with -6DS prescription. His near visual acu-

Supplementary Information The online version contains supplementary material available at https://doi.org/10.1007/978-981-19-7466-3_15.

A. Beniwal (✉) · K. Mahalingam · S. Gupta
Dr. Rajendra Prasad Centre for Ophthalmic Sciences, All India Institute of Medical Sciences, New Delhi, India

S. Gupta et al. (eds.), *Childhood Glaucoma*, https://doi.org/10.1007/978-981-19-7466-3_15

Table 15.1 Table highlighting differentials for subluxation of the lens and characteristic clinical features of respective conditions

	Differentials	Characteristics
Congenital	Marfan syndrome	Strong family history (Autosomal Dominant, FBN1 gene)
		Bilateral subluxation
		Can have associated angle dysgenesis
		7.7% incidence of glaucoma
		Wrist sign, thumb sign, aortic root dilation
	Ectopia lentis et pupillae	Autosomal recessive, ADAMTSL4 mutation
		Asymmetric eccentric pupils displaced opposite to direction of lens dislocation
		Oval ectopic poorly dilating pupil
		Glaucoma reported but exact incidence not quantified
	Weill Marchesani	Autosomal Recessive—ADAMTS10, ADAMTS17, LTBP2 genes
		Autosomal Dominant—FBN1 gene
		Microspherophakia
		Can have associated angle dysgenesis
		80% incidence of glaucoma
		Short, stout extremities, low stature
	Homocystinuria	Inferonasal subluxation of lens
		12% incidence of pupillary block glaucoma
		Failure to thrive, seizures, low IQ, and megaloblastic anemia
Acquired	Post-traumatic subluxation	History of trauma
		Other signs of trauma like sphincter tears, iridodialysis, etc.
		3.39%–7% incidence of glaucoma post-closed globe injury

ity was N12 in RE and N8 in LE. The intraocular pressure (IOP) was 24 mmHg (RE) and 26 mmHg (LE), respectively. There was significant superonasal subluxation in both eyes, right more than left but no anterior lens subluxation (Fig. 15.1). Gonioscopy revealed open angles with high iris insertion. There was 0.6:1 vertical cup disc ratio in right eye and 0.7:1 in LE. Axial length was 25.51 mm in the RE and 25.48 mm in the LE.

Systemic examination: The child had a large arm span to height ratio of 1.1, a high arched palate, and arachnodactyly. The wrist sign and thumb sign were positive (Fig. 15.2a–c).

Diagnosis: The patient was diagnosed with both eyes ectopia lentis with marfanoid features with developmental open angle glaucoma.

Differential diagnosis:

- Post-traumatic subluxation: would be unilateral usually, and other signs of trauma might be present, including rosette cataracts.
- Microspherophakia: the whole rim of the lens would be visible with adequate mydriasis.
- Homocystinuria: the child will present with developmental delay. There will be a failure to thrive and seizures.
- Marfanoid habitus is a constellation of symptoms resembling those of Marfan syndrome, like long limbs, high arm span to height ratio, etc. but often don't fit into the major criteria of Marfan syndrome.

Management: The IOP was managed medically with timolol eyedrops 0.5% BD. The patient was operated on with intralenticular lens aspiration in both eyes with the iris-claw lens under general anesthesia for visual rehabilitation. Six months post-surgery patient has IOP of 16 mmHg in BE. Vision has improved to 6/12 in both eyes.

Learning Points

- Ectopia lentis is seen in 50–60% of Marfan's patients and is a major cause of ocular morbidity. Ectopia lentis with marfanoid features could be associated with glaucoma due to associated angle dysgenesis. Most cases could be managed medically.
- In Marfan syndrome, the FBN1 gene is mutated leading to defective microfibrils

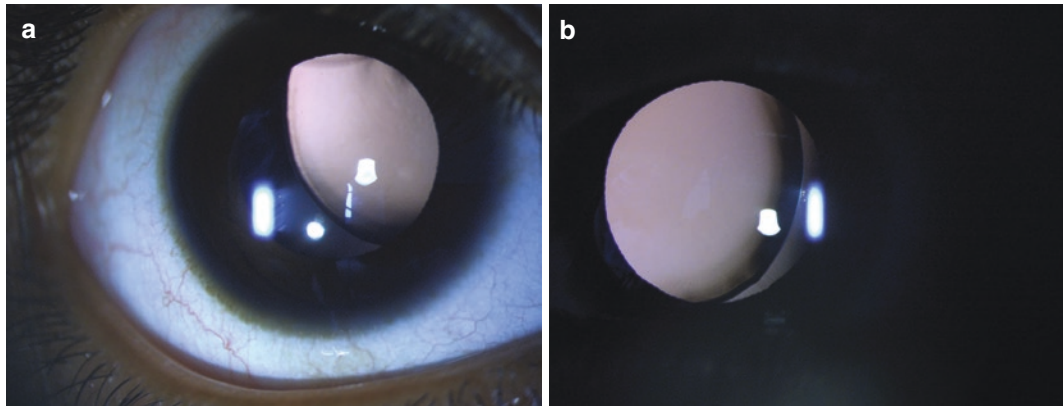

Fig. 15.1 (**a**) Right eye and (**b**) left eye of a child with ectopia lentis with marfanoid features. The zonules are stretched out

Fig. 15.2 (**a**) Clinical picture of a 16 year old boy with Marfanoid habitus showing large arm span to height ratio: 1.1 (normal ratio < 1.05) (**b**) Positive wrist sign—the terminal phalanx of little finger surrounded by thumb. (**c**) Positive thumb sign—terminal phalanx of thumb protruding through wrist

which can contribute to glaucoma through alterations in biomechanical properties of the trabecular meshwork. Hence targeting TGF β could be a potential therapeutic option.

- LTBP2 mutations may also lead to Marfan-like features, interfering with both fibrillin 1 and fibulin 5 binding.
- Constant rubbing of the mobile lens against the iris can also lead to associated pigment dispersion glaucoma (Fig. 15.3). In Marfan syndrome, the lens may subluxate anteriorly into the pupil or anterior chamber, causing pupillary block. Marfan may be associated with angle-closure glaucoma (Fig. 15.4). It is usu-

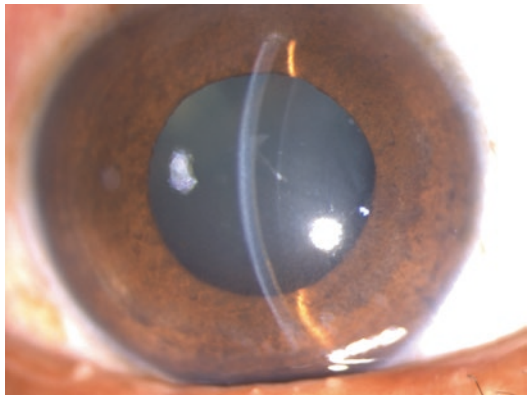

Fig. 15.3 Marfan with pigment dispersion syndrome slit lamp image, pigments can be seen on endothelium

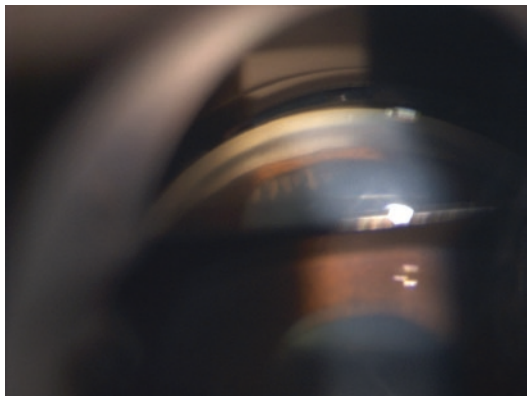

Fig. 15.4 Marfan with closed angle gonioscopic image

ally managed with pupillary dilation and then peripheral iridectomy with lens extraction.

- Open-angle glaucoma can be seen in Marfan's due to associated congenital angle dysgenesis. The longitudinal muscle is placed anteriorly and internally to the scleral spur, and its contraction may lead to the closure of the Schlemm's canal.
- Spontaneous dislocation of the lens in the vitreous cavity may rarely lead to inflammatory glaucoma, especially if the lens proteins are exposed to the external milieu.
- A high percentage of patients may require surgery for retinal detachment (scleral buckling or vitreoretinal surgery) in Marfan syndrome, which can lead to secondary glaucoma.
- Additionally, underlying connective tissue disorder may affect lamina cribrosa, due to which optic nerve exons may be damaged by compression at the exit site.

Case 15.2

An 11-year-old child presented with a diminution of vision in both eyes for 4–5 years.

On examination, he had best-corrected visual acuity of 6/24 in the right eye and no perception of light in the left eye. LE showed corneal decompensation. There were iridocorneal adhesions in LE and was aphakic. The intraocular pressures were raised, 26 mmHg in the right eye and 40 mmHg in the left eye. The patient was not fully dilated due to the risk of a pupillary block. The ultrasound biomicroscopy of RE revealed the lens' anteroposterior width of 5.5 mm and an equatorial diameter of 7 mm. The child had lenticular myopia of -14DS RE. There was 0.8:1 cupping in the right eye and total cupping in the left eye. Undilated slit-lamp examination of RE showed a 'Ɛ' sign (Fig. 15.5a) suggestive of microspherophakia, confirmed intraoperatively as the circumferential lens equator was seen in the dilated state (Fig. 15.5b). Right eye ultrasound biomicroscopy showed a shallow anterior chamber and increased anteroposterior diameter of the lens, confirming microspherophakia (Fig. 15.5c). Left eye cornea was decompensated (Fig. 15.5d).

Diagnosis: BE Microspherophakia with secondary angle closure glaucoma with LE aphakia with corneal decompensation.

Differential diagnosis:

- Weill-Marchesani syndrome - associated with microspherophakia and secondary glaucoma but also with short stature, brachycephaly, and joint stiffness.
- Microspherophakia metaphyseal dysplasia syndrome - associated with microspherophakia, myopia, lens coloboma, and retinal

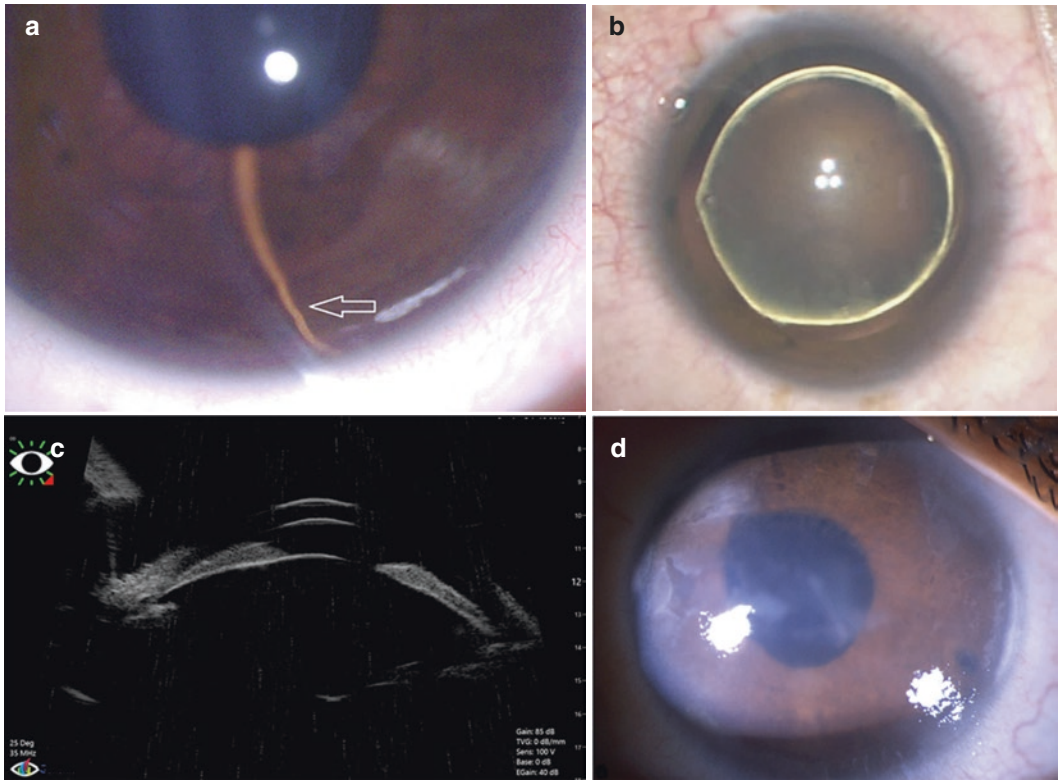

Fig. 15.5 (**a**) Right eye of a child showing "Ɛ" sign in microspherophakia (arrow). (**b**) The intraoperative clinical picture of a microspherophakia child with whole lens equator seen. (**c**) Right eye ultrasound biomicroscopy showing increased anteroposterior diameter and shallow anterior chamber. (**d**) left eye showing corneal decompensation

detachment. Long bones diaphyseal anomalies are seen.

- Axenfeld-Reiger syndrome - will be associated with iris anomalies, posterior embryotoxon, corectopia, polycoria, and systemic anomalies like maxillary hypoplasia.

Management: Patient underwent RE lens aspiration with PCIOL in bag with bag fixation to sclera using Cionni ring. The patient was started on 0.0015% tafluprost and betaxolol 0.5%, but IOP was not controlled. The right eye underwent trabeculectomy with mitomycin C 3 months later.

Learning Points

- Microspherophakia is a bilateral congenital anomaly of the lens. Due to the faulty development of secondary lens fibers during embryogenesis, zonular laxity occurs which leads to development of small spherical lenses causing high lenticular myopia. Despite it being congenital, the patients often present usually in their teens.
- It could be associated with numerous systemic conditions. Sometimes associated axial myopia can make a person prone to retinal pathologies. The equator of the lens is visible during the mydriatic state and can sometimes precipitate pupillary block.
- Three-fourths of patients with microspherophakia have closed angles (Fig. 15.6) and one-fourth have open angles. Only 15–20% of cases can be managed medically successfully.
- Fifty-nine percent of children present with glaucomatous disc damage. One-fifth of the affected eyes are blind due to glaucoma, which increases to one-third over time on follow-up,

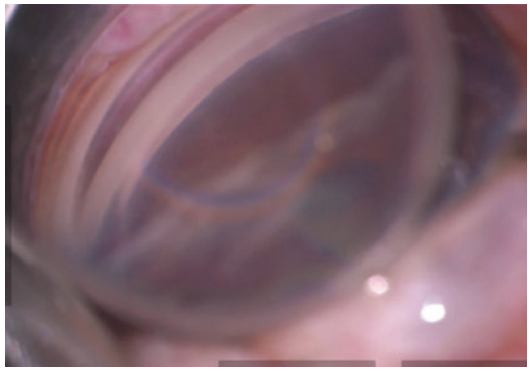

Fig. 15.6 Intraoperative gonioscopic image (using Swan Jacob lens) showing closed iridocorneal angle in a case of microspherophakia

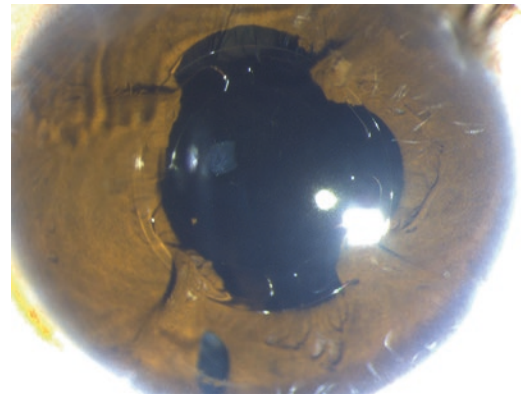

Fig. 15.7 Post-operative image of a case of microspherophakia managed with iris claw lens (Image credit: Dr. Kiranjeet Singh)

with two-thirds of blindness being attributed to glaucoma alone. Nearly three percent of the eyes with microspherophakia have associated corneal haze.

- The silhouette of the lens can be appreciated even in an undilated state because it is a small, spherical lens. It appears as a sudden dip in iris contour in the periphery all around, resembling the Latin "Ɛ" sign. This can help in suspecting the case in an undilated state and avoiding mydriasis-related pupillary block. Other investigations like ultrasound biomicroscopy can reveal elongated zonular fibers (>2 mm length as compared to normal less than 1 mm), increased lens sphericity, and ciliary body flattening in areas of missing zonules. The anteroposterior diameter of the lens will be larger >5 mm (normal: 3.5–4.5 mm), and the equatorial diameter will be shorter, an average of 6.75–7 mm (normal: 9 mm).
- Most eyes need surgical intervention even after laser iridotomy, especially in advanced cases, emphasizing that pupillary block is not the only mechanism leading to IOP rise in this condition, and lens extraction is needed for long-term IOP control. Lens extraction alone is not sufficient in chronic cases due to synechial angle closure.
- The technique of lens extraction (lensectomy with iris-claw lens (Fig. 15.7) (Video 15.1)/ scleral fixated IOL, anterior chamber IOL or bag fixation with sutured rings, and IOL implantation in the bag) is determined by the surgeon's choice and expertise as well as the extent of zonulopathy.

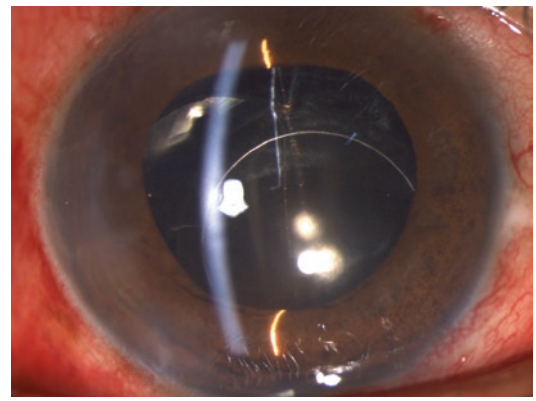

Fig. 15.8 Post-operative image of a patient with spherophakia presenting after 8 years of initial surgery showing decentered intraocular lens

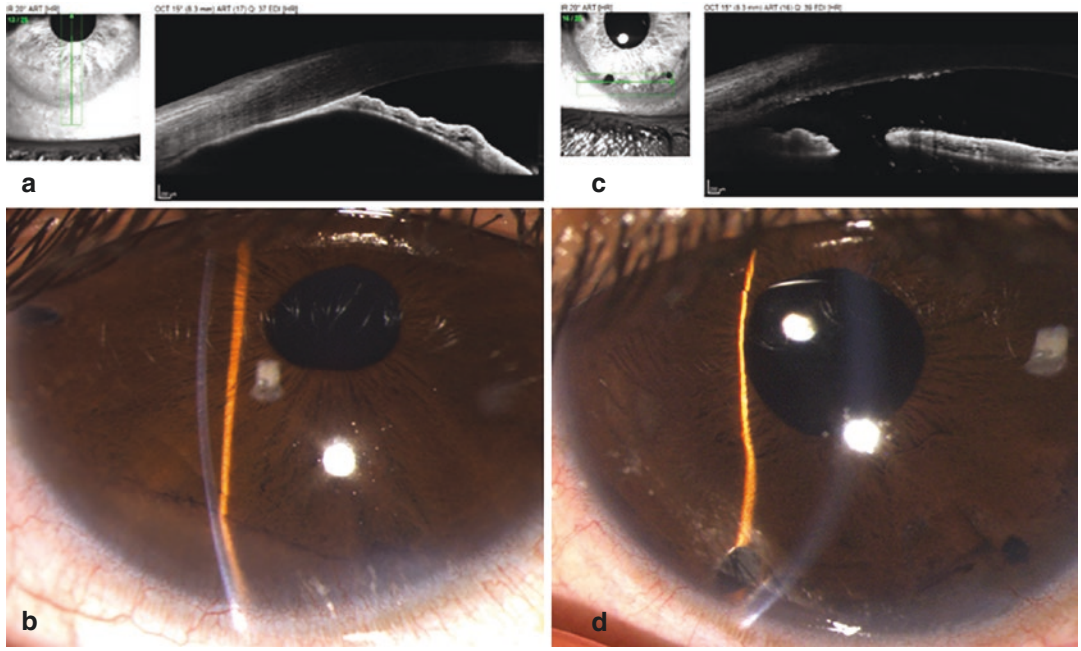

Fig. 15.9 Preoperative ASOCT (**a**) and slit-lamp imaging (**b**) shows irregular anterior chamber depth with inferior shallowing and peripheral anterior synechiae formation. Postoperatively with the help of localized surgical iridectomy, anterior chamber deepens regularly again as shown in ASOCT (**c**) and slit-lamp imaging (**d**). (Reproduced with permission: Gupta S, Mahalingam K, Ramesh P, Gupta V. Need of additional iridotomies despite lens extraction in spherophakes. BMJ Case Rep. 2021 Apr 19;14(4):e242838)

- Due to inherently weak zonules and the progressive condition, subluxation may worsen over time, and sutured CTR-bag complex may decenter over time requiring two-point fixation (Fig. 15.8).
- Despite lens extraction, additional iridotomies might be needed to prevent PAS formation and cause symmetric deepening of the anterior chamber (Fig. 15.9).
- Trabeculectomy, glaucoma drainage devices, and pars plana lensectomy and vitrectomy combined with transvitreal endocyclophotocoagulation are other options in advanced glaucomas.
- Younger age at presentation, higher IOP, and a greater number of glaucoma medications are associated with the risk of failure of lensectomy alone. Angle closure is the most common presentation; however, a possible developmental anomaly could lead to refractory open-angle glaucoma.

15.3 Management Algorithm for Phacotopic Glaucomas (Fig. 15.10)

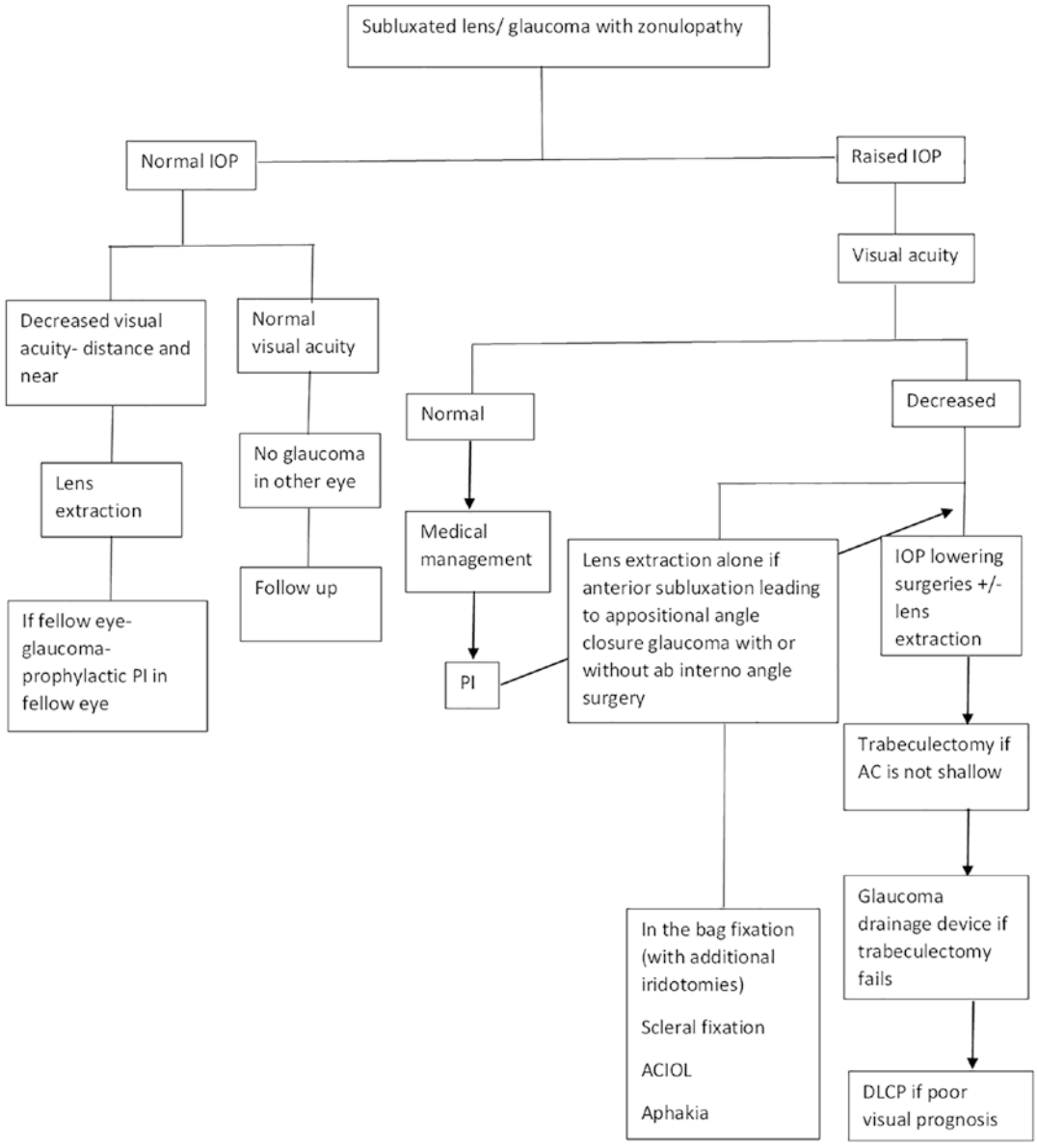

Fig. 15.10 Flowchart of management. *IOP* intraocular pressure, *PI* peripheral iridotomy, *DLCP* diode laser cyclophotocoagulation, *AC* anterior chamber, *ACIOL* anterior chamber intraocular lens

15.4 Conclusions

A case-by-case approach is essential in children with glaucoma associated with lenticular anomalies. The timing of intervention is very important. Lensectomy is important to control IOP despite the presence of patent iridotomy in most cases. Sometimes multiple iridotomies are required to prevent sectoral iris bombe. However, lensectomy alone may not be sufficient in all cases in controlling IOP, especially in eyes with late presentation with synechial angle closure. Such cases may additionally need filtration surgery. The control of IOP is very essential for visual rehabilitation in such children, and all the benefits of lensectomy could be negated by glaucoma, leading to poor vision. Along with the control of IOP, it is important to perform refraction at periodic intervals and prescribe glasses to prevent amblyopia.

Suggested Reading

Burian HM, Allen L. Histologic study of the chamber angle of patients with Marfan's syndrome: a discussion of the cases of Theobald, Reeh and Lehman, and Sadi de Buen and Velazquez. Arch Ophthalmol. 1961;65(3):323–33.

Dagi LR, Walton DS. Anterior axial lens subluxation, progressive myopia, and angle-closure glaucoma: recognition and treatment of atypical presentation of ectopia lentis. J Am Assoc Pediatr Ophthalmol Strabismus. 2006;10(4):345–50.

Ellant JP, Obstbaum SA. Lens-induced glaucoma. Doc Ophthalmol. 1992;81(3):317–38. https://doi.org/10.1007/BF00161770. PMID: 1483374.

Goel N, Sharma R, Sawhney A, Mandal M, Choudhry RM. Lensectomy, vitrectomy, and transvitreal ciliary body photocoagulation as primary treatment for glaucoma in microspherophakia. J Am Assoc Pediatr Ophthalmol Strabismus. 2015;19(4):366–8.

Gupta S, Warjri G, Gupta V. 'Ɛ' sign: a clinical clue to the diagnosis of microspherophakia. Eye. 2020;34(3):597–9.

Gupta S, Mahalingam K, Ramesh P, Gupta V. Need of additional iridotomies despite lens extraction in spherophakes. BMJ Case Rep. 2021;14(4):e242838.

Harasymowycz P, Wilson R. Surgical treatment of advanced chronic angle closure glaucoma in Weill–Marchesani syndrome. J Pediatr Ophthalmol Strabismus. 2004;41(5):295–9.

Heath P. Secondary glaucoma due to the lens. Arch Ophthalmol. 1941;25(3):424–37.

Mannino G, Abdolrahimzadeh B, Calafiore S, Anselmi G, Mannino C, Lambiase A. A review of the role of ultrasound biomicroscopy in glaucoma associated with rare diseases of the anterior segment. Clin Ophthalmol. 2016;10:1453.

Rao DP, John PJ, Ali MH, Kekunnaya R, Jalali S, Garudadri CS, Senthil S. Outcomes of lensectomy and risk factors for failure in spherophakic eyes with secondary glaucoma. Br J Ophthalmol. 2018;102(6):790–5.

Senthil S, Rao HL, Hoang NT, Jonnadula GB, Addepalli UK, Mandal AK, Garudadari CS. Glaucoma in microspherophakia: presenting features and treatment outcomes. J Glaucoma. 2014;23(4):262–7.

Yasar T. Lensectomy in the management of glaucoma in spherophakia: is it enough? J Cataract Refract Surg. 2003;29(6):1052–3.

16 Sturge-Weber Syndrome and Associated Syndromes with Glaucoma

Ananya Parampalli Ravindra,
Karthikeyan Mahalingam, and Shikha Gupta

16.1 Sturge-Weber Syndrome

16.1.1 Background

Encephalotrigeminal angiomatosis, more commonly known as Sturge-Weber syndrome (SWS), is a congenital neurocutaneous vascular syndrome, recognized by its signature port-wine birthmark involving part of the trigeminal nerve distribution. It also involves two more organs apart from the skin, namely, the eye and the brain. With no familial predisposition and appearing sporadically, SWS has not been associated with any specific inheritance pattern and has been hypothesized to occur as a result of postzygotic mutation (mutation during early embryogenesis). A somatic activating mutation (R183Q) in the *GNAQ* gene has been recently recognized as the etiology of vascular abnormalities in SWS. The prevalence is almost 1:50,000, and there is no gender predilection.

16.1.2 Pathogenesis

The pathogenesis of Sturge-Weber syndrome, including its effects on various organs, has been described in Fig. 16.1.

A. P. Ravindra (✉) · K. Mahalingam · S. Gupta
Dr. Rajendra Prasad Centre for Ophthalmic Sciences,
All India Institute of Medical Sciences,
New Delhi, India
e-mail: shikhagupta@aiims.edu

Theories regarding the pathogenesis of glaucoma in SWS patients are:

- Congenital malformation of the anterior chamber angle leading to increased resistance to outflow of aqueous
- Increase in the episcleral venous pressure (EVP) due to arteriovenous shunts into the episcleral hemangiomas
- Fluid hypersecretion either by the ciliary body or the choroidal hemangiomas
- Premature aging of the trabecular meshwork Schlemm's canal complex giving rise to abnormal hemodynamics of episclera and anterior chamber angle

Case 16.1
A 10-month-old male infant was brought by parents with complaints of a reddish birthmark over the left half of his face. He recently started squeezing his eyes in response to light, with incessant watering of the left eye. The eye involved was bigger in comparison with the fellow eye.

Examination: The child had a left-sided facial cutaneous vascular malformation (port-wine stain) involving the distribution of ophthalmic and maxillary division of the trigeminal nerve (Fig. 16.2a), with prominent epibulbar blood vessels in that eye. A thorough examination under anesthesia revealed corneal diameters of 10 × 10 mm in the right eye, 12 × 11.8 mm in the

S. Gupta et al. (eds.), *Childhood Glaucoma*, https://doi.org/10.1007/978-981-19-7466-3_16

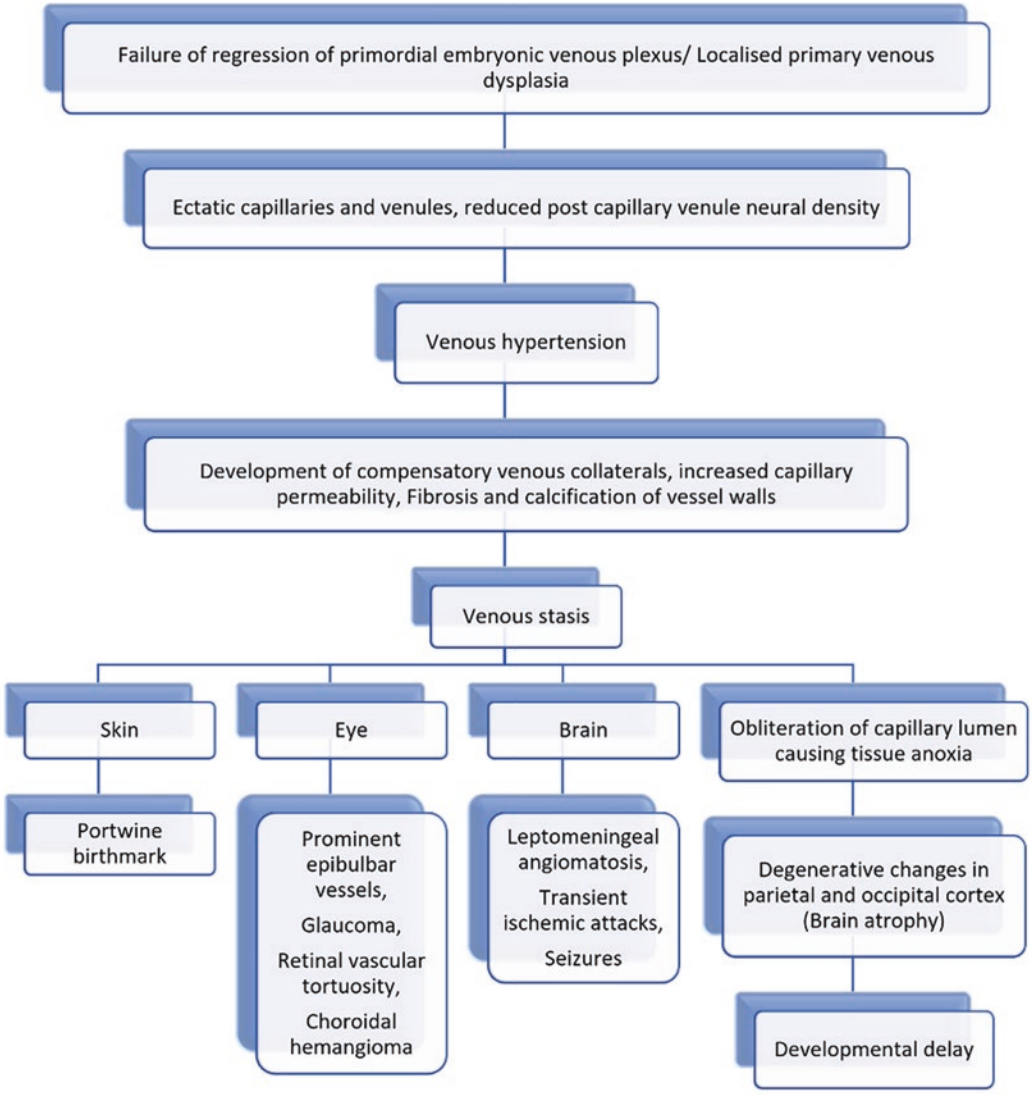

Fig. 16.1 A flowchart showing a brief description of the pathogenesis of Sturge-Weber syndrome and its clinical features

left eye, and intraocular pressure (IOP) of 12 mmHg and 24 mmHg in the right and left eyes, respectively, and on indirect ophthalmology, the left fundus showed orange-red glow (Fig. 16.2b), clear media, a tomato-ketchup appearance of the whole fundus suggestive of a diffuse choroidal hemangioma, and a vertical cup-disc ratio (CDR) of 0.8:1 with thinned out neuroretinal rim and tortuous retinal vessels. The fundus of the fellow eye was within normal limits.

Diagnosis: Sturge-Weber syndrome with left eye secondary congenital glaucoma.

Differential diagnoses:

- Klippel-Trenaunay syndrome: Port-wine stains are also located on a limb, along with varicose veins, abnormal bone, and soft-tissue growth. (Discussed in case 16.2)
- Cutis marmorata telangiectasia/Van Lohuizen syndrome: Marbled or fishnet appearance of the skin, especially of limbs and trunk, with

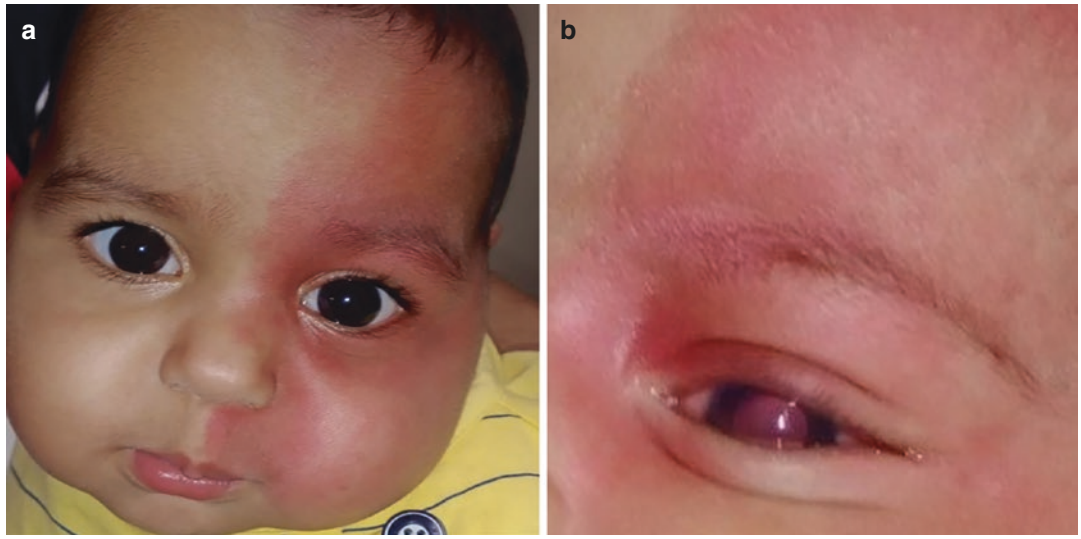

Fig. 16.2 (**a**) shows a left-sided facial cutaneous vascular malformation (port-wine stain) involving the distribution of ophthalmic and maxillary division of the trigeminal nerve, (**b**) reveals an orange-red choroidal reflex in the left eye

the face rarely involved, with under- or overgrowth of the involved area.

- Beckwith-Weideman syndrome: Facial naevus flammeus (port-wine stain) associated with macrosomia (infants larger than normal), macroglossia (large tongue), organomegaly, hemihypertrophy, omphalocele, or inguinal hernia due to an anterior abdominal wall defect.
- Neurofibromatosis 1 (NF-1/ Von Recklinghausen's disease): A neurocutaneous malformation where cutaneous lesions are colored similar to the appearance of coffee with milk, aptly known as café au lait spots, together with axillary and inguinal freckling, dermal and plexiform neurofibromata, and multiple neoplasms. (Fig. 16.3).
- Infantile hemangiomas: Historically called by various names like capillary hemangiomas, juvenile hemangiomas, hemangioblastomas, or strawberry nevi, these are benign vascular neoplasms that arise de novo (80% of which occur in the head and neck region) and undergo clonal proliferation, growing out of proportion to the somatic growth. They appear in the first few weeks of life as small flat plaques of telangiectatic vessels undergo rapid proliferation between 3 and 12 months of age and involute spontaneously from about 3 years of age (Fig. 16.4a, b).

Management

- The child was admitted for surgical management, and under anesthesia, the angles were assessed using a Swan-Jacob lens to look for angle anomalies and pre-trabeculotomy evaluation, and blood was visualized in the Schlemm's canal (Fig. 16.5a).
- A combined trabeculotomy-trabeculectomy was performed, taking care to avoid the conjunctival and episcleral prominent vessel loops (Fig. 16.5b, c).
- Postoperatively, the bleb was seen to be well-formed, with a deep anterior chamber and controlled IOP, and the child was discharged on topical antibiotics and steroids.
- On 3 months follow-up, the IOP was well controlled without any antiglaucoma medication.
- The treatment of glaucoma associated with SWS is challenging because of its early onset and associated severe visual field impairment, as well as unresponsiveness to standard medical treatment.
- The general treatment protocol for glaucoma associated with Sturge-Weber syndrome is as given in Fig. 16.6, which should be tailored to fit each patient, giving due consideration to

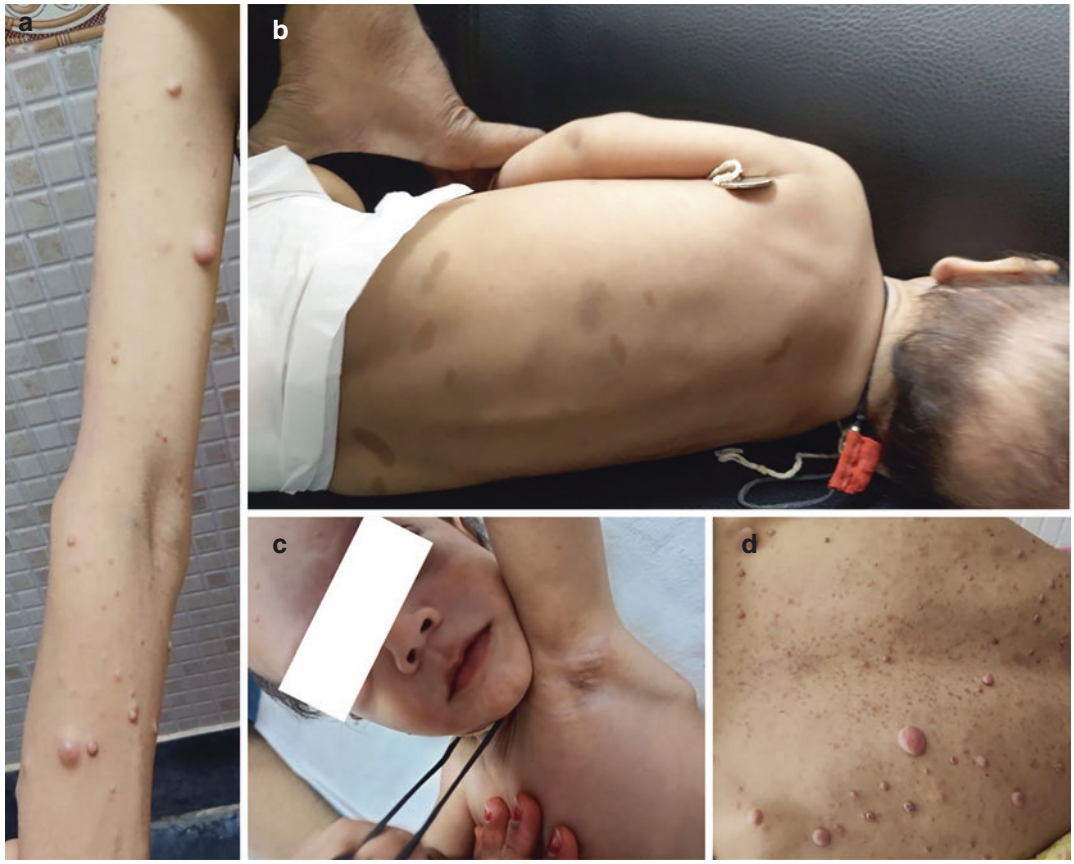

Fig. 16.3 (**a**) shows dermal neurofibromata on the arm of a child with Neurofibromatosis 1(NF-1), (**b**) shows Cafe au lait macules on the back of a child with NF-1, (**c**) shows axillary freckling, and (**d**) shows neurofibromata as well as cafe au lait spots on the back of a patient with NF-1

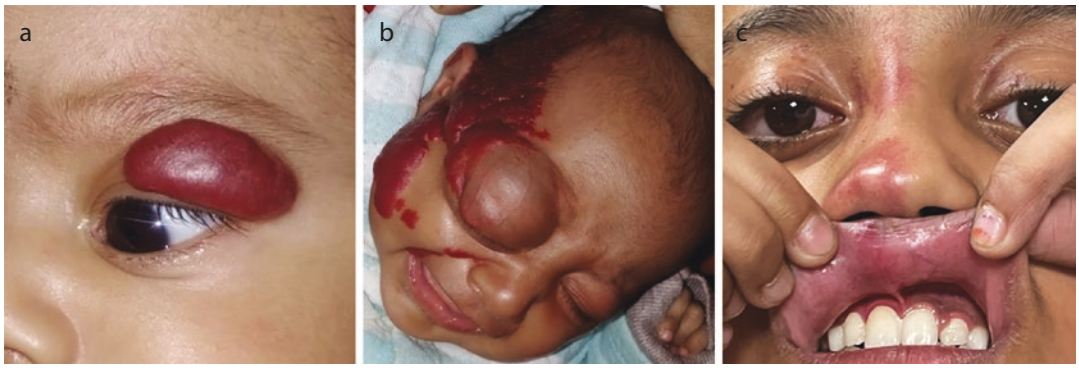

Fig. 16.4 (**a**) shows a clinical photograph of a child with infantile hemangioma of the upper eyelid, (**b**) is the clinical photograph showing the cutaneous involvement in an infant with PHACES (***p****osterior fossa malformations,* ***h****emangioma,* ***a****rterial anomalies,* ***c****oarctation of the aorta/****c****ardiac defects, and* ***e****ye abnormalities)* in the form of a segmental mixed hemangioma, (**c**) shows port-wine stain with labial and gingival involvement

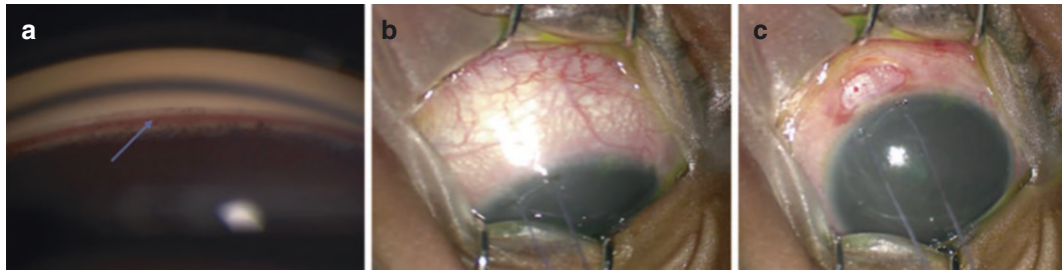

Fig. 16.5 (**a**) reveals a gonio-photograph showing blood in Schlemm's canal (blue arrow), (**b**), and (**c**) shows intraoperative photographs revealing prominent conjunctival, episcleral and scleral vessel loops

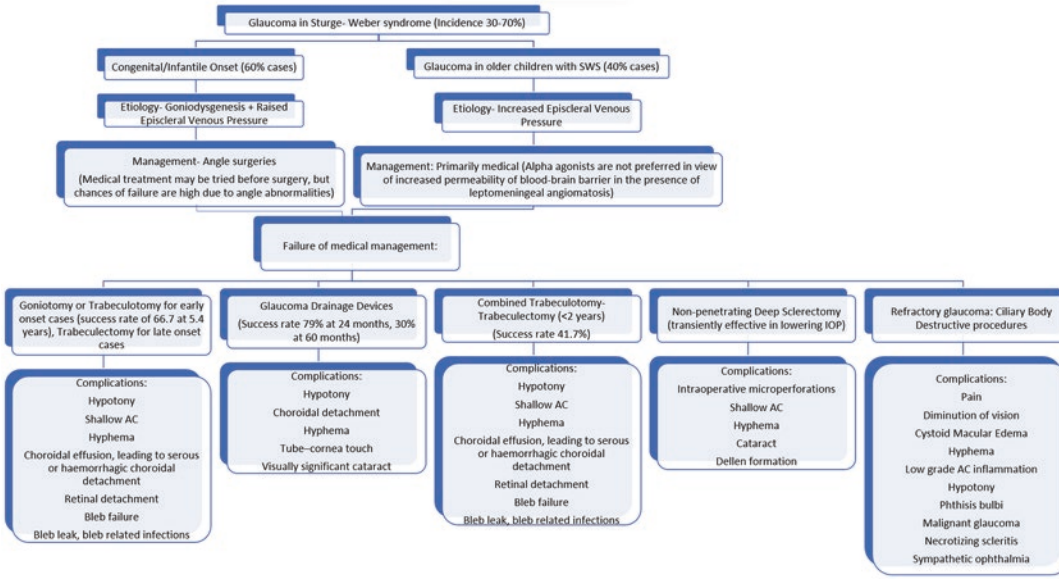

Fig. 16.6 A flowchart outlining the management of glaucoma in Sturge-Weber syndrome

the age of presentation, IOP, and coexistence of complications/sequelae.

Complications: Filtration surgeries carry a high risk of complications such as:

- *Cataract*: Cataracts can be preexistent in a patient with SWS as one of the associated anterior segment abnormalities but can also occur postoperatively due to tube-lens touch following glaucoma drainage devices, shallow anterior chamber following any angle/filtration surgery (Fig. 16.7), or following external beam radiotherapy for choroidal hemangioma. Any visually significant cataract needs to be managed surgically at the earliest to prevent the development or worsening of visual deprivation amblyopia. Lens aspiration should be performed, after which a posterior capsulorhexis with anterior vitrectomy can be done to reduce the occurrence of visual axis opacification, especially for children aged <6–8 years.
- *Choroidal effusion*: Filtration surgeries are associated with high risk of choroidal effusion (intraoperatively in 10–40%, postoperatively in 16.7%) (Fig. 16.8a, b), particularly in eyes with choroidal hemangioma, because the sudden fall in IOP intraoperatively may induce the transudation of fluid from a fragile vessel in the hemangioma.

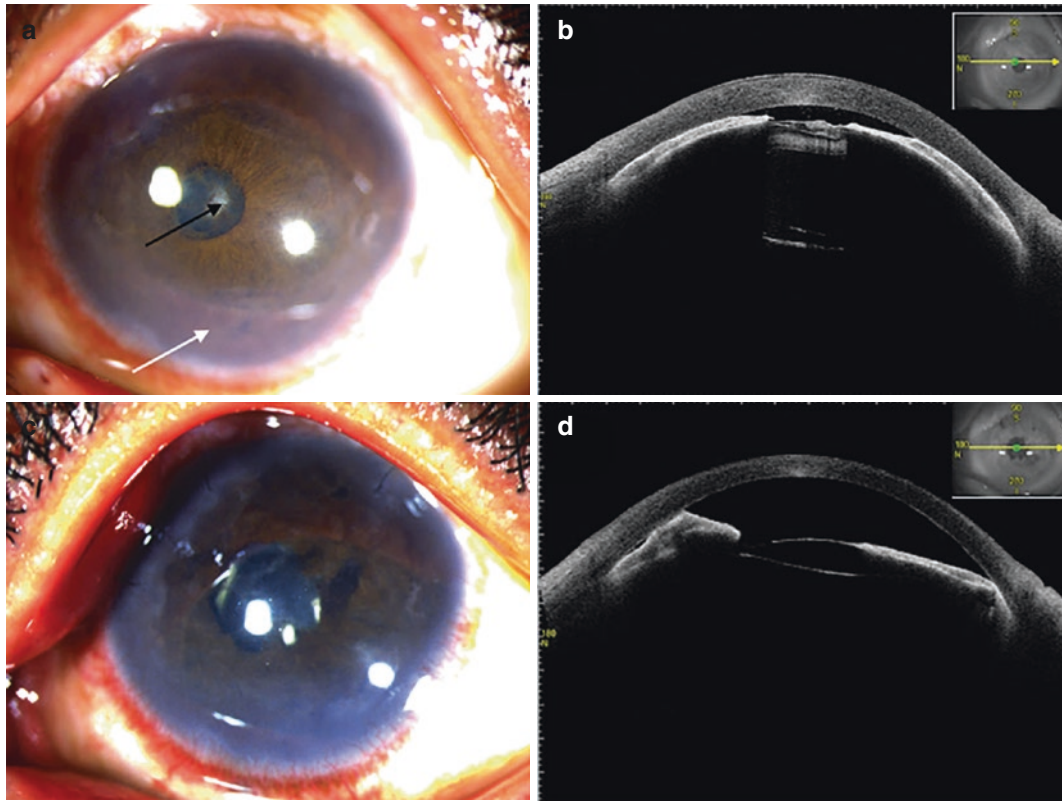

Fig. 16.7 (**a**) Shows a preoperative slit-lamp biomicroscopic image showing 360° peripheral anterior synechiae (white arrow) with shallow anterior chamber, with pigments over the anterior capsule of the lens and anterior subcapsular cataract (black arrow) in an eye with SWS operated for trabeculectomy in childhood following overfiltering bleb, (**b**) shows the AS-OCT image of the same eye revealing iridocorneal touch with the flat anterior chamber and cataractous lens. (**c**) is a postoperative slit-lamp biomicroscopic image showing PCIOL in situ following cataract extraction in the same eye, (**d**) shows the AS-OCT image of the same eye showing persistent iridocorneal touch nasally, temporally formed anterior chamber, and PCIOL in situ

Some of the prophylactic measures that can be taken to prevent the devastating complications of filtering surgery in SWS are:

- Usage of viscocohesive/viscoelastic to keep the anterior chamber formed viscocohesive viscoelastic at all times, AC maintainer to prevent rapid fall of IOP and fluid transudation from the choroidal layer
- Quick suturing of the flap (with the help of placing pre-placed sutures before making an osmium)
- The use of releasable sutures
- Pre-placed posterior sclerostomies
- Prophylactic laser photocoagulation, prophylactic radiotherapy
- Cauterization of the anterior episcleral vessel anomalies

Perioperative oral propranolol (i.e., 2 mg/kg of body weight daily in two divided doses, started 1 week before surgery and continued for 6 weeks after surgery) has been shown to be safe and effective in minimizing the development of sight-threatening choroidal effusion.

Cyclodiode treatment (diode laser cyclophotocoagulation) has been proposed as a safer alternative to filtration surgery because it avoids a sudden decrease of the IOP, reducing the risk of massive choroidal effusion. Other complications are mentioned in the flowchart (Fig. 16.6).

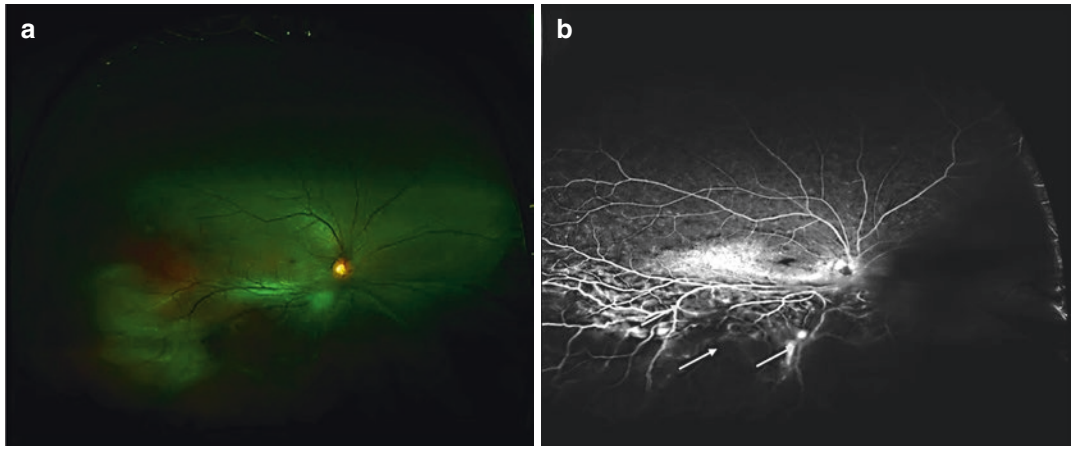

Fig. 16.8 (**a**) Shows an ultrawide field pseudocolor fundus photo of the right eye showing diffuse choroidal hemangioma with inferior and nasal exudative retinal detachment (**b**) shows the fluorescein angiography of the same eye in mid-venous phase showing inferior and nasal exudative retinal detachment. Note the peripheral capillary nonperfusion areas (blue arrow), venous dilatation (yellow arrow), and paravascular leaks (green arrow)

Case 16.2

A 17-year-old male came with complaints of diminution of vision in both eyes for the past 6 months. The patient had a red-colored birthmark over the face since birth, with a large nose and broad nasal bridge and large lips (Fig. 16.9), and similar nevi over the chest and left arm with increased length and girth of that arm with doughy consistency on palpation.

Examination: Ocular examination revealed intraocular pressures of 38 mmHg and 34 mmHg in the right and left eyes, respectively, dilated, tortuous conjunctival vessels, deep anterior chambers, reactive pupils, clear lenses, a vertical cup-disc ratio of 0.9:1 in both eyes, and a tomato ketchup appearance of the fundus, suggestive of a diffuse choroidal hemangioma in both eyes.

Diagnosis: Klippel-Trenaunay-Weber syndrome with B/E secondary open angle glaucoma due to raised episcleral venous pressure.

Treatment: The patient was started on E/d latanoprost HS (prostaglandin analogs increase uveoscleral outflow bypassing the obstacle to the passage of the aqueous humor due to raised episcleral venous pressure) and other glaucoma medications. As target IOP was not achieved, the patient was advised admission for trabeculectomy of the right eye, followed by left eye.

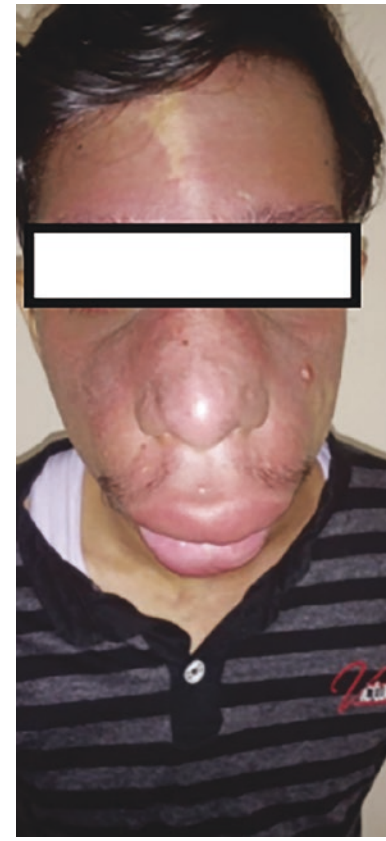

Fig. 16.9 Shows port-wine stain, large nose with broad nasal bridge, and large lips in a patient with Klippel-Trenaunay-Weber syndrome

16.2 Klippel-Trenaunay-Weber Syndrome

Klippel-Trenaunay-Weber syndrome, a rare (incidence—1:100,000), multisystem disorder, is characterized by the characteristic triad of a port-wine stain, varicose veins, and bony/soft-tissue hypertrophy (diagnosis can be made when at least two of the three are present, but 63% cases exhibit all three). When associated with arteriovenous shunting, the condition has also been called the **Parks-Weber syndrome**.

16.2.1 Ocular Signs

- Anterior segment: Conjunctival telangiectasias, iris coloboma, heterochromia, cataracts, glaucoma due to anterior chamber angle malformation, or elevated episcleral venous pressure (similar to glaucoma in SWS).
- Posterior segment: Persistent fetal vasculature, chiasmal, and bilateral optic nerve gliomas, optic disc drusen, myelinated nerve fibers, and retinal dysplasia, retinal varicosities and dilated retinal veins, and choroidal hemangiomas (most common ocular feature).

16.2.2 Systemic Signs

- Varicose veins, which may be complicated by lymphedema, thrombophlebitis, and venous ulcers. Involvement of internal organs like the colon, liver, spleen, or bladder can lead to internal hemorrhage leading to significant morbidity and mortality.
- Hypertrophy of soft tissues and bone (more often seen in the lower limbs, but any part of the body can be affected) may lead to massive overgrowth of that limb.
- Mental retardation, especially in patients with hemangiomas of the face and head.

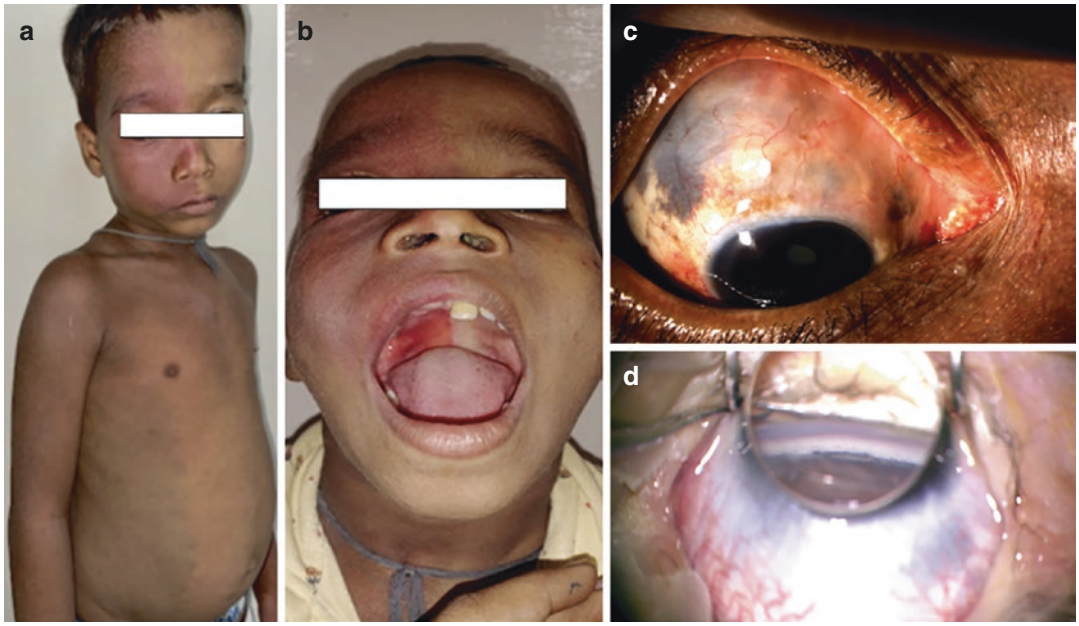

Fig. 16.10 (**a**) Shows clinical photographs of the child with port-wine stain and dermal melanosis (phakomatosis cesio flammea/phakomatosis pigmentovascularis II), (**b**) shows palatal involvement (**c**) Shows slit lamp biomicroscopic image of the right eye of the patient revealing the presence of nevus of Ota, (**d**) shows an intraoperative view of the anterior chamber angle through a Swan-Jacob Lens, demonstrating open angles with dense iris processes and increased trabecular pigmentation

16.2.3 Differential Diagnosis

Refer to Sturge-Weber syndrome (SWS).

16.2.4 Management

Similar to the management of glaucoma in SWS.

Case 16.3
A 7-year-old boy was referred from the department of dermatology for ophthalmological evaluation, after being diagnosed with phakomatosis pigmentovascularis. He had a large erythematous vascular nevus distributed over the right half of his face, with a similar distribution within the oral cavity, blue-gray pigmented lesion over his chest and right arm (Fig. 16.10a, b), along with multiple blue-gray-colored spots on the buttocks and lower back, and a depigmented patch on the upper back.

Examination: The patient had a visual acuity of 6/6 in both eyes, and intraocular pressures were 24 mmHg and 12 mmHg in the right and left eyes, respectively. While the left eye was within normal limits on slit-lamp biomicroscopy, the right eye showed a slate gray discoloration over the sclera (Fig. 16.10c), with a clear cornea, deep anterior chamber, and clear lens. On dilated fundoscopy, the right eye showed a CDR of 0.8:1, while the left eye had a CDR of 0.3:1. There were no associated choroidal hemangiomas.

Diagnosis: Phacomatosis pigmentovascularis with right eye secondary open angle glaucoma.

Treatment: The patient was admitted for surgical management, and under general anesthesia, the angles of the right eye visualized preoperatively using a Swan-Jacob Lens demonstrated open angles with dense iris processes and increased trabecular pigmentation (Fig. 16.10d). Gonioscopy-assisted transluminal trabeculotomy was performed, and the child was noted to have hyphema (~2 mm) on post-op day 1, with an IOP of 10 mmHg on NCT in the operated eye. The patient was advised propped up position and topical antibiotic-steroid combination along with pilocarpine and, on follow-up at 1 week, was found to have no hyphema and IOP of 10 mmHg in the right eye.

16.3 Phakomatosis Pigmentovascularis

Phakomatosis pigmentovascularis (PPV) is a rare (incidence: 0.2–0.5 per 10,000 live births) congenital syndrome characterized by the simultaneous existence of pigmentary naevi and vascular malformation.

16.3.1 Pathogenesis

The pathogenesis of PPV is still unclear. It has been suggested that genetic aberrations in vasomotor nerve cells and melanocytes, both derived from common neuroectodermal precursor cells, may be responsible for the association of vascular and pigmented nevi.

Another proposed model goes by the name twin spotting or didymosis. Twin spots are two different cutaneous areas (lesions) adjacent to one another, appearing as a result of the cells' loss of genetic heterozygosity, formed by mutant tissues that also differ from the rest of the normal tissue surrounding them. This can explain the coexistence of vascular and pigmented lesions.

16.3.2 Clinical Features

16.3.2.1 Dermatological Features

- Port-wine stain
- Melanocytic nevi/moles
- Epidermal nevi
- Dermal melanocytosis (areas of blue-gray discoloration)
- Nevus anemicus (areas of lighter skin)
- Hyperpigmentation (areas of darker skin)
- Cafe-au-lait spots
- Nevus of Ota
- Nevus of Ito (hyperpigmentation of shoulder and upper arm area, i.e., shoulder girdle)

Table 16.1 Classification of phakomatosis pigmentovascularis (Happle R. Phakomatosis pigmentovascularis revisited and reclassified. Arch Dermatol. 2005 Mar;141(3):385–8. doi: 10.1001/archderm.141.3.385. PMID: 15781681)

Traditional classification	Happle's classification	Vascular lesion	
PPV I	–	Nevus flammeus	Epidermal nevus
PPV II	Phakomatosis cesio flammea	Nevus flammeus ± Nevus anemicus	Dermal melanocytosis
PPV III	Phakomatosis spilorosea	Nevus flammeus ± Nevus anemicus	Nevus spilus
PPV IV	Unclassified	Nevus flammeus ± Nevus anemicus	Dermal melanocytosis ± Nevus spilus
PPV V	Phakomatosis cesio marmorata	Cutis marmorata telangiectasia congenita (CMTC)	Dermal melanocytosis

- Nevus spilus/naevoid lentigo (light brown patch of pigmentation containing multiple tiny dark brown spots within it)

16.3.2.2 Ocular Features

- Ocular melanosis along with nevus of Ota affecting one or both eyes, giving rise to complications like glaucoma and melanoma
- Iris hamartomas, iris mammillations, and iris nodules

16.3.2.3 Neurologic Abnormalities

- Developmental delay
- Seizures
- Intracranial calcifications
- Cerebral atrophy

16.3.2.4 Syndromic Associations

- Sturge-Weber syndrome
- Klippel-Trenaunay syndrome (Table 16.1)

16.3.3 Management

Skin lesions: Laser treatment (pulsed dye laser for nevus flammeus, Q-switched lasers for pigmentary nevus) has proved to be beneficial in improving the appearance of skin lesions. Early treatment is recommended since congenital lesions may grow in proportion with the body.

Congenital glaucoma: It can occur in both oculodermal melanosis (Naevus of Ota) and Sturge-Weber, Klippel-Trenaunay Weber syndromes, more often in the latter when the ophthalmic division is involved, suggesting that the vascular malformation predisposes more strongly to the development of glaucoma than the pigmented lesion. Accumulation of melanocytes in angle (as seen by electron microscopy) could be one possible mechanism for developing glaucoma secondary to oculodermal melanosis. Congenital glaucoma is more common when both are present at birth, extensively involving the globe. However, elevated lOP can also appear later in life, for which they should be examined thoroughly for associated conditions and should be kept on regular follow-up.

16.4 Conclusions

Glaucoma may occur in conjunction with multiple systemic phacomatosis such as, in association with Sturge-Weber Syndrome, Klippel-Trenaunay-Weber Sndrome and Phakomatosis pigmentovascularis. SWS is a congenital neurocutaneous vascular syndrome, and as the name explains, it affects the skin and the central nervous system, apart from the multiple ocular associations. Glaucoma occurring in infancy in SWS is refractory to medical treatment, due to the component of goniodysgenesis, and needs surgical therapy as first line of management, but on the

other hand, glaucoma presenting later in life can be managed medically and surgery is resorted to only in cases unresponsive to the same. Klippel-Trenaunay-Weber syndrome is characterised by the classical triad of a port-wine stain, varicose veins, and bony/soft-tissue hypertrophy and glaucoma can occur due to anterior chamber angle malformation, or elevated episcleral venous pressure, similar to that in SWS, and is managed similarly. PPV is a rare syndrome consisting of dermatological features like melanocytic nevi amongst others and ocular features like ocular melanosis along with Nevus of Ota which may be associated with glaucoma and melanoma.Timely management of glaucoma associated with these syndromes can yield a useful vision to the children.

Suggested Reading

Abdolrahimzadeh S, Scavella V, Felli L, Cruciani F, Contestabile MT, Recupero SM. Ophthalmic alterations in the Sturge-Weber Syndrome, Klippel-Trenaunay Syndrome, and the phakomatosis pigmentovascularis: an independent group of conditions? Biomed Res Int. 2015;2015:786519. https://doi.org/10.1155/2015/786519.

Dorairaj S, Ritch R. Encephalotrigeminal angiomatosis (Sturge-Weber Syndrome, Klippel-Trenaunay-Weber Syndrome): a review. Asia Pac J Ophthalmol. 2012;1(4):226–34. https://doi.org/10.1097/APO.0b013e31826080a9. PMID: 26107478.

Javaid U, Ali MH, Jamal S, Butt NH. Pathophysiology, diagnosis, and management of glaucoma associated with Sturge-Weber syndrome. Int Ophthalmol. 2018;38(1):409–16. https://doi.org/10.1007/s10792-016-0412-3.

Mantelli F, Bruscolini A, La Cava M, Abdolrahimzadeh S, Lambiase A. Ocular manifestations of Sturge-Weber syndrome: pathogenesis, diagnosis, and management. Clin Ophthalmol. 2016;10:871–8. https://doi.org/10.2147/OPTH.S101963.

Patrianakos TD, Nagao K, Walton DS. Surgical management of glaucoma with the Sturge Weber syndrome. Int Ophthalmol Clin. 2008;48(2):63–78. https://doi.org/10.1097/IIO.0b013e3181693582. PMID: 18427262.

Teekhasaenee C, Ritch R. Glaucoma in phakomatosis pigmentovascularis. Ophthalmology. 1997;104(1):150–7. https://doi.org/10.1016/s0161-6420(97)30346-7. PMID: 9022120.

Teekhasaenee C, Ritch R, Rutnin U, Leelawongs N. Glaucoma in oculodermal melanocytosis. Ophthalmology. 1990;97(5):562–70. https://doi.org/10.1016/s0161-6420(90)32540-x.

Thavikulwat AT, Edward DP, AlDarrab A, Vajaranant TS. Pathophysiology and management of glaucoma associated with phakomatoses. J Neurosci Res. 2019;97(1):57–69. https://doi.org/10.1002/jnr.24241. Epub 2018 Apr 1. PMID: 29607552.

17 Miscellaneous Secondary Childhood Glaucomas

Ananya Parampalli Ravindra,
Karthikeyan Mahalingam, and Shikha Gupta

A plethora of congenital conditions like intrauterine infections, developmental anomalies of the eye, and other underlying medical conditions have been known to be associated with early onset glaucomas. What sets them apart from primary glaucomas is the need to address other associations of such conditions in addition to managing glaucoma. In this chapter, we briefly discuss a few handpicked cases that had varied presentations, including glaucomas occurring secondary to congenital rubella syndrome, persistent fetal vasculature, keratomalacia, oculodermal melanocytosis, and microphthalmos.

Case 17.1

A 5-day-old female child was brought to the outpatient department of a tertiary eye clinic, with a history of watering and squeezing shut of eyes in response to bright light. There was no history of glaucoma in any family member. The mother had an episode of mild fever in the seventh week of pregnancy, during which she also had enlarged painful lymph nodes, which lasted for not more than 3 days, and for which she did not seek medical help.

Examination: An examination under anesthesia (EUA) was planned, and the child was detected to have an atrial septal defect during the pre-anesthesia checkup. The EUA revealed bilateral cloudy corneas with poor view of the intraocular structures. Intraocular pressure (IOP) was 36 mm Hg in the right eye and 32 mm Hg in the left eye. Corneal diameters were 12 × 12 mm and 11.8 × 12 mm in the right and left eyes, respectively (Fig. 17.1).

Keeping a high index of suspicion, Rubella serology was ordered for both mother and child, both of whom were found to have high titers of IgM antibodies.

Diagnosis: Congenital rubella syndrome with B/E secondary glaucoma.

Differential diagnoses:

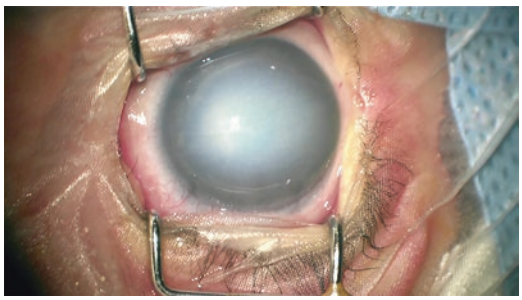

Fig. 17.1 Shows the clinical image of the right eye of the child, showing enlarged cornea with limbal stretching, with diffuse corneal haze

Supplementary Information The online version contains supplementary material available at https://doi.org/10.1007/978-981-19-7466-3_17.

A. P. Ravindra (✉) · K. Mahalingam · S. Gupta
Dr. Rajendra Prasad Centre for Ophthalmic Sciences, All India Institute of Medical Sciences, New Delhi, India
e-mail: shikhagupta@aiims.edu

S. Gupta et al. (eds.), *Childhood Glaucoma*, https://doi.org/10.1007/978-981-19-7466-3_17

- Neonatal primary congenital glaucoma: Presents within the first month of life, with the classic triad of epiphora, photophobia, and blepharospasm, and should be considered once intrauterine infections have been ruled out by serological tests.
- Congenital cytomegalovirus (CMV) infection with secondary glaucoma: Glaucoma is a rare manifestation of intrauterine infection with CMV, whose common ocular signs are chorioretinitis, optic atrophy, pigmentary retinopathy, and strabismus. Systemic features associated with it are petechiae, thrombocytopenia, hepatosplenomegaly, hyperbilirubinemia and jaundice, sensorineural hearing loss, microcephaly, intracranial calcifications manifesting as seizures, or fetal hydrops.
- Glaucoma associated with congenital syphilis: Presents late, secondary to chronic anterior uveitis and deep corneal stromal neovascularization associated with interstitial keratitis.

Treatment: The patient underwent combined trabeculotomy with trabeculectomy with 0.04% mitomycin C of the right eye followed by the left and with the exception of minimal hyphema on post-operative day 1 in the right eye, which resolved over the next 3 days, the course has been uneventful.

17.1 Congenital Rubella Syndrome

17.1.1 Background

Rubella (German Measles), a mild but highly contagious disease, is a viral illness (caused by Rubella virus, an enveloped, positive-stranded RNA virus) characterized by maculopapular rash, lymphadenopathy, and fever. However, maternal infection during the first trimester of pregnancy can cause a miscarriage, fetal death, or a wide spectrum of fetal malformations known as congenital rubella syndrome (CRS).

17.1.2 Pathogenesis

Ten percent of patients with congenital glaucoma syndrome develop glaucoma at some point, which may occur due to multiple reasons, some of which are outlined in Fig. 17.2.

17.1.3 Clinical Features

Congenital defects and glaucoma occur at a higher rate if the exposure is earlier in gestation: 100% in the first trimester, 30% in the second trimester, and no such risk in the third trimester, when organogenesis is almost complete.

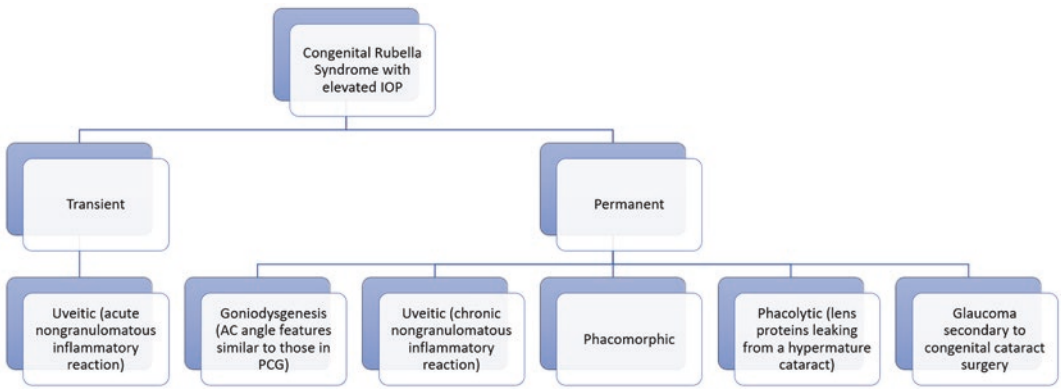

Fig. 17.2 Shows the pathomechanisms of elevated intraocular pressure (IOP) in congenital rubella. *AC* anterior chamber, *PCG* primary congenital glaucoma

17.1.3.1 Systemic Features

Systemic signs of congenital rubella present at birth consist of: classic rubella syndrome: Ocular, cardiac (partial pulmonary aretery stenosis or patent ductus arteriosus) and hearing defects where ocular defects are by far the commonest (78%)

- Sensorineural hearing loss (most common extraocular manifestation, seen in 66% cases)
- Congenital cardiac defects (58%)
- Microcephaly and mental retardation (42%)
- Intrauterine growth restriction (5–15%)
- "Blueberry muffin" rash
- Lymphadenopathy
- Thrombocytopenia
- Hepatosplenomegaly
- Interstitial pneumonia
- Radiolucent bone lesions

17.1.3.2 Ocular Features:

- Pigmentary retinopathy (most characteristic finding) (reported in 9–61% cases)
- Strabismus (9–60%)
- Cataract (seen in approximately 16–85% of cases) (Video 17.1)
- Microphthalmia and/or microcornea (which usually present concurrently, 10–63%)
- Chronic iridocyclitis
- Optic atrophy (9%)
- Corneal haze due to viral endotheliopathy. Congenital rubella syndrome with glaucoma presenting as cloudy cornea without buphthalmos is a ubiquitous presentation
- Glaucoma (seen in approximately 2–25% of cases) (can also present with corneal haze) (nearly one-third of these cases have associated cataract)
- Phthisis bulbi
- Double ring sign in iris due to peripheral iris hypoplasia is a pathognomonic feature of congenital rubella syndrome (Fig. 17.3). Most eyes with rubella and congenital glaucoma are microphthalmic; however, approximately 20% eyes may manifest with buphthalmos.

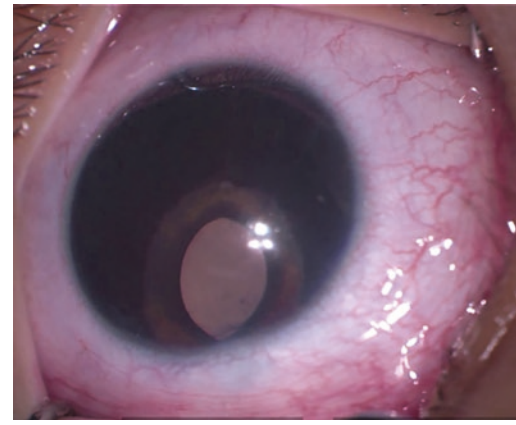

Fig. 17.3 Shows the clinical image of an eye with eccentric pupil, with peripupillary iris hypopigmentation secondary to peripheral iris hypoplasia giving rise to the characteristic 'double ring sign' of Congenital rubella

17.1.4 Investigations

- IgM antibodies to rubella can be detected by serology in cord blood.
- Though a raised IgG titer in throat culture or serum is not confirmatory since IgG can be transferred transplacentally, serially rising IgG titers may point toward the production of the same by the fetus, suggesting active infection.

17.1.5 Management

A summary of the approach to a case of congenital rubella with elevated intraocular pressures specific to the mechanism of glaucoma is outlined in Fig. 17.4.

Management of these patients should be tailored on a case-to-case basis.

Learning Points

- Fever with associated rash in an antenatal mother warrants investigations at the earliest, as many viral infections can have a devastating impact, both systemic and ocular, in the fetus.

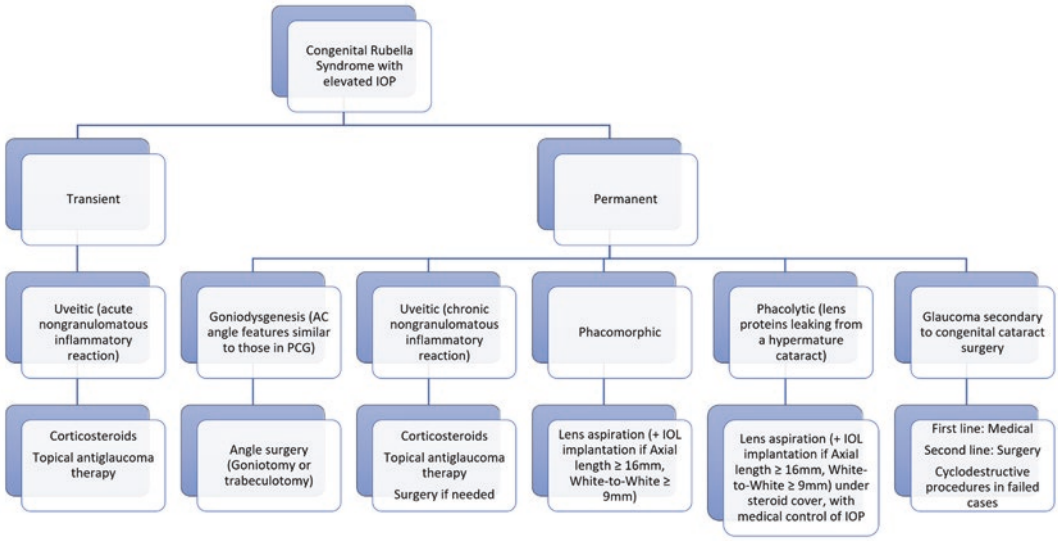

Fig. 17.4 Gives a guide to the management of elevated pressures in specific circumstances in case of congenital rubella syndrome. *IOP* intraocular pressure, *AC* anterior chamber, *PCG* primary congenital glaucoma, *IOL* intraocular lens, *WTW* white to white, *AL* axial length

- When glaucoma in a neonate presents with other ocular features, further investigations are necessary.
- Anti-rubella IgM antibodies are specific for acute infection in the child, while IgG antibodies could be transmitted transplacentally, but a serial rise in titers would point toward active infection in the child.
- A thorough systemic evaluation can lead to early detection of other organ involvement and prevention of severe morbidity.

Case 17.2

The parents of a 4-month-old male infant brought him to the emergency department of a tertiary care center for a second opinion after being diagnosed as a case of unilateral retinoblastoma at an outside hospital, where he was taken with complaints of white reflex in the left eye, and being advised to undergo enucleation. The child was a full-term, normal birthweight baby with an uneventful perinatal and postnatal period, with no family history of malignancy.

Examination findings: The corneal diameters of the left eye were 10 × 10 mm, with shallow AC, total white cataract and poor fundal glow on EUA (Fig. 17.5a). IOP was 34 mmHg using Perkin's applanation tonometer.

An ultrasound was performed for posterior segment examination, which showed a stalk-like structure connecting the posterior aspect of the cataractous lens with the posterior pole (Fig. 17.5b).

Diagnosis: Persistent fetal vasculature (previously known as persistent hyperplastic primary vitreous) with total white cataract with secondary buphthalmos.

Differential diagnoses:

- Retinoblastoma: The first differential to be considered in a case of leukocoria, which is usually associated with an increase in the size of the eyeball, a positive family history, and mass lesion with characteristic calcification seen on Ultrasonography (USG) or Computed Tomography (CT) (Fig. 17.6).
- Coat's disease: Typically seen in children of about 4–8 years of age, more in males than females, with exudative retinal detachment with normal size and shape of the globe and normal lens morphology.
- Retinal toxocariasis: Presents by the age of 2–8 years, with features of chronic endophthalmitis.

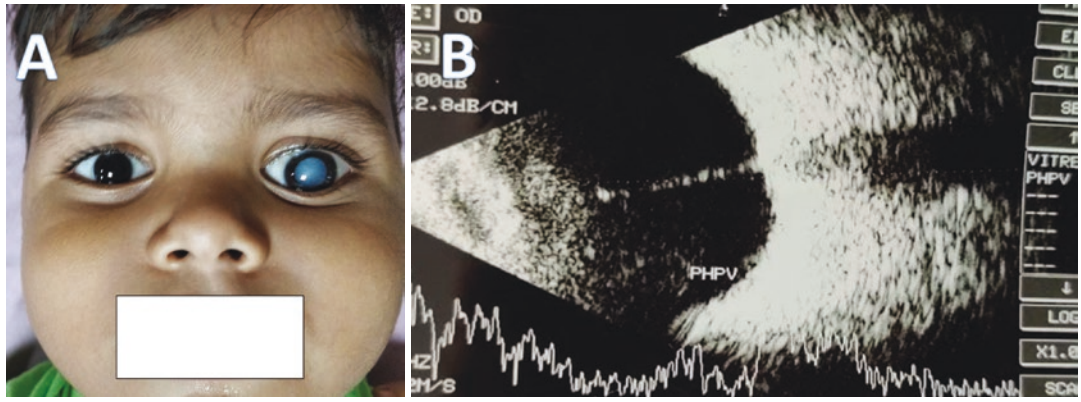

Fig. 17.5 (**a**) Shows the face photo of the child with left eye total white cataract with visibly enlarged left cornea. (**b**) Shows an image of the ultrasound (B and A) scans, showing a stalk-like structure in the vitreous cavity, connecting the cataractous lens to the optic nerve head, suggestive of persistent fetal vasculature

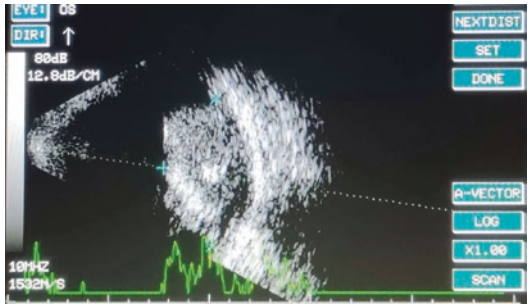

Fig. 17.6 Shows an ultrasound B scan image of a mass lesion in the vitreous cavity with the A scan showing high spikes (at gain 80dB) indicating calcification. (Image courtesy: Dr. Nimmy Raj)

- Retinopathy of prematurity: Classic history of premature birth, low birth weight, oxygen therapy (excess oxygen therapy in term neonates has also been shown to cause this retinopathy), and bilaterality.

Treatment: Our patient underwent left eye lens aspiration following which Fugo blade (Plasma knife) was used to cauterize the vascular stalk, and this was followed by implantation of PCIOL in sulcus, with simultaneous trabeculectomy, after which IOP normalized. He is now under regular follow-up.

17.2 Persistent Fetal Vasculature (PFV)

17.2.1 Background

The primary vitreous is formed during the first month of intrauterine life and is supplied by the hyaloid system of vessels. Formation of the avascular secondary vitreous commences at around 9 weeks of intrauterine life, during which the hyaloid artery begins to regress. Persistent fetal vasculature (PFV), as the name suggests, occurs due to incomplete regression of the embryonic vitreous and the hyaloid vasculature.

Bilateral cases (<10%) are usually combined anterior and posterior forms of PFV and may also be associated with bilateral microcornea, posterior megalolenticonus, and chorioretinal coloboma (MPPC syndrome).

17.2.2 Clinical Features

Systemic features: More often associated with bilateral cases, systemic features are found in genetic disorders (trisomy 13, Walker-Warburg syndrome, Norrie disease, inconti-

nentia pigmenti, Dandy-Walker syndrome, Angelman syndrome), metabolic diseases, such as glucose 6-phosphate dehydrogenase deficiency and perinatal infections (congenital cytomegalovirus infection and congenital rubella).

17.2.2.1 Ocular Manifestations

Usually unilateral, persistent fetal vasculature can have a wide range of presentations, ranging from:

- Microphthalmos
- Elongated ciliary processes
- Shallow anterior chamber
- Varying degrees of lenticular opacification (ranging from a Mittendorf dot on the posterior capsule to a total white cataract, as shown in Fig. 17.7)
- Retrolental fibrovascular mass
- Elevated vitreous membrane or stalk from optic nerve head (Bergmeister papilla)
- Disc drag (Fig. 17.8), retinal fold, retinal traction, or detachment
- Intraocular hemorrhage

Glaucoma may be present at the time of diagnosis, or it may develop over time associated with cataract or develop after cataract surgery. In such cases, the usually smaller eye with PFV is asymmetrically enlarged relative to the fellow eye due to stretching of the eye due to high IOP.

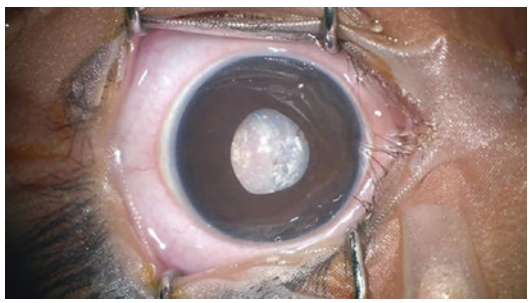

Fig. 17.7 Shows a total cataract with salmon pink sign reminiscent of cataract secondary to persistent fetal vasculature

17.2.3 Investigations

- Ultrasound B-scan (grayscale evaluation): Echogenic inhomogeneous band in the posterior segment, extending from the posterior surface of the posterior capsule of the lens to the optic disc, with no calcification or mass lesion, but a tractional retinal detachment may be noted (Fig. 17.5b).
- Color Doppler: Vascularity may be demonstrated along the abovementioned band (arterial flow, representing persistent hyaloid artery).
- Computed tomography (CT): Microphthalmia, a small or irregular lens, and tubular intravitreal density (Cloquet's canal).
- Magnetic resonance imaging (MRI): Shallow anterior chamber and retrolental vascular membrane (anterior type PFV), or microphthalmia, tubular Cloquet's canal, funnel-shaped retinal detachment, vitreous hemorrhage, and hypointense retrolental mass (posterior type PFV).

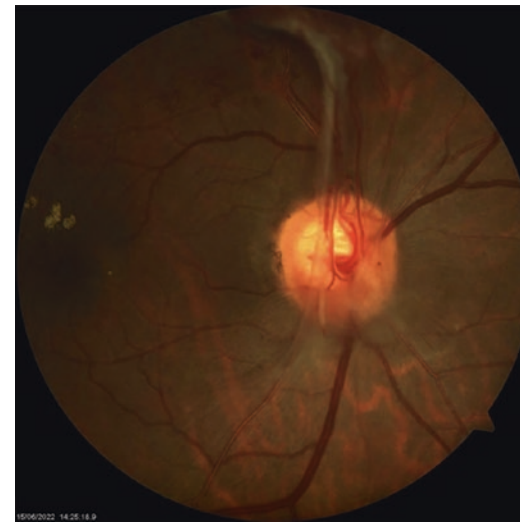

Fig. 17.8 Shows posterior persistent fetal vasculature (Bergmeister papilla) leading to disc drag and posterior retinal traction

17.2.4 Pathogenesis and Treatment of Glaucoma Secondary to Persistent Fetal Vasculature

Mild anterior involvement (nonprogressive, with clear visual axis and open angles) should only be observed regularly for development of secondary glaucoma (IOP measurement, assessment of AC depth), and early lensectomy should be avoided because of its guarded prognosis and risk of secondary glaucoma following cataract surgery.

In cases with severe posterior involvement, ciliary body detachment, eyes with no visual potential, etc., surgery is not usually indicated unless in cases of painful blind eyes or for cosmesis, where enucleation, followed by placement of an implant, may be performed. Figure 17.9 depicts a brief outline of the pathogenesis of glaucoma in association with persistent fetal vasculature and the principles of management in each of these cases.

Learning Points

- A good ocular ultrasound can go a long way in the diagnosis of posterior segment pathology in the presence of hazy media.
- Persistent fetal vasculature may present with a multitude of features, and deciding which of these need surgical management is of prime importance.

Case 17.3

An ophthalmology consult was sent regarding a protruding right eyeball with watering in a 3-year-old girl who was admitted in the Pediatrics ward because of Kwashiorkor. She had history of loss of vision BE when she was 2 months old. On general examination, the patient had sparse hair, a protruding belly, and lack of interest in her surroundings. The child's mother had not breastfed the child in infancy and had visible nutritional deficiency herself.

Ocular Examination: The child denied perception of light in the right eye with anterior staphyloma, with thickened congested conjunctiva with Bitot's spots; cornea was distorted, ectatic, and opaque, with peripheral vascularization and iridocorneal adhesion, and other details could not be assessed (Fig. 17.10). The fellow eye had minimal ambulatory vision and a large central nebulomacular corneal opacity. Applanation tonometry revealed pressures of 60 mmHg in RE (with distorted mires) and 18 mmHg in LE. Fundus details could not be assessed in either eye.

Diagnosis: Anterior staphyloma following healed sterile corneal melt secondary to keratomalacia and secondary glaucoma in RE with healed keratitis in LE.

Treatment: Our patient underwent RE diode laser cyclophotocoagulation under general anes-

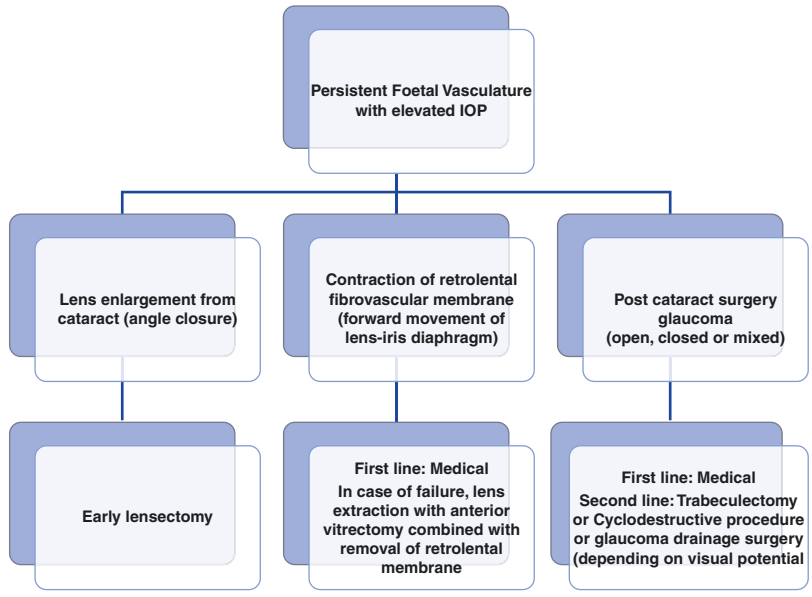

Fig. 17.9 A brief outline of pathogenesis of glaucoma in association with persistent fetal vasculature and the principles of management in each of these cases. *IOP* intraocular pressure

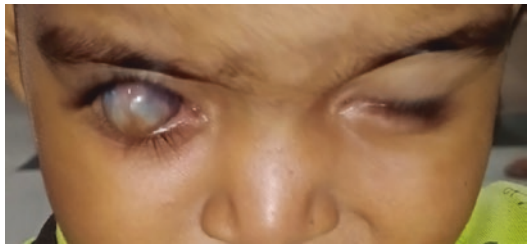

Fig. 17.10 Shows the face photo showing a bulging, distorted, ectatic, and opaque cornea of the right eye, with peripheral vascularization and iridocorneal adhesion

thesia and IOP is now maintained on one topical glaucoma medication. Cornea specialist opinion was sought for LE.

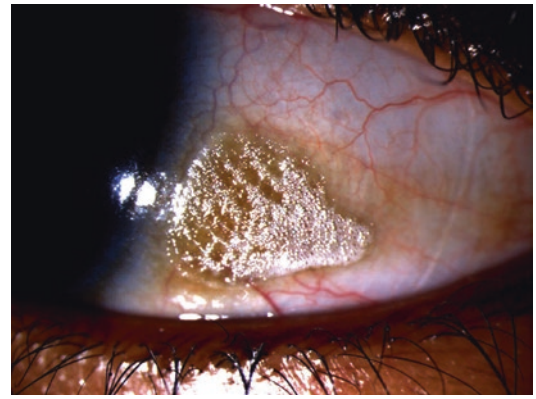

Fig. 17.11 Depicts a foamy appearing structure over the bulbar conjunctiva, which is triangular in shape with base toward the limbus, suggestive of a Bitot's spot

17.3 Keratomalacia

17.3.1 Background

Protein-energy malnutrition (PEM), quite rampant in developing and underdeveloped countries, especially in preschool children, increases vulnerability of the child to a multitude of diseases like respiratory infections, diarrhea, measles, etc. Vitamin A, a fat-soluble vitamin that cannot be produced endogenously, falls short in the body early in cases of PEM. Two forms of vitamin A are available in the human diet: preformed vitamin A (retinol and its esterified form, retinyl ester, which are obtained from animal sources) and provitamin A carotenoids (from plant sources, which are converted into the active form by our body). Dysfunction of corneal and conjunctival epithelial cell differentiation governed by vitamin A leads to abnormalities in the ocular surface ranging from punctate epithelial erosions to corneal perforation. Ocular manifestations of vitamin A deficiency are graded as follows:

- XN: Night blindness
- XIA: Conjunctival xerosis
- XIB: Bitot's spots (Fig. 17.11)
- X2: Corneal xerosis
- X3A: Corneal ulceration/keratomalacia less than one-third corneal surface
- X3B: Corneal ulceration/keratomalacia equal to or more than one-third corneal surface
- XS: Corneal scar
- XF: Xerophthalmic fundus

[Xerophthalmia grade X3B (keratomalacia) may progress to perforation with extrusion of intraocular contents leading to permanent distortion of the globe or phthisis bulbi, as shown in Fig. 17.12, or pseudocornea formation leading to anterior staphyloma.]

17.3.2 Pathogenesis

Pathogenesis of glaucoma is explained in Fig. 17.13.

17.3.3 Systemic Features

Follicular hyperkeratosis, anorexia, growth retardation, and increase in morbidity and mortality due to respiratory and diarrheal diseases.

Groups at risk of vitamin A inadequacy include premature infants, inadequately breastfed infants, and young children in developing countries, pregnant and lactating women, and people with lipid malabsorption (cystic fibrosis, h/o bowel resection).

Fig. 17.12 Shows a child with untreated keratomalacia (**a**) whose left eye developed a corneal melt and phthisis (**b**)

Fig. 17.13 Shows the outline of pathogenesis in glaucoma secondary to keratomalacia. *IOP* intraocular pressure

17.3.4 Differential Diagnoses

- Metabolic disorders with corneal abnormalities: mucopolysaccharidoses (Fig. 17.14), sphingolipidoses
- Corneal malformations: Dermoids, choristomas, sclerocornea, keratoglobus, buphthalmos
- Tumors: Pigmented conjunctival tumors, extraocular extension of a ciliary body melanoma
- Post perforating trauma/scleritis

17.3.5 Management

Treatment of vitamin A deficiency: Immediate, high-dose vitamin A supplementation should be commenced.

- Child <6 months: 50,000 IU of vitamin A on day 0 and day 1, and once again after 2 weeks which serves to replenish the hepatic stores of retinol.
- Child <12 months: 100,000 IU vitamin A on day 0, day 1, and at 2–4 weeks.
- Child >12 months: 200,000 IU on day 0, day 1 and at 2–4 weeks.
- Women of childbearing age; night blindness or Bitot's spots: 10,000 IU daily for 2 weeks *or* 25,000 IU weekly for 4 weeks (if corneal lesions are present, 200,000 IU on day 0, day 1, and at 2–4 weeks).
- In patients with severe anorexia or those in septic shock, in whom parenteral replenishment is essential, 55 mg of water miscible retinol palmitate can replace the first dose.

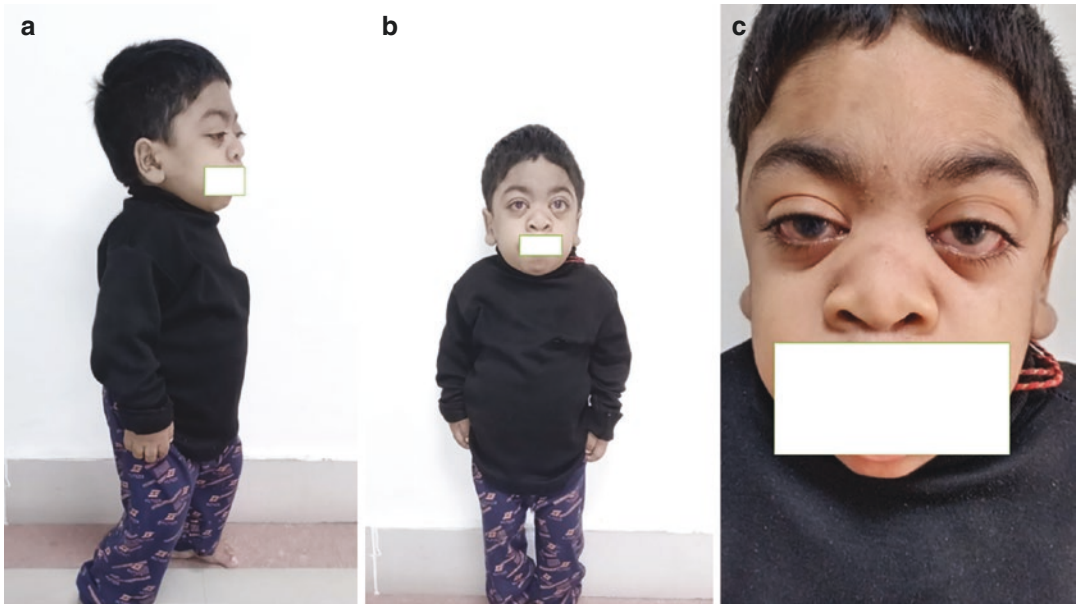

Fig. 17.14 (**a**–**c**) Shows a representative case of type 4 mucopolysaccharidosis

Fig. 17.15 Shows a child with a history of optical penetrating keratoplasty for corneal scarring secondary to keratomalacia, complicated by secondary glaucoma with graft failure and ectasia with right divergent squint

Supportive ocular therapy with aggressive lubrication and close follow-up is necessary to prevent secondary infection, melting, and perforation. Keratoplasty for optical rehabilitation in healed keratomalacia may be complicated by ocular surface problems and secondary glaucoma leading to failure of optical graft (Fig. 17.15).

17.3.6 Therapy

- Glaucoma is usually intractable and may not be amenable to medical or surgical therapy due to extensive anterior segment disorganization.
- Cyclodestructive procedures in eyes with poor visual potential are usually resorted to.
- Evisceration with placement of implant: can be performed for painful or disfiguring blind eyes.

Learning Points

- Ensuring adequate nourishment of pregnant and lactating women is of utmost importance in preventing the development of keratomalacia in children, which happens to be a preventable cause of blindness.
- Early recognition and prompt initiation of treatment may not only be sight-saving but also life-saving.
- Glaucoma associated with keratomalacia is usually intractable; thus, prevention, rather than treatment, should be the goal.

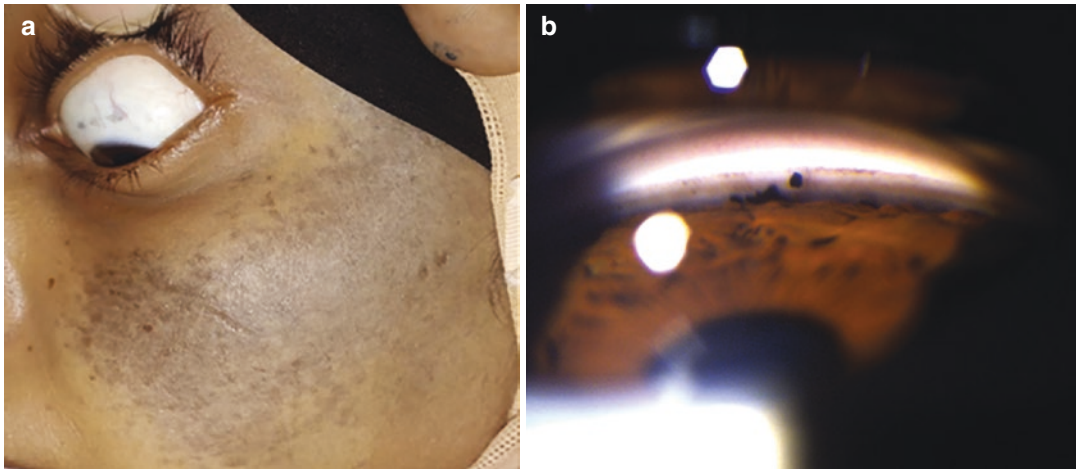

Fig. 17.16 (**a**) Shows a hyperpigmented lesion involving the skin along the distribution of ophthalmic and maxillary divisions of the trigeminal nerves was seen on the left side of the face, with patchy slate gray pigmentation over the left sclera; (**b**) is a gonio-photograph of the left eye of the patient showing open angles with areas of slate grey pigmentation obscuring details of the trabecular meshwork, suggestive of melanocytic infiltration of the trabecular meshwork with a single nevus in angle

Case 17.4

A 16-year-old female child was brought to the outpatient department of an ophthalmological hospital with the bystanders complaining of left-sided facial hyperpigmentation associated with slate gray pigmentation of the white area of the left eye, both of which were present since birth.

Examination: A hyperpigmented lesion involving the skin along the distribution of ophthalmic and maxillary divisions of the trigeminal nerves was seen on the left side of the face, with patchy slate gray pigmentation over the left sclera (Fig. 17.16a). Applanation tonometry revealed IOP of 12 mmHg and 24 mmHg in the RE and LE, respectively. Gonioscopic examination LE revealed open angles with velvety blackish pigmentation obscuring details of the trabecular meshwork (Fig. 17.16b). Fundus examination revealed a cup-disc ratio of 0.3:1 in RE and 0.6:1 in LE.

Diagnosis: Left-sided oculodermal melanocytosis (Nevus of Ota) with secondary open-angle glaucoma.

Management: Since our patient had no evidence of inflammation and open angles (with melanocytic infiltration), patient responded well to topical glaucoma medications. She was also referred to the Department of Dermatology for management of the dermal component for cosmesis.

17.4 Nevus of Ota

17.4.1 Background

Also known as oculodermal melanocytosis (ODM) or congenital ocular melanocytosis, Nevus of Ota is a congenital condition associated with hyperpigmentation of skin, mucosa, and eye [eyelid, tarsus, episcleral, conjunctiva, corneal epithelium, stroma and endothelium, anterior chamber angle/trabecular meshwork (causing glaucoma) iris (causing heterochromia iridis), pupil (leading to anisocoria, with the affected pupil being 1–1.5 mm smaller than the fellow pupil), lens, choroid] orbital tissue, and sometimes even leptomeninges along the distribution of ophthalmic, maxillary, and occasionally mandibular divisions of the trigeminal nerve (fifth cranial nerve), probably due to failure of migration of melanocytes from neural crest cells to their normal location within the basal layer of the epidermis.

Three clinical patterns have been described:

- Complete form (oculodermal melanocytosis)
- Dermal melanocytosis (dermal involvement alone)

Fig. 17.17 Shows a child with slate gray pigmentation only of sclera of the right eye, suggestive of ocular melanocytosis

- Ocular melanocytosis or melanosis oculi (ocular involvement alone) (Fig. 17.17)

17.4.2 Differential Diagnoses

- Nevus of Hori: Similar to Nevus of Ota but bilateral in distribution
- Nevus of Ito: Hyperpigmentation is seen over the neck, shoulders, axilla, and upper extremity

17.4.3 Pathogenesis and Treatment of Glaucoma in Oculodermal Melanocytosis (Fig. 17.18)

17.4.4 Management

Monitor regularly both for development of glaucoma and melanoma. No prophylactic measures need to be taken since only 10% of cases develop glaucoma.

Skin hyperpigmentation: Local application of camouflaging creams and concealers to mask it. Chemical peels, dermabrasion with carbon dioxide, cryotherapy, electrodissection, or Q-switched alexandrite laser therapy may help improve cosmesis.

Learning Points

- Oculodermal melanocytosis may affect almost every structure in the eye, but the potential for it to give rise to glaucoma and melanoma make it deserve a close watch. Those with scleral, choroidal or iris infiltration by melanocytes or those with palatal melanocytosis are more predisposed to developing melanoma.
- Associated developmental anomalies of the angle giving rise to elevated intraocular pressure warrant upfront surgical intervention.

Case 17.5

A 4-month-old male child was brought to the outpatient department of a tertiary eye care center with complaints of small-sized eyes noted at birth. The child was recently noted to have bluish appearance of the left eye associated with watering.

Examination: The eyes were found to be small, deeply set in the orbit (enophthalmic) and had narrow palpebral fissures, with normal appearing ocular structures but the left eye had a hazy cornea (Fig. 17.19). An ultrasound B-scan was performed for posterior segment evaluation, which showed optic nerve head cupping, and an axial length of around 15 mm in both the eyes. Sleeping IOP using a Tonopen was 26 mmHg in the right eye and 28 mmHg in the left eye.

Diagnosis: Simple microphthalmos with secondary glaucoma.

Treatment: Our case underwent a trabeculotomy combined with trabeculectomy with 0.02% mitomycin C under general anesthesia. Postoperatively, the child's IOP was controlled on 1 antiglaucoma medication and is currently doing well on regular follow-up.

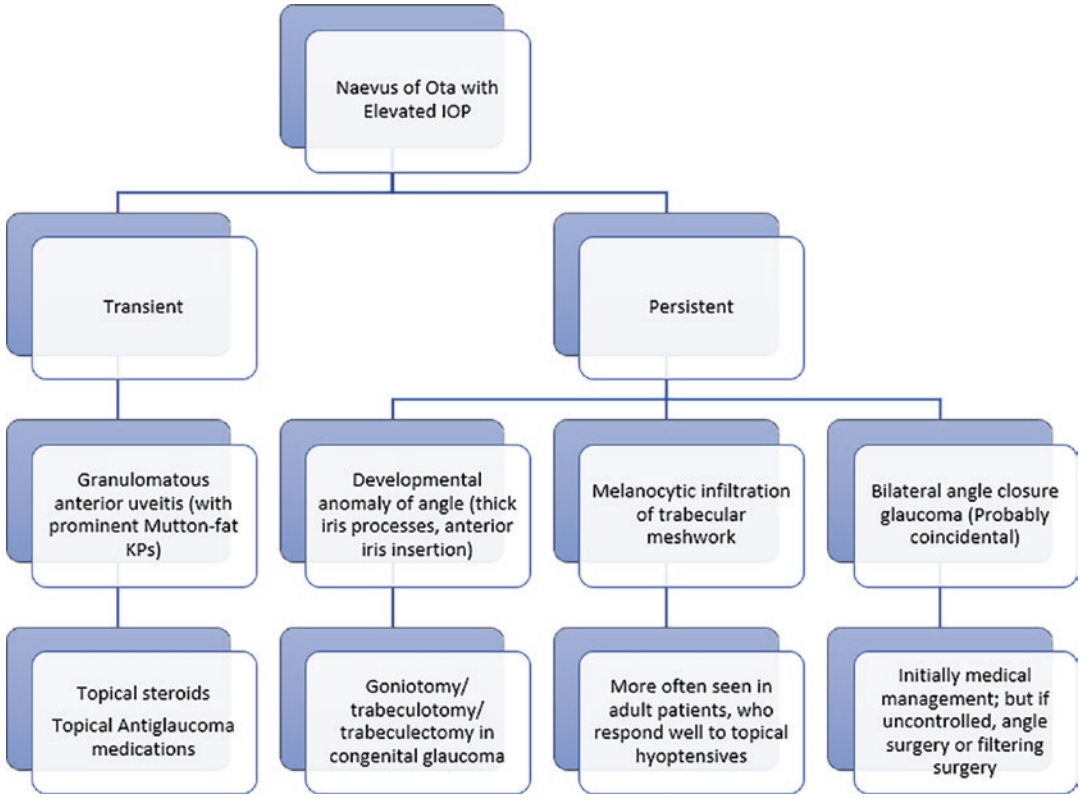

Fig. 17.18 Is a flowchart showing pathogenesis and management of glaucoma occurring in a case of Nevus of Ota. *IOP* intraocular pressure, *KPs* keratic precipitates

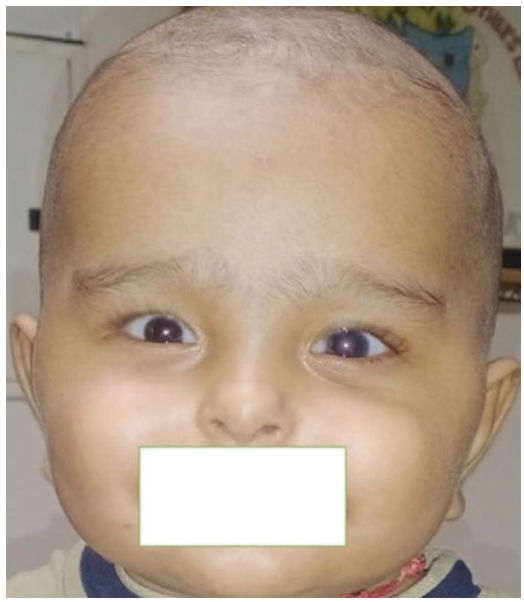

Fig. 17.19 Clinical picture of a child with microphthalmos showing bilateral small palpebral apertures with small, deeply set eyes and diffuse corneal haze in left eye

17.5 Microphthalmos

17.5.1 Background

Microphthalmos is described as an axial length of at least two standard deviations below the average for the patient's age [<15 mm in greatest diameter at birth (normal eye at birth varies between 16 and 19 mm) or 20 mm or less in an adult]. Histologically, it can have a wide range of appearances, ranging from near normal in nanophthalmos to rudimentary in clinical anophthalmos.

17.5.2 Types of Microphthalmos

- Simple microphthalmos or nanophthalmos: Eye is smaller than normal in size with no other gross abnormalities except for a high

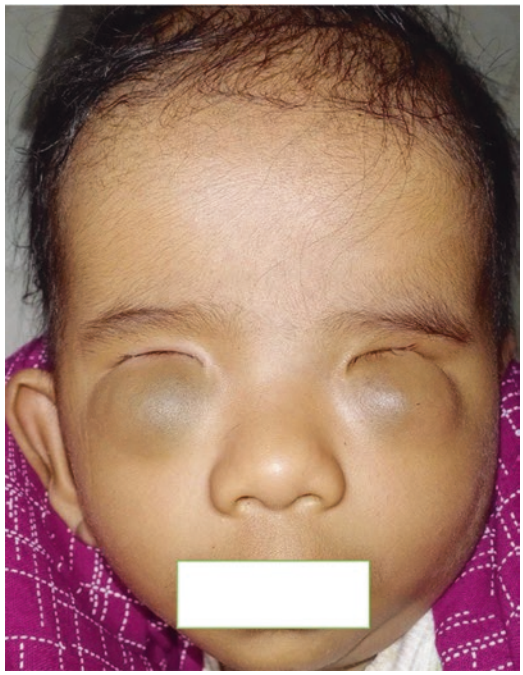

Fig. 17.20 Shows an infant with bilateral microphthalmos with cyst

lens/eye volume, thick sclera, macular hypoplasia, and hypermetropia. Nanophthalmos can also occur as part of a syndrome [oculo-dento-digital syndrome (ODD syndrome); Kenny-Caffey syndrome; nanophthalmos, retinitis pigmentosa, foveoschisis, and optic drusen syndrome; autosomal-dominant vitreoretinochoroidopathy (ADVIRC)].

- Complex microphthalmos, which is associated with other ocular abnormalities (microphthalmos with cyst, as shown in Fig. 17.20, microphthalmos associated with systemic anomalies, like congenital rubella, trisomy 13.

Disproportionate involvement of the anterior and posterior segments can give rise to relative anterior microphthalmos and relative posterior microphthalmos, respectively.

17.5.3 Differential Diagnosis

Atrophic bulbi: It is an acquired condition in which the eye is of normal size at birth but shrinks secondary to ocular disease.

17.5.4 Clinical Features

Ocular features: Bilateral and symmetrical condition, associated with shortened axial length; high corneal curvature; high lens/eye volume ratio raised from a normal value of 4% to up to 10–30% causing narrowing of anterior chamber angle; and high hyperopia (ranging from +8.00 to +25.00), which may lead to dense bilateral (isoametropic) amblyopia, nystagmus, and strabismus, usually non-accommodative esotropia, scleral thickening, and rudimentary foveal avascular zone (foveal hypoplasia). About 70% of these patients develop angle closure leading to glaucoma, so a close follow-up should be scheduled to detect and manage it early.

17.5.5 Investigations

17.5.5.1 Electroretinogram

Normal to variable degree of photopic and scotopic dysfunction.

17.5.5.2 OCT

Diffuse macular thickening or cystic changes, rudimentary foveal avascular zone, and schisis of the outer retinal layers.

17.5.5.3 Diagnosis of Glaucoma

Difficult due to a small crowded disc, inaccurate visual field testing due to high-plus lenses and reduced BCVA. Investigations like SD-OCT may detect subtle wedge-shaped loss of nerve fiber layer; HRT may help in monitoring the worsening of disc parameters; and stereo fundus photograph may help in documentation of disc morphology.

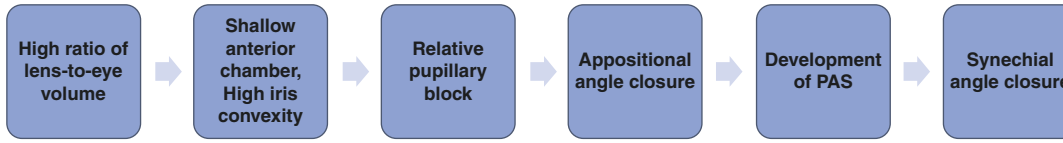

Fig. 17.21 Graphically represents the pathomechanism of development of angle closure in a microphthalmic eye. *PAS* peripheral anterior synechiae

17.5.6 Pathogenesis of Glaucoma

Development of angle closure in a case of microphthalmos occurs as shown in Fig. 17.21.

17.5.7 Management of Glaucoma Secondary to Microphthalmos

- Medical management: First-line therapy, though associated with high failure rates.
- Laser therapy: Nd:YAG laser peripheral iridotomy (LPI) in eyes with relative pupillary block and/or argon laser peripheral iridoplasty should be performed prophylactically (to prevent PAS formation) in eyes with plateau iris, (although less beneficial) and occludable angles and normal IOP.
- Cataract surgery: Phacoemulsification with IOL implantation, which may be combined with goniosynechialysis/ goniotomy/ MIGS or endoscopic cyclophotocoagulation, has been proved to be safe and effective.
- Glaucoma drainage device (with complete tube ligation to prevent hypotony) in cases in which glaucoma is not controlled after cataract surgery.
- Cyclodestructive procedures (diode cyclophotocoagulation) may be considered in advanced and high-risk cases.

(Drainage surgeries like trabeculectomy are usually not preferred due to high rate of complications like choroidal effusion, which may lead to secondary retinal detachment, intraocular hemorrhage, and malignant glaucoma. Performing 2–4 prophylactic sclerostomies to prevent sudden decompression and subsequent choroidal effusion can be performed.)

Post-surgery, there is high risk of malignant glaucoma in these eyes due to impaired ophthalmic venous reflex (thick sclera), pre-existing ciliary effusion, anterior rotation of ciliary body, a small ciliary ring, intraoperative complications, etc. About 60% of patients continue to have uncontrolled pressures after surgery.

Learning Points

- Choroidal effusion is a dreaded complication of surgeries in nanophthalmic eyes, and controlled lowering of IOP, minimizing the duration of hypotony intraoperatively, and prophylactic sclerostomies have been advised to lower the risk of the same.
- A close follow-up should be kept postoperatively in view of possible need for continued medical management.

17.6 Conclusions

A high degree of suspicion is essential in identifying glaucoma in various ocular conditions associated with multi-system pathologies. Handling the systemic manifestations of these conditions should be done at the earliest, but management of associated glaucoma should not take a back seat. A tailored approach is necessary to ensure that the coexisting ocular pathology is also dealt with appropriately.

Suggested Reading

Givens KT, Lee DA, Jones T, Ilstrup DM. Congenital rubella syndrome: ophthalmic manifestations and associated systemic disorders. Br J Ophthalmol. 1993;77(6):358–63.

Goldberg MF. Persistent fetal vasculature (PFV): an integrated interpretation of signs and symptoms associated with persistent hyperplastic primary vitreous (PHPV). LIV Edward Jackson Memorial Lecture. Am J Ophthalmol. 1997;124(5):587–626. https://doi.org/10.1016/s0002-9394(14)70899-2. PMID: 9372715.

Gupta V, Singh A, Gupta S. An iris heterochromia typical of rubella. Ophthalmology. 2022; 22:S0161–6420(22)00754-0.

McLaren DS, Kraemer K. Xerophthalmia. World Rev Nutr Diet. 2012;103:65–75. https://doi.org/10.1159/000185254. Epub 2012 Aug 27. PMID: 23008038.

Midha N, Sidhu T, Chaturvedi N, Sinha R, Shende DR, Dada T, Gupta V, Sihota R. Systemic associations of childhood glaucoma: a review. J Pediatr Ophthalmol Strabismus. 2018;55(6):397–402. https://doi.org/10.3928/01913913-20180905-01. PMID: 30452766.

Kaushik S, Choudhary S, Dhingra D, Singh MP, Gupta G, Arora A, Thattaruthody F, Pandav SS. Newborn glaucoma: A Neglected Manifestation of Congenital Rubella Syndrome. Ophthalmol Glaucoma. 2022;5(4):428–435.

Teekhasaenee C, Ritch R, Rutnin U, Leelawongs N. Glaucoma in oculodermal melanocytosis. Ophthalmology. 1990;97(5):562–70. https://doi.org/10.1016/s0161-6420(90)32540-x. PMID: 2342801.

Yang N, Jin S, Ma L, Liu J, Shan C, Zhao J. The pathogenesis and treatment of complications in nanophthalmos. J Ophthalmol. 2020;2020:6578750. https://doi.org/10.1155/2020/6578750. PMID: 32765903; PMCID: PMC7387986.

Part V

Acquired Secondary Childhood Glaucoma

Postsurgical Glaucoma

18

Niranjana Balasubramaniam,
Karthikeyan Mahalingam, and Shikha Gupta

Secondary glaucoma can occur following any ocular surgery. Common surgeries in the pediatric age group following which glaucoma can occur are cataract surgery, vitreoretinal surgery, scleral buckling, and penetrating keratoplasty among others.

18.1 Glaucoma Following Cataract Surgery

18.1.1 Introduction

Glaucoma following pediatric cataract surgery is the commonest cause of secondary childhood glaucoma. Though early cataract surgery results in better visual outcomes, there tends to be a higher incidence of postoperative glaucoma.

The incidence of glaucoma is higher in children less than 9 months of age. Table 18.1 summarizes the glaucoma incidence rates following pediatric cataract surgery according to Trivedi RH et al. Hence, younger children left aphakic are the ones most predisposed to the development of glaucoma. However, results from multivariate analyses show that a properly done primary posterior capsulotomy/anterior vitrectomy does not usually result in secondary glaucoma unless the primary diagnosis invites a higher risk of glaucoma.

N. Balasubramaniam (✉) · K. Mahalingam · S. Gupta
Dr. Rajendra Prasad Centre for Ophthalmic Sciences, All India Institute of Medical Sciences, New Delhi, India
e-mail: shikhagupta@aiims.edu

18.1.2 Mechanisms

Open-angle secondary glaucoma is fairly common following pediatric cataract surgery. The development of open-angle glaucoma involves one or more of the following mechanisms:

- Trabecular meshwork dysfunction with inflammatory and cellular obstruction
- High corticosteroid response
- Insult to developing angle structures from interaction with lens epithelial cells or vitreous leading to reduced outflow facility or developmental arrest
- Preexisting angle dysgenesis
- Trabecular meshwork collapse from loss of ciliary body support, following vitrectomy amongst aphakes

Angle-closure presentation is common in situations like microcornea, sulcus/iris-placed IOLs, poor mydriasis, prolonged postoperative inflammation especially in eyes with retained lens matter or inadequate vitrectomy with intracameral vitreous strands, and uveitis eyes due to either iris bombe formation following posterior synechiae formation or pupillary block. Angle-closure secondary to pupillary block, though a rare presentation, should be identified and treated early.

S. Gupta et al. (eds.), *Childhood Glaucoma*, https://doi.org/10.1007/978-981-19-7466-3_18

Table 18.1 Incidence rates of glaucoma following pediatric cataract surgery (Trivedi RH et al.)

Conditions	Incidence rates
Children younger than 9 months of age	37%
Children older than 9 months of age	6%
Aphakic eyes	17%
Eyes with a primary intraocular lens (IOL) implantation	3.8%

18.1.3 Risk Factors for Progression into Secondary Glaucoma in Eyes Undergoing Pediatric Cataract Surgery

1. Younger age of cataract surgery—especially before 4 months of age
2. Aphakia
3. Microcornea, microphthalmia
4. Extent of pupillary dilation—eyes with poor mydriasis
5. Need for secondary procedures like membranectomy or iridectomy
6. Residual lens matter
7. Chronic uveitis
8. Family history of glaucoma following pediatric cataract surgery
9. Conditions with coexistent cataracts and glaucomas like Marfan syndrome, congenital rubella syndrome, persistent fetal vasculature, oculo-cerebro-renal syndrome of Lowe, traumatic cataract, and glaucoma.

In some cases, open- and angle-closure mechanisms may also coexist to produce secondary glaucoma.

Case 18.1
A 5-year-old child with a history of bilateral congenital cataracts and microcornea operated on at 3 years of age with primary IOL implantation was found to have RE buphthalmos during second year of follow-up. Intraocular pressure (IOP) in the right eye (RE) was 38 mmHg and left eye (LE) 24 mmHg, with RE being larger than the left eye. Central corneal thickness (CCT) RE was 600 μm and LE 620 μm, and the child had large discs with a cup-disc ratio (CDR) in RE 0.9:1 and LE 0.6:1.

Management: The child was started on dorzolamide 2% + timolol maleate 0.5% combination BD and latanoprost 0.005% HS in RE. Follow-up after 1 month showed IOP RE 26 mmHg and LE 20 mmHg. Considering uncontrolled disease despite being compliant with medical management, trabeculectomy augmented with MMC 0.2 mg/mL was performed in RE. Figure 18.1a shows RE with PCIOL and low bleb, and Fig. 18.1b shows LE with PCIOL. Six months postoperatively, RE IOP was 12 mmHg, and LE was stable on medical treatment.

Case 18.2
A 5-year child presented with RE microcornea, aphakia, and secondary glaucoma. IOP was 30 mmHg on four topical glaucoma medications with vertical cup disc ratio (CDR) 0.8:1 in RE and LE was 0.5:1. The patient had a history of RE cataract surgery for unilateral congenital glaucoma at 2 months of age. At 11 months of age during examination under anesthesia, RE IOP was 26 mmHg and CDR of 0.6:1, so the child was started on two topical glaucoma medications, with the subsequent addition of another one, all of which proved ineffective in achieving the target IOP.

Management: The child underwent RE trabeculectomy augmented with MMC 0.2 mg/mL. At 2 years post-surgery, an IOP of 24 mmHg was recorded in RE on dorzolamide 2% and timolol 0.5%. Slit-lamp examination revealed a fibrosed flat bleb, and CDR was found to be 0.9:1. Considering the progression of the glaucomatous damage and failed trabeculectomy, RE superotemporal Ahmed glaucoma valve (AGV) implantation was performed. At 1-year postoperative follow-up, as shown Fig. 18.2, the AGV tube was in situ in the anterior chamber with no iris or corneal touch. IOP was recorded to be 10 mmHg on e/d timolol 0.5% bd only.

Case 18.3
An 8-year-old girl child was referred for a glaucoma opinion. She had a family history of congenital cataracts and was operated on at

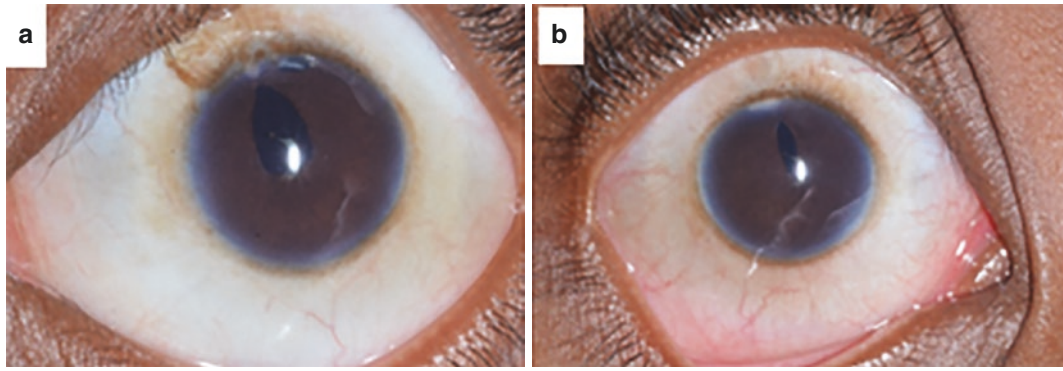

Fig. 18.1 (**a**, **b**) RE and LE with PCIOL. This figure also reveals low bleb and resolved corneal edema in RE

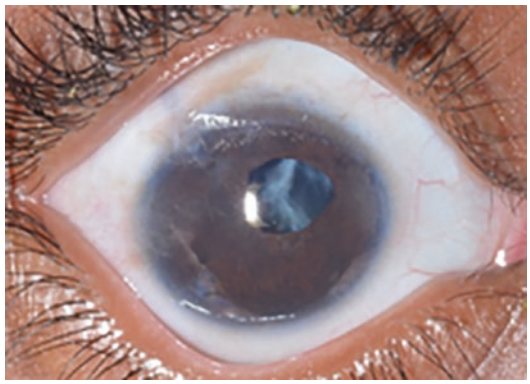

Fig. 18.2 Superotemporal AGV implant (with intracameral tube) in a microcorneal aphakic eye. There is visible posterior capsular opacification

11 months of age for sequential cataract surgery with primary IOL implantation and surgical iridectomy in both eyes as shown in Fig. 18.3a, b. She had microcornea with corneal diameters of approximately 9.5 mm both horizontally and vertically. She was started on betaxolol 0.5% drops at 5 years of age since the IOP recorded by rebound tonometry was 22 mmHg in RE and 20 mmHg in LE.

Management: After 3 years of starting medical management, the child's IOP was 18 mmHg in BE. The CCT in RE was 683 μm and in LE 690 μm. The CDR in RE was 0.5:1, and LE was 0.6:1 with a healthy neuro-retinal rim. There was no increase in CDR noted from the baseline. Hence, a decision was made to stop glaucoma medications with close periodical observation.

Learning Points

Standards for consideration in pediatric cataract surgery

- Prevention of hypotony—The risk of hypotony is higher in operated pediatric eyes due to simultaneous anterior vitrectomy performed during cataract surgery. The use of anterior chamber maintainer, separate infusion line as anterior chamber maintainer, tightly securing all ports with sutures, adding viscoelastic in the anterior chamber, and adding postoperative oral steroids help prevent hypotony-related choroidal effusions. An early hypotony is also a risk factor for bleb failure. And hence GDD may be the first choice for some surgeons compared to trabeculectomy in aphakic eyes with glaucoma.
- Control of inflammation—judicious use of topical steroids.
- Prophylactic peripheral iridectomy or iridotomy in the following situations:
  - Aphakic eyes
  - Sulcus inserted IOL
  - Uveitis/intraocular inflammation, where the probability for synechiae development is high
- Monitoring of post-cataract surgery eyes.

  Regular postoperative monitoring for IOP—either biannually or annually. In the presence of risk factors, two to four monthly monitoring is preferable.
- Role of central corneal thickness (CCT).

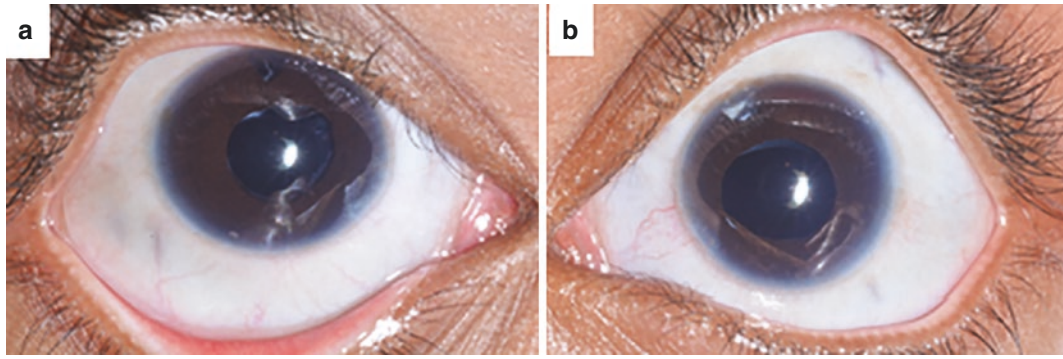

Fig. 18.3 (**a**, **b**) Right and left eye of the child with PCIOL in situ and superior surgical iridectomy

Following pediatric cataract surgery, an acquired increase in CCT is seen in many eyes. This may sometimes cause an overestimation of IOP. Hence, CCT adjustment may be needed in these situations, especially in eyes showing no progression in optic nerve cupping despite borderline high IOPs. However, in the event of symmetrical CCT in two eyes with consistent asymmetric high IOP in one of the two eyes, it needs to be treated irrespective of thick CCT. Due consideration should be given to other factors like changes in axial length, changes in IOP from baseline, and an increase in disc cupping before bringing about any therapeutic changes based on IOP reading alone.

18.2 Glaucoma Following Vitreoretinal Surgeries

Secondary glaucoma complicates retinal surgeries quite commonly. The underlying cause of glaucoma following vitreoretinal surgery is often multifactorial. The incidence of angle-closure glaucoma after the scleral buckling procedure has been reported to range from 1.4% to 4.4%. Postoperative elevation of IOP is a well-known complication in vitrectomy surgeries following intravitreal injection of expansile gases like sulfur hexafluoride (SF6) and perfluoropropane (C3F8) and also with silicon oil tamponade. In a study by DP Han et al., IOP >30 mmHg was found in up to 35% of patients following 48 h of pars plana vitrectomy (PPV).

18.2.1 Mechanism of Angle-Closure Post buckle Surgery

The changes in the eyeball leading to the development of angle closure in the eyes post encirclage or scleral buckling surgery are depicted in Fig. 18.4.

18.2.2 Intravitreal Tamponade Agents

Secondary glaucoma following intravitreal gas injection may occur either from both open-angle and/or closed-angle mechanisms. Figure 18.5 explains the causes for each of the mechanisms.

Secondary glaucoma following intravitreal injection of silicone oil may be due to pupillary block, inflammation, synechial angle closure, or migration of emulsified silicone oil in the anterior chamber with subsequent obstruction of the aqueous outflow pathway.

18.2.3 Management of Glaucoma After Scleral Buckling

- Therapy includes cycloplegics to shift the lens-iris diaphragm posteriorly and topical corticosteroids to reduce inflammation and peripheral anterior synechiae formation.
- Aqueous suppressants to reduce IOP include β-blockers, carbonic anhydrase inhibitors, and alpha-adrenergic agonists.

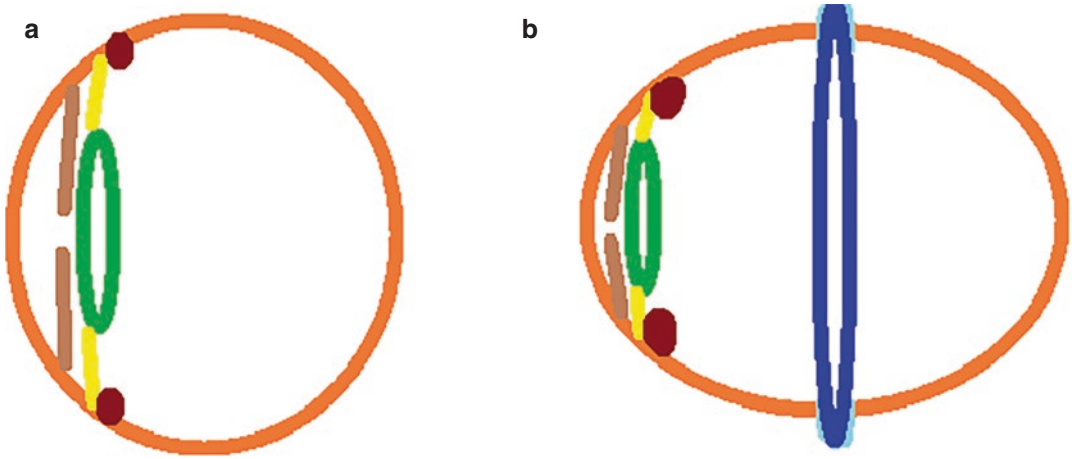

Fig. 18.4 Schematic diagram demonstrating the mechanism of angle closure after scleral buckling. (**a**) Normal anterior chamber depth (**b**) Forward displacement of iris-lens diaphragm leading to shallow anterior chamber post-buckling

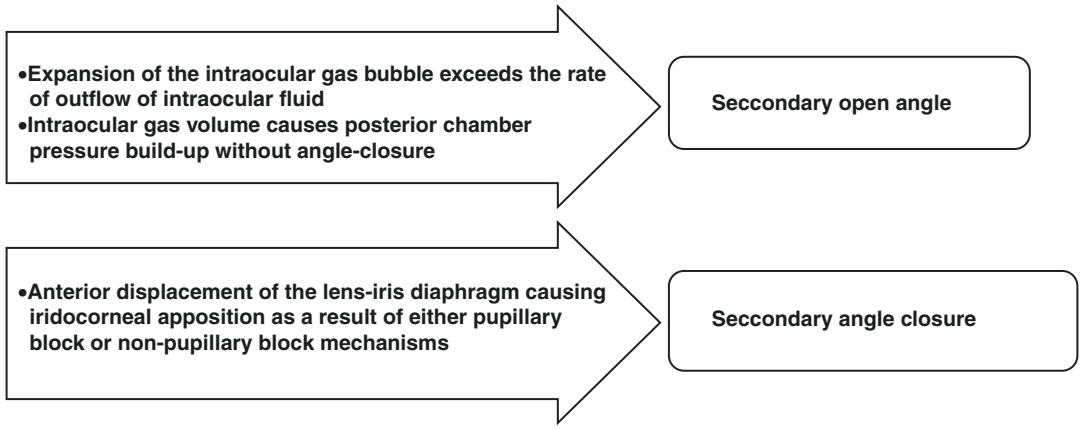

Fig. 18.5 Mechanism of glaucoma due to intravitreal tamponade agents

- Miotics should be avoided, as they can worsen inflammation and produce further angle narrowing via forward movement of the lens-iris diaphragm.

18.2.4 Management of Glaucoma Post-vitrectomy Surgery

- The prophylactic surgical iridectomy at the inferior 6 o'clock position (Ando's iridectomy) is done to prevent pupillary block, especially in aphakic eyes. In case of usage of heavy silicon oils, superior iridectomy is performed.
- The transient IOP spike depends on the postoperative inflammation (associated trabeculitis or choroidal effusion leading to anterior movement of lens iris diaphragm), steroid response, and the agents used for tamponade. This usually responds well to medical treatment.
- Medical therapy alone is successful in controlling IOP in many situations.
- Selective laser trabeculoplasty in older cooperative children in eyes with open-angle may help tide over the phase of acute rise in IOP.

- Conservative limited laser cyclophotocoagulation can also be done in silicone/gas-filled eyes as an interim measure in eyes with very high IOP rise despite medical therapy.
- However, silicone oil removal with or without glaucoma filtration surgery may also be required when medical management fails.
- Glaucoma drainage device (GDD) implantation is an important surgical option as there is a high risk of failure with standard filtering surgery. In such complex cases, simultaneous vitrectomy and AGV implantation with tube in the posterior segment may be an effective option. Insertion of the silicon tube of GDD through a pars plana scleral fistula after complete vitrectomy is particularly valuable in patients with extensive peripheral anterior synechiae.
- In refractory scenarios, cyclophotocoagulation or other laser techniques like micropulse laser and endoscopic cyclophotocoagulation can be performed for IOP control.

Case 18.4

An 11-year-old child with bilateral high myopia had BE rhegmatogenous retinal detachment. LE was treated by scleral buckling with intravitreal C3F8 2 years back, and in RE, vitreoretinal surgery with silicone oil tamponade was done 3 months back. Figure 18.6a, b show the development of inverse hypopyon in the anterior chamber and glaucomatous cupping of the optic nerve head post-surgery in RE. The child later developed secondary glaucoma in both the eyes and posterior subcapsular cataract in LE. Also, in LE multiple procedures like selective laser trabeculoplasty, trabeculectomy with MMC, and lens aspiration with IOL implantation were combined with 270° inferotemporal gonioscopy-assisted transluminal trabeculotomy (GATT) but failed to control IOP. Figure 18.6c, d show vascularized bleb post-augmented trabeculectomy with advanced glaucomatous cupping in LE.

Management: LE Aurolab aqueous drainage implant (AADI) was performed as in Fig. 18.6e. The IOP was 12 mmHg on the last follow-up. In the right eye, silicon oil removal with anterior chamber wash was performed. RE IOP by applanation tonometry was 20 mmHg on the last follow-up on maximum medical therapy (latanoprost, ripasudil, dorzolamide, and brimonidine + timolol combination).

Learning Points

- Glaucoma filtering surgeries offer a lesser success rate in secondary glaucoma following scleral buckling or vitreoretinal surgery with silicone oil tamponade, due to excessive conjunctival scarring (especially if encirclage/buckle has been placed) and due to ongoing inflammation. In a study by Gupta S et al., the long-term success of AGV implantation for glaucoma after vitreoretinal surgery with silicone oil insertion is better than that reported for trabeculectomy, though complication rates remain high. They reported a success of 62% at 12 months and 37% at 5 years in such eyes post-AGV implantation.
- In cases of raised IOP with silicon oil in situ especially in the presence of overfill, first silicon oil removal/replacement (if emulsified), partial removal (if there is overfill) should be considered and medical management with or without limited laser procedure (180–270° DLCP or micropulse) may be done in the interim waiting period.

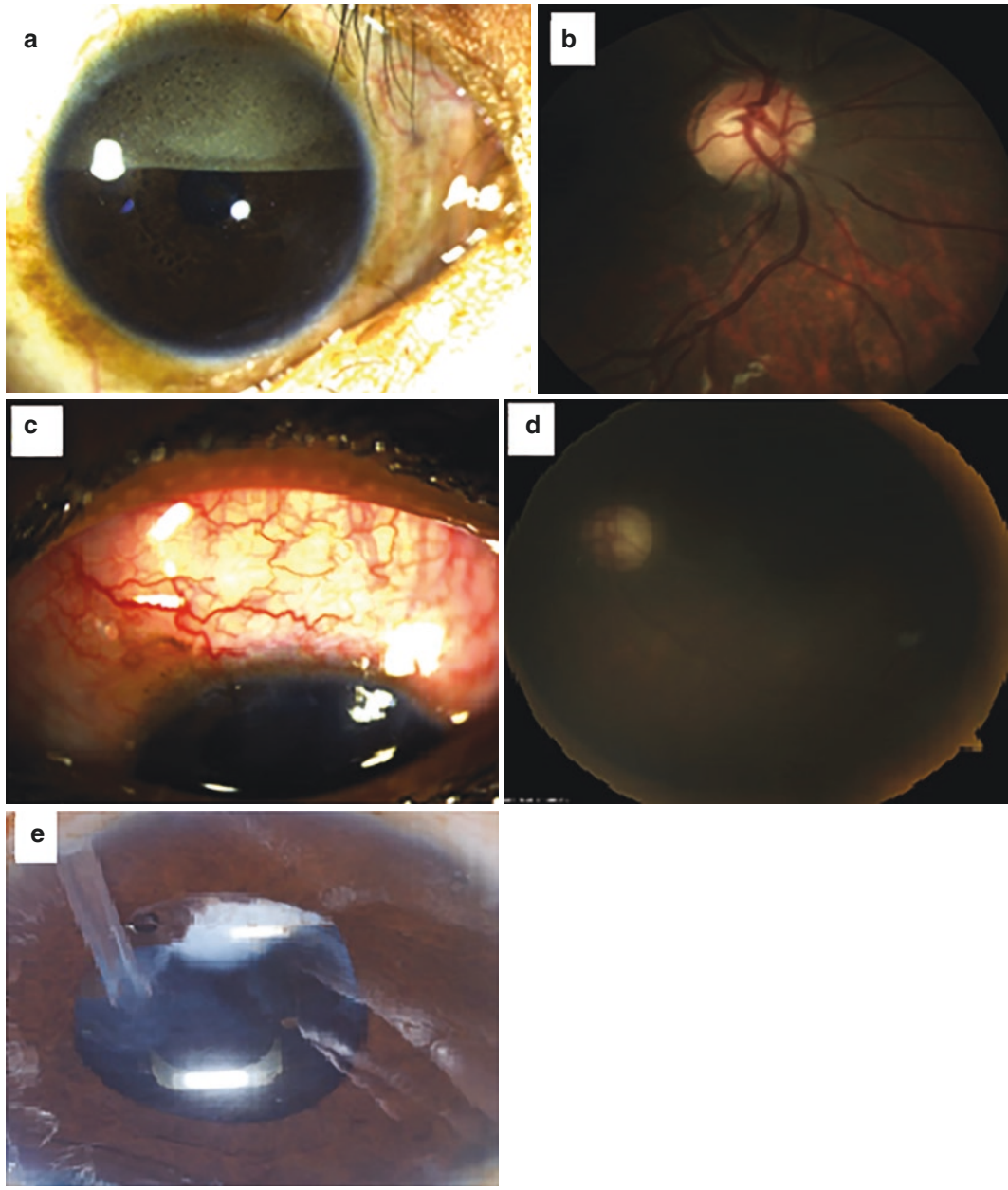

Fig. 18.6 (**a**, **b**) RE with inverse hypopyon and the fundus picture reveals CDR 0.6:1 and inferior NRR thinning. (**c**, **d**) Vascularized, flat bleb with advanced glaucomatous cupping in LE. (**e**) Status post superotemporal AADI implantation

18.3 Glaucoma Post-penetrating Keratoplasty

Pediatric keratoplasty is more challenging as compared to adult cases since it carries higher rates of graft rejection and poorer visual prognosis due to amblyopia. The most common cause of congenital corneal abnormalities in developed nations is Peter's anomaly (40.3%), followed by sclerocornea (18.1%), dermoid (15.3%), congenital glaucoma (6.9%), microphthalmia (4.2%), birth trauma, and metabolic diseases (2.8%). The other causes common in developing

countries include keratomalacia and corneal infection (ophthalmia neonatorum).

Glaucoma is a serious complication after corneal transplantation and itself a common cause of graft failure and a leading cause of vision loss post-keratoplasty due to corneal endothelial decompensation. Patients might also have preexisting glaucoma due to angle dysgenesis even before a corneal transplant. Endothelial keratoplasty procedures like Descemet's stripping automated endothelial keratoplasty (DSAEK) and Descemet membrane endothelial keratoplasty (DMEK) may be superior to penetrating keratoplasty (PKP) in terms of incidence of elevated IOP and development of glaucoma. The early and late post-operative causes for post-penetrating keratoplasty glaucoma are listed in Table 18.2.

Case 18.5

A 5-year-old child had corneal leucomatous opacity with cataract in the left eye following healed microbial keratitis. The child underwent optical PKP with lens extraction and IOL implantation in LE. The graft was performing well in the initial postoperative period as shown in Fig. 18.7. On review after 2 years, a drop in visual acuity of two lines in Snellen was noted in LE. Microcystic corneal edema reduced the graft clarity, and the IOP was recorded to be 32 mmHg on Tonopen in LE.

Management: The child was started on systemic carbonic anhydrase inhibitors according to body weight and topical betaxolol eye drops. Considering the persistent high IOP despite medical therapy and the higher likelihood of graft failure, the child underwent trabeculectomy augmented with MMC 0.4 mg/mL. The presence of healthy superior conjunctiva and a deep anterior chamber favored the surgical decision. Two months postoperatively, the child had a diffuse moderately vascular bleb, with an IOP of 14 mmHg on Tonopen and the graft edema resolved.

Table 18.2 The early and late causes of raised IOP following corneal transplantation

Early postoperative causes	Late postoperative causes
The following causes of IOP spikes need to be identified early and treated appropriately:	Peripheral anterior synechiae are seen in 87% of post-PKP eyes. They lead to progressive angle closure glaucoma that is often refractory
(a) Pupillary block	Factors anterior to the angle:
(b) Retained viscoelastic	(a) Distortion of the trabecular meshwork (TM) by tight and long sutures
(c) Iritis	
(d) Inflammatory reaction leading to the clogged trabecular meshwork	(b) Undersized donors resulting in angle crowding
(e) Hemorrhage	(c) Inflammation due to graft rejection
(f) Steroid response	Factors posterior to the angle:
(g) Malignant glaucoma	(a) Loss of the ciliary body-lens-support system allows for the collapse of the TM if it's a combined procedure

Case 18.6

Another 12-year-old male child presented with a history of optical PKP done for postinfectious adherent leucomatous opacity. The child's best-corrected visual acuity at 1-month post PKP was 3/60 and IOP was recorded to be 26 mmHg on Tonopen. The graft was mildly edematous and also showed deep vascularization in two quadrants. There were peripheral anterior synechiae in multiple areas. The child also had an inferior self-settled retinal detachment and macular scar. The CDR was hazily visualized to be 0.8:1. The child was diagnosed to have secondary angle-

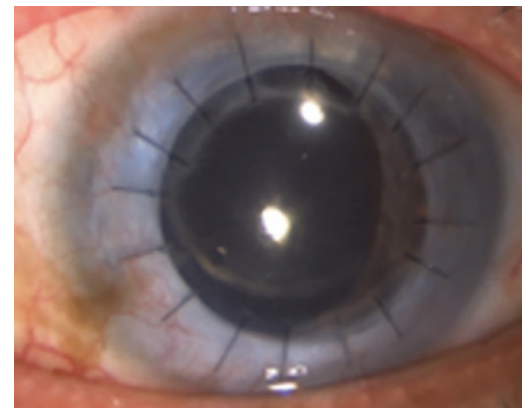

Fig. 18.7 Status post optical PKP with IOL implantation

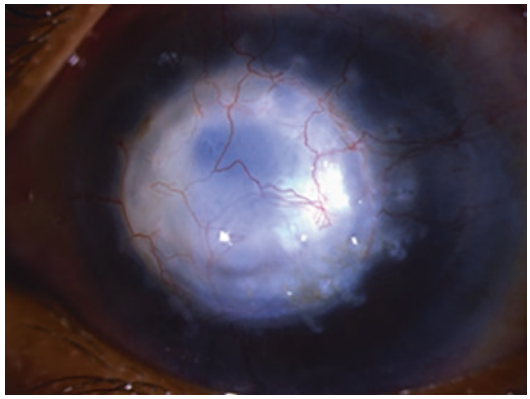

Fig. 18.8 Clinical picture of an eye with failed graft and secondary glaucoma showing total leucomatous opacity with vascularization in all quadrants

closure glaucoma and started on brimonidine with timolol eyedrops initially.

At 6 months postoperatively, the graft was diffusely edematous with increasing opacification and vascularization as shown in Fig. 18.8. The child complained of pain and headache. The visual acuity dropped to hand movements vision. IOP was 32 mmHg. Fundus could not be assessed. B scan showed optic disc cupping with inferior retinal detachment. The child underwent diode laser cyclophotocoagulation (DLCP) in 270°. At 1-year post-diode laser, the child maintained IOP in the mid-teens range on brimonidine and timolol with pain relief.

Learning Points

- Conditions with preexisting glaucoma like congenital glaucoma, keratomalacia, congenital hereditary endothelial dystrophy (CHED), etc. can be associated with glaucoma following keratoplasty, more often than eyes without preexisting glaucoma. In cases of preexisting glaucoma, adequate IOP control is needed for the success of a corneal transplant.
- Two principal causes of graft failure post-keratoplasty are graft rejection and secondary glaucoma development. Patients with preoperative glaucoma experience approximately twice to triple as many graft rejections as those without preexisting glaucoma.
- Filtering surgery with good functional blebs and optimum IOP control may fail post-keratoplasty.
- In cases planned for keratoplasty with high IOP (not controlled on medical management/failed glaucoma surgeries), limited quadrant DLCP or micropulse laser can be done as an interim measure to tide over pressure rise for at least 3 months following keratoplasty. Later on, glaucoma filtration surgery can be performed if IOP remains uncontrolled after keratoplasty.
- Both the surgeries for IOP control like glaucoma drainage device insertion and keratoplasty can also be performed in the same sitting in the event of total corneal opacity and uncontrolled IOPs at the time of surgery, albeit with higher chances of failure with both.

18.4 Management Algorithm (Fig. 18.9)

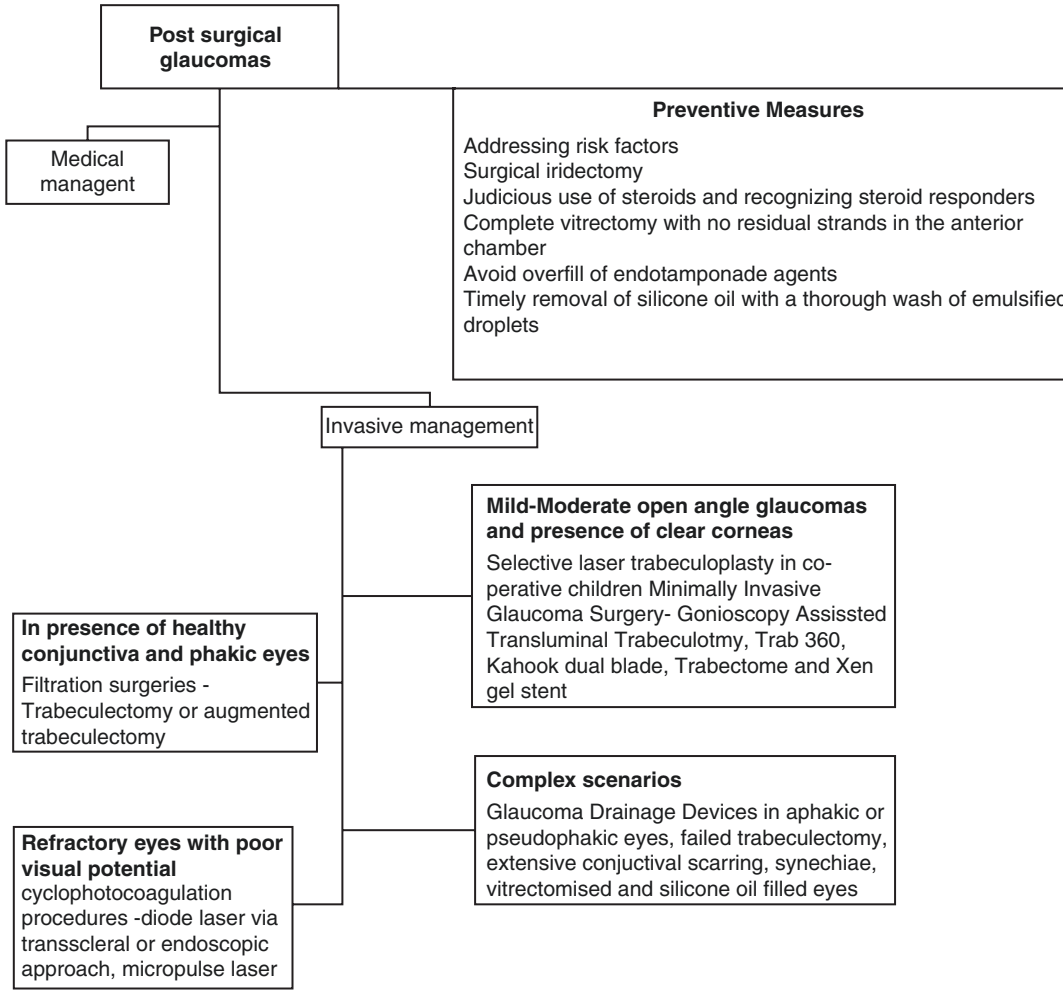

Fig. 18.9 Management algorithm of postsurgical glaucomas

18.5 Conclusions

Post-surgical glaucoma is a sight-threatening complication in pediatric eyes following intraocular surgery. Diagnostic difficulties in assessing IOP, visual fields, and optic nerve head changes may lead to delayed treatment unless the clinician is watchful of this complication. Medical, laser, and surgical treatments have a role in glaucoma management. These children need life-long care and the best management efforts to prevent blindness.

Suggested Reading

Abdolrahimzadeh S, Fameli V, Mollo R, Contestabile MT, Perdicchi A, Recupero SM. Rare diseases leading to childhood glaucoma: epidemiology, pathophysiogenesis, and management. Mantelli F, editor. Biomed Res Int. 2015;2015:781294. https://doi.org/10.1155/2015/781294.

Anders LM, Gatzioufas Z, Grieshaber MC. Challenges in the complex management of post-keratoplasty glaucoma. Ther Adv Ophthalmol. 2021;13:25158414211031396.

Banitt M, Lee RK. Management of patients with combined glaucoma and corneal transplant surgery. Eye. 2009;23(10):1972–9.

Chang EK, Gupta S, Chachanidze M, Miller JB, Chang TC, Solá-Del Valle DA. Combined pars plana glaucoma drainage device placement and vitrectomy using a vitrectomy sclerotomy site for tube placement: a case series. BMC Ophthalmol. 2021;21(1):106.

Gedde SJ. Management of glaucoma after retinal detachment surgery. Curr Opin Ophthalmol. 2002;13(2):103–9.

Gupta S, Chaurasia AK, Chawla R, Kapoor KS, Mahalingam K, Swamy DR, et al. Long-term outcomes of glaucoma drainage devices for glaucoma post-vitreoretinal surgery with silicone oil insertion: a prospective evaluation. Graefes Arch Clin Exp Ophthalmol. 2016;254(12):2449–54.

Han DP, Lewis H, Lambrou FHJ, Mieler WF, Hartz A. Mechanisms of intraocular pressure elevation after pars plana vitrectomy. Ophthalmology. 1989;96(9):1357–62.

Khokhar SK, Pillay G, Dhull C, Agarwal E, Mahabir M, Aggarwal P. Pediatric cataract. Indian J Ophthalmol. 2017;65(12):1340–9.

Kirwan C, Lanigan B, O'Keefe M. Glaucoma in aphakic and pseudophakic eyes following surgery for congenital cataract in the first year of life. Acta Ophthalmol. 2010;88(1):53–9.

Mangouritsas G, Mourtzoukos S, Portaliou DM, Georgopoulos VI, Dimopoulou A, Feretis E. Glaucoma associated with the management of rhegmatogenous retinal detachment. Clin Ophthalmol. 2013;7:727–34.

Müller M, Geerling G, Zierhut M, Klink T. [Glaucoma and retinal surgery]. Ophthalmologe. 2010;107(5):419–426.

Rezende RA, Uchoa UBC, Uchoa R, Rapuano CJ, Laibson PR, Cohen EJ. Congenital corneal opacities in a cornea referral practice. Cornea. 2004;23(6):565–70.

Sahin A, Caça I, Cingü AK, Türkcü FM, Yüksel H, Sahin M, et al. Secondary glaucoma after pediatric cataract surgery. Int J Ophthalmol. 2013;6(2):216–20.

Subasi S, Yuksel N, Karabas VL, Yilmaz Tugan B, Basaran E. Ahmed glaucoma valve implantation for secondary glaucoma post-vitrectomy. Int Ophthalmol. 2021;42:847.

Trivedi RH, Wilson MEJ, Golub RL. Incidence and risk factors for glaucoma after pediatric cataract surgery with and without intraocular lens implantation. J AAPOS. 2006;10(2):117–23.

Vanathi M, Panda A, Vengayil S, Chaudhuri Z, Dada T. Pediatric keratoplasty. Surv Ophthalmol. 2009;54(2):245–71.

Weinreb RN, Grajewski A, Papadopoulos M, Grigg J, Freedman AS, World Glaucoma Association. Childhood glaucoma. Consensus Series 9. Amsterdam: Kugler Publications; 2013.

Wong IBY, Sukthankar VD, Cortina-Borja M, Nischal KK. Incidence of early-onset glaucoma after infant cataract extraction with and without intraocular lens implantation. Br J Ophthalmol. 2009;93(9):1200–3.

Uveitic Glaucoma

19

Deeksha Rani, Karthikeyan Mahalingam, Shikha Gupta, and Pradeep Venkatesh

Uveitis is defined as the inflammation of the uveal tissue of the eye. Pediatric uveitis (5–10% of all uveitis) is less common when compared to adult uveitis. Children with uveitis usually suffer more severe visual morbidity as compared to adults. Up to 22% of all affected children develop at least one blind eye and 3% become legally blind before adulthood. Among pediatric uveitis, prevalence of various types includes:

- Anterior uveitis (iritis and iridocyclitis) 30–40%
- Intermediate uveitis (inflammation of vitreous body along with pars plana of ciliary body) 10–20%
- Posterior uveitis (retinochoroiditis or chorioretinitis) 40–50%
- Panuveitis (all the structures of the uveal network are involved) 5–10%

19.1 Etiology of Uveitis

The most common cause of uveitis in the pediatric age group is juvenile idiopathic arthritis. Other causative systemic diseases include sarcoidosis, tubulointerstitial nephritis and uveitis (TINU), and Blau syndrome.

D. Rani (✉) · K. Mahalingam · S. Gupta · P. Venkatesh
Dr. Rajendra Prasad Centre for Ophthalmic Sciences, All India Institute of Medical Sciences, New Delhi, India

The oligoarticular form of juvenile idiopathic arthritis (JIA) is often associated with an asymptomatic, bilateral, non-granulomatous anterior uveitis. JIA-related uveitis usually gets complicated with the development of cataract, band-shaped keratopathy and secondary glaucoma. The cases presenting with severe inflammation may also present with ocular hypotony due to the ciliary body shutdown. The cases with mild inflammation usually have elevated IOP. Figure 19.1 shows clinical features seen in a child with JIA-related uveitis and complications.

Early stages often present with open angles on gonioscopy, while long-standing cases may develop anterior synechial angle closure along with pupillary block due to posterior synechiae.

Management includes topical steroids, cycloplegics, and topical antiglaucoma medications. Severe cases may need regional or systemic steroids. Systemic steroids are used for management of short-term flare ups. Need for long-term anti-inflammatory therapy warrants the use of immunomodulators. Methotrexate is the first-line steroid sparing agent in children. Methotrexate is a dihydrofolate reductase inhibitor that exerts its anti-inflammatory activity by inhibiting the synthesis of purines and elevating levels of serum adenosine. The conventional dose is 8–12 mg/m^2/week. However, in certain cases, higher doses of up to 20–25 mg/m^2/week may be needed. This drug has a favorable side effect profile and is generally well tolerated in children.

S. Gupta et al. (eds.), *Childhood Glaucoma*, https://doi.org/10.1007/978-981-19-7466-3_19

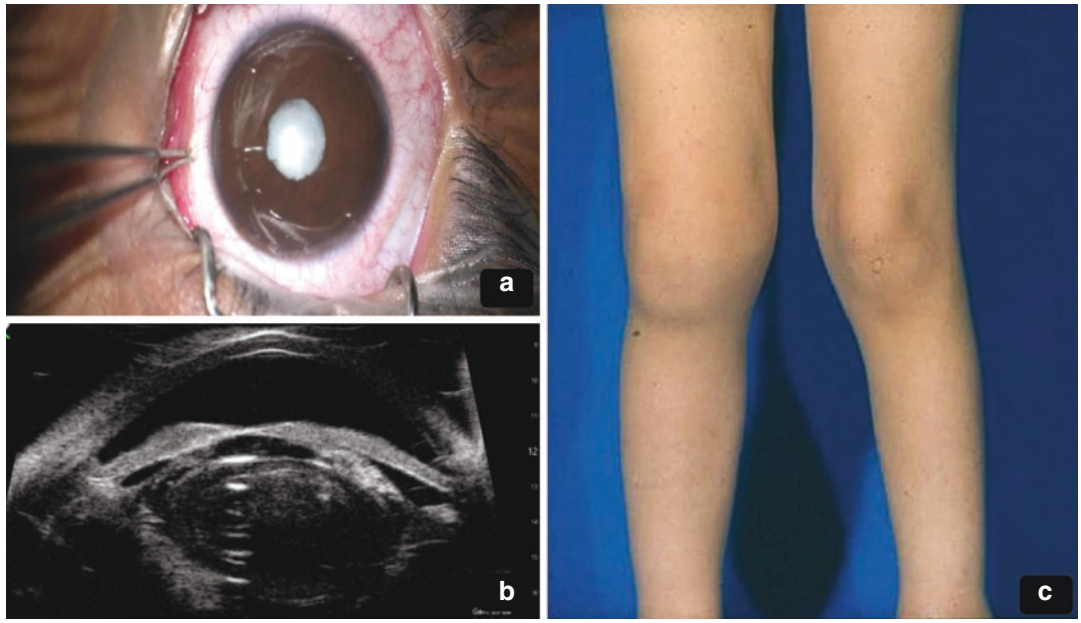

Fig. 19.1 (**a**) Clinical picture showing healed anterior uveitis with cataract and band-shaped keratopathy. (**b**) UBM picture shows total cataract with anterior subcapsular plaque. (**c**) The clinical picture shows swollen knees in a patient with oligoarticular arthritis

Leflunomide (20 mg/day) and sulfasalazine (30–50 mg/kg/day) are the alternative therapies for children who do not tolerate or fail to respond to methotrexate.

Six percent to 33% of cases of pediatric anterior uveitis are secondary to infections. Some of the infectious agents implicated are toxoplasma, rubella virus, varicella-zoster virus, herpes simplex virus, cytomegalovirus, Ebstein-Barr virus, and human herpes virus. Figure 19.2 shows a clinical picture of acute uveitis with mutton fat endothelial KPs in a case of infective uveitis (Fig. 19.2a) and its resolution with treatment (Fig. 19.2b).

Fuchs' heterochromic iridocyclitis is a chronic, idiopathic low-grade iridocyclitis causing atrophy of iris stroma leading to hypochromia in people with brown iris. The iris may be seen as hyperchromic in patients with light-colored iris due to increased visibility of posterior pigmented epithelium through the atrophied iris stroma. Most cases are unilateral, though bilaterality has been reported in about 13% of cases. Usually diagnosed in the third or fourth decade but in 8–20% of the cases, they are diagnosed before 16 years of age. Complications include secondary glaucoma (seen in 13–52% of cases) and posterior subcapsular cataract.

Retinoblastoma, leukemia, and juvenile xanthogranuloma can masquerade as chronic anterior uveitis in children. Open or closed globe injuries, intraocular foreign body, or retinal detachment may also present as anterior uveitis.

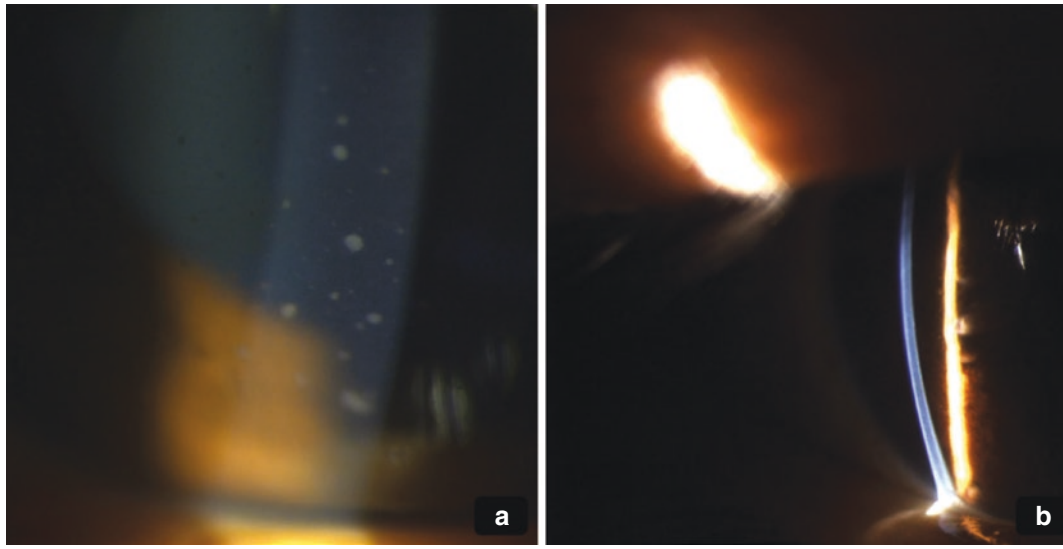

Fig. 19.2 Endothelial KPs (**a**) and resolution after treatment with topical steroids and cycloplegics (**b**)

19.2 Prevalence of Glaucoma in Uveitis

Various studies have been done, and the mean prevalence of pediatric glaucoma has been found to vary between 5% and 25% in patients with uveitis.

Higher incidence of uveitic glaucoma is seen in uveitis associated with juvenile idiopathic arthritis (JIA) and herpetic infections. Acute uveitis usually results in hypotony but cases with herpetic uveitis, fuch's heterochromic iridocyclitis and Posner Schlosmann syndrome may cause elevated IOP even during acute phase.

19.2.1 Hypotony:

Ten percent of patients with uveitis can develop hypotony during the course of their disease. Causes for hypotony include:

(a) Inflammation of the ciliary body causing a decrease in the production of aqueous humor. Chronic inflammation, edema of the ciliary body or tractional membranes causing ciliary body detachment may result in decreased blood circulation, thus causing ciliary body shutdown and eventual hypotony.
(b) Elevated uveoscleral outflow due to prostaglandin release can also result in lowering of IOP.

19.3 Pathophysiology of Uveitic Glaucoma

19.3.1 Open-Angle Mechanisms:

- Increased aqueous viscosity as **protein levels are elevated**
- **Pigment deposition/cells/debris/inflammatory nodules** in the irido-trabecular angle
- Inflammation (**trabeculitis**) of the trabecular meshwork
- **Increased trabecular resistance** following trabecular meshwork hypoperfusion in severe cyclitis
- **Corticosteroid-induced** trabecular meshwork **dysfunction, prescribed to treat acute uveitis**. (Corticosteroids inhibit the activity of

hyaluronidase which leads to the accumulation of extracellular matrix degradation products. These lead to trabecular swelling and decreased trabecular outflow. The influence of corticosteroids on outflow is more marked in those in whom outflow is already compromised.)
- Influence of cytokines on trabeculocytes (IL-1, TGF-β).

It has been found that most cases of elevated IOP were associated with chronic anterior uveitis (Sharon et al. 2010). Chronic open-angle glaucoma is the most common type of uveitic glaucoma. However certain conditions may present with high IOP during acute uveitis with open angles, such as Posner-Schlossman syndrome, herpetic keratouveitis, Fuchs' heterochromic iridocyclitis, bilateral acute iris transillumination (BAIT), and bilateral acute depigmentation of iris (BADI).

BAIT and BADI are two diseases of the same spectrum. BAIT is described as acute depigmentation of iris with pupillary sphincter defects. The pigment is lost from pigmented epithelium of iris in this condition. In BADI, the acute depigmentation of iris is associated with the absence of pupillary defects. There is no iris transillumination in these cases. The pigment is lost from iris stroma. In both the cases, there is pigment release in the anterior chamber. These pigments get deposited in the trabecular meshwork leading to acute rise of IOP.

19.3.2 Angle-Closure Mechanisms:

Prolonged inflammation in the anterior chamber leads to the formation of anterior or posterior synechiae. Development of anterior peripheral synechiae presents with chronic angle-closure glaucoma, while development of posterior synechiae may lead to the formation of occlusio or seclusio pupillae. This may lead to iris bombe formation that causes secondary pupillary block thus impeding aqueous outflow, and leading to pupillary block glaucoma.

Other mechanisms include forward displacement of lens-iris diaphragm due to uveal effusion and neovascularization.

19.4 Clinical Examples

Case 19.1

Case description: A 17-year-old female presented to us with complaints of diminution of vision in both eyes. She had a history of multiple episodes of redness and pain in both eyes for the last 2 years. At presentation, visual acuity in the right eye was 6/36 and in the left eye was perception of light (PL) negative. Intraocular pressure was 26 mmHg in the right eye and 32 mmHg in the left eye on maximum topical medication in both eyes. A clinical picture of the right eye shows 360° posterior synechiae with a cataractous lens (Fig. 19.3a), and the left eye shows a very shallow anterior chamber, atrophic iris, patent iridotomy, and posterior synechiae (Fig. 19.3c). Gonioscopy revealed increased and blotchy pigmentation with synechial angle closure in both the eyes (Fig 19.3b, d). Fundus examination of the left eye revealed total glaucomatous optic neuropathy.

Diagnosis: Both eyes healed anterior uveitis with right eye complicated cataract with secondary angle-closure glaucoma, left eye presented in absolute stage of angle closure glaucoma.

Treatment: Right eye lens aspiration with posterior synechiolysis and surgical peripheral iridectomy with implantation of the intraocular lens in the bag under general anaesthesia under steroid cover was done. A diode laser cyclodestructive procedure was performed for the left eye. On 3 months follow-up, distance visual acuity in the right eye was 6/9, and intraocular pressure was 14mmHg on two glaucoma medications.

Learning Points
- In healed uveitis with complicated cataract/posterior synechiae and uncontrolled secondary glaucoma, cataract surgery with iridectomy should be performed before planning for glaucoma filtration surgery. It relieves pupillary block component, prevents post-trabeculectomy shallowing of the anterior chamber and may avoid the need for future glaucoma filtration surgery if IOP remains controlled with or without medications.
- Prostaglandin analogues and miotics are relatively contraindicated for IOP control as they

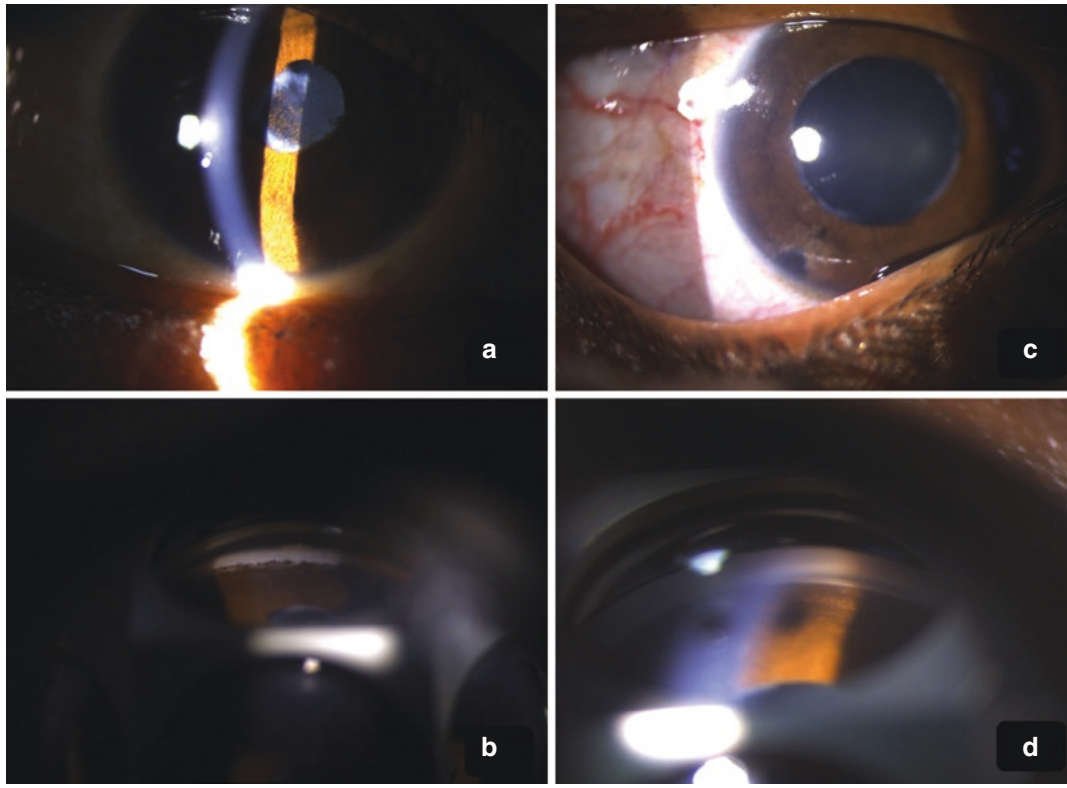

Fig. 19.3 (**a**) Clinical picture of right eye showing posterior synechiae and cataractous lens. (**b**) Gonio-photograph of right eye showing increased pigmentation and synechial angle closure. (**c**) Clinical picture of left eye shows multiple peripheral iridotomies with posterior synechiae. (**d**) Shows gonio-CP of left eye showing closed angles

may worsen inflammation. However they may also be instituted as a last resort.

- It is important to keep the pupil mobile postoperatively (short-acting cycloplegic-mydriatic combination, e.g., tropicamide-phenylephrine combination can be prescribed 3–4/day) to prevent reformation of posterior synechiae. Also the steroids are tapered more gradually over 6–8 weeks to avoid resurgence of inflammation. If the patient requires long term control of inflammation, institution of steroid sparing topical or oral agents should be looked into. The various immunomodulators include T cell inhibitors (Cyclosporine, Tacrolimus and Voclosporine); Antimetabolites (Methotrexate, Azathioprine and Mycophenolate mofetil), Alkylating agents (cyclophosphamide and chlorambucil) and biological response modifiers, which include TNF α inhibitors (Infliximab, adalimumab and etanercept); Tocilizumab- anti IL 6, Rituximab- anti CD 20, Secukinumab- anti IL 17A and Daclizumab- anti IL 2). Based on the side effect profile, methotrexate is the most commonly used steroid sparing agent in children. In cases where single drug fails to control the disease activity, biological response modifiers (e.g. adalimumab) may be added. There are upcoming reports on benefits of leflunomide in combination with biological agents for treating refractory uveitis associated with JIA. A multidisciplinary approach involving the paediatrician and rheumatologist is mandatory.

Case 19.2

Case description: A 15-year-old female child, who was a known case of JIA-related uveitis for the past 4 years, presented to the glaucoma clinic of our center with uncontrolled intraocular pressure on maximum topical medications. History of left ankle swelling 4 years back was present. The child was operated on for a complicated cataract at

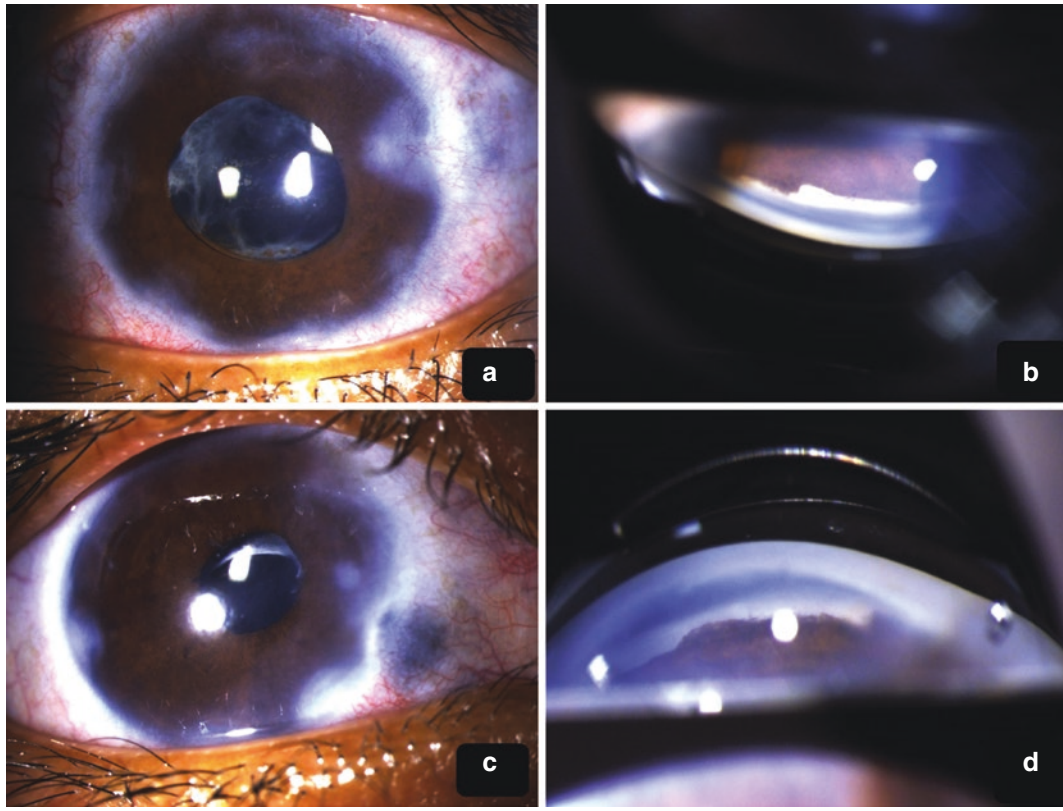

Fig. 19.4 (**a**) Right eye shows pseudophakia with multiple peripheral anterior synechiae with multiple Nebulo Macular Corneal Opacities (NMCOs), Band Shaped Keratopathy (BSK), scleral thinning with ciliary staphyloma. (**b**) Gonio-CP of the right eye shows a large peripheral anterior synechiae (PAS). (**c**) Clinical picture of the left eye showing pseudophakia with PCO with pannus and multiple PAS and circumferential thinning and scarring. (**d**) Gonio-CP of the left eye showing high peripheral anterior synechiae

the age of 6 years. On presentation, the best-corrected visual acuity in the right eye was 6/9 and in the left eye was PL positive, projection of rays (PR) inaccurate. Intraocular pressure in right and left eye was 28 mmHg (four topical hypotensive drugs) and 24 mmHg, respectively. Fundoscopy revealed a cup to disc ratio of 0.6:1 in the right eye and near-total cupping in the left eye. The clinical picture shows 360° posterior synechiae with multiple peripheral anterior synechiae and scleral thinning in both the eyes (Fig. 19.4a, c).

Gonio-CP showed peripheral anterior synechiae in all the quadrants (Fig. 19.4b, d).

Diagnosis: Both eyes healed anterior uveitis with both eye pseudophakia with right eye secondary glaucoma and left eye absolute stage of secondary angle closure glaucoma.

Treatment: The child underwent a right eye trabeculectomy with 0.04% mitomycin C under general anesthesia. IOP at 1-week follow-up was 13 mmHg in the right eye with circum-limbal congestion and three plus cells in the anterior chamber. The child was started on oral steroids at a dose of 1 mg/kg with weekly tapering. At 3 months follow-up, IOP was 10 mmHg with a well-formed bleb and formed anterior chamber.

Learning Points

- The eye should be quiet (at least for 3 months) during any intervention. Any surgical intervention in an inflamed eye can lead to exaggerated inflammation response. However in cases of intractable glaucoma, a glaucoma surgery can be performed even in an acute uveitis case if medications fail to control IOP.
- All surgical interventions in uveitic eyes should be done under strict systemic and topical steroid cover.
- During trabeculectomy in cases with scleral thinning, the scleral flap has to be made with adequate precautions as there are higher chances of scleral perforation. Areas away from scleral thinning can be chosen. Low-dose mitomycin C can be used.
- In cases of refractory glaucoma with/ without failed trabeculectomy, glaucoma drainage devices can be inserted.

Case 19.3

Case description: A 15-year-old male child, a known case of both eye anterior uveitis, was on regular follow-up in the glaucoma clinic of our center. The child had undergone cataract surgery for a complicated cataract at the age of 12 years. Two years later, because of uncontrolled IOP, both eyes trabeculectomy with MMC as an adjunct was done. The child was maintaining well on single antiglaucoma medication. Three weeks ago, on routine follow-up, high IOPs of 32 mmHg in the right eye and 26 mmHg in the left eye was documented. On slit-lamp examination, the bleb was well formed and functioning. Four plus cells were noted in the anterior chamber.

Diagnosis: Both eyes acute on chronic anterior uveitis with pseudophakia with operated trabeculectomy.

Treatment: The child was started on topical steroids (6 times/day), cycloplegic (Homatopine Bromide 2% four times a day), and three topical antiglaucoma medications. Oral acetazolamide 250 mg twice daily was given for 3 days. At 2 weeks follow-up, the anterior chamber reaction had improved to two plus AC cells. IOP in both the eyes had dropped to 12 mmHg and 14 mmHg, respectively on medications.

Learning Points

- Managing pediatric uveitic glaucoma is a challenge for an ophthalmologist. Long-term and regular follow-up is mandatory.
- In children with healed anterior uveitis, recording of high pressures on follow-up should raise a suspicion of recurrence of inflammation. In such cases, starting the treatment with topical steroids may lead to control of IOP, by taking care of the acute inflammation.

19.5 Management of Glaucoma

Management of glaucoma needs a multipronged therapy.

The following flowchart (Fig. 19.5) describes the management of uveitic glaucoma.

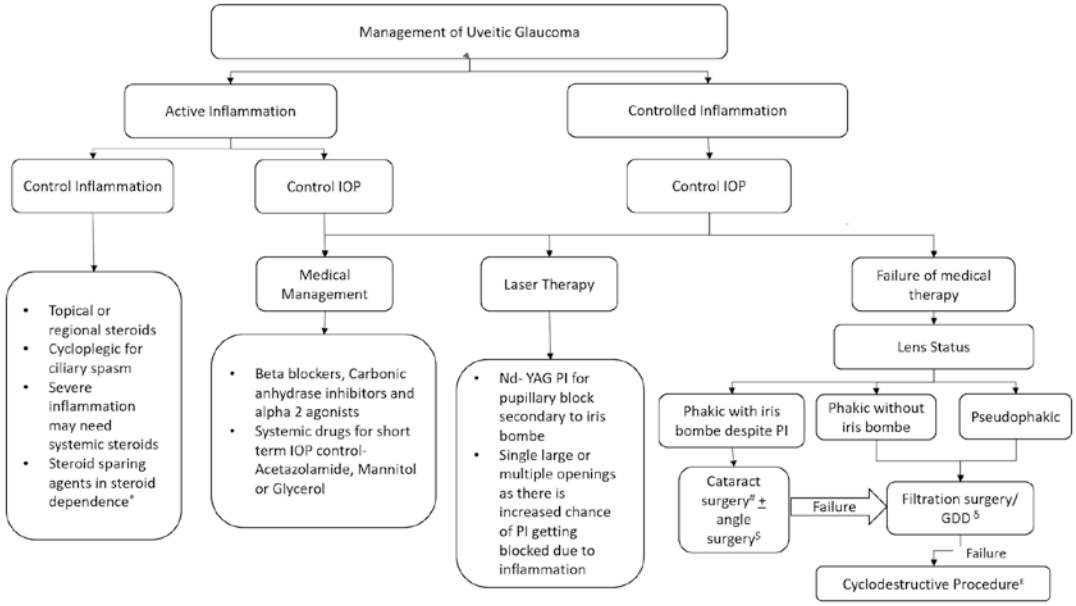

Fig. 19.5 Management of uveitic glaucoma. IOP - intraocular pressure, GDD - glaucoma drainage devices, PI - peripheral iridotomy/ iridectomy*—The safe steroid-sparing agents in pediatric cases include methotrexate (max dose of 20–25 mg/m^2/week); leflunomide (20 mg/day), and sulfasalazine (30–50 mg/kg/day)#—Cataract surgery should be done provided the eye is quiet for the past 3 months. It is specifically indicated in eyes with shallow or irregular anterior chamber depth due to synechiae. Surgery should always be done under strict oral steroid cover. In cases of uveitic cataract, IOL should always be implanted in the bag. Sulcus or angle implantation of IOL should be avoided as it can be associated with increased risk of flare up of uveitis$—Anterior and posterior synechiolysis, surgical PI, and goniotomy can be combined with cataract surgeryδ—Express glaucoma shunt diverts the aqueous from anterior chamber to subconjunctival space. This can be another option in uveitic glaucoma as it avoids iridectomy which may increase the risk of postoperative inflammationε—Since diode laser cyclophotocoagulation is associated with flare-up of inflammation, it is usually avoided but can be considered as the last resort when all other means have failed

19.6 Conclusions

Uveitic glaucoma can result from mechanisms which are open-angle, closed-angle, or a combination of both. The management of uveitic glaucoma requires careful observation and a collaborative approach. Steroids, cycloplegics, and glaucoma medications must be used with caution. Before considering any elective surgery, it is important to ensure that there is no active inflammation. Regular monitoring and the appropriate use of ocular hypotensive and anti-inflammatory treatments can help preserve vision in affected eyes.

Suggested Reading

Accorinti M, Spinucci G, Pirraglia MP, Bruschi S, Pesci FR, Iannetti L. Fuchs heterochromic iridocyclitis in an Italian Tertiary Referral Centre: epidemiology, clinical features, and prognosis. J Ophthalmol. 2016;2016:1458624. https://doi.org/10.1155/2016/1458624.

Birnbaum AD, Tessler HH, Schultz KL, et al. Epidemiologic relationship between fuchs heterochromic iridocyclitis and the United States rubella vaccination program. Am J Ophthalmol. 2007;144(3):424–8. https://doi.org/10.1016/j.ajo.2007.05.026.

Chan NSW, Chee SP. Demystifying viral anterior uveitis: a review. Clin Exp Ophthalmol. 2019;47(3):320–33. https://doi.org/10.1111/ceo.13417.

Edelsten C, Reddy MA, Stanford MR, Graham EM. Visual loss associated with pediatric uveitis in English primary and referral centres. Am J Ophthalmol. 2003;135:676–80.

Kimura SJ, Hogan MJ, Thygeson P. Fuchs' syndrome of heterochromic cyclitis. AMA Arch Ophthalmol. 1955;54(2):179–86. https://doi.org/10.1001/archopht.1955.00930020181003.

Mandeville JT, Levinson RD, Holland GN. The tubulointerstitial nephritis and uveitis syndrome. Surv Ophthalmol. 2001;46(3):195–208.

Nagpal A, Leigh JF, Acharya NR. Epidemiology of uveitis in children. Int Ophthalmol Clin. 2008;48(3):1–7.

O'Brien JM, Albert DM, Foster CS. Juvenile rheumatoid arthritis. In: Albert DM, Jakobiec FA, editors. Principles and practice of ophthalmology: clinical practice, vol. 5. Philadelphia, PA: WB Saunders; 1994. p. 2873–86.

Paivonsalo-Hietanen T, Tuominen J, Saari KM. Uveitis in children: population-based study in Finland. Acta Ophthalmol Scand. 2000;78(1):84–8.

Sfriso P, Caso F, Tognon S, Galozzi P, Gava A, Punzi L. Blau syndrome, clinical and genetic aspects. Autoimmun Rev. 2012;12(1):44–51.

Sharon Y, Friling R, Luski M, Campoverde BQ, Amer R, Kramer M. Uveitic glaucoma: long-term clinical outcome and risk factors for progression. Ocul Immunol Inflamm. 2017;25(6):740–7. https://doi.org/10.1080/09273948.2016.1255341.

Sng CCA, Barton K. Mechanism and management of angle closure in uveitis. Curr Opin Ophthalmol. 2015;26(2):121–7. https://doi.org/10.1097/ICU.0000000000000136.

Post-Traumatic Glaucoma

20

Harathy Selvan, Sudarshan Kumar Khokhar, and Shikha Gupta

Ocular trauma (both open globe and closed globe injury) is an important cause of secondary glaucoma that can manifest immediately or months to decades later. In open globe injuries, glaucoma can result from direct damage to angle structures, disruption of lens capsule, or from the reparative processes. On the other hand, closed globe injuries could have multiple mechanisms operating. The seven rings of trauma associated with blunt trauma are (1) sphincter tears, (2) iridodialysis, (3) trabecular meshwork (TM) tears, (4) angle recession, (5) cyclodialysis, (6) zonular dialysis, and (7) retinal dialysis. Advancing age, poor initial visual acuity, elevated baseline IOP, hyphema, lens injury, increased angle pigmentation, angle recession >180°, and a wider angle on ultrasound biomicroscopy (UBM) have been identified as early predictors of glaucoma following closed globe injury. The diverse mechanisms that could contribute to post-traumatic secondary glaucoma have been summarized in Fig. 20.1.

Inflammation associated with ocular trauma can manifest high intraocular pressure (IOP) by various ways. Trabeculitis and/or inflammatory clogging of TM remains the primary pathology in open-angle mechanism, while formation of posterior synechiae and peripheral anterior synechiae (PAS) contributes toward development of angle-closure glaucoma.

H. Selvan (✉)
Moorfields Eye Hospital NHS Foundation Trust, London, UK

S. K. Khokhar · S. Gupta
Dr. Rajendra Prasad Centre for Ophthalmic Sciences, All India Institute of Medical Sciences, New Delhi, India
e-mail: shikhagupta@aiims.edu

S. Gupta et al. (eds.), *Childhood Glaucoma*, https://doi.org/10.1007/978-981-19-7466-3_20

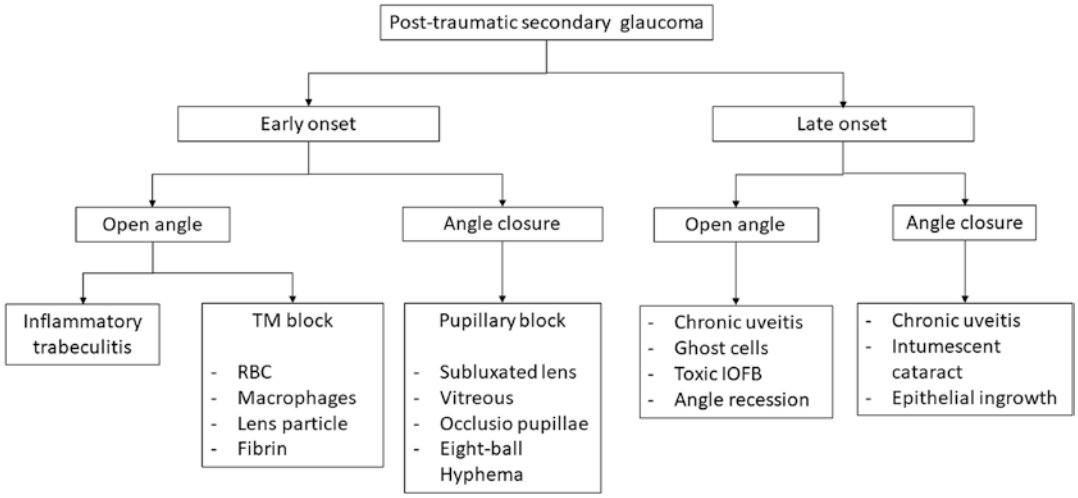

Fig. 20.1 Mechanisms of post-traumatic secondary glaucoma. *IOFB* intraocular foreign body, *TM* trabecular meshwork, *RBC* red blood cells

20.1 Case Examples

Case 20.1

A 16-year-old boy was brought to the casualty with complaints of sudden painful loss of vision and redness following trauma to the left eye by a cricket ball 3 hours ago. There was no history of any vomiting, loss of consciousness, or ear-nose-throat bleed.

Examination: Best-corrected visual acuity (BCVA) was 6/6 in right eye (RE) and perception of light with accurate projection of rays in left eye (LE). The LE upper lid showed ecchymosis, but on palpation, the orbital rim appeared intact with no subcutaneous emphysema or periorbital anesthesia. Ocular motility was full and free. The LE showed subconjunctival hemorrhage, clear cornea, and total hyphema (grade 4) (Fig. 20.2); RE examination was under normal limits, with a brisk direct and consensual pupillary reflex. Applanation IOP was 14 mmHg in RE and 40 mmHg in LE.

Investigations: (1) LE Ultrasound (USG) B scan showed echoes in the posterior segment suggestive of vitreous hemorrhage; retina was attached (2) X-ray face and orbit – no fractures were detected.

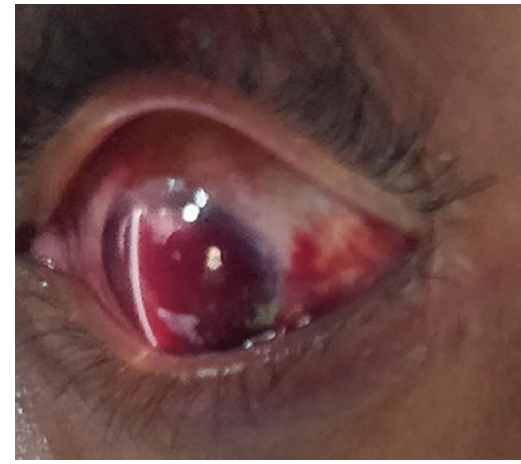

Fig. 20.2 Left eye of the patient showing subconjunctival hemorrhage and total hyphema

Diagnosis: LE total hyphema secondary to closed globe injury with secondary post-traumatic glaucoma

Differential diagnosis: Sudden hyphema in children without history of preceding trauma should raise the suspicion of the following:

- Retinoblastoma: A mass with calcification in the retina, with/without a positive family history is diagnostic.

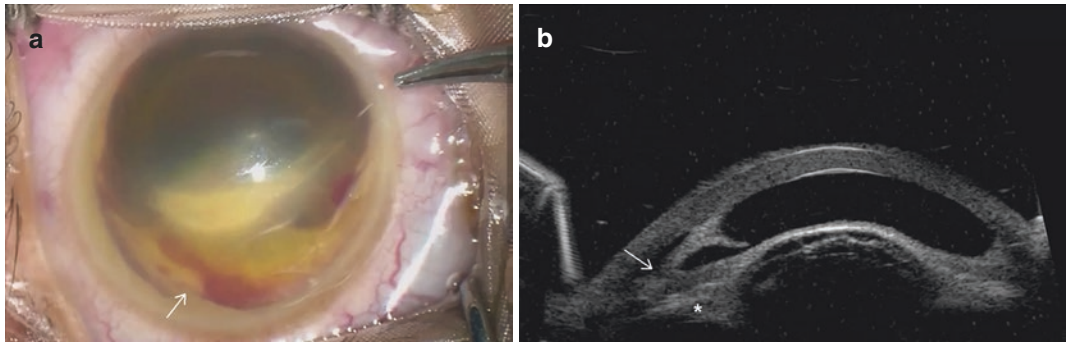

Fig. 20.3 A case of Juvenile Xanthogranuloma. (**a**) Intra-operative photograph showing a dense layered-hyphema at different stages due to recurrent hemorrhage (white arrow) (**b**) Ultrasound biomicroscopy showing dense inferior membranes in the angle (white arrow) and behind the iris (*) due to hemorrhage and mass lesion, causing secondary angle closure

- Juvenile xanthogranuloma (Fig. 20.3): A mass may or may not be detectable on clinical examination. UBM scan can identify a lesion in the iris.
- Systemic bleeding disorders: A full blood count, peripheral blood smear, and entire bleeding and clotting profile can identify inborn or acquired hematological disorders.
- Shaken baby syndrome: A discordant history and multiple tri-layered retinal hemorrhages could be a diagnostic feature.

Treatment

- Immediate treatment: Propped-up position. Intravenous mannitol 20% 1 g/kg and oral acetazolamide 500 mg stat dose, fixed-dose combination of brimonidine 0.2% + timolol maleate 0.5%BD, dexamethasone QDS, and homatropine 2% TDS.
- Definitive treatment: Anterior chamber (AC) washout followed by close monitoring for incidence of rebleeds and IOP status is required. If the IOP remains uncontrolled even after a thorough AC wash, an urgent trabeculectomy with mitomycin C (MMC) is warranted.

In young children with post-traumatic total hyphema and high IOP where serial monitoring would require examination under anesthesia each time, an anterior chamber irrigation aspiration along with trabeculectomy can be considered in the same sitting.

Other Examples: Figs. 20.4, 20.5

Learning Points

- Post-traumatic hyphema usually results from tearing of the major arterial circle vessels present at the iris base.
- Hyphema is graded as microscopic (suspended red blood cells), grade 1 (<1/3 of AC), grade 2 (1/3–1/2 AC), grade 3 (1/2–near total), and grade 4 (total/eight-ball hyphema).
- Indications for surgical intervention include:
  - IOP > 60 mmHg for 2 days, > 50 mmHg for 5 days, > 35 mmHg for 7 days, or near-total/total hyphema with IOP > 25 mmHg for 5 days
  - Failure of hyphema to resolve to <50% of anterior chamber volume by 8 days
  - Sickle cell disease/trait and mean IOP > 24 mmHg for ≥24 hours or IOP spikes repeatedly >30 mmHg
  - Preexisting glaucomatous optic neuropathy and unacceptable IOP
  - Corneal blood staining
- Rebleeding can occur in up to one-third of patients, frequently 2–5 days after injury.

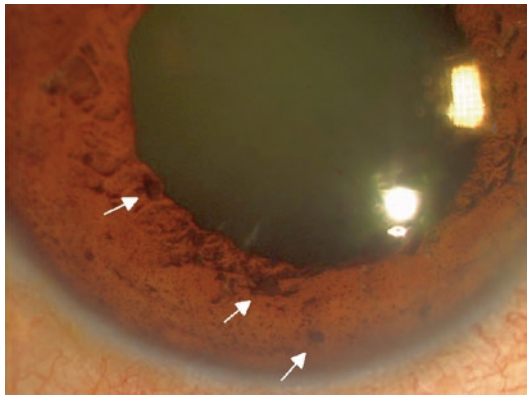

Fig. 20.4 Slit-lamp photograph of a post-traumatic eye with organizing hyphema showing blood clots on the iris surface (white arrows)

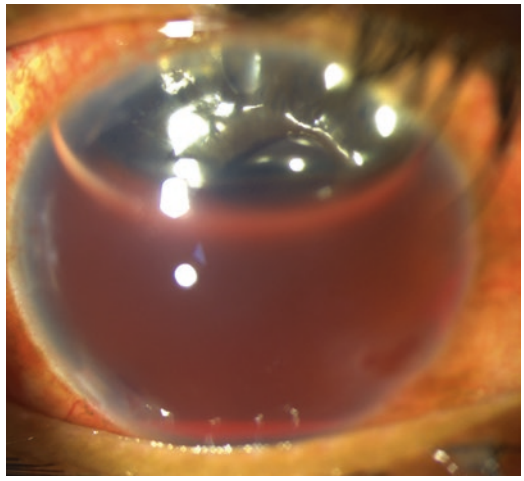

Fig. 20.5 Slit-lamp photograph of a case of iatrogenic hyphema following gonioscopy assisted transluminal trabeculotomy (GATT) procedure for pediatric glaucoma, creating a risk of secondary glaucoma. An anterior chamber wash out was performed

- The development and severity of glaucoma depend upon the amount of hyphema. About 10% of eyes with ≤50% hyphema develop glaucoma, while 25% with >50% hyphema do so. Total and eight-ball hyphema carry a risk of 50% and 100% of glaucoma development, respectively. Hence, it is advisable to perform simultaneous trabeculectomy at the time of hyphema drainage in the latter situation.

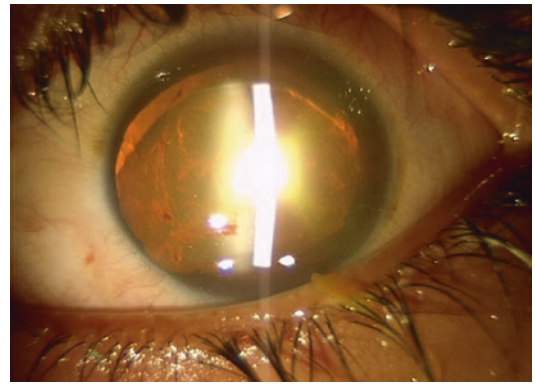

Fig. 20.6 Slit-lamp photograph showing an anteroinferiorly subluxated cataractous lens

Case 20.2

A 15-year-old boy presented with complaints of pain and progressive worsening of vision in his RE over the past 10 days, following injury to the eye by fist.

Examination: Unaided visual acuity (VA) RE 3/60; LE 6/6. Pupillary reflexes were normal both eyes (BE). On examination, RE had a clear cornea with irregular AC depth (deep superiorly, shallow inferiorly), cells 0.5+, no flare, sphincter tears+, and cataractous lens showing phacodonesis. The LE was within normal limits. Applanation IOP was 34 mmHg in RE and 14 mmHg in LE. Gonioscopy showed 180° angle recession in RE. On dilated examination, the RE cataractous lens was anteroinferiorly displaced with visible 180° zonular loss superiorly (Fig. 20.6). Indirect ophthalmoscopy examination did not show any retinal breaks or detachments, cup-disc ratio (CDR) was 0.3:1. Repeat applanation IOP after dilation showed RE 26 mmHg and LE 12 mmHg.

Investigations: (1) BE axial length, keratometry, and automated biometry (2) RE UBM to assess the true extent of zonular deficiency.

Diagnosis: RE post-traumatic subluxated cataractous lens with secondary angle-closure glaucoma.

Differential diagnosis:

- Microspherophakia: Small globular lenses with lax zonules can result in pupillary capture or

complete anterior dislocation leading to glaucoma. They could be an isolated ocular defect or be a part of Weil-Marchesani syndrome.
- Systemic syndromes with zonular weakness: Marfan syndrome, homocystinuria, hyperlysinemia, sulfite oxidase deficiency, etc. The subluxation in Marfan syndrome is typically superotemporal, while in homocystinuria, it is usually infero-nasal.

Treatment:

- Interim management: Rest in supine position. RE atropine 1% TDS and fixed dose combination of brimonidine 0.2% + timolol maleate 0.5% BD.
- Definitive management: RE lens aspiration aided with capsular support ring systems/Cionni ring fixation + posterior chamber intraocular lens (PCIOL) +/− anterior vitrectomy.

Other Examples (Figs. 20.7, 20.8, 20.9, 20.10, 20.11, 20.12, 20.13, and 20.14)

Learning Points
- Secondary angle closure glaucoma caused due to anterior lens displacement and subsequent pupillary block is a type of "inverse glaucoma" that improves with mydriatic cycloplegics (due to posterior displacement of the lens), in contrast to primary angle-closure disease. It causes phacotopic type of glaucoma.
- "Reverse pupillary block" is another mechanism observed in cases of pigment dispersion syndrome. In this scenario, due to a one-way valve effect at the plane of iris and lens, the communication of aqueous between the anterior and posterior chamber is blocked, leading to a relatively higher pressure in the anterior chamber and subsequent backward bowing of the peripheral iris. This effect can be relieved by creation of a peripheral iridotomy.
- The selection of capsular stabilization technique for displaced cataractous lenses, though is surgeon skill based, can be summarized depending upon the extent of zonular weakness:
  - 1 clock hour: Multipiece IOL haptic alignment ± capsular tension ring (CTR)
  - 1–3 clock hours: CTR
  - 4–6 clock hours: Single eyelet Cionni ring fixation
  - 7–9 clock hours: Bi-point fixation with double eyelet Cionni ring/CTR + capsular tension segment (CTS) or lensectomy with IOL (anterior chamber/iris claw/scleral-fixated intraocular lens). In eyes with pre-

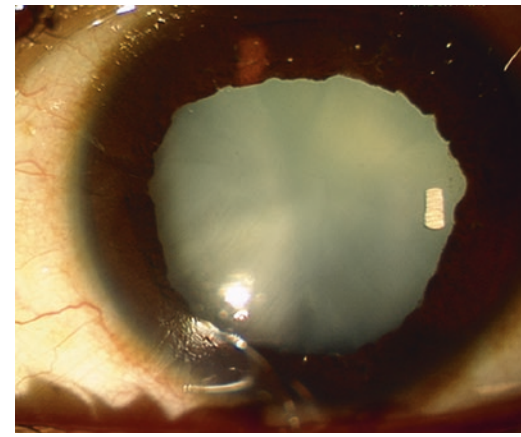

Fig. 20.7 Slit-lamp photograph of an eye with angle recession glaucoma showing additional signs of trauma such as post-traumatic cataract, traumatic mydriasis and multiple sphincter tears

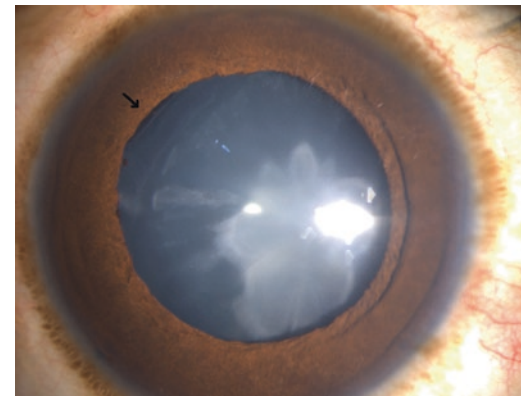

Fig. 20.8 Slit-lamp photograph of an eye showing post-traumatic rosette cataract with nasal subluxation. The black arrow indicates the region of zonular deficiency (2–3 clock hours)

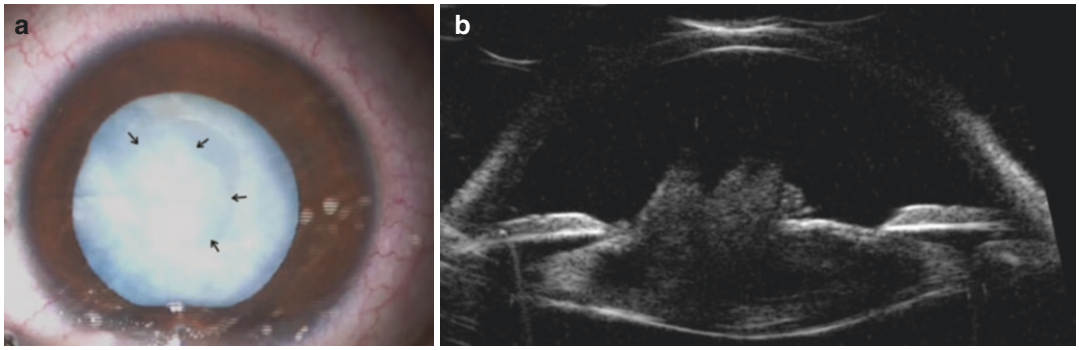

Fig. 20.9 (**a**) Photograph of an eye with post-blunt trauma white cataract with anterior capsular rupture and prolapsed lens matter into the anterior chamber (black arrows) causing secondary inflammatory glaucoma. (**b**) UBM examination of the eye delineated the extent of anterior capsular breach and confirmed the presence of an intact posterior capsule and taut zonules

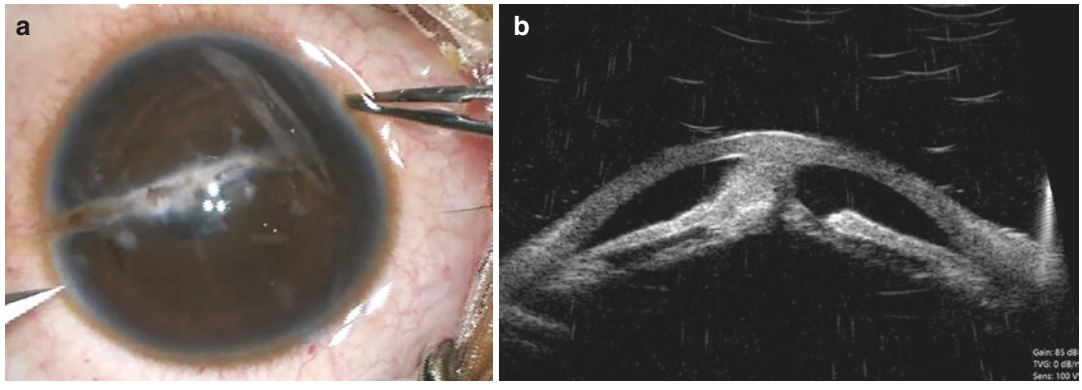

Fig. 20.10 (**a**) Intra-operative photograph showing an eye with healed repaired corneal laceration, non-dilating irregular pupil and an underlying traumatic cataract. (**b**) UBM of the eye showed a partially absorbed cataractous lens with formation of lenticulo-irido-corneal adhesions, causing secondary angle closure glaucoma

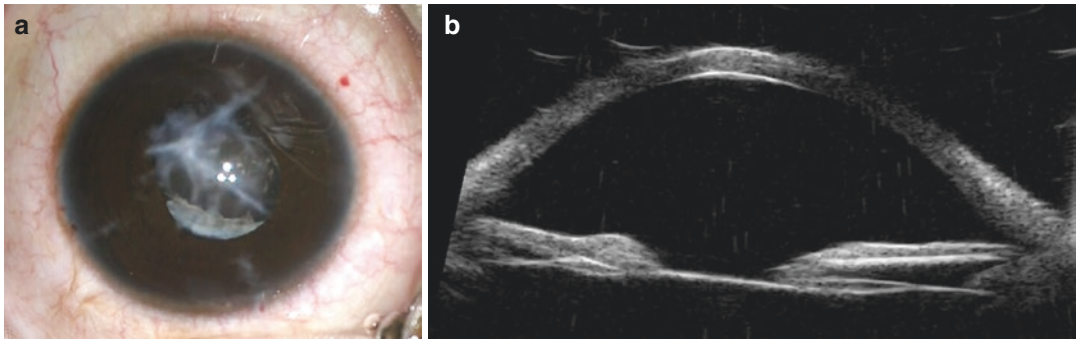

Fig. 20.11 (**a**) Intra-operative photograph showing a healed repaired tri-radiate corneal laceration, posterior synechiae, and a cataract. (**b**) UBM of the eye revealed a post-traumatic membranous cataract

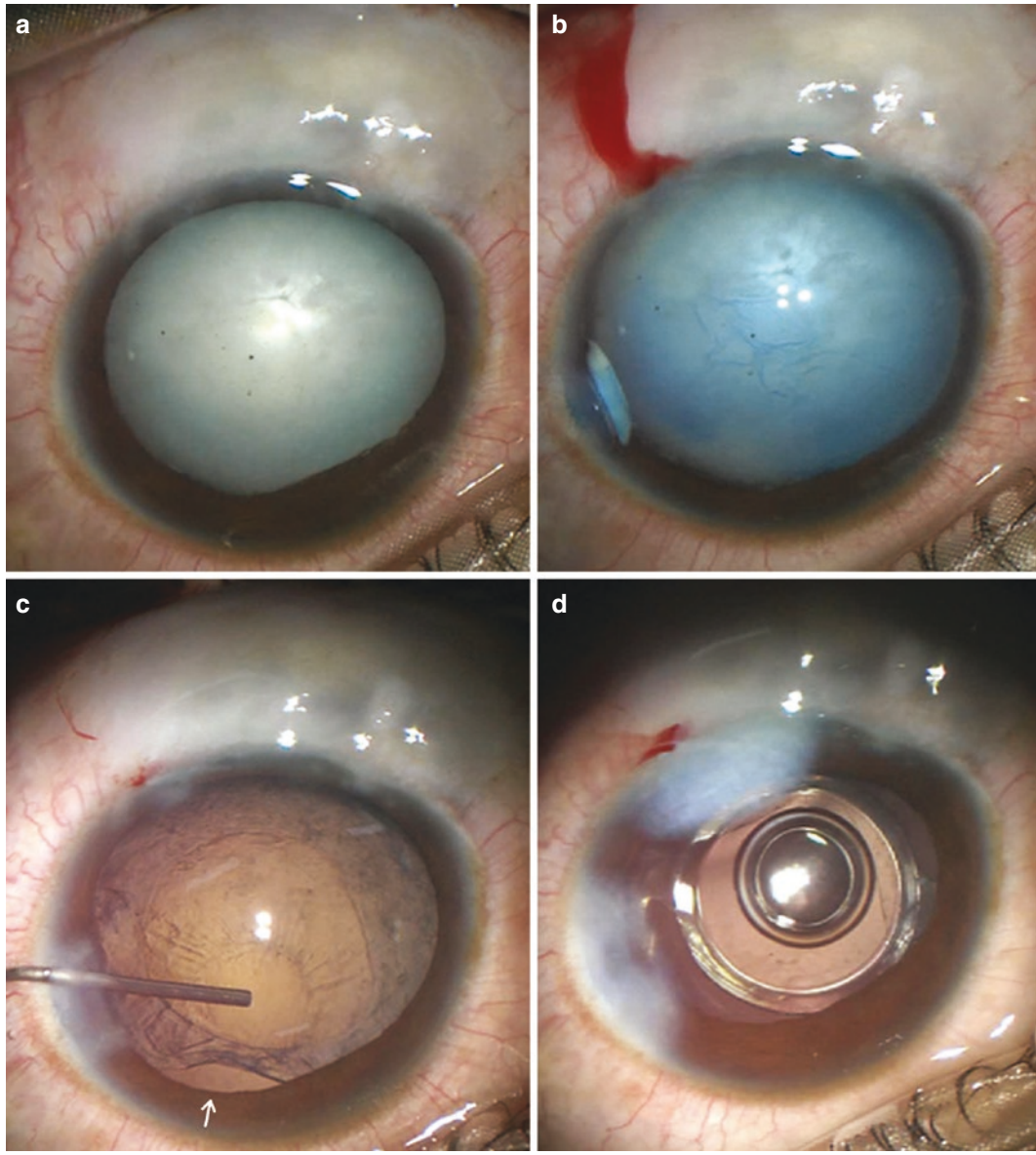

Fig. 20.12 (**a**) Post-traumatic white cataract in an eye with pre-existing trabeculectomy bleb. (**b**) Intraoperative trypan blue staining highlighted wrinkling of anterior capsule. (**c**) Two clock hours inferior subluxation was identified (white arrow). Posterior capsule also showed prominent wrinkling inferiorly. (**d**) The eye was successfully managed with a capsular tension ring and posterior chamber IOL

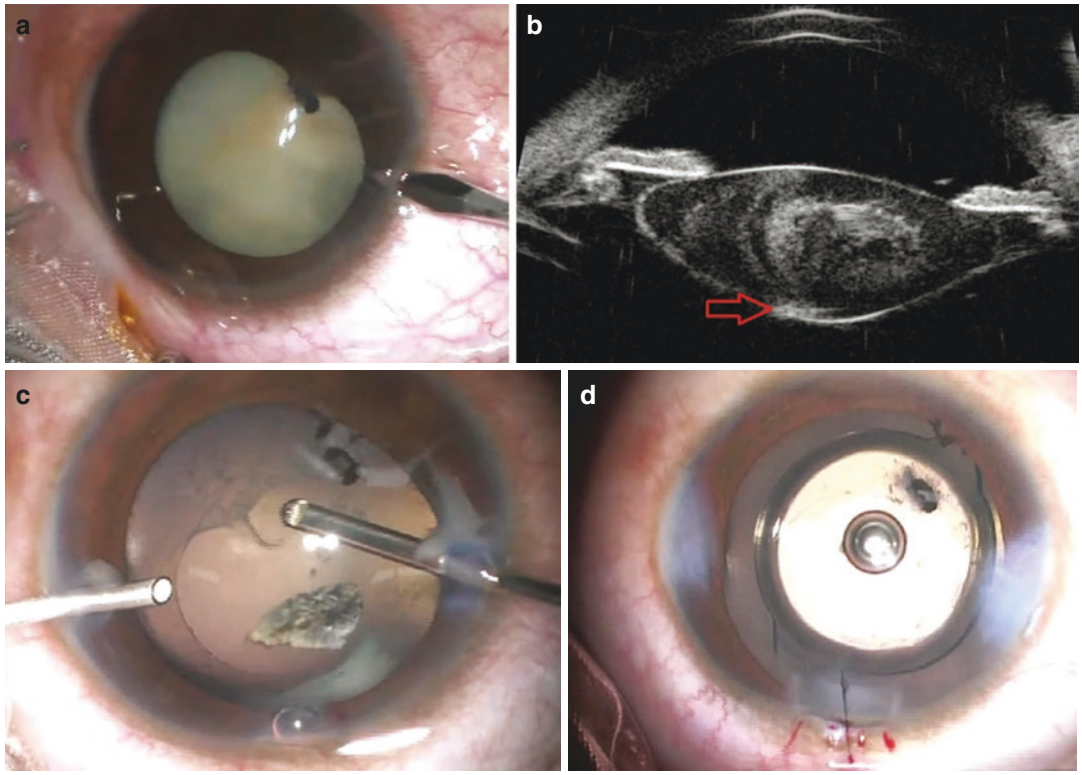

Fig. 20.13 (**a**) Post-traumatic white cataract and high intraocular pressures following an open globe injury. (**b**) UBM showed a hyperechoic structure near the posterior capsule (red arrow). (**c**) Following removal of the cataract, a retained metallic intraocular foreign body was identified. (**d**) The foreign body was removed using forceps, and a posterior chamber intraocular lens was inserted

existing bleb, avoid placing the Cionni suture fixation in the area of bleb.
  - > 9 clock hours: Pars plana lensectomy or intracapsular cataract extraction with anterior chamber/iris claw/scleral-fixated intraocular lens.
- Post-traumatic cataractous lenses with capsular disruption can result in inflammatory glaucoma or lens particle glaucoma.
- Most lens-induced glaucomas can be readily treated with lens extraction ± anterior vitrectomy, which tends to clear the pupillary block, relieve angle closure, and resolve the inflammation, thereby lowering the IOP. However, if the disease had been long-standing, TM damage could occur, necessitating a combined/sequential cataract + glaucoma surgery.

Case 20.3

A 17-year-old girl presented with complaints of dull eye pain and redness in RE for 1 year. There was a history of blunt trauma (shuttle cork injury) to the eye a year back, which was managed conservatively.

Examination: BCVA RE 6/12, LE 6/6. Applanation IOP: RE 44 mmHg and LE 16 mmHg. The RE showed mild corneal edema, a very deep AC as compared to the fellow eye, traumatic mydriasis, and a clear lens; the LE was within normal limits. On gonioscopy, RE showed irregular widening of the ciliary body band (CBB) (angle recession) over 6 clock hours, while the LE showed a normal open angle up to CBB all over (Fig. 20.15). Dilated fundus

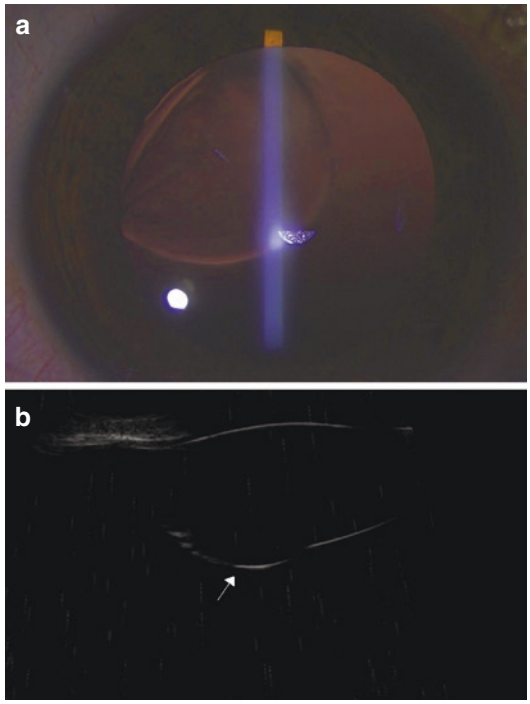

Fig. 20.14 (**a**) Slit-lamp photograph shows a post-traumatic posterior lenticonus with high pressures (**b**) UBM image confirms focal outpouching of the posterior lens capsule (white arrow) (Reproduced with permission from Desai A, Yadav MA, Gupta V, Gupta S. Wavefront analysis to diagnose blunt trauma-induced Weigert ligament dialysis: Isolated peripheral posterior lenticonus. J Cataract Refract Surg. 2018 Nov;44(11):1390–1393. doi: 10.1016/j.jcrs.2018.06.058)

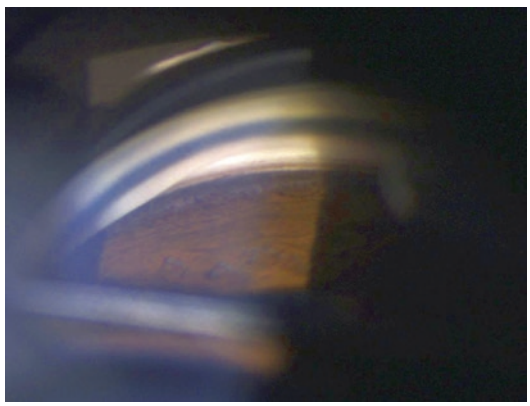

Fig. 20.15 Goniophotograph of right eye showing irregular widening of the CBB suggestive of angle recession

examination showed a CDR of 0.9:1 in RE and 0.3:1 in the LE; peripheral retina was normal BE.

Investigations: Humphrey visual field 30–2 SS of RE – arcuate scotoma

Diagnosis: RE post-traumatic angle recession glaucoma

Differential diagnosis:

- Pigmentary glaucoma: A densely pigmented angle could be confused with widened ciliary body band. The presence of Krukenberg spindle, concave iris configuration, and symmetry between the eyes may aid in differentiation.
- Uveitic glaucoma: Chronic inflammation may result in irregularly dense trabecular pigmentations that could be mistaken for angle recession. Keratic precipitates, AC cells and flare, posterior synechiae, and retrolental cells may aid in diagnosis. Unilateral, subtle uveitis with episodes of very high IOP can point to Posner-Schlossman syndrome.
- Steroid-induced glaucoma: History of topical steroid drops or ointments, periocular/intravitreal injections, nasal sprays, skin creams, and oral steroids should be elicited. A positive history along with a physiologically wide CBB could be a close mimic. Sometimes, a steroid response could exacerbate the severity of other glaucomas.
- Juvenile open-angle glaucoma (JOAG): Unilateral JOAG could be a differential diagnosis as nearly one-fourth may present with unilateral disease. A positive family history and careful gonioscopy will help in exclusion of the disease. Secondary glaucomas are more likely unilateral and should be ruled out before labeling it a case of primary glaucoma.

Treatment: Intravenous mannitol 20% 1 g/kg stat dose, oral acetazolamide 250 mg TDS, topical latanoprost HS, and fixed-dose combination of brimonidine 0.2% + timolol maleate 0.5% BD followed by listing for early trabeculectomy with mitomycin C RE if IOP remains uncontrolled.

Learning Points

- Comparison of gonioscopy findings with the fellow eye is important to identify abnormal and/or irregular broadening of the CBB, indicative of angle recession. Sometimes, a wide CBB may be physiological in both eyes.
- Angle recession can be seen in nearly 8% of eyes without glaucoma and 35% of eyes with glaucoma.
- The greater the extent of angle recession, the higher is the likelihood of glaucoma. 4–9% of patients with angle recession >180° can develop chronic glaucoma and therefore need long-term monitoring.
- More than 70% of eyes with traumatic hyphema may have angle recession. Gonioscopy is usually advised at least 2–6 weeks after injury when ocular inflammation/hyphema has resolved and pain has minimized.

Case 20.4

A 17-year-old boy presented with complaints of sudden blurring of vision in RE following a close-range firecracker injury.

Examination: Unaided VA of RE was 6/60, improving with pinhole to 6/18; LE 6/6. Goldmann IOP: RE 6 mmHg and LE 16 mmHg. Examination of RE showed Bowman corneal folds, normal AC depth, cells 0.5+ flare 1+, superotemporal iridodialysis, a D-shaped pupil, and a cataractous lens (Fig. 20.16). There was no phacodonesis. A gentle indirect gonioscopy

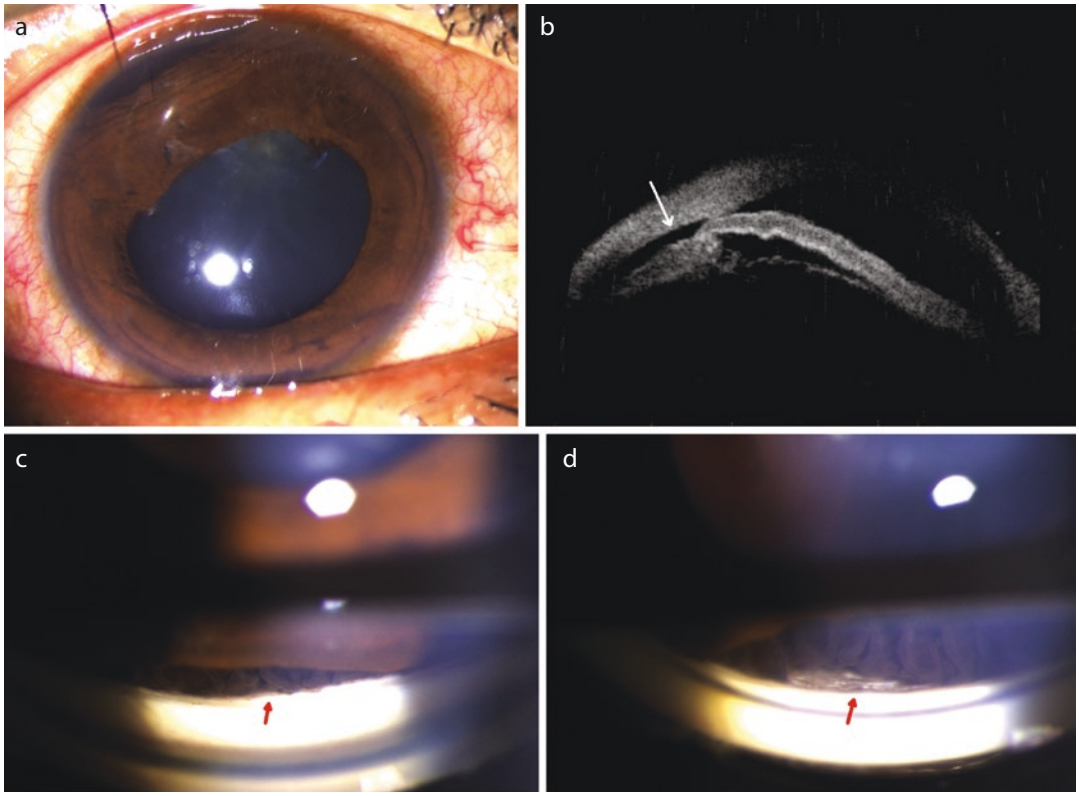

Fig. 20.16 (**a**) Clinical photograph showing superotemporal iridodialysis, D-shaped pupil, and cataractous lens (**b**) Ultrasound biomicroscopy (50 MHz, 85 dB) revealing cyclodialysis behind an intact iris (white arrow) that was undetectable clinically (**c**) Indirect gonioscopy in primary gaze showing an area of suspicious cleft (red arrow) (**d**) Dynamic gonioscopy opening up the maximum dimensions of the cleft like a rising crescent (red arrow) (Reproduced with permission from Gupta S, Selvan H, Agrawal S, Gupta V. Dynamic gonioscopy and ultrasound biomicroscopy for diagnosis of latent or low-lying cyclodialysis clefts. Clin Exp Ophthalmol. 2018; 46(8):960–962)

of RE showed a suspicious cleft in the superior quadrant. Dynamic gonioscopy opened the cleft spanning over 2 clock hours, and also identified an adjacent latent cleft of 2 more clock hours. Fundus examination showed a blurred disc margin with CDR 0.2:1, hypotonic maculopathy, and peripheral shallow choroidal detachments. LE examination was within normal limits.

Investigations: (1) Circumferential swept-source anterior segment OCT (SS-ASOCT) – Superior cyclodialysis cleft spanning over 5 clock hours. The apparently attached area between the two clinically identified clefts also had ciliary body detachment behind the intact iris, communicating on either sides (2) circumferential ultrasound biomicroscopy (UBM): findings same as SS-ASOCT. Additionally, shallow choroidal detachments were noted. (3) BE axial length (noncontact technique), keratometry, and biometry.

Diagnosis: RE post-traumatic cataract with iridodialysis and cyclodialysis

Differential diagnosis:

- Posterior scleral rupture: Post-traumatic hypotonic eyes without any identifiable cause could harbor a posterior globe rupture. A gentle USG B scan can clinch the diagnosis.
- Ciliary body shutdown: A severely injured eye with chronic inflammation may develop cyclitic membranes, resulting in hypotony and subsequent atrophic bulbi.
- **Treatment:** RE lens aspiration with IOL in bag + modified sewing machine endocyclopexy + stroke and dock iris repair.

Other Examples (Figs. 20.17 and 20.18)

Learning Points

- A cyclodialysis cleft should be looked for in an eye with chronic post-traumatic hypotony without other identifiable causes.
- Identifying the exact location, full extent and maximum dimensions of cyclodialysis clefts are crucial in planning their management.
- The surgical options for cleft repair include exocyclopexy, exocyclotamponade, endocyclopexy, and endocyclotamponade. The ab interno techniques are easier to perform, efficacious, and safer when compared to *ab externo* methods.
- Modified sewing machine technique of endocyclopexy can be performed in cases of coexisting posterior capsular rupture or zonular dialysis.
- In view of the transient hyperopic shift, IOL power calculation in hypotonic eyes is better based on their pre-injury measurements or the fellow eye biometry (if symmetric) to avoid postoperative refractive surprises.

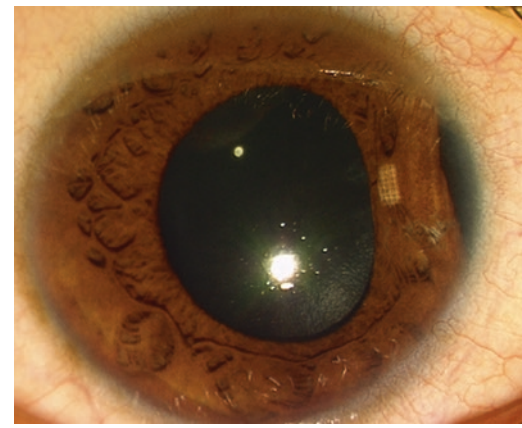

Fig. 20.17 Slit-lamp photograph of a case of isolated iridodialysis post blunt trauma

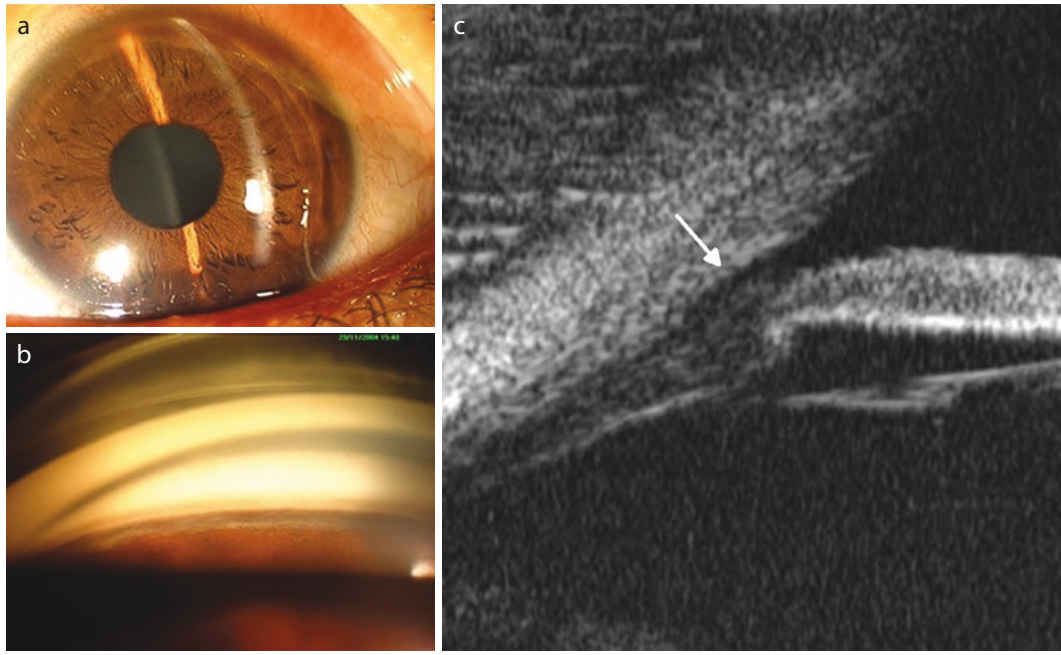

Fig. 20.18 A case of isolated cyclodialysis: (**a**) Slit-lamp photograph of anterior segment. (**b**) Goniophotograph showing the cleft (**c**) UBM image showing disinsertion of ciliary body from the scleral spur (white arrow)

20.2 Management Strategies (Figs. 20.19 and 20.20)

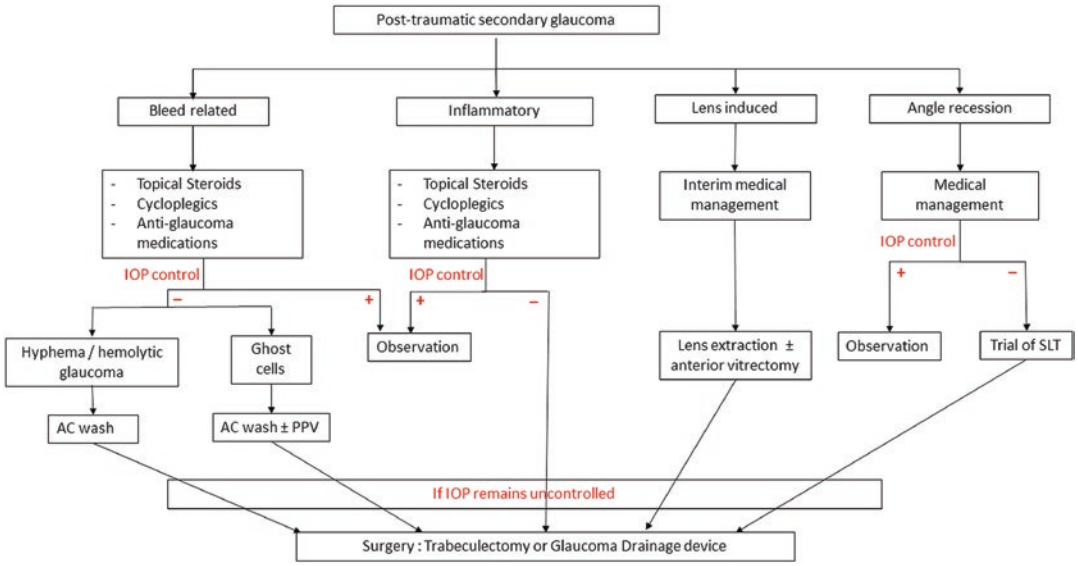

Fig. 20.19 Management strategies for post-traumatic glaucoma. *AC* anterior chamber, *IOP* intraocular pressure, *PPV* pars plana vitrectomy, *SLT* selective laser trabeculoplasty. + IOP controlled, - IOP uncontrolled

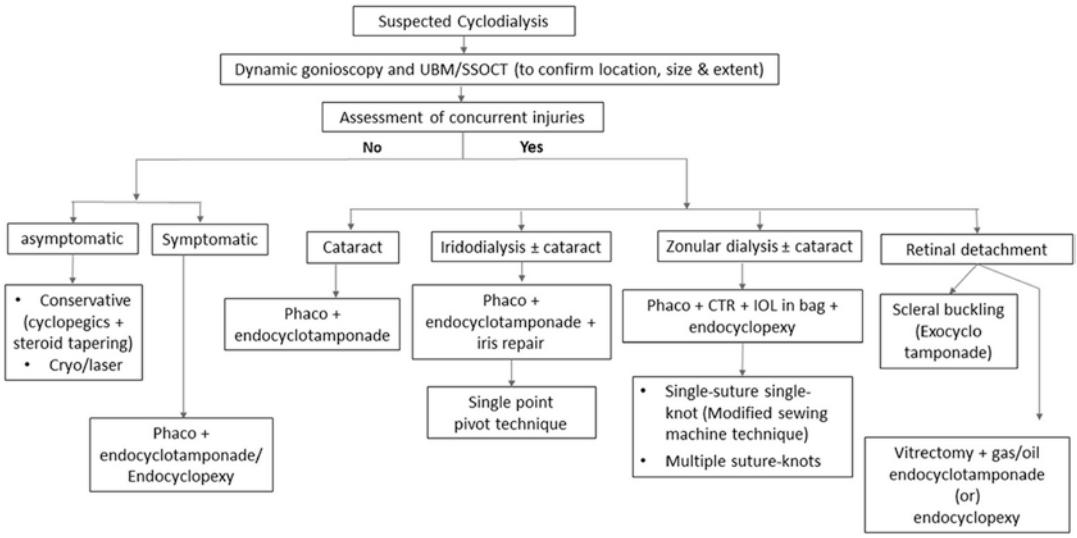

Fig. 20.20 Generalized management algorithm for cyclodialysis clefts. *CTR* capsular tension ring, *IOL* intraocular lens, *Cryo* Cryopexy, *Phaco* Phacoemulsification, *SSOCT* swept source anterior segment optical coherence tomography, *UBM* ultrasound biomicroscopy (Reproduced with permission from Selvan, H., Gupta, V. and Gupta, S. (2019), Cyclodialysis: an updated approach to surgical strategies. Acta Ophthalmol, 97: 744–751. https://doi.org/10.1111/aos.14210)

20.3 Conclusions

In conclusion, trauma is an important cause of secondary glaucoma. It may have multiple factors contributing and can occur at any time point. A detailed work-up, well-planned management, and life-long monitoring are crucial for optimal outcomes.

Suggested Reading

Girkin CA, McGwin G Jr, Long C, Morris R, Kuhn F. Glaucoma after ocular contusion: a cohort study of the United States eye injury registry. J Glaucoma. 2005;14(6):470–3. https://doi.org/10.1097/01.ijg.0000185437.92803.d7.

Gupta S, Selvan H, Agrawal S, Gupta V. Dynamic gonioscopy and ultrasound biomicroscopy for diagnosis of latent or low-lying cyclodialysis clefts. Clin Exp Ophthalmol. 2018;46(8):960–2. https://doi.org/10.1111/ceo.13316.

Kalamkar C, Mukherjee A. Incidence, clinical profile, and short-term outcomes of post-traumatic glaucoma in pediatric eyes. Indian J Ophthalmol. 2019;67(4):509–14. https://doi.org/10.4103/ijo.IJO_655_18.

Khokhar S, Gupta S, Yogi R, Gogia V, Agarwal T. Epidemiology and intermediate-term outcomes of open- and closed-globe injuries in traumatic childhood cataract. Eur J Ophthalmol. 2014;24(1):124–30. https://doi.org/10.5301/ejo.5000342.

Selvan H, Gupta V, Gupta S. Cyclodialysis: an updated approach to surgical strategies. Acta Ophthalmol. 2019;97(8):744–51. https://doi.org/10.1111/aos.14210.

Shingleton BJ, Hersh PS, Kenyon KR. Chapter 9-10 Eye trauma. St.Louis: Mosby-Year Book; 1991.

Sihota R, Kumar S, Gupta V, Dada T, Kashyap S, Insan R, Srinivasan G. Early predictors of traumatic glaucoma after closed globe injury: trabecular pigmentation, widened angle recess, and higher baseline intraocular pressure. Arch Ophthalmol. 2008;126(7):921–6. https://doi.org/10.1001/archopht.126.7.921.

Walton W, Von Hagen S, Grigorian R, Zarbin M. Management of traumatic hyphema. Surv Ophthalmol. 2002;47(4):297–334. https://doi.org/10.1016/s0039-6257(02)00317-x.

Glaucoma in Retinopathy of Prematurity

21

Nawazish Shaikh, Ruchir Tewari, and Parijat Chandra

21.1 Introduction

Retinopathy of prematurity (ROP) is a potentially blinding disease affecting the retinal vasculature of preterm babies and is emerging as an important cause of childhood blindness worldwide. The most important risk factors for ROP development are prematurity and low birth weight. The other common risk factors are respiratory distress, necrotizing enterocolitis, twin pregnancy, patent ductus arteriosus, poor weight gain, hypoxia, anemia, intraventricular hemorrhage, hypotension, blood transfusions, hypoxia, episodes of apnea, mechanical ventilation, acidosis, and sepsis.

An ROP screening program is the best way to detect treatable ROP in time. The international screening guidelines suggest screening of babies <30 weeks of gestational age (GA) and <1500 g birth weight (BW) within the first 4 weeks of life; bigger babies with risk factors can also be screened at the discretion of the neonatologist. Since bigger babies may develop ROP in the presence of high risk factors, modified screening guidelines are used in India, which suggest screening babies <34 weeks of GA or <2000 g BW or even bigger babies having risk factors (as above). First, screening is recommended at 4 weeks of birth but may be done as early as 2–3 weeks of birth in very small neonates with GA <28 weeks or BW <1200 g.

Laser therapy of the avascular retina has been the mainstay of treatment for the last few decades. With the changing profile of ROP involving small zones (Zone 1/Zone 2 posterior), and occurrence of severe variants like aggressive ROP (AROP), the use of intravitreal anti-VEGF drug injections (like ranibizumab / bevacizumab / aflibercept) is getting popular. Landmark trials such as the BEAT-ROP and RAINBOW trials have demonstrated the utility of anti-VEGF injections in Zone 1 and Zone 2 ROP. Vitreoretinal surgery is needed for cases developing advanced disease with retinal detachment. Stage 5 ROP is the last stage of blinding ROP and has poor prognosis.

21.2 Glaucoma in ROP

ROP is a potentially treatable disease with good visual outcomes if managed in time. The development of complications such as glaucoma in ROP is an important cause of morbidity in such eyes, hence the disease requires a prolonged follow-up. Clinically, any subtype of glaucoma in association with ROP in infancy will present with corneal clouding, Haab's striae, watering, and enlarged corneal diameter along with size disparity between the two eyeballs. The anterior

N. Shaikh · P. Chandra (✉)
Dr. Rajendra Prasad Centre for Ophthalmic Sciences, All India Institute of Medical Sciences, New Delhi, India

R. Tewari
Tewari Eye Centre, Ghaziabad, Uttar Pradesh, India

S. Gupta et al. (eds.), *Childhood Glaucoma*, https://doi.org/10.1007/978-981-19-7466-3_21

chamber may be open in those coexisting with primary trabeculodysgenesis/those presenting post-vitrectomy or it may be shallow/flat in eyes with closed angles with/without iris neovascularization, especially in patients with neovascular glaucoma/closed funnel retinal detachment.

Since patients may develop secondary angle-closure glaucoma at later time periods ranging from as early as weeks to years after intervention (cryotherapy, laser therapy, and vitrectomy), follow-up is essential in all patients.

21.3 Etiopathogenesis of Glaucoma in ROP

Glaucoma in association with ROP is observed in the following scenarios:

1. **Secondary glaucoma: Advanced disease (Stage 4/5 ROP)**

   The prevalence of secondary glaucoma in advanced stages of ROP (Stage 4A,4B and 5) is as high as 30%, being the predominant patho-mechanism responsible for glaucoma in association with ROP. These children may present with corneal edema and shallow to flat anterior chamber with raised intraocular pressure (IOP) as early as the first year of life to as late as adulthood. The predominant mechanism of glaucoma is secondary angle closure caused by the anterior displacement of iris-lens diaphragm due to contraction of retrolental membranes. Other proposed mechanisms include neovascular glaucoma, pupillary block, and ciliary block glaucoma.
2. **Secondary glaucoma: Post-laser therapy for ROP**

   Laser photocoagulation has been the mainstay of management of ROP, but it may lead to transient increase in IOP which usually normalizes in a few days (Fig. 21.1). These neonates may present with raised IOP, corneal edema, shallowing of anterior chamber, formation of synechiae, and increased corneal diameter. The proposed mechanisms behind angle-closure glaucoma following laser therapy are thermal injury to choroidal vasculature causing choroidal congestion and ciliary body edema that causes anterior displacement of iris-lens diaphragm. Other contributory mechanisms include increased lens size and intraocular inflammation causing posterior synechiae leading to pupillary block. Transient increase in IOP is usually self-limiting and only in a few cases it may persist in the post-laser period. The ETROP study showed prevalence of glaucoma post-laser at 6 years to be 1.67%, whereas the CRYO-ROP study (with cryotherapy) showed the prevalence of glaucoma at 5.5 years examination to be 2.9% in treated eyes and 6.1% in untreated eyes.
3. **Secondary glaucoma: Post-surgery for advanced ROP**

   Post-vitreoretinal surgery glaucoma in ROP has an incidence as high as 14.5% with median time intervals reported in different studies varying between 2.5 and 5 months. These children present with watering, corneal edema, enlargement of corneal diameters, and usually a normal to deep anterior chamber. The proposed mechanisms of glaucoma

Fig. 21.1 Laser treatment of ROP being performed in the operation theatre under general anaesthesia using Laser Indirect Ophthalmoscope and 28D lens

include surgical trauma, intraocular inflammation, steroid responsiveness, goniodysgenesis, and oxidative damage to trabecular meshwork.

4. **Secondary glaucoma: Post-intravitreal anti-VEGF injection for ROP**

   Transient IOP rise due to increase in intraocular volume may occur following intravitreal anti-VEGF injection in ROP and is rarely managed with anterior chamber paracentesis. Iatrogenic needle injury by improper technique can lead to injury of the lens, retina, or choroid, which can lead to inflammatory reaction and secondary glaucoma as well. Other possible mechanisms could be prolonged raised intraocular volume and harmful effect of anti-VEGF to retinal nerve fiber layer, but this is a rare scenario.

5. **Primary congenital glaucoma (PCG) coexistent with ROP**

   The reported prevalence of primary congenital glaucoma coexistent with ROP is 0.08% and provides a unique situation which has been rarely reported. These neonates present early due to corneal edema, Haab's striae, and watering. Routine retina screening is done based on screening criteria, but examination, diagnosis, and management are challenging due to hazy media. The proposed mechanism of glaucoma in such cases is goniodysgenesis.

21.4 Management of Glaucoma in ROP Eyes

The diagnosis of glaucoma in ROP has multiple challenges. Measurement of intraocular pressure (IOP) is perhaps the best parameter to assess optic nerve head damage as visual field testing is not possible, but IOP measurement in all preterm neonates may not be possible in a high-volume setting. The use of Goldmann applanation tonometer is not possible, and Perkin's tonometer may need sedation or anesthesia, whereas Tono-pen may not correlate well with the gold standard, especially when used with a speculum in a crying distressed baby. Gonioscopy in these premature neonates is arduous and characteristically classifying as open- or angle-closure glaucoma is difficult. By the time parents notice increased corneal size, clouding of the cornea and watering, the diagnosis of glaucoma has already been delayed. These premature eyes have elastic collagen tissue with incomplete development of lamina cribrosa, therefore, even small changes in IOP can present with advanced cupping which may reverse with adequate reduction of IOP.

High IOP is detrimental to ganglion cells which affects the visual function of affected neonates. Control of IOP is essential for improvement in visual function. Management options include medical management with topical medications, trabeculectomy, combined trabeculectomy and trabeculotomy, peripheral iridectomy, lensectomy with anterior vitrectomy and cilioablative procedures. Despite management and control of IOP, visual acuity outcomes in these patients may be poor.

21.5 Case Examples

Case 21.1: Secondary Glaucoma after Stage 4 ROP Surgery

A female child born at 29 weeks of GA with 1228 g BW was first evaluated at 34 weeks of post-menstrual age (PMA) and was diagnosed as both eye (BE) Zone 2 Stage 3 ROP with plus disease and underwent laser therapy of avascular retina BE. Right eye (RE) regressed whereas the left eye (LE) progressed to Stage 4A ROP at 38 weeks. 25G lens-sparing vitrectomy (LSV) was done in LE. At 4 weeks after LSV, parents noticed watering from LE and presented to us.

Examination and Diagnosis: The child had corneal edema and increased corneal diameters (CD) in LE (11 mm LE compared to 10 mm RE). Detailed examination revealed increased sleeping IOP of 28 mmHg LE with increased cupping (0.9:1) (Fig. 21.2a). She was diagnosed as LE secondary glaucoma at 42 weeks of PMA.

Treatment and Outcome: Patient was prescribed topical betaxolol 0.25% twice a day and dorzolamide 2% thrice a day in LE. At last follow-up of 6 months following topical therapy, the IOP was 12 mmHg on medications, the cor-

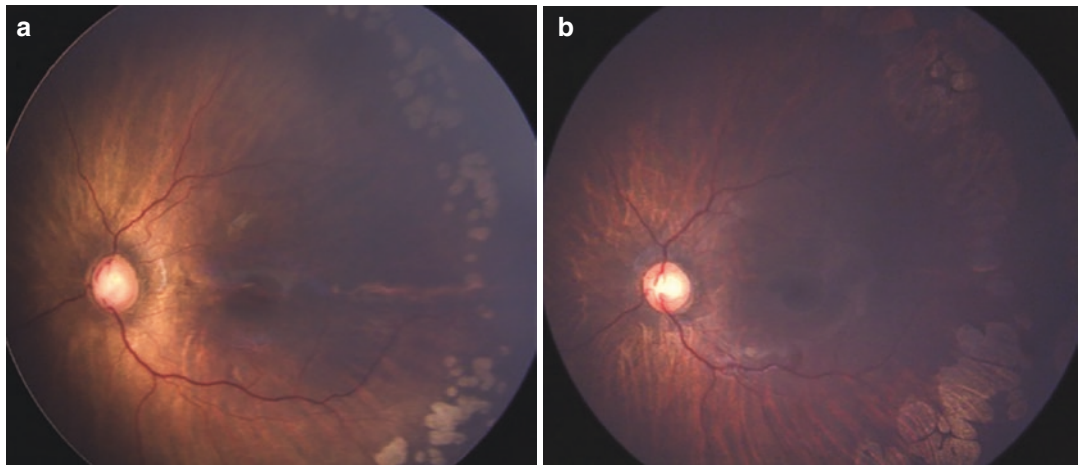

Fig. 21.2 Clinical picture of LE showing increased vertical cup disc ratio (approximately 0.8:1) at 42 weeks of PMA (**a**) and follow-up on medical therapy showing reduced vertical cup disc ratio to 0.5:1 after 6 months with medically controlled IOP (**b**). (Reproduced with permission from: Chandra P, Tewari R, Salunkhe N, Kumawat D, Chaurasia AK, Gupta V. Short-term incidence and management of glaucoma after successful surgery for Stage 4 retinopathy of prematurity. Indian Journal of Ophthalmology. 2019 Jun;67(6):917)

nea was clear with stable CD of 11 mm and reversed cupping of 0.5:1 in LE. (Fig. 21.2b).

Learning Points

- Increase in IOP can cause increase in eye size. Corneal edema with watering may provide an early clue to the diagnosis of glaucoma.
- Reversal of cupping can occur with adequate control of IOP.
- Due to absence of dysgenesis in ROP associated secondary glaucoma (following vitrectomy/injections or laser), IOP may respond well to medications unlike congenital glaucoma associated with angle dysgenesis.

Case 21.2: Late Secondary Glaucoma After Stage 4 ROP Surgery

A male child born at 30 weeks of GA with BW of 1600g was first evaluated at 35 weeks of PMA and diagnosed with BE Zone 2 posterior Stage 3 ROP with plus disease and underwent prompt laser photocoagulation. RE regressed uneventfully but LE progressed requiring a LSV at 37 weeks of PMA. The child presented at 5 months' follow-up with parents noticing increased globe size and cloudiness of the cornea in LE since one week.

Examination and diagnosis: The child had corneal edema and increased corneal diameter in LE (13 mm LE vs. 11 mm in RE). Detailed evaluation revealed an increased IOP of 24 mmHg with increased cupping of 0.7:1 in LE (Fig. 21.3a.) He was diagnosed as LE secondary glaucoma at 58 weeks of PMA.

Treatment and outcome: He was prescribed topical betaxolol 0.25% BD and latanoprost 0.005% OD initially in LE. On follow-up at 61 weeks of PMA, IOP was still 24 mmHg in LE on medical management with persistent corneal haze. The child underwent an uneventful filtering surgery (combined trabeculotomy-trabeculectomy with mitomycin-C) in LE. At 3 months' follow-up, IOP was 14 mmHg with stabilization of corneal diameters (13 mm) and cupping (0.7:1), with gonioscopy showing a patent ostium in LE (Fig. 21.3b, blue arrow).

Learning Points

- Postsurgical glaucoma may present as late as 20 weeks after LSV with irreversible increase in corneal diameters. Hence, regular follow-ups following surgery are paramount.
- Management with topical glaucoma medication alone may not suffice, and filtering surgery like combined trabeculotomy-trabeculectomy with mitomycin-C may be needed.

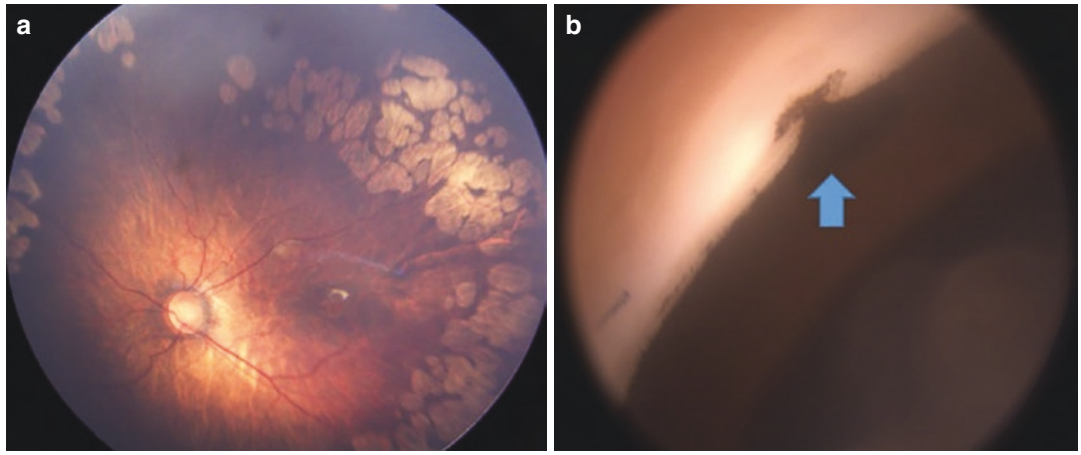

Fig. 21.3 Clinical picture of LE showing increased vertical cup disc ratio (0.7:1) at 20 weeks after LSV (58 weeks of PMA) (**a**). The child was managed with topical medications and underwent a filtering surgery with patent ostium (blue arrow indicating iris adhered partially to the site of filter) seen at 3 months after filtering surgery (**b**). (Reproduced with permission from: Chandra P, Tewari R, Salunkhe N, Kumawat D, Chaurasia AK, Gupta V. Short-term incidence and management of glaucoma after successful surgery for Stage 4 retinopathy of prematurity. Indian Journal of Ophthalmology. 2019 Jun;67(6):917)

Case 21.3: Disc Suspect with Anti-VEGF Injection in ROP

A male child born at 28 weeks of GA with 1000 g BW was first evaluated at 40 weeks of PMA and diagnosed with BE Zone 2 posterior Stage 3 ROP with plus disease with extensive neovascularization with a cupping of 0.6:1 (Fig. 21.4a, b) and underwent BE intravitreal half dose anti-VEGF injection (Ranibizumab 0.25 mg) under topical anesthesia in operation theater under monitored anaesthesia care.

Examination and diagnosis: At 44 weeks of PMA, the child was noted to have similar vertical cup disc ratio as on presentation (0.6:1) in BE (Fig. 21.4c, d). Sleeping IOP was 12 mmHg in RE and 10 mm of Hg in LE with corneal diameters of 10 mm in both eyes. He was diagnosed as glaucoma disc suspect in BE.

Treatment and outcome: The child was advised close follow-up and the cupping was found to be stable with no change in corneal diameters with IOP maintained in a range of 10–14 mmHg in BE. However, reactivation of ROP was noted at 48 weeks of PMA, and the child underwent prompt laser therapy with uneventful regression in both eyes. At last follow-up at 56 weeks of PMA, the child had an IOP of 10 mmHg with stable corneal diameters (10 mm) and cupping in BE (0.6:1).

Learning Points

- Increased vertical cup disc ratio of the disc can be observed without a rise in IOP, which needs no further intervention.
- If increased cupping is noted, serial measurements for corneal diameters, fundus, and IOP on Examination under Anesthesia are essential.
- Premature neonates may present with pseudoglaucomatous cupping (possibly due to some degree of subtle periventricular leukomalacia). Family history and genetic factors also play an important role in such cases. If this cupping remains stable over time with no progression, no further intervention is needed.

Case 21.4: Secondary Glaucoma After Anti-VEGF Injection and Laser in AROP

A male child born at 28 weeks of GA with 900 g BW was evaluated at 35 weeks of PMA and diagnosed as BE Zone 1 aggressive ROP (AROP) and underwent prompt BE intravitreal half dose anti-VEGF injection (ranibizumab 0.25 mg) under topical anesthesia followed by BE laser therapy

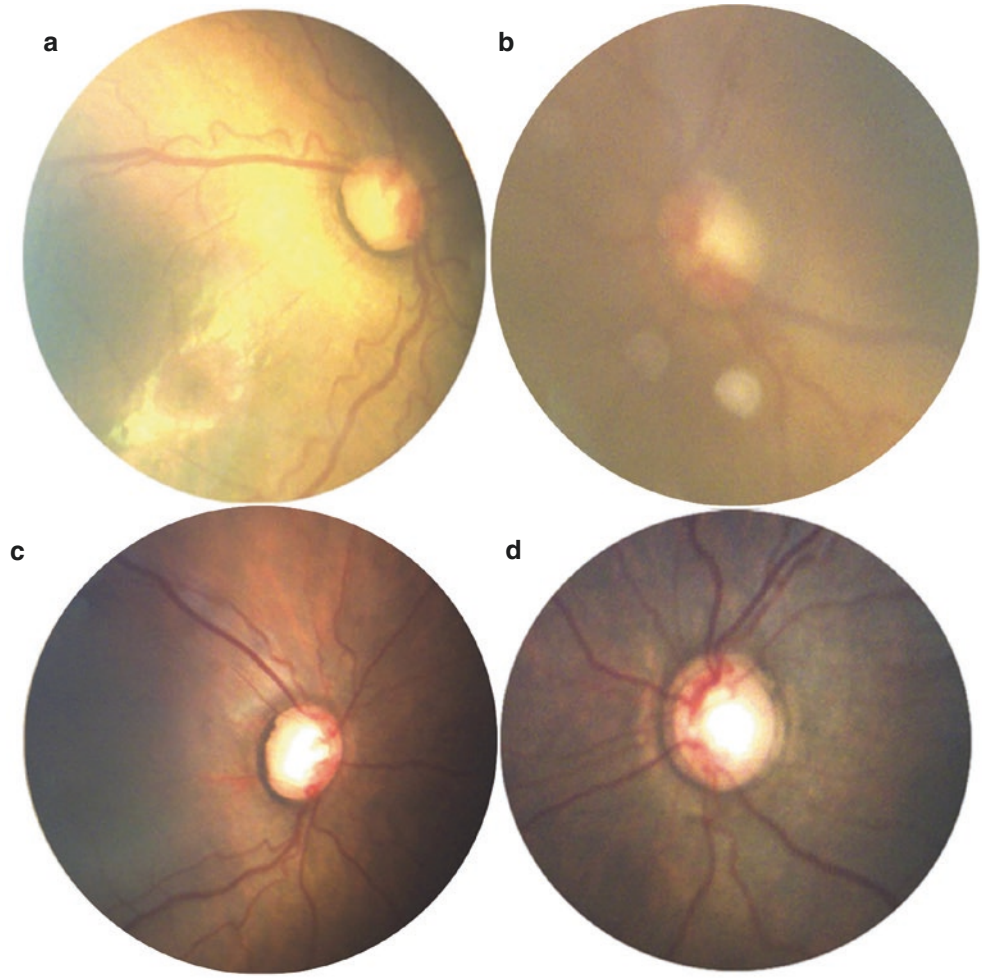

Fig. 21.4 Clinical picture of BE showing vertical cup disc ratio of 0.6:1 at 40 weeks of PMA with poor media clarity (**a**, **b**). Similar vertical cup disc ratio of 0.6:1 in RE and 0.6:1 in LE with superior baring of blood vessel was confirmed 1 month after intravitreal anti-VEGF injection as regression of plus disease occurred providing better media clarity for disc assessment (**c**, **d**)

at 44 weeks of PMA. At 48 weeks of PMA, he presented with BE lamellar cataract and Zone 2 posterior Stage 3 ROP with plus disease suggestive of ROP reactivation (Fig. 21.5a, b). The child underwent prompt laser augmentation at 48 weeks of PMA.

Examination and diagnosis: Detailed evaluation revealed both eye corneal diameters of 9.5 mm with sleeping IOP of 22 mm of Hg with an increased cupping (0.9:1) in RE. He was diagnosed with secondary glaucoma in RE. LE IOP was within normal limits.

Treatment and outcome: He was prescribed topical betaxolol 0.25% twice a day and latanoprost 0.005% once a day in RE. The ROP status was stable. The retinal status and IOP was stable on next visit at 1 week, following which the child was lost to follow-up.

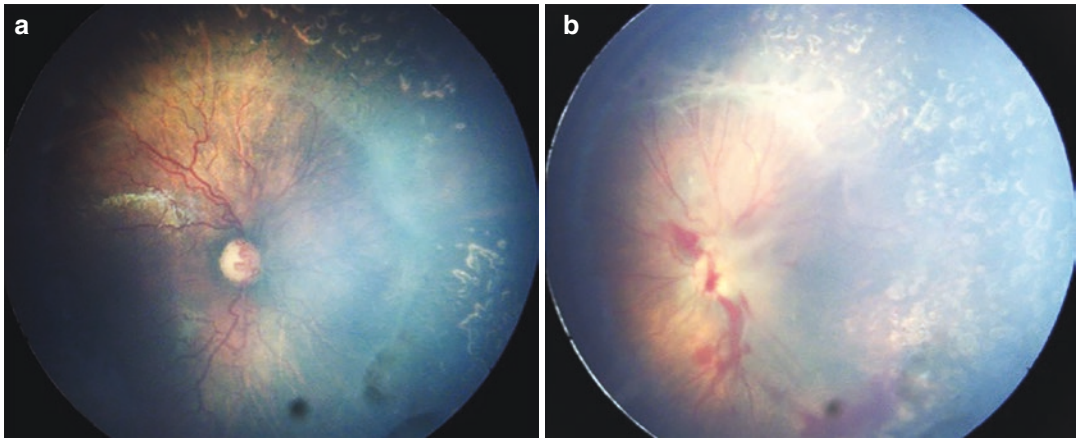

Fig. 21.5 Clinical picture of RE (**a**) showing ROP reactivation with increased vertical cup disc ratio (0.9:1) in RE at 48 weeks of PMA with tortuosity of blood vessels at the disc (plus disease). He was diagnosed as RE secondary glaucoma. LE showed proliferative membranes at disc with tortous blood vessels (plus disease)

Learning Points

- Glaucoma can occur at any time following treatment of AROP. Close monitoring of the disc status, corneal diameters and IOP is important.

21.6 Conclusions

Glaucoma in ROP is unusual but may occur either as primary congenital or as secondary glaucoma and requires a high degree of suspicion for diagnosis. Follow-up is essential to appropriately manage both co-existent conditions in premature babies. Timely intervention is of utmost importance to maximize visual outcome and reduce ocular morbidity.

Suggested Reading

Axer-Siegel R, Bourla D, Friling R, Shalev B, Sirota L, Benjamini Y, et al. Intraocular pressure variations after diode laser photocoagulation for threshold retinopathy of prematurity. Ophthalmology. 2004;111(9):1734–8.

Blencowe H, Moxon SA, Gilbert C. Update on blindness due to retinopathy of prematurity globally and in India. Indian Pediatr. 2016;53:S89–92.

Bremer DL, Rogers DL, Good WV, Tung B, Hardy RJ, Fellows R. Glaucoma in the early treatment for retinopathy of prematurity (ETROP) study. J AAPOS. 2012;16(5):449–52.

Chandra P, Tewari R, Salunkhe N, Kumawat D, Chaurasia AK, Gupta V. Short-term incidence and management of glaucoma after successful surgery for stage 4 retinopathy of prematurity. Indian J Ophthalmol. 2019;67(6):917–21.

Chiang MF, Quinn GE, Fielder AR, Ostmo SR, Chan RP, Berrocal A, Binenbaum G, Blair M, Campbell JP, Capone A Jr, Chen Y. International classification of retinopathy of prematurity. Ophthalmology. 2021;128(10):e51–68.

Cryotherapy for Retinopathy of Prematurity Cooperative Group, Multicenter trial of cryotherapy for retinopathy of prematurity. Snellen visual acuity and structural outcome at 5 1/2 years after randomization. Arch Ophthalmol. 1996;114(4):417–24.

Fierson WM, American Academy of Pediatrics Section on Ophthalmology, American Academy of Ophthalmology, American Association for Pediatric Ophthalmology and Strabismus, American Association of Certified Orthoptists. Screening Examination of Premature Infants for Retinopathy of Prematurity. Pediatrics. 2018;142(6):e20183061.

Good WV. Early treatment for retinopathy of prematurity cooperative group. Final results of the early treatment for retinopathy of prematurity (ETROP) randomized trial. Trans Am Ophthalmol Soc. 2004;102:233–48; discussion 248–250.

Guidelines for universal eye screening in newborns including retinopathy of prematurity [internet]. Rashtriya bal. swasthya karyakram; 2017. [cited 2022 Jun 1]. https://www.nhm.gov.in/images/pdf/programmes/RBSK/Resource_Documents/Revised_ROP_Guidelines-Web_Optimized.pdf.

Hartnett ME, Gilbert MM, Hirose T, Richardson TM, Katsumi O. Glaucoma as a cause of poor vision in severe retinopathy of prematurity. Graefes Arch Clin Exp Ophthalmol. 1993;231(8):433–8.

Hartnett ME, Katsumi O, Hirose T, Richardson TM, Walton DS. Improved visual function in retinopathy of

prematurity after lowering high intraocular pressure. Am J Ophthalmol. 1994;117(1):113–5.

Iwahashi-Shima C, Miki A, Hamasaki T, Otori Y, Matsushita K, Kiuchi Y, et al. Intraocular pressure elevation is a delayed-onset complication after successful vitrectomy for stages 4 and 5 retinopathy of prematurity. Retina. 2012;32(8):1636–42.

Lee GA, Lee LR, Gole GA. Angle-closure glaucoma after laser treatment for retinopathy of prematurity. J AAPOS. 1998;2(6):383–4.

Michael AJ, Pesin SR, Katz LJ, Tasman WS. Management of late-onset angle-closure glaucoma associated with retinopathy of prematurity. Ophthalmology. 1991;98(7):1093–8.

Senthil S, Balijepalli P, Garudadri C, Jalali S. Clinical presentation and management outcomes of coexistent congenital glaucoma and retinopathy of prematurity. J Glaucoma. 2019;28(1):20–6.

Senthil S, Balijepalli P, Mohamed A, Rani PK, Nayak S, Garudadri C, et al. Management outcomes of secondary glaucoma due to retinopathy of prematurity: A 19-year prospective study at a tertiary eye care Institute. The Indian Twin cities ROP Screening (ITCROPS) database report number 8. PloS One. 2020;15(9):e0238633.

Stahl A, Lepore D, Fielder A, Fleck B, Reynolds JD, Chiang MF, et al. Ranibizumab versus laser therapy for the treatment of very low birthweight infants with retinopathy of prematurity (RAINBOW): an open-label randomised controlled trial. Lancet. 2019;394(10208):1551–9.

Trigler L, Grey Weaver R, O'Neil JW, Barondes MJ, Freedman SF. Case series of angle-closure glaucoma after laser treatment for retinopathy of prematurity. J AAPOS. 2005;9(1):17–21.

Steroid-Induced Glaucoma

22

Toshit Varshney, Pankhuri Dudani, and Viney Gupta

22.1 Introduction

Steroid responsiveness was initially defined as an intraocular pressure (IOP) rise >5 mmHg or an absolute value of >24 mmHg after steroid exposure. However, an IOP rise ≥10 mmHg over baseline with clinical significance has recently been adopted as the definition by the US FDA for defining steroid responsiveness.

Following exposure to steroids, the IOP usually rises over a few weeks, but an acute rise (within hours) may also occur. An increase in IOP is most often seen after topical (Table 22.1), intraocular, or periocular routes of steroid administration but, less commonly, can also occur after oral, intravenous, transcutaneous (especially, periocular, and facial skin), inhaled, and nasal routes. Rarely, it is caused by excessive endogenous production of glucocorticoids, like in the case of Cushing's disease.

On instillation of topical corticosteroids, their anti-inflammatory effect and the amount of IOP rise do not have a linear relationship. Efficacy depends on penetration and durability, in addition to intrinsic potency. Acetate preparations are more lipophilic than those with phosphate and hence have a greater corneal penetration. For

Table 22.1 Relative anti-inflammatory efficacy[a] of various topical ocular corticosteroids (in decreasing order) and associated IOP rise

Topical ocular glucocorticoids	Range of IOP increase (mmHg)	The proportion of patients in whom hypertension developed (%) (QID dose regimen)
Difluprednate 0.05% emulsion	10–>21	3
Dexamethasone acetate 0.1%[b]	9–22	45.8
Prednisolone acetate 1.0% suspension	9–22	4.8–44
Dexamethasone alcohol 0.1%[b]	–	–
Dexamethasone sodium phosphate 0.1%[b]	–	–
Betamethasone sodium phosphate 0.1%	5–16	13
Prednisolone sodium phosphate 1.0% solution	–	–
Loteprednol etabonate 0.38% or 0.5%	<10–>10	0.8–16
Fluorometholone acetate 0.1%	2.9–6	2–8.3
Fluorometholone alcohol 0.1%	–	–
Loteprednol etabonate 0.2%	–	–

[a] Efficacy depends on penetration and durability, in addition to intrinsic potency

[b] No significant difference has been noted in the IOP rising side effects between different dexamethasone salts

T. Varshney (✉) · V. Gupta
Dr. Rajendra Prasad Centre for Ophthalmic Sciences, All India Institute of Medical Sciences, New Delhi, India

P. Dudani
Department of Dermatology, All India Institute of Medical Sciences, New Delhi, India

S. Gupta et al. (eds.), *Childhood Glaucoma*, https://doi.org/10.1007/978-981-19-7466-3_22

example, prednisolone acetate is six times less potent on a molar basis than dexamethasone; however, due to the acetate preparation, topical prednisolone acetate 1% provides greater anti-inflammatory effect than dexamethasone phosphate 0.1%.

Topical drugs associated with a higher rise in IOP include difluprednate, dexamethasone, betamethasone, and prednisolone acetate. A lower rise in IOP is seen with fluorometholone and loteprednol, as these drugs are rapidly metabolized after exerting their therapeutic effects, thus resulting in fewer adverse effects.

22.2 Mechanisms of Corticosteroid-Induced Increase in IOP

There is a high concentration of steroid specific receptors in the trabecular meshwork (TM). The glucocorticoid (GC) receptor has an α and a ß isoform, with the α-isoform being mainly responsible for ligand-dependent activation of GC-responsive genes. A higher GCα:GCß ratio is thought to be responsible for steroid responsiveness, especially in patients with a history of glaucoma.

IOP elevation is due to a reduction in the aqueous outflow facility via the following proposed mechanisms:

1. Increased deposition of extracellular material like fibronectin, elastin, and glycosaminoglycans (GAGs) in the TM. GC tends to stabilize lysosomal membranes, which are usually responsible for the depolymerization of GAGs like hyaluronate.
2. Increase in trabecular meshwork (TM) stiffness and decrease in its contractility due to reorganization of cytoskeletal network and cross-linking of actin filaments.
3. Impaired phagocytosis in the endothelial cells of the TM.
4. Increased expression of the TIGR gene (trabecular meshwork inducible glucocorticoid response gene, now called MYOC gene) and TIGR glycoprotein (now called myocilin). However, recent studies have shown that myocilin does not play a major role in glucocorticoid-induced ocular hypertension.

22.3 Risk Factors

1. Age—Children (especially age < 6 years), due to structural and functional immaturity of TM. Asian children and those with vernal keratoconjunctivitis (mixed variant followed by palpebral variant) are more steroid responsive. Elderly individuals are also at an increased risk (Bimodal distribution).
2. Glaucoma—history of primary glaucomas or family history of glaucoma in first-degree relatives of these individuals. **Angle-recession glaucoma** is also a reported risk factor.
3. Connective tissue disease.
4. High myopia.
5. Type 1 diabetes mellitus.

22.4 Case Examples

Case 22.1

A 10-years-old female child, known case of vernal keratoconjunctivitis, presented with complaints of redness and itching. The child had been on fluorometholone eye drops intermittently for the last 4 years. On examination, her best corrected visual acuity (BCVA) was 6/9 in the right eye (RE) and 6/18 in the left eye (LE), with an IOP of 28 mmHg and 34 mmHg in RE and LE, respectively. Active papillae were noted in bilateral palpebral conjunctiva with limbal nodules (Fig. 22.1a). On fundus examination, cup-disk ratio (CDR) was 0.6:1 in RE (Fig. 22.1b) and 0.8:1 in LE, with the rest of the fundus within normal limits.

Diagnosis: Both eyes (BE) have steroid-induced glaucoma with vernal keratoconjunctivitis (VKC).

Treatment: Initially started on BE timolol BD, brinzolamide TDS, and oral acetazolamide 250 mg (1/2) tablet TDS.

Topical fluorometholone was discontinued. Topical alcaftadine 0.25% OD and cyclosporine 0.05% BD were started for VKC. However, due

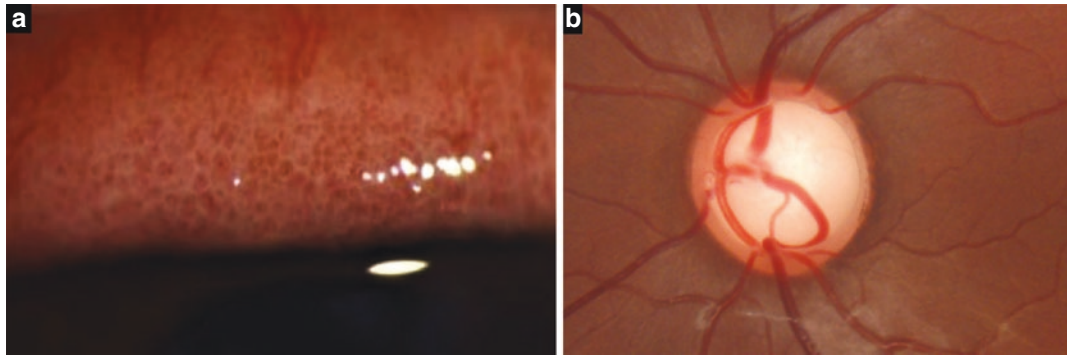

Fig. 22.1 Clinical picture (**a**) of the right eye showing the presence of active papillae. Left eye fundus image (**b**) showing vertical cup-disk ratio of 0.8:1 with neuroretinal rim thinning

to the inability to control IOP on topical medications, medical management had to be followed up with BE trabeculectomy augmented with mitomycin C 0.04% under general anesthesia.

Table 22.2 Results of studies by Becker and Armaly

Feature/parameter	Becker	Armaly
Topical ocular corticosteroid used	Betamethasone 0.1% QID for 6 weeks	Dexamethasone 0.1% TDS for 4 weeks
Parameter	Final IOP	IOP change
Types of responders • Low • Intermediate • High	<20 mmHg (58%) 20–31 mmHg (36%) >31 mmHg (6%)	<6 mmHg (66%) 6–15 mmHg (29%) >15 mmHg (5%)

Learning Points

- Almost about 45% of patients on topical dexamethasone or prednisolone have a risk of developing ocular hypertension. While newer topical steroids like loteprednol etabonate and difluprednate have an improved safety profile, they can still cause an increase in IOP in 3–16% of patients, and the clinicians must take caution.
- Studies done by Becker and Armaly (Table 22.2) showed that 5–6% of the general population can develop a marked increase in IOP after the use of topical ocular steroids and should be considered high responders.
- One-third of VKC children may present with unilateral blindness due to indiscriminate use of steroids; hence, a comprehensive ocular examination is a must for all children with VKC.
- A reduction in IOP may be seen as early as 2–4 weeks after discontinuation of therapy unless irreversible TM changes have occurred; these tend to occur if the drug has been administered usually for over a year. In the above mentioned case, long-standing steroid use lead to irreversible TM changes, requiring surgical intervention for IOP control, despite withholding steroids at this stage.
- If patients do not respond to anti-histaminic eye drops, then low-potency steroids (like fluorometholone acetate 0.1%, loteprednol etabonate 0.5%, and rimexolone 1%) are the first-line steroids to be used in active VKC cases due to their better side effect profile. Only a short course of low-potency steroids should be used to downregulate conjunctival inflammation and is indicated in cases with persistent severe symptoms, thick mucus discharge with moderate to severe corneal involvement, numerous and inflamed limbal infiltrates, giant papillae, or before taking up for surgery.
- In addition to topical antihistamines, a short course of low-potency topical steroids is usually replaced with immunomodulators (calcineurin inhibitors) like topical cyclosporine (0.05%, 0.1%, 1%, 2%) or topical tacrolimus (0.03%, 0.1%) (off-label use) for long-term allergy abatement.
- Sometimes, these children may show a spurious steroid response when administered steroids post-filtering surgery or angle surgery. Hence, IOP should be kept under close watch following surgery and potent steroids should be replaced with milder steroids which are tapered quickly as well.

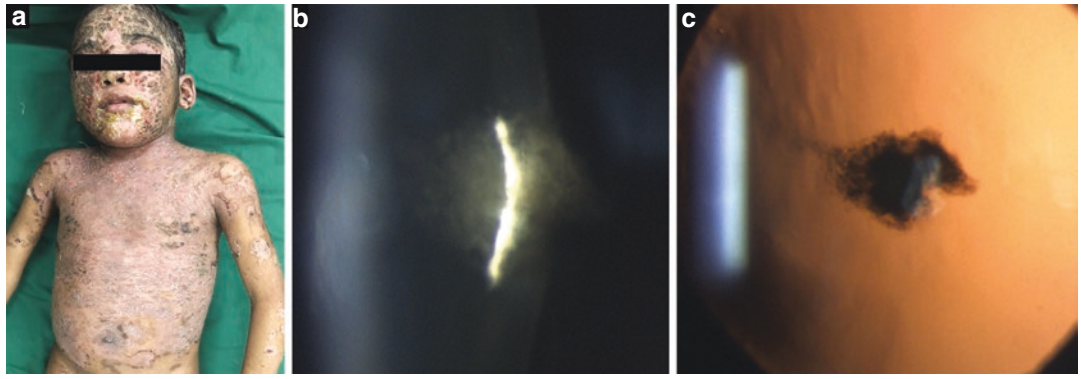

Fig. 22.2 Clinical picture (**a**) of a 7-year-old male child with pemphigus vulgaris predominantly involving facial and truncal areas, with crusted and healing erosions. Slit-lamp clinical picture of the right eye showing posterior subcapsular cataract on diffuse illumination (**b**) and retro-illumination (**c**)

Case 22.2

A 7-year-old male child was referred from the dermatology clinic for eye evaluation as he complained of glare disability in RE. He had a history of intake of oral prednisolone for the past 6 months for pemphigus vulgaris, which subsequently resolved. (Fig. 22.2a).

On examination, his BCVA was 6/24 in RE and 6/12 in LE with an IOP of 28 mmHg in BE. There was the presence of posterior subcapsular cataract in BE (Fig. 22.2b, c). On fundus examination, he had a cup-disk ratio of 0.3:1 with the rest of the fundus within normal limits.

Diagnosis: Both eyes have steroid-induced posterior subcapsular cataract with oral steroid induced ocular hypertension (secondary to oral steroids consumed for treatment of pemphigus vulgaris).

Treatment: With consultation with the dermatology department, oral prednisolone was replaced with oral azathioprine. He was started on eye drop timolol BE and underwent BE lens aspiration with IOL implantation with good visual outcomes. IOP was controlled within 3 months of discontinuation of steroid therapy, and topical glaucoma medications were gradually tapered off.

Learning Points

- Long-term prednisolone can induce ocular hypertension (OHT) in 4.9–10% of cases, with onset seen between 1 and 11 months (Table 22.3). There is a cumulative dose-dependent rise in IOP, with a dose of ≥80 mg/day having maximum odds of developing OHT.
- There should be a baseline IOP measurement before the initiation of any systemic steroid therapy. The IOP should then be measured at 2 weeks' follow-up and then every 4–6 weeks' interval.
- Systemically administered steroids more often lead to cataractogenesis, while topical steroids more often cause glaucoma.

Table 22.3 Average time taken for IOP rise after administration of various corticosteroids

Route	Onset of OHT
Topical	2–6 weeks
IV TA 4 mg	1–20 weeks
IV fluocinolone acetonide 0.59 mg	2–4 weeks
IV dexamethasone 0.7 mg	1–12 weeks
Oral	<1–11 months
Intravenous	1 day
Percutaneous	2–5 years
Inhalation/nasal route	1–4 months

IV intravitreal, *TA* triamcinolone acetonide

Case 22.3

A 16-years-old girl presented to uvea clinic with diminution of vision in both eyes. She had a past history of bilateral wrist swelling (Fig. 22.3a) which resolved after a few months of oral steroid therapy administration and was subsequently diagnosed as juvenile idiopathic arthritis with positive antinuclear antibody. She had been diagnosed with BE uveitis with cystoid macular edema three months ago and was on BE prednis-

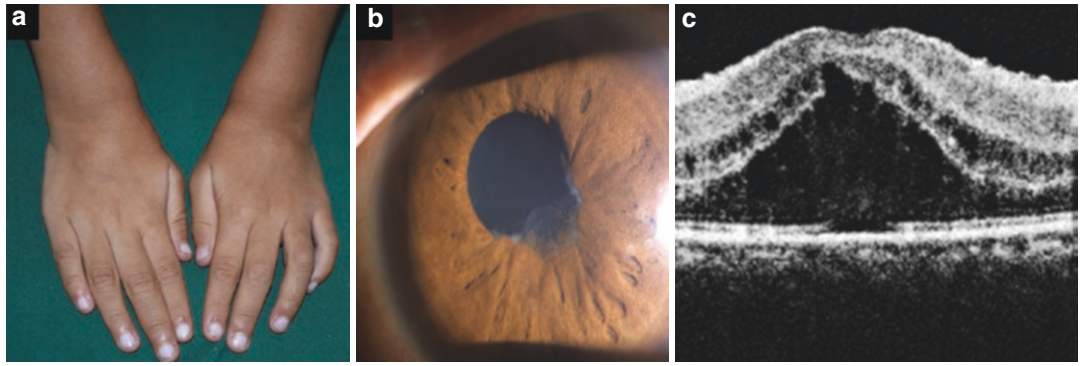

Fig. 22.3 Clinical picture (**a**) showing bilateral asymmetric wrist swelling. Slit-lamp clinical picture (**b**) of the left eye showing posterior synechiae. SD-OCT image (**c**) of the left eye showing cystoid macular edema

olone phosphate 1%, 6 times a day tapered over past 3 months to two times per day, and had received posterior sub-tenon triamcinolone acetonide injection in both the eyes 2 months ago.

On examination, BCVA was 6/36 in RE and 6/60 in LE with an IOP of 16 mmHg BE. Anterior segment examination of both her eyes showed 2 + cells and flare with fine keratic precipitates on endothelium and posterior synechiae (Fig. 22.3b). The posterior segment examination showed macular edema in both eyes, with a central retinal thickness of 465 in RE and 522 μm in LE (Fig. 22.3c). As macular edema was not responsive to topical steroid therapy and periocular subtenon steroid injection, an intravitreal 0.7 mg dexamethasone implant was implanted in LE first (planned for RE later). Four weeks later, the inflammation in her LE improved; however, an IOP of 54 mmHg was noted with a vertical cup-disk ratio of 0.6:1. Despite maximal medical therapy, the LE IOP continued to persist at around 32–36 mmHg over the next 2–3 weeks.

Diagnosis: Both eyes have juvenile idiopathic arthritis-related uveitis with cystoid macular edema with LE steroid-induced glaucoma (post-intravitreal dexamethasone implant).

Treatment: A pediatric rheumatology consultation was made in view of starting oral steroids/immunomodulators. Selective laser trabeculoplasty was administered to the visible angle. This also failed to bring the IOP down. At 3 months' post-dexamethasone implant injection, a filtration surgery was performed to control IOP. Post surgery the LE IOP was maintained in normal range.

Learning Points

- Intravitreal dexamethasone sustained-release implant (eg Ozurdex) has a better side effect profile as compared to intravitreal fluocinolone acetate implants (eg Retisert). However, OHT can be seen in up to 26.5% of patients.
- While a majority of the patients who develop OHT can be treated with glaucoma medications to control IOP, 0.2–3.2% may require filtration or any other IOP lowering surgery.
- Ozurdex is a biodegradable implant and can last in vitreous cavity for upto 6 months. In cases with intractable IOP rise, the implant may be removed via a 23G transconjunctival vitrectomy, preserving the conjunctiva for future surgeries.
- Another management plan is to retain the intravitreal implant (as it takes care of inflammation) and perform a glaucoma filtration surgery (if needed). It bypasses an additional performance of vitrectomy surgery.

Case 22.4

A 30-year-old woman presented with complaints of ocular discomfort and headache for 11 months. There was associated facial puffiness and truncal obesity with striae formation over the bilateral axillae, thigh, and hips (Fig. 22.4a). There was no history of use of exogenous steroids or a positive family history of glaucoma.

On examination, the BCVA was 6/6 BE (power of glasses -1.75DS RE and -1DS/-1 DC at 180^0 in LE) with an IOP of 28 and 36 mmHg in RE and LE, respectively. Gonioscopy showed an

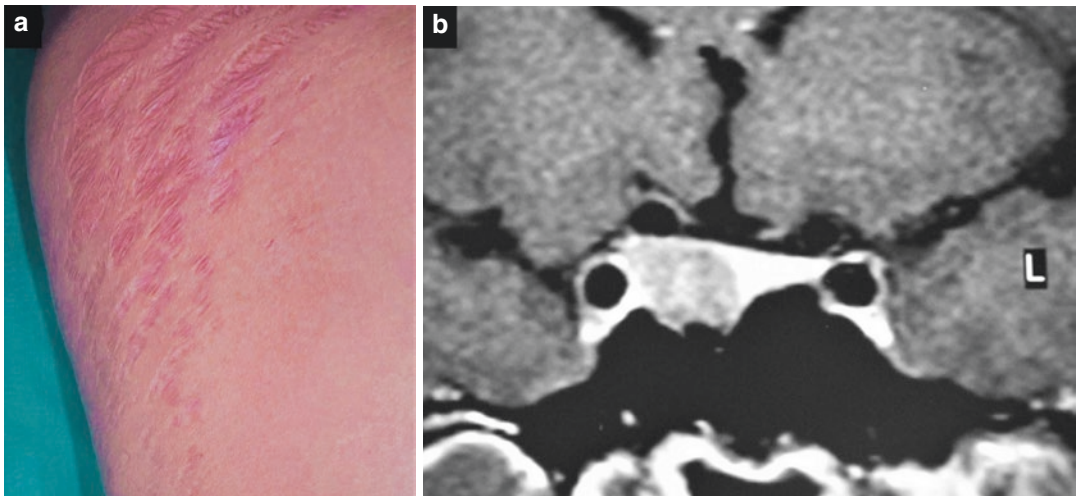

Fig. 22.4 Clinical picture of a patient with Cushing's disease (secondary to pituitary adenoma) (**a**) showing active striae seen on the medial aspect of the left thigh. Contrast-enhanced magnetic resonance imaging (coronal view) (**b**) showing well-defined focal lesion in the right adenohypophysis

open angle in BE. A few iris processes with a visible ciliary body band were seen in the LE. On fundus examination, the cup-disk ratio (CDR) was 0.4:1 with a healthy neuroretinal rim in both eyes.

Visual field evaluation by Humphrey field analyzer 30–2 was within normal limits. The systemic evaluation revealed raised blood pressure (200/110 mmHg consistently) and elevated blood sugar levels. Endocrine investigations showed elevated plasma cortisol. Overnight dexamethasone suppression test (2 mg) confirmed raised serum cortisol level. Magnetic resonance imaging depicted a small well-defined focal lesion in the right adenohypophysis (Fig. 22.4b).

Diagnosis: Both eyes have endogenous steroid-induced ocular hypertension with Cushing's disease (secondary to pituitary adenoma).

Treatment: Her IOP was controlled on maximal topical glaucoma medications and her blood pressure and sugar were controlled medically till she underwent transsphenoidal hypophysectomy. Glaucoma medications were subsequently tapered off postsurgery as her serum cortisol levels dipped and as she attained normal IOP.

Differential diagnosis for steroid-induced glaucoma (Table 22.4):

- Juvenile onset open-angle glaucoma (JOAG)
- Traumatic glaucoma

Table 22.4 Differences between Steroid Induced Glaucoma (SIG), Juvenile-onset Open Angle Glaucoma (JOAG), and traumatic glaucoma

	SIG	JOAG	Traumatic glaucoma
History	• History of steroid use/ over-the-counter medication use • History of seasonal/ chronic red eye, itching, skin disorders, and systemic diseases like asthma/nephrotic syndrome • Family history of glaucoma may be present	• Family history of glaucoma may be present	• Ocular trauma
Laterality	Mostly bilateral	Mostly bilateral	Mostly unilateral
Intraocular pressure (IOP)	IOP rise ≥10 mmHg over baseline	High IOPs >21 mmHg, usually between 30 and 40 mmHg	Variable
Gonioscopy	Open angle	• Normal appearing open angle in 34% of eyes • Rest may have gonioscopic features like – Prominent iris processes—ciliary body band is not visible behind the iris processes (vs. normal iris processes) – High iris insertion – Featureless angle	Angle recession
Other associated findings	Posterior subcapsular cataract	Large-sized disk with deep cupping, myopia	Hyphema, sphincter tear, iridodialysis, zonular dialysis, vitreous base avlasion, vitreous hemorrhage, retinal dialysis

22.5 Management

SIG should be prevented by regular follow-up and IOP evaluation for patients on steroid therapy. When ocular hypertension develops (Fig. 22.5), steroid therapy should be discontinued where possible or switched to low-potency or steroid-sparing agents. Wherever practical, removal of depot steroid preparations may be considered. The medical management of SIG is similar to that of POAG. Intractable SIG requires surgical management, with trabeculectomy being the preferred surgery.

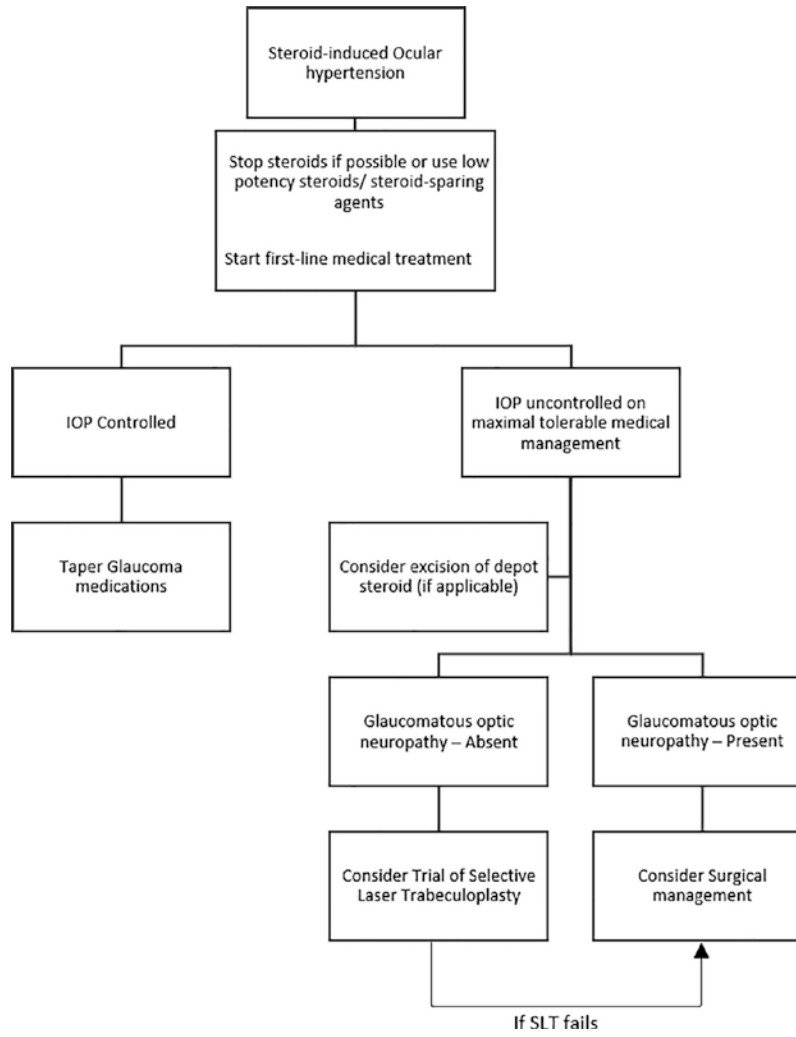

Fig. 22.5 Flow chart explaining the management protocol for steroid-induced ocular hypertension/ glaucoma

22.6 Conclusions

The IOP of patients on any form of steroid therapy should be regularly screened for steroid responsiveness. The clinician needs to be even more vigilant in those individuals who are at increased risk of steroid induced glaucoma, like children, elderly or those with previous history of glaucoma. Timely intervention by steroid cessation, or substitution with low potency steroids (or steroid sparing agents) allows IOP management with short term glaucoma medications before irreversible changes set in the trabecular meshwork.

Suggested Reading

Armaly MF. Statistical attributes of the steroid hypertensive response in the clinically normal eye: I. the demonstration of three levels of response. Invest Ophthalmol Vis Sci. 1965;4(2): 187–97.

Becker B. Intraocular pressure response to topical corticosteroids. Invest Ophthalmol Vis Sci. 1965;4(2):198–205.

François F, Victoria-Troncoso V. Mucopolysaccharides and pathogenesis of cortisone glaucoma [in German]. Klin Monatsbl Augenheilkd. 1974;165(1):5–10.

Gagen D, Filla MS, Clark R, Liton P, Peters DM. Activated αvβ3 integrin regulates αvβ5 integrin–mediated Phagocytosis in trabecular meshwork cells. Invest

Ophthalmol Vis Sci. 2013;54(7):5000–11. https://doi.org/10.1167/iovs.13-12084.

Garbe E, LeLorier J, Boivin JF, Suissa S. Risk of ocular hypertension or open-angle glaucoma in elderly patients on oral glucocorticoids. Lancet. 1997;350(9083):979–82. https://doi.org/10.1016/S0140-6736(97)03392-8.

Gupta S, Shah P, Grewal S, Chaurasia AK, Gupta V. Steroid-induced glaucoma and childhood blindness. Br J Ophthalmol. 2015;99(11):1454–6. https://doi.org/10.1136/bjophthalmol-2014-306557.

Heinz C, Koch JM, Zurek-Imhoff B, Heiligenhaus A. Prevalence of uveitic secondary glaucoma and success of nonsurgical treatment in adults and children in a tertiary referral center. Ocul Immunol Inflamm. 2009;17(4):243–8. https://doi.org/10.1080/09273940902913035.

Jain A, Wordinger RJ, Yorio T, Clark AF. Role of the alternatively spliced glucocorticoid receptor isoform GRβ in steroid responsiveness and glaucoma. J Ocul Pharmacol Ther. 2014;30(2–3):121–7. https://doi.org/10.1089/jop.2013.0239.

Kumari N, Parchand S, Kaushik S, Singh R. Intractable glaucoma necessitating dexamethasone implant (Ozurdex) removal and glaucoma surgery in a child with uveitis. Case Rep. 2013;2013:bcr2013201293. https://doi.org/10.1136/bcr-2013-201293.

Leibowitz HM, Kupferman A, Stewart RH, Kimbrough RL. Evaluation of dexamethasone acetate as a topical ophthalmic formulation. Am J Ophthalmol. 1978;86(3):418–23. https://doi.org/10.1016/0002-9394(78)90249-0.

Mark BA, Salim B. Corticosteroids in ophthalmic practice. In: Albert & Jakobiec's principles and practice of ophthalmology, vol. 1. 3rd ed. Philadelphia, PA: Saunders/Elsevier; 2008. p. 249–58.

Patel GC, Phan TN, Maddineni P, et al. Dexamethasone-induced ocular hypertension in mice: effects of myocilin and route of administration. Am J Pathol. 2017;187(4):713–23. https://doi.org/10.1016/j.ajpath.2016.12.003.

Pleyer U, Ursell PG, Rama P. Intraocular pressure effects of common topical steroids for post-cataract inflammation: are they all the same? Ophthalmol Ther. 2013;2(2):55–72. https://doi.org/10.1007/s40123-013-0020-5.

Roberti G, Oddone F, Agnifili L, et al. Steroid-induced glaucoma: epidemiology, pathophysiology, and clinical management. Surv Ophthalmol. 2020;65(4):458–72. https://doi.org/10.1016/j.survophthal.2020.01.002.

Selvan H, Gupta S, Wiggs JL, Gupta V. Juvenile-onset open-angle glaucoma a clinical and genetic update. Surv Ophthalmol. 2021b;67(4):1099. https://doi.org/10.1016/j.survophthal.2021.09.001.

Sendrowski DP, Jaanus SD, Semes LP, Stern ME. Anti-inflammatory drugs. In: Bartlett JD, Jaanus SD, editors. Clinical ocular pharmacology. 5th ed. Waltham: Butterworth-Heinemann; 2008.

Senthil S, Thakur M, Rao HL, et al. Steroid-induced glaucoma and blindness in vernal keratoconjunctivitis. Br J Ophthalmol. 2020;104(2):265–9. https://doi.org/10.1136/bjophthalmol-2019-313988.

Singhal D, Sahay P, Maharana PK, Raj N, Sharma N, Titiyal JS. Vernal keratoconjunctivitis. Surv Ophthalmol. 2019;64(3):289–311. https://doi.org/10.1016/j.survophthal.2018.12.001.

Yamamoto Y, Komatsu T, Koura Y, Nishino K, Fukushima A, Ueno H. Intraocular pressure elevation after intravitreal or posterior sub-tenon triamcinolone acetonide injection. Can J Ophthalmol. 2008;43(1):42–7. https://doi.org/10.3129/i07-186.

Yemanyi F, Baidouri H, Burns AR, Raghunathan V. Dexamethasone and glucocorticoid-induced matrix temporally modulate key integrins, caveolins, contractility, and stiffness in human trabecular meshwork cells. Invest Ophthalmol Vis Sci. 2020;61(13):16. https://doi.org/10.1167/iovs.61.13.16.

Retinoblastoma with Glaucoma

23

Neiwete Lomi, Nimmy Raj, and Navneet Sidhu

Retinoblastoma is the most common intraocular malignant tumor in children. The reported incidence ranges from 1 in 15,000 to 16,000 live births (Bishop and Madsen 1975). Retinoblastoma presents bilaterally in about 25–35% of the cases, with the average age of diagnosis being around 18 months (Shields and Shields 1992). Leukocoria is the most common presentation, followed by strabismus, painful red eye, poor vision, secondary glaucoma, and orbital cellulitis. Retinoblastoma if not diagnosed and treated early can lead to vision-threatening complications and even death due to intracranial and distant metastasis. There are three tumor growth patterns:

- Endophytic: tumor grows into the vitreous cavity. The retinal vessels are not seen over the tumor surface.
- Exophytic: tumor grows toward the subretinal space, leading to retinal detachment, and retinal vessels are seen over the tumor surface.
- Mixed: combination of both tumor growth patterns.
- Diffuse infiltrating retinoblastoma: generally seen as a small focus of tumor in the peripheral retina from which free tumor cells enter the anterior chamber and infiltrate the iris, ciliary body, and trabecular meshwork. It commonly presents with pseudouveitis, pseudohypopyon, and raised intraocular pressure with inability to visualize an intraocular mass.

The association between glaucoma and retinoblastoma was first reported in 1965 (Howard and Ellsworth 1965). Various literature reports have documented prevalence of raised intraocular pressure (IOP) in the eyes with retinoblastoma to be approximately 2–23% (Howard and Ellsworth 1965; Stafford et al. 1969; Yoshizumi et al. 1978). Glaucoma in retinoblastoma indicates a delayed diagnosis and advanced nature of disease. Majority of the cases of retinoblastoma associated with glaucoma usually require secondary enucleation after adjuvant systemic chemotherapy. The signs and symptoms of glaucoma in children with retinoblastoma remain the same as that of primary congenital glaucoma. There is often buphthalmos, lacrimation, and blepharospasm especially when retinoblastoma involves the eye at age < 2 years. Haab's striae formation is often seen secondary to corneal stretch in refractory cases.

23.1 Pathophysiology

There are primarily five basic mechanisms that induce glaucoma in retinoblastoma (Yoshizumi et al. 1978; Shields et al. 1987):

1. **Iris neovascularization secondary to ischemia**
   Neovascularization of the iris in retinoblastoma is seen in around 30–44% (Yoshizumi

N. Lomi (✉) · N. Raj · N. Sidhu
Dr. Rajendra Prasad Centre for Ophthalmic Sciences, All India Institute of Medical Sciences, New Delhi, India

S. Gupta et al. (eds.), *Childhood Glaucoma*, https://doi.org/10.1007/978-981-19-7466-3_23

et al. 1978; Walton and Grant 1968). Intraocular retinoblastoma with endophytic growth pattern which involve the posterior pole and extend into the area of central retinal vessels or large vascularized tumors which grow into the vitreous cavity or both can cause ischemia secondary to vascular involvement. This may lead to iris and angle neovascularization, subsequently causing raised IOP, hyphema, vitreous hemorrhage, or fibrovascular membrane formation which can contract to cause ectropion uvea and peripheral anterior synechiae (PAS), resulting in end stage angle-closure glaucoma.

2. **Massive exudative retinal detachment causing secondary angle-closure glaucoma**

   A total or closed funnel retinal detachment with massive exudation (exophytic type retinoblastoma) causes anterior displacement of the lens and iris diaphragm resulting in pupillary block and PAS formation and subsequently secondary angle-closure glaucoma.

3. **Uveitis and/or necrotic tumor tissue cells in the anterior chamber**

   Inflammatory cells and/or necrotic tumor cells may be seen in the anterior chamber, infiltrating and clogging the tubercular meshwork, which can lead to raised IOP. This phenomenon is commonly seen in diffuse infiltrating retinoblastoma and often masquerades as anterior uveitis.

4. **Tumor angiogenesis factor**

   Angiogenesis factors like vascular endothelial growth factor (VEGF) and its receptors are expressed within the tumor cells and are essential for tumor growth and metastasis. It may induce iris and angle neovascularization, thus producing neovascular glaucoma.

5. **Combination or mixed mechanism**

   A combination of the first and the second mechanisms most commonly causes the development of glaucoma in these children.

23.2 Case Examples

Case 23.1

A two-year-old boy presented with a white reflex in the left eye for 3 months. Clinical findings on examination under anesthesia (EUA) are shown in Fig. 23.1. IOP on applanation tonometry

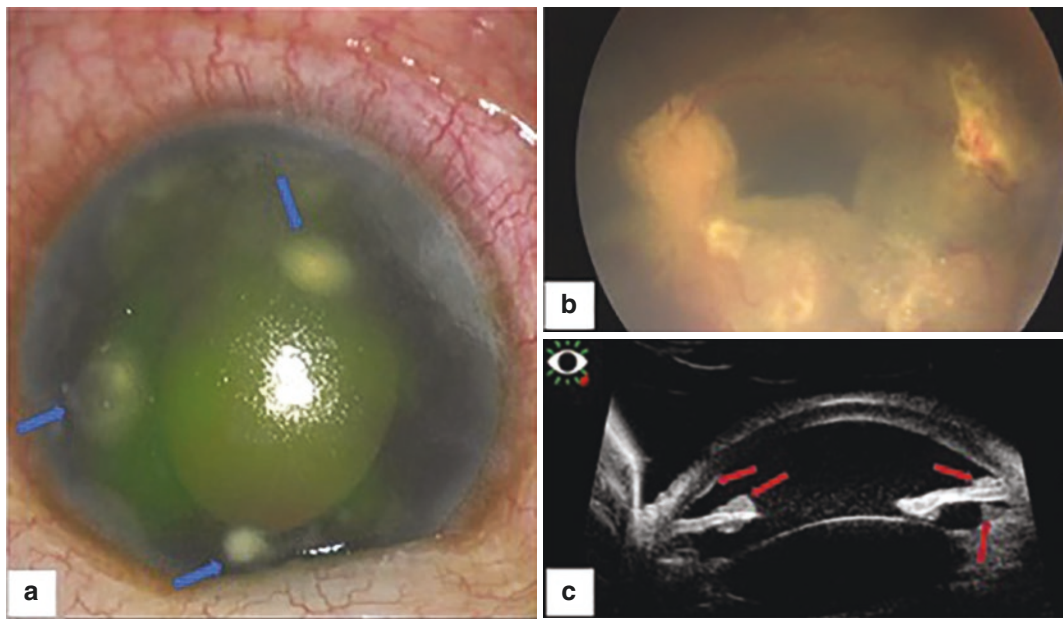

Fig. 23.1 (**a**). Operating microscope picture of the left eye shows hazy and cloudy cornea with circumciliary conjunctival congestion with absent red glow. Blue arrows show retinoblastoma tumor seedings on corneal endothelium with dispersed anterior chamber involvement (**b**). RetCam fundus picture showing tumor involving the posterior pole, obscuring the optic disk (**c**). Ultrasound biomicroscope (UBM) picture shows the tumor seedings involving the corneal endothelium, anterior chamber angle, iris, and ciliary body (red arrows)

(Perkin's) measured 10 mmHg in the right eye and 32 mmHg in the left eye.

Further investigations: MRI brain and orbit with contrast-enhanced and fat-suppressed scans suggested no extraocular extension of tumor.

Diagnosis: Right eye, fellow eye; left eye, group E retinoblastoma with glaucoma secondary to necrotic tumor tissue in the anterior chamber.

Treatment: Primary enucleation with orbital implant and adjuvant systemic chemotherapy based on the histopathological report to look for high-risk factors (HRF) was done. Regular follow-up with advice for sibling screening.

Case 23.2

A 3-year-old boy presented with gradual enlargement of the left eye associated with pain and redness since 3 weeks. His mother gave a history of leukocoria noticed in his left eye since 2 months. He had no history of any past ocular injury or treatment. Clinical findings on examination under anesthesia are given in Fig. 23.2. IOP on applanation tonometry (Perkin's) measured 12 mmHg in the right eye and 38 mmHg in the left eye.

Further investigations: MRI brain and orbit with contrast-enhanced and fat-suppressed scans shows a homogeneous intraocular mass in left eye suggestive of an extraocular retinoblastoma with optic nerve involvement (Fig. 23.3). Systemic involvement was ruled out during metastatic workup.

Diagnosis: Right eye, fellow eye; left eye, extraocular retinoblastoma with secondary angle-closure glaucoma.

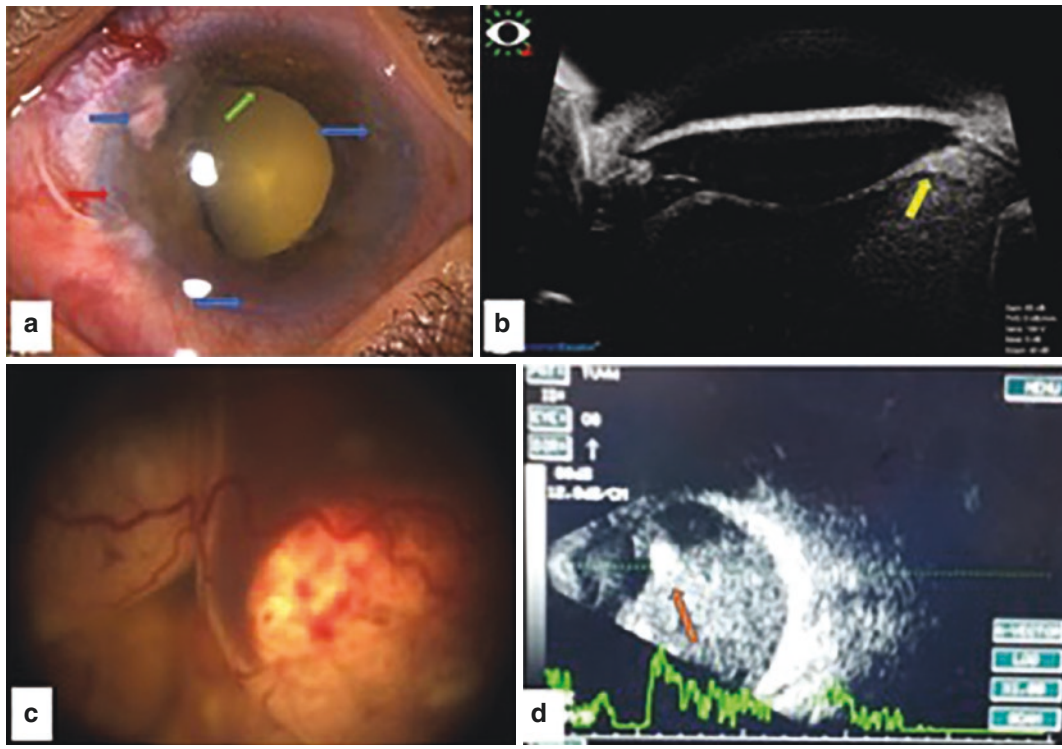

Fig. 23.2 (**a**) The clinical picture of the left eye shows limbal stretching and perilimbal conjunctival congestion with a corneal vascularized infiltrate and supero-temporal engorged episcleral vessel. Blue arrows show inflammatory or necrotic tumor cells in the anterior chamber, red arrow indicates the iris neovascularization and green arrow shows the ectropion uvea. (**b**) Ultrasound biomicroscopy of the left eye shows the tumor mass displacing the ciliary body (yellow arrow) and pushing the iris anteriorly, thus causing a shallow anterior chamber. (**c**) Fundus picture of the left eye on RetCam photography shows exophytic tumor mass with exudative retinal detachment. (**d**) B/A scan ultrasound picture of the same eye shows a heterogenous retinal mass growing into the vitreous cavity with intralesional specks of calcification indicated by high reflectivity spikes on A-scan (orange arrow) suggesting of retinoblastoma

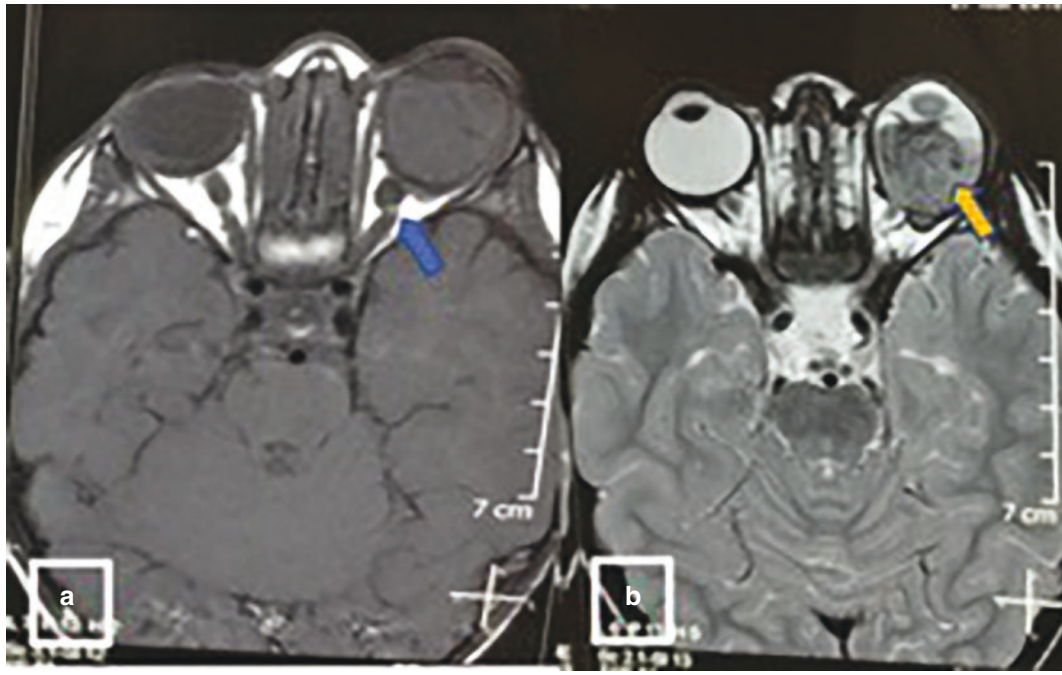

Fig. 23.3 (**a**) T1-weighted MRI scan showing left buphthalmic eye with iso-intense intraocular mass almost filling the globe with thickened and tortuous optic nerve (blue arrow). (**b**) T2-weighted image showing hypointense intraocular mass in the left eye, pushing the lens iris diaphragm anteriorly on the nasal side (yellow arrow)

Treatment: He was advised to undergo three cycles of high-dose systemic chemotherapy and topical dorzolamide 2% with timolol 0.5% combination drops twice a day followed by enucleation with adjuvant total 12 cycles of systemic chemotherapy and 20 cycles external beam radiotherapy.

Case 23.3

A seven-month-old girl presented with both eyes' white reflex, along with enlargement, redness, and watering in the right eye for 3 weeks. The clinical picture of both eyes is depicted in Fig. 23.4.

Investigation: On examination under anesthesia (EUA), IOP on Perkin's applanation tonometry measured 36 mmHg in the right eye and 18 mmHg in the left eye. Corneal diameters, vertical-horizontal (V:H), in the right eye were 13 × 14 mm while in left eye were 11 × 12 mm. Ultrasound of both eyes showed an intraocular mass filling the whole globes with intralesional calcification. MRI brain and orbit also showed intraocular masses in both eyes with no extraocular extension.

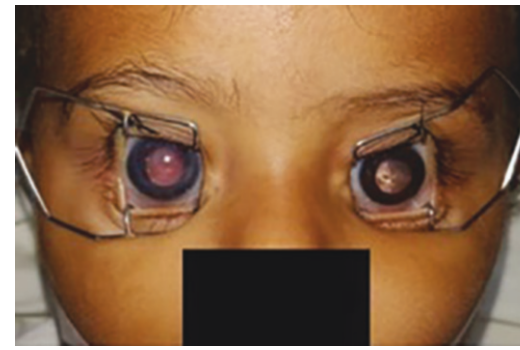

Fig. 23.4 Clinical picture of the right eye shows a reddish-white reflex with an accompanying hazy cornea and enlarged eyeball with circumferential Haab's striae. The left eyes shows leukocoria with yellowish-white reflex

Diagnosis: Both eyes had intraocular group E retinoblastoma along with right eye complicated with secondary glaucoma and buphthalmos.

Treatment: Systemic chemotherapy with regular follow-up and sibling screening was done. Patient was started on topical dorzolamide 2% bd and timolol 0.25% twice a day In both eyes. Depending on tumor response to initial three cycles of systemic chemotherapy, further treatment strategy would be decided whether to go for enucleation or for salvaging the eye.

Learning Points

- Glaucoma associated with retinoblastoma indicates advanced intraocular disease and usually has a poor prognosis.
- Detailed fundus examination with indirect ophthalmoscopy of both eyes under general anesthesia is a must to rule out retinoblastoma in a child presenting with leukocoria, as there could be several other differentials for the same (Table 23.1)
- Early diagnosis and treatment are paramount for retinoblastoma management, with or without glaucoma.

Table 23.1 Childhood ocular diseases presenting with leukocoria

Differential diagnosis for leukocoria
Retinoblastoma
Coats' disease
Persistent fetal vasculature (PFV) or Persistent hyperplastic primary vitreous (PHPV)
Vitreous hemorrhage
Toxocariasis
Familial exudative vitreoretinopathy
Retinal detachment
Congenital cataract
Coloboma
Astrocytic and combined hamartoma
Endogenous endophthalmitis
Retinopathy of prematurity
Medulloepithelioma
X-linked retinoschisis
Incontinentia pigmenti
Juvenile xanthogranuloma
Norrie's disease

23.3 Conclusions

- Glaucoma is an important clinical issue in retinoblastoma management.
- It is usually managed with systemic chemotherapy along with aqueous suppressants.
- Once neovascularization or anterior chamber infiltration develops, medical management fails, and enucleation is the treatment of choice.
- For advanced intraocular retinoblastoma presenting with glaucoma, the chances of ocular salvage with intravenous chemotherapy are better when the age at diagnosis is <6 months, duration of symptoms is <10 weeks, IOP is <27 mmHg, and there is absence of buphthalmos and sterile orbital inflammation (Rao et al. 2019).
- Glaucoma filtration surgery is absolutely contraindicated in retinoblastoma as there is a risk for the extraocular spread of active tumor cells. Hence before any glaucoma surgery, ruling out any intraocular tumor is mandatory especially in the eyes with unilateral secondary congenital glaucoma with or without neovascularization.
- Patients presenting with glaucoma and/or buphthalmia have a significantly higher risk for the occurrence of pathological high-risk factors, including those resulting in microscopically residual disease.

Suggested Reading

Bishop JO, Madsen EC. Retinoblastoma. Review of current status. Surv Ophthalmol. 1975b;19:342–66.

Chantada Guillermo L, Andrea G, Adriana F, et al. Some clinical findings at presentation can predict high-risk pathology features in unilateral retinoblastoma. J Pediatr Hematol Oncol. 2009b;31(5):325–9.

de Leon JM, Walton DS, Latina MA, Mercado GV. Glaucoma in retinoblastoma. Semin Ophthalmol. 2005b;20(4):217–22.

Howard GM, Ellsworth RM. Differential diagnosis of retinoblastoma. Am J Ophthalmol. 1965b;60:618–21.
Rao R, Honavar SG, Reddy VP. Preservation of retinoblastoma group E eyes with neovascular glaucoma using intravenous chemotherapy: risk factors and outcomes. Br J Ophthalmol. 2019b;103:1856–61.
Shields JA, Shields CL. Intraocular tumors—a text and atlas. Philadelphia, PA: WB Saunder Company; 1992b.
Shields CL, Shields JA, Shields MB, Augsburger JJ. Prevalence and mechanism of secondary intraocular pressure elevation in eyes with intraocular tumors. Ophthalmology. 1987b;94:839–46.
Stafford WR, Yanoff M, Parnell BL. Retinoblastoma initially misdiagnosed as primary ocular inflammation. Arch Ophthalmol. 1969b;82:771–3.
Walton DS, Grant WM. Retinoblastoma and neovascularization. Am J Ophthalmol. 1968b;65:598–9.
Yoshizumi MO, Thomas JV, Smith TR. Glaucoma-inducing mechanisms in eyes with retinoblastoma. Arch Ophthalmol. 1978b;96:105–10.

Part VI

Ancillary Investigations

24 Anterior Segment Imaging in Childhood Glaucoma

Somya Kumari, Abhishek Singh, Shikha Gupta, Karthikeyan Mahalingam, and Viney Gupta

24.1 Introduction

Anterior segment imaging in childhood glaucoma allows an objective method for visualization of anterior segment angle, iris configuration, lens morphology, and its relationship with adjacent structures. Two commonly used modalities for imaging in children are ultrasound biomicroscopy (UBM) and anterior chamber optical coherence tomography (ASOCT).

24.2 Ultrasound Biomicroscopy

It is primarily used for imaging the anterior segment of the eye. It uses a higher-frequency transducer (35–50 MHz) with a depth of penetration up to 4–5 mm. It is a noninvasive modality to visualize the cornea, iris, anterior chamber angle, scleral spur, ciliary body, lens, and anterior vitreous face and can be used for quantitative measurements of these structures. The ciliary body, ciliary processes, zonules, and lens behind the posterior pigment epithelium of the iris can be visualized on UBM, in contrast to ASOCT (Fig. 24.1, Table 24.1).

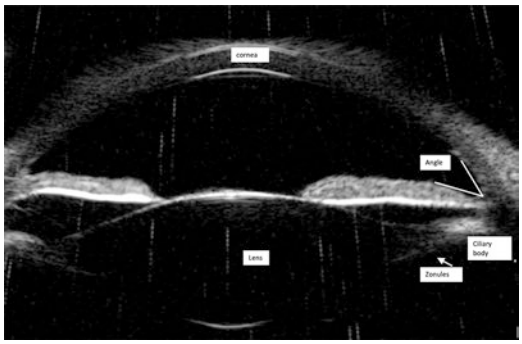

Fig. 24.1 Clinical picture demonstrating normal anterior segment structures on ultrasound biomicroscopy (UBM) imaging in a child during examination under anaesthesia. In the picture, the cornea, the angle, and the lens with posterior capsule are visualized. The ciliary body is appreciated along with processes and zonules.

Supplementary Information The online version contains supplementary material available at https://doi.org/10.1007/978-981-19-7466-3_24.

S. Kumari (✉) · A. Singh · S. Gupta · K. Mahalingam · V. Gupta
Dr. Rajendra Prasad Centre for Ophthalmic Sciences, All India Institute of Medical Sciences, New Delhi, India

S. Gupta et al. (eds.), *Childhood Glaucoma*, https://doi.org/10.1007/978-981-19-7466-3_24

Table 24.1 Table demonstrating the imaging comparison between UBM and ASOCT

	UBM	ASOCT
Principle	Based on high-frequency ultrasound waves (35-100MHz)	Based on low-coherence interferometry (1310nm)
Method	Contact procedure: a water bath is required	Noncontact
Patient position	Supine	Sitting position, supine position (in FLEX module, handheld OCT devices, microscope-integrated OCT systems)
Coupling media	Silicone eye cup filled with fluid, interface required	No coupling agent required
Advantages	Other than all anterior segment structures, can also visualize structures posterior to the posterior pigment epithelium of the iris like ciliary body, zonules, and peripheral lens and anterior hyaloid face	1. High-resolution 3D imaging 2. Requires less patient cooperation and less operator skill 3. Useful in immediate postoperative period
Disadvantages	1. Cannot be used in immediate postoperative period or following open globe injury 2. Contact procedure 3. Requires a skilled operator	Cannot be used for imaging the ciliary body, zonules, peripheral lens, or anterior hyaloid face

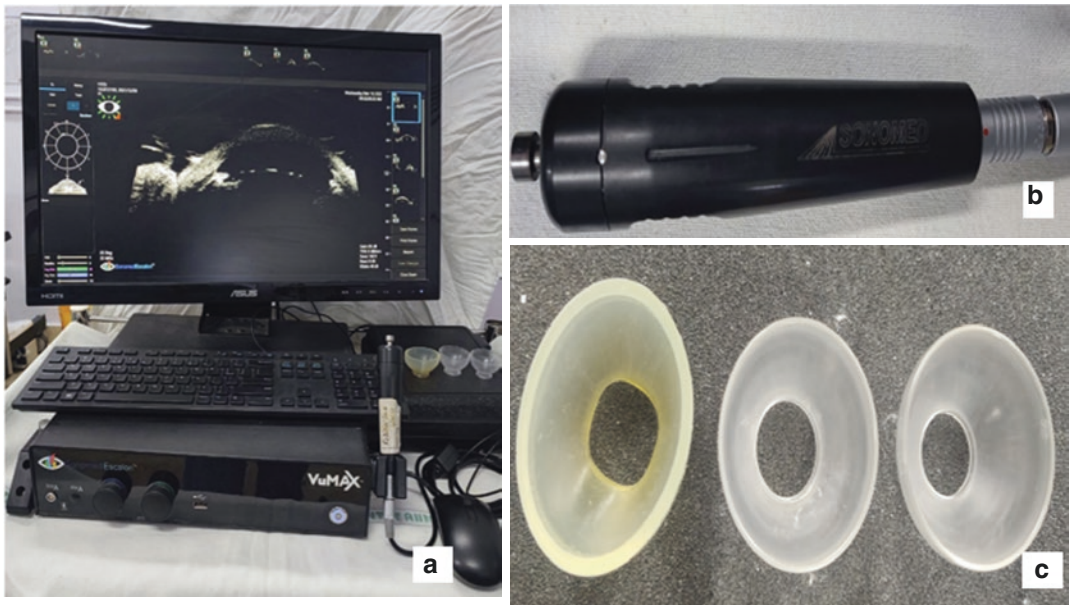

Fig. 24.2 (**a**) UBM (VuMAX, Sonomed Escalon, New York) equipment; (**b**) Oscillation probe, (**c**) Silicone cups for water bath

24.2.1 Procedure for UBM (VuMAX, Sonomed Escalon, New York)

Variable sizes of silicone cups are available which are used to create a water bath with saline as a coupling agent over the surface of the eye (Video 24.1). The patient lies in the supine position, a topical anesthetic drop is instilled (general anesthesia also administered in case of younger/uncooperative children), the cup is fit in the palpebral aperture, and the oscillating probe is introduced into the water bath (Figs. 24.2 and 24.3). Based on UBM probe orientation, axial and limbal (transverse) scans can be obtained. For axial scan, the probe is placed axially at the center of the cornea to achieve horizontal and vertical scans. For transverse scans, the probe is placed at the limbus, at four quadrants, 3,6,9 and 12 o'clock to cover the nasal, inferior, temporal and superior quadrant.

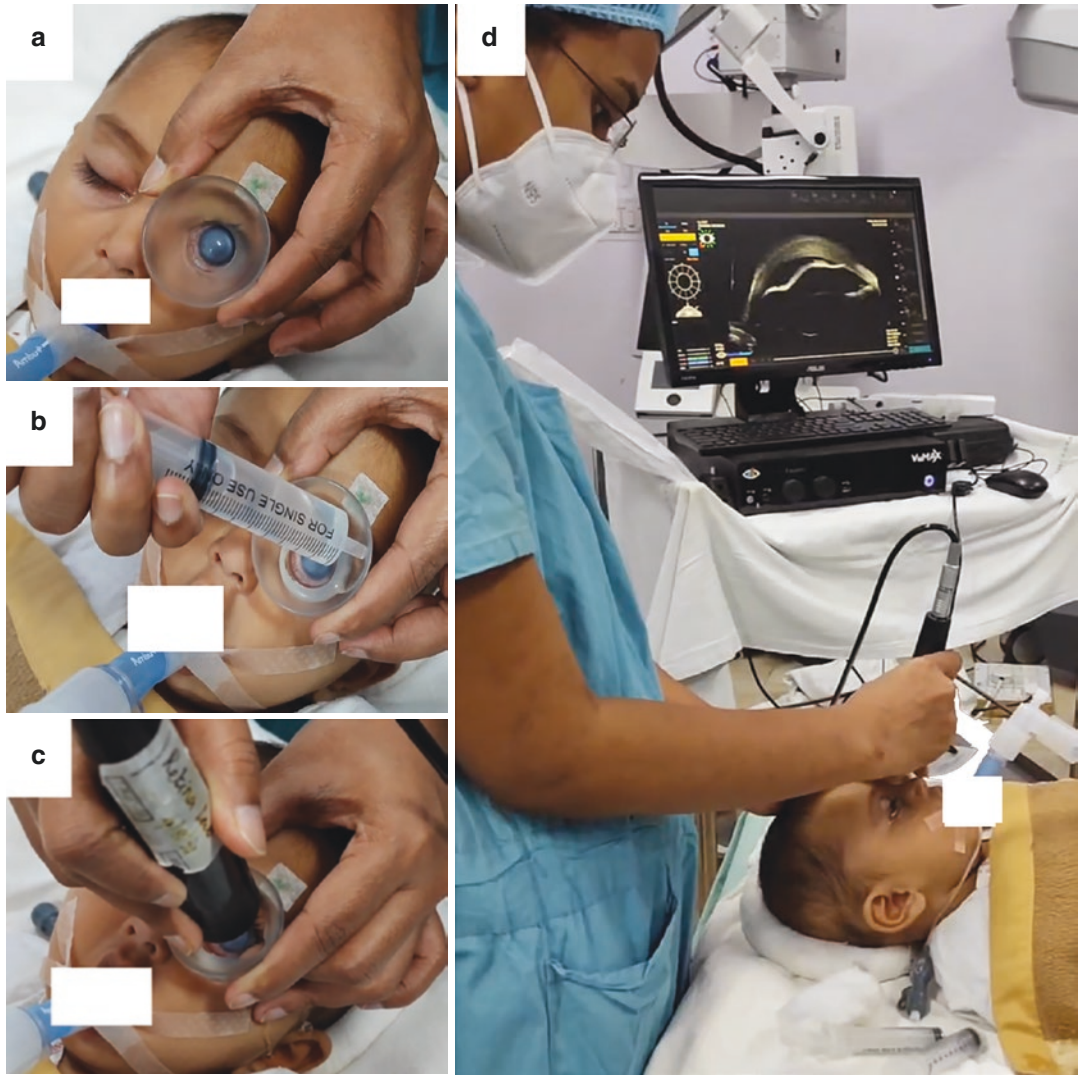

Fig. 24.3 Procedure for performing UBM. (**a**) Silicone cups are placed in the palpebral aperture. (**b**) The cup is filled with saline for the water bath. (**c**) Probe introduced into the water bath perpendicular to the ocular surface for the axial scan. (**d**) Scanning being done

24.3 Anterior Chamber Optical Coherence Tomography (ASOCT)

ASOCT (Fig. 24.4) is a high-resolution cross-sectional imaging technology which uses a wavelength of 1310 nm. It provides information about the cornea, conjunctiva, iris, angle, lens, intraocular lenses, and extraocular muscles. It can be done in both cooperative older children (sitting position) and in a supine position under EUA for younger/uncooperative children.

1. ASOCTs which can be obtained while in sitting position:
   (a) Heidelberg Spectralis OCT (Heidelberg Engineering, Germany).
   (b) CASIA 2 (Tomey Corporation, Japan).
   (c) Topcon ASOCT (Topcon Corporation, Japan).
   (d) Visante ASOCT (Carl Zeiss Meditec, Dublin, CA).
   (e) SOLIX (CAREGROUP, Gujarat, India).
   (f) ANTERION (Heidelberg Engineering, Germany), Heidelberg: It automatically

Fig. 24.4 (**a**) Heidelberg Spectralis ASOCT (Heidelberg Engineering, Germany); (**b**) CASIA 2 ASOCT (CASIA 2, Tomey Corporation, Nagoya, Japan); (**c**) Heidelberg Spectralis FLEX OCT (Heidelberg Engineering, Germany). D. Topcon ASOCT (Topcon Corporation, Japan)

marks the scleral spurs and ciliary body but has a resolution less than that of UBM.

2. ASOCTs which can be performed while in supine position:
   (a) Mobile stand mounted: FLEX module of Spectralis, Heidelberg Engineering, Germany: it provides the additional function of performing aqueous angiography
   (b) Portable handheld OCT device (Envisu, Leica Microsystem, Germany) can improve accessibility and provide scope for telemedicine.
   (c) Microscope-integrated OCT (Mi-OCT, Zeiss Rescan 700, USA) provides a real time cross-sectional imaging during various steps of surgery and assists in surgical decision-making.

24.4 Uses of Anterior Segment Imaging in Glaucoma

It helps in determining the mechanism of glaucoma by demonstrating the close relationships between anterior segment structures, like cornea, iris and trabecular meshwork.

24.4.1 In Cases of Corneal Opacities

Congenital Glaucoma (CG)

Congenital glaucomas can be associated with non-resolving corneal opacities or Haab's striae. Haab's striae are tears in the Descemet membrane (DM) pathognomonic of congenital glaucoma appearing as tram-track appearance (Fig. 24.5). A rupture of DM can cause acute hydrops resulting in acute corneal opacification in a child. A 1-month-old child presented with a sudden-onset, whitish corneal discoloration for 2 days. On examination, the patient was diagnosed as buphthalmos with corneal opacity. On UBM (Fig. 24.6), a type I DMD (descemet membrane detachment) was diagnosed with a simultaneous detachment of both DM and Pre-descemet layer (PDL). Intraocular pressure (IOP) was lowered by external trabeculotomy. Another presentation of acute hydrops can be a central dewdrop appearance in the cornea as seen on UBM (Fig. 24.7).

Imaging can also help to visualize angle dysgenesis in the form of high iris insertion (Fig. 24.8a) and probably a Barkan's membrane covering the angle (Fig. 24.8b) in eyes with con-

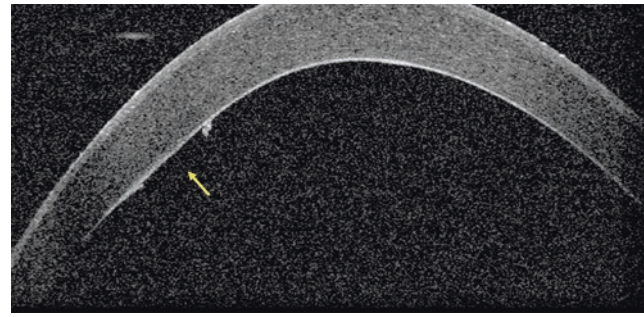

Fig. 24.5 ASOCT in a child with primary congenital glaucoma showing Haab's striae (yellow arrow). They are tears in the DM, clinically appearing as tram-track lines parallel to the limbus

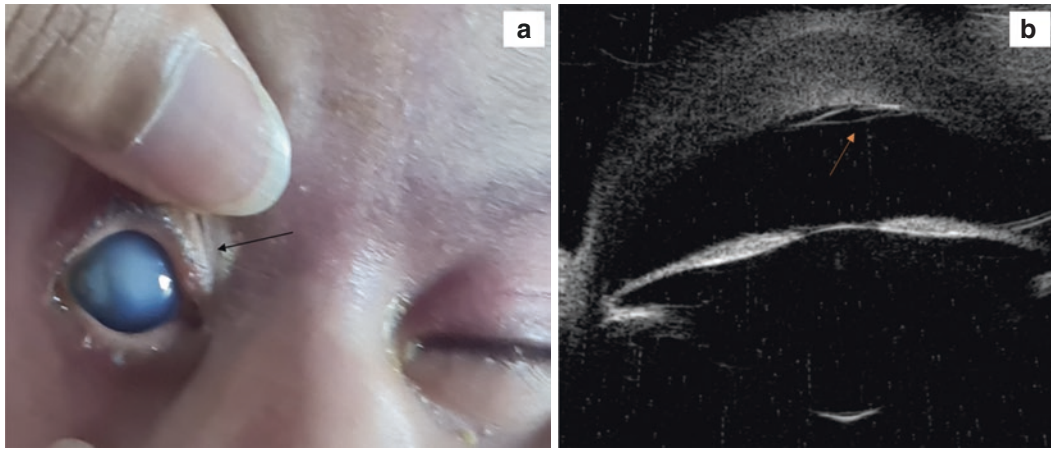

Fig. 24.6 (**a**) Clinical picture of a 1-month-old child with primary congenital glaucoma presenting with acute hydrops in right eye. On UBM (**b**), two hyperreflective lines are seen (orange arrow): the Descemet membrane (DM) and the pre-Descemet layer (PDL) along with corneal edema. The patient was diagnosed with type I DM detachment where DM and PDL are detached simultaneously

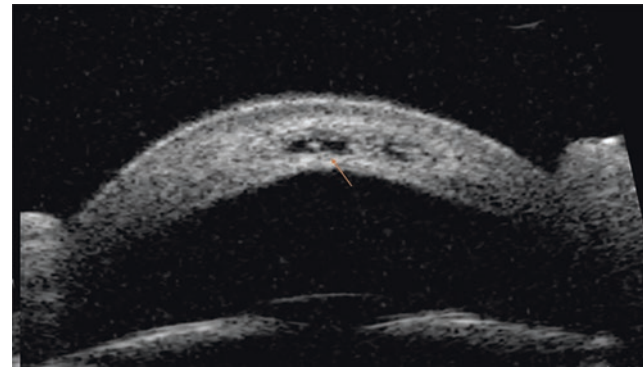

Fig. 24.7 UBM image of an acute hydrops in PCG showing a typical dewdrop appearance. There is thickened central cornea with peripheral clearing with central dewdrop appearance (arrow)

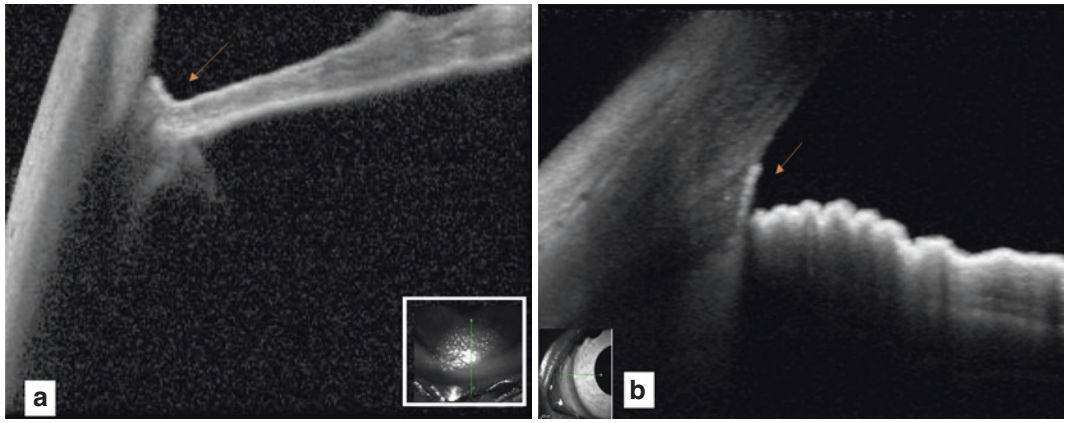

Fig. 24.8 (**a**) ASOCT of angle in a child with primary congenital glaucoma (PCG). The figure shows high iris insertion (red arrow). (**b**) ASOCT in an eye with PCG showing the presence of hyperreflective membranous structure covering the angle (red arrow). The Schlemm's canal and trabecular meshwork could not be discerned

Table 24.2 Differences between CHED and PCG in a child presenting with corneal edema based on anterior segment imaging)

No.	Congenital Hereditary Endothelial Dystrophy	Primary Congenital Glaucoma
1.	Diffuse increase in corneal thickness, usually >1000 µm	Asymmetrical increase in corneal thickness, mostly central with peripheral clearing (Fig. 24.6). Central dewdrop edema could be seen (Fig. 24.7)
2.	OCT shows thickened epithelial layer with underlying irregular Bowman's membrane, increased stromal thickness, and abnormally thickened and hyporeflective Descemet membrane. Long-standing CHED cases can show scarring at Descemet's membrane level on OCT	Horizontal parallel lines of Descemet's membrane rupture (Haab's striae), with secondary stromal and epithelial edema in cases with high IOP
3.	Angle morphogenesis appears normal, unless complicated with glaucoma	Goniodysgenesis in form of an abnormal membrane over the trabecular meshwork or absence of Schlemm's canal present
4.	Iris and ciliary body appear normal	Thin and stretched iris and ciliary body

genital glaucoma. Anomalies of the trabecular meshwork and Schlemm's canal can also be seen on ASOCT imaging.

Congenital Hereditary Endothelial Dystrophy (CHED)

Corneal transparency can be objectively estimated by studying light backscattering on ASOCT. Primary congenital glaucoma (PCG) may be differentiated from other causes of congenital corneal opacities confused with glaucoma such as CHED using anterior segment imaging (Fig. 24.9, Table 24.2).

Peters Anomaly

Peters anomaly is an anterior segment dysgenesis leading to central corneal opacity and glaucoma. Type 1 Peters has iridocorneal adhesions (Fig. 24.10a, d), while type 2 Peters has additional lenticular abnormalities (Fig. 24.10c). Classically, it is bilateral but can rarely present unilaterally. Posterior keratoconus can be one of the associations with Peters (Fig. 24.10e, f).

Peters plus syndrome is associated with systemic abnormalities, namely, short stature, cleft lip, cleft palate, umbilical hernia, facial dysmorphism, and intellectual disability.

Learning Points

- UBM/ASOCT in Peters anomaly can detect shallow anterior chamber, iridocorneal adhesions, corneo-lenticular touch, posterior corneal hyperreflectivity, hyperechoic lens, and

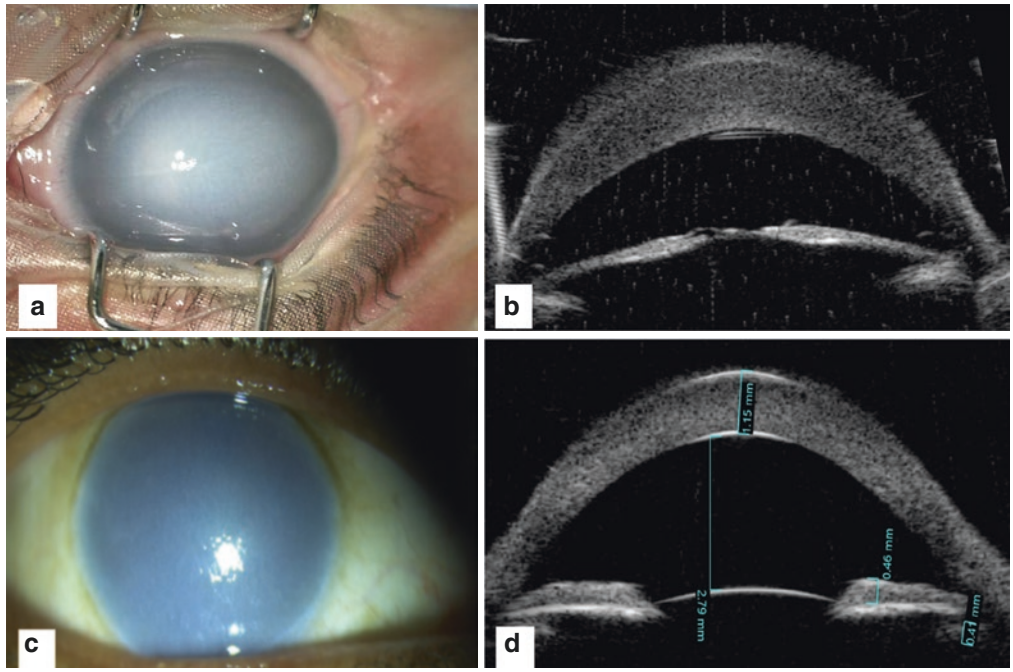

Fig. 24.9 UBM in two children along with their clinical picture distinguishing PCG from CHED. (**a**) Clinical picture of PCG showing central corneal edema with peripheral clearing, (**b**, **c**) UBM of the same child showing DM/PDL detachment, (**c**) Clinical picture of CHED showing limbus to limbus corneal edema with uniformly thick cornea (no peripheral clearing) measuring over 1000 microns as visualized in UBM (**d**) and Rest of the anterior segment structures appear normal

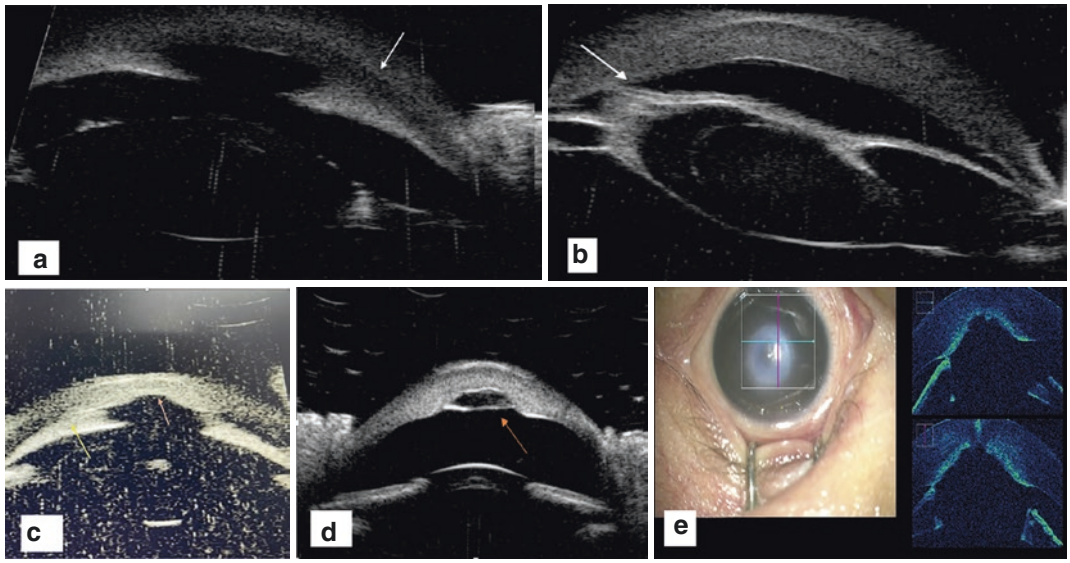

Fig. 24.10 (**a**) UBM in a child with type 1 Peters anomaly showing iridocorneal adhesions (white arrow). (**b**) UBM of a 2 year old child with corneal opacity and high intraocular pressure showing iridocorneal and lenticular corneal adhesions (white arrow). The patient also had a umbilical hernia. Because of systemic association, the patient was diagnosed with Peters plus syndrome. (**c**) UBM in a child with Peters anomaly. Posterior corneal defect (orange arrow) is present and central iridocorneal adhesions (yellow arrow) can be seen. The lens appears to be normal and thus the patient is diagnosed to have type 1 Peters. (**d**) UBM in a child with type 1 Peters anomaly showing posterior corneal defect. (**e**) iOCT (Rescan 700, Carl Zeiss, USA) in a Peters disease, showing posterior corneal excavation indicating a defect in the endothelium and Descemet layer with iridocorneal adhesions

Table 24.3 Classification of Peters anomaly based on ASOCT by Hong et al. (2017)

Disease severity	Corneal thickness	Defects in corneal layers	Iridocorneal adhesions	Angle morphology
Mild	Irregular corneal thickness	Defect in Descemet and endothelial layer	No iridocorneal adhesion	Angle is open
Moderate	Irregular corneal thickness	Defect in Descemet and endothelial layer	Iridocorneal adhesions in 1–3 quadrants	Variable extent of angle closure
Severe	Irregular corneal thickness	Defect in Descemet and endothelial layer	Lenticulo-corneal adhesion	Complete closure of all quadrants of the anterior chamber angle

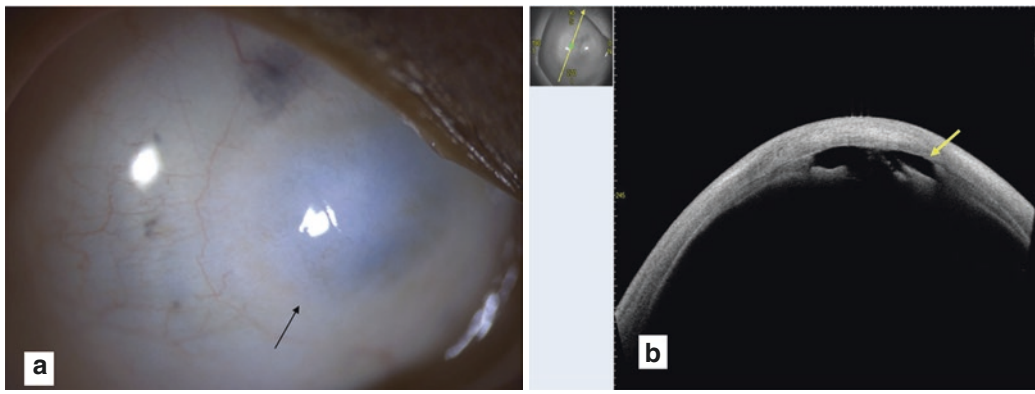

Fig. 24.11 The clinical picture (**a**) shows corneal opacification and flat corneal curvature (Cornea plana) (black arrow). There is limbal abnormality with obscured border between the cornea and sclera. (**b**) ASOCT shows anterior segment dysgenesis (arrow), without visualisation of limbal palisades or a distinct corneoscleral border. A co-existing congenital aphakia with sclerocornea is seen.

lens luxation. It can detect early corneal edema and the absence of Descemet membrane.

- iOCT in Peters can help in intraoperative anatomical evaluation, severity, grading, and surgical decision-making.
- Based on ASOCT, Hong et al. (2017) classified Peters anomaly as mild, moderate, and severe (Table 24.3).
- Imaging helps in establishing/confirming the diagnosis and to determine the developmental morphology of the angle. In an eye with extensive adhesions, filtering surgery or glaucoma drainage device implantation remains better options compared to milder cases with open angles, where goniotomy can be attempted (can be assisted by endoscope in eyes with dense large corneal opacities).
- Intraoperatively in these cases with corneal opacities and iridocorneal adhesions, UBM may help in localizing a relatively clear site with absent adhesions for proceeding with trabeculectomy or glaucoma drainage device implantation.

Sclerocornea

Sclerocornea is a congenital condition where the cornea is opaque and vascularized and resembles the sclera. Glaucoma in sclerocornea is said to be due to goniodysgenesis due to abnormal neural crest cell migration. An 8-year-old girl presented with whitish opacification of both eyes since birth along with involuntary eye movements. ASOCT showed a flat cornea (cornea plana) and anterior segment dysgenesis with sclerocornea (Fig. 24.11).

Congenital Aphakia

Congenital aphakia is a rare entity, the possibility of which should be kept in mind while dealing with eyes with corneal ectasia with opacification and vascularization. It can be isolated or associated with microphthalmia and/or sclerocornea. UBM helps to show the absence of the lens with or without absence of the iris, ciliary body, and trabecular meshwork (Fig. 24.11).

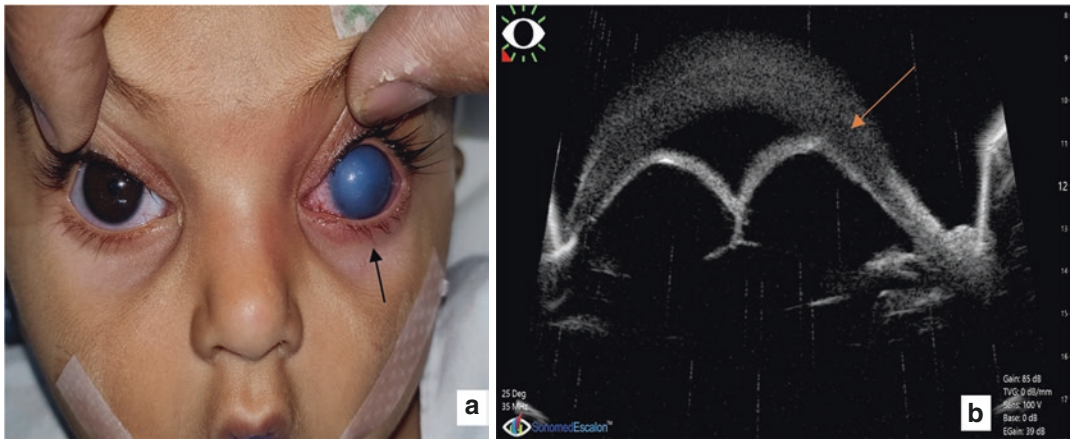

Fig. 24.12 (**a**) Clinical picture of a child with unilateral corneal opacity (black arrow). (**b**) UBM showing iris bombe (orange arrow) and posterior synechiae

Uveitis

Inflammation in the anterior or posterior chamber can cause posterior synechiae formation leading to iris bombe and secondary angle closure. The cause of inflammation could be idiopathic or secondary to causes such as retinoblastoma, uveitis, trauma, infection, etc. in a child. Anterior chamber cell quantification can also be performed on high-resolution HDOCTs, especially of benefit in the eyes with corneal opacity.

Case example: A 1-year-old child presented with unilateral corneal opacity with raised IOP. UBM showed the presence of iris bombe leading to severe corneal edema and secondary glaucoma (Fig. 24.12). The presence of exudative retinal detachment on ultrasound led to the diagnosis of likely Coats disease with secondary glaucoma.

Learning Points

- Imaging helped to arrive at the correct diagnosis in this child and appropriate treatment in the form of surgical iridectomy could be provided.
- Sometimes, long-standing chronic uveitis can lead to band-shaped keratopathy in the cornea where the anterior chamber details become unclear.
- UBM holds a special role in cases of uveitis to look at cilio-tractional membranes, whenever attempting any surgical intervention in these eyes. Any surgical intervention in the presence of these membranes can lead to ciliochoroidal detachment and chronic refractory hypotony.

24.4.2 To Look at the Iris and its Configuration (Especially Useful in Certain Situations Like Plateau Iris or Aniridia)

Aniridia

The term aniridia is a misnomer; often, a rudimentary iris stump is present (Fig. 24.13a, b). Glaucoma in aniridia can be seen in 50–75% because of primary angle dysgenesis or rotation of the stump causing obstruction of the trabecular meshwork and aqueous outflow.

Learning Points

- ASOCT and UBM can help elaborate the mechanism of glaucoma, viz., open or closed angle in aniridia. Various degrees of lens subluxation or tilt can be seen and objectively measured using CASIA ASOCT (swept-source OCT). Increased corneal thickness and associated abnormalities can also be seen in aniridia-associated keratopathy.
- Aniridic eyes show significantly smaller ciliary body length and thickness along with iris root thickness that can be measured on UBM.

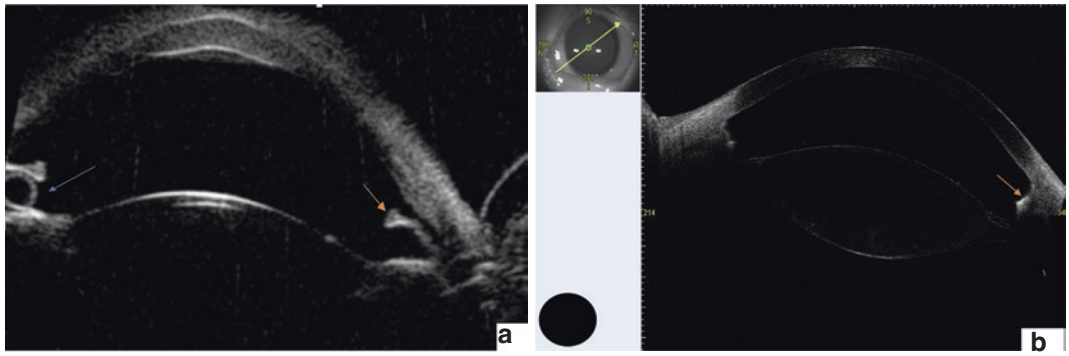

Fig. 24.13 (**a**) UBM of a child with aniridia shows a rudimentary iris stump (orange arrow). Corneal edema and incidental ciliary body cyst (blue arrow) can also be appreciated. (**b**) ASOCT of a child with aniridia showing iris stump (arrow).

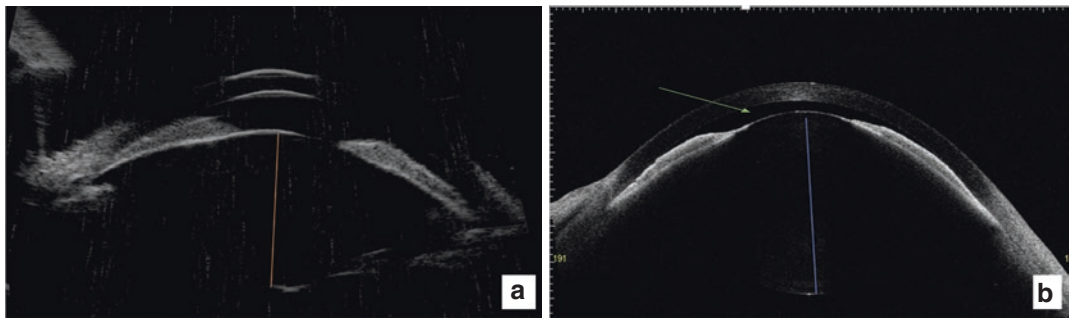

Fig. 24.14 (**a**) UBM in a 10-year-old girl diagnosed as microspherophakia with glaucoma. UBM shows a shallow anterior chamber and increased anteroposterior diameter of the lens. (**b**) ASOCT in a child with microspherophakia with anterior subluxated lens causing shallow anterior chamber (arrow) and secondary angle closure glaucoma

24.4.3 To Evaluate Biometry

Microspherophakia

Microspherophakia is characterized by increased anteroposterior diameter and reduced equatorial diameter of the crystalline lens. Weak zonular fibers lead to lack of tension in the equatorial plane; thus, the lens remains spherical and does not acquire a biconvex shape. This spherical configuration of the lens in concurrence with a generalised zonulopathy causes a shallow anterior chamber and, often, angle-closure glaucoma owing to lenticular subluxation (Fig. 24.14a). Other signs seen on UBM include elongation of zonules, angle status, degree of lens tilt, etc. A 10-year-old child presented with near-total cupping in both eyes. On examination, the anterior chamber was shallow. ASOCT confirmed increased anteroposterior diameter of the lens. The small spherical lens was subluxated in the anterior chamber and caused intermittent pupillary block leading to glaucomatous optic neuropathy (Fig. 24.14b). The child was managed with both eyes intralenticular lens aspiration with iris-fixated claw lens which controlled IOP in both eyes without the need for trabeculectomy.

Mucopolysaccharidosis (MPS)

These are rare lysosomal disorder characterized by accumulation of glycosaminoglycans (GAG) due to enzymatic dysfunction within the lysosomes. Within the eye, abnormal accumulation of

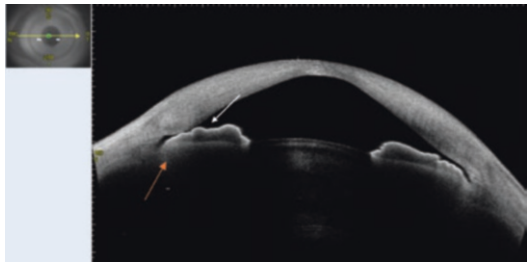

Fig. 24.15 ASOCT in a child with Hurler syndrome. The patient had ground-glass cornea and increased peripheral corneal thickness can be appreciated in the ASOCT scan. Anterior chamber crowding (white arrow) occurs because of GAG accumulation causing thickened iris and ciliary body (orange arrow) leading to secondary angle closure

glycosaminoglycans is seen within the trabecular meshwork, sclera, and even lamina cribrosa. All these act to increase IOP by open-angle mechanism commonly and eventually induce glaucomatous optic neuropathy. Anterior chamber crowding also occurs due to GAG deposition in the peripheral cornea, iris, and ciliary body which again can result in angle-closure glaucoma (Fig. 24.15). Glaucoma can be seen in MPS types 1, 4, and 6, namely, Hurler syndrome, Morquio syndrome, and Maroteaux-Lamy syndrome, respectively. Serial follow-up examination with ASOCT enables objective evaluation of disease progression in MPS.

24.4.4 To Examine the Ciliary Body Details Through UBM

Ciliary Body Cysts

Rarely ciliary body cysts may cause shallow anterior chamber. The condition is termed as "pseudo-plateau iris." However, they generally result in angle-closure glaucoma during late teens or early adulthood (Fig. 24.16). Likewise, primary iris cyst of the pigment epithelium or iris stroma (Fig. 24.17) can be confirmed on ASOCT. Secondary iris cyst due to inclusion cyst or use of miotics can be confirmed on UBM when they tend to masquerade something else.

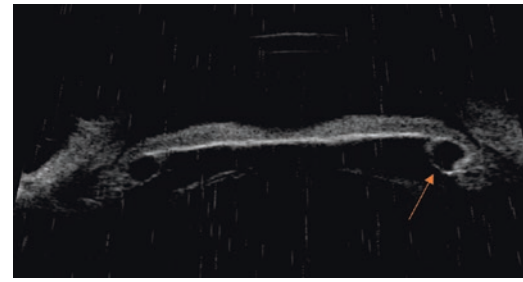

Fig. 24.16 UBM in a child showing single cyst (orange arrow) within the ciliary body causing pseudo-plateau iris configuration with angle closure

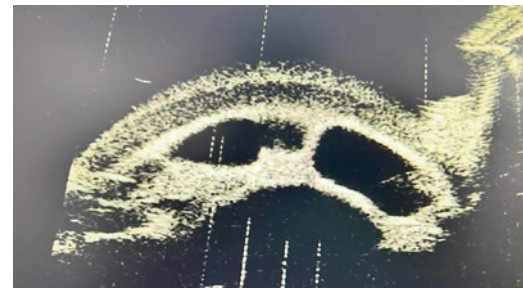

Fig. 24.17 UBM imaging showing multiloculated congenital iris cysts with flat anterior chamber and extensive irido-corneal adhesions in a child presenting with high IOP and ocrneal opacity

Ciliary Body Tumor

Ocular tumors like retinoblastoma, xanthogranuloma, or rarely melanoma in children can cause invasion of the ciliary body. Forward displacement of lens-iris diaphragm by the protruding ciliary body is the most common cause of glaucoma. Direct invasion of the anterior chamber angle by the tumor can cause mechanical obstruction and secondary glaucoma. Angle seeding and pigment dispersion from pigmented tumors are other mechanisms of secondary open-angle glaucoma.

Case example: A 14-year-old female child presented with unilateral (left eye) raised IOP with irregular anterior chamber. Dilated examination showed a brownish mass in nasal quadrant. UBM confirmed an irido-ciliary mass (Fig. 24.18). Thus, the child was diagnosed with glaucoma secondary to ocular malignancy.

Learning Points

- UBM has a diagnostic role in case of small tumors situated anteriorly that are not visualized on a slit lamp or with an indirect ophthalmoscope.
- UBM can also differentiate solid from cystic lesions.

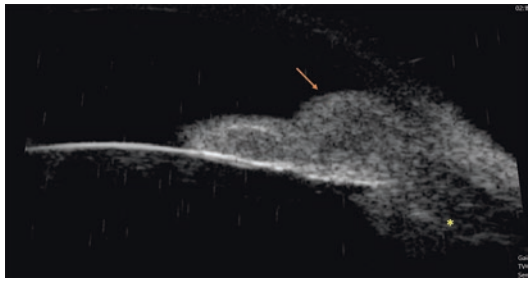

Fig. 24.18 UBM in a 14-year-old female child showing ciliary body* and iris mass (arrow), likely tumor in the left eye

24.4.5 To Study Angle Anatomy in Children as Adjunct to Gonioscopy

Axenfeld-Rieger Anomaly or Syndrome (ARS)

High iris insertion or high peripheral anterior synechaie can be seen in ARS on gonioscopy (Fig. 24.19a). Iris abnormalities include iris hypoplasia, corectopia, or polycoria (Fig. 24.19b, c). Anteriorly displaced Schwalbe's line called posterior embryotoxon can be sometimes visualized on ASOCT (Fig. 24.19d).

Learning Points

- The typical anterior segment anomalies of Axenfeld-Rieger syndrome include iris atrophy, posterior embryotoxon, peripheral bridging tissue bands, trabecular meshwork elongation, and high insertion of the iris root into the posterior trabecular meshwork and can be visualized on ASOCT images.

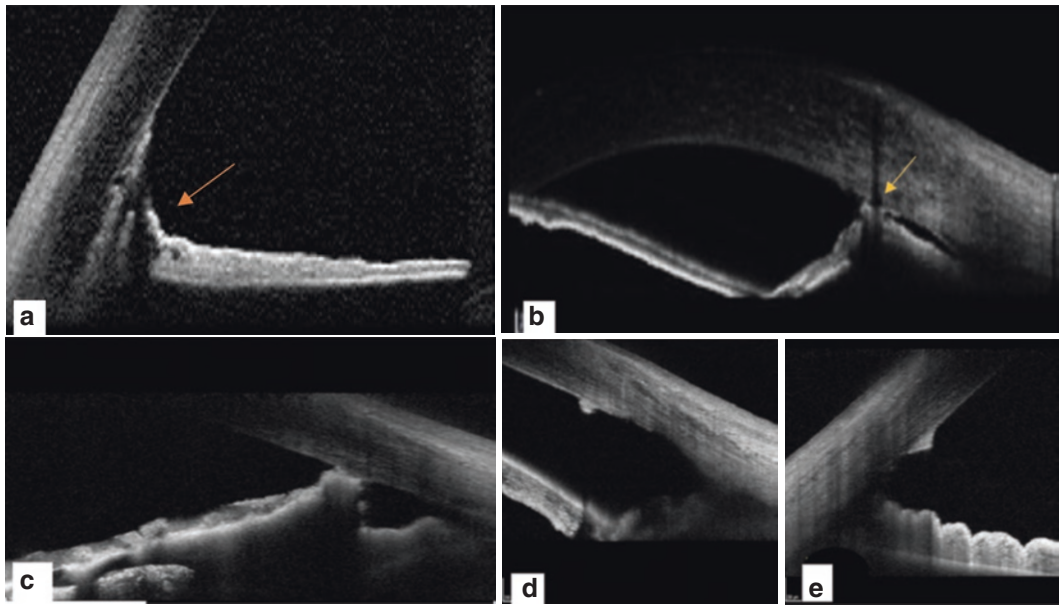

Fig. 24.19 (**a**) ASOCT in a child with Axenfeld-Rieger anomaly showing high iris insertion (arrow). (**b**) ASOCT in a child with Axenfeld-Rieger syndrome showing iris hypoplasia, and peripheral strands of iris adhered at the anteriorly displaced Schwalbe's line (posterior embryotoxon, arrow). (**c**) ASOCT in another child with Axenfeld-Rieger syndrome, with peripheral strands of iris adhered at the posterior embryotoxon. (**d**, **e**) ASOCT in two different individuals with Axenfeld-Rieger anomaly showing posterior embryotoxon

Specifically, the high-resolution mode of the ASOCT program had improved performance in outlining finer structures such as the distinctive endothelial membrane covering the iris in which enables better understanding of the pathophysiology in the patient.

- Based on ultrasound biomicroscopy, Chen et al. (2020) classified infants with Peters and Axenfeld-Reiger anomaly into the four types as given in Table 24.4

Table 24.4 Ultrasound biomicroscopy (UBM) classification of infants with Peters and Axenfeld-Reiger anomaly by Chen et al. (2020)

Type	Characteristics
UBM Dx type 1	DM and endothelium with heterogenous or discontinuous echo, with corneal stroma echo-enhanced or shallow anterior chamber
UBM Dx type 2	The echoes of the DM and the endothelium were continuous, with corneal stroma echo-enhanced, an abnormal strand of peripheral iris extends to the protruding Schwalbe line, often accompanied by iris stroma or pupil heteromorphism, with a shallow or flat anterior chamber
UBM Dx type 3	The echoes of the DM and the endothelium were continuous, with corneal stroma echo-enhanced, an abnormal strand of peripheral iris extends to the protruding Schwalbe line, often accompanied by iris stroma or pupil heteromorphism, with a shallow or flat anterior chamber
UBM Dx type 4	The echoes of the DM and the endothelium were continuous, with corneal stroma echo-enhanced, an abnormal strand of peripheral iris extends to the protruding Schwalbe line, often accompanied by iris stroma or pupil heteromorphism, with a shallow or flat anterior chamber

DM Descemet membrane

Juvenile-Onset Open-Angle Glaucoma (JOAG)

Though gonioscopy can show a normal angle, there can still be subtle angle dysgenesis which can be picked up on ASOCT in eyes with JOAG. The signs of dysgenesis in such cases could be in the form of a hyperreflective membrane seen in a few eyes or the absence of a Schlemm's canal (Fig. 24.20). A few eyes of JOAG may show a normal Schlemm's canal, seen as a hyporeflective area on ASOCT (Fig. 24.20).

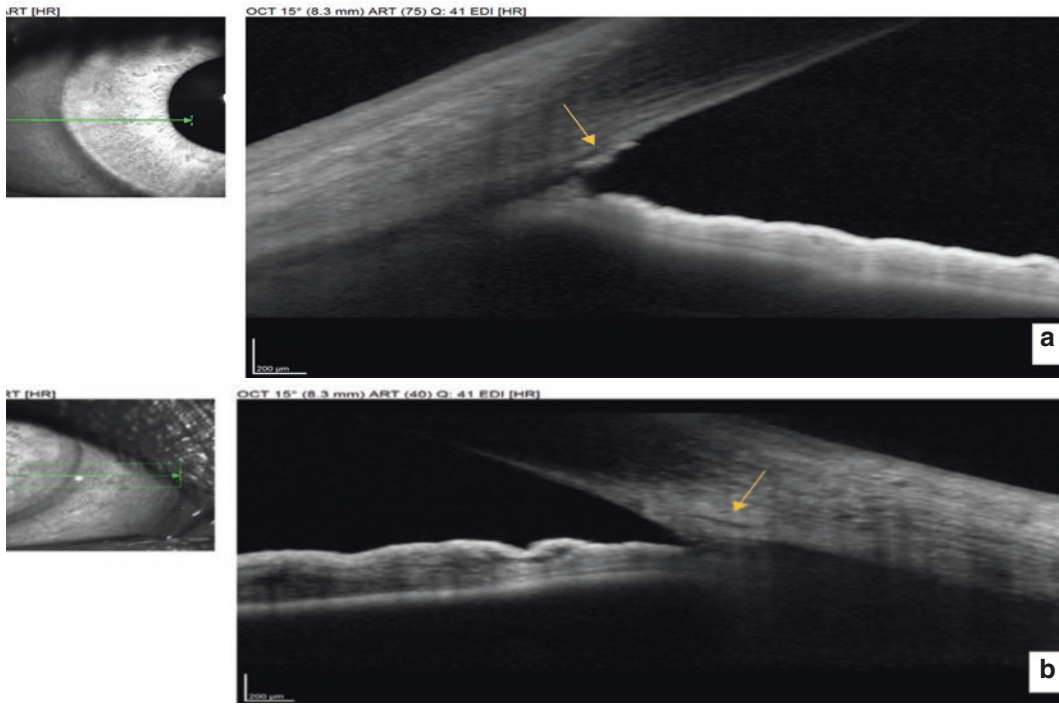

Fig. 24.20 (**a**) ASOCT image of a 28-year-old male diagnosed as juvenile-onset open-angle glaucoma. Abnormal tissue or hyperreflective membrane is seen (arrow). The Schlemm's canal is not visualized. (**b**) Normal Schlemm's canal as a hyporeflective line (arrow) as seen in few cases of JOAG

24.4.6 Other Uses

Effectiveness of Angle Surgery

Postoperatively, visualization of de-roofed Schlemm's canal in angle surgery can be imaged using ASOCT (Fig. 24.21).

Sturge-Weber Syndrome (SWS)

Glaucoma in Sturge-Weber has a bimodal presentation, pathophysiology being primary angle dysgenesis in infants while raised episcleral venous pressure in a teenager. They present with buphthalmos on the side of the port wine stain.

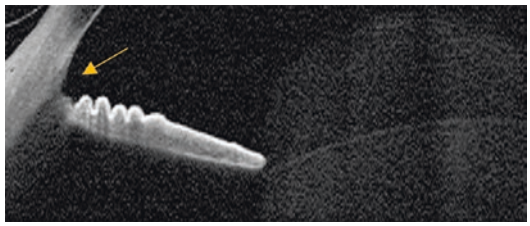

Fig. 24.21 ASOCT in a child of primary congenital glaucoma, an intraoperative picture showing deroofed Schlemm's canal (arrow) after GATT (gonioscopy-assisted transluminal trabeculotomy)

Learning Points

- Dilated superficial and intrastromal vessels can be seen in open-angle SWS supporting the pathomechanism of raised episcleral venous pressure (Fig. 24.22). UBM can be used to see supraciliary effusion which can occur in SWS.
- Episcleral hemangiomas, especially at the limbus, are biomarkers of the occurrence of glaucoma in Sturge-Weber syndrome (Fig. 24.22).

Uveal Effusion in Nanophthalmos

The abnormal scleral collagen fibers cause increased resistance to transscleral fluid outflow, leading to fluid accumulation in supraciliary and suprachoroidal space. Nanophthalmos is a rare differential of angle closure in the young (Fig. 24.23).

Imaging the Eyes with Glaucoma Following Ocular Trauma

ASOCT being noninvasive can be safely done in immediate post-injury period. A cyclodialysis cleft is a disinsertion of the ciliary body from scleral spur, allowing aqueous humor flow into the suprachoroidal space (Fig. 24.24) Angle recession, zonular dialysis, iridodialysis, vitreous in the anterior chamber, and anterior chamber reaction are other telltale signs of trauma on imaging.

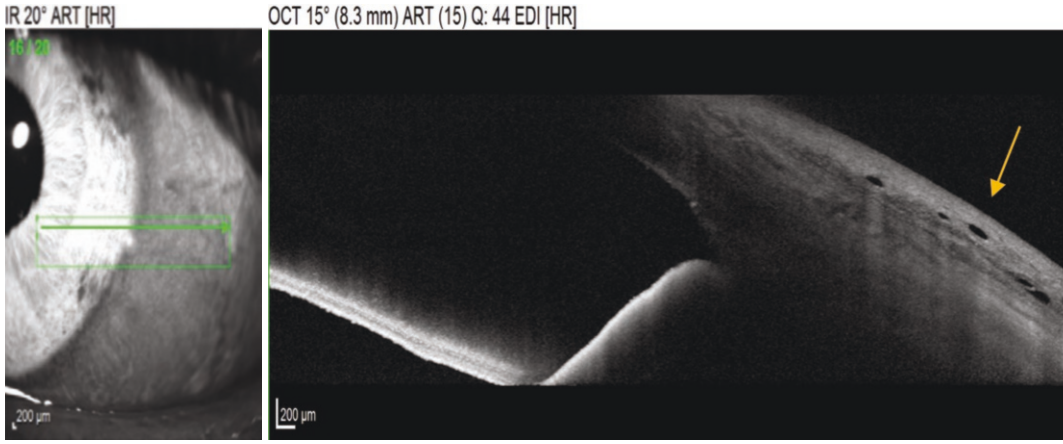

Fig. 24.22 ASOCT of the sclera in a child with Sturge-Weber syndrome. Dilated episcleral vessels could be seen as a string of pearls (arrow)

Fig. 24.23 UBM in a 16-year-old boy with nanophthalmos showing accumulation of supraciliary fluid (arrow)

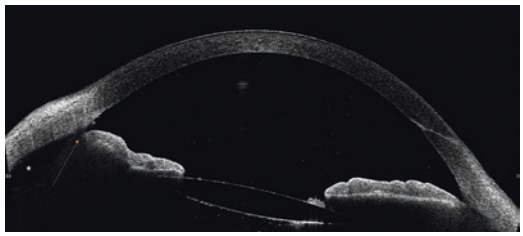

Fig. 24.24 ASOCT in a child presenting with post-traumatic ocular hypotony. The figure shows disinsertion of the ciliary muscle from the scleral spur (arrow) causing fluid collection in suprachoroidal space (asterisk)

24.5 Conclusions

The advent of anterior segment imaging, ASOCT, and UBM in glaucoma has revolutionized diagnosis and management in glaucoma patients. They provide objective quantitative method for evaluation. With further advances in technology, they will play a bigger role in understanding the mechanisms of various types of glaucoma.

Suggested Reading

Chen WS, Xiang DM, Hu LX. Ultrasound biomicroscopy detects Peters' anomaly and Rieger's anomaly in infants. J Ophthalmol. 2020;2020:8346981. https://doi.org/10.1155/2020/8346981.

Dada T, Gadia R, Sharma A, Ichhpujani P, Bali SJ, Bhartiya S, Panda A. Ultrasound biomicroscopy in glaucoma. Surv Ophthalmol. 2011;56(5):433–50. https://doi.org/10.1016/j.survophthal.2011.04.004.

Gupta V, Jha R, Srinivasan G, Dada T, Sihota R. Ultrasound biomicroscopic characteristics of the anterior segment in primary congenital glaucoma. J AAPOS. 2007;11(6):546–50. https://doi.org/10.1016/j.jaapos.2007.06.014.

Gupta V, Chaurasia AK, Gupta S, Gorimanipalli B, Sharma A, Gupta A. In vivo analysis of angle dysgenesis in primary congenital, juvenile, and adult-onset open angle glaucoma. Invest Ophthalmol Vis Sci. 2017;58(13):6000–5. https://doi.org/10.1167/iovs.17-22695.

Gupta S, Warjri G, Gupta V. "Ɛ" sign: a clinical clue to the diagnosis of microspherophakia. Eye (Lond). 2020;34(3):597–9.

Hong J, Yang Y, Cursiefen C, Mashaghi A, Wu D, Liu Z, Sun X, Dana R, Xu J. Optimising keratoplasty for Peters' anomaly in infants using spectral-domain optical coherence tomography. Br J Ophthalmol. 2017;101(6):820–7. https://doi.org/10.1136/bjophthalmol-2016-308658.

Jat NS, Tripathy K. Peters anomaly. In: StatPearls [internet]. Treasure Island, FL: StatPearls Publishing; 2022.

Mannino G, Abdolrahimzadeh B, Calafiore S, Anselmi G, Mannino C, Lambiase A. A review of the role of ultrasound biomicroscopy in glaucoma associated with rare diseases of the anterior segment. Clin Ophthalmol. 2016;10:1453–9. https://doi.org/10.2147/OPTH.S112166.

Maslin JS, Barkana Y, Dorairaj SK. Anterior segment imaging in glaucoma: an updated review. Indian J Ophthalmol. 2015;63(8):630–40. https://doi.org/10.4103/0301-4738.169787.

Mehta N, Ramappa M. Novel proposed algorithm in congenital hereditary endothelial dystrophy. Semin Ophthalmol. 2023;38(2):108–15. https://doi.org/10.1080/08820538.2022.2094713.

Panigrahi A, Huang A, Arora M, Kumari S, Mahalingam K, Gupta V, et al. Indocyanine green aided Schlemm's canal identification during gonioscopic assisted transluminal trabeculotomy. J Glaucoma. 2022;31:e69.

Varshney T, Azmira K, Gupta S, Mahalingam K, Singh A, Angmo D, Gupta V. In vivo imaging of the schlemm's canal and the response to selective laser trabeculoplasty. Am J Ophthalmol. 2022;234:126–37. https://doi.org/10.1016/j.ajo.2021.07.002.

Wang KJ, Simpson TL, Fonn D. Objective measurements of corneal light-backscatter during corneal swelling, by optical coherence tomography. Invest Ophthalmol Vis Sci. 2004;45(10):3493–8. https://doi.org/10.1167/iovs.04-0096.

Wang D, Wang M, Console JW, He M, Seider MI, Lin SC. Distinctive findings in a patient with Axenfeld-Rieger syndrome using high-resolution AS-OCT. Ophthalmic Surg Lasers Imaging. 2009;40(6):589–92. https://doi.org/10.3928/15428877-20091030-10.

Posterior Segment Optical Coherence Tomography

25

Rahul Sangwan, Karthikeyan Mahalingam, and Shikha Gupta

25.1 Introduction

Optical coherence tomography (OCT) is a noninvasive/noncontact, highly reproducible, objective medical diagnostic imaging tool. Posterior segment OCT is a promising additional diagnostic and prognosticator modality in glaucoma. It can be used to mitigate the subjectivity and reproducibility concerns of traditional diagnostic modalities, especially in the pediatric population.

25.2 Principle

OCT works on the principle of partial coherence interferometry. Low-coherence infrared light from a super-luminescent diode laser (830 nm) is directed to an optical beam splitter, which acts as an interferometer (Fig. 25.1). It splits half of the beam to the reference mirror placed at a known distance, and the rest is transmitted to the tissue. Light backscattered from the tissue

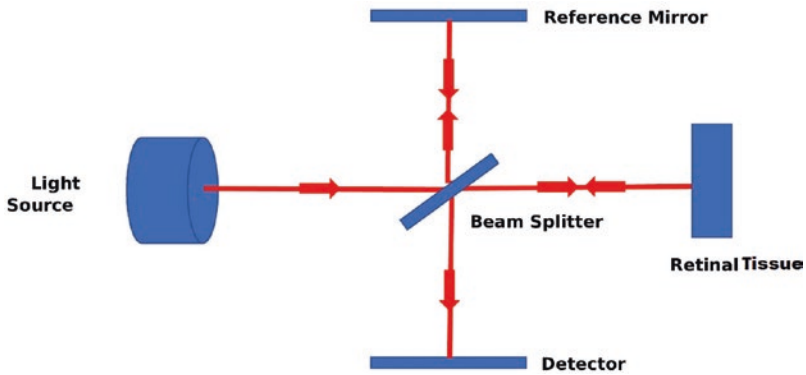

Fig. 25.1 Schematic diagram of optical coherence tomography

R. Sangwan (✉)
Dr. Rajendra Prasad Centre for Ophthalmic Sciences, All India Institute of Medical Sciences, New Delhi, India

K. Mahalingam · S. Gupta
Dr. Rajendra Prasad Centre for Ophthalmic Sciences, All India Institute of Medical Sciences, New Delhi, India
e-mail: shikhagupta@aiims.edu

S. Gupta et al. (eds.), *Childhood Glaucoma*, https://doi.org/10.1007/978-981-19-7466-3_25

Table 25.1 Comparison of specifications between swept-source, spectral-domain, and time-domain OCT

	Swept-source OCT	Spectral-domain OCT	Time-domain OCT
Light source	Swept-source tunable laser (1040–1060 nm)	Super-luminescent diode (SLD), 840 nm	Super-luminescent diode (SLD),820 nm
Axial resolution	Optical 6.3 μm Digital 1.95 μm	5 μm	10 μm
Transverse resolution	20 μm	15 μm	20 μm
Maximum A-scans per B-scan	300	245	128
Scan depth	3 mm	2 mm	2 mm
Scan speed	1,00,000 A-scans/sec	27,000–68,000 A-scans/sec	400 A-scans/s
Resolution	1280 × 1024 dpi	1280 × 1024 dpi	1024 × 768 dpi

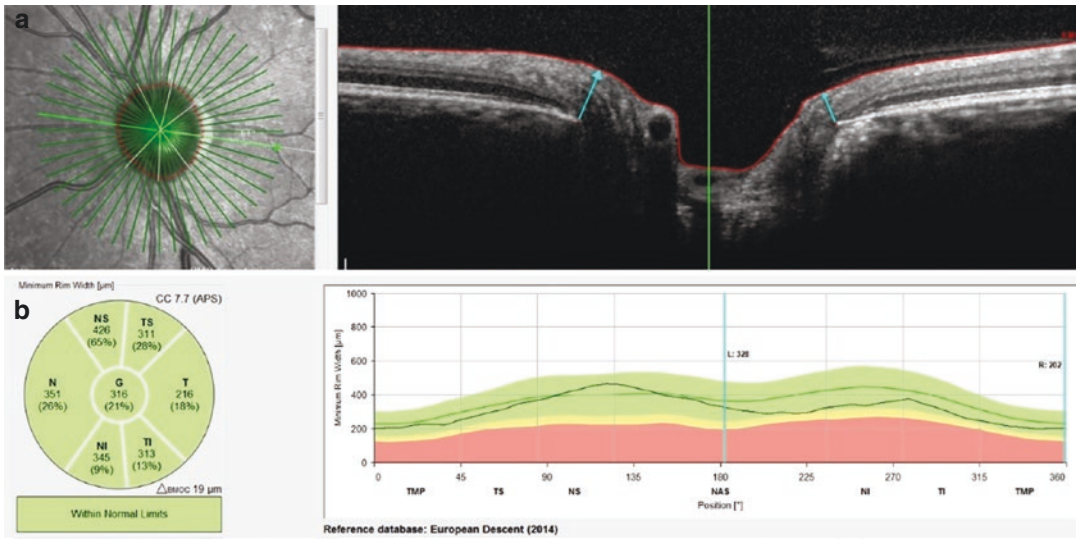

Fig. 25.2 (**a**) Represent radial scans on BMO (Bruch's membrane opening) and BMO-MRW (minimum rim width) on B-scan. The blue arrow represents BMO-MRW, which is the shortest distance between BMO and the ILM, (**b**) BMO-MRW classification charts (right), and thickness profile (left). (Green, within normal; yellow, borderline, red, outside normal limit)

and reference mirror is superimposed which makes an interference pattern of low and high light intensities, measured by a light-sensitive detector. The difference in echo time delay and reflecting properties of different layers are used to generate a two-dimensional cross-section image with successive longitudinal sequential scans. Optical Coherence Tomography (OCT) has evolved through distinct technologies (Table 25.1). Time-Domain OCT (TD-OCT) employs mechanical depth scanning, Spectral Domain OCT (SD-OCT) utilizes a spectrometer for simultaneous depth capture, and Swept-Source OCT (SS-OCT) rapidly sweeps spectral range for high-speed imaging, especially valuable in ophthalmology.

25.3 Applications of Posterior Segment Optical Coherence Tomography in Glaucoma

OCT is the most promising tool in the objective assessment of the optic nerve head (ONH), retinal nerve fiber layer thickness (RNFL), and structural assessment of the macula and posterior pole asymmetry, which can aid in the diagnosis and monitoring of glaucoma.

25.3.1 Optic Nerve Head Assessment

Bruch's membrane opening (BMO) is an important landmark in identifying the optic nerve head

Table 25.2 Macular scan protocols and parameters of commonly available OCT machines

Instrument	Macular scan protocol	Macular thickness measurements
1 Cirrus 5000 HD-OCT (Carl Zeiss Meditec, Inc., Dublin, CA)	• Macular cube 200 × 200 protocol (6 × 6 mm square grid) containing 200 B-scans (200 A-scan lines) • Macular cube 512 × 128 protocol (128 B-scans, 512 A-scans per B-scan) • The macular thickness data are calculated on 13–14 mm^2 elliptical annulus area centered on the fovea	**Ganglion cell OU analysis** • Thickness map (GCL + IPL) • Deviation map (GCL + IPL)
2 SPECTRALIS HRA + OCT (Heidelberg Engineering, Inc., Heidelberg, Germany)	• Average retinal layers measurement of each 8 × 8 mm (3 × 3°) sector (64 sectors) • 61 line scans (1024 A-scans/line)	**Structural assessment of the macula** • Thickness map (retina, RNFL, GCL, IPL) • Thickness deviation map (retina, RNFL, GCL, IPL) • Classification chart (retina, RNFL, GCL, IPL)
3 DRI OCT triton	• **3D macula (H)** 7.0*7.0 mm with a scan resolution of 512*256 • **3D macula (V)** 7.0*7.0 mm with scan resolution 512*128	**Glaucoma analysis in the macula** • **3D macula (H)** • **3D macula (V)** – SuperPixal-600 (RNFL, GCL+, GCL++) – SuperPixal-200 (RNFL, GCL+, GCL++)

GCL+ between the RNFL/GCL-IPL/INL boundaries, *GCL++* between the ILM-IPL/INL boundaries. *GCL* ganglion cell layer, *IPL* inner plexiform layer, *RNFL* retinal nerve fiber layer, *ILM* internal limiting membrane, *INL* inner nuclear layer

(ONH) boundary. The neuroretinal rim (NRR) thickness can be accessed by capturing 24 radial OCT scans centered on the BMO, and the blue arrow represents BMO-MRW, which is the shortest distance between BMO and the ILM (Fig. 25.2a). In a healthy eye, the thickness profile of the BMO-minimum rim width (BMO-MRW) should show a slight double hump (Fig. 25.2b). Tilted and myopic disks may exhibit an altered profile with a single hump.

25.3.2 Ganglion Cell Complex (GCC)

Macular ganglion cell complex (GCC) includes all three innermost retinal layers, potentially involved in the glaucomatous damage (RNFL, ganglion cell layer (GCL), and inner plexiform layer (IPL)). The GCC thickness analysis is confirmed to be superior to macular thickness in detecting glaucoma.

Ganglion cell density at the foveal center ranges between 31,00 and 37,800 cells/mm. About 50% of the retinal ganglion cells are located within 4.5 mm of the foveal center. Ganglion cell loss appears in an arcuate fashion with the corresponding area of the neuroretinal rim on the optic nerve head. With the introduction of Fourier-domain and swept-source OCT technology, several manufacturers proposed the evaluation of the ganglion cell layer using different protocols (Table 25.2).

25.3.3 RNFL Assessment

RNFL analysis has a great diagnostic ability to detect early glaucoma; most of the OCT platforms measure RNFL values from a fixed distance (3.5 mm) from the optic disk and gives circular cross-sectional thickness well centered around the optic nerve. The 4.1 mm and 4.7 mm scans can offer reliable diagnostic measurements when the traditional 3.5 mm RNFL scan is confounded by pathology. RNFL thickness generally follows the ISNT rule (i.e., maximum inferiorly and minimum temporally) with a "double hump" configuration (Fig. 25.3a). Clinically, RNFL loss in the superior and inferior quadrants appears as wedge-shaped defect; as you can see in the fundus photo (Fig. 25.4a (30°) and 4b (10°), red arrows), this can be confirmed by OCT RNFL thickness profile which also represents borderline superior (Fig. 25.3b, early glaucomatous changes) sectoral defect.

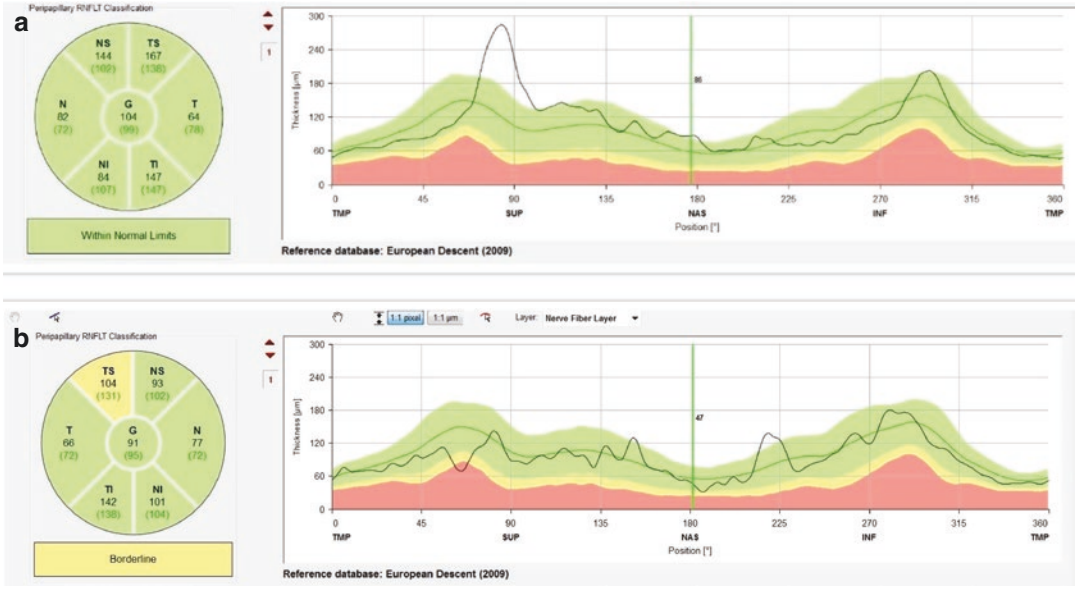

Fig. 25.3 Classification chart of RNFL (retinal nerve fiber layer) thickness in different sectors and average thickness profile graph of a normal eye (**a**) and borderline superior sectoral defect in early glaucomatous changes (**b**)

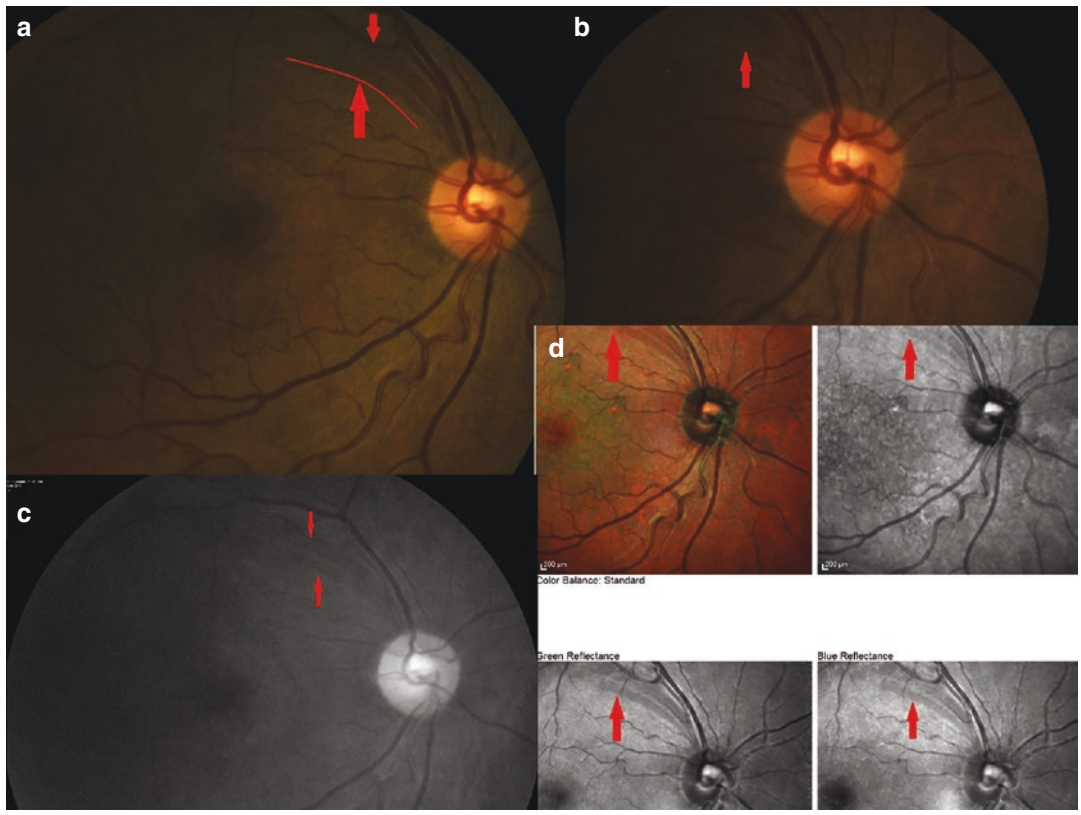

Fig. 25.4 Colored fundus photograph of early glaucomatous patient showing superior arcuate wedge-shaped defect (**a** 45°, **b** 30° red arrows); red-free (**c**) and multicolor (**d**) imaging also shows arcuate-shaped defects as blue and green reflectance, in particular, may offer the highest level of RNFL(retinal nerve fiber layer) visibility to improve diagnostic accuracy

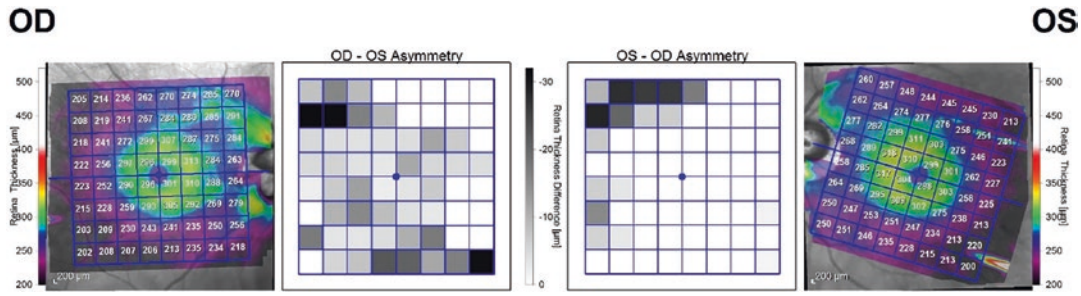

Fig. 25.5 Glaucoma patient showing high degree of retinal thickness asymmetry between the superior and inferior half of the same eye (macular) and between the right and left eye as well

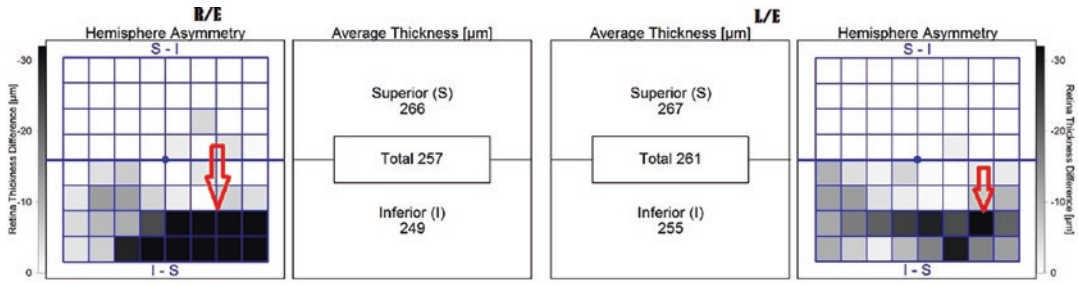

Fig. 25.6 Asymmetry map between the superior and inferior hemispheres of the same eye; the darker the square, the greater is the asymmetry

Multicolor imaging also shows arcuate-shaped defects (Fig. 25.4c, d) as blue- and green-reflectance and red-free images, which in particular, may offer the highest level of RNFL visibility to improve diagnostic accuracy.

Studies report that the eyes with congenital glaucoma have thinner RNFL compared to control eyes. The RNFL loss Is more in congenital glaucoma eyes, which have higher baseline intraocular pressure (IOP) and visual field defects.

25.3.4 Posterior Pole Asymmetry

Asymmetry between the two eyes is a hallmark of glaucoma. The full retinal thickness asymmetry analysis quantifies imbalances between the inferior and superior macula, as well as between the left and the right eye, serving as an aid in identifying potential glaucomatous damage (Fig. 25.5). Figure 25.6 depicts asymmetric retinal thinning of the superior and inferior hemispheres in both the left and right eye of a glaucoma patient. The superior hemisphere is overall thicker than the inferior hemisphere in both eyes.

25.4 Factors Associated with Signal Strength and Image Quality

25.4.1 Patient-Dependent Factors that Can Cause Poor Scan Quality

- Pupil size: small pupil size can limit scan quality
- Dry eyes
- Cataract
- Asteroid hyalosis
- Floaters and vitreous opacities
- Low visual acuity
- Effect of high refractive error, astigmatism, and axial length
- Blink reflex

- Motion artifacts
- Signal strength and signal/noise ratio: Scans with ratios >6–7 should be chosen
- Peripapillary atrophy

25.4.2 Operator-Dependent Factors

- Smudged OCT lens
- Inaccurate axial alignment of the OCT image, leading to only partial inclusion of ocular tsructures and truncation of the ocular structures.

25.4.3 Device-Dependent Factors

- Inaccurate optic disk margin delineationt e.g., overestimation in scans with peripapillary atrophy and underestimation from interference by blood vessels and motion artifacts, all causing scan circle displacement
- Inaccurate retinal layer segmentation
- Angular distribution of retinal nerve fiber layer bundles

25.5 Case Examples

Case 25.1
An 18-year-old male patient with high myopia (−9.00DS B/E) was referred to the glaucoma clinic due to an increased cup-disk ratio (0.7:1). Intraocular pressure (IOP) was 14 mmHg (RE) and 12 mmHg (LE), and the central corneal thickness (CCT) was 535 µm (RE) and 540 µm (LE). RNFL OCT shows RE within normal limits and LE indicates defects (Borderline, Fig. 25.7 red arrow), but the topography of macular ganglion cells (Fig.25.8) along with thickness map (Fig. 25.9a) and hemisphere asymmetry map (Fig. 25.9b) of both eyes were normal.

Learning Points

In cases of high myopia, RNFL thinning can erroneously be labelled as glaucoma because of mechanical stretching and retinal degeneration.

Current OCT machines do not incorporate high refractive errors in their database; therefore, RNFL analysis of such eyes may show false-positive localized RNFL defects. Due to this false-positive error, sometimes non-glaucomatous eyes are erroneously labeled as glaucomatous (**red disease**).

Some of the reasons for false-positive errors on OCT are listed:

- Circumpapillary RNFL thinning
- Temporal displacement of RNFL peaks
- Poor centration of measurement circle on the optic disk
- Lack of normative data in the machine database
- Parapapillary atrophy
- Magnification factors while scanning ONH
- Variations in disk and shape
- RNFL segmentation on the superior and inferior poles of the disk

In such special cases, a macular scan (ganglion cell complex) can aid in correct diagnosis (if there is no other macular pathology). OCT accurately calculates the GCL thickness or any other loss (cell body and dendrites of ganglion cells) before the axonal loss (RNFL).

Case 25.2
An 18-year-old female with raised intracranial pressure presented with IOP of 20 mmHg in

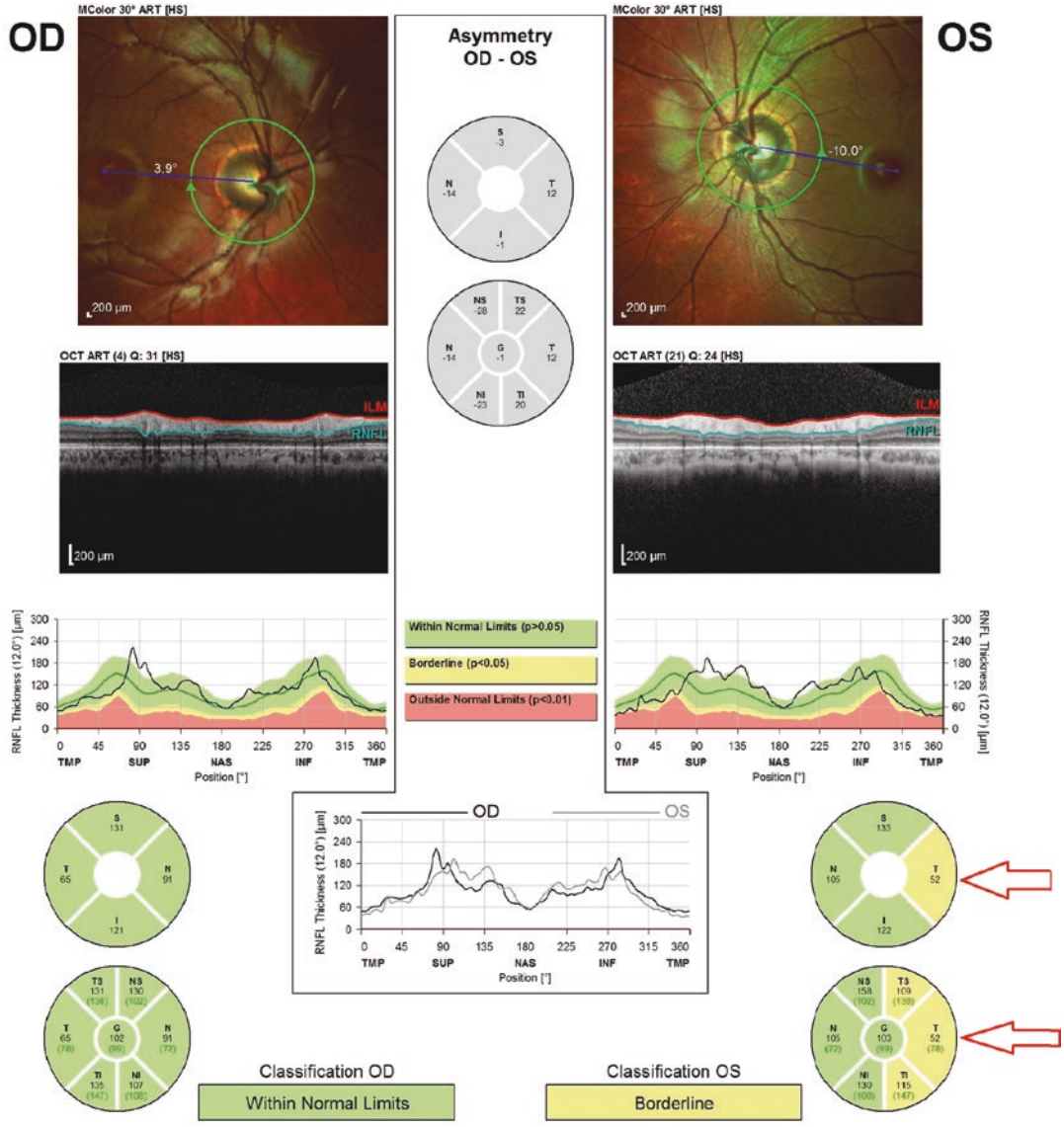

Fig. 25.7 RNFL (retinal nerve fiber layer) report showing thickness profile and classification chart of the high myopic patient. It represents RNFL thinning in the temporal quadrant half of the left eye

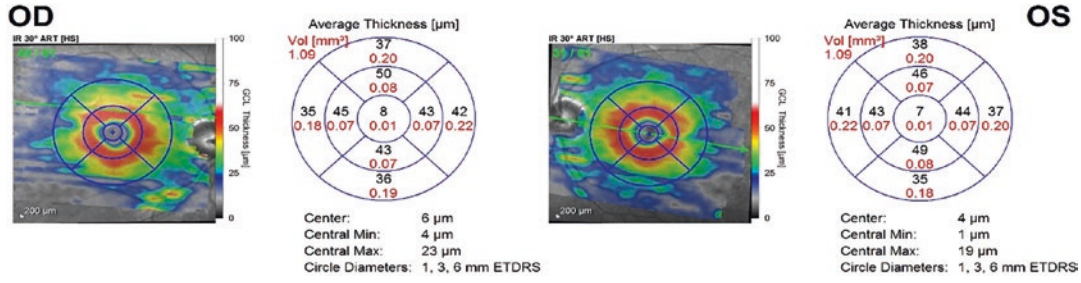

Fig. 25.8 OCT macula report showing normal GCL (ganglion cell layer) represented in hot colors of red and yellow, measuring approximately 50–75 µm thickness. And average thickness of ganglion cell layer in structural assessment of the macula

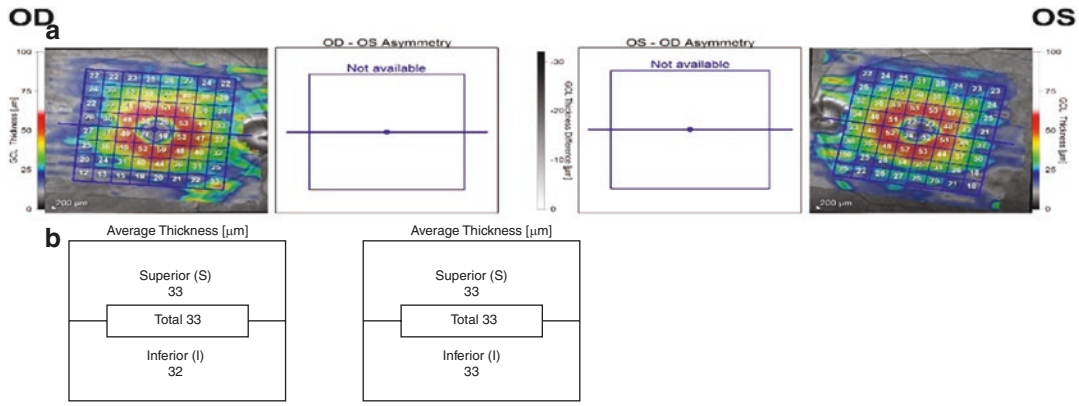

Fig. 25.9 Thickness map (**a**) and hemisphere asymmetry map (**b**) showing absence of asymmetry in the superior and inferior half of the myopic eye

both eyes (BE); fundus examination showed bilateral Frisen grade 4 papilledema. OCT showed increased RNFL thickness in the **superior** and **inferior** quadrants of the optic nerve head (Fig. 25.10). In addition, GCL maps (Fig. 25.11) indicated abnormally increased thickness of the ganglion cell layer over the macular region, probably due to axonal edema from papilledema.

This error in RNFL thickness and GCL thickness can hide an underlying glaucomatous change and show an erroneously 'false-negative green disease' on OCT.

Some of the other reasons for false-negative errors are:

- Tilted disks
- Traction at the optic disk
- Posterior vitreous detachment and epi-retinal membrane
- Retinal detachments and segmentation errors
- Macular edema

Case 25.3

An 18-year-old boy who had episodes of intermediate uveitis LE presented with IOP of 16 mmHg (RE) and 24 mmHg (LE). Fundus examination revealed vertical CDR of 0.7:1 in RE and 0.8:1 with epi-retinal membrane (ERM) in LE. OCT showed ERM (B-scan Fig. 25.12 red arrows) with posterior vitreous detachment. Superior-inferior and average global peripapillary thicknesses were significantly higher even in the presence of glaucomatous changes on the disk.

Learning Points

ERM can cause distortion and thickening of the retina, which results in erroneously high RNFL and macular thickness, resulting in 'false negative green disease' on OCT.

If ERM and glaucoma are present simultaneously, the results of the automated RNFL measurement should be critically evaluated.

The temporal increase in RNFL thickness and segmentation error is more common with ERM. Schisis of RNFL in ERM also results in increased thickness of RNFL.

Factors inducing segmentation error:

- Media opacities (Fig. 25.13)
- Epi-retinal membranes and vitreoretinal tractions
- Miotic pupils
- Long axial length
- Advanced glaucoma
- Scan decentration

Figure 25.13 shows a segmentation error due to media opacity causing red disease (despite normal GCL thickness (Fig. 25.14) which can be corrected manually (Fig. 25.15).

In advanced glaucomas, as axonal degeneration progresses, the major vessels begin to protrude out of the thinned RNFL (anteriorly towards the vitreous and posteriorly into the distal retina)

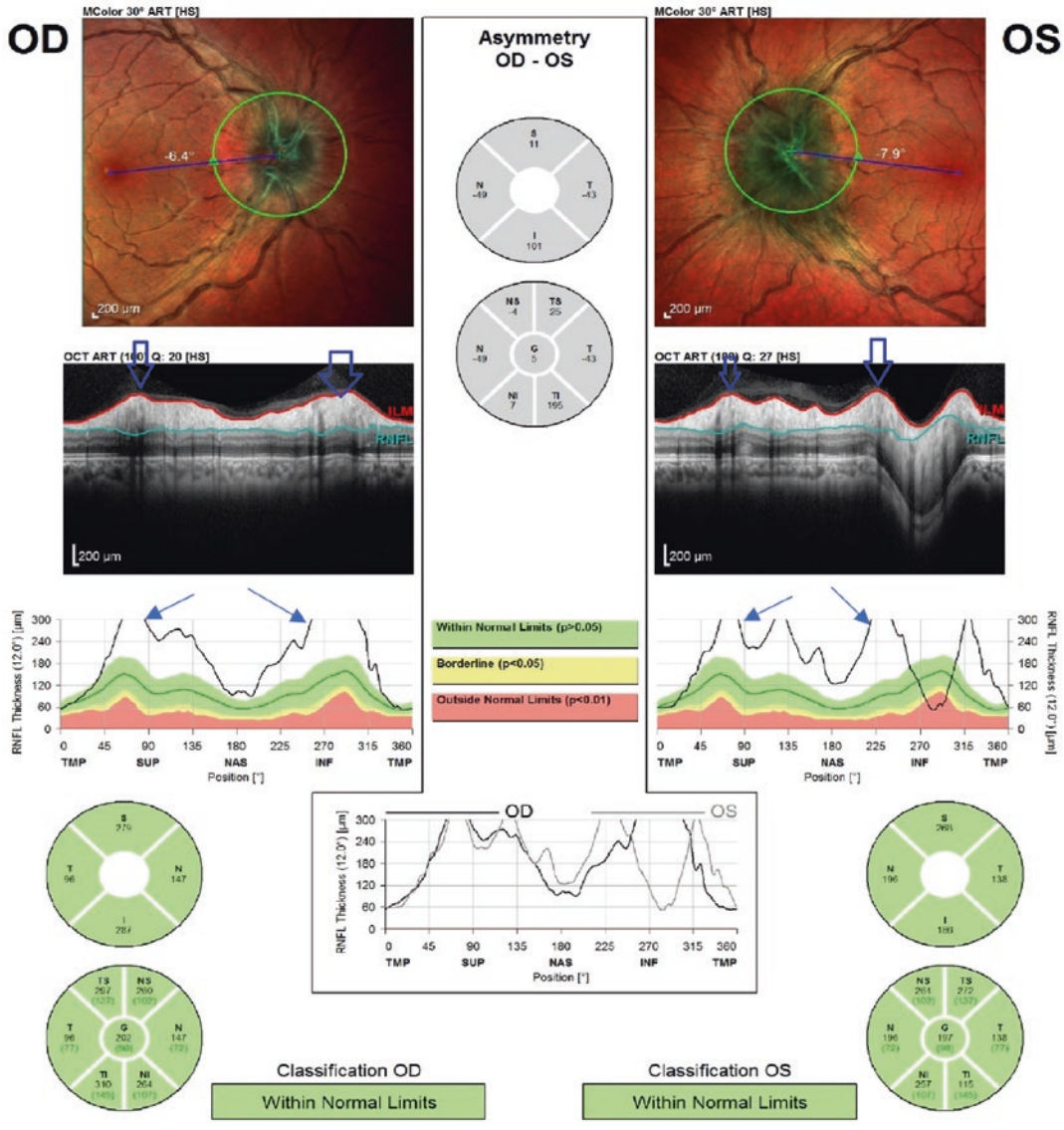

Fig. 25.10 RNFL (retinal nerve fiber layer) thickness profile and B-scan along with average thickness of circumpapillary RNFL show abnormal high thickness (blue arrows) due to edema

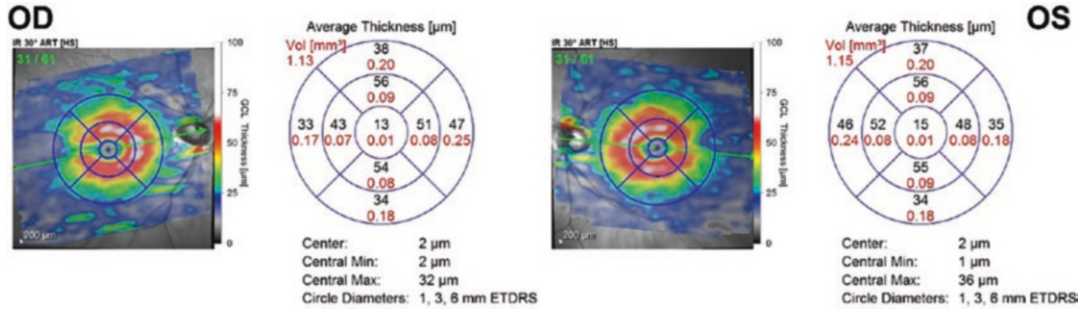

Fig. 25.11 Ganglion cell layer thickness map and color-coding map showing excessive high thickness of the ganglion cell layer over the macula due to axonal edema in the initial stage of papilledema

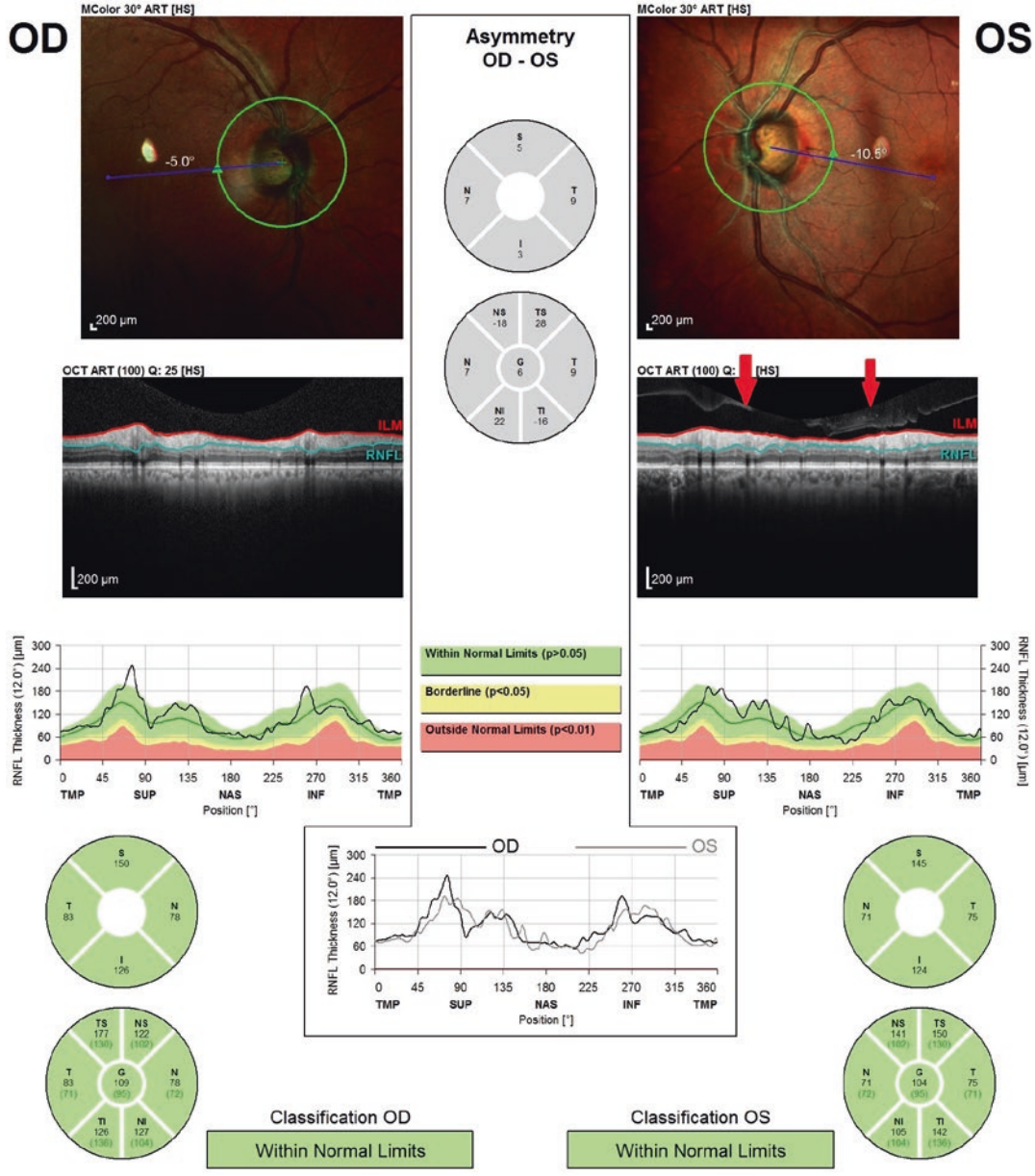

Fig. 25.12 In this case, left eye B-scan showing ERM (epi-retinal membrane) (red arrow) and elevated RNFL (retinal nerve fiber layer) thickness profile in a patient with PVD (posterior vitreous detachment)

creating additional challenges for the automated segmentation algorithms.

Case 25.4

Fundus examination of an 18-year-old boy with high myopia (−9.00 DS/−1.00 DC R/E, −9.75 DS/−0.75 DC) revealed tilted disks, temporal crescent, and parapapillary atrophy (Fig. 25.16) BE. Global RNFL thickness profile shows a superior-nasal defect in the right eye and superior-temporal sector defect in the left eye (Fig. 25.17). BMO-MRW analysis shows an abnormal thickness in the inferior sector of RE (Fig. 25.18).

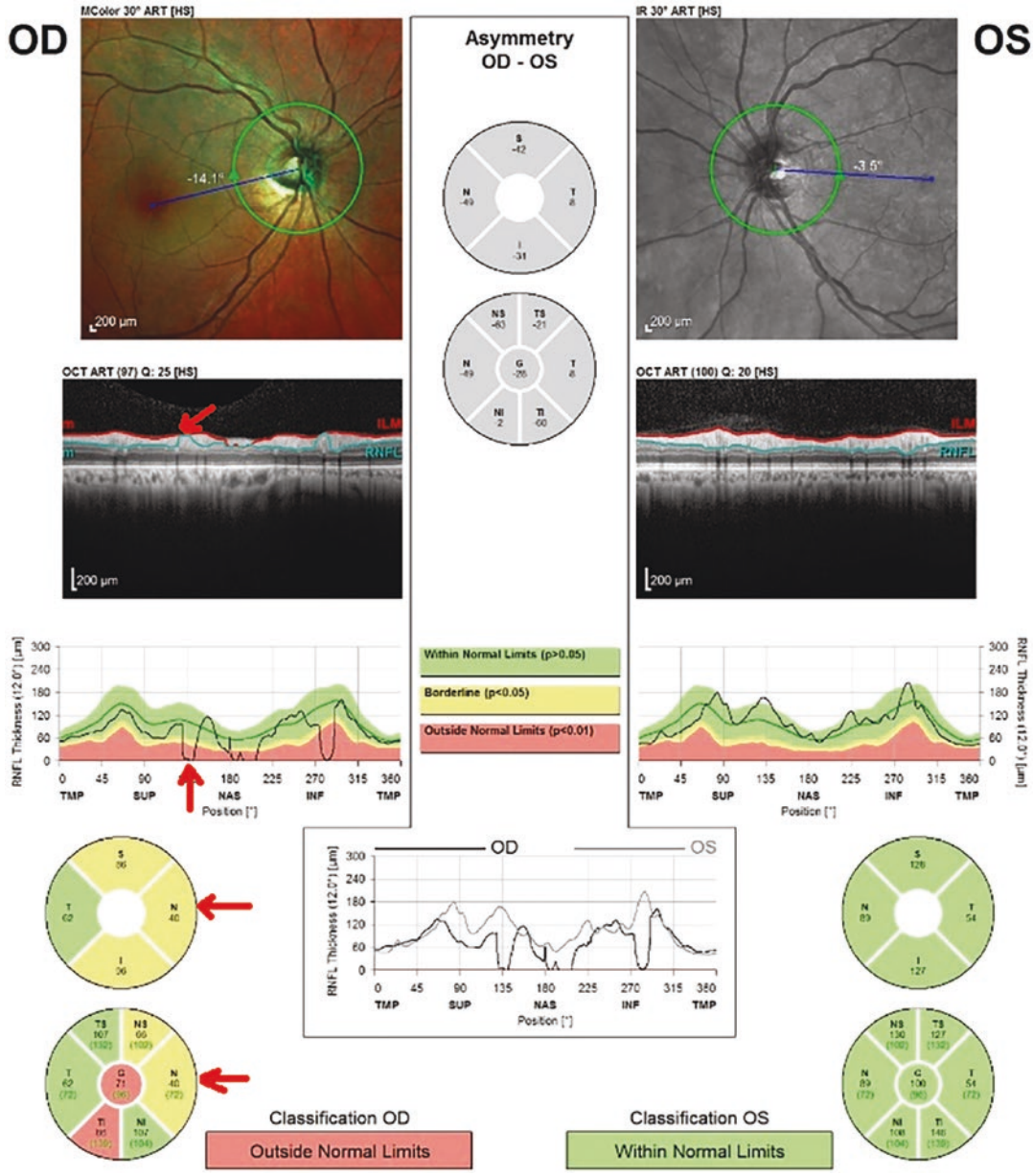

Fig. 25.13 Shows an example of the right eye in which errors in the automated segmentation (red arrows) resulted in an underestimation of sectoral RNFL thickness values at baseline

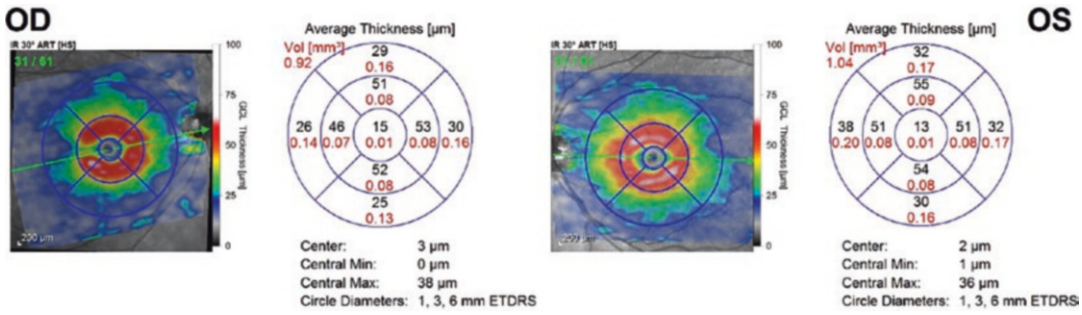

Fig. 25.14 Normal thickness of macular GCL (ganglion cell layer) profile in both eyes despite segmentation error with abnormal RNFL (retinal nerve fiber layer) defects

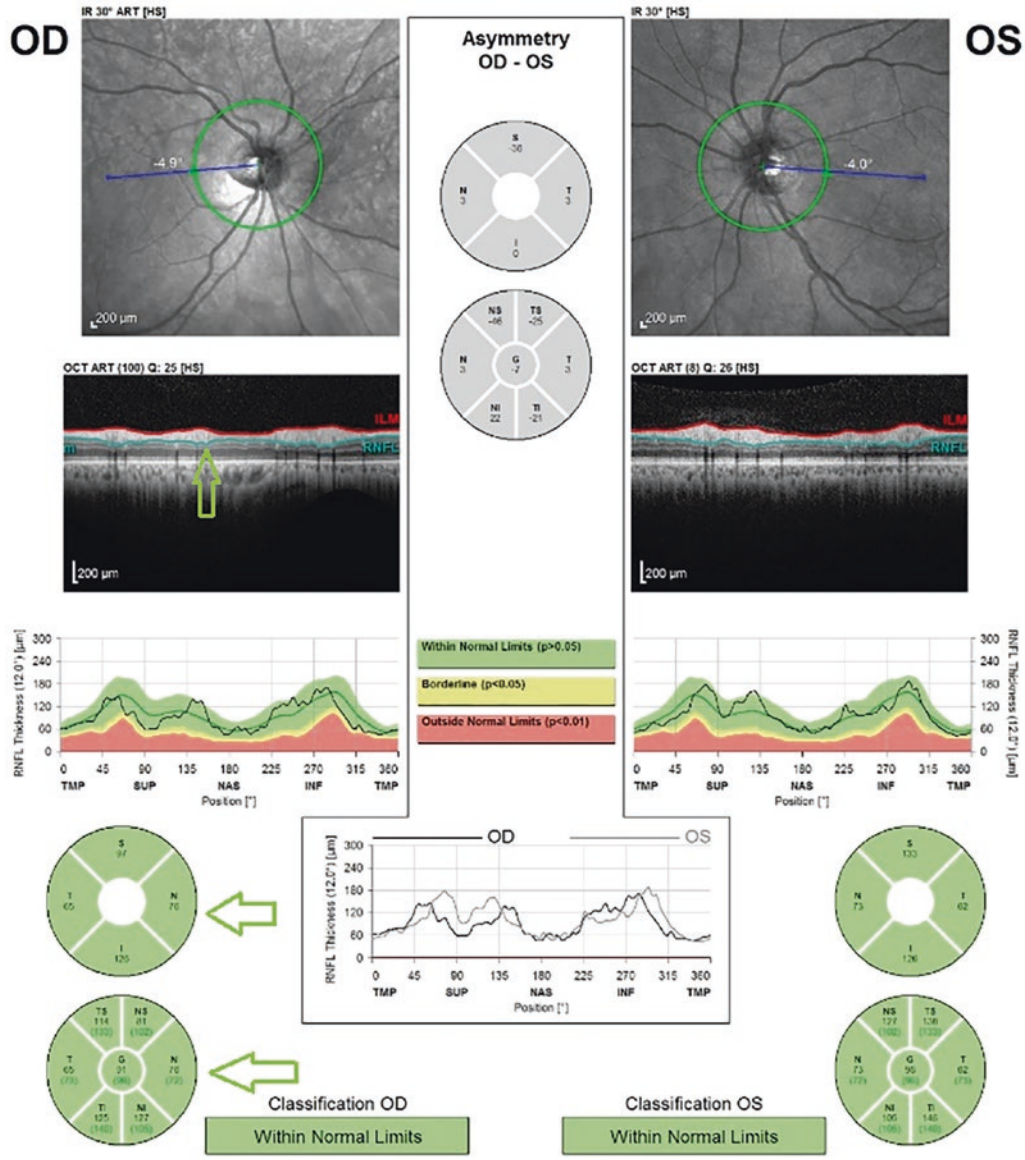

Fig. 25.15 Manually corrected automated segmentation error, which shows normal RNFL (retinal nerve fiber layer) thickness profile (green arrows)

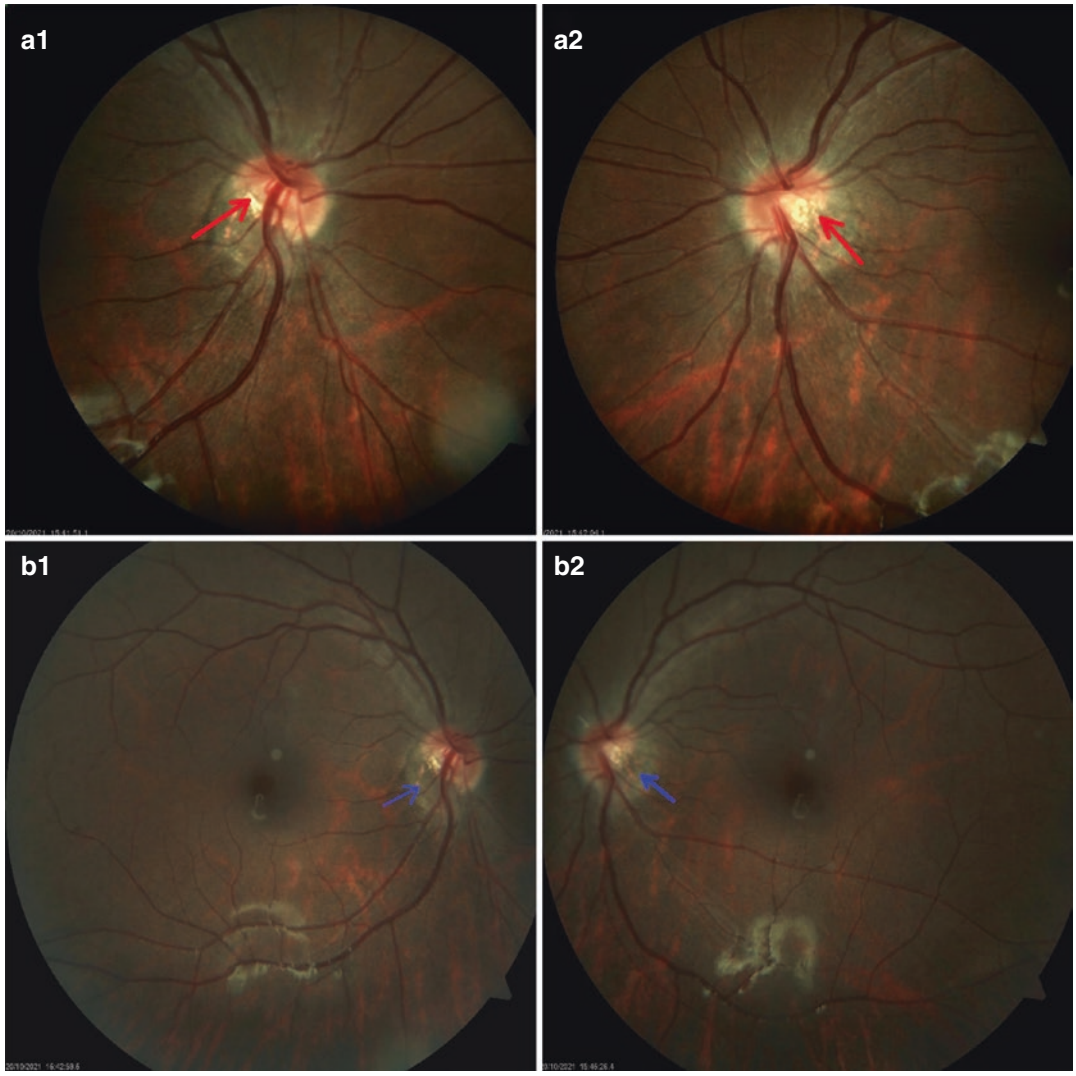

Fig. 25.16 30°(a1 and a2) and 45°(b1 and b2) fundus photos show the clinical characteristics of tilted disk, temporal crescent (Both eyes, red arrow), and parapapillary atrophy (Both eyes, blue arrow)

Learning Points

- Optic disk tilt (ODT) is a common finding in the general population which is caused by the malclosure of the embryonic optic fissure.
- The tilted optic disk is often associated with abnormal peripapillary RNFL thickness as well as visual field defects, leading to diagnostic difficulties due to similarities with glaucomatous disks.
- Studies show that there is a significantly low superior-temporal, superior-nasal, temporal, and global RNFL thickness in the tilted disk group as compared to normal disk. However, there were no significant differences in the ganglion cell layer and ganglion cell-inner plexiform layer thickness between the tilted and normal optic disks.
- The characteristics of the peripapillary RNFL thickness also depends on the degree of temporal myopic ODT. Hence, while interpreting the RNFL thickness in myopic eyes, the degree of myopic ODT should be considered.

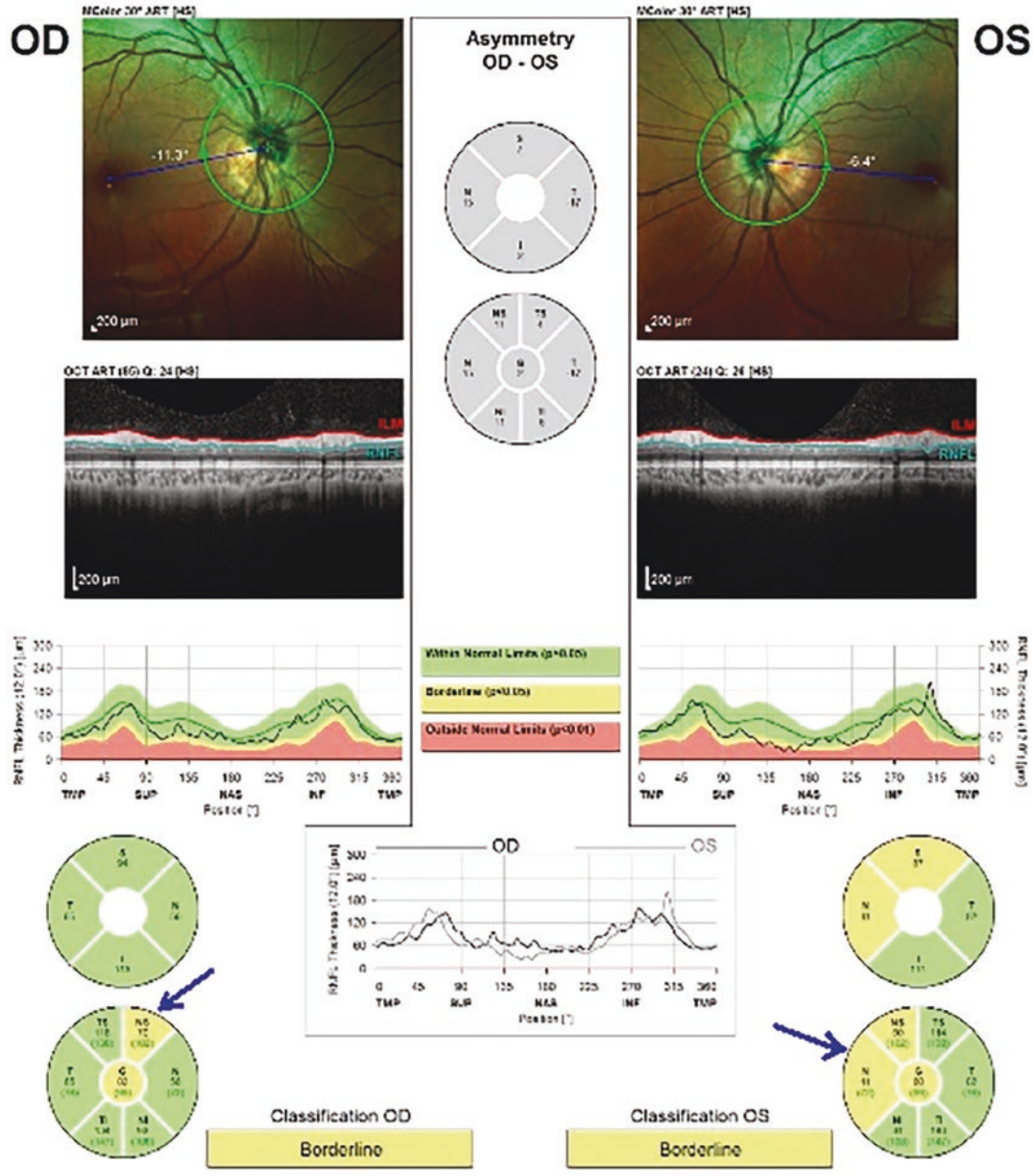

Fig. 25.17 A patient with tilted disk (both eyes) reveals abnormal parapapillary RNFL (retinal nerve fiber layer) thickness (blue arrows show sectoral defects) and significantly low RNFL thickness in different quadrants (viz. superior-temporal (R/E) and superior-nasal (LE))

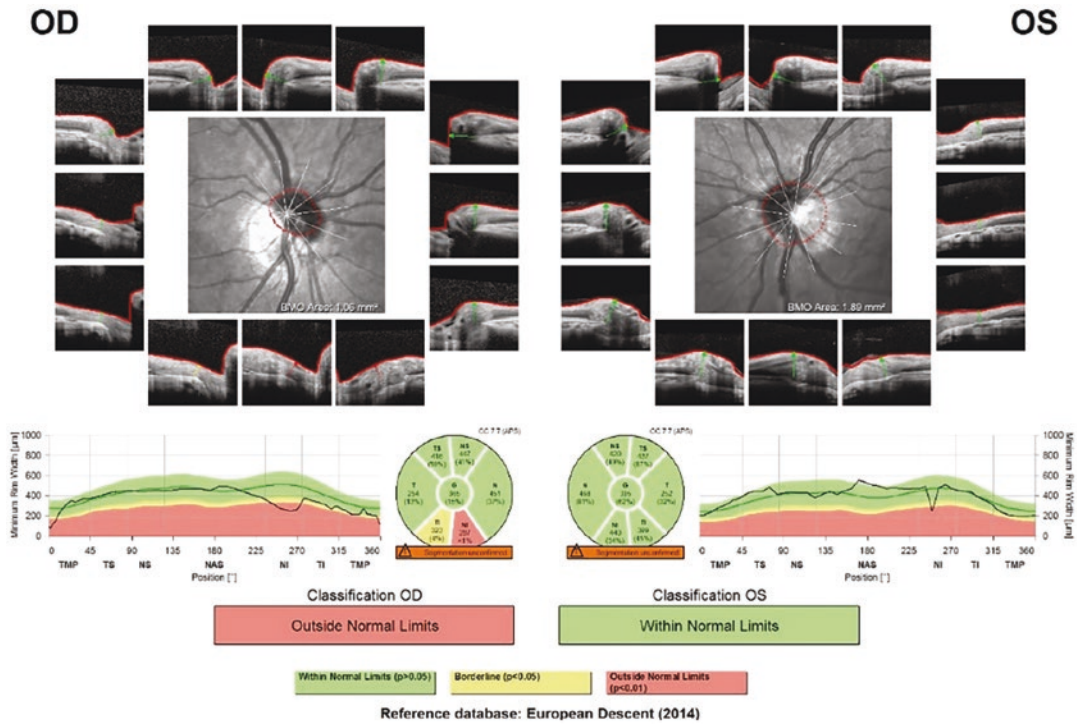

Fig. 25.18 BMO-MRW (Bruch's membrane opening-minimum rim width) analysis also shows an abnormal thickness in the inferior sector of RE

25.6 Conclusions

Poster segment OCT is a non-invasive diagnostic tool, helpful in the evaluation of glaucoma. OCT's applications include objective evaluation of optic nerve head (ONH), retinal nerve fiber layer thickness (RNFL), and structural characteristics of the macula and the ganglion cell complex (GCC). Though a normative database is unavailable for all age groups at present, OCT still serves as a valuable tool to look for progression in childhood glaucoma.

Suggested Reading

Chen JJ, Kardon RH, Biousse V, Galetta S. Avoiding clinical misinterpretation and artifacts of optical coherence tomography analysis of the optic nerve, retinal nerve fiber layer, and ganglion cell layer. J Neuroophthalmol. 2016;36(4):417–38. https://doi.org/10.1097/WNO.0000000000000422.

Gude NN, Gardiner KS, Fortune B, Demirel S, Mansberger SL. Optical coherence tomography segmentation errors of the retinal nerve fiber layer persist over time. J Glaucoma. 2019;28(5):368–74. https://doi.org/10.1097/IJG.0000000000001222.

Kim YC, Moon JS, Park LHY, Park CK. Three Dimensional evaluation of posterior pole and optic nerve head in tilted disc. Sci Rep. 2018;8(1):1121. https://doi.org/10.1038/s41598-018-19242-z.

Lee KM, Lee EJ, Kim TW, Kim H. Comparison of the abilities of SD-OCT and SS-OCT in evaluating the thickness of the macular inner retinal layer for glaucoma diagnosis. PLoS One. 2016;11(1):e0147964. https://doi.org/10.1371/journal.pone.0147964.

Naik A, Sihota R, Mahalingam K, Angmo D, Dada T, Kumar A, Kumar A, Gupta A. Evaluation of visual field changes with retinal nerve fiber layer thickness in primary congenital glaucoma. Indian J Ophthalmol. 2022;70(10):3556–61. https://doi.org/10.4103/ijo.IJO_396_22.

Scuderi G, Fragiotta S, Scuderi L, Iodice CM, Perdicchi A. Ganglion cell complex analysis in glaucoma patients: what can it tell us? Eye Brain. 2020;12:33–44. https://doi.org/10.2147/EB.S226319.

Shin HY, Park LHY, Park CK. The effect of myopic optic disc tilt on measurement of spectral-domain optical coherence tomography parameters. Br J Ophthalmol. 2015;99(1):69–74. https://doi.org/10.1136/bjophthalmol-2014-305259. Epub 2014 Aug 4.

Sihota R. Practical approach to glaucoma: case-based. 1st ed. Delhi: Thieme Publishers; 2022.

Singh K. Challenges in optical coherence tomography interpretation for diagnosing glaucoma in myopic eyes. DJO. 2020;31:9–17. https://doi.org/10.7869/djo.584.

Heidelberg Retinal Tomography

26

Harathy Selvan, Abhishek Singh, and Shikha Gupta

The Heidelberg retinal tomography (HRT, Heidelberg Engineering GmbH, Heidelberg, Germany) is a type of optic nerve head (ONH) imaging based on the concept of confocal scanning laser ophthalmoscopy (CSLO) (Fig. 26.1).

It performs a 3-D structural assessment of the ONH and generates quantitative data such as the disc area, cup area, rim area, cup-disc ratio, cup-disc area ratio, rim-disc area ratio, rim volume, cup volume, cup depth, mean retinal nerve fiber layer (RNFL) thickness, RNFL cross-sectional area, etc., as global and sectoral indices (Fig. 26.2). Comparison of the results against their respective ethnic normative database aids in the diagnosis of glaucoma. In addition, longitudinal follow-up of the scans can assist in the early detection of structural progression.

To differentiate between a normal and a glaucomatous ONH, two built-in software programs, the Moorfields regression analysis (MRA) and glaucoma probability score (GPS), are useful (Figs. 26.3 and 26.4 respectively). Their features have been summarized in Table 26.1. The reports are generated as "within normal limits," "borderline," or "outside normal limits" aiding in easy diagnosis.

The diagnosis of childhood glaucoma is primarily clinical, based on serial fundus evaluation and tonometry, as children may not be able to perform reliable diagnostics. The lack of a normative pediatric database for structural tests limits their utility in establishing an initial diagnosis. Therefore, when performing HRT on a child, the MRA and GPS formulated against the adult normative database should be interpreted with caution. However, a study of serial scans to detect deviations that have occurred from baseline remains valuable. It also avoids erroneous interpretation due to isolated artifacts.

H. Selvan (✉)
Moorfields Eye Hospital NHS Foundation Trust, London, UK

A. Singh · S. Gupta
Dr. Rajendra Prasad Centre for Ophthalmic Sciences, All India Institute of Medical Sciences, New Delhi, India

S. Gupta et al. (eds.), *Childhood Glaucoma*, https://doi.org/10.1007/978-981-19-7466-3_26

Fig. 26.1 Image of a child being examined on Heidelberg retinal tomograph

To assess progression, two algorithms, namely, the topographic change analysis (TCA) and stereometric trend analysis (TA), are helpful. In TCA, the progression is predicted based on the probability of change in surface height of each super-pixel cluster between the baseline and follow-up scans. Significant surface depressions are seen as red clusters, while elevations are denoted as green clusters. Changes in the area and volume of each cluster over time can also be studied on individual graphs. On the other hand, TA uses the stereoparametric progression chart to identify changes in normalized topographic parameters

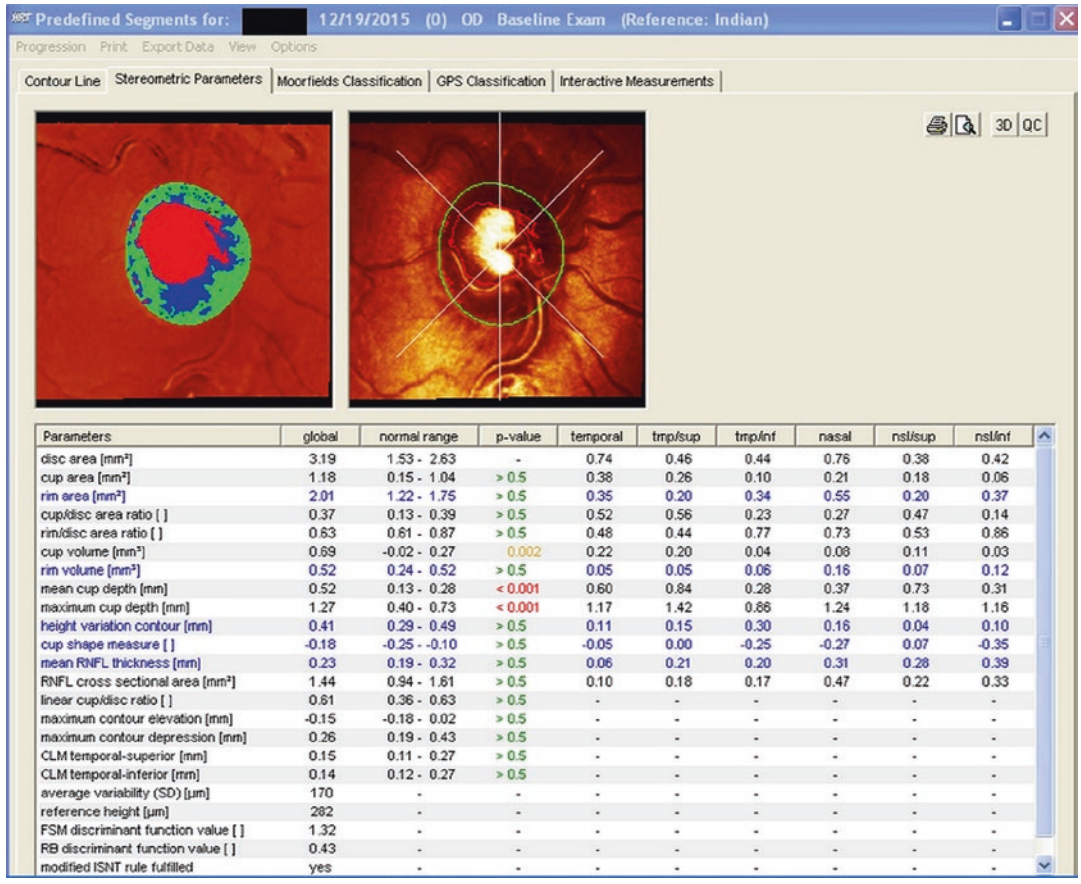

Parameters	global	normal range	p-value	temporal	tmp/sup	tmp/inf	nasal	nsl/sup	nsl/inf
disc area [mm²]	3.19	1.53 - 2.63	-	0.74	0.46	0.44	0.76	0.38	0.42
cup area [mm²]	1.18	0.15 - 1.04	> 0.5	0.38	0.26	0.10	0.21	0.18	0.06
rim area [mm²]	2.01	1.22 - 1.75	> 0.5	0.35	0.20	0.34	0.55	0.20	0.37
cup/disc area ratio [ ]	0.37	0.13 - 0.39	> 0.5	0.52	0.56	0.23	0.27	0.47	0.14
rim/disc area ratio [ ]	0.63	0.61 - 0.87	> 0.5	0.48	0.44	0.77	0.73	0.53	0.86
cup volume [mm³]	0.69	-0.02 - 0.27	0.002	0.22	0.20	0.04	0.08	0.11	0.03
rim volume [mm³]	0.52	0.24 - 0.52	> 0.5	0.05	0.05	0.06	0.16	0.07	0.12
mean cup depth [mm]	0.52	0.13 - 0.28	< 0.001	0.60	0.84	0.28	0.37	0.73	0.31
maximum cup depth [mm]	1.27	0.40 - 0.73	< 0.001	1.17	1.42	0.86	1.24	1.18	1.16
height variation contour [mm]	0.41	0.29 - 0.49	> 0.5	0.11	0.15	0.30	0.16	0.04	0.10
cup shape measure [ ]	-0.18	-0.25 - -0.10	> 0.5	-0.05	0.00	-0.25	-0.27	0.07	-0.35
mean RNFL thickness [mm]	0.23	0.19 - 0.32	> 0.5	0.06	0.21	0.20	0.31	0.28	0.39
RNFL cross sectional area [mm²]	1.44	0.94 - 1.61	> 0.5	0.10	0.18	0.17	0.47	0.22	0.33
linear cup/disc ratio [ ]	0.61	0.36 - 0.63	> 0.5	-	-	-	-	-	-
maximum contour elevation [mm]	-0.15	-0.18 - 0.02	> 0.5	-	-	-	-	-	-
maximum contour depression [mm]	0.26	0.19 - 0.43	> 0.5	-	-	-	-	-	-
CLM temporal-superior [mm]	0.15	0.11 - 0.27	> 0.5	-	-	-	-	-	-
CLM temporal-inferior [mm]	0.14	0.12 - 0.27	> 0.5	-	-	-	-	-	-
average variability (SD) [µm]	170	-	-	-	-	-	-	-	-
reference height [µm]	282	-	-	-	-	-	-	-	-
FSM discriminant function value [ ]	1.32	-	-	-	-	-	-	-	-
RB discriminant function value [ ]	0.43	-	-	-	-	-	-	-	-
modified ISNT rule fulfilled	yes	-	-	-	-	-	-	-	-

Fig. 26.2 Report of optic disc and retinal nerve fiber layer stereoparameters generated on the Heidelberg retinal tomography

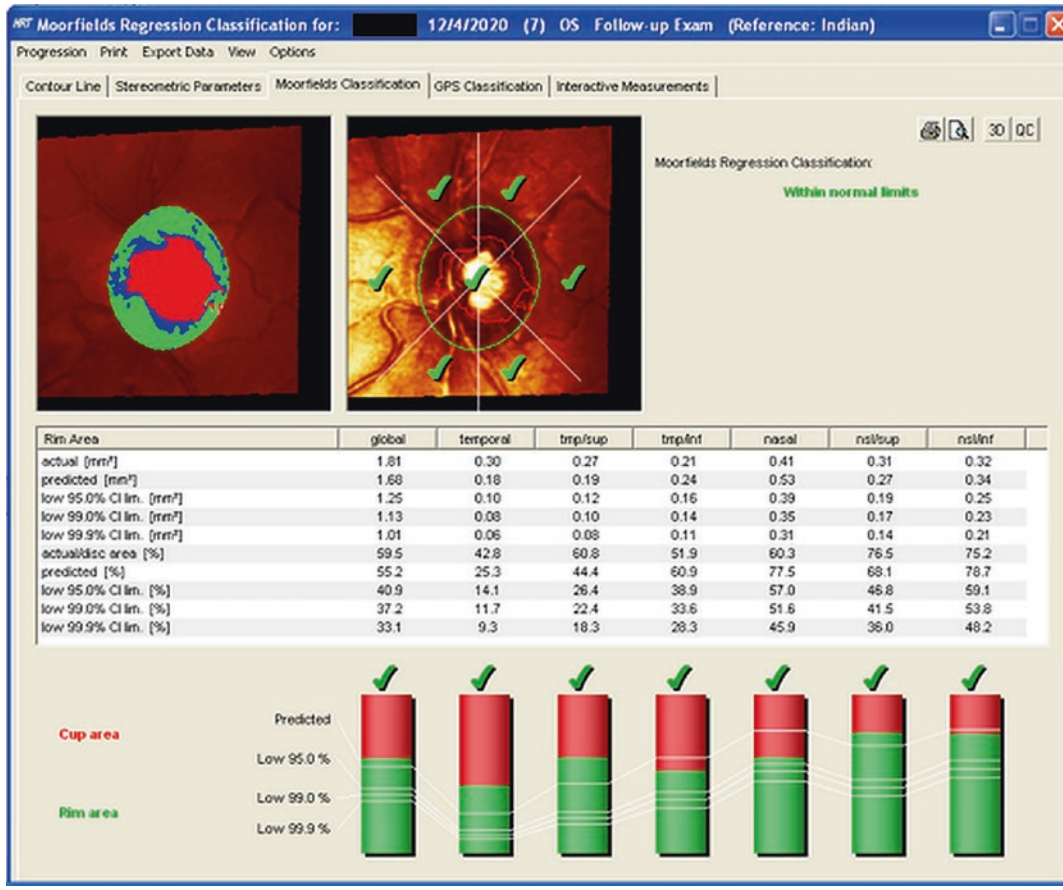

Fig. 26.3 Shows report of a Moorfields regression analysis as within normal limits

over time. A downward trend line of the global or sectoral indices by more than 0.2 implies progression (Fig. 26.5).

Structural progression could be detected by HRT and optical coherence tomography (OCT). While the latter primarily characterizes the peripapillary retinal nerve fiber layer or the macular ganglion cell complex, the HRT measures the disc and peripapillary RNFL parameters. They may also show variable agreement, as indicated by examples discussed in the later section of this chapter. The HRT may hold an advantage in cases of high myopia, where the peripapillary retina and macula are thinner and prone to progressive change due to myopia progression. A study of disc parameters in such cases is more helpful; however, the overall precision of glaucoma diagnosis in myopic discs is lower than in normal subjects. Functional studies should be considered in such challenging eyes, but when poor visual acuity does not allow functional measurement, structural tests can be monitored. The pros and cons of HRT versus perimetry in childhood glaucoma have been summarized in Table 26.2.

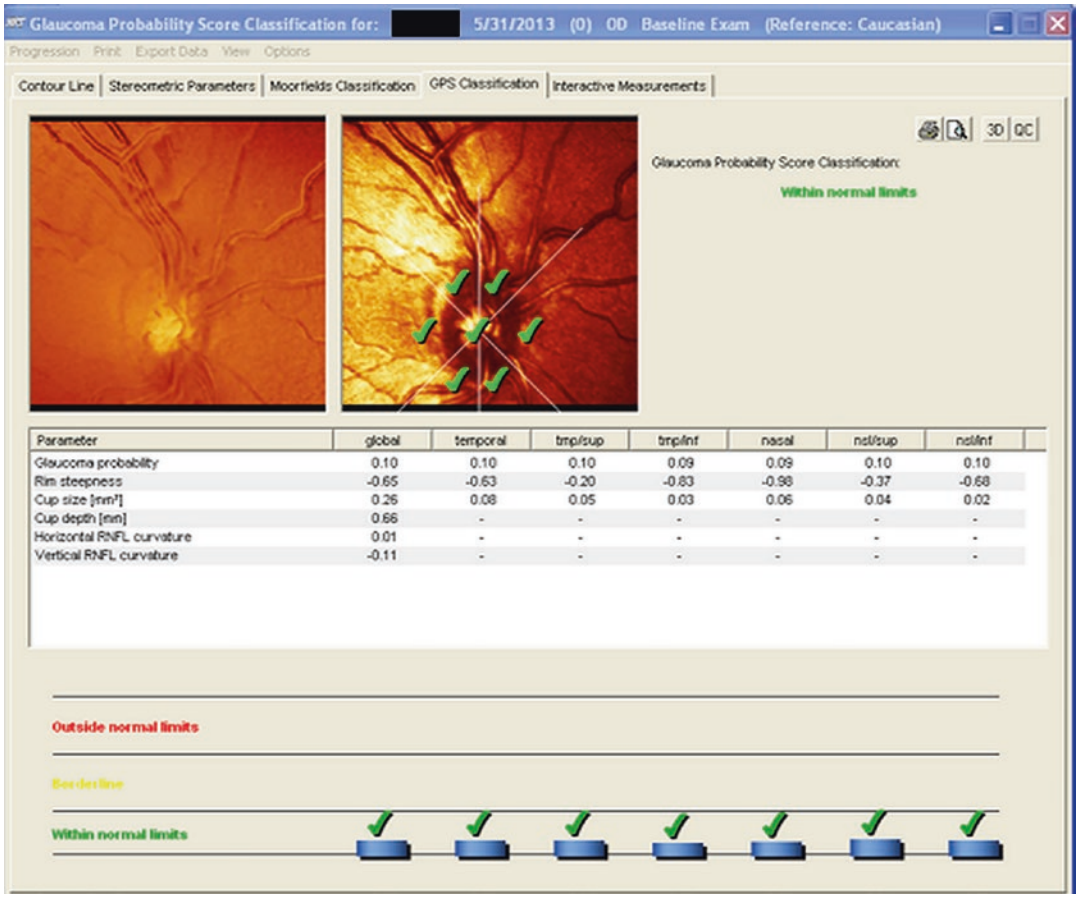

Fig. 26.4 Shows the report of Glaucoma Probability Score as within normal limits

Table 26.1 Comparison of Moorfields Regression Analysis (MRA) and Glaucoma Probability Score (GPS) in Heidelberg Retinal Tomography (HRT)

S.no	Moorfields regression analysis (MRA)	Glaucoma probability score (GPS)
1.	The optic disc contour line needs to be manually drawn by the technician and hence is amenable to subjective judgment	Measurements based on automatic detection of the optic disc, which is then fitted to that of a model optic disc. Does not need a manual contour line drawing
2.	A reference plane is used to deduce the measurements	Reference plane not used
3.	Experienced operator required (to draw the exact contour line)	Operator independent
4.	MRA uses a logarithmic relationship between the neuroretinal rim and optic disc areas to generate the report	GPS utilizes the whole topographic image of the optic disc, including the cup size, cup depth, rim steepness, and horizontal/vertical RNFL curvature
5.	Good reproducibility	Good reproducibility. Image quality does not affect overall GPS report
6.	Individual stereoparameters maybe affected by altered disc shape and high refractive errors	Reproducibility not affected by refraction, disc size, tilted disc morphology, peripapillary atrophy, or disease stage
7.	Present in all HRT versions	Present in HRT-3 (latest version)

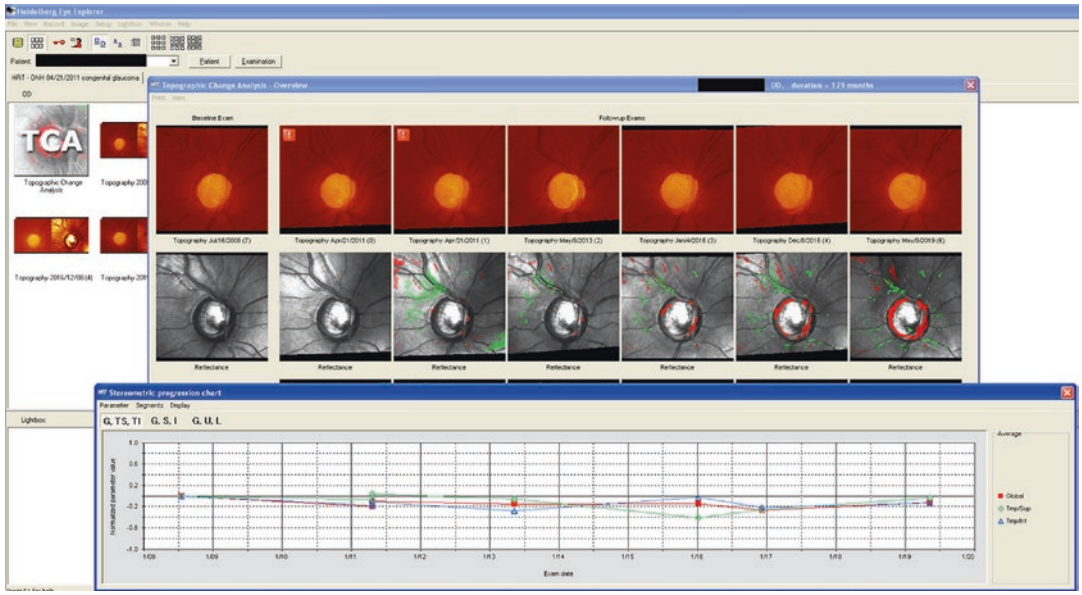

Fig. 26.5 Upper part of the image shows topographic change analysis, where evolution of red super-pixel clusters can be seen. Lower part of the image shows trend analysis (stereoparametric progression chart), where changes in numerical parameters are plotted against time

Table 26.2 Comparison of Heidelberg Retinal tomography (HRT) and perimetry for childhood glaucoma

S.no	HRT in children	Perimetry in children
1.	Identifies structural topographic changes of the optic disc	Identifies functional visual field changes
2.	Objective testing	Subjective testing
3.	Easier positioning	Difficult positioning
4.	Quick (performed in less than a minute)	Takes longer to perform (4–10 min)
5.	Requires minimal cooperation from the child and so can be performed on young children	Requires active participation from the child. Therefore, it can only be performed on children with a good understanding
6.	Minimal chances of poor image quality in the absence of media haze.	There are significant chances of unreliable tests due to loss of fixation and false-positive and false-negative responses
7.	Less laborious	More laborious. Several tests may be required before a good baseline can be set up
8.	Can be performed in the eyes with moderate visual acuity impairment too	Requires visual acuity better than 6/18 for performing static perimetry
9.	Moderate technician skills required	Highly skilled technicians required (especially for Goldmann fields)
10.	Lacks pediatric normative database	Lacks pediatric normative database
11.	Topographic change analysis and stereometric trend analysis are used to study progression	Overview analysis and guided progression analysis (GPA) are used to study progression

26.1 Case Examples

Case 26.1

A 16-year-old boy, a known case of bilateral primary congenital glaucoma who had undergone bilateral trabeculotomy with trabeculectomy and mitomycin-c (MMC) at 2 years of age, presented for his routine checkup. His baseline records revealed an initial intraocular pressure (IOP) of 28 mmHg in the right eye (RE) and 32 mmHg in the left eye (LE), with a cup-disc ratio (CDR) of 0.8:1 in both eyes (BE).

Examination: Best-corrected visual acuity (BCVA) was 6/12 BE; applanation IOP was RE 14 mmHg and LE 18 mmHg. BE had superior diffuse functional blebs, large corneal diameters, paracentral Haab's striae, deep anterior chamber (AC), and clear lenses. Fundus examination showed a CDR of 0.6:1 in RE and 0.8:1 in LE; the macula was normal in BE. Diurnal variations showed IOP fluctuation of up to 24 mmHg in LE.

Investigations: (1) Ultrasound pachymetry, RE 500 μm, LE 505 μm (2) cycloplegic refraction, RE -2DS/-2 DC@ 100°, LE -1.5 DS/−1.5 DC @ 80° and (3) HRT: MRA RE ✓ in all sectors and LE x in all sectors except temporal and inferotemporal. The LE had shown worsening as compared to baseline (Fig. 26.6a, b). Trend Analysis: The stereoparametric progression chart showed RE to be stable, but the LE showed significant downward trend of global, supero-temporal and inferotemporal sectors, indicating progression (Fig. 26.6c). (4) Humphrey visual fields (HVF) and Goldmann fields could not be reliably performed.

Diagnosis: BE primary congenital glaucoma, operated combined trabeculotomy and trabeculectomy; RE stable, LE structural progression.

Treatment: LE topical latanoprost 0.005% HS and timolol maleate 0.5% bd were started.

Learning Points

- Detection of structural progression by objective tests is important in pediatric glaucomas as children may not be able to perform a reliable perimetry.
- Reversal of optic disc cupping may or may not occur in primary congenital glaucoma after surgical lowering of IOP. This can be monitored on the HRT.
- Acquisition of reflectance and topographic disc images gives a good measure of simultaneous fundus photography that can also be serially followed up. Reports suggest that discs with progressive glaucoma with or without myopia can also undergo morphological variations over time.

Case 26.2

A 20-year-old girl, a known case of RE familial juvenile open-angle glaucoma (JOAG), presented for her 6-month checkup. The family history was significant for JOAG in her father, and subsequent family screening identified her early disease at the age of 6. Her baseline IOP was RE 28 mmHg and LE 24 mmHg, and baseline CDR was 0.7:1 RE and 0.5:1 LE. Baseline HRT showed MRA ✓ in all sectors BE. Baseline HVF showed a superior nasal step in RE and normal study in the LE. She was started on medical management with BE latanoprost 0.005% HS and RE timolol maleate 0.5% BD, and the IOPs have remained within the target range since then.

Examination: BE BCVA 6/6 and applanation IOP 18 mmHg. BE AC was deep, iris showed normal pattern, and gonioscopy revealed prominent iris processes. Optic discs showed RE CDR of 0.7:1 with inferior NRR thinning and LE 0.5:1 with healthy rims.

Investigations: (1) Ultrasound pachymetry: RE 520 μm and LE 523 μm (2) HVF 30–2 SS: RE superior nasal step and LE within normal limits; GPA, no progression detected in BE. (3) HRT: MRA RE x in the inferotemporal and inferonasal sectors and ✓ in all other sectors; LE showed ✓ in all sectors. TCA: The RE showed evolution of a red super-pixel cluster

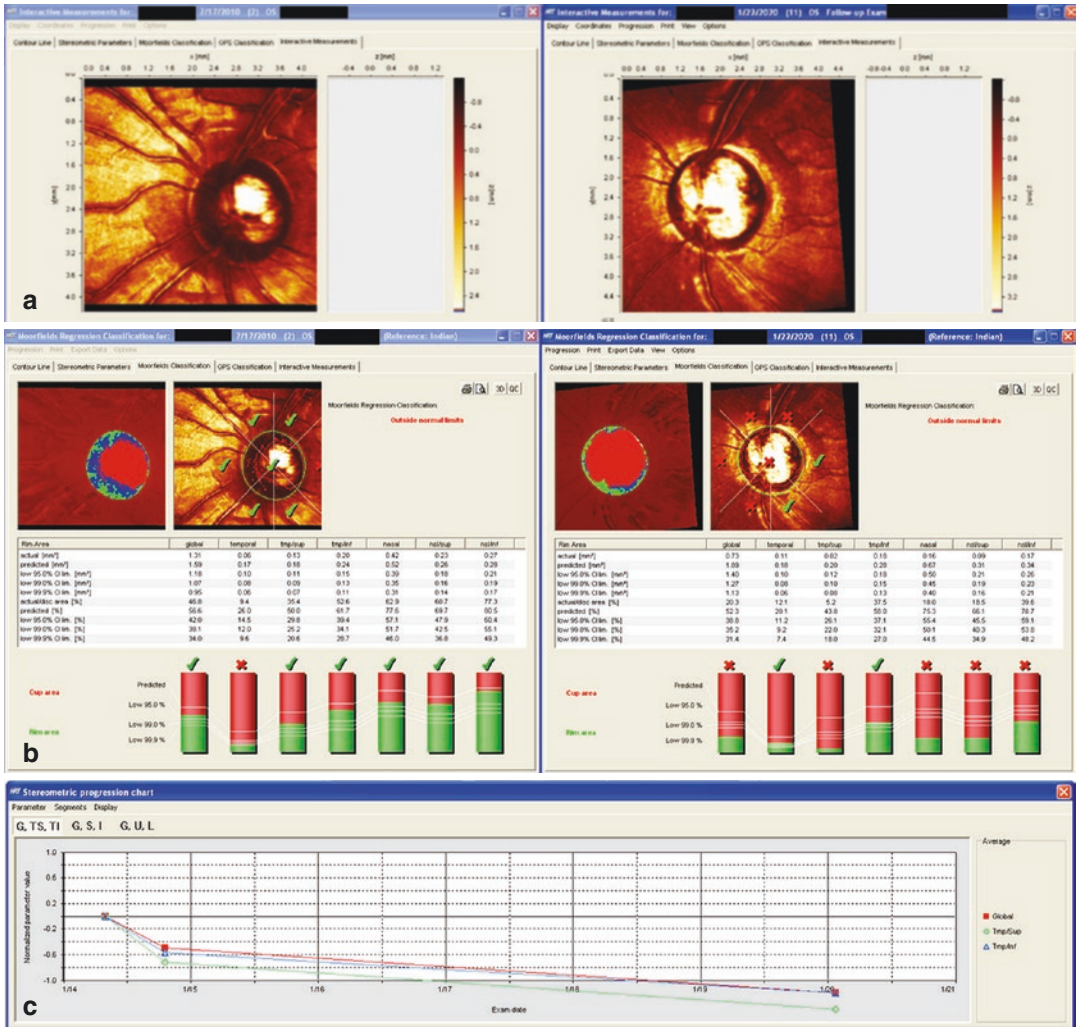

Fig. 26.6 HRT report of Case 26.1. (**a**) Comparison of reflectance image between baseline and follow-up visits 10 years apart shows significant NRR thinning. (**b**) Comparison of MRA report between baseline and follow-up shows deterioration of disc parameters. (**c**) Stereoparametric chart (trend analysis) shows significant downward trend of global, supero-temporal and infero-temporal sectors, suggestive of progression

involving the inferior NRR and the peripapillary retina, gradually increasing in size. Numerical study of the change by means of a graphical plot showed 2× change in volume over time, indicating structural progression (Fig. 26.7). The LE had remained stable.

Diagnosis: RE JOAG with structural progression, LE stable JOHT (Juvenile Ocular hypertension).

Treatment: RE addition of brimonidine 0.2% BD to preexisting therapy.

Learning Points

- Structural progression can precede functional progression.
- Identification of structural progression at an early stage facilitates treatment and halting of further progression.

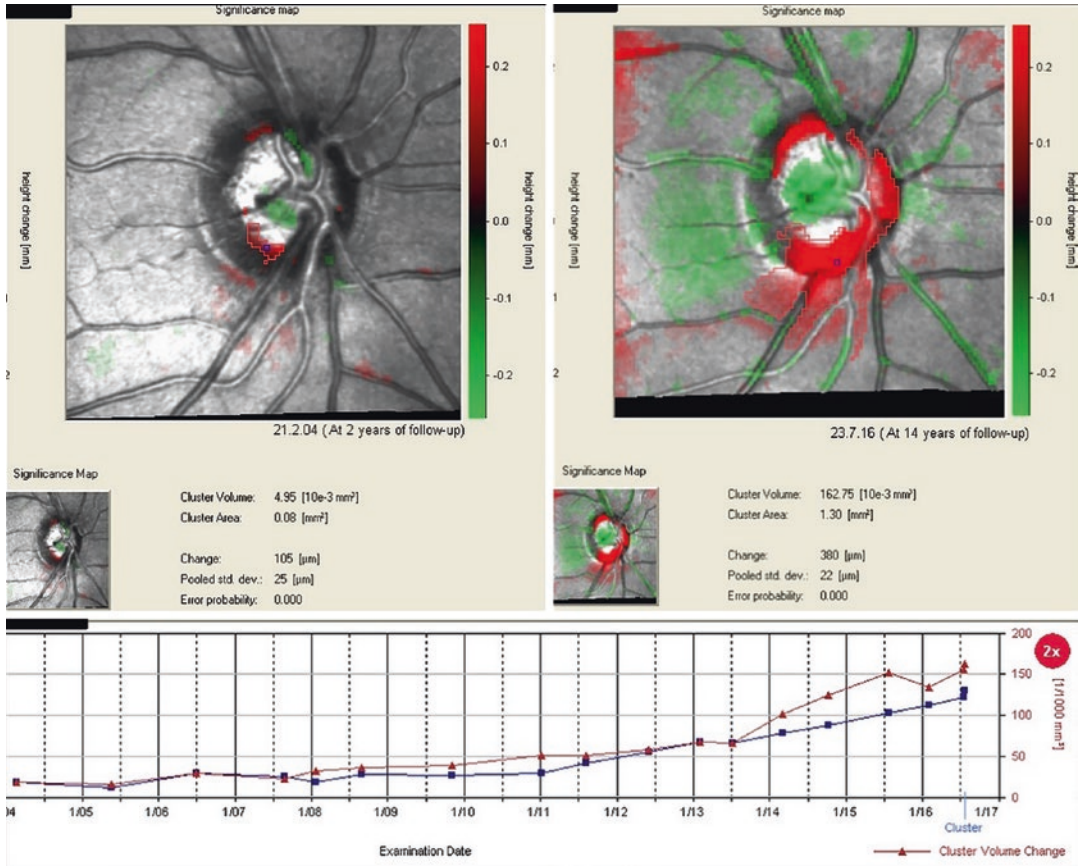

Fig. 26.7 Heidelberg retinal tomography report of Case 26.2: Comparison of the baseline and follow-up images (14 years later) shows formation of a red super-pixel cluster involving the inferior NRR and the peripapillary retina. The graphical plot of the cluster shows 2× increase in cluster area and volume over time, suggesting progression

26.2 Other Examples

Many a times, imaging reports can have variable agreement. In such cases, it is important to look for clinical correlation and interpret the reports with caution. Examples of concordance and discordance between different programs within the same machine (HRT) and between different machines (HRT and OCT) have been shown below for a better understanding:

1. HRT MRA and GPS showing concordance (Fig. 26.8) and discordance (Fig. 26.9)
2. HRT and OCT showing concordance (Fig. 26.10) and discordance (Fig. 26.11)

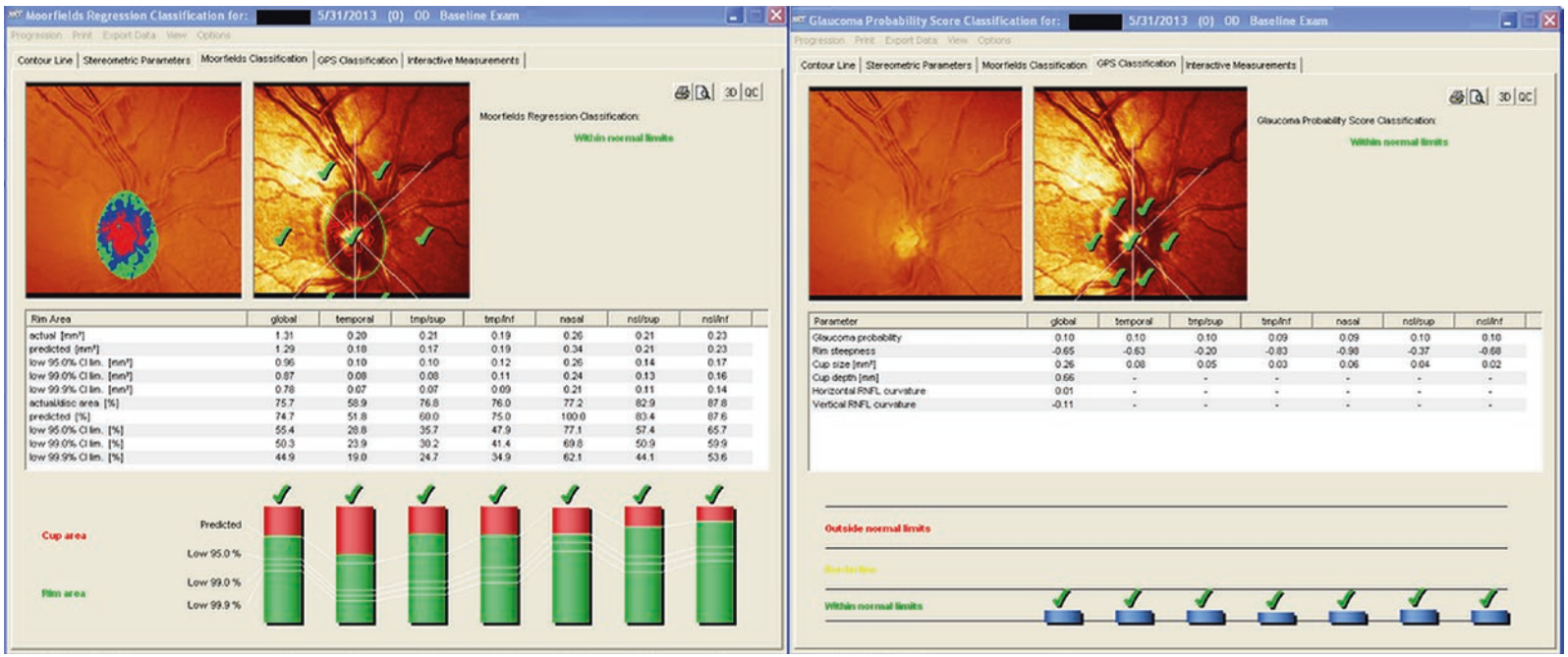

Fig. 26.8 The Moorfields Regression Analysis and Glaucoma Probability Score report of the same eye, showing ✓ in all sectors, and report "within normal limits"

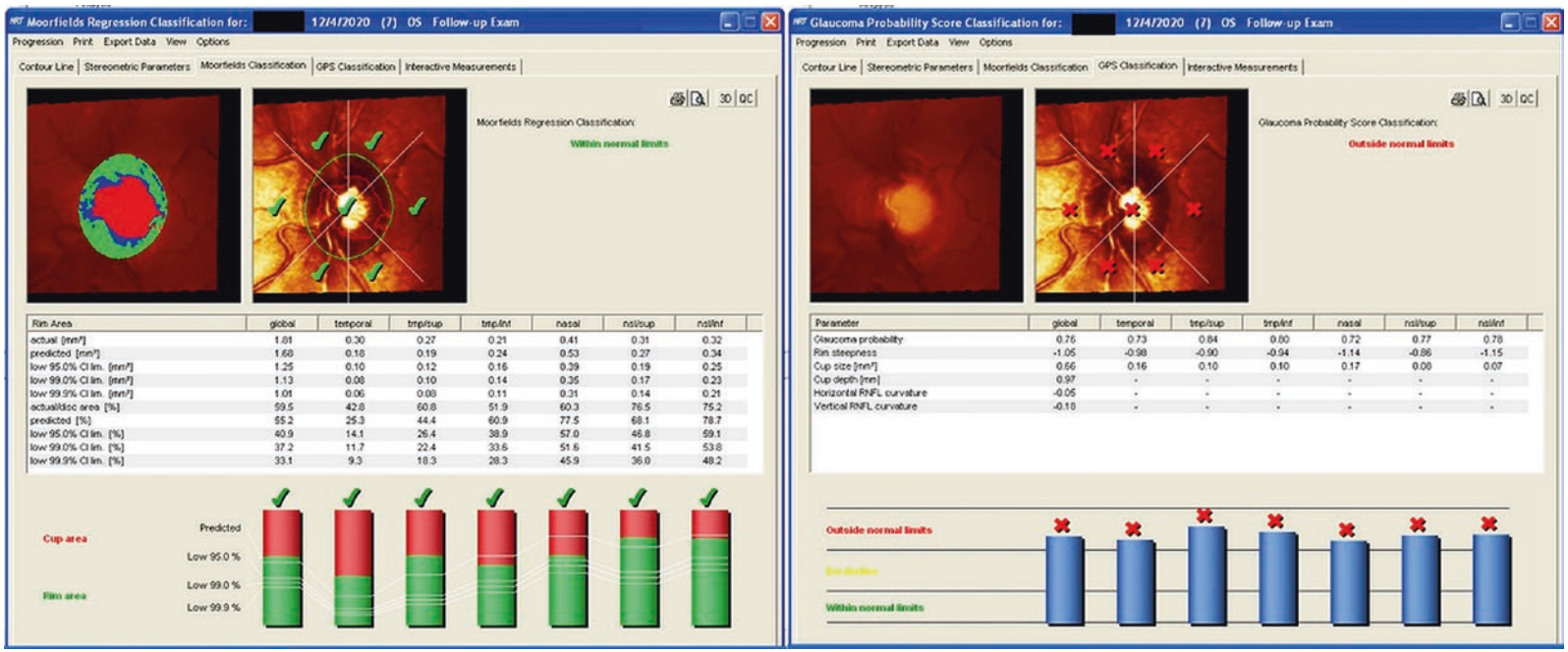

Fig. 26.9 The Moorfields Regression Analysis (MRA) and Glaucoma Probability Score (GPS) report of the same eye shows different results in the same examination. While the MRA reports ✓ in all sectors and "within normal limits," the GPS shows in all x sectors and report "outside normal limits." This shows that the reports should be interpreted with caution. This may be because of different reference planes used to calculate the stereometric parameters by the two softwares

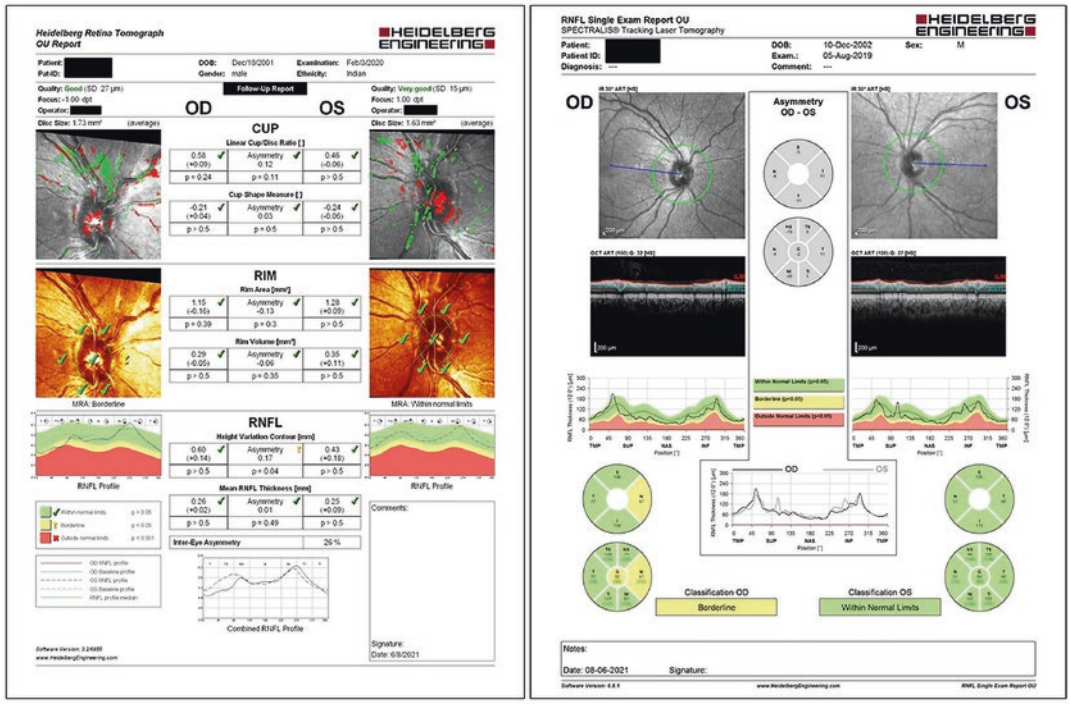

Fig. 26.10 Heidelberg retinal tomography report and retinal nerve fiber layer OCT report of the same patient showing RE nasal thinning, with all other sectors and LE being under normal limits - shows concordance between different scanning modalities

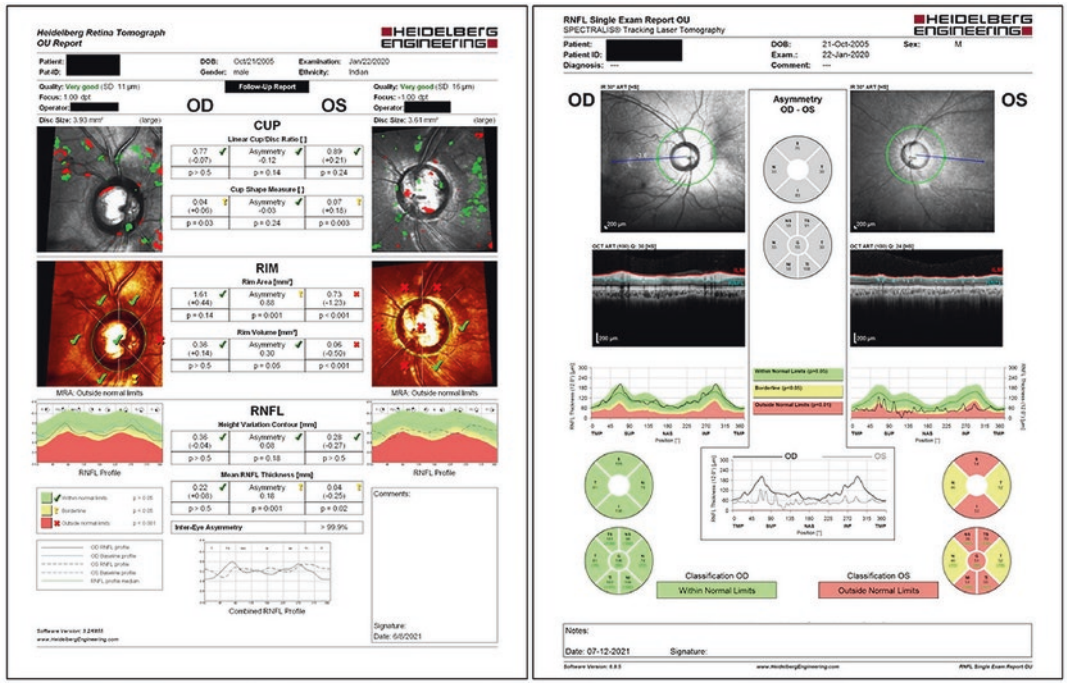

Fig. 26.11 Heidelberg retinal tomography and retinal nerve fiber layer OCT report of the same patient showing discordance between the two investigative modalities. In the RE, nasal "x" and inferonasal "!" indicate thinning. However, in the OCT, RE parameters are all shown under normal limits. Similarly, while the LE HRT report shows ✓ in temporal and inferotemporal sectors, the OCT reports thinning. Therefore, these reports should be clinically correlated and interpreted with caution

26.3 Summary (Fig. 26.12)

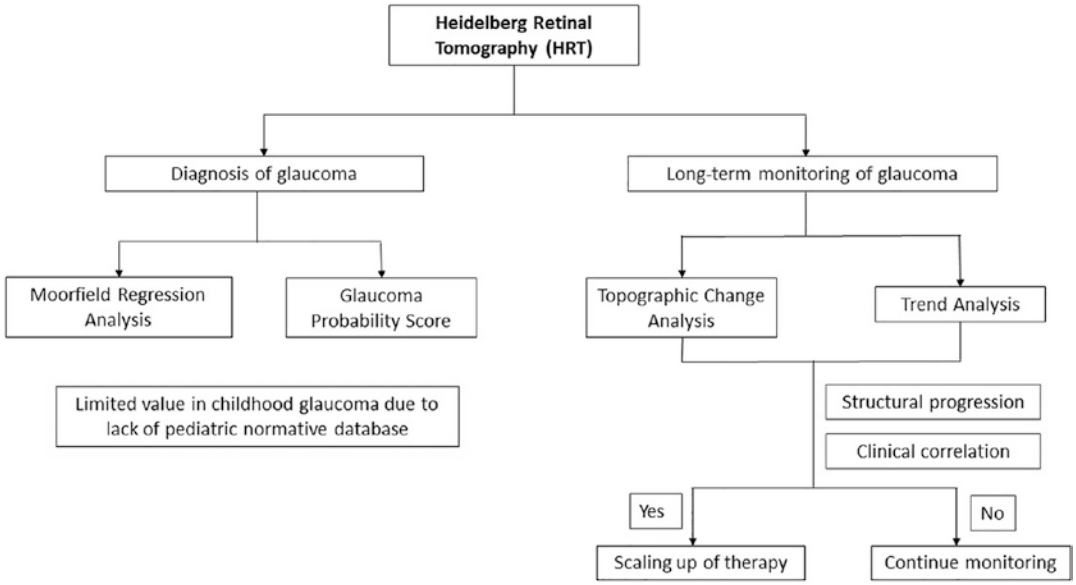

Fig. 26.12 Summary

26.4 Conclusions

HRT provides 3-dimensional structural imaging of the optic nerve head and surrounding peripapillary retina. The quantitative data generated is compared against an age-matched normative database to identify eyes with and at risk of glaucoma. Further sequential scans and longitudinal analysis aid in identifying structural progression. Though a normative database is unavailable for all age groups at present, HRT still serves as a valuable tool to look for progression in childhood glaucoma.

Suggested Reading

Gupta S, Singh A, Mahalingam K, et al. Myopia and glaucoma progression among patients with juvenile onset open angle glaucoma: a retrospective follow up study. Ophthalmic Physiol Opt. 2021b;41(3):475–85. https://doi.org/10.1111/opo.12805.

Maslin JS, Mansouri K, Dorairaj SK. HRT for the diagnosis and detection of glaucoma progression. Open Ophthalmol J. 2015b;9:58–67. https://doi.org/10.2174/1874364101509010058.

Strouthidis NG, Garway-Heath DF. New developments in Heidelberg retina tomograph for glaucoma. Curr Opin Ophthalmol. 2008b;19(2):141–8. https://doi.org/10.1097/ICU.0b013e3282f4450b.

Vizzeri G, Weinreb RN, Martinez de la Casa JM, Alencar LM, Bowd C, Balasubramanian M, Medeiros FA, Sample P, Zangwill LM. Clinicians agreement in establishing glaucomatous progression using the Heidelberg retina tomograph. Ophthalmology. 2009b;116(1):14–24. https://doi.org/10.1016/j.ophtha.2008.08.030.

In Vivo Confocal Microscopy in Childhood Glaucoma

27

Manasi Tripathi, Ram Kishore, and Shikha Gupta

27.1 Introduction

Corneal confocal microscopy is a non-invasive imaging modality that provides in vivo cross-sectional images of the ultrastructure of the cornea (Fig. 27.1). In vivo confocal microscopy (IVCM) enables visualization of the various layers of the corneal epithelium, Bowman's layer with nerves and K-structures (collagen fibers), limbal epithelial cells, stroma, Descemet's membrane (DM), and corneal endothelial cells. The confocal arrangement comprises of two slits—one slit illuminates the tissue on a small area using an objective lens and the second slit filters the reflected rays from unfocused layers. The illumination and the detection lie in the same focal plane, hence the term "confocal."

IVCM has a potential utility in aiding the diagnosis in eyes with decompensated corneas where diagnosis is unclear.

Although it has been widely used in the diagnosis, management, and research of corneal pathologies, the role of confocal microscopy in the realm of childhood glaucoma is relatively nascent.

- Higher intraocular pressure (IOP) can cause Descemet's membrane tear (Haab's striae) and pathological endothelial changes. IVCM can be used to assess these changes (Fig. 27.2).

Fig. 27.1 In vivo confocal microscopy being done in a child with Axenfeld-Rieger syndrome

- The use of topical hypotensive medications or even surgery can cause chronic inflammation of the ocular surface, causing the following changes in conjunctival and corneal epithelium: loss of goblet cells, squamous metaplasia, inflammatory cell infiltrates, dendritic cell activation, and stromal fibrosis. IVCM can be used to assess these changes within the ocular surface.
- Among the congenital glaucomas, certain diseases such as primary congenital glaucoma and Axenfeld-Rieger syndrome are characterized by pathognomonic corneal IVCM features.
- On IVCM, reduced mean stromal keratocyte and reduced mean endothelial density have been observed in the eyes with primary congenital glaucoma. The presence of discontinu-

M. Tripathi (✉) · R. Kishore · S. Gupta
Dr. Rajendra Prasad Centre for Ophthalmic Sciences, All India Institute of Medical Sciences, New Delhi, India

S. Gupta et al. (eds.), *Childhood Glaucoma*, https://doi.org/10.1007/978-981-19-7466-3_27

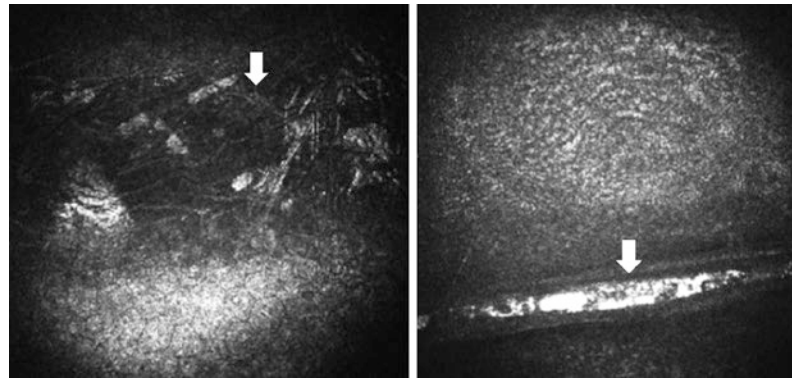

Fig. 27.2 In vivo confocal microscopy images showing Haab's striae (**a**). Notice stretched endothelium (white arrow) and thickened pre-Descemet's layer (**b**, white arrow) along the Haab's striae

Table 27.1 Corneal characteristics in the eyes with childhood glaucoma as compared to the normal cornea

	Normal cornea	Childhood glaucoma
Epithelium	• Superficial cells are polygonal and exhibit small bright rounded nuclei, surrounded by a darker cytoplasm with a perinuclear hypo-reflective dark ring and a well-defined cell border • Wing cells are characterized by bright cell borders and a bright cell nucleus • Basal cells have uniformly bright cell borders with a dark cytoplasmic mass (Fig. 27.3a)	• Mostly within normal limits (Fig. 27.4a). More hyperreflective areas may be seen, as in Axenfeld-Rieger syndrome (Fig. 27.5a)
Bowman's layer	• Featureless and gray • Discrete, parallel nerve bundles of the subbasal nerve plexus traversing the field of view (Fig. 27.3b)	• Distorted and broken arrangement of subbasal nerve fibers (Fig. 27.5b)
Stroma	• Keratocytes (white pointer, Fig. 27.3c) appear bean-like in anterior stroma and oval shaped in the posterior stroma (Fig. 27.3c) • Nuclei are 5–30 μm in diameter	• Distorted stromal architecture with relatively reduced density of keratocytes (Fig. 27.5c)
Pre-Descemet's layer	• Acellular	• Acellular
Descemet's membrane	• Whorled pattern (Fig. 27.3d)	• Hyperreflective DM with a whorled pattern may be seen (Figs. 27.4d, 27.5d)
Endothelium	• Endothelial cells appear hexagonal or polygonal • Bright cell bodies with dark cell borders • Cell nuclei are rarely recognizable (Fig. 27.3e)	• Relatively more hypolucent or hyperlucent areas as compared to normal endothelium suggestive of endothelial cell drop (Figs. 27.4e, 27.5e) • Polymegathism, pleomorphism seen (Fig. 27.4e) • Tractions and bands may be seen on the endothelial side, as in primary congenital glaucoma (Fig. 27.4f)

ous hyperreflective structures overhanging the endothelial layer at the level of the Descemet's membrane, representing Haab's striae, is also known.

- However, confocal microscopy appearance of corneal characteristics of glaucomatous eyes with Axenfeld-Rieger syndrome is relatively unknown.

Table 27.1 summarizes the differentiating features of the normal eyes and eyes with childhood glaucoma with IVCM (unpublished study).

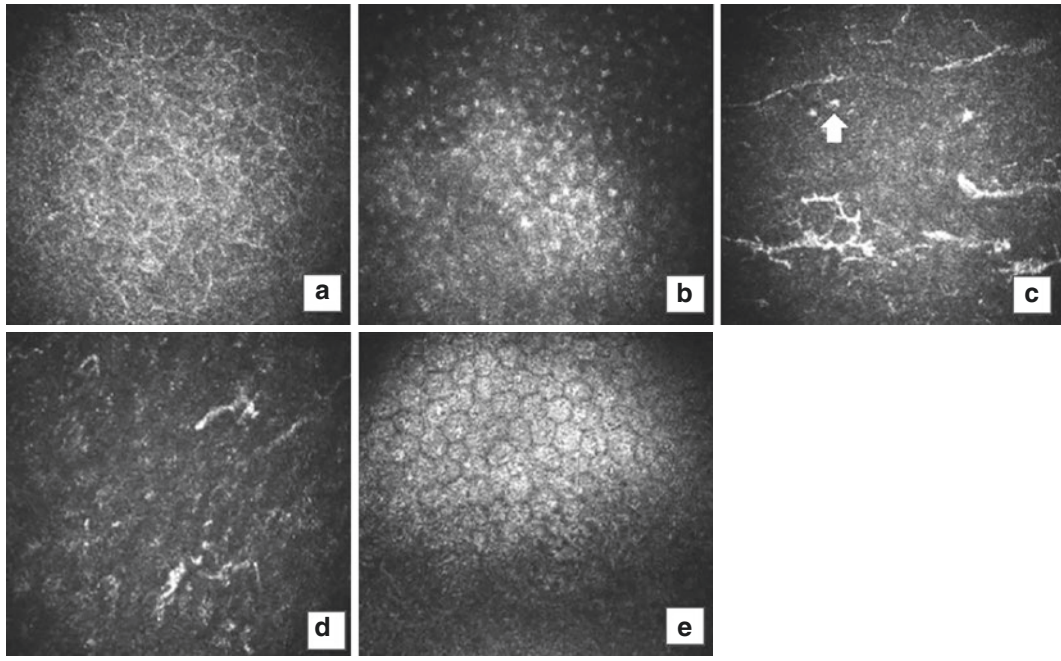

Fig. 27.3 In vivo confocal microscopy images showing normal corneal morphology. The figure displays the corneal epithelial layer (**a**), Bowman's layer (**b**), corneal stroma (**c**), Descemet's layer (**d**), and endothelium (**e**). Normal keratocytes can be visualized in the corneal stroma (white pointer, fig **c**)

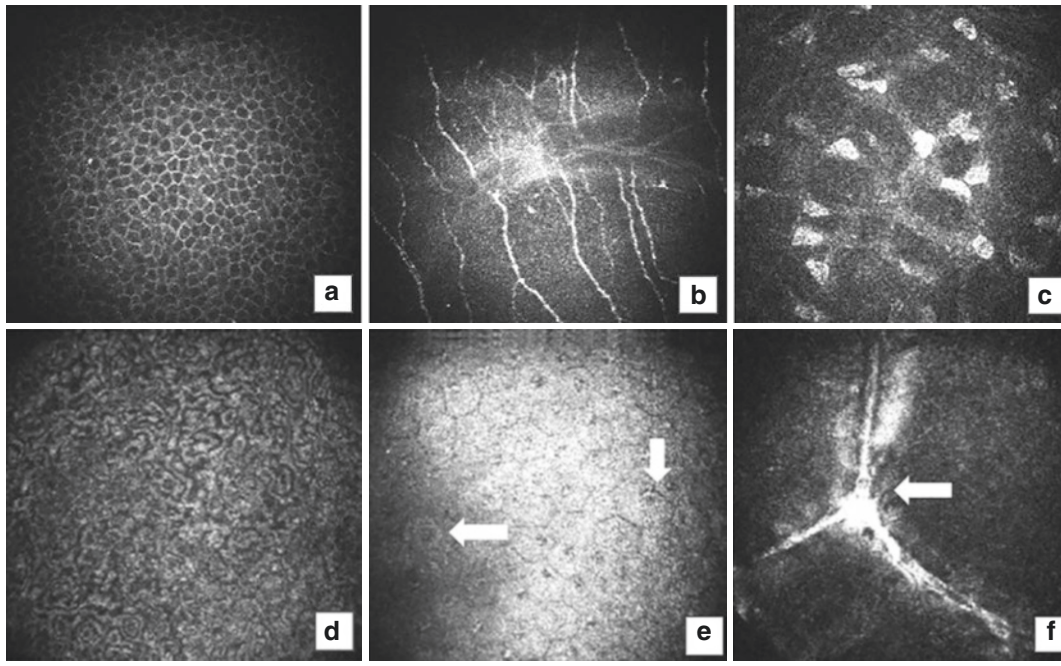

Fig. 27.4 In vivo confocal microscopy images of a child with primary congenital glaucoma showing corneal epithelium (**a**), Bowman's layer (**b**), corneal stroma (**c**), Descemet's layer (**d**) and relatively hypo-lucent endothelium with significant polymegathism and polymorphism with nucleated endothelial cells (arrow) (**e**–**f**). Fig f shows hyper-lucent traction band (arrow) at the level of corneal endothelium

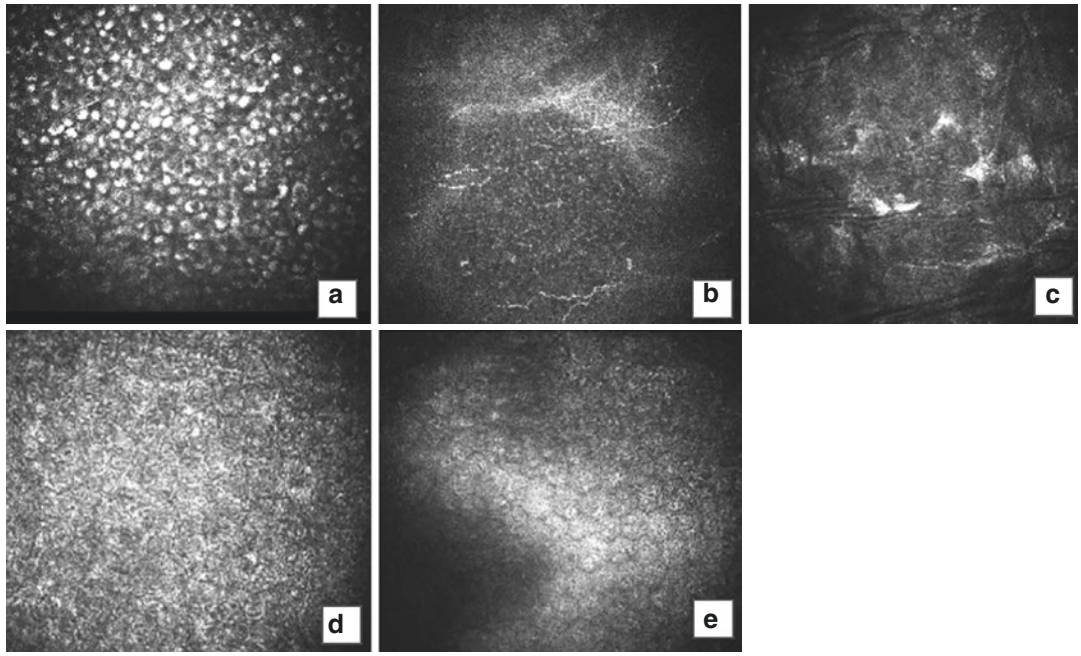

Fig. 27.5 In vivo confocal microscopy images of a child with Axenfeld-Rieger syndrome showing hyperreflective corneal epithelium (**a**), broken sub-epithelial nerve fibres (**a**), distorted Bowman's layer (**b**), hypocellular and distorted corneal stroma (**c**), hyper-reflective Descemet's layer (**d**) and hyperlucent endothelium with polymegathism (**e**)

27.2 Case Examples

Case 27.1

A 5-year-old male child had bilateral primary congenital glaucoma. The IVCM scans of the child are as follows:

- Epithelium: Normal morphology of corneal epithelial cells was seen in both eyes (Fig. 27.4a).
- Bowman's membrane: Normal architecture with a parallel arrangement of subbasal corneal nerves could be seen in both eyes (Fig. 27.4b).
- Stroma: Fig. 27.4c shows normal arrangement of stromal lamellae and normal keratocyte density.
- Descemet's membrane: Normal whorled pattern of the DM was conspicuous (Fig. 27.4d).
- Endothelium: This layer is relatively hypolucent. Polymegathism was a significant feature (Fig. 27.4e; white pointer). Figure 27.4f shows a hyperlucent traction band at the level of the endothelium. Nucleated endothelial cells may also be visualized.

Case Summary

- IVCM reveals abnormality of the endothelium in the eyes with primary congenital glaucoma.
- Traction bands at the level of the endothelium are a conspicuous feature, due to presence of Haab's striae.

Case 27.2

The in vivo confocal microscopy scan of a 12-year-old female treated for high IOP secondary to Axenfeld-Rieger syndrome showed:

- Corneal epithelium: Hyperreflectivity of the corneal epithelium was noted on IVCM (Fig. 27.5a). The normal architecture of the epithelial cells could not be appreciated with hyperreflectivity apparent within cell bodies.
- Bowman's membrane: Fig. 27.5b shows an irregular, nonparallel arrangement of subbasal nerve fibers. Many distorted, beaded, and broken (arrows) nerve fibers can also be seen. This is in stark contrast to eyes with primary con-

genital glaucoma (Fig. 27.4b), where a parallel arrangement of nerve fibers was preserved.
- Stroma: Distorted stromal architecture and marked loss of keratocytes (Fig. 27.5c). Multiple hypo-reflective linear streaks of unknown significance could be observed.
- Descemet's membrane: Granular hyperreflectivity is conspicuous within the DM (Fig. 27.5d).
- Endothelium: Polymegathism with nucleated (arrows) endothelial cells seen (5e; note white arrows). Moreover, this endothelial cell layer is relatively more hyperlucent in comparison to Case 27.1 (Fig. 27.4d). There are no traction bands.

Case Summary

- The hyperreflective corneal epithelium is seen on IVCM in patients with Axenfeld-Rieger syndrome.
- Irregular and broken subbasal nerve bundles and marked loss of keratocytes are conspicuous.
- Polymegathism is noted, however, unlike PCG traction bands are usually not a feature as association with Haab's striae is rare.
- Profound diminution of sub-basal corneal nerves in late-stage Fuchs endothelial corneal dystrophy and pseudophakic bullous keratopathy on IVCM has also been documented. However, unlike these two pathologies, the corneas of Axenfeld-Rieger syndrome do not affect subbasal nerve density unless complicated by edema.

Case 27.3

The following are IVCM images of a 14-year-old boy with B/E congenital aniridia with secondary glaucoma. The cornea was markedly thickened.

1. Corneal epithelium: Loss of normal architecture of superficial, wing cells and basal layer was seen on IVCM (Fig. 27.6a). It was associated with hyperreflectivity of the subepithelial layer associated with hyperreflective dots (Fig. 27.6b). Congenital aniridia is often associated with limbal stem cell deficiency, which

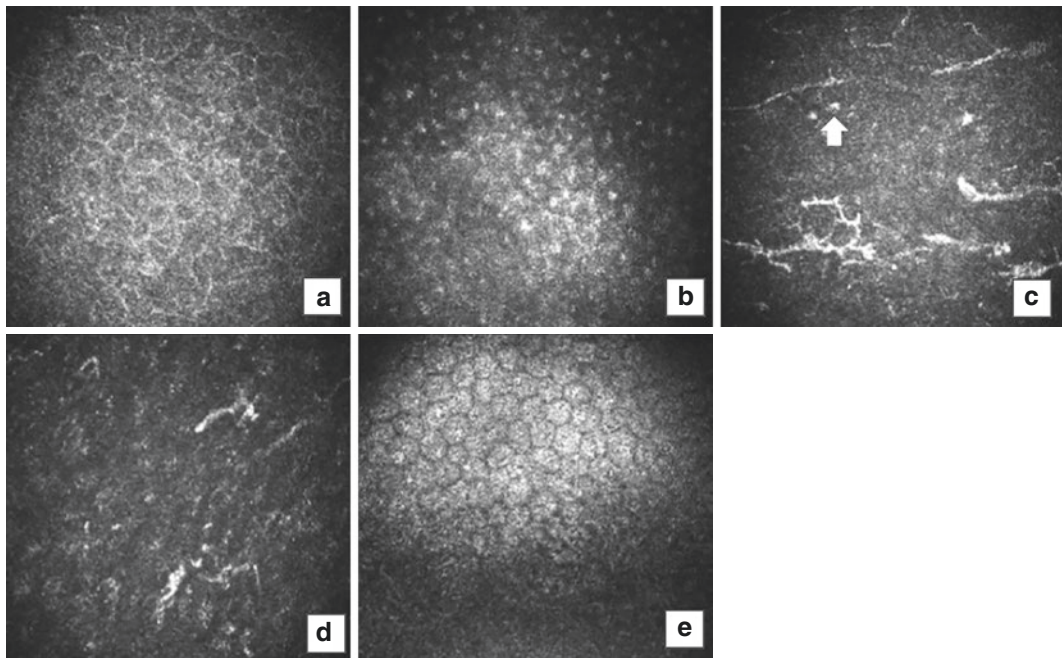

Fig. 27.6 In vivo confocal microscopy images of a patient with congenital aniridia with secondary glaucoma showing loss of normal architecture of corneal epithelium and sub-epithelial layer (**a**–**b**) and bowman's layer (**c**), indistinguishable keratocytes in the corneal stroma (**d**), and relatively normal endothelium (**e**)

leads to poor health and regeneration of the corneal epithelium.
2. Bowman's layer: Normal parallel arrangement of subbasal nerve plexus was lost with reduced density of nerve fibers (Fig. 27.6c). The existing nerve fibers appeared thickened. Infiltration of dendritic cells was visible (Fig. 27.6c; white arrow).
3. Stroma: Stromal keratocytes were indistinguishable (Fig. 27.6d). There was an increased stromal thickness.
4. Endothelium: Endothelial cells appeared normal (Fig. 27.6e).

Case Summary

- Corneal epithelial architecture may be lost in aniridia, especially in aniridia-associated keratopathy.
- Reduced density of subbasal nerve plexus with infiltration of dendritic cells is a feature.
- Endothelial cells are usually not affected. But in later stages of IOP-associated corneal endothelial decompensation, endothelial changes become inevitable.
- Both increased and decreased densities of sub-basal nerves have been reported in the literature in cases of congenital aniridia. However, this possibly depends on the stage of aniridia-associated keratopathy (AAK) that the patient has at the time of observation. More long-term studies with larger sample sizes are required to ascertain the same.

27.3 Conclusions

- In vivo confocal microscopy (IVCM) can be used to study and identify the morphology of the corneal layers in the eyes with childhood glaucoma.
- The differential corneal features may be further explored to understand the pathogenesis of these entities.

Suggested Reading

Aggarwal S, Cavalcanti BM, Regali L, Cruzat A, Trinidad M, Williams C, et al. In vivo confocal microscopy shows alterations in nerve density and Dendritiform cell density in Fuchs' endothelial corneal dystrophy. Am J Ophthalmol. 2018;196:136–44.

Doozandeh A, Yazdani S, Ansari S, Pakravan M, Motevasseli T, Hosseini B, et al. Corneal profile in primary congenital glaucoma. Acta Ophthalmol. 2017;95(7):e575–81.

Edén U, Fagerholm P, Danyali R, Lagali N. Pathologic epithelial and anterior corneal nerve morphology in early-stage congenital Aniridic keratopathy. Ophthalmology. 2012;119(9):1803–10.

Le Q, Deng SX, Xu J. In vivo confocal microscopy of congenital aniridia-associated keratopathy. Eye. 2013;27(6):763–6.

Mahelková G, Filouš A, Odehnal M, Cendelín J. Corneal changes assessed using confocal microscopy in patients with unilateral Buphthalmos. Investig Opthalmol Vis Sci. 2013;54(6):4048.

Mastropasqua L, Carpineto P, Ciancaglini M, Nubile M, Doronzo E. In vivo confocal microscopy in primary congenital glaucoma with megalocornea. J Glaucoma. 2002;11(2):83–9.

28 Specular Microscopy in Childhood Glaucoma

Monika Arora, Abhishek Singh, and Arnav Panigrahi

28.1 Principle

Specular microscopy allows in vivo analysis of corneal endothelial cells (density and morphology). It works on the principle of light reflection using a mirror where the angle of incidence equals the angle of reflection. As light ray passes from a medium with higher refractive index (cornea) to a medium with lower refractive index (aqueous humor), the endothelium-aqueous interface reflects back 0.022% of the projected light, which is then focused onto a film plane for viewing on a real-time monitor (Fig. 28.1). By design, the specular microscope does not allow non-specular light rays to be observed. The light that is reflected from the endothelial surface is collected by the same objective lens and focused onto a film plane or a video monitor screen for examination.

The instruments currently available for use in clinics are of two types: contact and noncontact models, which capture the image and analyze the endothelial cell morphology. In contact specular microscopes, a contact lens is used with a coupling agent, of refractive index similar to that of the cornea, to eliminate reflection from the corneal surface. Although it provides a good resolution and magnification, it carries a higher risk of infection and may cause artifacts, especially in weak and diseased corneas. Heyer-Schulte corneal endothelial camera (Model HS CEM 3) with an Olympus OMI camera unit is a classic example of contact specular microscope. The non-contact instruments are Nidek CEM -530 (NIDEK Co Ltd., Japan, Fig. 28.2a) and Topcon (TOPCON, SP-1P, Tokyo, Japan).

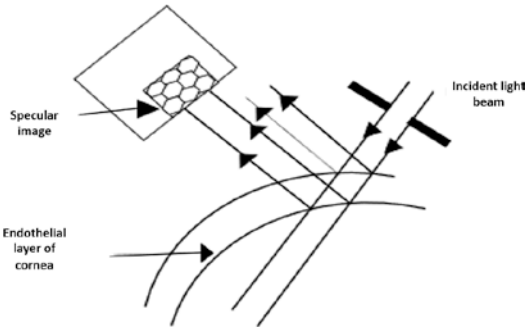

Fig. 28.1 A schematic representation of the optics for visualization of the endothelial mosaic produced on slit-lamp biomicroscopy

The specular scans analyse the following parameters (Fig. 28.2b):

1. Number: The average number of cells assessed in the frame (75 to 100).
2. Endothelial cell density (ECD) (cells/mm^2): The number of cells present in 1 mm^2 area. The corneal endothelial cell density declines

M. Arora (✉) · A. Singh · A. Panigrahi
Dr. Rajendra Prasad Centre for Ophthalmic Sciences, All India Institute of Medical Sciences, New Delhi, India

S. Gupta et al. (eds.), *Childhood Glaucoma*, https://doi.org/10.1007/978-981-19-7466-3_28

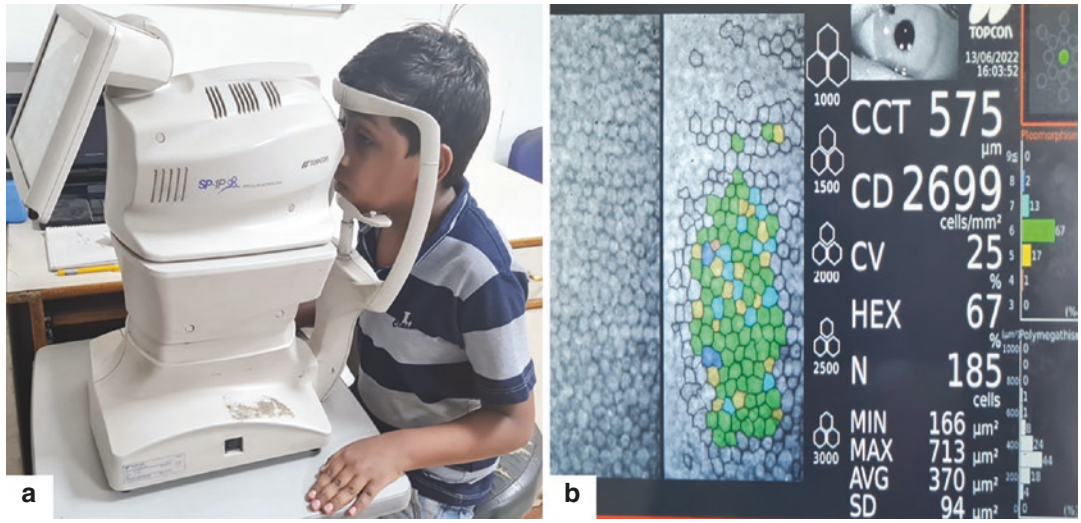

Fig. 28.2 (**a**) A non-contact specular microscope (CEM -530, NIDEK CO. LTD., Japan). Scanning a child's corneal endothelium. (**b**) Specular scan showing normal endothelial parameters. *N*: number of cells, *CCT*: central corneal thickness, *MIN*, *MAX*, *AVG*: minimum, maximum, and average cell area, *CD*: cell density, *SD*: standard deviation, *CV*: coefficient of variation, *HEX*: hexagonality percentage

throughout life at an average rate of 0.6% per year. At birth, human endothelial cell density is approximately 5000–6000 cells/mm^2, but gradually decreases to about 3500 cells/mm^2, by 5 years of age, 3000 cells/mm^2 by the age 14–20 years, and 2500 cells/mm^2 in late adulthood. This is due to age-related increase in corneal dimensions and normal senescence of the endothelial cells. It has been observed that when the number of endothelial cells reaches a critical level (approximately 500–1000 cells/mm^2), the cornea loses its transparency. This critical level is known as the "corneal decompensation threshold level."

3. AVG: It represents the average cell area of a determined population of the studied cells (µm^2), approximately ranging from 200 to 500 µm^2.
4. Max: It is the area of the largest cell.
5. Min: It is the area of the smallest cell.
6. SD (standard deviation): It is the standard deviation of the cell area.
7. Coefficient of variation (CV): It is the standard deviation in cell area/average cell area. The normal CV value is <30%. A lower CV shows uniformity in the endothelial cell arrangement, while a higher CV indicates polymegathism. A higher CV signifies endothelial cells under stress.
8. HEX (percentage of hexagonality): It is the number of hexagonal cells/total number of cells counted in the scan (Fig. 28.3). The normal percentage of hexagonal cells in healthy individuals is 70–80%. During pathological stress, endothelial cells undergo readaptation resulting in cells with fewer than six sides. When there is

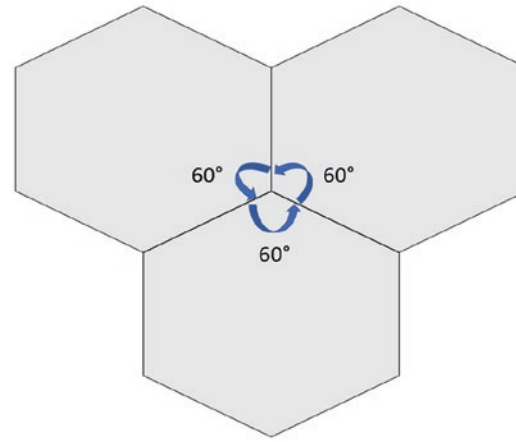

Fig. 28.3 A schematic representation of a hexagonal endothelial cell intersecting in a way that results in three angles of intersection, each approximately 60°

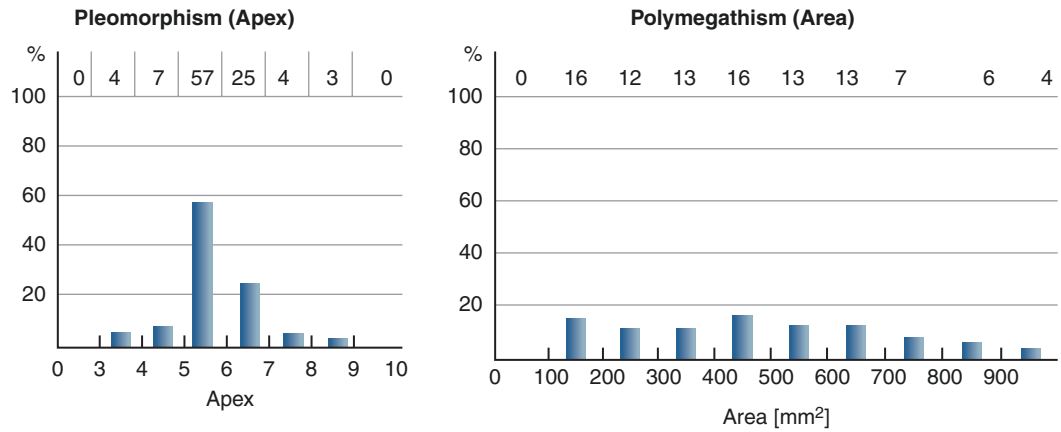

Fig. 28.4 Histogram showing the percentage of hexagonal cells (57% of total cells have six sides) and percentage of the area of endothelial cells (maximum number of cells occupy the area in the range of 150 to 350 μm^2)

50% or more cells with fewer than 6 sides, it indicates clinically significant pleomorphism.

9. Histogram: Pleomorphism and polymegathism are displayed in histogram (Fig. 28.4).

28.2 Role of Specular Microscopy in Childhood Glaucoma

In congenital glaucoma, the stretched posterior cornea is under stress due to high intraocular pressure (IOP) which leads to breaks in the Descemet's membrane, thereby forming Haab's striae. This consequently leads to distortion and stretching of the endothelial cells which heal by scarring, consequently leading to low ECD. Even if Haab's striae do not form, endothelial cell loss occurs secondary to high IOP. According to Tamcelik et al. (2022), primary congenital glaucoma (PCG) eyes with Haab's striae had lesser mean ECD (1705 ± 591 vs. 2406 ± 600 cells/mm^2) and thinner mean central corneal thickness (CCT) (526 ± 50 vs. 570 ± 61 μm) as compared to those without Haab's striae.

Similarly, the specular microscopy of Axenfeld-Rieger syndrome (ARS) patients with long-standing glaucoma may show mild to moderate variation in the endothelial size and shape with up to 15–20% cells harboring corneal guttae.

Further, ECD in adolescents with juvenile open-angle glaucoma (JOAG) is significantly lower than their normal counterparts of similar age group. Increased IOP for a prolonged duration before glaucoma treatment may affect the endothelium directly or indirectly by causing hypoxic damage. The main mechanisms are:

1. Elevated IOP influences the metabolically active pumping mechanism, thus reducing resistance to aqueous flow to the stroma and consequently causing stromal edema.
2. High IOP causes morphological cellular damage, for example, cellular rupture, swelling of the mitochondria, disorganization of endoplasmic reticulum, and formation of myelin bodies.

According to the study by Lee HM et al (2020), ECD can decrease after Ahmed glaucoma valve (AGV) implantation also, with a mean rate of ECD change of −18.82 ± 22.97%/year, which is greater in the superior temporal area than in the central area (−30.38 ± 26.18%/year vs. −17.82 ± 25.01%/year, $p < 0.001$). This decrease may be induced by retrograde flow from the encapsulated reservoir to the anterior chamber, anterior chamber reaction, occasional tube-corneal contact, turbulence at the tube tip, and foreign body response toward the tube material. Apart from the above factors, multiple intraocular surgeries can also decrease ECD significantly.

Thus, specular endothelial microscopy is an important tool to evaluate the functional status of endothelial cells in follow-up cases of childhood glaucoma. Around 3.7% of cornea in patients with congenital glaucoma eventually decompensates with time (Silva et al. 2011).

28.3 Case Examples

Case 28.1

A case of a 7-year-old male child with unilateral PCG, with a history of the right eye (RE) operated combined trabeculotomy and trabeculectomy (CTT) at the age of 2 months.

Slit-lamp examination revealed RE Haab's striae with corneal enlargement (Fig. 28.5), with normal features in LE. Corneal diameter was 13×13 mm in RE and 11.5×11 mm in LE. Specular microscopy revealed the following parameters: RE N = 40 cells, ECD = 2111 cells/mm^2, LE N = 137 cells, ECD = 3124 cells/mm^2, along with localised endothelial cell loss (in areas of Haab's striae), polymegathism (CV RE = 44%, LE = 24%) with poor differentiation of the cells (hexagonality RE = 60%, LE = 71%), and thinner central corneal thickness in RE compared to LE (CCT RE = 484 μm, LE = 600 μm).

Learning Points

1. In PCG, prolonged exposure of immature endothelial cells to elevated IOP in the intrauterine and early postnatal period can cause a reduction in endothelial cell density, indicating endothelial cell dysfunction due to stress.
2. Corneal endothelial cellularity diminishes during the prenatal period, and this drop happens at a faster pace in PCG eyes than in healthy corneas in the first 2 years of life.
3. The other cause of decreased ECD in patients with PCG seems to be long-term corneal distension secondary to elevated IOP in young eyes.
4. The onset and duration of the disease to elevated IOP, duration of medication use, and the timing of surgery are some of the other factors responsible for endothelial cell loss.
5. Areas with Haab's striae may have a further reduction in ECD compared to areas without Haab's striae.

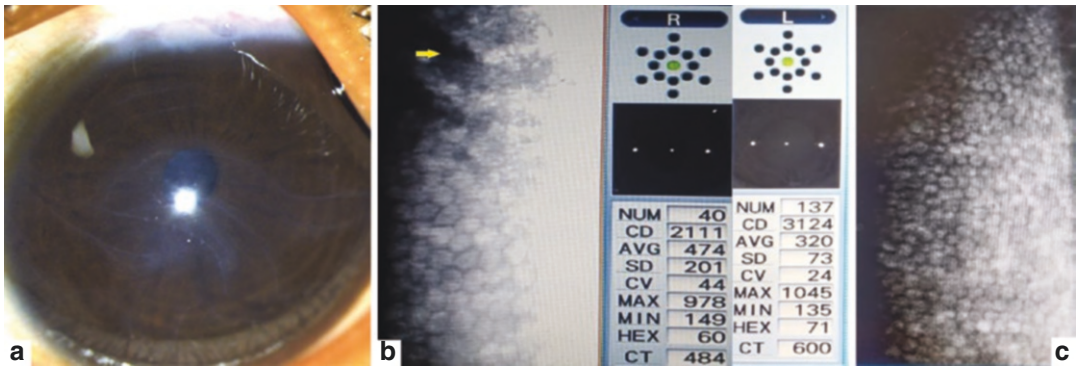

Fig. 28.5 (**a**) Slit-lamp biomicroscopy image under diffuse illumination of RE showing Haab's striae. (**b**) Specular endothelial scan of RE showing endothelial free cell area around Haab's striae (yellow arrow). (**c**) Specular endothelial cell scan of the fellow eye without glaucoma or Haab's striae

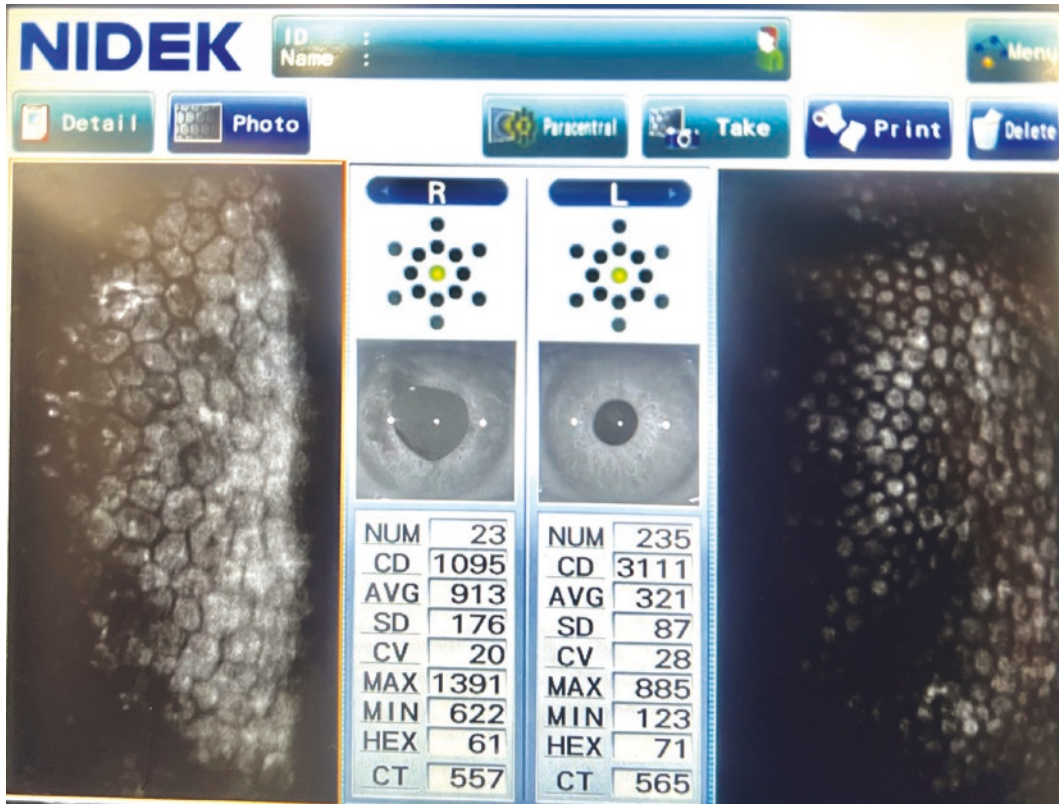

Fig. 28.6 Specular scan of BE. Scan of RE (left panel) shows pleomorphism and polymegathism, whereas that of LE (right panel) reveals more uniform cells with distinct cell margins and fewer dropout cells

Case 28.2

A 9-year-old girl, having unilateral (RE) Axenfeld-Rieger anomaly with glaucoma presented for routine examination. Her baseline IOP was 46 mmHg and 18 mmHg in RE and LE respectively. RE trabeculectomy was done 4 years back and now IOP is controlled in both eyes (BE). A specular microscopy scan for endothelium revealed RE N = 23 cells, ECD = 1095 cells/mm^2 compared to LE N = 235 cells, and ECD = 3111 cells/mm^2, respectively (Fig. 28.6). Right eye scan showed significant polymegathism with minimal pleomorphism, the abnormal cells being significantly more in RE with few dropouts in LE. The plausible cause behind the variation in the endothelium of both eyes could be long-standing higher baseline IOP in RE as compared to LE or congenital corneal involvement.

Learning Points

1. Asymmetry in the quality and quantity of endothelial cells indicates a direct role of high IOP in endothelial cell damage.
2. ARS patients with glaucoma also show endothelial cell pleomorphism, polymegathism, and endothelial guttae.

Case 28.3

A 9-year-old female diagnosed case of BE JOAG, with history of BE trabeculectomy 6 years back. The baseline IOP before initiation of therapy was RE 38 mmHg and LE 24 mmHg, which are now controlled post surgery.

The specular scan of RE revealed a significant decrease in the number of cells as well as ECD, with RE N = 24 cells, ECD = 767 cells/mm^2 as compared to LE N = 83 cells, ECD = 2028 cells/mm^2, respectively. The aver-

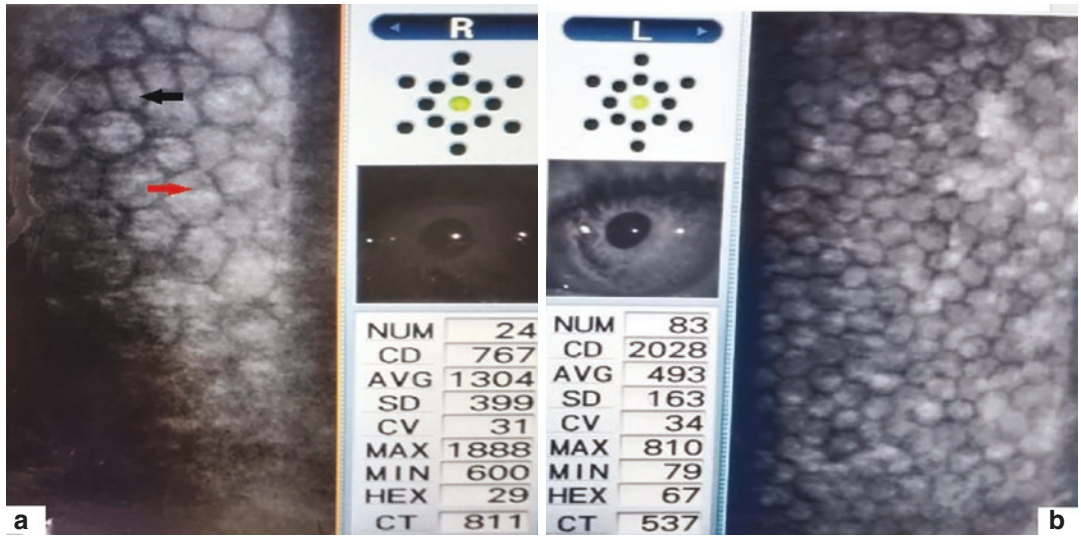

Fig. 28.7 Specular endothelial scan of juvenile open-angle glaucoma (BE). (**a**) Specular endothelial scan of RE showing polymegathism (red arrow) with pleomorphism (black arrow). (**b**) Specular endothelial scan of LE showing endothelial cells with greater uniformity and distinct cell margins

age cell size was increased in RE to 1304 μm^2 showing polymegathism (red arrow). In RE, significant pleomorphism (black arrow) was present with HEX = 29%, as compared to relatively normal values in LE (HEX = 67%) (Fig. 28.7).

Case 28.4

A 9-year-old male child diagnosed with unilateral congenital ectropion uveae with secondary glaucoma underwent trabeculectomy in the right eye, with a baseline IOP of 36 and 16 mmHg in the RE and LE respectively.

The specular scan in RE revealed endothelial cell status as: N = 41 cells, ECD = 1754 cells/mm^2 while that in the fellow eye was: N = 262 cells, ECD = 3224 cells/mm^2. HEX in RE was non-recordable. The histogram graph of RE showed polymegathism (black arrow) with significant pleomorphism (red arrow) as maximum cells had reduced number of sides, whereas the histogram of LE showed a high hexagonality index at 71% (Fig. 28.8).

Case 28.5

A 10-year-old boy had BE aniridia with secondary glaucoma. Specular microscopy of RE was captured. Corresponding scans of LE could not be obtained due to poor fixation.

The specular scan of RE had N = 113 cells, ECD = 1913 cells/mm^2. The maximum cellular area noted was 1168 μm^2, showing polymegathism with a HEX percentage of 67% (Fig. 28.9). Despite the reduced number and lack of uniformity in cell size, they retained their uniformity in cell shape with a preserved hexagonality index.

Specular microscopy characteristics in other endothelial disorders:

1. Fuch's endothelial corneal dystrophy: Specular microscopy shows dropout areas which correspond to guttae with reduced ECD (Fig. 28.10a).
2. Posterior polymorphous endothelial disorder: Specular microscopy reveals bands, reduced endothelial cell density, and increased mean cell area (Fig. 28.10b).

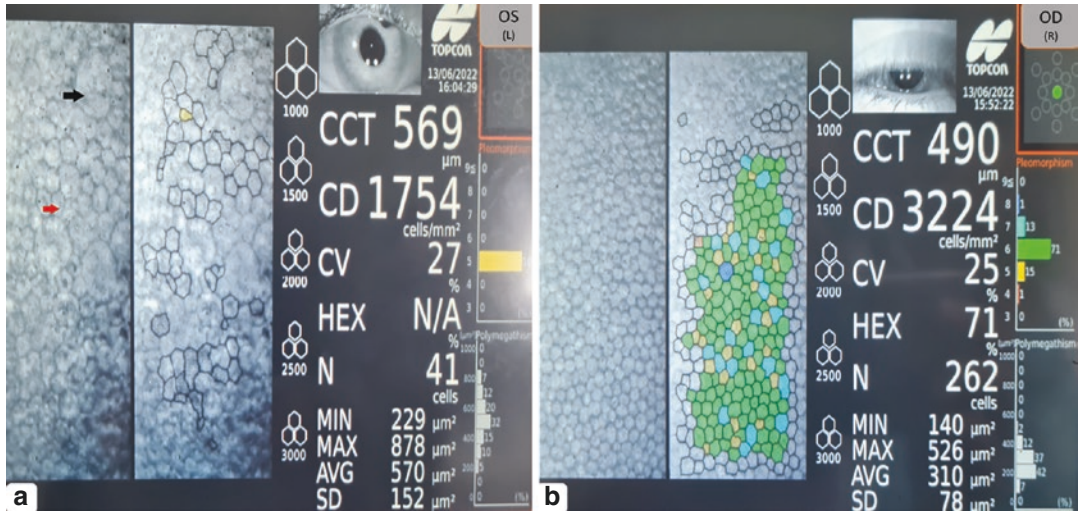

Fig. 28.8 Specular endothelial scan of (RE) having congenital ectropion uveae with secondary glaucoma. (**a**) Endothelial scan in RE showed endothelial cells having significant pleomorphism (red arrow) and polymegathism (black arrow). (**b**) Normal specular endothelial scan with distinct endothelial cell margins and uniformity in fellow LE

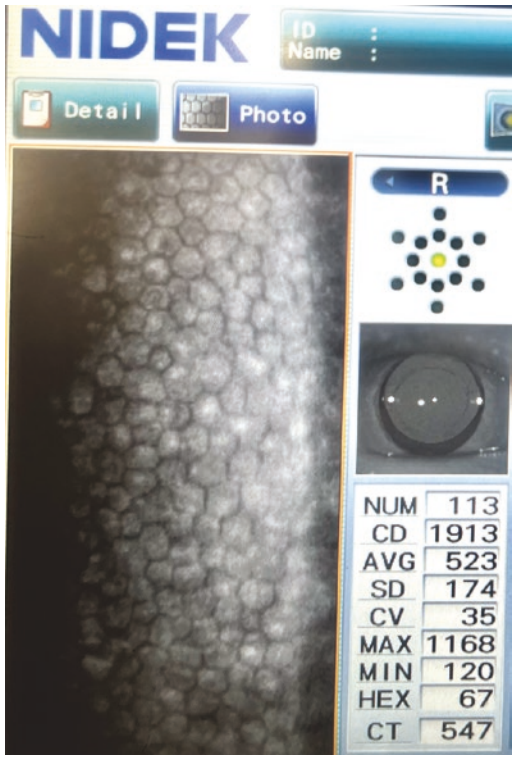

Fig. 28.9 Specular scan of RE of the patient, showing polymegathism

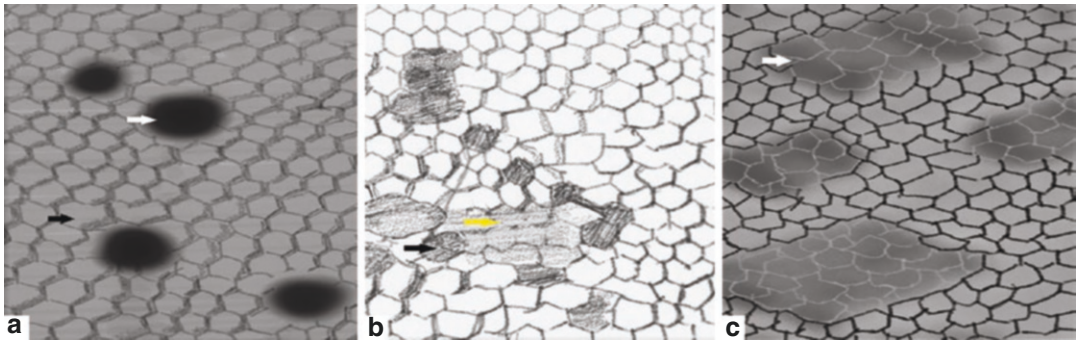

Fig. 28.10 Schematic drawings of specular endothelial scans in certain disease states. (**a**) Specular microscopy of Fuchs endothelial corneal dystrophy showing dropout areas (black arrow) with polymegathism (white arrow). (**b**) Specular microscopy of posterior polymorphous endothelial disorder showing the band. In the area of vesicles (black arrow) and bands (yellow arrow) endothelial cells are not visualized. (**c**) Specular microscopy of iridocorneal endothelial syndrome showing the characteristic dark-light reversal pattern (white arrow) (the endothelial cell border is seen in white instead of black, and the inside of the cell is seen as black instead of white) of the normal endothelium

3. Irido-corneal endothelial (ICE) syndrome: Specular microscopy reveals enlarged endothelial cells, rounding off of the cellular boundaries and increased blackout areas within the cells with a characteristic dark-light reversal pattern (Fig. 28.10c).

28.4 Conclusions

Long-term exposure to high IOP during intrauterine period and or at an early age causes structural and functional changes in naive infant cornea. The specular microscopy parameters of healthy subjects and childhood glaucoma differ significantly. Thus, specular microscopy is an important tool for assessing the functional status of endothelial cells in follow-up cases of childhood glaucoma

Suggested Reading

Chaurasia S, Vanathi M. Specular microscopy in clinical practice. Indian J Ophthalmol. 2021;69(3):517–24. https://doi.org/10.4103/ijo.IJO_574_20; PMID: 33595465; PMCID: PMC7942069.

de Silva DJ, Khaw PT, Brookes JL. Long-term outcome of primary congenital glaucoma. J AAPOS. 2011;15(2):148–52. https://doi.org/10.1016/j.jaapos.2010.11.025.

Doughty MJ, Müller A, Zaman ML. Assessment of the reliability of human corneal endothelial cell-density estimates using a noncontact specular microscope. Cornea. 2000;19(2):148–58. https://doi.org/10.1097/00003226-200003000-00006.

Gatzioufas Z, Labiris G, Stachs O, Hovakimyan M, Schnaidt A, Viestenz A, Käsmann-Kellner B, Seitz B. Biomechanical profile of the cornea in primary congenital glaucoma. Acta Ophthalmol. 2013;91(1):e29–34. https://doi.org/10.1111/j.1755--3768.2012.02519.x; Epub 2012 Aug 31.

Lee HM, Kim KN, Park KS, Lee NH, Lee SB, Kim CS. Relationship between tube parameters and corneal endothelial cell damage after Ahmed glaucoma valve implantation: a comparative study. J Clin Med. 2020;9(8):2546. https://doi.org/10.3390/jcm9082546; PMID: 32781635; PMCID: PMC7464728.

Novak-Stroligo M, Alpeza-Dunato Z, Kovacević D, Caljkusić-Mance T. Corneal thickness in congenital glaucoma. Coll Antropol. 2011;35(Suppl 2):305–6.

Shields MB. Axenfeld-Rieger syndrome: a theory of mechanism and distinctions from the iridocorneal endothelial syndrome. Trans Am Ophthalmol Soc. 1983;81:736–84; PMID: 6676983; PMCID: PMC1312467.

Tamçelik N, Batu Oto B, Mergen B, Kiliçarslan O, Gönen B, Arici C. Corneal endothelial changes in patients with primary congenital glaucoma. J Glaucoma. 2022;31(2):123–8. https://doi.org/10.1097/IJG.0000000000001909.

Urban B, Bakunowicz-Łazarczyk A, Michalczuk M, Krętowska M. Evaluation of corneal endothelium in adolescents with juvenile glaucoma. J Ophthalmol. 2015;2015:895428. https://doi.org/10.1155/2015/895428; Epub 2015 Jan 6. PMID: 25642345; PMCID: PMC4302359.

29 Histopathology in Childhood Glaucoma

Seema Sen and Venkatesh Nathiya

A histological understanding of the layers of the eye is essential for appreciating disease pathophysiology and also understanding certain therapeutic approaches. Tissue preparation is a key step for histopathological evaluation. The tissue of the eye and orbit can undergo preparation in several different ways for analysis. For light microscopy, 10% neutral buffered formalin is used, while glutaraldehyde is the standard choice for electron microscopy. The widely used hematoxylin and eosin stain is used, staining the nucleus dark purple. The periodic acid-Schiff stain detects carbohydrates in tissue and can be used to visualize basement membranes.

Neural crest cells give rise to all connective tissues anterior to the lens epithelium including corneal stromal cells, corneal and trabecular mesothelial cells, iris stromal cells, and iris melanophores. These cells constitute a continuous layer which extends from the corneal to trabecular meshwork mesothelium and onto the anterior surface of the iris. The Descemet's membrane is an acellular layer made of type IV collagen that serves as a modified basement membrane of the corneal endothelium. The corneal endothelium is a one cell thick layer made of cuboidal cells.

Aqueous humor and its fluid mechanics play a crucial role in maintaining intraocular pressure (IOP). The aqueous humor is produced by ciliary processes of the ciliary body (CB) and drains through the trabecular pathway located anatomically at the internal junction of the cornea and sclera. This outflow pathway consists of trabecular meshwork (TM), Schlemm's canal (SC), intrascleral channels, and episcleral and conjunctival veins. Hence, the histopathology of the trabecular meshwork is an important part of glaucoma research since the cause of most glaucomas is suspected in or around this corneoscleral filtration meshwork. Normal trabecular beams have a lamellar arrangement of collagen fibers with clear intervening spaces and interspersed trabecular endothelial cells (TECs). Due to the less well-defined lamellar arrangement of the trabecular beams, the resistance progressively increases from the intracameral to the scleral side (Fig. 29.1a–c).

S. Sen (✉)
Ocular Pathology, Dr. Rajendra Prasad Centre for Ophthalmic Sciences, All India Institute of Medical Sciences, New Delhi, India
e-mail: drseemasen@aiims.gov.in

V. Nathiya
Department of Ophthalmology, Dr. Rajendra Prasad Centre for Ophthalmic Sciences, All India Institute of Medical Sciences, New Delhi, India

S. Gupta et al. (eds.), *Childhood Glaucoma*, https://doi.org/10.1007/978-981-19-7466-3_29

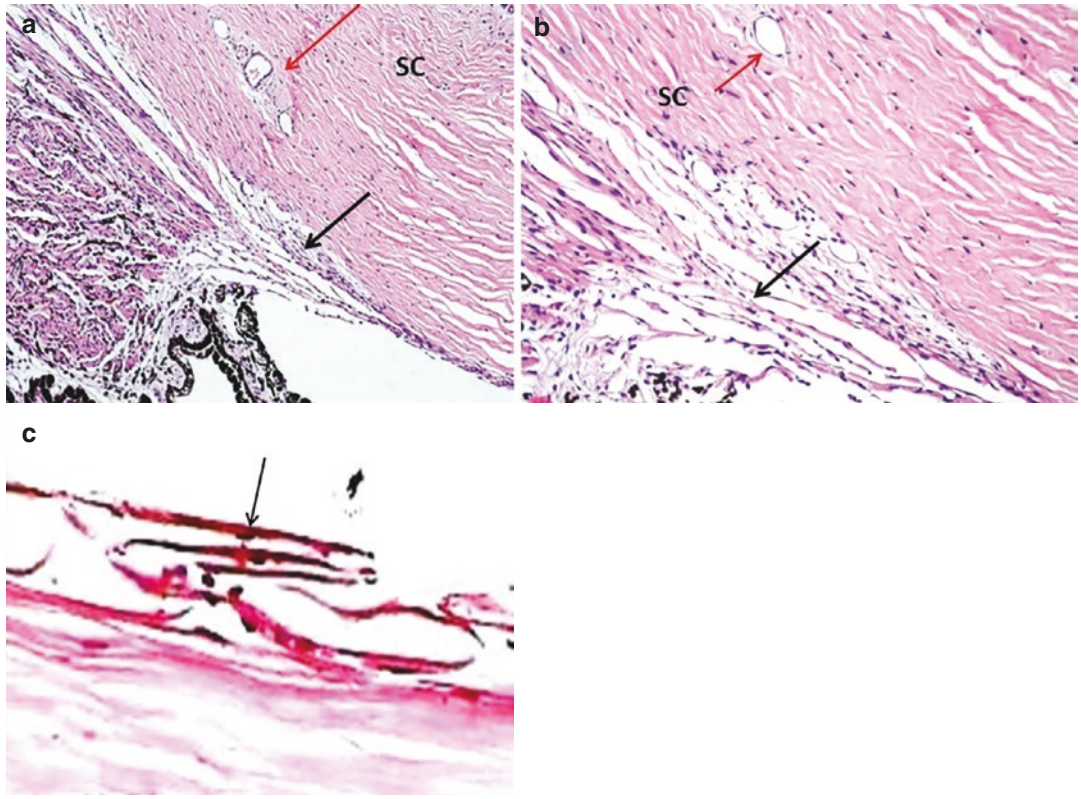

Fig. 29.1 (**a**) Normal trabecular meshwork (black arrow) and Schlemm's canal (SC, red arrow) (hematoxylin and eosin stain-H&E×100). (**b**) Higher magnification to show trabecular meshwork (black arrow) and Schlemm's canal (red arrow) (H&E×200). (**c**) Normal trabecular beams with intervening spaces and endothelial cells (arrow) (H&E×400)

The TM is methodically studied from cameral to scleral side at high power magnification for the presence of an eosinophilic membrane (EM), arrangement of trabecular beams, quality and number of trabecular endothelial cells (TECs), and presence of intervening spaces with respect to glaucoma.

The aqueous side of the specimen is determined by the presence of trabecular beams and/or melanin-containing uveal tissue from CB. The scleral side is identified by haphazard arrangement of the collagen fibers with near absence of intervening cells. In high cellular specimens, the cellular component constitutes more than the non-cellular component; in low cellular specimens, the ratio is reversed, and in moderately cellular specimens, both components are comparable.

29.1 Primary Congenital Glaucoma

Several classification systems for Primary Congenital Glaucoma (PCG) have been proposed by Shaffer-Weis, De Luise-Anderson, and Hoskins-Shaffer-Hetherington anatomically. However, these grading systems are cumbersome and carry few prognostic or therapeutic implications. Recently, Hollander classified goniodysgenesis in PCG as mild, moderate, and severe.

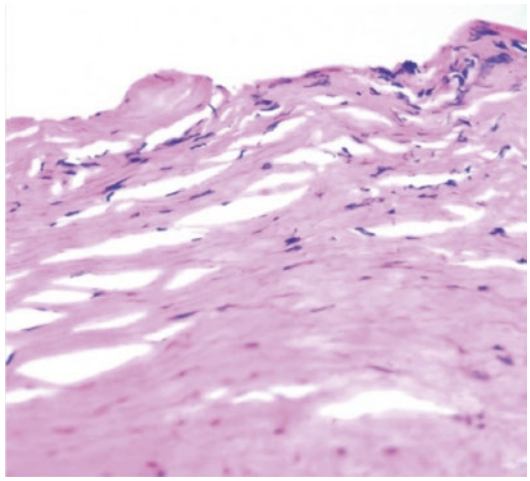

Fig. 29.2 Fibrosed trabecular beams and reduced intertrabecular space in a case of primary congenital glaucoma (hematoxylin and eosin stain- H&E×400)

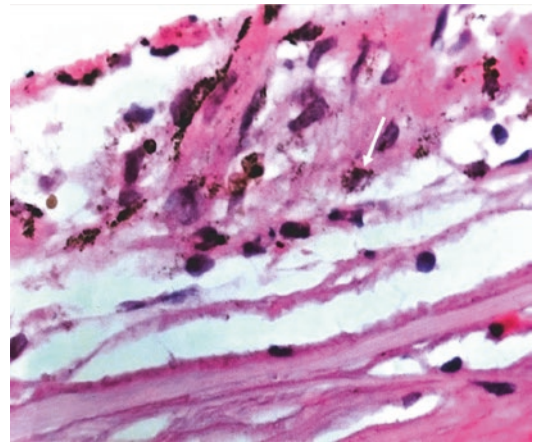

Fig. 29.3 Dysmorphic subcanalicular tissue with uveal pigment laden cells (white arrow) in a case of primary congenital glaucoma (hematoxylin and eosin stain- H&E×600)

According to this classification, severe goniodysgenesis is characterized by agenesis of SC and relative hypoplasia of TM. It presents with early severe forms of the disease and requires multiple surgeries for the control of IOP; moderate and mild goniodysgenesis are categorized by abnormal tissue band on the outer TM and deposition of extracellular substance in juxtacanalicular tissue, respectively.

The disorganization of TM is attributable to its embryological immaturity and deposition of amorphous extracellular substance (collagen and proteoglycan) on the inner wall of SC; the absence of SC can also be attributed to its collapse during surgical manipulation or tissue preparation, variability in its histological localization, or to its abnormal development.

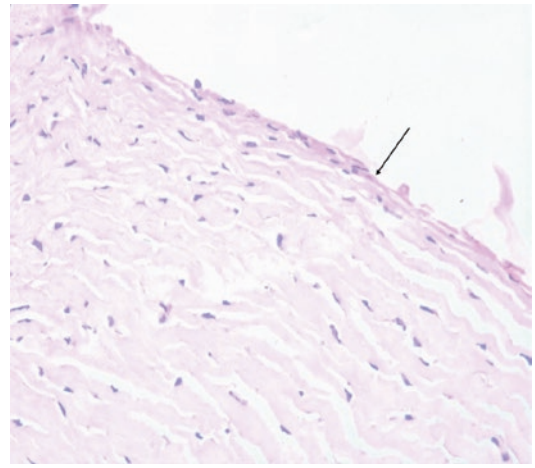

Fig. 29.4 Fused trabecular beams (arrow), which are normocellular in a case of primary congenital glaucoma (hematoxylin and eosin stain- H&E×400)

Case 29.1

Fused trabecular beams with decreased intertrabecular spaces (Fig. 29.2) are the major finding in PCG. Thickened and dysmorphic subcanalicular tissue could cause obstruction to the aqueous outflow in PCG eyes (Fig. 29.3). The inner layers of the filtration zone are affected by greatest oxidative insult in PCG. In the study by Agarwal et al. 2022, it has been reported that few intervening spaces present on the scleral side of the specimens also get blocked by this thickened and non-yielding subcanalicular tissue.

Case 29.2

Normal residual TECs histologically may have imperceptible functional disturbance which causes raised IOP even in normocellular specimens (Fig. 29.4).

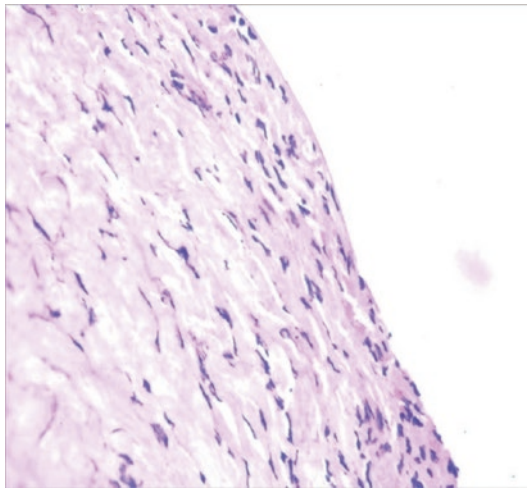

Fig. 29.5 Hypercellularity, pleomorphism, and fused trabecular beams in a case of primary congenital glaucoma (hematoxylin and eosin stain- H&E×400)

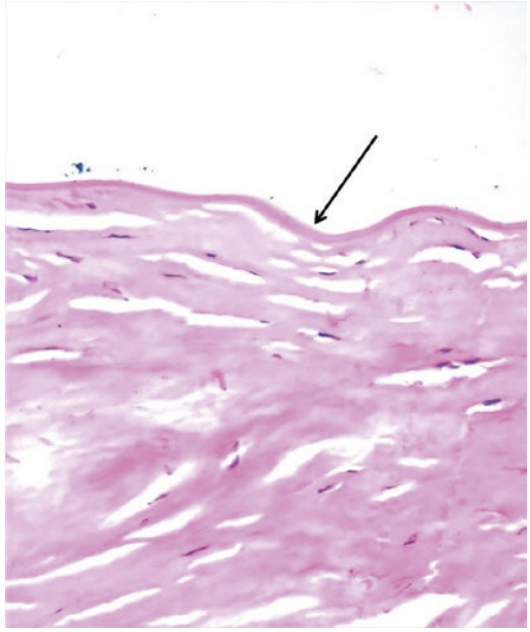

Fig. 29.6 Hypocellular trabecular beams and eosinophilic membrane (basement membrane-like material) (arrow) on intracameral side in a case of primary congenital glaucoma (hematoxylin and eosin stain-H&E×400)

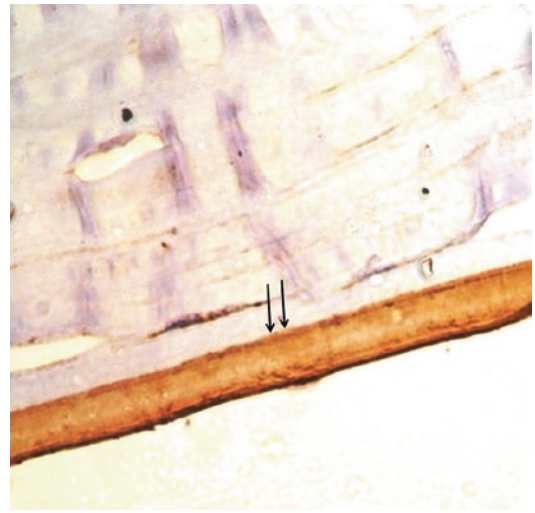

Fig. 29.7 A case of Primary Congenital Glaucoma showing collagen IV positivity in the Descemet's membrane. Note the pre-Descemet's layer (arrows) (Avidin-Biotin X 600)

Case 29.3

The various histological changes in TM cause abnormal compensatory division of TECs. These cells appear to be pleomorphic and possibly not functionally capable of causing remodelling of the acellular component. This has been observed as pleomorphism and thickening of high-cellularity specimens (Fig. 29.5).

Case 29.4

A hypocellular trabecular meshwork with an eosinophilic membrane may also be observed (Fig. 29.6).

Case 29.5

The Descemet's membrane consists of many extracellular matrix protein types, including collagen type IV, fibronectin, and laminin. Therefore, collagen 4 immunostaining of the Descemet's membrane is quite useful, especially in ophthalmic clinical research (Fig. 29.7).

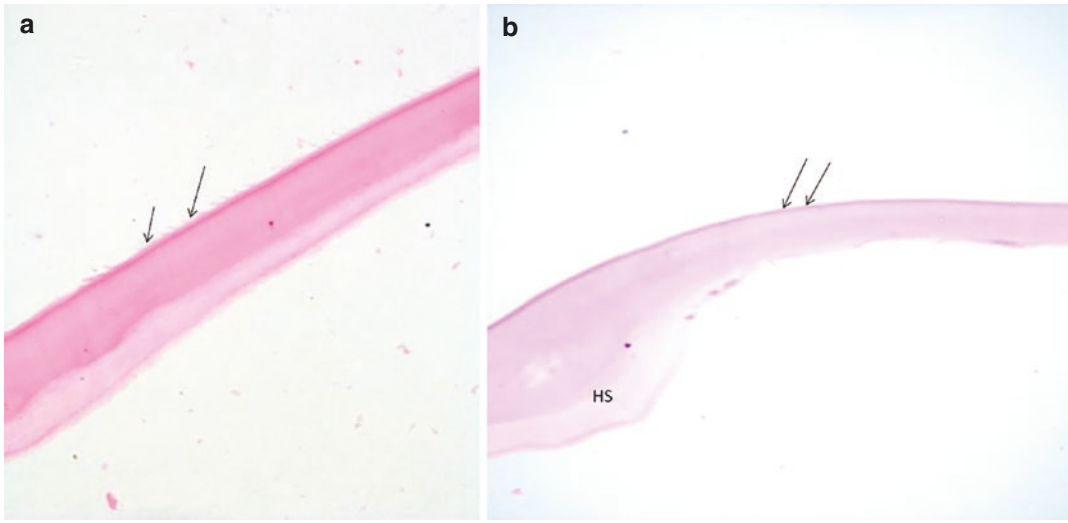

Fig. 29.8 (**a**) Continuous dark band of pre-Descemet's layer (PDL; Dua's layer) (arrows) seen anterior to the Descemet's membrane in primary congenital glaucoma. (**b**) PDL is seen markedly thickened (hematoxylin and eosin stain- H&E×600) Haab's striae region (HS) showing thickened Descemet's layer and prominent PDL (arrows) (H&E×400)

Some cases of PCG also show a prominent pre-Descemet's layer. Breaks in the Descemet's membrane, Haab's stria, are also seen due to elevated intraocular pressure (Fig. 29.8).

29.2 Axenfeld-Rieger Syndrome (ARS)

Because of developmental arrest, there is retention of primitive endothelial tissue on the iris and angle of the anterior chamber. Atypical basement membrane is produced near the corneo-limbal junction, causing prominent Schwalbe's line. There is incomplete maturation of TM and SC due to failure of the intertrabecular spaces to develop (Fig. 29.9a). Several histopathological studies describe that the iris insertion and anterior ciliary body overlap over the posterior portion of the trabecular meshwork. During chamber angle development, the iris and the ciliary body fail to recede posteriorly. In addition, an increase in extracellular matrix has been described in the trabecular meshwork.

Corneal changes include interlayer splitting of the Descemet's membrane with hypoplastic iris, uneven thickness of DM, and absence of endothelium due to decompensation (Fig. 29.9b).

Case 29.6

The trabecular meshwork in ARS shows incomplete maturation (Fig. 29.9a), and the cornea shows posterior absence of endothelial cells. Another case of ARS shows posterior corneal stroma and uneven Descemet's membrane with loss of endothelial cells (Fig. 29.9b).

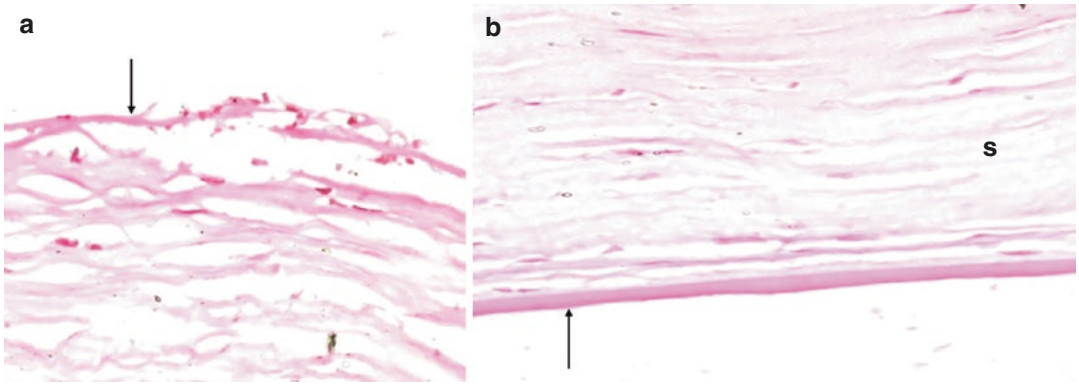

Fig. 29.9 (**a**) Trabecular meshwork from a case of Axenfeld-Rieger Syndrome (ARS) shows scant intertrabecular spaces (arrow). (**b**) Posterior corneal stroma (s) with Descemet's membrane of uneven thickness from another case of ARS shows absence of endothelial cells (hematoxylin and eosin stain- H&E×600)

29.3 Peters Anomaly

In Peters anomaly, pathology is primarily the mesenchymal dysgenesis of the anterior ocular segment resulting from the abnormal development of neural crest cells. Defects in the endothelium, Descemet's membrane, and posterior stroma are observed. Lens material may be seen in the defective corneal stroma.

Case 29.7
The anterior chamber space is not formed, and the iris pigment is seen adherent to the posterior surface of the peripheral cornea (Fig. 29.10a, b).

Case 29.8
The anterior chamber space is poorly formed, and the iris pigment and lens material are seen adherent to the posterior surface of the peripheral cornea (Fig. 29.10c, d).

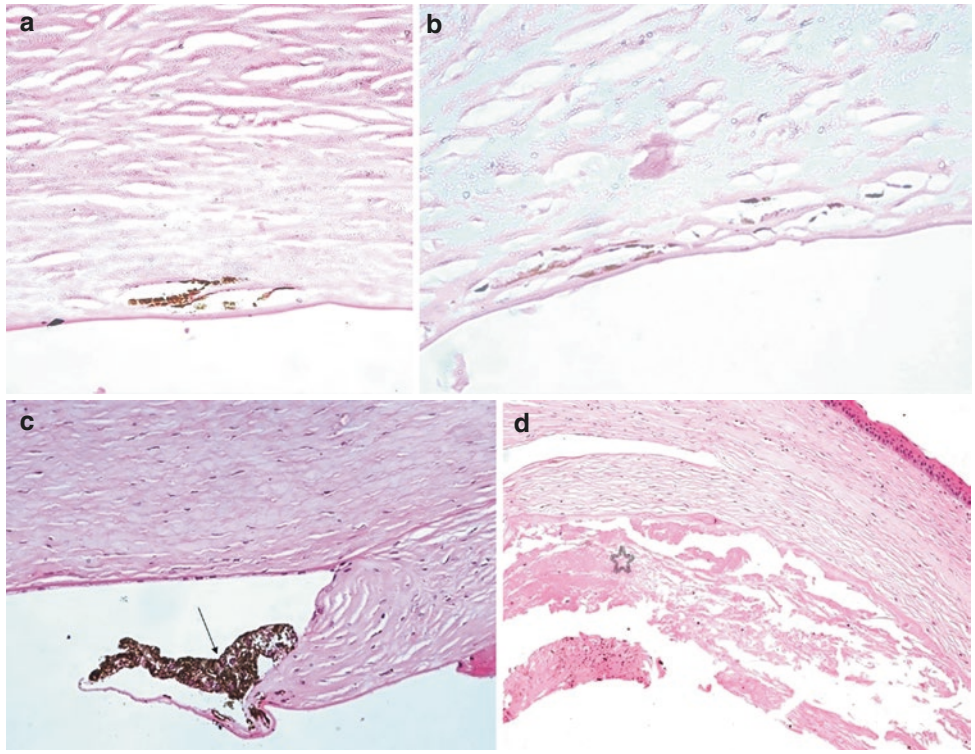

Fig. 29.10 (**a**, **b**) Iris pigment adherent to the peripheral cornea in a case of Peters anomaly (hematoxylin and eosin stain- H&E×400). (**c**) Undifferentiated iris stroma (arrow) (H&E×200) and (**d**) degenerative lens (asterisk) adherent to defective central cornea in another case of Peters anomaly (H&E×100)

29.4 Conclusions

The spectrum of histopathological changes seen in congenital glaucoma includes:

- Loss of the normal lamellar arrangement of trabecular beams. This may include fusion/disorganization, fibrosis, and deposition of extracellular substance, resulting in blocking of the trabecular spaces.
- Trabecular endothelial cells lining the beams may have normal, hypo-, or hypercellularity which may be associated with pleomorphism.
- The Schlemm's canal may be normal, hypoplastic, or absent and could be combined with deposition of extracellular substance/subcanalicular tissue. An eosinophilic membrane is often seen on the intracameral side, over the trabecular beams.
- In ARS, trabecular meshwork is immature, with abnormal basement membrane near the limbus.
- Corneal changes in primary congenital glaucoma include thickening of PDL, presence of Haab's striae, loss of endothelium, and irregular DM.
- In Peters anomaly, defects in the DM and posterior corneal stroma with adherent lenticular/iris tissue may be seen.

Suggested Reading

Agarwal R, Sen S, Kashyap S, et al. Correlation of histopathology of trabecular meshwork with clinical features in primary congenital glaucoma. Br J Ophthalmol. 2022;106:60–4.

Agha B, Shajari M, Slavik-Lencova A, Kohnen T, Schmack I. Outcome of Descemet membrane endothelial keratoplasty for graft failure after Descemet stripping automated endothelial keratoplasty. Clin Ophthalmol. 2019;13:553–9.

Alvarado J, Murphy C, Polansky J, et al. Age-related changes in trabecular meshworkcellularity. Invest Ophthalmol Vis Sci. 1981;21:714–27.

Anderson DR. The development of the trabecular meshwork and its abnormality inprimary infantile glaucoma. Trans Am Ophthalmol Soc. 1981;79:458–85.

Ascher KW. Veins of the aqueous humor in glaucoma. Boll Ocul. 1954;33:129–44.

Ashton N, Brini A, Smith R. Anatomical studies of the trabecular meshwork of the normal human eye. Br J Ophthalmol. 1956;40:257–82.

Azari AA, Syed NA, Albert DM. Examining and processing eye specimens. Methods Mol Biol. 2014;1180:377–96.

Bakunowicz-Lazarczyk A, Sulkowska M, Sulkowski S, et al. Ultrastructural changes inthe trabecular meshwork of congenital glaucoma. J Submicrosc Cytol Pathol. 2001;33:17–22.

Bonanno JA. Molecular mechanisms underlying the corneal endothelial pump. Exp Eye Res. 2012;95(1):2–7.

Chen SY, Terry MA. Step-by-step Descemet's membrane endothelial keratoplasty surgery. Taiwan J Ophthalmol. 2019;9(1):18–26.

deLuise VP, Anderson DR. Primary infantile glaucoma (congenital glaucoma). SurvOphthal. 1983;28:1–19.

Gupta V, Chaurasia AK, Gupta S, et al. In vivo analysis of angle dysgenesis in primary congenital, juvenile, and adult-onset open angle glaucoma. Invest Ophthalmol Vis Sci. 2017;58:6000–5.

Gupta S, Chaurasia AK, Sen S, Bhardwaj M, Mandal S, Titiyal JS, Gupta V. The Descemet membrane in primary congenital glaucoma. Cornea. 2021;40(2):172–8.

Hollander DA, Sarfarazi M, Stoilov I, et al. Genotype and phenotype correlations in congenital glaucoma. Trans Am Ophthalmol Soc. 2006;104:183–95.

Hoskins HD, Shaffer RN, Hetherington J. Anatomical classification of the developmental glaucomas. Arch Ophthalmol (Chic IL, 1960). 1984;102:1331–6.

Knepper PA, Goossens W, McLone DG. Ultrastructural studies of primary congenital glaucoma in rabbits. J PediatrOphthalmol Strabismus. 1997;34:365–71.

Matsubara A, Ozeki H, Matsunaga N, et al. Histopathological examination of two cases of anterior staphyloma associated with Peters' anomaly and persistent hyperplastic primary vitreous. Br J Ophthalmol. 2001a;85:1421–5.

Matsubara A, Ozeki H, Matsunaga N, Nozaki M, Ashikari M, Shirai S, Ogura Y. Histopathological examination of two cases of anterior staphyloma associated with Peters' anomaly and persistent hyperplastic primary vitreous. Br J Ophthalmol. 2001b;85(12):1421–5.

Maumenee AE. The pathogenesis of congenital glaucoma: a new theory. Trans Am Ophthalmol Soc. 1958;56:507–70.

Rojas B, Ramírez AI, de Hoz R, et al. Structural changes of the anterior chamber angle in primary congenital glaucoma with respect to normal development. Arch Soc Espanola Oftalmol. 2006;81:65–71.

Shaffer R, Weiss D. Congenital and pediatricglaucomas. Saint Louis, MI: Mosby; 1970.

Shields MB. Axenfeld-Rieger syndrome: a theory of mechanism and distinctions from the iridocorneal endothelial syndrome. Trans Am Ophthalmol Soc. 1983;81:736–84.

Tamm ER. The trabecular meshwork outflow pathways: structural and functional aspects. Exp Eye Res. 2009;88:648–55.

Tandon A, Watson C, Ayyala R. Ultrasound biomicroscopy measurement of Schlemm's canal in pediatric patients with and without glaucoma. J AAPOS. 2017;21:234–7.

Tawara A, Inomata H. Developmental immaturity of the trabecular meshwork in congenital glaucoma. Am J Ophthalmol. 1981;92:508–25.

Yu T, Dai Z, Peng R, et al. Axenfeld-Rieger syndrome: a novel histopathologic finding associated with corneal abnormalities. BMC Ophthalmol. 2022;22(1):514. https://doi.org/10.21203/rs.3.rs-1681755/v1.

Zhang J. Histo- and ultrahisto-pathology of the anterior chamber angle in congenital glaucoma. Zhonghua Yan Ke Za Zhi Chin J Ophthalmol. 1991;27:151–3.

Part VII

Management and Rehabilitation

30 Medical Management in Childhood Glaucoma

Shakha, Karthikeyan Mahalingam, and Shikha Gupta

30.1 Introduction

Childhood glaucomas are heterogeneous in their causation as well as in their responses to different glaucoma medications. The role of medical treatment in childhood glaucoma treatment varies with the type of glaucoma as well as specific features of the affected child and eye(s). As a primary treatment for glaucoma, medications alone rarely show sustained efficacy in infants and young children, due to associated angle dysgenesis. There is a high nonresponder rate as well as a lack of long-term safety profile. These factors contribute to the limited use of medical treatment in pediatric glaucoma. The role of medical management in congenital glaucomas is, therefore, generally supportive.

They may help by reducing the corneal edema just before surgery, facilitating angle surgery in some cases or acting as an adjunct to maximize intraocular pressure (IOP) reduction postoperatively. While surgery is the mainstay of glaucoma treatment in infants and young children, medical therapy may be considered a first-line treatment in some cases of childhood glaucoma (e.g., juvenile open-angle glaucoma (JOAG), secondary childhood glaucomas, etc.).

Challenges in pediatric cases as compared to the adult population:

1. Childhood glaucomas are heterogeneous in their causation; hence, their responses to different glaucoma medications are also variable.
2. Systemic pharmacokinetics:
   (a) While the ocular volume of a child and an adult is similar, that of a neonate is approximately half of an adult.
   (b) A child's plasma volume is lesser compared with that of an adult.
   (c) Hence, when the drug is absorbed systemically (mostly through the nasal mucosa), the dosage is diluted by a much smaller volume of blood, leading to higher systemic concentrations in children than in their adult counterparts.
   (d) Only a few drugs have been evaluated for pharmacokinetics in children.
   (e) Simple maneuvers can help reduce systemic absorption of topical medications:

   - Having care providers close the lids, remove excess liquid, and perform nasolacrimal occlusion after drop instillation, whenever possible (Fig. 30.1, Video 30.1).

Supplementary Information The online version contains supplementary material available at https://doi.org/10.1007/978-981-19-7466-3_30.

Shakha (✉) · K. Mahalingam · S. Gupta
Dr. Rajendra Prasad Centre for Ophthalmic Sciences, All India Institute of Medical Sciences, New Delhi, India
e-mail: shikhagupta@aiims.edu

S. Gupta et al. (eds.), *Childhood Glaucoma*, https://doi.org/10.1007/978-981-19-7466-3_30

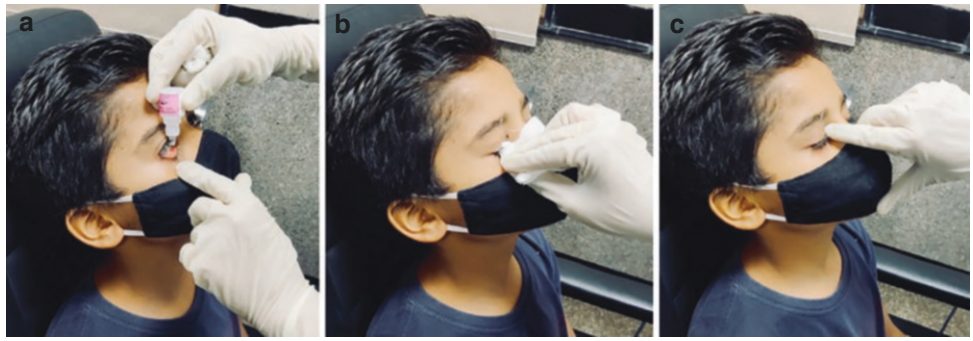

Fig. 30.1 Instillation of eye drops in a cooperative child. (**a**) The child is asked to look upward and lower lid retracted down. (**b**) Excessive drop wiped off. (**c**) Punctal occlusion

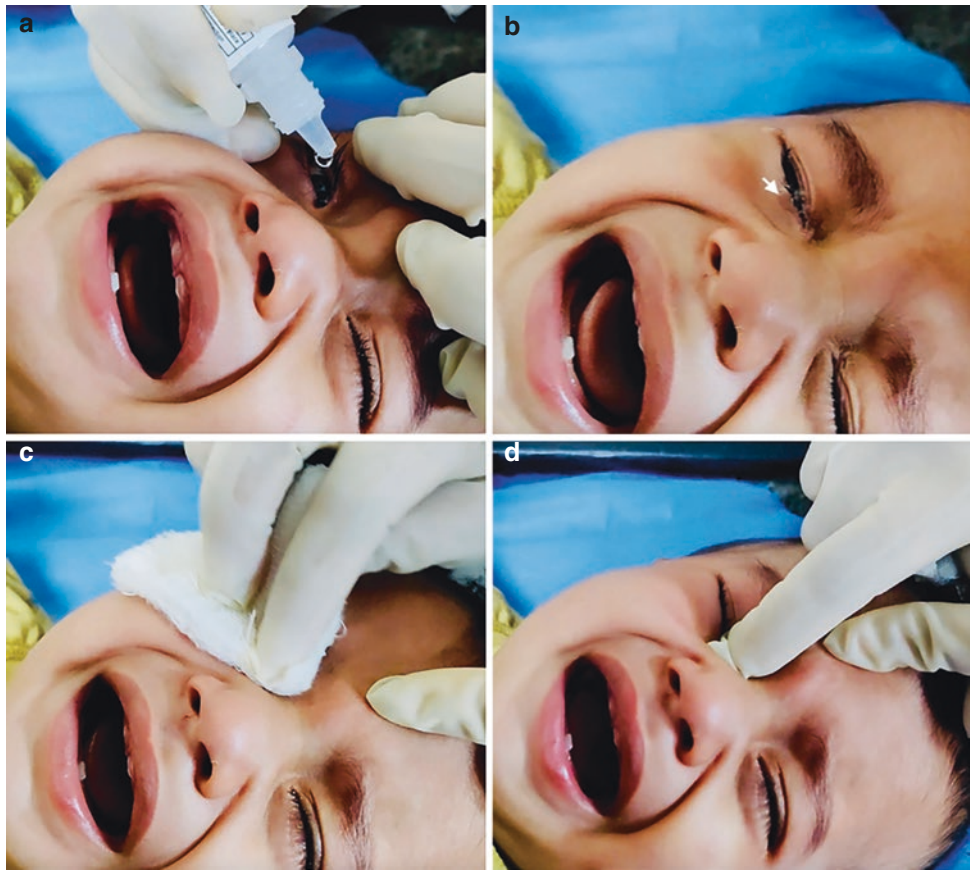

Fig. 30.2 Instillation of eye drops in an uncooperative child. (**a**) Separation of lids and instilling eye drops. (**b**) Closing the lids. Excess drops seen (arrow). (**c**) Wiping off excess drops. (**d**) Applying punctal pressure

- Using the minimum frequency and lowest concentration of a given glaucoma drug that is needed to achieve the target IOP.
- Parents must be well informed about potential side effects of prescribed glaucoma medications.
- In uncooperative children:
  - The drops can be instilled either by separating the lids (Fig. 30.2, Video 30.1).
  - Or the drops can be instilled on the medial canthus followed by separation of lids, which allows the medications to enter the eye (Fig. 30.3).

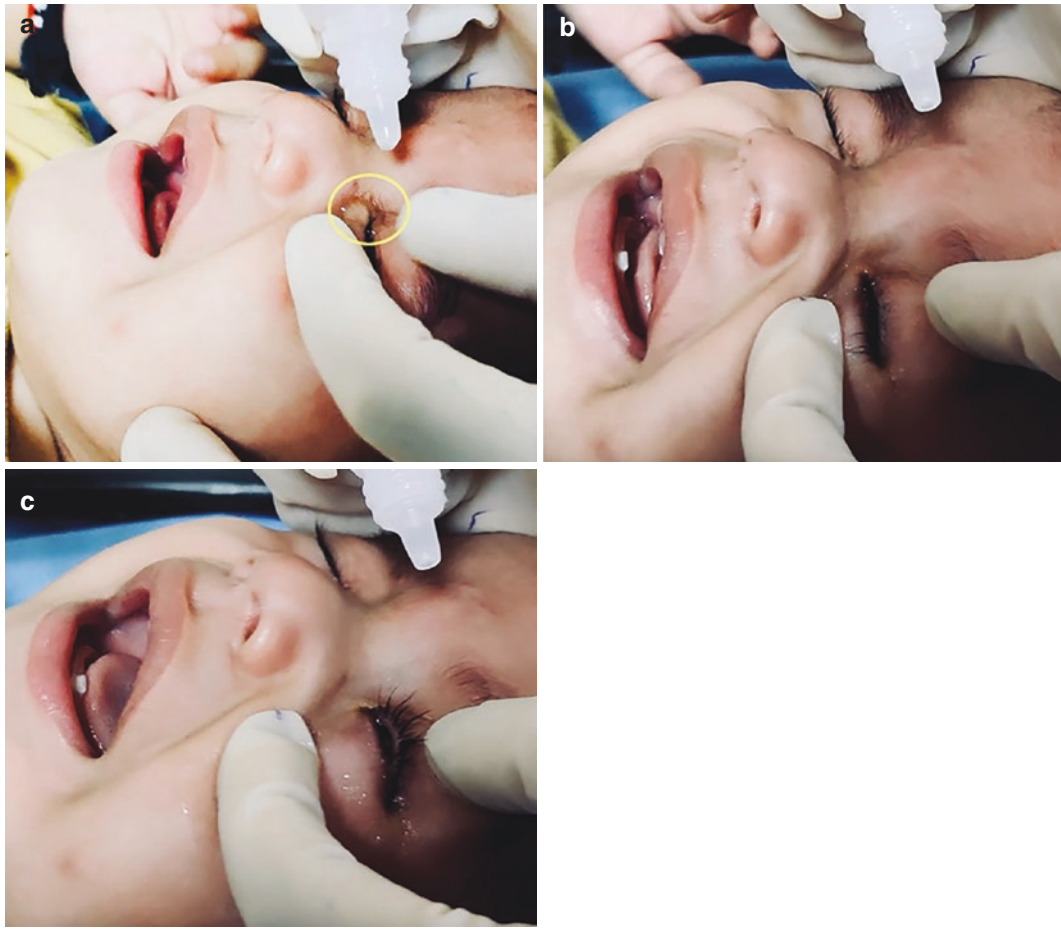

Fig. 30.3 Instillation of eye drops in an uncooperative child. (**a**) Putting drops on the medial canthus of eye. (**b**, **c**) Separation of the upper and lower lids so that the drop enters the eye

3. Compliance:
   (a) Highly dependent on the caregivers and parents.
   (b) High chance of possible lack of cooperation in the administration of treatment.

30.2 Medications

The various classes of drugs and their mechanism of action, dosage, and side effects are described in the table (Table 30.1).

Case 30.1
A 5-year-old male child with both eyes (BE) late-onset primary congenital glaucoma was referred to a glaucoma clinic. IOP was 24 mmHg and 28 mmHg in right eye (RE) and left eye (LE) (on brimonidine + timolol combination BD, dorzolamide TDS and pilocarpine TDS). The mother complained of excessive sleepiness and lethargy after using topical medications. A diagnosis of brimonidine-induced central nervous system toxicity was made. The patient was advised to stop brimonidine and was planned for glaucoma filtration surgery in BE.

Learning Points
- Brimonidine is highly lipophilic, absorbed through the cornea, and also passes through the blood-brain barrier in neonates and infants, producing central nervous system toxicity.

Table 30.1 Mechanism of action, dosage, and side effects of antiglaucoma drugs

Class of drugs	Mechanism of ocular action	Dosage	Side effects and contraindications
Beta-blockers	• **Nonselective β-blockers (timolol, levobunolol, carteolol):** – Decrease aqueous production by binding to β-adrenergic receptors on the ciliary epithelium and inhibiting cyclic adenosine monophosphate – May bind to β-2-adrenoceptors in the anterior ciliary artery wall, causing vasoconstriction and thus indirectly decreasing aqueous humor secretion • **β1-selective (betaxolol):** – Acts by reaching sufficient concentration to block β-1-adrenoceptors in the ciliary epithelium – Neuroprotective action by relaxing the smooth muscles on the wall of retinal arterioles	• **Timolol:** – 0.25% and 0.5% concentrations available – Administered BD – Also available as a viscous formulation, gel-forming solution, which makes them possible to dose as once-daily drugs – In a small child, administer the lowest effective dose possible. Observe the child for adverse effects for 1–2 h in the office on first-time instillation – It can be increased up to 0.5% in children up to 6 years of age • **Betaxolol**: – 0.25% and 0.5% concentrations • **Levobunolol:** – 0.25% and 0.5% concentrations	• **Ocular:** – Burning pain and discomfort (more with betaxolol) – Conjunctival hyperemia – Superficial punctate keratitis and dry eye • **Systemic:** – High risk of apnea and bradycardia in premature infants and newborns – Exacerbation of respiratory symptoms, especially in children with "reactive airways" – Contraindications: bradycardia, second- or third-degree atrioventricular block, and active bronchoconstrictive disease – Betaxolol: less bronchospasm vs. nonselective β-blockers. Hence, it is preferred in children. It can be given in low doses and with punctal occlusion for lesser systemic side effects
Carbonic anhydrase inhibitors (CAIs)	Inhibits carbonic anhydrase inhibitor of the ciliary epithelium and decreases aqueous production **Dorzolamide:** has both free sulfonamide and amine group, hence the right amount of lipid and aqueous solubility for good corneal penetration. Inhibits CA II and IV. Little crossover effect is seen, hence local rather than systemic action. In pediatric cases despite being less effective than oral acetazolamide, it worked in most of the cases with lesser systemic side effects **Brinzolamide:** CA II inhibitor. Suspension form has better permeability, less surface irritation, increased pressure reducing activity, and prolonged duration of action	**Systemic CAIs:** • Acetazolamide: 10–15 mg/kg/day (maximum dose 20 mg/kg/day) with meals, divided BD to QID (5 to 10 mg/kg every 6 to 12 h) • Methazolamide: < 2 mg/kg/day, divided BD **Topical CAIs:** • Dorzolamide 2% TDS • Brinzolamide 1% TDS	• **Ocular:** – Stinging – Allergy – Superficial punctate keratitis and dry eye – Transient myopia – Corneal thickening and even decompensation in the diseased cornea • **Systemic:** – Lethargy – Loss of appetite – Gastrointestinal disturbance – Metabolic acidosis – Failure to thrive – Bedwetting – Hypersensitivity reactions (including urticaria, angioedema, and bronchospasm) – Stevens-Johnson syndrome – Bitter taste – Urolithiasis – Growth suppression – Other possible side effects (reported in adults) include neutropenia and aplastic anemia – Contraindicated in patients with sickle cell anemia (hyphema-induced ocular hypertension) When an infant is receiving topical CAIs, it should be determined whether the child is feeding well and gaining weight. In the event of their occurrence, CAI should be immediately stopped, because these may be the earliest symptoms of acidosis in an infant

Class of drugs	Mechanism of ocular action	Dosage	Side effects and contraindications
Adrenergic agonists	Increase uveoscleral outflow by relaxing the ciliary smooth muscles Decrease aqueous humor production by decreasing activity of adenylate cyclase and causing vasoconstriction Improves conventional outflow facility • **Apraclonidine:** derivative of clonidine, action similar to clonidine but structural modification reduces the ability of the drug to penetrate the blood-brain barrier. Has both α1 and α2 action Mechanism: – Decreases episcleral venous pressure – Increases trabecular meshwork outflow – Decreases aqueous production • **Brimonidine:** α2−selective agent. More lipophilic, hence easily crosses the blood-brain barrier Mechanism: – Decreases aqueous production – Increases uveoscleral outflow – Neuroprotection	• Apraclonidine (0.5%) TDS • Brimonidine (generic brimonidine 0.2 %, Alphagan P 0.15%, 0.10%) TDS	• **Ocular:** – Redness – Itching – Allergy – Ocular surface disease • **Systemic:** – Somnolence – Central nervous system depression – Respiratory depression – Apnea – Bradycardia – Hypothermia – Hypotension Brimonidine is contraindicated in children less than 2 years of age. Better to avoid it till 6 years of age, in children with cognitive impairment, and children with a weight < 15 kg
Prostaglandin analogues	Increase in the uveoscleral outflow Increases metalloproteinase production, leading to extracellular matrix remodelling, widening of intramuscular spaces in longitudinal ciliary muscle bundles, and dissolution of collagen types I and III Prostamides: increase the trabecular outflow	• Latanoprost 0.005%, • Travoprost 0.004%, Bimatoprost 0.03%–0.01% (prostamide) • Tafluprost 0.0015% (preservative-free), • Unoprostone 0.15% PGAs in children are dosed HS When administered with pilocarpine, the bedtime dose of pilocarpine should be administered 1 h after the dose of latanoprost for maximum efficacy	• **Ocular:** – Lash growth and hyperemia (Fig. 30.4) – Iris pigmentation change – Hyperemia – Allergy (Fig. 30.5) – Uveitis – Periocular hyperpigmentation • **Systemic:** – Headache, upper body muscle aches – Abnormal liver function tests – Cough More side effects (ocular) seem to occur with travoprost and bimatoprost compared with latanoprost (mostly anecdotal), so most providers prefer to begin PGA treatment with latanoprost. Orbital fat atrophy has been described in adults Avoided in unilateral cases due to local side effects and the cosmetic concern

(continued)

Table 30.1 (continued)

Class of drugs	Mechanism of ocular action	Dosage	Side effects and contraindications
Parasympathomimetic agonist	Stimulates the ciliary muscle (direct-acting parasympathomimetic) and opens the trabecular meshwork outflow channels Since the majority of pediatric glaucomas result from structural and developmental abnormalities of the angle and associated structures, not much IOP lowering effect of pilocarpine in these cases is seen The main uses are: • To induce miosis in preoperative preparation for laser iridotomies or angle surgery • To minimize synechiae formation, post-angle surgery	Pilocarpine: 1–2%, BD or TDS	• **Ocular:** – Brow ache – Miosis – Variably increased myopia (ciliary spasm). (Pseudophakic or aphakic patients have fewer side effects) – Retinal detachment – Pigment hypertrophy • **Systemic:** – Bronchial spasm – Nausea, vomiting, abdominal pain – Weakness, fatigue, muscle spasm – Sweating, salivation, lacrimation – Hypotension, bradycardia – Nightmares, depression, delusions
ROCK inhibitors	• Increase aqueous outflow by decreasing trabecular meshwork resistance (decreases smooth muscle contraction, disrupting actin fibers) Netarsudil also inhibits norepinephrine transporter leading to additional benefits: • Decrease in episcleral venous pressure • Reduction in aqueous humor production	• Ripasudil 0.4% BD • Netarsudil 0.02% OD	• **Ocular:** – Transient conjunctival hyperemia (in. approx. 50% of cases) – Conjunctival hemorrhage – Mild corneal staining – Eyelid erythema – Blurry vision – Instillation site pain/erythema – Corneal epithelial edema – Reticular edema of the corneal epithelium (Fig. 30.6) • **Systemic:** – Headaches

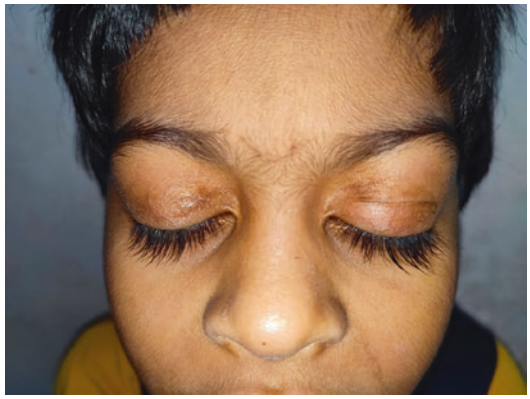

Fig. 30.4 Hypertrichiasis following use of topical PG analogues

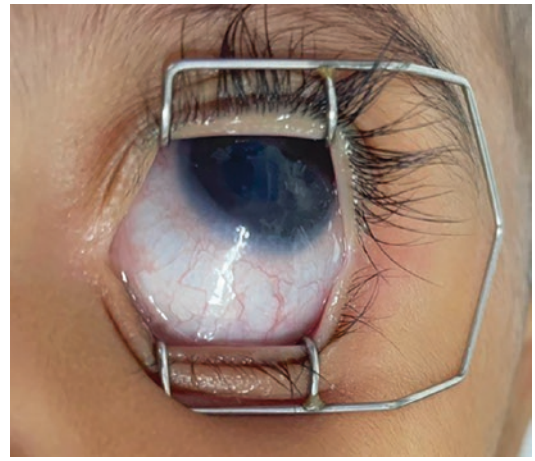

Fig. 30.5 Allergic reaction to prostaglandin eye drops

Since children have smaller plasma volumes, excessive systemic absorption, immature metabolism and excretion, immature blood-brain barrier, and increased receptor sensitivity, they are at a higher risk of having central nervous system effects.

- Neurological symptoms reported are somnolence, respiratory depression, apnea, and even coma. Those effects usually happen 30–60 min after administration and recover without sequelae.
- Naloxone has been reported to reverse those symptoms after being administered in cases of severe central nervous system involvement. The central nervous system side effects can be exacerbated in children taking topical beta-blockers and brimonidine together.
- Allergic blepharoconjunctivitis is a common adverse effect of brimonidine.

Case 30.2

A 15-year-old juvenile-onset open-angle glaucoma patient visited for a routine checkup. His IOP was 12 mmHg in BE on (bimatoprost HS, dorzolamide + timolol BD). Enlarged eyelashes and conjunctival congestion were noted in both eyes (Fig. 30.5). Fundus examination revealed cup-disk ratio of 0.6:1 (RE) and 0.7:1 (LE). Bimatoprost was suspected to be the cause of trichomegaly and allergy.

Learning Points

- Prostaglandin analogues are known to cause eyelash trichomegaly.
- It has been shown to stimulate the growth of hair follicles (induce anagen phase in resting follicles) and follicular melanocytes.
- Bimatoprost 0.03% was approved by the Food and Drug Administration for the cosmetic treatment of eyelash hypotrichosis.

Case 30.3

A 9-year-old patient female with BE juvenile open-angle glaucoma presented with LE vision 1/60 and IOP of 52 mmHg (on maximal topical hypotensive medications including netarsudil). There was conjunctival congestion, corneal epithelial edema (Fig. 30.6) and fundus revealed total glaucomatous optic neuropathy. Despite anterior chamber paracentesis, corneal epithelial edema persisted. Oral acetazolamide and intravenous mannitol were started, netarsudil was stopped, and the patient was planned for RE glaucoma filtration surgery. On the day of surgery (3 days after stopping netarsudil), corneal epithelial edema disappeared and vision improved to 6/12. Hence, a diagnosis of netarsudil-induced epithelial edema (epithelial honeycombing) was made.

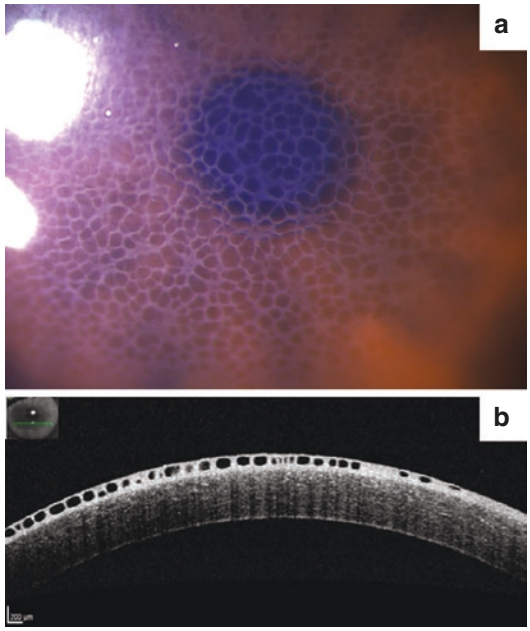

Fig. 30.6 Corneal epithelial edema after use of topical netarsudil (reproduced with permission. Mahalingam K, Joshi S, Vanathi M, Gupta V, Gupta S. Honeycomb ensemble of corneal epithelium. Clin Exp Optom. 2022 Mar 31:1–2). (**a**) Slit-lamp image showing honeycomb appearance. (**b**) ASOCT showing edema in the superficial epithelium layer of cornea after netarsudil use

Learning Points

- ROCK inhibitors have been shown to increase endothelial cell count and reduce corneal edema in the eyes with Fuchs endothelial dystrophy.
- On the contrary, many cases of netarsudil-induced corneal epithelial edema are reported. Most of these cases had high IOP and corneal edema. So, it was postulated that the netarsudil would have effluxed the posterior stromal fluid into AC (increased endothelial pumps) and anterior stromal fluid into the epithelium (increased permeability of tight junctions), causing epithelial edema.
- Corneal epithelial edema caused by netarsudil usually disappears after discontinuation of the drug.

30.3 Conclusions

Medical management has a supportive role in cases of congenital glaucoma. These drugs have drastically different pharmacokinetics and pharmacodynamics in pediatric cases, and hence one has to be cautious in regard to the dosing and monitoring of side effects of these drugs when used in children.

Suggested Reading

Anon. n.d.-a. Clinical Experience With Timolol in Childhood GlaucomalJAMA OphthalmologyIJAMA Network. [cited 2021 Sep 26]. https://jamanetwork.com/journals/jamaophthalmology/article-abstract/635643.

Anon. n.d.-b. A randomized trial assessing Dorzolamide in patients with glaucoma who are younger than 6 yearsIGlaucomalJAMA OphthalmologyIJAMA Network. [cited 2021 Sep 26]. https://jamanetwork.com/journals/jamaophthalmology/article-abstract/417240.

Anon. n.d.-c. Indications for surgical management of hyphema in patients with sickle cell trait. JAMA Ophthalmol. JAMA Network. [cited 2021 Sep 26]. https://jamanetwork.com/journals/jamaophthalmology/article-abstract/635018.

Black AC, Jones S, Yanovitch TL, Enyedi LB, Stinnett SS, Freedman SF. Latanoprost in pediatric glaucoma—pediatric exposure over a decade. J AAPOS. 2009;13(6):558–62.

Boger WP, Walton DS. Timolol in uncontrolled childhood Glaucomas. Ophthalmology. 1981;88(3):253–8.

Gupta S, Mahalingam K, Arora M, Singh A, Kumari S, Gupta V. Netarsudil induced corneal honeycombing in childhood glaucomas. J AAPOS. 2022;S1091-8531(22):00424.

Konowal A, Morrison JC, Brown SVL, Cooke DL, Maguire LJ, Verdier DV, et al. Irreversible corneal decompensation in patients treated with topical dorzolamide. Am J Ophthalmol. 1999;127(4):403–6.

Mahalingam K, Joshi S, Vanathi M, Gupta V, Gupta S. Honeycomb ensemble of corneal epithelium. Clin Exp Optom. 2022;1:1–2.

McMahon CD, Hetherington J, Hoskins HD, Shaffer RN. Timolol and pediatric glaucomas. Ophthalmology. 1981;88(3):249–52.

Morris S, Geh V, Nischal KK, Sahi S, Ahmed M, a. S. Topical dorzolamide and metabolic acidosis in a neonate. Br J Ophthalmol. 2003;87(8):1052–3.

Olson RJ, Bromberg BB, Zimmerman TJ. Apneic spells associated with timolol therapy in a neonate. Am J Ophthalmol. 1979;88(1):120–2.

Passo MS, Palmer EA, Van Buskirk EM. Plasma timolol in glaucoma patients. Ophthalmology. 1984a;91(11):1361–3.

Passo MS, Palmer EA, Van Buskirk EM. Plasma timolol in glaucoma patients. Ophthalmology. 1984b;91(11): 1361–3.

Portellos M, Buckley EG, Freedman SF. Topical versus oral carbonic anhydrase inhibitor therapy for pediatric glaucoma. J AAPOS. 1998;2(1):43–7.

Raber S, Courtney R, Maeda-Chubachi T, Simons BD, Freedman SF, Wirostko B. Latanoprost systemic exposure in pediatric and adult patients with glaucoma: a phase 1, open-label study. Ophthalmology. 2011;118(10):2022–7.

Sabri K, Levin AV. The additive effect of topical Dorzolamide and systemic acetazolamide in pediatric glaucoma. J AAPOS. 2006;10(5):464–8.

Yanovitch TL, Enyedi LB, Schotthoeffer EO, Freedman SF. Travoprost in children: adverse effects and intraocular pressure response. J AAPOS. 2009;13(1):91–3.

Zimmerman TJ, Kooner KS, Morgan KS. Safety and efficacy of timolol in pediatric glaucoma. Surv Ophthalmol. 1983;28:262–4.

Combined Trabeculectomy with Trabeculotomy

31

Karthikeyan Mahalingam, Antriksh Wahi, and Shikha Gupta

31.1 Introduction

Almost all patients with childhood glaucoma need surgical intervention. Early intervention helps to reverse the corneal edema and preserve a healthy optic disc. Compared to adult glaucoma surgeries, challenges faced in childhood glaucoma surgeries are as follows:

- Need of examination under anesthesia before (planning) or after (monitoring/managing complications) surgery.
- Differences in anatomy: Small palpebral fissure, large eyeball, less rigid and thin sclera, and stretched limbus causing alteration in usual landmarks.
- Lower success rate due to the immense healing response and a longer life.

Angle-based surgeries (goniotomy/trabeculotomy) or guarded filtration surgeries (trabeculectomy) performed alone have a limited success rate in severe cases of childhood glaucomas. So, Luntz first proposed the concept of combined trabeculectomy with trabeculotomy for childhood glaucomas as it provides a dual outflow (through Schlemm's canal and trabeculectomy fistula), thus increasing the success rate. Elder et al. reported the 2-year success rate of primary trabeculectomy to be 72% and the 2-year success rate increased to 93.5% for combined trabeculectomy with ab externo trabeculotomy (CTT). The use of antimetabolites (mitomycin C) further increases the success rate of glaucoma filtering surgeries.

31.2 Indications

- As a primary intervention for severe primary congenital glaucoma (PCG) (as proposed by Gupta V et al. 2022):
  - Neonatal-onset PCG
  - Corneal diameter ≥ 13 mm
  - Axial length (AL) ≥ 24 mm
  - Total or significant corneal haze/opacity (no anterior chamber structures visible)
- Failed goniotomy or other minimally invasive angle surgeries.
- Failed trabeculectomy.
- Severe congenital glaucomas without significant peripheral anterior synechiae not precluding trabeculotomy.
- <2 years age, as in children more than 2 years, a stand-alone trabeculectomy is preferred.

Supplementary Information The online version contains supplementary material available at https://doi.org/10.1007/978-981-19-7466-3_31.

K. Mahalingam · A. Wahi · S. Gupta (✉)
Dr. Rajendra Prasad Centre for Ophthalmic Sciences, All India Institute of Medical Sciences, New Delhi, India
e-mail: shikhagupta@aiims.edu

S. Gupta et al. (eds.), *Childhood Glaucoma*, https://doi.org/10.1007/978-981-19-7466-3_31

31.3 Preoperative Considerations

1. Thorough clinical examination preoperatively or during EUA is necessary to look at corneal diameters, baseline untreated intraocular pressure (IOP), corneal opacity, fundus, AL, etc. Postoperatively, it is important to detect early/late surgical failure and in following up the children for optimal IOP control.
2. Posterior segment examination is mandatory before the surgery. In cases of hazy media where posterior segment examination cannot be done using either direct or indirect ophthalmoscopy, B-scan ultrasonography should be performed.
   (a) To explain prognosis based on damage to the optic disc.
   (b) To rule out intraocular tumor presenting with secondary glaucoma (where glaucoma filtration surgery is contraindicated).
   (c) To look for retinal detachment, vitreous hemorrhage, and other pathologies.
3. In cases of uveitic glaucoma, the eye should be quiet for at least 3 months before elective surgery, however in cases with medically uncontrolled glaucoma, immediate IOP loweing surgery needs to be performed.
4. Use a short course of low-dose topical steroids (fluorometholone) preoperatively to optimize ocular surface, if there is conjunctival inflammation (due to the use of topical glaucoma medications or secondary to vernal keratoconjunctivitis or if glaucoma is secondary to previous surgery).

31.4 Surgical Steps (Video 31.1, Fig. 31.1)

Surgery is performed under general anesthesia.

- To expose the surgical site, either a corneal traction suture or a superior rectus bridle suture is placed (Figs. 31.1a and 31.2a, b).
- Look for conjunctival mobility (if the eye has been previously operated, buckling surgery, previous trabeculectomy) and choose the site without fibrosis. Avoid areas where the sclera is thin or staphylomatous. As a rule, the superonasal quadrant is preferred so that superotemporal quadrant can be utilized for a re-surgery.
- Either a limbal-based (incision 8 to 10 mm posterior to the limbus) or fornix-based (incision at the limbus) peritomy could be created (Table 31.1) (Fig. 31.2c, d). However, due to the logistics of the requirement of general anesthesia in children for any repeat intervention like nonabsorbable suture removal, bleb leaks, etc. (both of which more with fornix-based surgeries), limbal-based approach is preferred in children where the peritomy is closed with conjunctiva-conjunctiva suturing with absorbable sutures like 8′0 Vicryl. On the contrary, fornix-based flaps require cornea-conjunctival suturing, preferred with non-absorbable sutures like monofilament nylon to ensure tight wound closure and is preferred for older children.
- Conjunctiva and tenon's are dissected from the sclera. Antimetabolites like mitomycin C 0.02% (primary surgery) to 0.04% (secondary surgery) are placed subconjunctivally for 1 to 3 min to reduce postoperative fibrosis. Although the use of mitomycin C increases the success rate of surgeries, caution must be applied to the dose and duration of its use because of long-term complications like thin cystic bleb, leak, and risk of endophthalmitis. We prefer to apply mitomycin C both subconjunctivally (3 min) and subsclerally (1 min) in a dose of 0.004% in very young children with reducing dose and duration for older children. Mitomycin C should be applied in a wider posterior area (to decrease the risk of a "ring of steel" forming, with a thin ischemic anterior bleb). After application, care should be taken to wash it off thoroughly with at least 20 mL balanced salt solution (BSS). Application of a higher dose of mitomycin C in younger individuals (as they have a greater healing response) can also predispose to thin bleb formation, and the risk of infection increases every year of the person's life. So, it is necessary to titrate its risk-benefit ratio.
- After achieving hemostasis, a triangular-, rectangular-, or trapezoid-shaped scleral flap (Fig. 31.1c) is made (based on the surgeon's preference) in the superonasal (preferred) or superotemporal quadrant. Flap width vary from

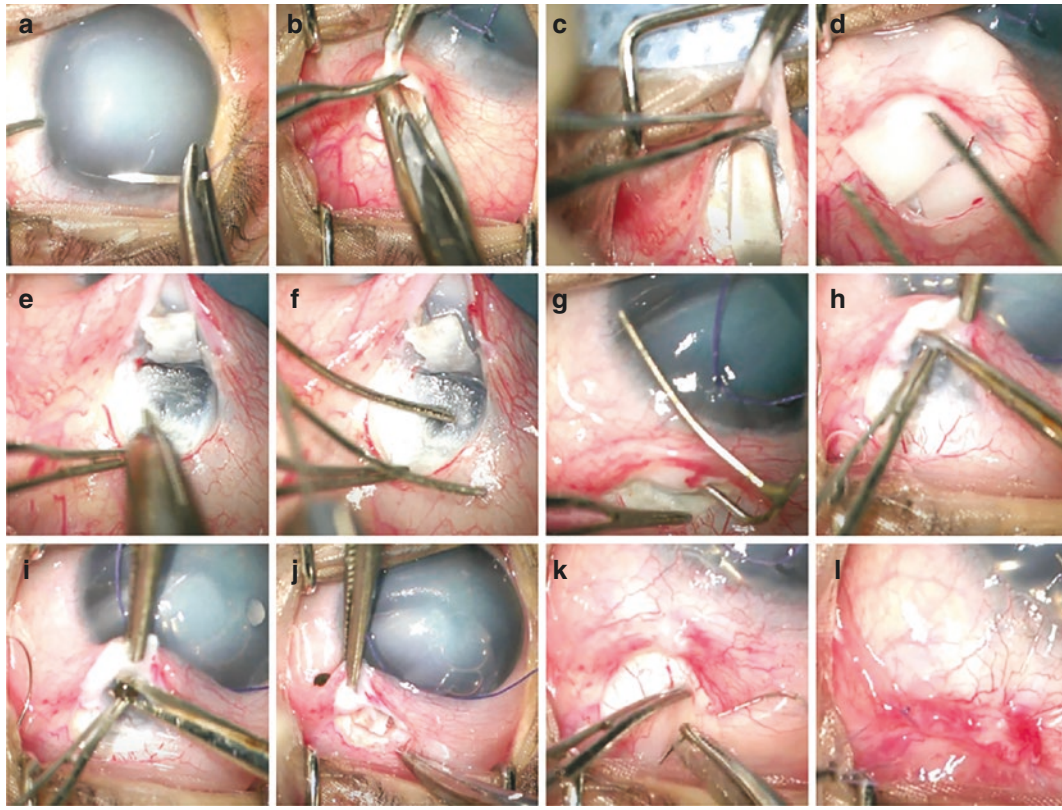

Fig. 31.1 Intraoperative images showing steps of combined trabeculectomy with trabeculotomy augmented with mitomycin C. (**a**) Corneal traction suture, (**b**) limbal-based conjunctival flap, (**c**) scleral flap, (**d**) application of mitomycin C using Merosel sponge, (**e**) radial incision over scleral spur, (**f**, **g**) trabeculotomy done aided through Harm's trabeculotome on each side, (**h**) sclerostomy done using Vannas scissors, (**i**) peripheral iridectomy through Vannas scissors, (**j**) suturing scleral flap using 10′0 Vicryl suture, (**k**) suturing conjunctiva using 8′0 running closure of vicryl suture, (**l**) corneal wound closed using 10′0 MFN

3 to 4.5 mm and length from 3 to 4 mm to allow adequate visualizion of the Schlemm's canal. Bard-Parker handle with a blade or a disposable crescent knife can be used for fashioning the flap. Following this, mitomycin C is also applied subsclerally (Fig. 31.1d) and is washed out completely. After this, some surgeons may perform deep sclerectomy (Video 31.2), but due to lack of concrete evidence regarding its usefulness, it is not routinely performed during CTT.

- Scleral spur is identified externally as the junction between the narrow grayish-blue band (trabecular meshwork) and the white opaque sclera. A radial incision is made over the scleral spur to cut the external wall of the Schlemm's canal (Fig. 31.1e). The distal arm of Harms trabeculotomy probe is introduced into the canal (proximal arm acts as a guide) and rotated internally to disrupt the internal wall of the Schlemm's canal and trabecular meshwork, taking care to keep the inserted arm pulled up toward the roof to minimize complication risk (Fig. 31.1f, g). This procedure is carried on either side to affect an overall 100° to 120° angle cleavage.
- Anterior chamber (AC) paracentesis is done, miosis achieved with 2% pilocarpine and air injected in AC. An AC maintainer, infusing constant pressure air/BSS, can also be placed at this point of time to avoid AC collapse anytime during or after scleral ostium creation.
- The permanent/releasable flap sutures can be pre-placed to avoid prolonged AC shallowing. A block of the sclera/angle is removed at the grayish-blue transition zone using a sharp blade and Vannas scissors or Kelly Descemet punch (Fig. 31.1h). Then, peripheral iridectomy is car-

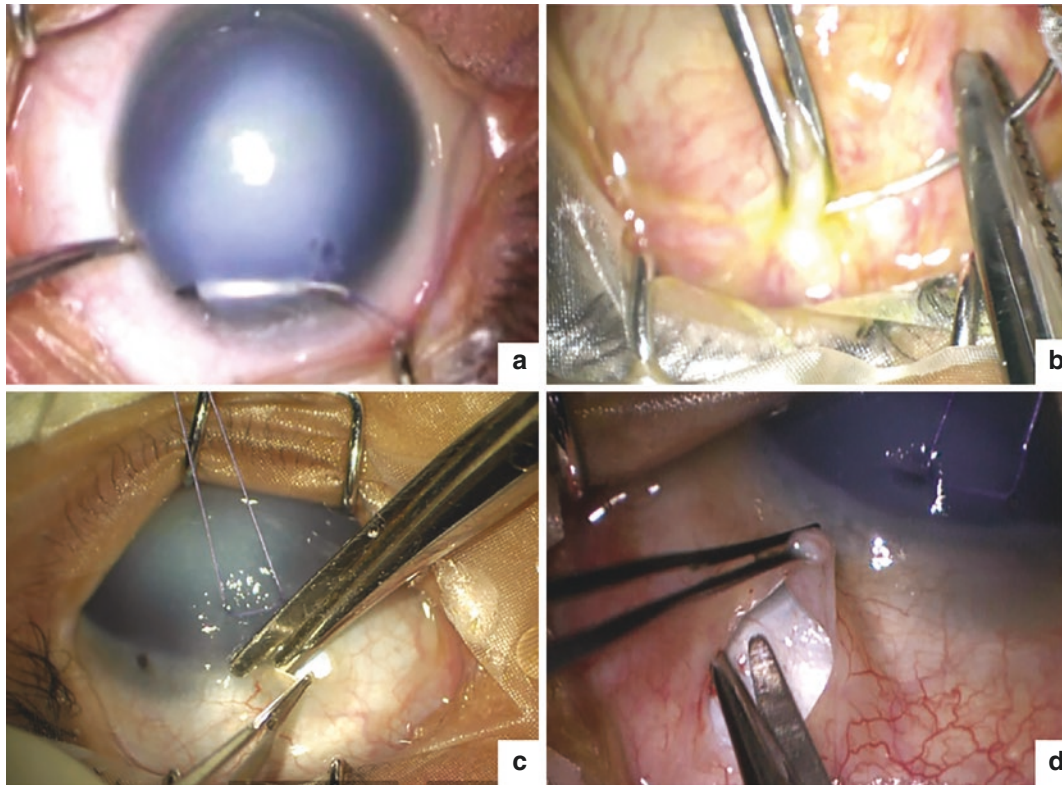

Fig. 31.2 Intraoperative image showing corneal traction suture (**a**), superior rectus bridle suture (**b**), fornix- (**c**) and limbal- (**d**) based conjunctival flaps

Table 31.1 Advantages and disadvantages of limbal- and fornix-based flaps

Limbal-based flaps	Fornix-based flaps
Advantages: • Use of absorbable sutures, Less postoperative discomfort and irritation • Provide a watertight closure, fewer chances of bleb leaking from early suture resorption as wound is posterior • Preferred in younger children, do not require repeat visit to operation theatre for suture removal	Advantages: • Posteriorly directed bleb • Easy to dissect the sclera and place releasable sutures • Favored in older children and those who have undergone previous surgeries who can allow suture removal on an outpatient basis
Disadvantages: • Exposure of surgical field hampered by the conjunctival flap • More chances of the localized bleb, limited by the ring of steel and hence greater risk of avascular bleb with bleb-related infections (BRI)	Disadvantages: • More chances of early postoperative discomfort and irritation due to non-absorbable suture • Astigmatism due to the sutures used to appose the conjunctiva with the corneal limbus • Chances of early wound leak and conjunctival retraction due to faster suture resorption

ried out (Fig. 31.1i), keeping the base of iridectomy a little more than the size of ostium to prevent it from being closed in the future.

- The scleral flap is closed at both ends with 10–0 monofilament nylon or 9 or 10′0 Vicryl absorbable sutures based on surgeon preference (Fig. 31.1j). In general, monofilament sutures incite less inflammation and fibrosis, but absorbable poly-filament sutures may dissolve faster to allow better scleral filtra-

tion. Releasable sutures can be used especially in high-risk cases like Sturge-Weber syndrome or aniridia or when the child is cooperative enough to allow slit-lamp removal.
- In the case of limbal-based flaps, the conjunctiva is closed with absorbable running 8–0 Vicryl suture (Fig. 31.1k). Suture is also passed through the sclera to anchor the bleb posteriorly and prevent anterior shifting of the bleb postoperatively. In the case of fornix-based flaps, nonabsorbable 10–0 monofilament nylon sutures are used as wing and mattress sutures to achieve corneal-conjunctival watertight closure.

31.5 Postoperative Medications

- Topical antibiotic and steroid (prednisolone or betamethasone) combination is given 6 to 8 times per day for the first 2 weeks and tapered over 6–8 weeks.
- Short-acting cycloplegics like tropicamide are prescribed in cycles twice a day to keep the pupil mobile, prevent posterior synechiae formation, reduce ciliary spasm, and deepen the anterior chamber.

31.6 Intraoperative Complications

31.6.1 Anterior Chamber Entry While Passing Corneal Traction Suture

- It can occur if traction suture is passed over the thin cornea (because of Haab's striae/scarring).
- Precaution: While passing traction suture, avoid thin areas in the cornea, and pass only partial thickness through the cornea.
- Management: Inject air in the anterior chamber; if it is not maintained, take a suture over the injection tract.

31.6.2 Conjunctival Buttonhole Formation

- It can occur if traumatic instruments (toothed forceps/Lims forceps) are used to handle the conjunctiva. Application of a high dose of mitomycin C for a longer duration can also predispose to thinning of the conjunctiva. Incidence 1.1%.
- Precaution: Use atraumatic forceps (Fechtner conjunctival forceps) to handle the conjunctiva.
- Management: Make a purse-string suture around the buttonhole with 10–0 absorbable/nonabsorbable suture. Bandage contact lens can be placed (if there is a small buttonhole near the limbus), glue such as cyanoacrylate or fibrin glue can also be used in some cases. In cases with large buttonholes, conjunctival grafting (autograft) can aslo be used.

31.6.3 Scleral Flap Buttonhole Formation/Disinsertion

- It usually occurs if a thin scleral flap is made. Use of traumatic forceps while handling the scleral flap can also cause buttonhole formation. Incidence 0.7%.
- Precaution: Make scleral flap of adequate thickness, use atraumatic forceps to hold the flap.
- Management: Suture the torn end of the scleral flap or create a scleral flap in a new site and use. If the defect is large, scleral patch graft can be used.

31.6.4 Vitreous Prolapse (Video 31.3, Fig. 31.3)

- It can occur if the corneal traction suture is not released during ostium creation or if the ostium is created posteriorly.
- Precaution: Release the corneal traction suture while making scleral ostium and peripheral iridectomy. Scleral ostium to be made as anteriorly as possible.

- Management: Vitrectomy to be done with the scissors. If the ostium is not filtering, another ostium is made more anteriorly into the cornea and the previous ostium is sutured one with non-absorbable 10–0 nylon.

31.6.5 Intraoperative Bleeding

- There is high chance of intraoperative bleeding in neovascular glaucoma, uveitic glaucoma, and if there is conjunctival inflammation (due to topical glaucoma drugs). Incidence: 8.4% (Fig. 31.4a).

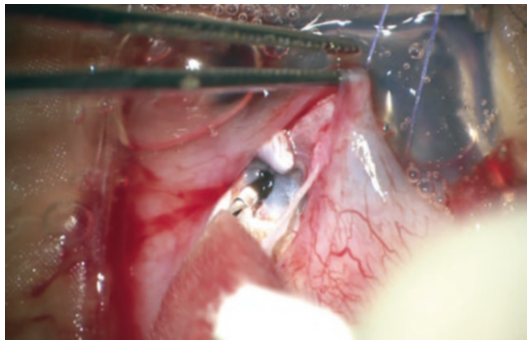

Fig. 31.3 Intraoperative image showing vitreous prolapse during trabeculectomy. Vitreous is confirmed by touching it with cotton swab and lifting it

- Precaution: Preoperative anti-VEGF to be given in neovascular glaucoma (Fig. 31.4b). Preoperative topical steroids can be given to reduce the inflammation.
- Management: Adequate cautery to be done intraoperatively.

31.6.6 Suprachoroidal Hemorrhage

- It is a rare complication. Occurs in high-risk cases like aphakia, vitrectomized eyes, patients on anticoagulants, pathological myopia, high preoperative IOP, sudden intraoperative hypotony and uncontrolled systemic hypertension. Incidence of intraoperative suprachoroidal hemorrhage is 0.15% (incidence during postoperative period varies from 1.6% to 6.1%). Intraoperatively it is diagnosed by the following signs: sudden shallowing of anterior chamber, altered fundal glow/reflex and increased IOP with firming of the eye.
- Precaution: Gradual lowering of intraocular pressure, preoperative mannitol injection, intraoperative AC depth maintenance, use of AC maintainer, and control of blood pressure are to be done to reduce incidence of suprachoroidal hemorrhage.
- Management: Initially it is managed conservatively with ocular hypotensive drugs, steroids,

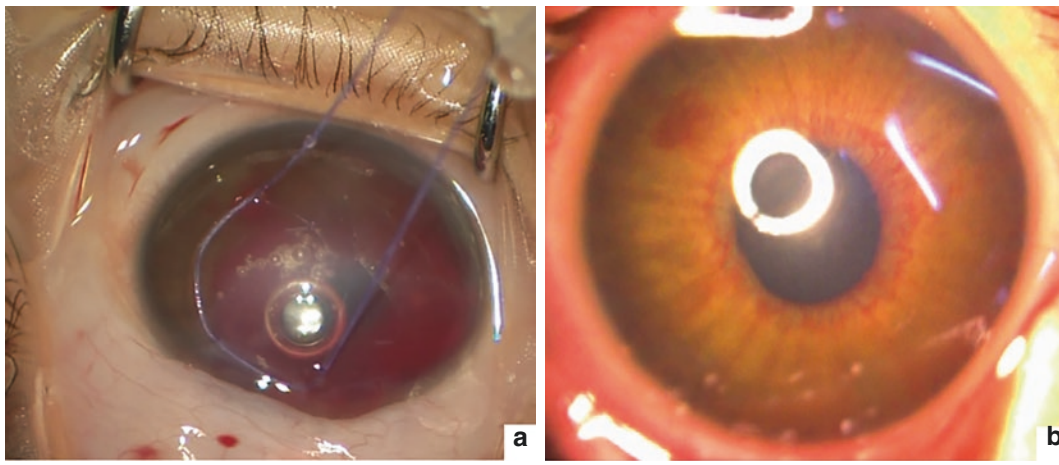

Fig. 31.4 (**a**) Intraoperative hyphema during trabeculectomy. (**b**) Clinical picture of an eye with neovascular glaucoma (which has high risk of intraoperative bleeding) showing corneal edema (due to high intraocular pressure) and neovascularisation of iris

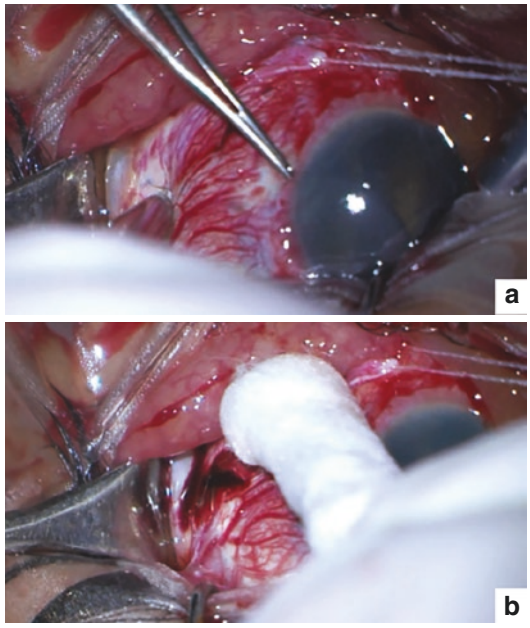

Fig. 31.5 Drainage of suprachoroidal hemorrhage: Lims forceps is used to hold the globe at limbus, conjunctival retractor is used to expose the surgical site. (**a**) Incision is made in the sclera with blade at the place where the choroidal detachment is highest (confirmed using ultrasonography), (**b**) pressure given with cotton swab to express the hemorrhage

and cycloplegics. If conservative managment fails, drainage of suprachoroidal hemorrhage will be the last resort (Fig. 31.5, Video 31.4).

31.6.7 Complications While Doing Trabeculotomy

- Arms of Harms trabeculotomy probe can pass behind iris causing iridodialysis (especially if iris is anteriorly inserted). Other complications include Descemet's membrane detachment, cyclodialysis, etc. These complications usually occur if the arms of Harms trabeculotomy probe are not positioned appropriately or if the anatomy of the buphthalmic eye is abnormal.
- Precaution: Confirm the position of the Harms trabeculotomy probe before cleaving the Schlemm's canal. Also make a small pass first against the scleral roof superiorly before tearing it apart.

Intraoperative and postoperative complications (Videos 31.5, 31.6, 31.7, 31.8; Figs. 31.6 and 31.7) are summarised in the Table 31.2).

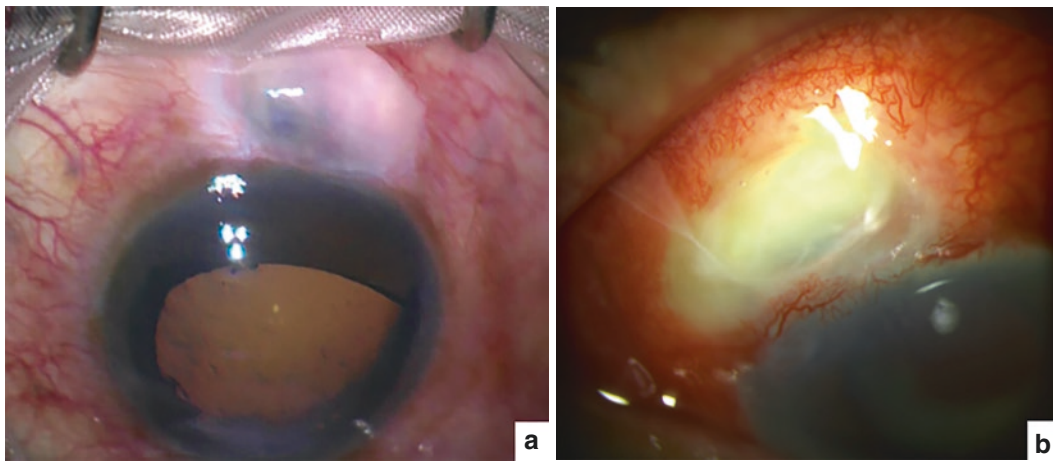

Fig. 31.6 (**a**) Clinical picture showing thin cystic avascular bleb post-trabeculectomy, (**b**) Clinical picture of bleb-related endophthalmitis (in a case of thin cystic avascular bleb) showing white (bleb) on red (inflammed vessels) appearance

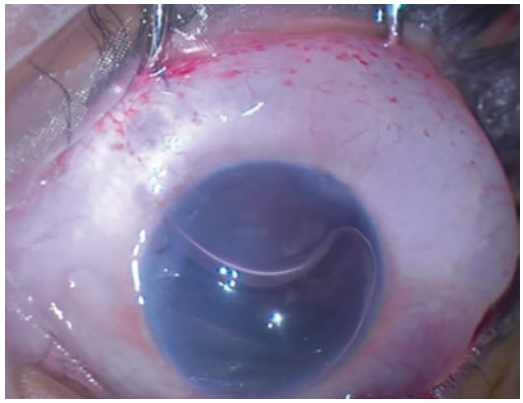

Fig. 31.7 Intraoperative image showing shallowing of anterior chamber due to over filtering bleb

Table 31.2 Intraoperative and postoperative complications of combined trabeculectomy with trabeculotomy

Intraoperative complications	Postoperative complications
Anterior chamber entry while passing corneal traction suture	Shallowing of the anterior chamber
Conjunctival buttonhole formation	Bleb leak (Video 31.5)
Scleral flap buttonhole formation/disinsertion, scleral perforation	Overfiltration
Intraoperative bleeding Hyphema	Flat bleb: • Tight flap sutures • Iris/blood/exudate/ vitreous plugging ostium
Iris prolapse Vitreous prolapse	Hyphema
Descemet's membrane detachment Iridodialysis Cyclodialysis	Localized encysted bleb (Video 31.6) Cystic avascular bleb (Video 31.7) Bleb-related endophthalmitis (Fig. 31.6) Overhanging bleb causing astigmatism
Suprachoroidal hemorrhage	Hypotonic maculopathy
Recurrent shallowing of the anterior chamber (Video 31.8, Fig. 31.7)	Serous choroidal detachment Suprachoroidal hemorrhage
Malignant glaucoma	Malignant glaucoma

31.7 Conclusions

As children have an immense healing response, trabeculectomy is combined with trabeculotomy to increase the success rate of surgery. Combined trabeculectomy with trabeculotomy is one of the most widely performed surgeries for childhood glaucoma. The surgeon should individualise his treatment plan to tailor to each child's unique requirements.

Suggested Reading

Al-Hazmi A, Zwaan J, Awad A, Al-Mesfer S, Mullaney PB, Wheeler DT. Effectiveness and complications of mitomycin C use during pediatric glaucoma surgery. Ophthalmology. 1998;105(10):1915–20. https://doi.org/10.1016/S0161-6420(98)91041-7.

Elder MJ. Combined trabeculotomy-trabeculectomy compared with primary trabeculectomy for congenital glaucoma. Br J Ophthalmol. 1994;78:78745–8.

Gupta V, Bhandari A, Gupta S, Singh A, Gupta A. Consanguinity and severity of primary congenital glaucoma. J AAPOS. 2022;26(3):119.e1–5.

Jampel HD, Musch DC, Gillespie BW, et al. Perioperative complications of trabeculectomy in the collaborative initial glaucoma treatment study (CIGTS). Am J Ophthalmol. 2005;140(1):16–22. https://doi.org/10.1016/j.ajo.2005.02.013.

Khan AO. A surgical approach to pediatric glaucoma. Open Ophthalmol J. 2015;9:104–12. https://doi.org/10.2174/1874364101509010104; Published 2015 May 15.

Mandal AK, Bhatia PG, Gothwal VK, Reddy VM, Sriramulu P, Prasad MS, et al. Safety and efficacy of simultaneous bilateral primary combined trabeculotomy–trabeculectomy for developmental glaucoma in India. Indian J Ophthalmol. 2002;50:13–9.

Mandal A, Matalia J, Nutheti R, et al. Combined trabeculotomy and trabeculectomy in advanced primary developmental glaucoma with corneal diameter of 14 mm or more. Eye. 2006;20:135–43. https://doi.org/10.1038/sj.eye.6701817.

Morales J, Al Shahwan S, Al Odhayb S, Al Jadaan I, Edward DP. Current surgical options for the management of pediatric glaucoma. J Ophthalmol. 2013;2013:763735. https://doi.org/10.1155/2013/763735.

Mullaney PB, Selleck C, Al-Awad A, Al-Mesfer S, Zwaan J. Combined Trabeculotomy and trabeculectomy as an initial procedure in uncomplicated congenital glaucoma. Arch Ophthalmol. 1999;117(4):457–60. https://doi.org/10.1001/archopht.117.4.457.

Vaziri K, Schwartz SG, Kishor KS, Fortun JA, Moshfeghi DM, Moshfeghi AA, Flynn HW Jr. Incidence of postoperative suprachoroidal hemorrhage after glaucoma filtration surgeries in the United States. Clin Ophthalmol. 2015;9:579–84. https://doi.org/10.2147/OPTH.S78359.

Goniotomy

32

Ashok Kumar Singh and Sushmita Kaushik

32.1 Introduction

Childhood glaucoma is a potentially blinding condition. Although numbers are less, it is the second-largest cause of blind-person years, next only to cataracts. Approximately 40% of childhood blindness is avoidable. This makes early diagnosis and prompt intervention more critical in patients with childhood glaucoma. Medical management is supplementary, and surgical intervention is the definitive treatment.

The choice of surgery for childhood glaucoma depends on multiple factors such as the clarity of the cornea, degree of goniodysgenesis, and associated ocular or systemic abnormalities. Angle surgeries are preferred in patients with clear cornea where trabecular meshwork (TM) can be seen. Type I goniodysgenesis where TM is visible is more amenable to angle surgeries than type II goniodysgenesis. Angle surgeries are also preferred in primary congenital glaucoma (PCG) and non-acquired childhood glaucoma patients.

Goniotomy is one of the oldest surgical techniques described for childhood glaucoma, being performed for the first time by De Vincentiis in 1893 for all types of glaucoma. However, Barkan is credited with providing more elaborate details of the surgery, combining it with the gonioscopy view and also providing details of the surgical outcome. Introduction of viscoelastic materials has further enhanced the safety of the surgery while also providing visco-tamponade of any intraoperative bleed. When done on patients optimally selected for goniotomy, results are promising.

Barkan in 1953 described an 80% success rate with adequate intraocular pressure (IOP) control in 188 patients treated over 17 years. Shaffer described a 94% success rate in 287 eyes who underwent one or two goniotomies. Other series from the western literature also report very high success rates (over 90%). However, the success rate decreases sharply after 2 years, thus making case selection very important for goniotomy.

32.2 Indications

Primary congenital glaucoma (PCG) is the most common indication for goniotomy. It is usually performed as the initial procedure for intraocular pressure (IOP) control. Other non-acquired or acquired conditions require open angle or partial-angle closure. The common indications are summarized below:

Supplementary Information The online version contains supplementary material available at https://doi.org/10.1007/978-981-19-7466-3_32.

A. K. Singh · S. Kaushik (✉)
Glaucoma Services, Advanced Eye Centre, Postgraduate Institute of Medical Education and Research, Chandigarh, India

S. Gupta et al. (eds.), *Childhood Glaucoma*, https://doi.org/10.1007/978-981-19-7466-3_32

1. Primary congenital glaucoma (PCG).
2. Glaucoma associated with non-acquired ocular anomalies with open angles or limited angle closure:
   (a) Congenital ectropion uveae with open angles
   (b) Aniridia with open-angle or limited angle closure
   (c) Congenital iris hypoplasia with open angles
3. Glaucoma associated with non-acquired systemic disease or syndrome.
   (a) Sturge-Weber syndrome
   (b) Klippel-Trenaunay-Weber syndrome
4. Acquired glaucoma if angles are open.
   (a) Uveitic glaucoma
   (b) Steroid-induced glaucoma
5. Aphakic or pseudophakic secondary glaucoma with open angles.
6. Prophylactic goniotomy is sometimes done in non-glaucomatous aniridic eyes, especially in young patients, which is thought to prevent further closure and secondary glaucoma (Chen and Walton 1999).

32.3 Contraindications

Conditions that preclude the surgeon from viewing angle structures clearly, particularly the trabecular meshwork, are contraindicated for goniotomy or other angle surgeries. The following situations would usually preclude angle surgery:

1. The eyes with corneal scarring or cloudy cornea with a poor angle view.
2. Older children with advanced stage of the disease. These patients are at increased risk of bleeding due to dilated vessels and occasionally due to established collateral circulation.
3. The eyes with very large eyes in which the Schlemm's canal and aqueous outflow channels may be obliterated.

32.4 Preoperative Considerations

1. Complete ophthalmic examination in the clinic and during examination under anesthesia (EUA) is mandatory. Baseline IOP, pachymetry, axial length, keratometry, corneal clarity, corneal diameters, and gonioscopy, especially to look for the trabecular meshwork, are evaluated.
2. Posterior segment examination is mandatory before the surgery. In cases of hazy media, B-scan ultrasonography should be done. The patient should be screened for any tumor, mass lesion, retinal detachment, vitreous hemorrhage, or other retinal pathologies.
3. In the case of uveitic glaucoma, the eye should be quiet for at least 3 months before surgery.
4. A short course of systemic acetazolamide at 25 mg/kg/body weight in three divided doses may decrease corneal edema before surgery. This reduces corneal haze and facilitates better visualization of angle structures during surgery.

32.5 Surgical Details

32.5.1 Principles of Goniotomy

1. Goniotomy is an ab interno angle surgery.
2. Angle structures are visualized directly using surgical goniolens.
3. The nonfunctional trabecular meshwork is sliced using a knife or blade.
4. This provides a conduit for the aqueous to bypass the trabecular meshwork and exit the eye through the Schlemm's canal and collector channels.

32.5.2 Goniolens

Intraoperatively, angle structures are visualized using surgical direct goniolenses. Various goniolenses that are commonly used in clinical practice are shown in Fig. 32.1a–d.

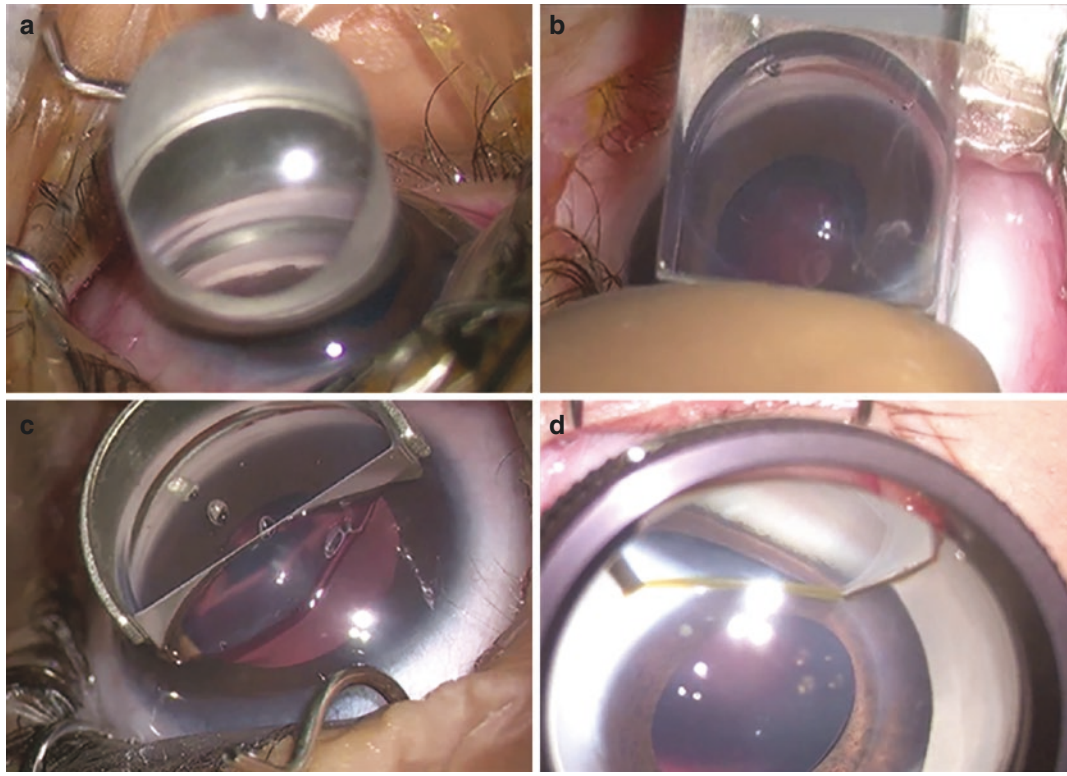

Fig. 32.1 (**a**) Swan Jacob goniolens, (**b**) Mori's upright lens, (**c**) Ritch goniolens, (**d**) Abrahams goniolens

32.6 Preparation in the Operating Room

Preparation for surgery is the essential part of an angle surgery. Position of patient, surgeon, and degree of tilt of microscope have implications on how smooth the surgery goes:

- The microscope is tilted approximately around 45° (Fig. 32.2).
- The head of the patient is tilted to the opposite side.
- The surgeon sits directly opposite the angle to be operated (Fig. 32.2).

Fig. 32.2 Microscope is tilted at 45° and the surgeon sits directly opposite to the angle to be treated

32.7 Surgical Steps (Video 32.1)

1. The surgery in infants is performed under general anesthesia.
2. The side port is made using a microvitreoretinal (MVR) or goniotomy knife 180° away from the angle to be treated. The nasal angle is preferred for initial goniotomy, so the paracentesis port is made temporally in the clear cornea (Fig. 32.3a).
3. Pilocarpine 2% is injected into the anterior chamber through a paracentesis port to constrict the pupil. This protects the lens during intraocular maneuvering.

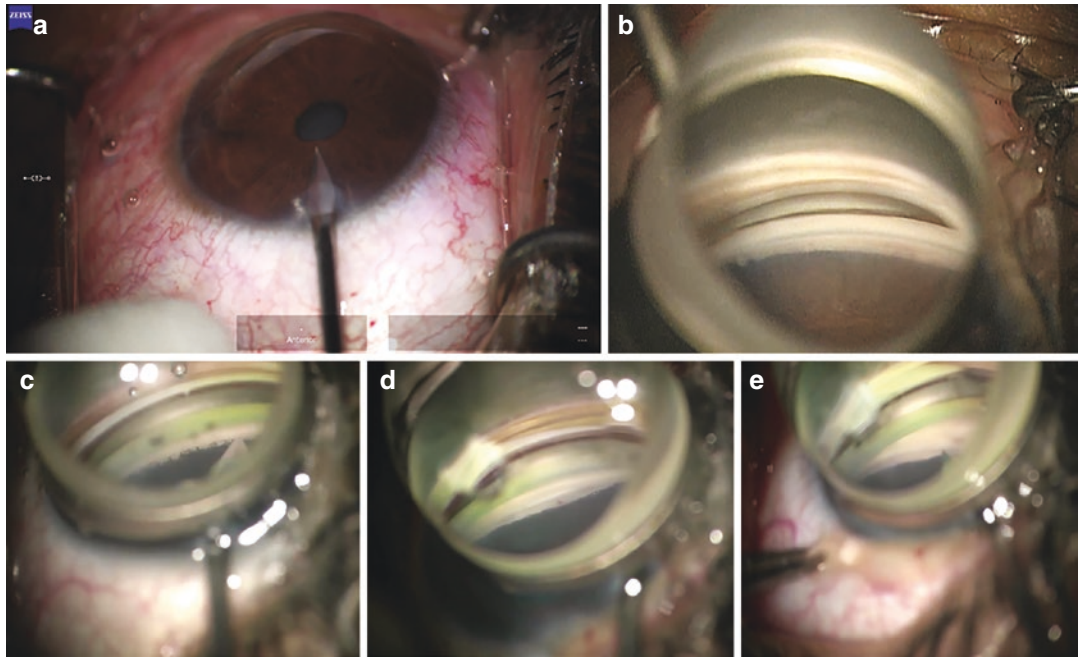

Fig. 32.3 (**a**) Paracentesis port is made in the clear cornea using MVR blade. (**b**) Swan Jacob goniolens placed directly over the cornea to get a clear view of the angle before proceeding with the surgery. (**c**) The tip of the blade/needle is engaged into the middle to the anterior trabecular meshwork. (**d**) Formation of goniocleft and falling back of the iris indicating successful goniotomy. (**e**) Rotation of the eye by the assistant in both directions to bring the untreated angle into surgeon's view for maximum possible goniotomy

4. The angle is visualized using the Swan Jacob lens or any other goniolens. A mound of sodium hyaluronate is placed over the cornea. This is followed by placing the Swan Jacob goniolens over the cornea to get a clear view of the angle (Fig. 32.3b). About 2 mm of the cornea should be left exposed after placing goniolens for comfortable and nontraumatic entry of microvitreoretinal (MVR) or goniotomy knife or 24-gauge needle.
5. The anterior chamber is deepened using cohesive viscoelastic material.
6. Goniotomy is performed using an MVR blade or a 24-gauge needle mounted on a syringe loaded with a dispersive viscoelastic (hydroxypropyl methylcellulose 2%). The tip of the blade/needle is engaged into the middle to the anterior trabecular meshwork and is moved in either direction as far as corneal wound and angle view permit (Fig. 32.3c).
7. Successful goniotomy is indicated by the formation of goniocleft and falling back of the iris (Fig. 32.3d). The incision should be superficial and smooth. The surgeon should see the incision rather than feel a cutting sensation, which indicates that the cut may be too deep.
8. The eye is rotated by the assistant in either direction to bring the untreated angle into view of the surgeon. This allows treatment of maximum angle possible around 150–180° (Fig. 32.3e).
9. The side port is sutured using 10–0 nylon or 10–0 polyglactin suture.

32.8 Postoperative Care

1. Parents should be instructed and taught to keep the child's head tilted toward the side of the surgery to ensure that any hyphema if

occurred, should be away from the raw area created.
2. Topical steroids are started, 2 hourly tapered over 4–6 weeks.
3. Tobramycin 0.3% drops q.i.d is started for 2–3 weeks and then stopped.
4. Cycloplegics or mydriatics should be strictly avoided postoperatively.
5. Pilocarpine 2% may be instilled for a short time postoperatively. The rationale for its use after the goniotomy procedure is its miotic effect by which the iris is pulled away from the incision and theoretically may prevent the formation of peripheral anterior synechiae. Peripheral anterior synechiae can lead to the closure of the cleft created during goniotomy, which may lead to the failure of the procedure. While the theoretical benefit of pilocarpine has been proposed, its actual benefit is yet to be proved.

32.9 Advantages

1. Goniotomy is a faster and less traumatic procedure than other glaucoma surgeries. Shorter operating time decreases the patient's exposure to general anesthesia.
2. The surgical limbus, conjunctiva, and sclera remain intact with goniotomy, unlike trabeculectomy or ab externo trabeculotomy.
3. There is minimal intraocular manipulation, unlike ab interno trabeculotomy, thus decreasing the possible intraoperative complications.

32.10 Disadvantages

1. Goniotomy is a technically demanding procedure that requires considerable surgical experience to master.
2. Special instrumentation and proper patient selection are necessary.
3. Goniotomy requires a clear view of angle structures, which precludes its use in patients with a cloudy cornea.
4. It is less useful in severe or advanced glaucoma.

32.11 Complications

1. Hyphema
   (a) Most common complication.
   (b) The intraoperative bleed may limit the view and the amount of angle treated.
   (c) Mostly, it resolves spontaneously; however, a full chamber hyphema that fails to resolve or hyphema threatening corneal staining or uncontrolled IOP should undergo an anterior chamber (AC) washout.
2. Injury to the iris and lens
   (a) Most likely to occur while passing MVR blade or goniotomy blade if the AC remains shallow.
   (b) Intracameral dispersive viscoelastic should be used to deepen the anterior chamber.
3. Iridodialysis or cyclodialysis
   (a) It occurs if the incision is made too posterior or too deep.
   (b) The surgeon should be familiar with the anterior segment anatomy and angle structures.
   (c) Surgery should be performed only in areas viewed adequately.

32.12 Options After Failed Surgery

1. If primary goniotomy does not satisfactorily control the patient's glaucoma, secondary goniotomy may be planned for the untreated area.
2. The untreated angle can be treated by an ab externo procedure, i.e., trabeculectomy or combined trabeculotomy-trabeculectomy.
3. Since the conjunctiva and sclera are not incised during goniotomy, a glaucoma drainage device may be placed, or a second trabeculectomy may be performed if deemed necessary for extremely refractive cases.

32.13 Conclusions

In conclusion, goniotomy is a valuable surgical approach in the armamentarium against glaucoma. Goniotomy is a viable initial approach, especially in primary congenital glaucoma, and has its place in other surgeries such as trabeculectomy, drainage implants, and laser treatments.

Suggested Reading

Anderson DR. Trabeculotomy compared to goniotomy for glaucoma in children. Ophthalmology. 1983;90(7):805–6.

Barkan O. Technique of goniotomy. Arch Ophthalmol. 1938;19:217–21.

Barkan O. Surgery of congenital glaucoma; review of 196 eyes operated by goniotomy. Am J Ophthalmol. 1953;36(11):1523–34.

Chen TC, Walton DS. Goniosurgery for prevention of aniridic glaucoma. Arch Ophthalmol. 1999;117(9):1144–8.

De Vincentis C. Incisions dell Angolo video nel glaucoma. Ann Ophthalmol. 1893;22:540–2.

Gilbert C, Foster A. Childhood blindness in the context of vision 2020: the right to sight. Bull World Health Organ. 2001;79:227–32.

Kaushik S, Gupta G, Thattaruthody F, Dhingra D, Kumari K, Arora A, Snehi S, Raj S, Pandav SS. Goniotomy for initial and re-surgery for childhood glaucoma in northern India. Indian J Ophthalmol. 2021;69(8):2088–94.

SD MP Jr, Berry DP. Goniotomy vs. external trabeculotomy for developmental glaucoma. Am J Ophthalmol. 1983;95(4):427–31.

Shaffer RN. Prognosis of goniotomy in primary infantile glaucoma (trabeculodysgenesis). Trans Am Ophthalmol Soc. 1982;80:321–5.

Walton DS, Hodapp E. Angle surgery: goniotomy. surgical management of childhood glaucoma. 2018:49–55.

33 Illuminated Microcatheter-Assisted Trabeculotomy

Tanuj Dada and Saurabh Verma

33.1 Introduction

Goniotomy and trabeculotomy are the primary procedure of choice in non-severe primary congenital glaucoma. While ab externo trabeculotomy can be performed in hazy corneas, goniotomy is often difficult as corneal haze in congenital glaucoma precludes visualization of angle structures. The conventional trabeculotomy technique of using rigid metallic instruments for the aforementioned procedures can open up to 1/3 angle in a single sitting. Determining the accurate placement of trabeculotomy in the Schlemm's canal is often difficult, and false passage into the anterior chamber and suprachoroidal space can happen. Sometimes, multiple procedures are required before target IOP is achieved, leading to conjunctival scarring which can adversely affect the outcome of any future filtration surgery, if needed.

To overcome these limitations of conventional techniques, 360° (circumferential, ab externo) trabeculotomy was first described using a 6–0 polypropylene suture. Retrieval of the leading end from the original cut-down site and contrast of blue-colored suture leading to better visualization via gonioscopy even in hazy cornea helped in ensuring correct suture placement. Deroofing the whole circumference of the Schlemm's canal leads to improved functional results. Long-term studies have proven the higher efficacy of this approach over conventional trabeculotomy. However, complications such as false passage and incomplete canalization are still major concerns. This was later improved by the development of a flexible illuminated microcatheter. Illuminated microcatheter allows trans-scleral visualization, unlike suture which requires gonioscopic visualization, thus reducing the risk of false passage. Since most serious complications of suture technique can be avoided by using an illuminated microcatheter, and it has been proved to have better surgical outcomes than conventional trabeculotomy and goniotomy, this procedure is now the preferred surgical approach as primary surgery for congenital glaucoma.

Two types of illuminated microcatheters have been used for performing 360° trabeculotomy:

- Glaucolight (DORC, Netherland; Fig. 33.1) has a 40 G/15-micron diameter shaft with an integrated battery-powered LED light source at the leading edge.

Supplementary Information The online version contains supplementary material available at https://doi.org/10.1007/978-981-19-7466-3_33.

T. Dada
Glaucoma Services, Dr. Rajendra Prasad Centre for Ophthalmic Sciences, All India Institute of Medical Sciences, Delhi, India

S. Verma (✉)
Dr. Rajendra Prasad Centre for Ophthalmic Sciences, All India Institute of Medical Sciences, Delhi, India

S. Gupta et al. (eds.), *Childhood Glaucoma*, https://doi.org/10.1007/978-981-19-7466-3_33

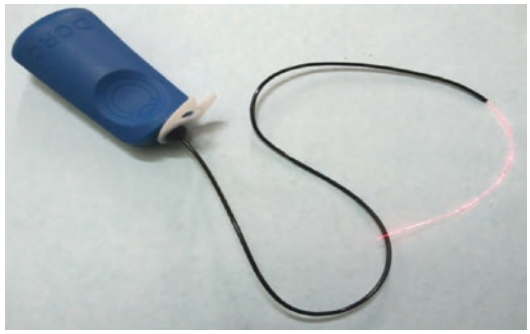

Fig. 33.1 Glaucolight, DORC International, Netherlands

Table 33.1 Harms trabeculotomy vs. illuminated microcatheter-assisted trabeculotomy

Harms trabeculotomy	Illuminated microcatheter-assisted trabeculotomy
1. Can open only up to 1/3 angle in a single sitting	1. 360° angle can be treated in single sitting
2. Cost-effective	2. Costly equipment
3. Short surgical time	3. Longer surgical time
4. Relatively easy to learn	4. Steep learning curve
5. Higher rate of the Descemet's membrane detachment and iridodialysis due to rigid instrument	5. Higher rate of hyphema
6. Causes conjunctival scarring	6. Spares the superior conjunctiva for future trabeculectomy if needed
7. Difficult to ascertain correct positioning in the Schlemm's canal	7. Illuminated tip results in easy identification of correct placement and advancement
8. Can be combined with trabeculectomy	8. Usually done as a standalone procedure
9. Partial opening of the Schlemm's canal leads to a lower reduction in IOP as compared to circumferential opening	9. Studies have supported a higher success rate than Harms trabeculotomy

- iTrack (Ellex, Menlo Park, California) consists of a 250-micron shaft enclosing a guidewire and fiber-optic illuminated tip.

Both devices have an atraumatic tip for smooth passage through the Schlemm's canal. iTrack has the added advantage of having an integrated screw-type ophthalmic viscosurgical device (OVD) injector which allows for viscodilation and enlargement of distal drainage/collector channels. The advantages and disadvantages of illuminated microcatheter-assisted trabeculotomy over conventional trabeculotomy have been described in Table 33.1.

33.2 Indications for Illuminated Microcatheter Circumferential Trabeculotomy

1. As initial surgery for the management of primary congenital glaucoma (successful IOP reduction has been reported in 80 to 90% of cases).
2. As a second procedure following failed angle surgeries (studies have proven it to be a reasonable choice for repeat surgical treatment with a success rate reaching almost 80%).
3. As a combined procedure with trabeculectomy (studies have supported higher efficacy of combined surgeries over either procedure alone).
4. This procedure may also be useful in certain conditions such as Sturge-Weber syndrome which has a high incidence of choroidal hemorrhage/effusions with conventional full-thickness filtration surgery.

33.3 Contraindications

Conditions such as angle-closure glaucoma, neovascular glaucoma, angle recession glaucoma and uveitic glaucoma which have synechial angle-closure or angle scarring are not suitable for this procedure.

33.4 Preoperative Considerations

1. Though the ab externo approach is the more widely followed, recently ab interno approach is also being increasingly used. The choice between the two is primarily decided by corneal haze as the ab interno procedure is difficult in such a scenario (Fig. 33.2).

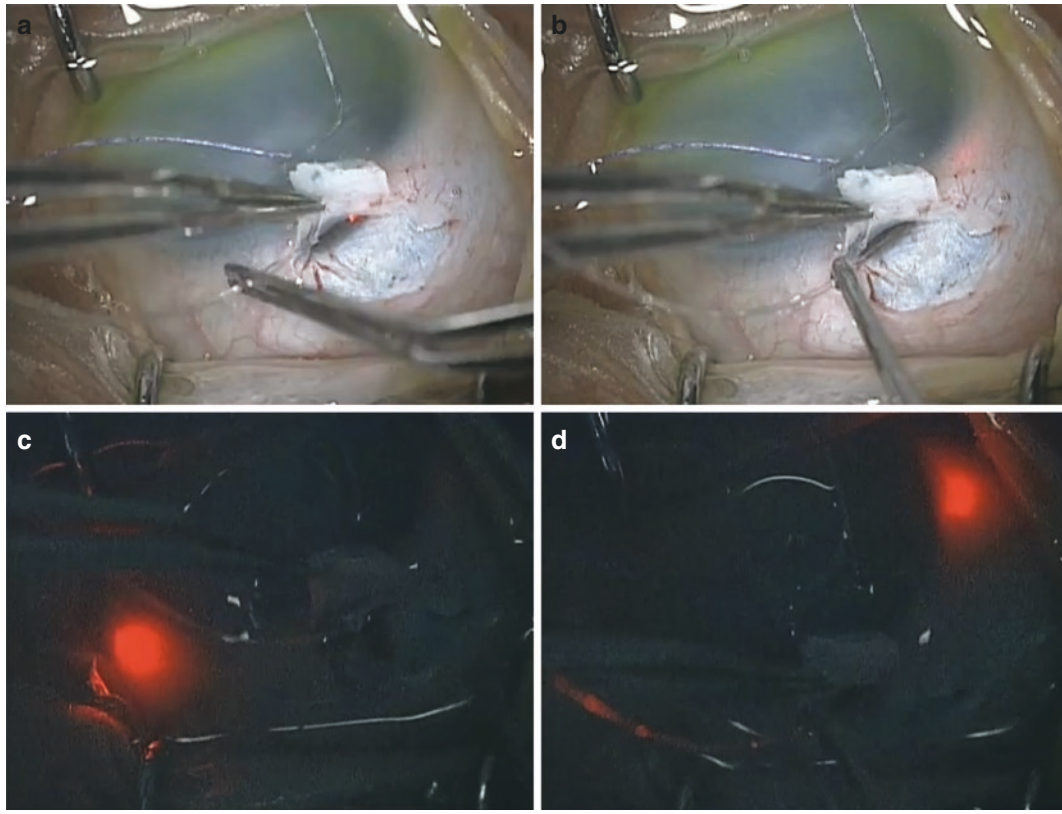

Fig. 33.2 Illuminated microcatheter-assisted trabeculotomy being performed in the hazy cornea. After fornix-based peritomy, creation of a scleral flap, and identification of the Schlemm's canal, a microcatheter is introduced into the canal. Note the easy visualization of advancing illuminated microcatheter tip in the canal (**a**–**d**)

2. Trabeculotomy is a bleb-less technique. This is especially desirable in children who otherwise are prone to a lifelong risk of blebitis and endophthalmitis.

33.5 Surgical Steps

Ab externo microcatheter-assisted trabeculotomy (Videos 33.1 and 33.2).

A temporal location is preferred for trabeculotomy as that leaves the superior conjunctiva intact for a future trabeculectomy if required:

1. A corneal stay suture is applied using spatulated 8–0 polyglactin.
2. A fornix-based localized peritomy is performed in the temporal quadrant. Hemostasis is achieved using wet field cautery.
3. A 4×4-mm superficial scleral flap is raised. This is followed by the creation of a deep scleral flap to identify and deroof the Schlemm's canal.
4. Viscoelastic is injected at the cut end of the Schlemm's canal to make space for catheter insertion.
5. A microcatheter is introduced and advanced slowly within the Schlemm's canal with direct trans-scleral visualization of the microcatheter tip (Fig. 33.3).
6. After the completion of successful 360° catheterization, the catheter is retrieved from the other cut end of the Schlemm's canal (Fig. 33.4).
7. Paracentesis followed by air injection in the anterior chamber is done to maintain the anterior chamber during further steps.

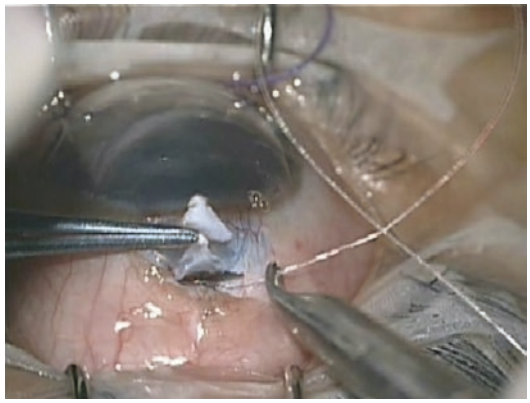

Fig. 33.3 Introduction of the tip of an illuminated microcatheter into the Schlemm's canal

8. A 360° circumferential trabeculotomy is completed by pulling the two ends of the catheter like a purse string (Fig. 33.5).
9. In cases of incomplete catheterization owing either to tip obstruction or misdirection, a repeat attempt can be made from the other end. In case of obstruction in both directions, conjunctival incision followed by scleral cut down can be performed over the leading tip of the catheter, and trabeculotomy is performed in the direction in which greater advancement is achieved.
10. Scleral flaps are closed using 10–0 monofilament nylon suture.

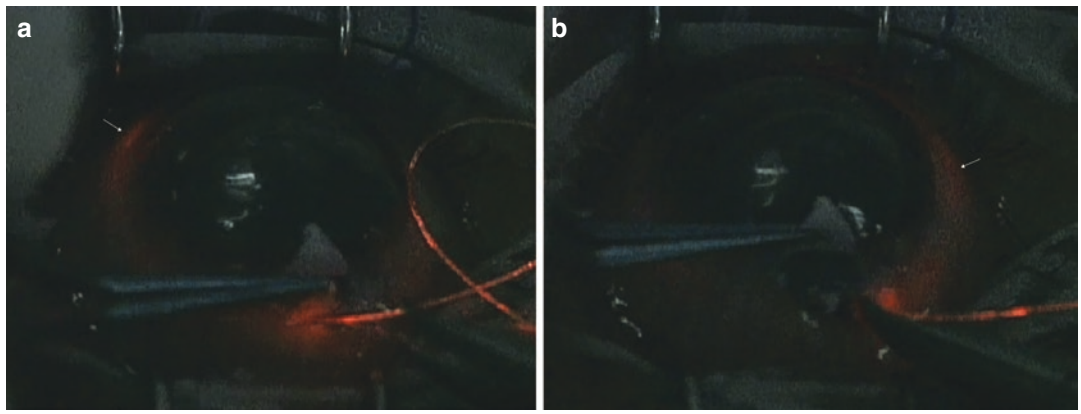

Fig. 33.4 (**a**, **b**) Illuminated microcatheter being inserted in the Schlemm's canal with a red light at tip marking the progression (white arrow)

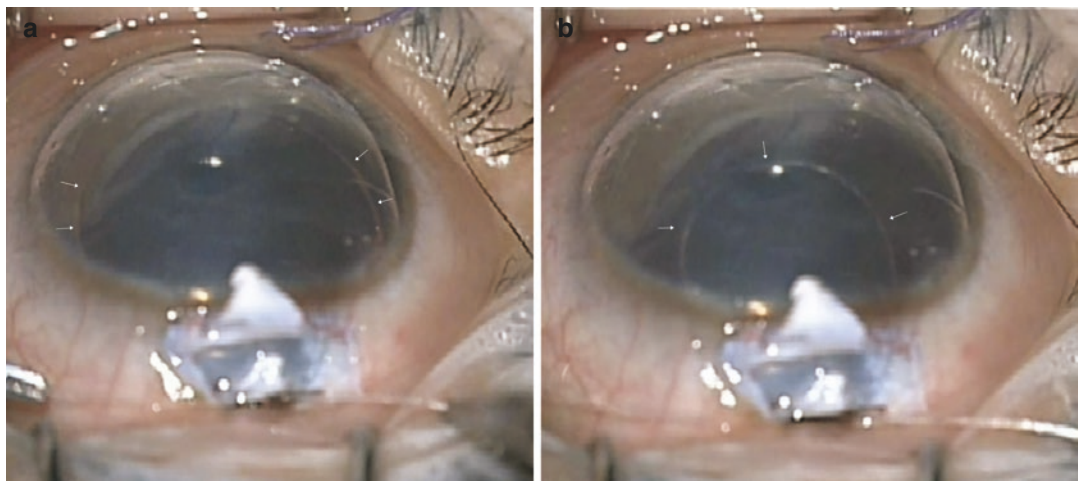

Fig. 33.5 After successful 360°catheterization of the Schlemm's canal (demonstrated by the exit of microcatheter from the other cut end of canal); (**a**) the two ends of microcatheter being pulled resulting in circumferential tension (white arrows) on the inner wall of the Schlemm's canal; (**b**) microcatheter (white arrows) in the anterior chamber after circumferential tearing of the canal

11. Peritomy is closed by continuous interlocking 8–0 round-bodied absorbable polyglactin sutures.

Ab interno microcatheter-assisted trabeculotomy:

1. Paracentesis followed by injection of viscoelastic in the anterior chamber is done through a temporal corneal incision.
2. A microcatheter is inserted in the anterior chamber through a track in the superonasal or inferonasal quadrant.
3. A 1–2 mm goniotomy is created at the nasal angle using a 25-G microsurgical (MVR) blade under gonioprism-assisted visualization.
4. A microsurgical forceps is used to hold the microcatheter and insert it in the Schlemm's canal from the site of goniotomy.
5. The microcatheter is advanced circumferentially under visualization.
6. After 360° catheterization, the distal tip is held and externalized through the temporal corneal incision creating a 360° circumferential ab interno trabeculotomy.
7. In case of obstruction leading to partial canalization, trabecular meshwork can be cut down, and a microcatheter can be brought into the anterior chamber to perform partial trabeculotomy.
8. Viscoelastics are then washed out and corneal wounds are hydrated.
9. If the microcatheter becomes misdirected or obstructed, its distal end is retrieved under direct gonioscopic visualization.

Important differences between ab interno and ab externo approaches have been summarized in Table 33.2.

Table 33.2 Ab externo vs. ab interno microcatheter-assisted trabeculotomy

Ab externo microcatheter-assisted trabeculotomy	Ab interno microcatheter-assisted trabeculotomy
1. No gonioscope lens is required 2. Can be performed in the hazy cornea 3. Some conjunctival scarring will occur. However, the temporal approach is used to spare the superior conjunctiva for future surgeries if needed 4. Similar success rate to ab interno approach with lesser incidence of early postoperative IOP spike and reduced risk of lens touch	1. Requires tilting of the microscope and the eye and an assistant to hold the gonioscope lens 2. Difficult to perform in the hazy cornea 3. Ab interno approach spares the conjunctiva, thus avoiding conjunctival scarring and allowing for future filtration surgeries 4. Ab interno approach has a higher incidence of postoperative IOP spike. Possible retention of our viscoelastic results in ab interno approach and leaking of the aqueous through the scleral incision in ab externo approach constitute the possible reasons

33.6 Intraoperative Complications

Complications up to the creation of a scleral flap are the same as that of any standard trabeculectomy procedure. This procedure has a steep learning curve and often requires a longer intraoperative time when compared to trabeculectomy or Harms trabeculotomy. Failure to identify the Schlemm's canal is a frequent challenge experienced by new learners. Other complications are as follows:

1. Studies have reported a success rate of 50–90% in achieving 360°catheterization. Incomplete catheterization can be due to obstruction or premature breakthrough into the anterior chamber. Destruction of the angle from previous surgeries and severe malformation of angle/Schlemm's canal are the main causes of incomplete catheterization due to obstruction. The fact that previous surgeries compromise surgical outcomes of microcatheter-assisted trabeculotomy has supported its use as the primary surgery for congenital glaucoma.
2. Some degree of hyphema can be seen in almost all cases in the intraoperative and postoperative period. A thorough anterior chamber wash must be given at the end of the procedure.
3. The risk of misdirection of the catheter in suprachoroidal space leads to suprachoroidal hemorrhage or in subretinal space leads to subretinal hemorrhage and retinal detachment. To avoid this complication, one must carefully observe the movement of the leading end of the illuminated microcatheter.
4. Iris manipulation and iris/lenticular damage are more common in the ab interno approach. Precaution: They can be avoided by keeping the anterior chamber formed with viscoelastic and careful visualization and manipulation of instruments/catheter during the surgery.

33.7 Postoperative Care

1. Patient can experience mild pain, watering, and discomfort in the first few days. Overnight patching of the operated eye is usually done. Corneal clarity, anterior chamber depth intraocular pressure, hyphema, and scleral flap site are to be carefully examined in the postoperative period. Usually, postoperative follow-up is done on day 1, day 7, 1 month, 3 months, and then every 6 months, and this follow-up is modified according to IOP control.
2. Topical antibiotics (e.g., moxifloxacin, ciprofloxacin) are given for a period of 2 to 4 weeks.
3. Topical steroids (e.g., prednisolone, betamethasone) are given for 4 to 6 weeks. They are usually started at a frequency of 6 to 8 times a day and tapered every week.
4. Pilocarpine (2%) three times a day for up to 3 months is used by some surgeons to prevent the development of peripheral anterior synechiae.

33.8 Surgical Outcomes

Shakarwal et al. compared outcomes of illuminated microcatheter-assisted circumferential trabeculotomy vs. conventional rigid probe partial trabeculotomy in 40 eyes with primary congenital glaucoma. They were able to achieve 360° cannulation in 80% of the eyes in the circumferential trabeculotomy group. At the end of 1 year, the eyes in which target IOP was achieved without or with antiglaucoma medications were 80% and 90% in the circumferential trabeculotomy group and 60% and 70%, respectively, in the conventional rigid probe partial trabeculotomy group.

Temkar et al. compared outcomes of illuminated microcatheter-assisted circumferential trabeculotomy vs. combined mitomycin C-augmented trabeculectomy-trabeculotomy in the surgical management of 30 patients with bilateral primary congenital glaucoma. One eye of each patient was randomized to either treatment. Both groups had comparable IOP reduction at the end of 1 year. Improvement in corneal clarity and cup-disc ratio was also comparable in both groups at the end of 1 year. Hyphema was the only complication more frequently encountered in the circumferential trabeculotomy group.

A recent meta-analysis by Ling et al. evaluated five studies and concluded that microcatheter-assisted circumferential trabeculotomy resulted in excellent IOP control, higher success rates, and lower need for antiglaucoma mediations than conventional trabeculotomy.

These findings favor the use of illuminated microcatheter-assisted circumferential trabeculotomy as the primary surgery for childhood/congenital glaucoma.

Habash et al. retrospectively evaluated surgical outcomes of microcatheter-assisted trabeculotomy as a secondary procedure in 16 eyes with primary congenital glaucoma. Complete catheterization was achieved in 69% of cases. Transient postoperative hyphema was encountered in 6 eyes (37.5%) eyes. Mean IOP reduced from 31.8 ± 6.6 mmHg to 15.6 ± 3.7 mmHg over a mean follow-up period of almost 20 months. Sixty-two percent of eyes did not require any antiglaucoma medications in the follow-up. In a similar study, Shi et al. were able to achieve IOP control in 17 out of 22 eyes undergoing microcatheter-assisted trabeculotomy as a secondary procedure. This suggests that illuminated microcatheter-assisted circumferential trabeculotomy is an effective and safe secondary surgical option for primary congenital glaucoma treatment after failed primary glaucoma surgery.

33.9 Conclusions

Circumferential microcatheter trabeculotomy has become the go-to procedure for the management of primary congenital glaucoma. It is a procedure with a high success rate and minimal long-term complications and retains the superior conjunctiva for a subsequent trabeculectomy if required. The high cost of the catheter remains a major drawback for its widespread application, and suture trabeculotomy is a useful alternative.

Suggested Reading

Al Habash A, Otaif W, Edward D, Al JI. Surgical outcomes of microcatheter-assisted trabeculotomy as a secondary procedure in patients with primary congenital glaucoma. Middle East Afr J Ophthalmol. 2020;27(3):145. https://doi.org/10.4103/meajo.MEAJO_317_20.

Al-Hazmi A. Correlation between surgical success rate and severity of congenital glaucoma. Br J Ophthalmol. 2005;89(4):449–53. https://doi.org/10.1136/bjo.2004.047761.

Broughton WL, Parks MM. An analysis of treatment of congenital glaucoma by Goniotomy. Am J Ophthalmol. 1981;91(5):566–72. https://doi.org/10.1016/0002-9394(81)90054-4.

Elwehidy AS, Bayoumi NHL, Abd Elfattah D, Hagras SM. Surgical outcomes of visco-circumferential-suture-trabeculotomy versus rigid probe Trabeculotomy in primary congenital glaucoma: a 3-year randomized controlled study. J Glaucoma. 2021; https://doi.org/10.1097/IJG.0000000000001944; Publish Ahead of Print.

Girkin CA, Marchase N, Cogen MS. Circumferential Trabeculotomy with an illuminated microcatheter in congenital Glaucomas. J Glaucoma. 2012a;21(3):160–3. https://doi.org/10.1097/IJG.0b013e31822af350.

Girkin CA, Rhodes L, McGwin G, Marchase N, Cogen MS. Goniotomy versus circumferential trabeculotomy with an illuminated microcatheter in congenital glaucoma. J AAPOS. 2012b;16(5):424–7. https://doi.org/10.1016/j.jaapos.2012.05.013.

Ling L, Ji K, Li P, et al. Microcatheter-assisted circumferential Trabeculotomy versus conventional Trabeculotomy for the treatment of childhood glaucoma: a meta-analysis. Biomed Res Int. 2020;2020:1–9. https://doi.org/10.1155/2020/3716859.

Luntz MH, Livingston DG. Trabeculotomy ab Externo and trabeculectomy in congenital and adult-onset glaucoma. Am J Ophthalmol. 1977;83(2):174–9. https://doi.org/10.1016/0002-9394(77)90612-2.

Neely DE. False passage: a complication of 360° suture Trabeculotomy. JAAPOS. 2005;9(4):396–7. https://doi.org/10.1016/j.jaapos.2005.05.003.

Sarkisian SR. An illuminated microcatheter for 360-degree trabeculectomy in congenital glaucoma: a retrospective case series. J AAPOS. 2010;14(5):412–6. https://doi.org/10.1016/j.jaapos.2010.07.010.

Shakrawal J, Bali S, Sidhu T, Verma S, Sihota R, Dada T. Randomized trial on illuminated-microcatheter circumferential Trabeculotomy versus conventional Trabeculotomy in congenital glaucoma. Am J Ophthalmol. 2017;180:158–64. https://doi.org/10.1016/j.ajo.2017.06.004.

Shi Y, Wang H, Yin J, et al. Outcomes of microcatheter-assisted trabeculotomy following failed angle surgeries in primary congenital glaucoma. Eye. 2017;31(1):132–9. https://doi.org/10.1038/eye.2016.212.

Shi Y, Wang H, Oatts J, et al. Ab interno vs ab externo microcatheter-assisted trabeculotomy for primary congenital glaucoma with clear cornea. Clin Exp Ophthalmol. 2020;48(9):1201–9. https://doi.org/10.1111/ceo.13868.

Temkar S, Gupta S, Sihota R, et al. Illuminated microcatheter circumferential Trabeculotomy versus combined Trabeculotomy-trabeculectomy for primary congenital glaucoma: a randomized controlled trial. Am J Ophthalmol. 2015;159(3):490–497.e2. https://doi.org/10.1016/j.ajo.2014.12.001.

Vastardis I, Kontopoulou K, Fili S, Gatzioufas Z, Kohlhaas M. Comparison of performance between two microcatheter systems in ab externo canaloplasty: a retrospective comparison study. Eur J Ophthalmol. 2020;30(3):487–93. https://doi.org/10.1177/1120672119833547.

Gonioscopy-Assisted Transluminal Trabeculotomy

34

Shikha Gupta, Karthikeyan Mahalingam, and Antriksh Wahi

Ab interno and ab externo angle surgeries are the initial surgical treatment of choice for congenital glaucoma, whenever feasible, especially in milder cases with preserved angle anatomy. Ab interno procedures can only be performed in the eyes with relatively clear cornea as it requires gonioscopy-aided angle visualization.
The ab interno procedures can be listed as:

- Incisional goniotomy (using a microvitreoretinal blade)
- Circumferential ab interno trabeculotomy: Gonioscopy-assisted transluminal trabeculotomy (GATT)
- Excisional gonio-surgeries using:
  - Trabectome, an electrosurgical ablative device (Neomedix Corporation, Tustin, CA).
  - Kahook Dual Blade (KDB, New World Medical Inc., CA).
  - Bent 26 G needle (bent ab interno needle goniectomy, BANG).

These procedures (Excisional gonio-surgeries using Trabectome, KDB, BANG) usually treat 120° to 150° of the angle (up to 180°). They involve excising a strip of the trabecular meshwork as they are advanced around the angle, minimizing chances of closure of the excised TM leaflets over time.

34.1 Circumferential Ab Interno Trabeculotomy

In 2014, Grover et al. described the gonioscopy-assisted transluminal trabeculotomy (GATT) using a flexible illuminated microcatheter (iTrack, Ellex, Menlo Park, California, USA), which could treat up to 360° angle. The main disadvantage of the procedure was the high cost of the disposable microcatheter.

In 2015, the Trab360™ (Sight Sciences, Menlo Park CA, USA) was devised which could perform 360° ab interno trabeculotomy. It uses OMNI viscosurgical systems which consists of retractable suture microcatheter with bent canula and viscoelastic reservoir for single port viscocanaloplasty as well trabeculotomy (Fig. 34.1).

Suture GATT: In 2016, Grover et al. described a novel technique for performing GATT using a thermal cautery modified round-tipped 4-0 nylon suture (5 and 6-0 polypropylene suture have also been used for the same). The surgical procedure of suture GATT is similar to that of microcatheter-aided GATT with added

Supplementary Information The online version contains supplementary material available at https://doi.org/10.1007/978-981-19-7466-3_34.

S. Gupta (✉) · K. Mahalingam · A. Wahi
Dr. Rajendra Prasad Centre for Ophthalmic Sciences, All India Institute of Medical Sciences, New Delhi, India
e-mail: shikhagupta@aiims.edu

S. Gupta et al. (eds.), *Childhood Glaucoma*, https://doi.org/10.1007/978-981-19-7466-3_34

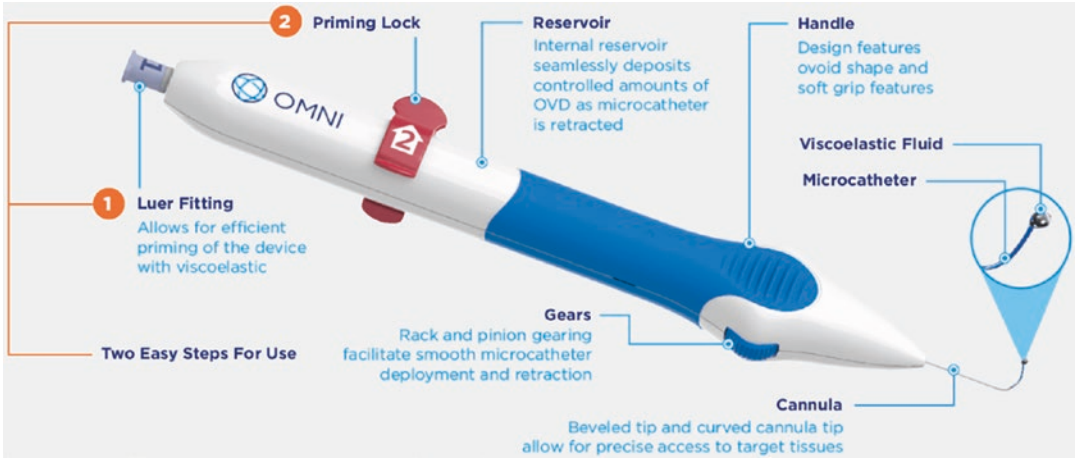

Fig. 34.1 Trab360™, OMNI™ surgical system (Sight Sciences, Menlo Park CA, USA) (www.sightsciences.com)

advantage of being cost-effective, albeit with absence of LED-guided suture advancement. Hence, by offering equivalent efficacy and safety at significantly lower cost (US$20 for suture vs. US$700 to US$1000 for microcatheter), suture GATT is the preferred procedure by most surgeons.

The indications and contraindications of GATT are usually similar to those for goniotomy surgery (mentioned in the previous chapter). The patient should preferably be aged <2 years, with mild to moderate glaucoma and a relatively clear cornea, and the angle should be open with structures visible and minimal angle distortion.

34.2 Surgical Procedure (Video 34.1)

- Surgery is performed under general anesthesia, with the surgeon sitting temporally. Following intubation, the patient's head is tilted opposite to the direction of the surgeon's position to maximize visibility of nasal angle structures.
- Patient positioning (Fig. 34.2):
  - The surgeon should be seated on the temporal side of the eye to be operated.
  - The patient's head should be tilted to the opposite side.
  - The microscope is tilted towards the surgeon by approximately 45°.
- Two side ports are made with a microvitreoretinal blade (MVR) in such a manner that the Schlemm's canal is cannulated in the superior-inferior direction. Hence, for surgery on RE, the ports are preferably made inferotemporally (for the forceps) and superonasally (for the suture), while for LE surgery, the ports are preferably fashioned in the inferonasal (suture entry) and the superotemporal (forceps entry) quadrants.
- Preservative-free pilocarpine 2% is injected intracamerally to constrict the pupil. It helps in the opening of the angle by pulling the iris away and prevents injury to the lens in phakic eyes. This is followed by instillation of a cohesive viscoelastic (Healon, Alcon) to aid angle deepening and tamponade angle bleeding, if any.
- Next, gonioscopy is performed with a direct gonioprism such as, Swan Jacob gonioprism (Ocular Instruments, USA) to visualize angle structures. In such stretched eyes, appreciation of angle structures may be suboptimal due to (Fig. 34.3):
  - Altered angle anatomy in buphthalmic eyes
  - Angle dysgenesis: presence of featureless angle or membrane over the angle precluding adequate visualization
  - Corneal opacity/Haab's striae/corneal edema in untreated eyes
  - High iris insertion, etc.

Fig. 34.2 (**a**) Patient's head tilted to the left side for angle surgery on the right eye. (**b**) Microscope is angulated down toward the surgeon. (**c**) The angulation of the microscope (red dotted line) and head position of the patient (black dotted line) demonstrated which are needed for maximal nasal angle visualization

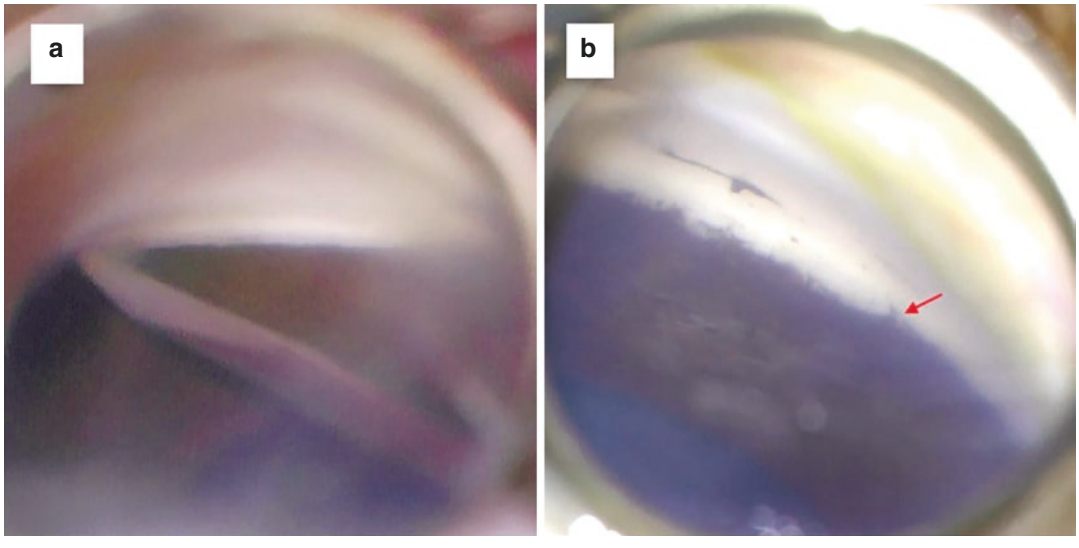

Fig. 34.3 Intraoperative gonioscopy images showing featureless angle (**a**) in primary congenital glaucoma and (**b**) in a case of Axenfeld Rieger Syndrome showing high iris insertion and large peripheral anterior synechiae. Both these cases pose a difficulty in the correct identification of trabecular meshwork (reproduced with permission: Panigrahi A, Huang AS, Arora M, Kumari S, Mahalingam K, Gupta V, Gupta S. Indocyanine Green Aided Schlemm Canal Identification During Gonioscopic Assisted Transluminal Trabeculotomy. J Glaucoma. 2022 Aug 1;31 (8):e69-e71. doi: 10.1097/IJG.0000000000002047)

The following methods can be used for correct identification of trabecular meshwork in young eyes of congenital glaucoma:

- Ipsilateral external jugular vein compression can cause engorgement of the ipsilateral Schlemm's canal, which is then seen as a circumferential tangential red streak (Fig. 34.4).
- Intracameral injection of indocyanine green dye (0.2%) causes band-like staining of both the anterior and the posterior trabecular meshwork with a forest green color. It can also aid identification of angle structures in the eyes with hazy cornea (Fig. 34.5).

• Preparation of the suture: A 5-0/6-0 polypropylene suture is cut into a short length, and the end is rounded with a bipolar diathermy set at high voltage to produce an umbrella tipped suture, minimizing injury to angle structures as the suture is advanced (Fig. 34.6).

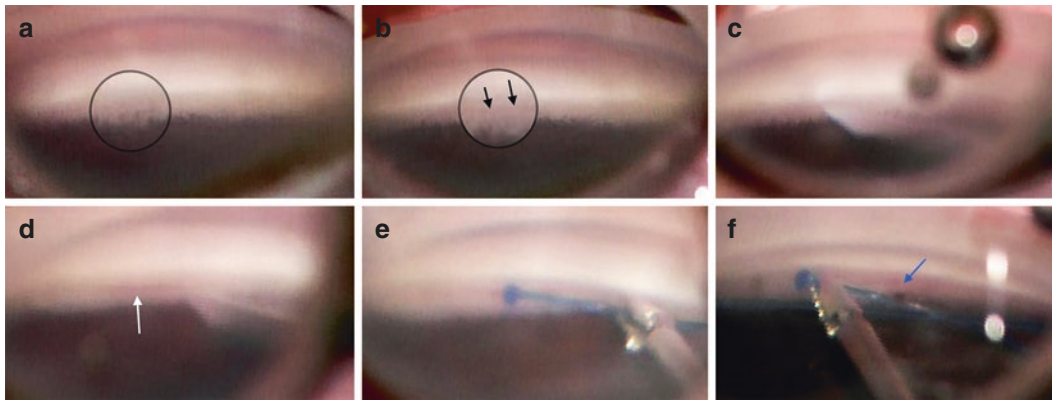

Fig. 34.4 Intraoperative clinical photograph of a 6-month-old patient with primary congenital glaucoma undergoing gonioscopicassisted transluminal trabeculotomy. The child has a featureless angle (**a**), with no angle structures seen (magnified inset). A circumferential tangential red line is seen post external jugular vein compression (**b**, black arrows), which corresponds to the engorged Schlemm's canal (SC). Goniotomy at the red line (**c**) leads to egress of blood from SC, resulting in the appearance of a blood-streaked band (**d**, white arrow), confirming the accuracy of the site of goniotomy. A 6-0 polypropylene suture is guided into the SC via the goniotomy incision (**e**), and is pulled out from it from an adjacent site (**f**). Blood streaked band can be seen adjacent to the site of the suture exit (blue arrow). (Reproduced with permission: Gupta S, Panigrahi A, Mahalingam K, Kumari S, Gupta V. External Jugular Vein Compression Aided Gonioscopy Assisted Transluminal Trabeculotomy in Eyes With Congenital Glaucoma. J Glaucoma. 2022;31(7):e43–e45. https://doi.org/10.1097/IJG.0000000000002036)

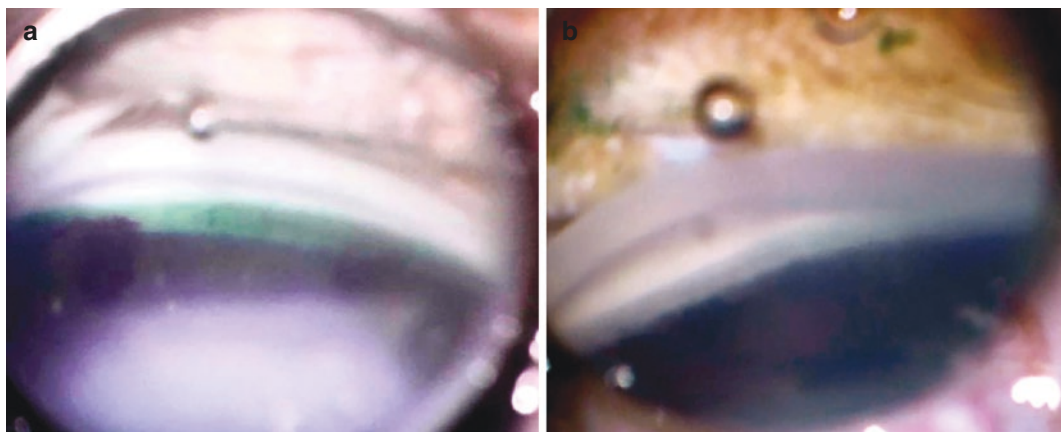

Fig. 34.5 (**a**, **b**) Intraoperative images after use of indocyanine green dye, showing 'forest green' colored staining of trabecular meshwork (reproduced with permission: Panigrahi A, Huang AS, Arora M, Kumari S, Mahalingam K, Gupta V, Gupta S. Indocyanine Green Aided Schlemm Canal Identification During Gonioscopic Assisted Transluminal Trabeculotomy. J Glaucoma. 2022 Aug 1;31 (8):e69-e71. doi: 10.1097/IJG.0000000000002047)

- The anterior chamber is filled with a viscocohesive OVD (e.g., sodium hyaluronate 1%). Sodium hyaluronate is also placed in between the gonioprism and cornea. The MVR is used to make an adequate 1–2 clock hours goniotomy incision over the anterior trabecular meshwork within the nasal angle.
- The umbrella tipped suture is passed intracamerally through one of the side ports. Then, with the help of microsurgical forceps (e.g., a bent end grasping or scleral fixation IOL forceps), it is inserted into the Schlemm's canal through the small goniotomy and advanced 360° through the Schlemm's canal till it comes out of the other end (Fig. 34.7). Care is taken that the plane of the suture is parallel to the iris and the bluish hue of the suture is visible through the translucent trabecular meshwork as it is advanced to confirm it's position in the right plane. In some eyes, pigmented trabecu-

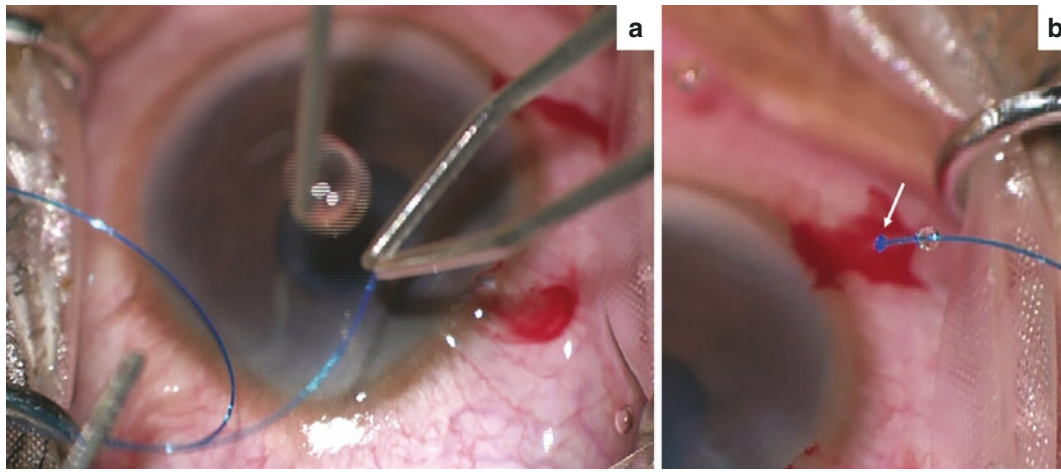

Fig. 34.6 Preparation of suture. Wet-field thermal cautery is done (**a**) to produce umbrella tip (**b**)

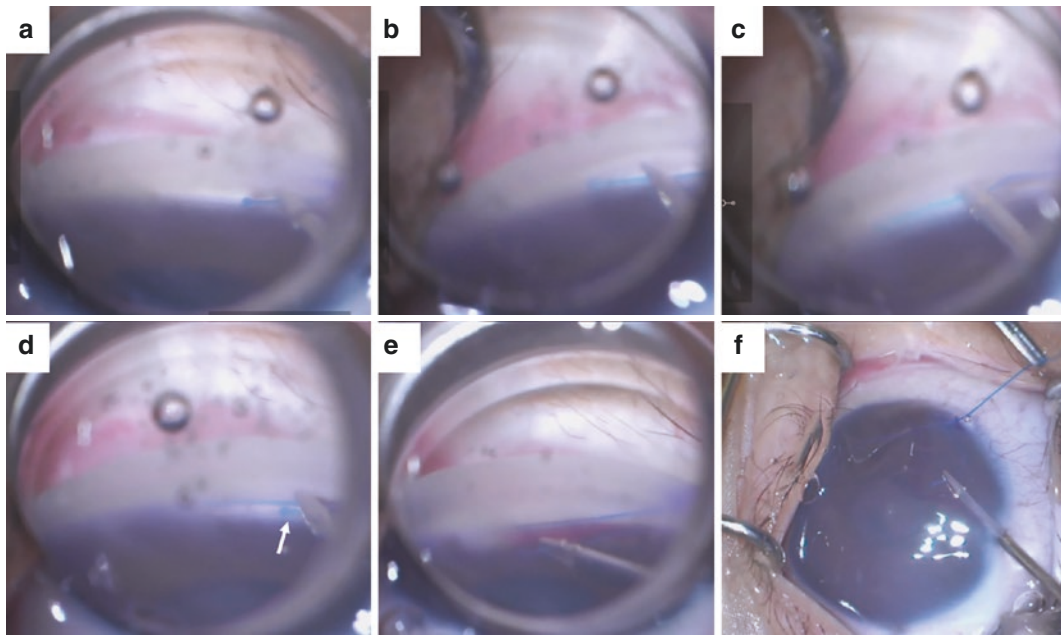

Fig. 34.7 Intraoperative gonioscopy-aided view showing insertion of suture through the goniotomy and advancement in the Schlemm's canal (**a**–**c**) till it comes out of other end (**d**, arrow). Then it is exteriorized and pulled (**e**), while the other end is held firmly (**f**)

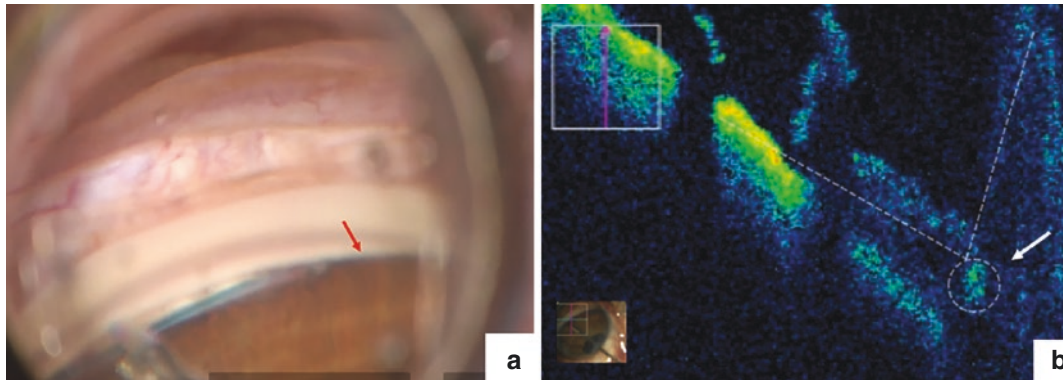

Fig. 34.8 (**a**) Intraoperative gonioscopic image showing the advancement of 6-0 Prolene suture. Red arrow shows pigmented trabecular meshwork obscuring the suture. (**b**) Intraoperative OCT aids in identifying suture (white arrow) as a dot within the trabecular meshwork eliciting a typical inverted Ångström (Å) sign (reproduced with permission: Mahalingam K, Gupta V, Gupta S. Inverted Ångström sign on iOCT: cannulated Schlemm's canal during gonioscopy-assisted transluminal trabeculotomy. BMJ Case Rep. 2022 Jul 15;15 (7):e250219. doi: 10.1136/bcr-2022-250,219)

lar meshwork can preclude the visualization of the suture as it is advanced in the Schlemm's canal. Intraoperative optical coherence tomography (iOCT) can help in the correct identification of the suture, where it is visible as an inverted Å sign (Fig. 34.8).

- The end of the suture (after passing through 360° of the Schlemm's canal) is exteriorized and pulled out using a McPherson's suture, while the other end is held firmly with the end grasping forceps. This causes 360° deroofing of the trabecular meshwork/internal wall of the Schlemm's canal. In some cases, where there is some obstruction felt during suture cannulation, then the Schlemm's canal is deroofed using an MVR in that area, and the suture is exteriorized to create a partial internal trabeculotomy. Another option is to try passing the suture from the other end (Video 34.2). Superior to inferior direction of cannulation helps in retrieving the advancing end of the suture from the inferior angle while being seated superiorly in cases of partial Schlemm's canal cannulation.
- Then, irrigation and aspiration are done to remove the viscoelastic or blood and air left in situ. The side ports are hydrated/sutured. The intraocular pressure (IOP) should be kept on the higher side to prevent hyphema in the postoperative period, which can occur if IOP is low. Sometimes, in cases of recurrent bleed from the angle, some amount of visco-cohesive OVD can be left in situ. Care is taken to suture the side ports, especially in young babies.
- Subconjunctival injection (antibiotic + steroid) is given at the end of the surgery.

34.3 Postoperative Care

- Topical antibiotic and steroid combination is given for 2 to 4 weeks, with a frequency of six times per day for at least 1–2 weeks and then tapered over another 1–2 weeks. Some children may show acute IOP spike due to prescribed steroids, and in such cases, they should be tapered rapidly and replaced with nonsteroidal anti-inflammatory agents supplemented with appropriate glaucoma medications.
- We prefer to give topical pilocarpine 2% in the morning and afternoon and topical tropicamide 1% at night time for at least a week. Pilocarpine constricts the pupil and prevents peripheral anterior synechia formation at the raw junction of the ruptured Schlemm's canal and also provides IOP lowering effect, while tropicamide keeps the pupil mobile, preventing posterior synechiae formation.

- In cases with unilateral partial cannulation (nasal), children are advised to be made to sleep with the nasal angle higher to prevent blood clotting within the treated angle due to gravity for at least a week or two.
- Any kind of Valsalva maneuver or excessive crying should be avoided (if possible) to prevent postoperative blood reflux from the torn Schlemm's canal, especially in the immediate postoperative period.

34.4 Complications

- Hyphema: It is the most common intra- and postoperative complication. Microhyphema is innocuous and resolves on its own. The presence of postoperative macrohyphema can affect the success rate negatively and needs to be drained, especially if it doesn't resolve with conservative management (Video 34.3).
- Iridodialysis/cyclodialysis (Fig. 34.9, Video 34.4): Proper identification of the trabecular meshwork/Schlemm's canal with the help of dye or external jugular vein compression and confirmation of passage of suture in the Schlemm's canal with the help of iOCT can prevent these complications. It occurs if the suture is advanced at plane, more posterior than the intended one.
- Cannulation in suprachoroidal space: Again posterior advancement of suture can cause cannulation in supra-choroidal space. To prevent this complication, it is important that the suture is advanced in a direction parallel to the iris. Besides, visualization of the advancing end in relatively nonpigmented eyes or iOCT-aided confirmation of suture advancement within the Schlemm's canal, whenever available, can be helpful.
- Other rare complications include accidental injury to the iris/lens.

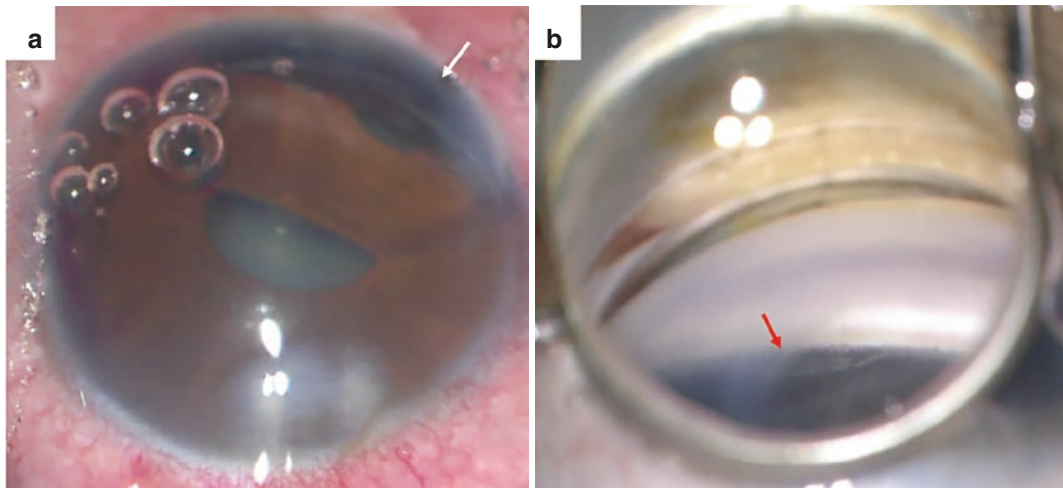

Fig. 34.9 (**a**) Intraoperative image showing iridodialysis (white arrow). (**b**) Intraoperative gonioscopy image showing cyclodialysis (red arrow)

34.5 Outcomes

Grover et al. (2015) performed GATT (illuminated microcatheter assisted) on 14 eyes of primary congenital glaucoma and juvenile open-angle glaucoma. They reported a significant decrease in intraocular pressure (IOP) from 27.3 mmHg to 14.8 mmHg and a decrease in the mean number of glaucoma medications used from 2.6 to 0.86 at a mean follow-up of 20.4 months.

None of the studies have reported the outcomes of suture GATT in childhood glaucoma. Aktas et al. assessed the efficacy of GATT (6-0 Prolene) in moderate to advanced open-angle glaucoma (n = 104), and surgical success was achieved in 83.7% of the cases over an average follow-up of 19.4 months. Grover et al. (2017) reported that GATT was successful in treating 60–70% with prior incisional glaucoma surgeries and significantly reduced IOP (and the number of glaucoma medications required) at 2 years of follow-up.

Qiao et al. compared the efficacy of GATT with Kahook Dual Blade (KDB) excisional goniotomy in 46 juvenile open-angle glaucoma eyes. At 6 months, the partial/complete success rate was 65.6%/44.7% in the GATT group and 30.8%/15.4% in the KDB group. They concluded that GATT has a greater reduction in IOP and the number of glaucoma medications used compared to KDB. On the contrary, Hirabayashi et al. reported that at 6 months' follow-up GATT and KDB had similar IOP reduction and reduction in the number of glaucoma medications.

In authors' experience, it offers good IOP reduction when 360° cannulation is successful in primary congenital glaucoma eyes aged less than 2 years.

34.6 Conclusions

GATT is a safe and effective procedure for ab interno circumferential trabeculotomy in childhood glaucoma. It is not only useful as an initial surgical procedure but can be used as a secondary procedure in eyes with prior failed glaucoma surgeries. The introduction of suture GATT has made it a cost-effective intervention, along with retention of safety.

Suggested Reading

Aktas Z, Ucgul AY, Bektas C, Sahin KS. Surgical outcomes of Prolene Gonioscopy-assisted transluminal Trabeculotomy in patients with moderate to advanced open-angle glaucoma. J Glaucoma. 2019;28(10):884–8. https://doi.org/10.1097/IJG.0000000000001331.

Areaux RG Jr, Grajewski AL, Balasubramaniam S, Brandt JD, Jun A, Edmunds B, Shyne MT, Bitrian E. Trabeculotomy ab Interno with the Trab360 device for childhood Glaucomas. Am J Ophthalmol. 2020;209:178–86. https://doi.org/10.1016/j.ajo.2019.10.014.

Go MS, Freedman SF. Minimally invasive glaucoma surgery in childhood glaucoma. Curr Opin Ophthalmol. 2022;33(2):91–6. https://doi.org/10.1097/ICU.0000000000000827.

Grover DS, Fellman RL. Gonioscopy-assisted transluminal trabeculotomy (GATT): thermal suture modification with a dye-stained rounded tip. J Glaucoma. 2016;25(6):501–4. https://doi.org/10.1097/IJG.0000000000000325.

Grover DS, Godfrey DG, Smith O, Feuer WJ, Montes de Oca I, Fellman RL. Gonioscopy-assisted transluminal trabeculotomy, ab interno trabeculotomy: technique report and preliminary results. Ophthalmology. 2014;121(4):855–61. https://doi.org/10.1016/j.ophtha.2013.11.001.

Grover DS, Smith O, Fellman RL, Godfrey DG, Butler MR, Montes de Oca I, Feuer WJ. Gonioscopy assisted transluminal trabeculotomy: an ab interno circumferential trabeculotomy for the treatment of primary congenital glaucoma and juvenile open angle glaucoma. Br J Ophthalmol. 2015;99(8):1092–6. https://doi.org/10.1136/bjophthalmol-2014-306269.

Grover DS, Godfrey DG, Smith O, Shi W, Feuer WJ, Fellman RL. Outcomes of Gonioscopy-assisted transluminal Trabeculotomy (GATT) in eyes with prior incisional glaucoma surgery. J Glaucoma. 2017;26(1):41–5. https://doi.org/10.1097/IJG.0000000000000564.

Gupta S, Panigrahi A, Mahalingam K, Kumari S, Gupta V. External jugular vein compression aided Gonioscopy assisted transluminal Trabeculotomy in eyes with congenital glaucoma. J Glaucoma. 2022;31(7):e43–5. https://doi.org/10.1097/IJG.0000000000002036.

Hirabayashi MT, Lee D, King JT, Thomsen S, An JA. Comparison of surgical outcomes of 360° circumferential Trabeculotomy versus sectoral excisional Goniotomy with the Kahook dual blade at 6 months. Clin Ophthalmol. 2019;13:2017–24. https://doi.org/10.2147/OPTH.S208468.

Mahalingam K, Gupta V, Gupta S. Inverted Ångström sign on iOCT: cannulated Schlemm's canal during gonioscopy-assisted transluminal trabeculotomy. BMJ Case Rep. 2022;15(7):e250219. https://doi.org/10.1136/bcr-2022-250219.

Panigrahi A, Huang AS, Arora M, Kumari S, Mahalingam K, Gupta V, Gupta S. Indocyanine green aided schlemm canal identification during Gonioscopic assisted transluminal Trabeculotomy. J Glaucoma. 2022;31(8):e69–71. https://doi.org/10.1097/IJG.0000000000002047.

Qiao Y, Tan C, Chen X, Sun X, Chen J. Gonioscopy-assisted transluminal trabeculotomy versus goniotomy with Kahook dual blade in patients with uncontrolled juvenile open-angle glaucoma: a retrospective study. BMC Ophthalmol. 2021;21(1):395. https://doi.org/10.1186/s12886-021-02159-z.

35 Ab Interno Goniectomy with Trabectome

Suneeta Dubey and Prerna Garg

35.1 Introduction

Traditionally, angle surgery (goniotomy and/or trabeculotomy) has been the first choice for surgical management of primary congenital glaucoma (PCG). Goniotomy has shown approximately 85% success in mild to moderate PCG. However, since goniotomy is an incisional procedure, there is a possibility of scarring of the trabecular meshwork (TM) by residual leaflets (Table 35.1).

With the advancement in technology and advent of minimally invasive glaucoma surgeries (MIGS), we now have various other options to treat the angle. Trabectome (NeoMedix Corporation, Tustin, CA), an electrosurgical handheld gonio-ablative device, is used to perform excisional goniotomy, also known as irrigating goniectomy; it has the theoretical advantage of decreased risk of cicatricial closure of the trabecular cleft. However, there is a paucity of qualitative and quantitative data about the role of MIGS in childhood glaucoma. Trabectome combines irrigation, aspiration, and ablation capabilities within a disposable handpiece which is controlled by a foot pedal and is approved by the FDA in 2004 for clinical use. It works by ablating the trabecular meshwork and the inner

Table 35.1 Comparison of goniotomy and trabectome-assisted goniectomy

	Goniotomy	Trabectome-assisted goniectomy
Mechanism	It's an incisional procedure	It's an excisional procedure
Scarring	Leaflets of TM remain on either side of the incision which can undergo scarring	TM is ablated and excised, with less chance of residual scarring
Hyphema	No irrigation/aspiration system which increases the chance of intraoperative hyphema and postoperative synechiae formation	It incorporates irrigation/aspiration which increases intraoperative visibility, maintains AC stability, and decreases blood reflux
Cost	Cheaper technique	Expensive technique (around 700-800 USD)

Supplementary Information The online version contains supplementary material available at https://doi.org/10.1007/978-981-19-7466-3_35.

S. Dubey (✉) · P. Garg
Dr. Shroff's Charity Eye Hospital, New Delhi, India

S. Gupta et al. (eds.), *Childhood Glaucoma*, https://doi.org/10.1007/978-981-19-7466-3_35

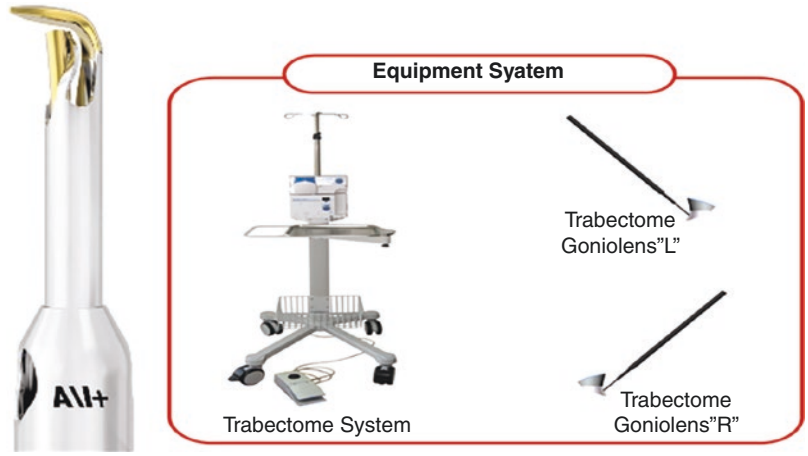

Fig. 35.1 Figure showing the equipment system and trabectome probe. (Copyright NeoMedix Corporation, San Juan Capistrano, CA, USA; reproduced with permission)

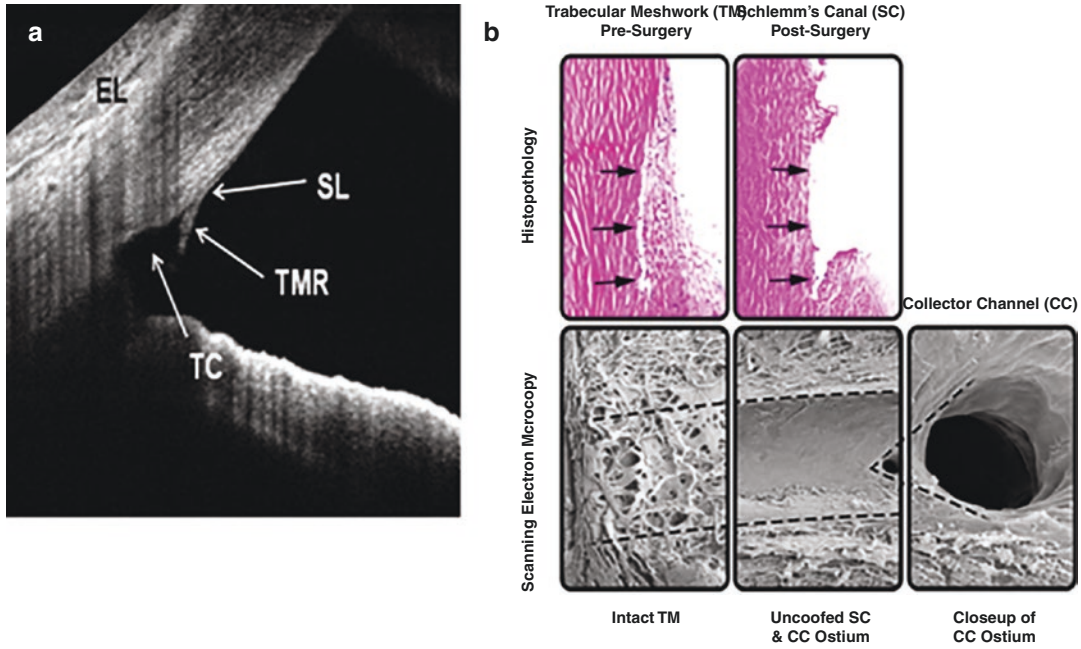

Fig. 35.2 (**a**) Histopathology images of the trabecular meshwork and Schlemm's canal before and after the trabectome procedure. (**b**) Electron microscopy images of the anterior chamber angle structures before and after the trabectome procedure. (Copyright NeoMedix Corporation, San Juan Capistrano, CA, USA; reproduced with permission)

wall of the Schlemm's canal using an ab interno approach with a bipolar 550 kHz electrode and thus helps to restore the original aqueous outflow pathway. Unlike cautery, plasma has a highly confined heat dissipation cone with minimal thermal transfer to the adjoining structures. Ablation is applied for 120–140° of the trabecular meshwork to allow for the reestablishment of the drainage pathway (Figs. 35.1, 35.2, and 35.3).

Indications and contraindications are the same as for goniotomy.

35.1.1 Indications

1. Mild to moderate primary infantile, developmental, and juvenile open-angle glaucoma
2. Other glaucoma

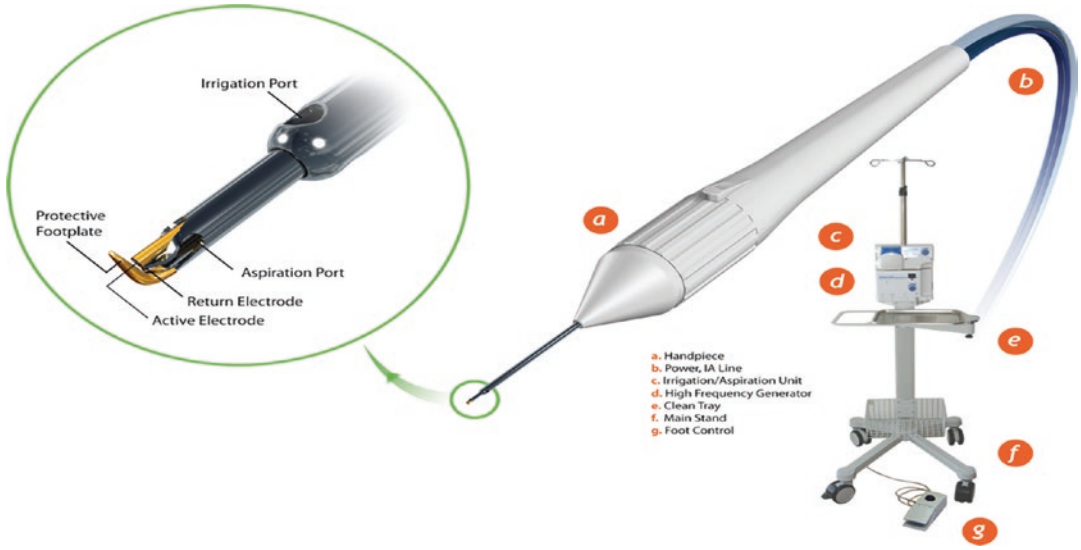

Fig. 35.3 Trabectome console and foot pedal. (Copyright NeoMedix Corporation, San Juan Capistrano, CA, USA; reproduced with permission)

(a) Associated with non-acquired systemic disease or syndrome, e.g., Sturge-Weber syndrome and neurofibromatosis 1
(b) Associated with non-acquired ocular anomalies, e.g., Axenfeld-Rieger syndrome, aniridia, and Peters syndrome
(c) Associated with congenital cataract surgery
(d) Associated with acquired conditions, e.g., trauma, uveitis, andsteroid use

35.1.2 Contraindications

1. Advanced congenital glaucomas
2. Corneal diameter >13 mm
3. Presence of corneal opacification/edema—angle structures not visualized
4. Neonatal glaucoma—presenting at birth or <1 month of age
5. Angles with peripheral anterior synechiae (PAS), in which trabecular meshwork can't be ascertained

35.2 Surgical Procedure

- Position and setup: best view of TM is achieved when the angle of the microscope and the patient's eye equals 70°. Tilt the microscope toward the surgeon ~30–35°. Rotate the patient's head away 30–35° to maximize the gonioscopic view (Fig. 35.4).

35.2.1 Surgical Steps (Video 35.1)

Step 1: Clear Corneal Incision (Fig. 35.5a)

- Create a 1.8 mm clear corneal incision with a keratome

Step 2: Lower Anterior Chamber (AC) Intraocular Pressure (IOP) to Visualize the Schlemm's Canal (SC)

- Open corneal incision to allow aqueous humor to leave AC, lowering IOP
- Blood refluxes into the SC to promote visualization of the trabecular meshwork (TM)
- Reform AC by injecting a saline solution

Step 3: Microscope Tilt and Head

- Tilt the microscope toward the surgeon 40°
- Sitting temporally, turn the patient's head away 30°

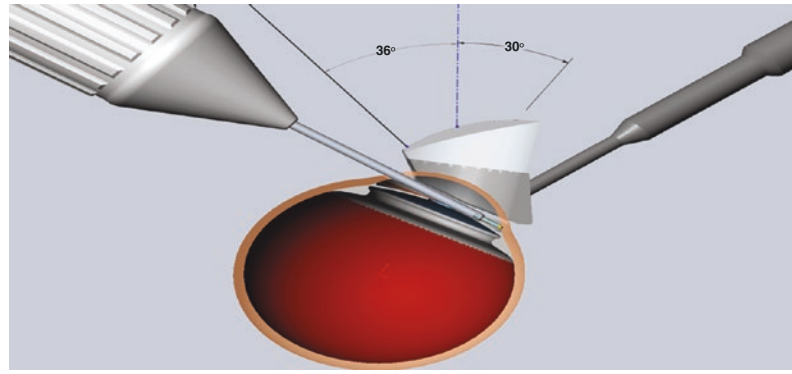

Fig. 35.4 Position and setup while performing trabectome ablation

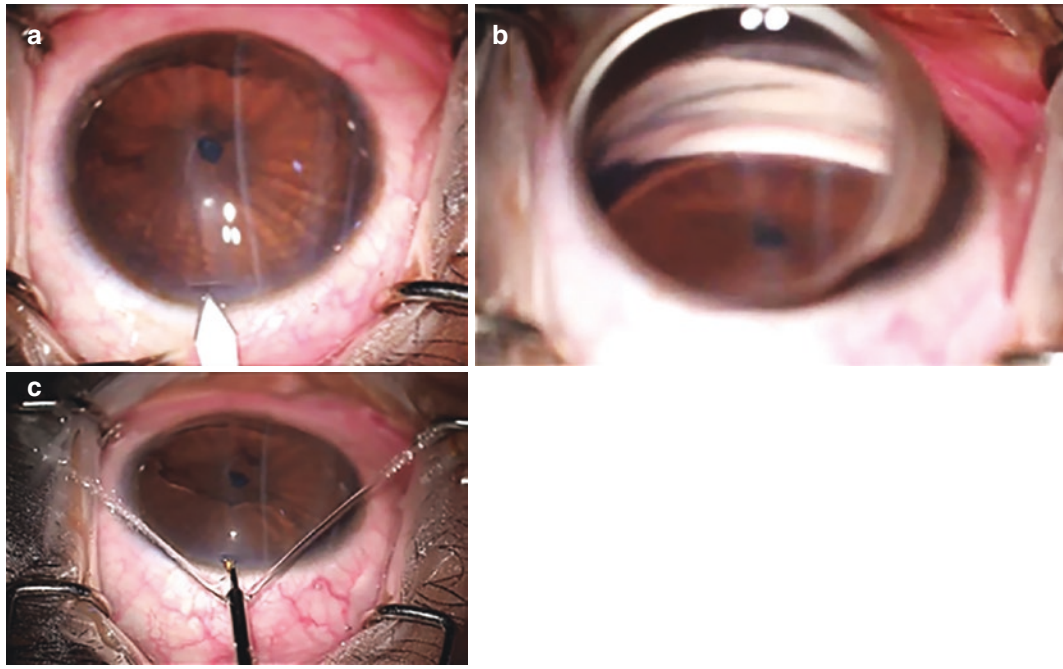

Fig. 35.5 Temporal clear corneal incision (**a**), visualization of TM with gonioscope (**b**), entering the AC with the trabectome irrigation/aspiration probe (**c**)

Step 4: Goniolens Placement (Fig. 35.5b, c)

- Place the goniolens on the cornea and identify the TM—enhanced by Step 2
- Remove the goniolens and insert the tip with irrigation on
- Advance the tip 1/4 of the way across the AC toward the TM
- Replace the goniolens and continue advancing the tip, contacting the TM

Step 5: Removal of the Trabecular Meshwork (Figs. 35.6 and 35.7)

- Gently insert tip into the SC highlighted with blood congestion.
- Depress the foot pedal to activate aspiration and electrosurgical power.
- Advance the trabectome tip clockwise within the SC to remove the TM.
- Bring the trabectome tip in the center of the AC and rotate 180°.
- Repeat in a counterclockwise direction to remove the TM.
- Ablation of approximately 120–140° of the trabecular meshwork is performed under gonioscopy. Ablation is done by pointing the tip of

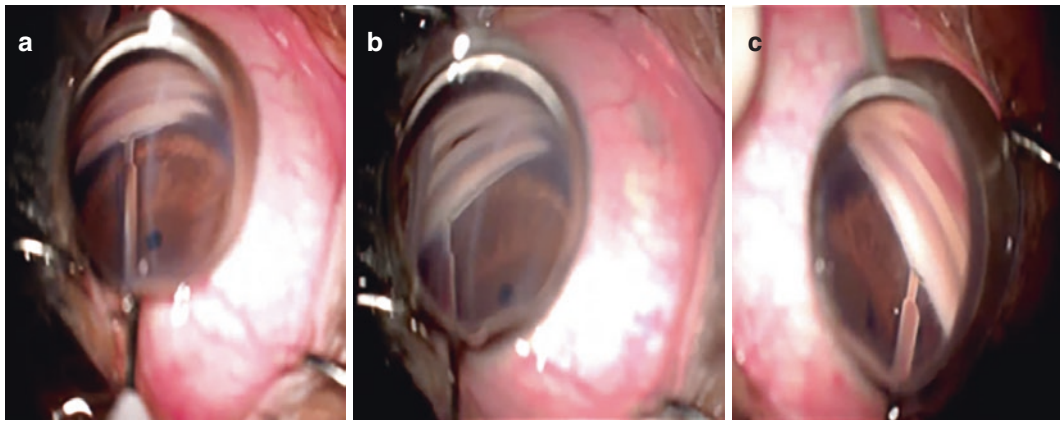

Fig. 35.6 Excisional Goniectomy with trabectome blade. (**a**) Gently insert tip into the SC, depress the foot pedal to activate aspiration and electrosurgical power. (**b**) Advance the trabectome tip clockwise within the SC to remove the TM. (**c**) Bring the trabectome tip to the center of the AC and rotate 180°, repeat counterclockwise to remove the TM to complete 120–140 degrees of ablation

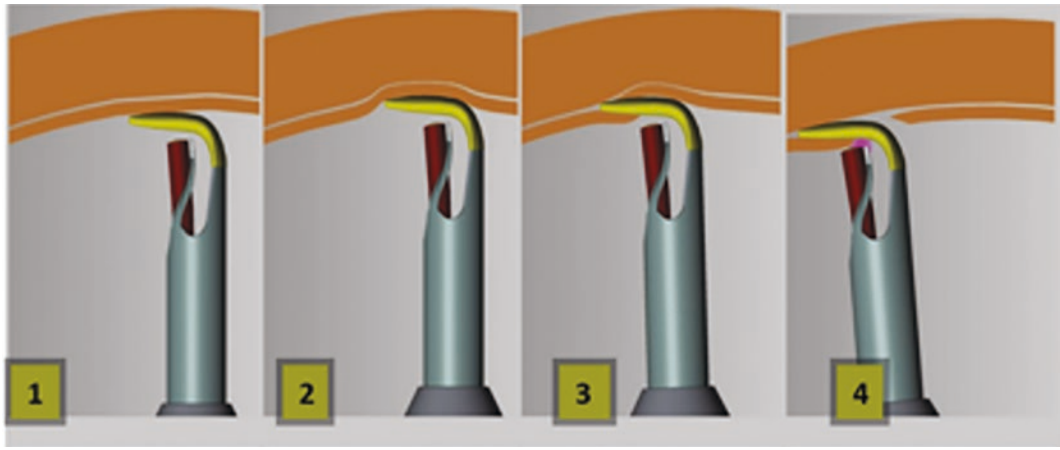

Fig. 35.7 (1) Visual contact with meshwork (2) Minimal pressure and gentle compression of meshwork (3) Enter tip through wrinkle in meshwork arcing into Schlemm's canal (4) Slowly advance the tip in Schlemm's Canal to take out the middle third of the width of the trabecular meshwork

footplate forward and rotating along the arc and the foot plate within the Schlemm's canal acting as guide. Continual handpiece withdrawal toward the surgeon helps to minimize the friction on posterior wall of the Schlemm's canal while advancing along the arc.

Step 6: Irrigate, Aspirate, and Suture (Fig. 35.8)

- Irrigate and aspirate.
- Suture the port with 10-0 nylon suture.

Postoperative care includes topical antibiotic QID for 1 week, topical steroid in tapering doses for 1 month, and antiglaucoma medications for 1 month while the eye heals. Usually, only one antiglaucoma medication is required in most cases. Some surgeons also use pilocarpine 1–2% in tapering doses for 1–3 months postop to avoid the formation of PAS. Routine follow-up of the patient is done at day 1, week 1, 1 month, 3 months, and 6 months thereafter.

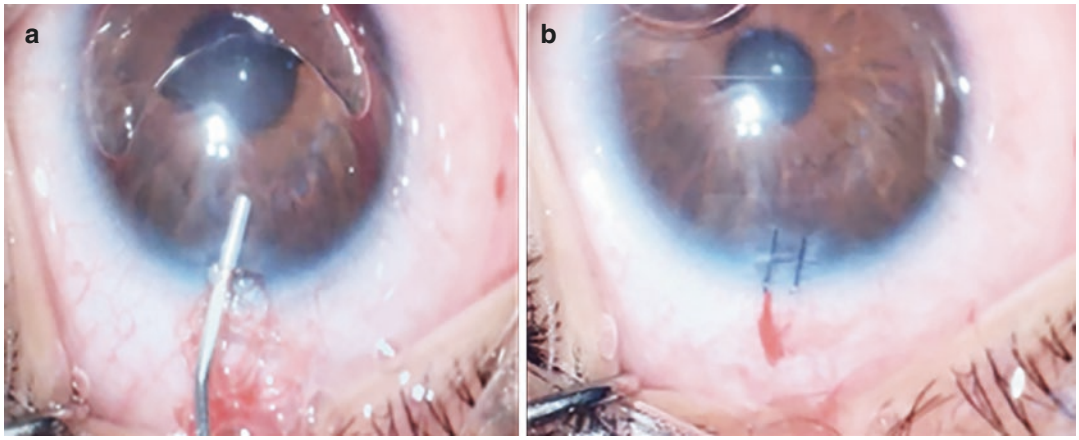

Fig. 35.8 (**a**) AC wash and (**b**) suturing of the wound

35.3 Review of the Literature

- Minckler et al. reported that trabectome surgery in primary and secondary open-angle glaucoma (n = 15) lowered IOP from 22.6 ± 4.7 mmHg to 16.3 ± 2.0 mmHg with a reduction in the mean number of medications from 1.2 to 0.1 over 1 year. Although they noted the success rate to be 50%, the 1-year success rates have varied significantly in different studies, ranging from 36% to 94%.
- Currently, there is no published data on the use of trabectome in childhood glaucoma; however, results of other ab interno procedures like GATT (gonioscopy-assisted transluminal goniotomy) and KDB (excisional goniectomy with Kahook Dual Blade) have been reported in patients of juvenile open-angle glaucoma.
- Helen et al. reported an overall success of 77% with goniotomy in 17 eyes with a mean follow-up of 7.8 years.
- Stangos et al. showed that primary viscocanalostomy is effective in lowering IOP in cases of medically uncontrolled JOAG. They studied 20 eyes of 20 patients with medical refractory JOAG and found an 80% overall surgical success associated with no serious postoperative complications.
- In 2015, Grover et al. published the preliminary results of GATT in 14 eyes (10 JOAG and 4 PCG) with a decrease in IOP from 27.3 to 14.8 mmHg and a decrease in the number of medications from 2.6 to 0.86. Five eyes had a drop in IOP ≥15 mmHg.
- Two recent studies have reported the results of MIGS angle procedures like GATT and KDB in JOAG:

  – Wang et al. reported complete and qualified success rates of 70.8% and 81.2% at 12 months and 58.6% and 81.2% at 18 months, respectively, with GATT in 59 eyes of JOAG.
  – Qiao et al. compared the efficacy and safety of GATT and Kahook Dual Blade (KDB) excisional goniotomy in patients with uncontrolled juvenile open-angle glaucoma (JOAG). The cumulative proportion of partial and complete success was 65.6% and 44.7% in the GATT group and 30.8% and 15.4% in the KDB group at 6 months. Additional procedures were required in 13.9% of cases after GATT and in 61.5% after KDB (P = 0.001).

We studied preliminary results of ab interno goniectomy using trabectome in 11 pediatric glaucoma eyes (unpublished data).

- The diagnosis was primary congenital glaucoma in seven eyes, JOAG in two eyes, and glaucoma associated with the non-acquired

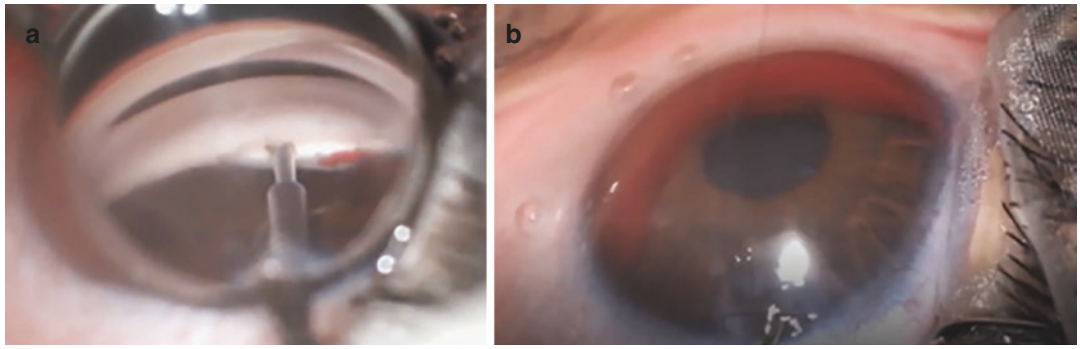

Fig. 35.9 (**a**) Intraoperative blood reflux from Schlemm's canal while performing trabectome ablation. (**b**) Intraoperative hyphema

systemic syndrome (Axenfeld-Rieger syndrome) in two eyes.

- Overall success was 86%. An average IOP reduction of 39.7% was achieved in all categories with a reduction of 46.4 % in PCG (failure of 1/7 eyes).
- **In PCG, one eye that failed was** a seven-month-old male child, who had advanced glaucoma with an IOP of 38 mmHg, a corneal diameter of 14.5 mm, and axial length of 24.51 mm. The child eventually underwent trabeculotomy plus trabeculectomy with mitomycin-C (MMC). The probable cause of poor prognosis in these advanced cases may be the extension of resistance to aqueous flow to collector channels beyond the TM.
- There may be interspersed synechial closure at the site of trabectome cleft, which could be attributed to exaggerated inflammatory response postsurgery.

35.4 Complications

- Intraoperative hyphema (Fig. 35.9): 78–90%
  - Usually mild due to the reflux of blood from the Schlemm's canal and is indicative of a successful procedure, hence should not be classified as a complication.
- PAS formation: 14–25%
- Postoperative transient IOP spike: 5.8%
- Hypotony: 1.5%
- Cataract progression: 1.2%
- Minor iris injury: 1.3%
- Aqueous misdirection: 0.09%
- Postoperative hyphema: rare
- Cyclodialysis cleft: very rare

Serious complications associated with conventional filtering surgery like infection, wound leak, bleb formation, choroidal effusion, choroidal hemorrhage, or visual acuity decrease of more than two lines are rare with trabectome surgery.

35.5 Conclusions

Further studies are required to assess the efficacy and safety of ab interno goniectomy with trabectome in the pediatric population. As of now, the technique though costly seems effective.

Suggested Reading

Administration FDA. FDA 510 (k) Database Entry Neomedix NMX-1000 (Trabectome). 2012. Available http://www.accessdata.fda.gov/scripts/cdrh/cfdocs/cfPMN/pmn.cfm?ID=K040584.

Berk TA, An JA, Ahmed IIK. Inadvertent cyclodialysis cleft and hypotony following ab-interno trabeculotomy using the Trabectome device requiring surgical repair. J Glaucoma. 2017;26(8):742–6.

Bowman RJ, Dickerson M, Mwende J, Khaw PT. Outcomes of goniotomy for primary congenital glaucoma in East Africa. Ophthalmology. 2011;118(2):236–40.

Francis BA, Minckler D, Dustin L, Kawji S, Yeh J, Sit A, et al. Combined cataract extraction and trabeculotomy by the internal approach for coexisting cataract and open-angle glaucoma: initial results. J Cataract Refract Surg. 2008;34(7):1096–103.

Grover DS, Smith O, Fellman RL, et al. Gonioscopy assisted transluminal trabeculotomy: an ab interno circumferential trabeculotomy for the treatment of primary congenital glaucoma and juvenile open angle glaucoma. Br J Ophthalmol. 2015;99(8):1092–6. https://doi.org/10.1136/bjophthalmol-2014-306269.

Hu K, Shah A, Virgili G, Bunce C, Gazzard G. Ab interno trabecular bypass surgery with Trabectome for open-angle glaucoma. Cochrane Database Syst Rev. 2021;2(2):CD011693. https://doi.org/10.1002/14651858.CD011693.pub3.

Jordan JF, Wecker T, van Oterendorp C, Anton A, Reinhard T, Boehringer D, et al. Trabectome surgery for primary and secondary open angle glaucomas. Graefes Arch Clin Ex Ophthalmol. 2013;251(12):2753–60. Pubmed Central PMCID: 3889259.

Mandal AK, Chakrabarti D. Update on congenital glaucoma. Indian J Ophthalmol. 2011;59(1):S148–57.

Minckler D, Mosaed S, Dustin L, Ms BF, Trabectome Study G. Trabectome (trabeculectomy-internal approach): additional experience and extended follow-up. Trans Am Ophthalmol Soc. 2008;106:149–59; discussion 59–60. Pubmed Central PMCID: 2646453.

Minckler DS, Baerveldt G, Alfaro MR, Francis BA. Clinical results with the Trabectome for treatment of open-angle glaucoma. Ophthalmology. 2005;112(6):962–7.

Osman EA, AlMobarak F. Ciliochoroidal effusion with persistent hypotony after trabectome surgery. Indian J Ophthalmol. 2015;63(3):272–4. Pubmed Central PMCID: 4448246.

Qiao Y, Tan C, Chen X, Sun X, Chen J. Gonioscopy-assisted transluminal trabeculotomy versus goniotomy with Kahook dual blade in patients with uncontrolled juvenile open-angle glaucoma: a retrospective study. BMC Ophthalmol. 2021;21(1):395. https://doi.org/10.1186/s12886-021-02159-z.

Stangos AN, Whatham AR, Sunaric-Megevand G. Primary viscocanalostomy for juvenile open-angle glaucoma. Am J Ophthalmol. 2005;140:490–6.

Ting JL, Rudnisky CJ, Damji KF. Prospective randomized controlled trial of phaco-trabectome versus phaco-trabeculectomy in patients with open angle glaucoma. Can J Ophthalmol. 2018;53(6):588–94. https://doi.org/10.1016/j.jcjo.2018.01.033.

Wang Y, Wang H, Han Y, et al. Outcomes of gonioscopy-assisted transluminal trabeculotomy in juvenile-onset primary open-angle glaucoma. Eye. 2021;35(10):2848–54. https://doi.org/10.1038/s41433-020-01320-0.

Yeung HH, Walton DS. Goniotomy for juvenile open-angle glaucoma. J Glaucoma. 2010;19(1):1–4. https://doi.org/10.1097/IJG.0b013e3181a2fa31.

Glaucoma Drainage Devices

36

Karthikeyan Mahalingam, Shikha Gupta, and Viney Gupta

Glaucoma drainage devices (GDD) are usually preferred in refractory childhood glaucomas when the initial surgical procedures like angle surgeries and glaucoma filtration surgery fail to control intraocular pressure (IOP) or as a primary procedure in cases where there is a higher chance of failure of angle surgeries and glaucoma filtration surgeries.

36.1 Indications for GDD in Childhood Glaucoma

- Refractory childhood glaucoma (after multiple failed angle/glaucoma filtration surgeries)
- Post-keratoplasty with secondary glaucoma
- Post-vitreoretinal surgery with secondary glaucoma
- Uveitic glaucoma
- Post-traumatic glaucoma
- Anterior segment dysgenesis (multiple iridocorneal adhesions) with glaucoma
- Aphakic/pseudophakic glaucoma
- Sturge-Weber syndrome
- Eyes with conjunctival fibrosis
- Neovascular glaucoma (rare in pediatric age group)

Various GDDs available are (summarized in Table 36.1) classified into non-valved devices including the Aurolab aqueous drainage implant device (AADI, Aurolab, India), the Baerveldt implant (Advanced Medical Optics Inc., CA), Molteno implant (Molteno Ophthalmic Ltd., Dunedin, New Zealand), the Ahmed ClearPath (ACP, New World Medical Inc., CA), and valved devices including Ahmed glaucoma valve (AGV, New World Medical Inc., CA) and Krupin slit valve (Hood Laboratories, Pembroke, MA). Pediatric versions are available in some GDDs, while the adult versions are used in the rest.

Supplementary Information The online version contains supplementary material available at https://doi.org/10.1007/978-981-19-7466-3_36.

K. Mahalingam · S. Gupta · V. Gupta (✉)
Dr. Rajendra Prasad Centre for Ophthalmic Sciences, All India Institute of Medical Sciences, New Delhi, India

S. Gupta et al. (eds.), *Childhood Glaucoma*, https://doi.org/10.1007/978-981-19-7466-3_36

Table 36.1 Summary of different glaucoma drainage devices

Glaucoma drainage device	Molteno	Baerveldt	AADI	ACP	AGV	Krupin
Material	Silicone/ polypropylene	Silicone (barium-impregnated)	Silicone	Silicone (barium-impregnated)	Silicone/ polypropylene	Silicone
Resistance mechanism	Available only in ridged version/ Molteno 3	None	None	None	Venturi valve	Slit valve
Surface area	135 mm^2, 175 mm^2 double plate 270 mm^2, 230 mm^2	250 mm^2, 350 mm^2 double plate 500 mm^2	350 mm^2	250 mm^2, 350 mm^2	FP8 (96 mm^2), FP7 (184 mm^2) double plate FX1 (364 mm^2)	184 mm^2
Pediatric size availability	Yes	No	No	No	Yes (FP8)	No
Success rate in pediatric glaucoma	44–85% (1–10 years)	58–86.7% (1–4 years)	41.8–81.7% (1–3 years)	57% (1 year)	42–85% (1–4 years)	NA

AADI Aurolab aqueous drainage implant device, *ACP* Ahmed ClearPath, *AGV* Ahmed glaucoma valve, *NA* Not Available

36.2 Preoperative Considerations

- Pediatric size or adult size of the GDD has to be chosen according to the size of the eye.
- Stretched limbus and thin sclera in the eyes with congenital glaucoma will make the surgery a bit more difficult compared to other adult glaucomas.
- If there is a history of vitreoretinal surgery with encirclage or scleral buckling, an opinion can be sought from the vitreoretinal surgeon if the encirclage or buckle can be removed to place the GDD. If removal is not possible, the plate can be placed on top of the buckle itself.
- Either autologous sclera, corneoscleral graft, or pericardial graft should be placed over the GDD tube (to prevent erosion). Corneoscleral graft has better availability and placement of the cornea gives better cosmesis.
- The lens status of the eye should be noted. In pseudophakic/aphakic patients, the GDD tube is preferably placed in the sulcus, and in phakic patients, the tube is placed in the anterior chamber. Placement of the tube in the sulcus reduces the risk of corneal touch and decompensation. In vitrectomized eyes with anterior segment dysgenesis, pars plana tubes may be placed using a pars plana clip.
- Choose the quadrant with minimal conjunctival scarring to place the GDD. Usually, the superotemporal quadrant is chosen due to ease of accessibility during surgery and follow-up for needling/capsulectomy. Placement of GDD in the superonasal quadrant gives a better cosmesis.
- The tube positions are prone to more fluctuations in children due to expanding globe size in buphthalmic eyes leading to corneal touch or tube extrusion from intracameral space. Hence, a longer tube segment may be left intracamerally in young glaucoma eyes expected to grow significantly in the future to prevent tube extrusion.

36.3 Surgical Procedure for AGV/ Any Other Valved Device (Fig. 36.1, Video 36.1)

- Surgery is performed under general anesthesia.
- A 6-0 Vicryl suture is passed near the superior limbus and the eye pulled down to expose the surgical field.
- A limbal-based peritomy is made in either the superotemporal or superonasal quadrant. A 1–2 mm of conjunctival frill can be left behind for the ease of suturing.
- The conjunctiva and tenon's capsule are dissected using a tenotomy scissor. A relaxing incision is given in the conjunctiva to access the posterior sclera and to allow the placement

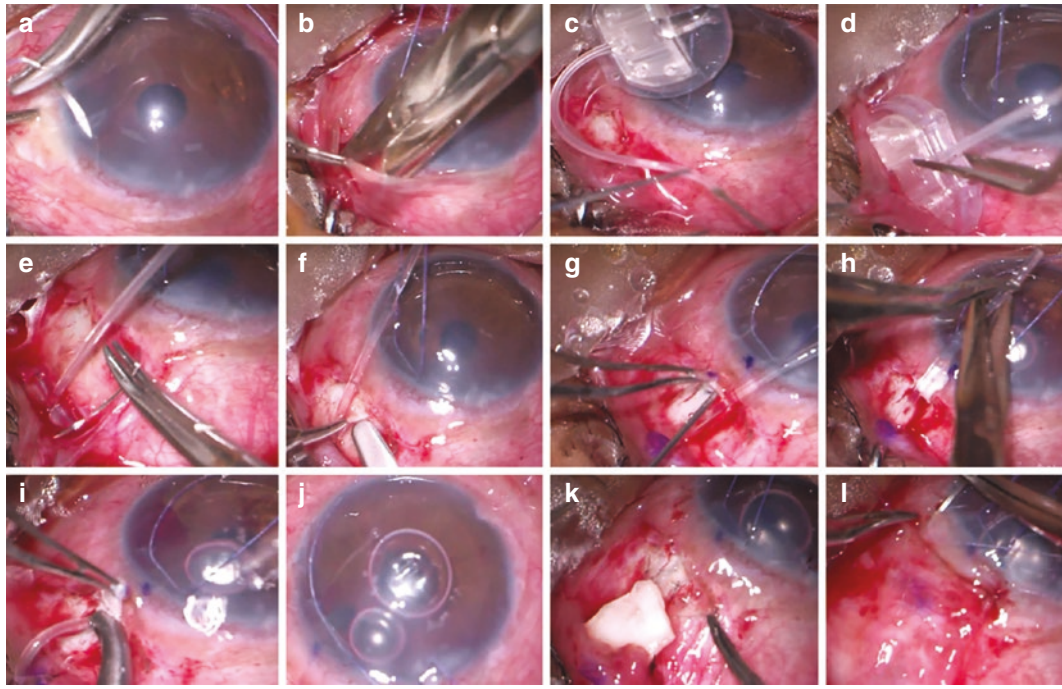

Fig. 36.1 Intraoperative images showing steps of Ahmed glaucoma valve surgery. (**a**) Corneal traction suture. (**b**) Localized peritomy. (**c**) Priming of Ahmed glaucoma valve tube. (**d**, **e**) Implantation of Ahmed glaucoma valve plate 8–10 mm posterior to the limbus. (**f**, **g**) Scleral flap and sclerostomy. (**h**) Trimming of the tube. (**i**, **j**) Insertion of Ahmed glaucoma valve tube. (**k**) Corneoscleral patch graft placed. (**l**) Conjunctival wound closed

of the GDD plate. Cautery is done to stop the bleeders.

- Priming: Sterile balanced salt solution is injected via a 26-G cannula into the GDD draining tube. Priming is complete when the fluid flows out through the holes of the plate.
- The plate is implanted 8–10 mm posterior to the limbus and the plate is secured to the sclera with nonabsorbable 6-0 nylon or 6-0 Prolene sutures.
- To place the tube in the anterior chamber, entry is made with a 23-G needle 1–1.5 mm posterior to the limbus. For placement in the sulcus, entry is made 1.5–2 mm posterior to the limbus. A partial-thickness scleral flap can be made around the entry site as per the convenience of the surgeon.
- The AGV tube should be trimmed to an adequate length with the creation of a beveled edge. Through the 23-G needle track smoothened with a viscoelastic, the tube is inserted with the help of AGV tube passing forceps.
- The AGV tube can be buried under the partial-thickness scleral tunnel or covered with the help of a corneoscleral patch graft. The patch graft should be chiselled into a thin tissue apt to cover the entire length and breadth of tube. Else, the tube can also be buried inside the grooved long scleral tunnel created right from the beginning of the tube from the AGV plate till it enters inside the eye.
- After insertion of the AGV tube, traction should be released to see the intraocular position of the tube. If the tube length is long, it can be trimmed with micro-vitreoretinal scissors and forceps (Fig. 36.2; Video 36.2). During sulcus placement of the tube, if there are iridocapsular (in aphakic) or iridolenticular (pseudophakic) adhesions blocking the tube drainage, basal iridectomy can be done, and the tube can be pulled out into the anterior chamber or the adhesions should be released. The patency of the tube should be ensured by looking at the tube lumen before closing.
- Conjunctival wound is secured using 8-0 Vicryl or 10-0 nylon sutures.
- An antibiotic-steroid combination is injected subconjunctivally at the end of surgery.

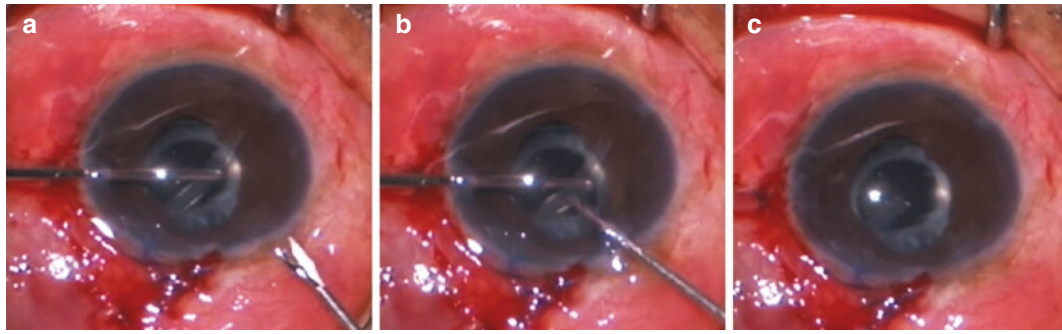

Fig. 36.2 Intraoperative trimming of the tube of Ahmed glaucoma valve (AGV). (**a**) AGV tube held with micro-vitreoretinal forceps, (**b**) the AGV tube is trimmed (note the distal end has to be held with the forceps), (**c**) final image after trimming

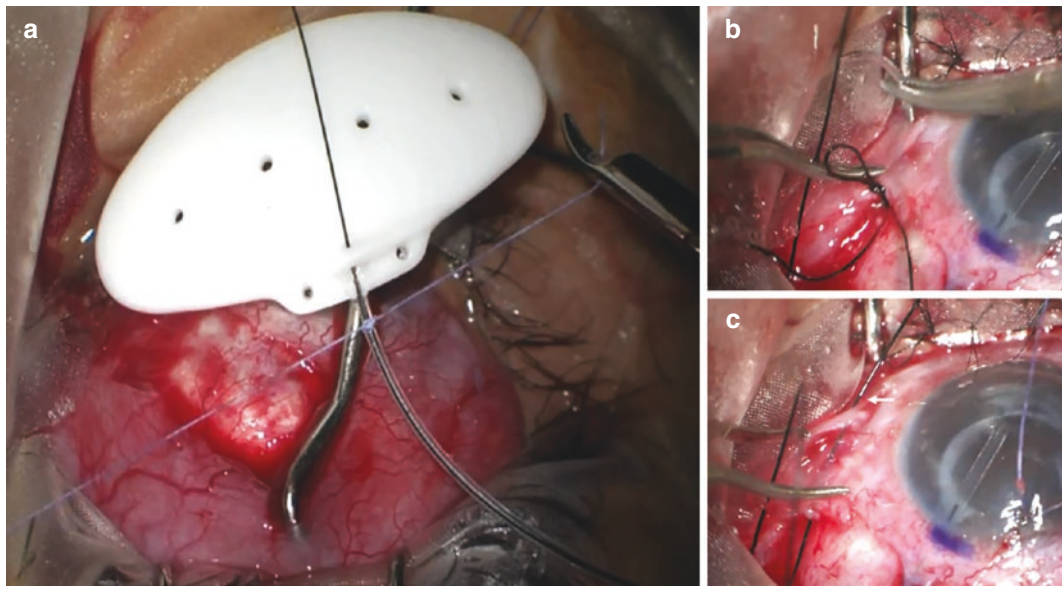

Fig. 36.3 Intraoperative images showing the ripcord suture (4-0 silk) inserted into the lumen of the tube (**a**) and passed out of the conjunctiva (**b**, **c**, white arrow)

36.4 Surgical Procedure for AADI/ Any Other Non-valved Device (Video 36.3)

Most of the steps are the same as AGV surgery except for the placement of the GDD plate and the use of ligation sutures.

- Placement of AADI plate: Usually placed in the superotemporal quadrant. The plate is placed 8–10 mm posterior to the limbus. The adjacent recti muscles are hooked and the wings of the endplate are inserted beneath the insertion of the muscles.
- To prevent hypotony (due to absence of valve) in the early postoperative period, following strategies are followed:
  - Following a two-staged procedure for surgery, i.e., in the first stage, the plate is implanted over the sclera, and in the second stage (after 4–6 weeks), the tube is inserted into the anterior chamber.
  - A ripcord suture (4-0 silk) is inserted into the lumen of the tube (Fig. 36.3a) with or

without ligation of the tube using 7-0 or 8-0 Vicryl suture. The other end of the ripcord is passed out of the conjunctiva (Fig. 36.3b) and it can be pulled later (3–6 weeks after surgery) to facilitate complete drainage.
  - A tube ligature suture: Absorbable 6-0 Vicryl suture just tight enough to curtail drainage initially but not too tight to break the tube into two.
- Till the implantation of the tube or till the removal of the ripcord suture, antiglaucoma medications should be continued. The use of ripcord suture is always better than a two-staged procedure as it avoids second surgery. In cooperative children, the ripcord suture can be pulled out as an outpatient procedure, and in younger uncooperative children, it can be done during a short examination under anesthesia.

36.5 Postoperative Care

- Topical antibiotic-steroid combinations (moxifloxacin + dexamethasone) are used for 4–8 weeks tailored according to each case. Cycloplegics are given for 2–4 weeks.
- The position of the tube should be checked on subsequent follow-ups (Fig. 36.4) for any signs of tube retraction, extrusion, erosion, or tube-corneal or tube-lens touch.

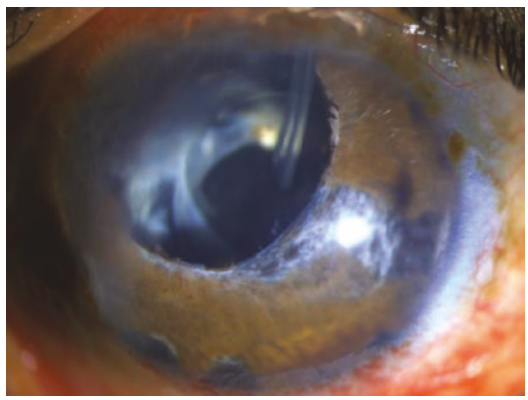

Fig. 36.4 Postoperative image in a child with Axenfeld-Rieger syndrome showing Ahmed glaucoma valve tube in position

36.6 Complications

Complications specific to glaucoma drainage devices are mentioned here. Other common complications are mentioned in previous chapters.

36.6.1 Intraoperative Complications

- Recurrent shallowing of the anterior chamber if the tube entry port is larger than the tube. The use of a 23-G needle for entry helps in this case, or in case of a larger entry site, it can be sutured with nylon monofilament suture before covering with scleral flap or tunnel.
- Misdirection of silicone tube into the anterior chamber when planned for sulcus placement or vice versa or into pars plana region (Fig. 36.5). The tube can be passed with a smaller-bore needle (trocar of the 24-G intravenous cannula) as a guide or the new entry port has to be made in another place with appropriate measurement (Video 36.2).
- If there is tube corneal touch, the scleral graft can be placed beneath the tube and sclera to change the direction of the tube toward the iris.
- During sulcus placement of the tube, it can get stuck between iridolenticular/iridocapsular adhesions. Then basal iridectomy can be done and the tube can be pulled out into the anterior chamber.

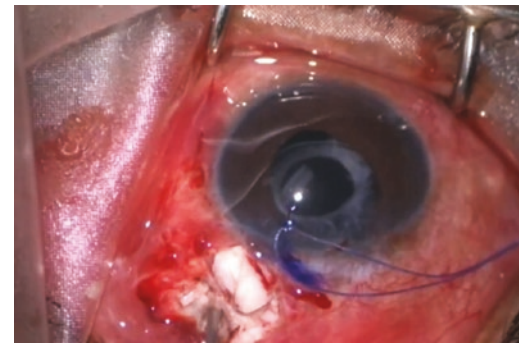

Fig. 36.5 Placement of tube behind the intraocular lens

36.6.2 Postoperative Complications

- Hypotony (4–47%): It can be minimized by the use of valved devices. In the case of non-valved devices, the use of a ripcord ligation, tube ligature suture, or a two-staged procedure should be done.
- Tube erosion (7%): It can be repaired by covering it with a donor tissue like a scleral patch graft and conjunctiva. Sometimes, in cases of scarred conjunctiva, a relaxing posterior partial-thickness horizontal incision can be given in the conjunctiva to bring it down. Else, an autologous conjunctival graft from the same or the contralateral eye may be required in severe cicatrized conjunctiva.
- Plate erosion (1–11.7%): It is more difficult to treat compared to tube erosion. The plate can be cut short and the overlying healthy conjunctiva or a conjunctival autograft can be used. In cases not amenable to repair, GDD must be removed and placed elsewhere (Fig. 36.6).
- Tube corneal touch: It can lead to corneal decompensation (15–35%) if not treated early (Figs. 36.7 and 36.8). The tube can be directed posteriorly with the help of 9-0 Prolene sutures anchored at 10 and 2 o'clock positions under two partial-thickness scleral flaps near the limbus. In pseudophakic and aphakic patients with overlying iris defects, a transscleral supracapsular anchor suture can be used to facilitate repositioning of the tube within the ciliary sulcus. A remnant of the cut tube can also be placed underneath the tube entry site to redirect it. Else, intracameral tube can be redirected through an iridectomy to redirect it in the sulcus in pseudophakic and aphakic eyes.
- Encapsulated bleb (15 to 69.2%): Usually, after 4–6 weeks after surgery, a hypertensive phase due to the formation of a fibrous capsule around the plate can occur. Aqueous suppressants are prescribed initially; if IOP remains uncontrolled, needling of the bleb may be required. If the above measures fail, then capsulectomy is advised (Fig. 36.9, Videos 36.4 and 36.5).
- Diplopia (2–18%): It can occur due to restriction of extraocular movements after placement of large plate implants where the muscle has been manipulated for placement of the plate. Increased height of the bleb also can cause diplopia. Choosing the correct size of the implant with minimal manipulation of the muscles can avoid this complication.
- Endophthalmitis (1–2%): It can occur due to improper conjunctival suturing/rubbing of the eyes by the child leading to conjunctival dehiscence and tube/plate erosion. Management options include topical/intravitreal/systemic antibiotics, pars plana vitrectomy of endophthalmitis, and removal of GDD. The management should be tailored according to individual cases.
- Tube can be blocked (4.7%) by vitreous, blood, iris, or silicone oil (Fig. 36.10). In case of emulsified silicone oil globules (tube meniscus sign), intracameral vent and flush technique can be used to remove the blockade (Fig. 36.11, Video 36.6). Intracameral venting incision is made in the tube with 20-G straight blade and flushing is done with 26-G cannula. Vitreous/blood blockade can be removed by anterior vitrectomy/irrigation and aspiration/Nd:Yag laser. Iridectomy or tube repositioning is needed in cases of iris blockade.

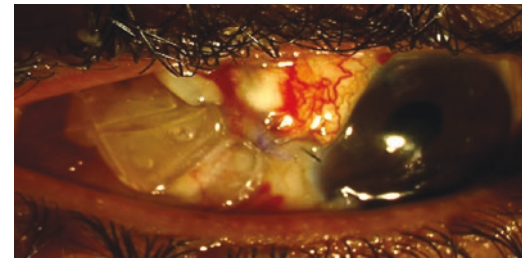

Fig. 36.6 Clinical picture showing plate erosion in a patient with operated Ahmed glaucoma valve

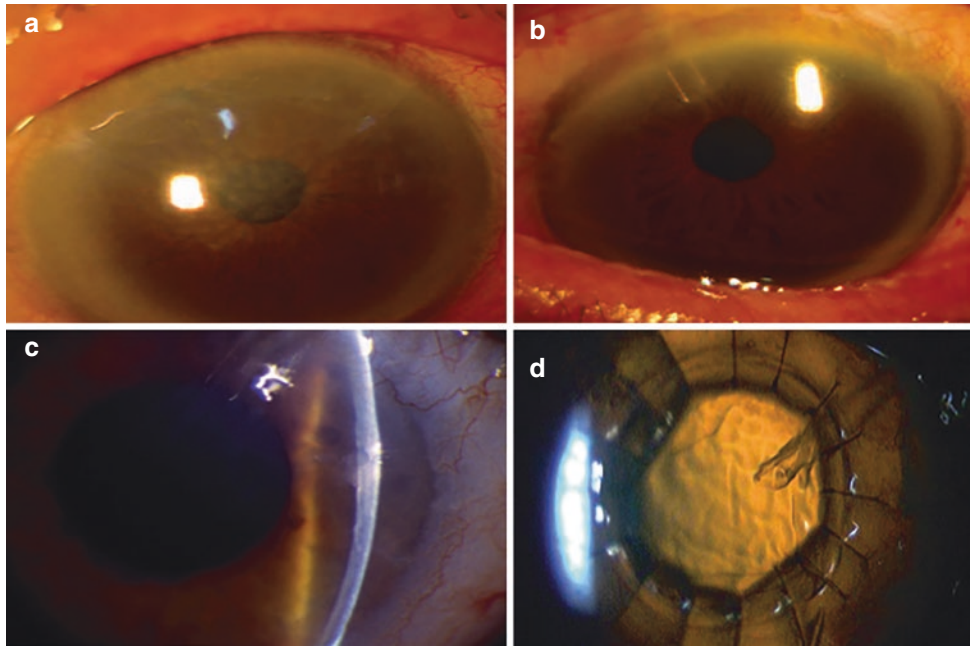

Fig. 36.7 Slitlamp biomicroscopy clinical picture showing tube corneal touch in various eyes after Ahmed glaucoma valve causing corneal decompensation. (**a**, **b**) Diffuse illumination picture showing tube-corneal touch with corneal decompensation more in (**a**). (**c**) Slit illumination picture showing tube-corneal touch, (**d**) diffuse illumination picture showing tube-corneal (graft) touch in post penetrating keratoplasty glaucoma

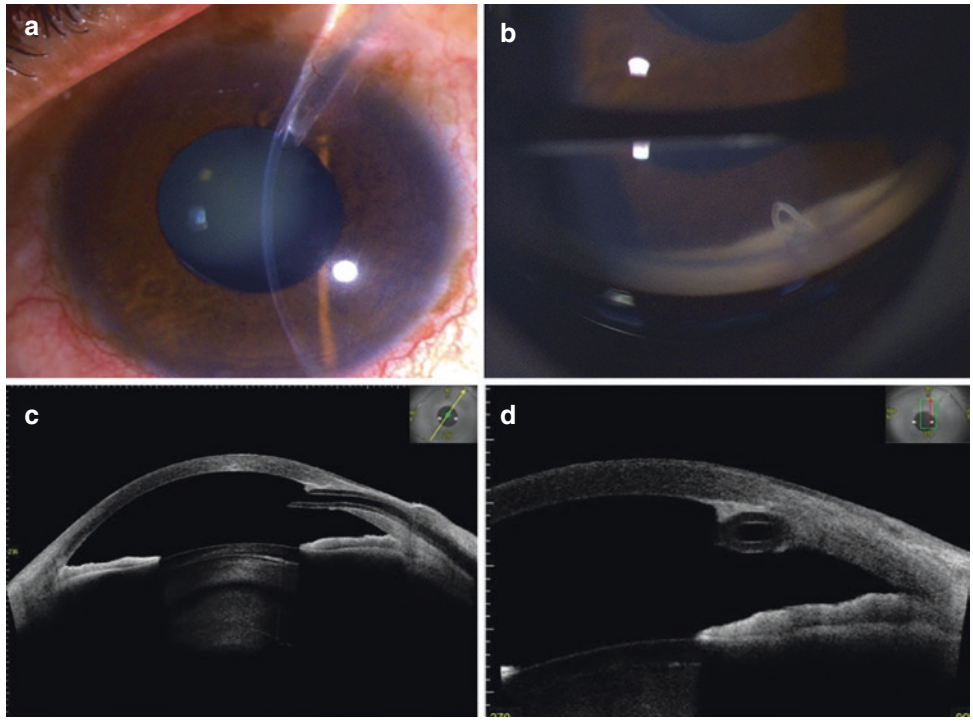

Fig. 36.8 Slit lamp (**a**), gonioscopy (**b**), anterior segment OCT (**c**, **d**) image showing Ahmed glaucoma valve tube corneal touch

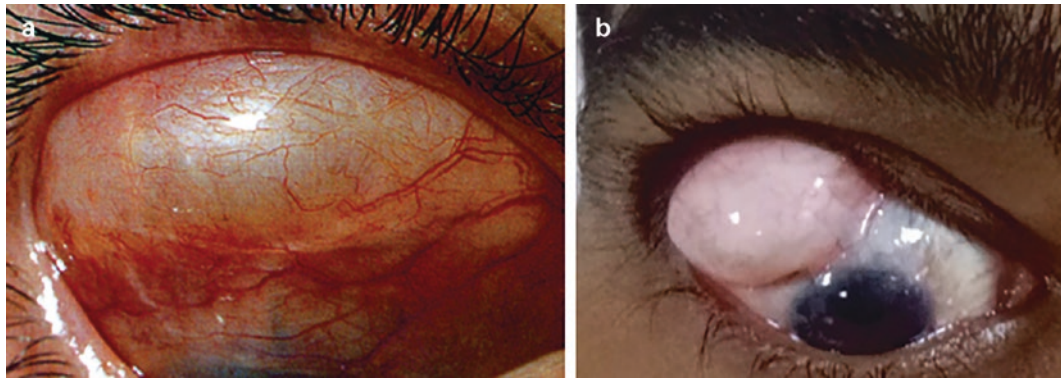

Fig. 36.9 Clinical picture showing diffuse vascularised (**a**) and localised (**b**) encapsulated bleb

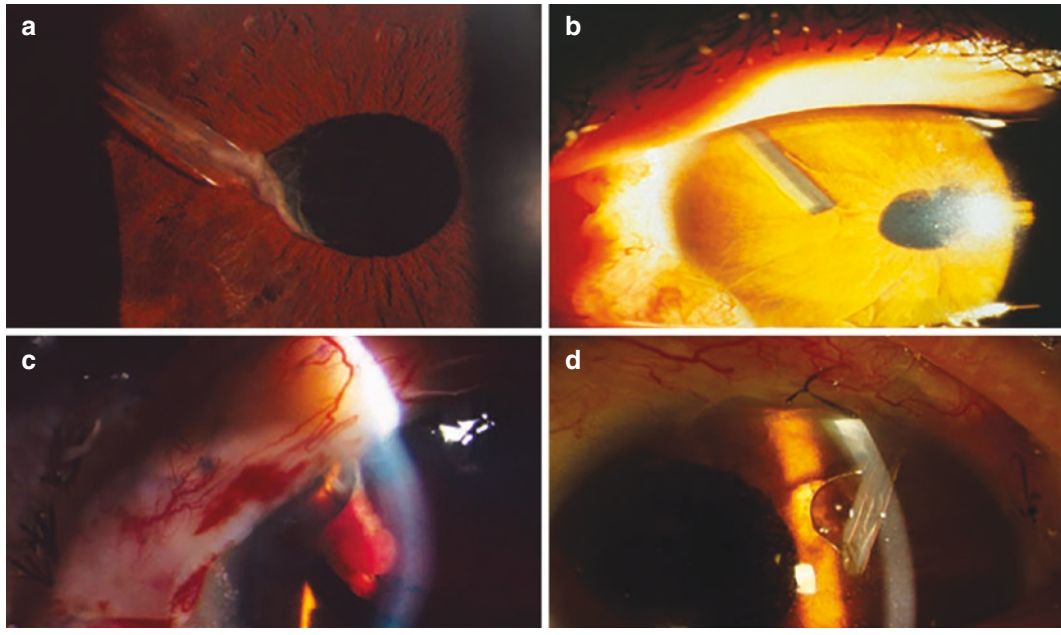

Fig. 36.10 Slit lamp photography showing vitreous (**a**), iris (**b**), blood clot (**c**), and silicone oil (**d**) blocking the Ahmed glaucoma valve tube

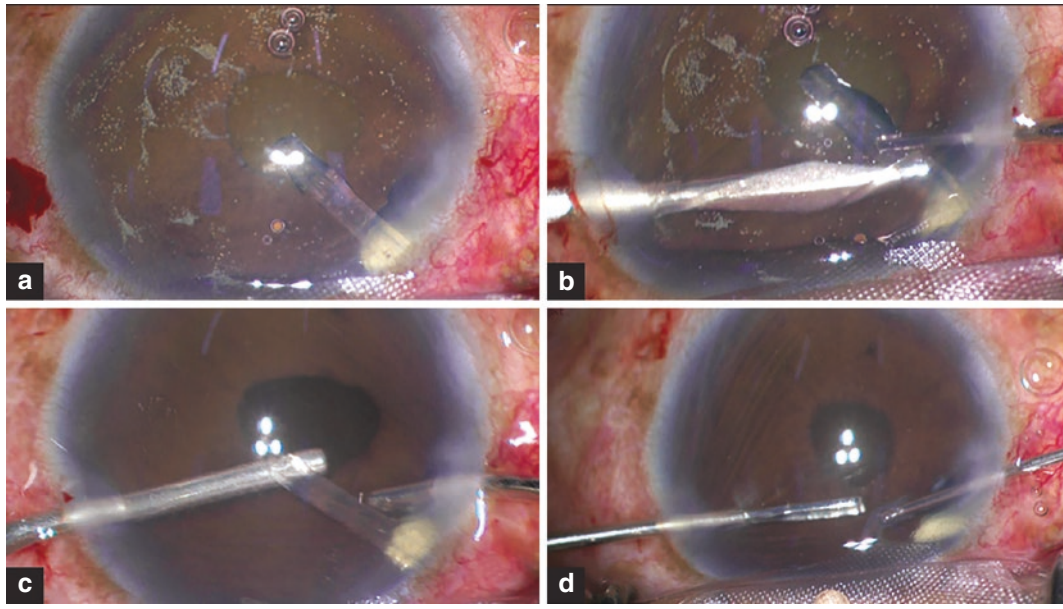

Fig. 36.11 (**a**) Intraoperative image showing silicone oil in and around the tube. (**b**) Vent incision in the AGV tube with the help of 20-G straight blade and micro-vitreoretinal forceps. (**c**) Aspiration of oil around the surface of AGV tube. (**d**) Irrigation of AGV tube with basic salt solution. (Reproduced with permission from: Namdev V, Panigrahi A, Arora M, Gupta V, Gupta S. Intracameral vent and flush technique for silicone oil blockade in Ahmed glaucoma valve. Indian J Ophthalmol. 2022 May;70(5):1812-1814. doi: 10.4103/ijo.IJO_2677_21)

36.7 Long-Term Outcomes

Mandalos et al. compared the outcome and complication of GDDs (Baerveldt/Molteno) in children (69 eyes) and adults (145 eyes) over a mean period of 3–4 years. They stated that postoperatively the mean IOP and number of glaucoma medications used reduced significantly in both groups. Both groups had similar failure rates. Children had more frequent encapsulation (due to increased healing response) and a higher rate of endophthalmitis, while adults had more frequent corneal decompensation.

Khan et al. compared the surgical outcomes of AADI (56 eyes) with AGV (70 eyes) in refractory pediatric glaucoma. They concluded that both had a similar success rate (AGV 69.9%, AADI 66.8%) at 2 years, but in AADI, there was less need for glaucoma medications or glaucoma reoperations at the end of 1 year. The pros and cons of valved (AGV) vs. non-valved (AADI/Baerveldt) implants are mentioned in Table 36.2.

Reiser et al. compared the outcomes of AGV (41) with Baerveldt (48) implant retrospectively in pediatric refractory glaucoma. At 1 year, 20% of AGV and 2% of Baerveldt implant failed. At 5 years, 80% of AGV and 50% of Baerveldt implant failed. They concluded that Baerveldt implant showed greater, more sustained IOP reduction over time with lesser postsurgical complications and lower failure rates. However, Budenz et al. conducted a randomized controlled trial to compare the 5-year outcomes of AGV (143) with Baerveldt (133) implant in refractory adult glaucoma and reported that both groups had similar rate of surgical success. Also, Baerveldt group had a greater IOP reduction but more failures (due to safety issues) compared to AGV group.

Elhusseiny et al. evaluated the short-term outcomes (median follow-up 12 months) of ACP valveless glaucoma drainage device (Fig. 36.12) in childhood glaucoma (7 eyes) and reported a IOP reduction from 36 ± 3.5 mmHg (on 2.7 ± 0.6

Table 36.2 Pros and cons of non-valved (Baerveldt/AADI/ACP) vs. valved (AGV) implants

	Baerveldt/AADI/ACP	AGV
Inserting device beneath the recti	Yes; hence, muscle hooking required	No
Ripcord/ligature suture	Required	Not required
Two-staged procedure	Tube is inserted intracamerally at 4–6 weeks apart. It may be required if a ligation suture is not used	Not required
IOP control	Better IOP reduction compared to AGV	Lesser IOP reduction; greater chances of bleb fibrosis, encapsulation and failure
Hypotony	Higher chances of early postoperative hypotony compared to AGV	Lesser chances of hypotony
Implantation	Larger surface area making implantation difficult in buphthalmic eyes with small orbits or in eyes with extensive conjunctival fibrosis	Easier implantation due to lesser surface area and availability of pediatric size

AADI Aurolab aqueous drainage implant device, *ACP* Ahmed ClearPath, *AGV* Ahmed glaucoma valve

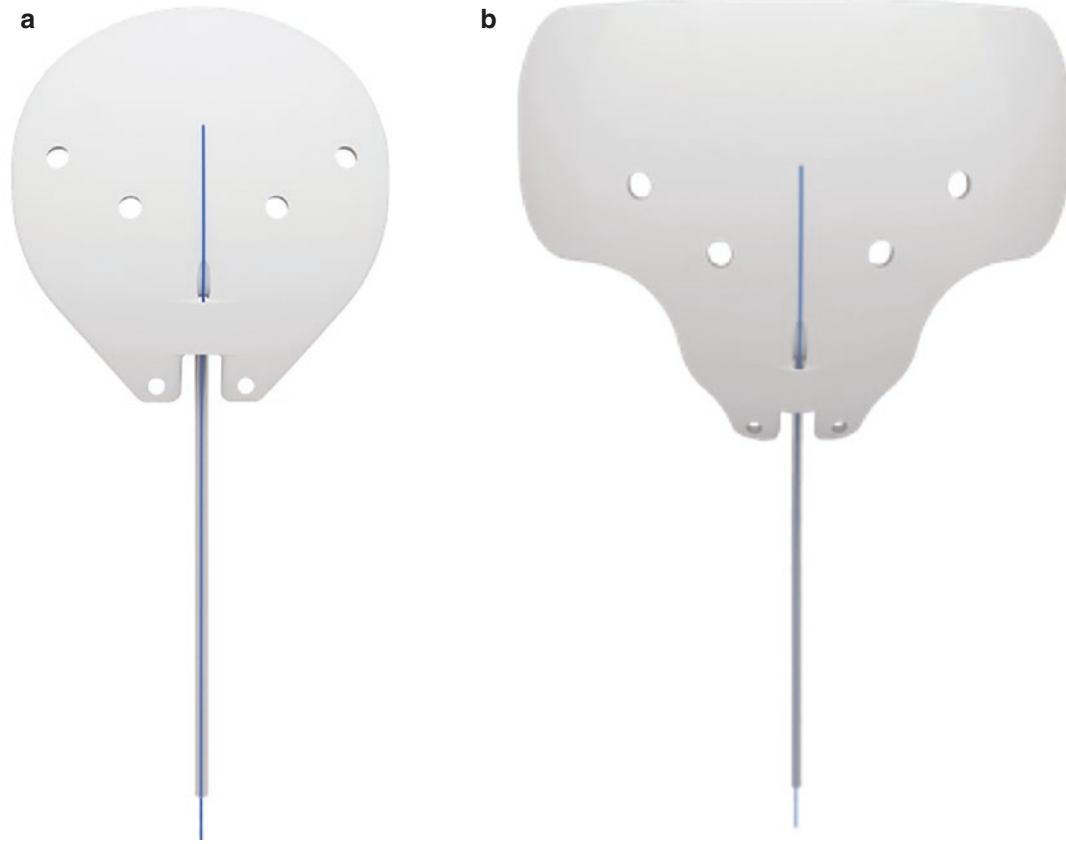

Fig. 36.12 Ahmed ClearPath (New World Medical Inc., CA) (**a**) 250 mm^2 and (**b**) 350 mm^2 with a threaded 4-0 polypropylene ripcord suture

glaucoma medications) to 12.4 ± 2.8 mmHg (on 0.7 ± 0.8 glaucoma medications) at the final follow-up. Complete success was achieved in four eyes (out of seven).

None of the studies have compared the GDD vs. trabeculectomy in childhood glaucoma. The "Tube Versus Trabeculectomy" (TVT) study compared the efficacy of Baerveldt vs. trabeculectomy with mitomycin C in adult glaucomas. The 5-year results do not demonstrate a clear superiority of one surgery over another. The tube shunt surgery had a higher success rate compared to trabeculectomy with mitomycin C in eyes with previous cataract surgery and/or glaucoma surgery. Both procedures were similar with regard to the need for additional medications and effectively lowering IOP.

36.8 Conclusions

GDD has become the procedure of choice for managing pediatric glaucomas after failed angle/filtration surgeries or as a primary procedure in cases where there is high risk of failure with angle/filtration surgeries. Non-valved GDDs have better IOP control, lesser chances of bleb encapsulation/failure but higher chances of hypotony as compared to valved GDDs.

Suggested Reading

Ayyala RS, Zurakowski D, Smith JA, Monshizadeh R, Netland PA, Richards DW, Layden WE. A clinical study of the Ahmed glaucoma valve implant in advanced glaucoma. Ophthalmology. 1998;105(10):1968–76. https://doi.org/10.1016/S0161-6420(98)91049-1.

Budenz DL, Barton K, Gedde SJ, Feuer WJ, Schiffman J, Costa VP, Godfrey DG, Buys YM, Ahmed Baerveldt Comparison Study Group. Five-year treatment outcomes in the Ahmed Baerveldt comparison study. Ophthalmology. 2015;122(2):308–16. https://doi.org/10.1016/j.ophtha.2014.08.043.

Christakis PG, Kalenak JW, Tsai JC, Zurakowski D, Kammer JA, Harasymowycz PJ, Mura JJ, Cantor LB, Ahmed II. The Ahmed versus Baerveldt study: five-year treatment outcomes. Ophthalmology. 2016;123(10):2093–102. https://doi.org/10.1016/j.ophtha.2016.06.035.

Elhusseiny AM, VanderVeen DK. Early experience with Ahmed clear path glaucoma drainage device in childhood glaucoma. J Glaucoma. 2021;30(7):575–8. https://doi.org/10.1097/IJG.0000000000001855.

Elhusseiny AM, Van der Veen DK. Outcomes of glaucoma drainage devices in childhood glaucoma. Semin Ophthalmol. 2020;35(3):194–204. https://doi.org/10.1080/08820538.2020.1781906.

Gedde SJ, Schiffman JC, Feuer WJ, Herndon LW, Brandt JD, Budenz DL, et al. Treatment outcomes in the Tube Versus Trabeculectomy (TVT) study after five years of follow-up. Am J Ophthalmol. 2012;153(5):789–803.

Gupta S, Chaurasia AK, Chawla R, Kapoor KS, Mahalingam K, Swamy DR, Gupta V. Long-term outcomes of glaucoma drainage devices for glaucoma post-vitreoretinal surgery with silicone oil insertion: a prospective evaluation. Graefes Arch Clin Exp Ophthalmol. 2016;254(12):2449–54. https://doi.org/10.1007/s00417-016-3469-9.

Gupta S, Markan A, Azmira K, Dada T, Gupta V. Supracapsular fixation for repositioning Ahmed glaucoma valve in case with tube-endothelial touch. Eur J Ophthalmol. 2020;30(1):212–6. https://doi.org/10.1177/1120672119834491.

Gupta S, Saluja G, Chaurasia AK, Behera AK, Gupta V. Transcorneal tube extrusion: anterior segment optical coherence tomography-aided management. Indian J Ophthalmol. 2019;67(1):126–7. https://doi.org/10.4103/ijo.IJO_416_18.

Khan AM, Ahmad K, Alarfaj M, et al. Surgical outcomes of the Aurolab aqueous drainage implant (AADI) versus the Ahmed glaucoma valve for refractory paediatric glaucoma in Middle Eastern children. BMJ Open Ophthalmol. 2021;6:e000831. https://doi.org/10.1136/bmjophth-2021-000831.

Kumar H, Gupta A, Gupta V. A microinvasive technique for management of corneal edema secondary to glaucoma drainage device tube-corneal touch. Indian J Ophthalmol. 2018;66(6):861–2. https://doi.org/10.4103/ijo.IJO_987_17.

Mandalos A, Sung V. Glaucoma drainage device surgery in children and adults: a comparative study of outcomes and complications. Graefes Arch Clin Exp Ophthalmol. 2017;255(5):1003–11. https://doi.org/10.1007/s00417-017-3584-2.

Namdev V, Panigrahi A, Arora M, Gupta V, Gupta S. Intracameral vent and flush technique for silicone oil blockade in Ahmed glaucoma valve. Indian J Ophthalmol. 2022;70(5):1812–4. https://doi.org/10.4103/ijo.IJO_2677_21.

Patel S, Pasquale LR. Glaucoma drainage devices: a review of the past, present, and future. Semin Ophthalmol. 2010;25(5-6):265–70. https://doi.org/10.3109/08820538.2010.518840. PMID: 21091010.

Patil TS, Mani B, Balekudaru S, George RJ, Lingam V. Effect of immediate shallow anterior chamber after Ahmed glaucoma valve implantation on intermediate-term intraocular pressure control. Indian J Ophthalmol. 2022;70(8):2915–21. https://doi.org/10.4103/ijo.IJO_3071_21.

Reiser BJ, Murakami Y, Choe JY, Contractor D, Reid M. The Ahmed-Baerveldt comparison (ABC) study for pediatric refractory glaucoma. J Am Assoc Pediatr Ophthalmol Strabismus. 2018;22(4):e8. https://doi.org/10.1016/j.jaapos.2018.07.020.

Tseng VL, Coleman AL, Chang MY, Caprioli J. Aqueous shunts for glaucoma. Cochrane Database Syst Rev. 2017;7(7):CD004918. https://doi.org/10.1002/14651858.CD004918.pub3.

van Overdam KA, de Faber JT, Lemij HG, de Waard PW. Baerveldt glaucoma implant in paediatric patients. Br J Ophthalmol. 2006;90(3):328–32. https://doi.org/10.1136/bjo.2005.078832.

Cyclodestructive Procedures

37

Vaibhav Namdev, Karthikeyan Mahalingam, and Shikha Gupta

37.1 Introduction

Childhood glaucoma is mainly a surgical disease as medical therapy seldom helps in intraocular pressure control. Various surgical modalities in clinical practice are angle surgeries (goniotomy/trabeculotomy), trabeculectomy, and glaucoma drainage devices. However, owing to an aggressive scarring response after filtering surgery in children compared to adults, higher failure rates are observed. In the case of refractory glaucomas (after the failure of two or more surgical procedures), cyclodestructive procedures often remain the procedure of choice, especially in eyes with poor visual potential. As the name suggests, cyclodestruction involves damaging the ciliary body, thus enabling decreased production of aqueous humor. Cyclodestruction is based on two mechanisms: heating (cyclophotocoagulation) and freezing (cyclocryotherapy).

Cyclocryotherapy was prevalent before the advent of cyclophotocoagulation. It is associated with intracellular ice crystal formation and ischemic necrosis of ciliary body. It offers poor outcomes in pediatric glaucomas with success rates of only about 30% (Al Faran et al. 1990). Besides, it also causes significant scleral thinning. Due to its poor outcomes and complications, it is not preferred nowadays.

- Currently, semiconductor diode lasers, with wavelength ranging between 750 and 850 nm, are being used extensively for transscleral cyclophotocoagulation because of their compact size, low cost, low maintenance requirement, and greater absorption by uveal melanin pigment.
- The advent of micropulse technology has made application of cyclodestruction possible in eyes with better visual potential.
- The development of endoscopic cyclophotocoagulation (ECP) has facilitated a more targeted approach to the ciliary body processes, thus limiting collateral damage.

Supplementary Information The online version contains supplementary material available at https://doi.org/10.1007/978-981-19-7466-3_37.

V. Namdev (✉) · K. Mahalingam · S. Gupta
Dr. Rajendra Prasad Centre for Ophthalmic Sciences, All India Institute of Medical Sciences, New Delhi, India

S. Gupta et al. (eds.), *Childhood Glaucoma*, https://doi.org/10.1007/978-981-19-7466-3_37

37.1.1 Laser-Tissue Interaction in Cyclophotocoagulation

Cyclophotocoagulation (CPC) involves thermal injury to the tissue. In simple words, laser-tissue interaction involves transfer of light energy to the tissue, which in turn heats it, thus causing denaturation of proteins and eventually its destruction (coagulation). The effect depends upon the composition of the laser and the chromophore. A chromophore is a molecule that absorbs light of a certain wavelength in a manner that generates heat. Hemoglobin, melanin, and xanthophyll are chromophores naturally present in our body.

Cyclophotocoagulation involves the destruction of ciliary body tissue and surrounding blood vessels due to excellent absorption of red/green/yellow or infrared light by chromophore melanin and hemoglobin, respectively. Different sources of laser with different wavelengths have variable effects on trabecular meshwork tissue which determines therapeutic effects of that particular laser and its efficacy.

37.2 Classification of Various Cyclophotocoagulation Techniques

The Fig. 37.1 summarises the different modalities of cyclophotocoagulation procedures. The Table 37.1 summarises the different aspects of various contact laser delivery systems.

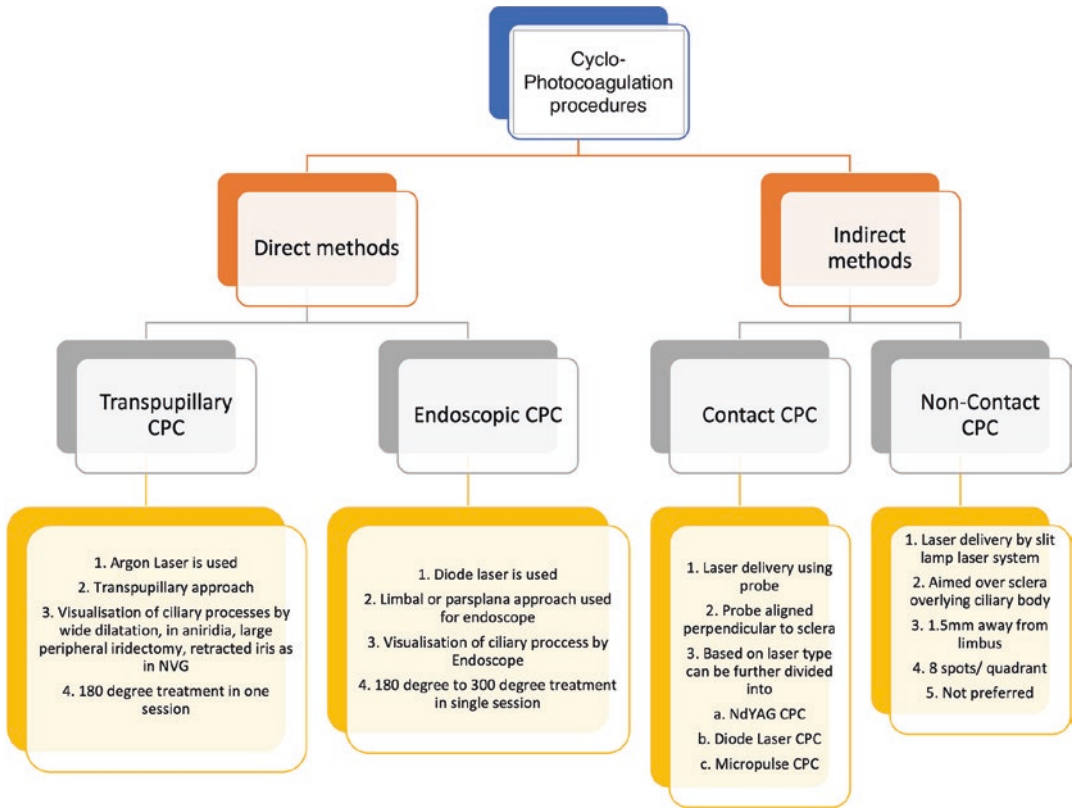

Fig. 37.1 Classification of cyclophotocoagulation procedures. (*CPC* cyclophotocoagulation, *NVG* neovascular glaucoma)

Table 37.1 Table summarising and comparing various contact laser systems

	Nd YAG contact CPC	Continuous-wave/conventional diode laser CPC	Micropulse diode laser CPC
Laser type	Single-frequency Nd YAG laser	Diode laser	Diode laser with micropulse delivery
Wavelength	1024 nm	750–850 nm	810 nm
Power	7000 mW	1250–2000 mW	2000–2400 mW
Pulse duration	0.7 seconds	2 seconds	On time: 0.5 msec Off time: 1.1 msec
Probe	G probe	G-Probe with illuminator probe	Micropulse P3 delivery device (round body probe with notch)
Laser application	Probe based on the sclera overlying the ciliary body with probe	Probe based on the sclera overlying the ciliary body	Sweeping motions over the sclera overlying the ciliary body
Advantages	• Less scatter through sclera • Compact size	• High efficiency • Low maintenance • Compact size • Greater absorption by melanin	• Less inflammation • Moderate efficacy • Can be used in advanced glaucoma with good visual acuity • Less damage to adjacent tissue
Disadvantages	• Low absorption through the sclera • Lesser absorption by uveal tissue • Commercially unavailable	• Waning effect over time • Need of multiple sessions • More inflammation	• Waning effect over time • Need of multiple sessions

37.2.1 Semiconductor Diode Laser Cyclophotocoagulation

Contact-based semiconductor diode laser cyclophotocoagulation with a continuous wave is the most commonly performed cyclodestructive procedure which is popularly called diode laser cyclophotocoagulation (DLCP).

Instrument

The Oculight SLx (Iris Medical Instruments Inc., CA) is a continuous-wave contact delivery diode laser system with a wavelength of 810 nm, a maximum power output of 2.5–3 W and a maximum duration of 9.9 seconds. The G-Probe consists of 600-micron quartz fiberoptic, protruding 0.7 mm from a handpiece, which is fabricated to center the fiberoptic 1.2 mm behind the surgical limbus and parallel to the visual axis.

37.2.1.1 Procedure (Fig. 37.2, Video 37.1)

- Anesthesia: It is always performed in general anesthesia unless the child is older enough to be cooperative for a peribulbar block. As it is quite a painful procedure, 2–4 ml of peribulbar block in addition to general anesthesia is administered to reduce perioperative pain. At our center, peribulbar block of the local anesthetic solution is prepared by mixing 1500 IU of hyaluronidase in 30 ml 2% lignocaine solution and then mixing 5 ml of this solution with 5 ml of 0.75% of ropivacaine. Performing bilateral laser therapy simultaneously is generally not performed, unless associated with high risk of anesthesia-related complications.
- Lid speculum to be placed.
- Viscoelastic devices can be used to coat the cornea/conjunctiva to prevent it from drying and also help in protecting from conjunctival burns.

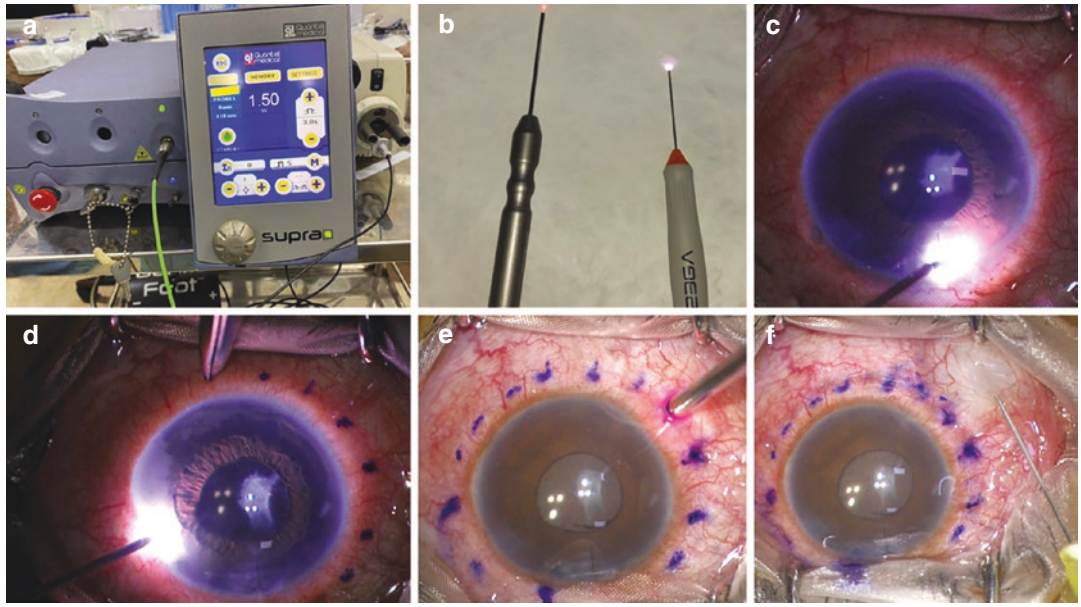

Fig. 37.2 Conventional diode laser cyclophotocoagulation (DLCP): Image (**a**) showing the DLCP console (Supra 810, Quantel Medical, France) with power setting of 1500 mW and pulse duration of 3 seconds. Image (**b**) shows probes used in DLCP. The right-side probe represents the illuminator probe and left-side probe is the laser probe. Image (**c**) shows intraoperative view of the eye in a dark room setting to illuminate the margin of the ciliary body by keeping the illumination probe at the limbus. The trans-illuminated margin (representing the ciliary processes) can be marked with gentian blue as shown in the image (**d**). The laser is delivered at each marked point for desired 270° cyclophotocoagulation sparing the 3 and 9'o clock position as depicted in the image (**e**). At the end of the procedure, subconjunctival depot injection containing cycloplegic agents and steroids should be given (**f**)

- The G-Probe footplate is placed on the conjunctiva with the short side facing the surgical limbus. The proper probe positioning ensures that the fiberoptic is lying 1.2 mm behind the limbus. Alternatively, the correct position can be identified by keeping the illuminator in the limbus and marking the junction of the light and dark zone. Later, laser probe can be placed in the marks and the laser energy can be delivered (Fig. 37.2).
- Usually, initial settings are kept at 1750 mW and 2 second duration. With initial application, if a popping sound is heard, the power is reduced by 250 mW, and if no popping sound is heard, the power is increased by the similar amount until the sound is heard followed by a reduction by 250 mW. In darkly pigmented irises like that seen in Asians and Africans, the energy required is usually higher than that in lightly pigmented irises.
- The popping sound is associated with tissue coagulation and destruction of the ciliary process, and it is believed that this audible indicator represents excessive tissue damage. Power setting of one level below this indicator represents optimum treatment.
- After the laser application, the G-Probe is moved circumferentially and placed adjacent to the indentation mark of the previous fiberoptic placement.
- Laser application at 3 and 9'o clock positions should be avoided as it may cause damage to the long posterior ciliary vessels which can result in anterior segment ischemia and the co-located, long ciliary nerves which may cause immense pain.
- We prefer six laser applications per quadrant covering 270° in single session and usually spare the superior conjunctival area for future trabeculectomy if required. The original protocol also recommended 17–19 applications for 270°. However, 24 applications for 360° may provide more effective IOP control according to Shields et al.

- Because of significant postoperative inflammation, subconjunctival injection of steroid/atropine/cycloplegic can be given at the end of the procedure.

37.2.1.2 Postoperative Measures

As postoperative inflammation and pain are significant issues associated with DLCP, topical steroids and homatropine 2% or eye ointment atropine 1%, respectively, are prescribed along with analgesic medication for at least 2–4 weeks in tapering doses. Preoperative glaucoma medications may be instituted at follow-up (except miotics and prostaglandin analogs) if required. Oral acetazolamide can also be given immediately after the procedure. Postoperative IOP evaluation is to be done a few hours after the procedure, the following day, 3 weeks later, and then thereafter as required.

The utility of continuous-wave transscleral DLCP for the management of refractory glaucoma (defined as uncontrolled glaucoma despite prior surgical treatments and/or medical therapy alone) has been well established for over 30 years. It is well tolerated among children with few complications reported.

Kirwan et al. studied the efficacy of conventional DLCP in refractory pediatric glaucoma (77 eyes) and demonstrated a sustained control of IOP to <21 mmHg in 72% of the eyes at 1 year and 51% at 2 years after treatment (mean of 2.3 treatment sessions per eye). Autrata et al. studied the efficacy of conventional DLCP in refractory pediatric glaucoma (69 eyes) and reported a clinically effective reduction in IOP in 79% of eyes (with repeat treatment) at 1 year.

37.2.2 Micropulse Diode Laser Cyclophotocoagulation

Micropulse diode laser system is a new modality launched in the US market in 2015 by Iridex Co. Micropulse® laser therapy is a tissue-sparing alternative for the treatment of retinal diseases and glaucoma. With micropulse, a continuous-wave laser beam is chopped into a train of short, repetitive, low-energy pulses separated by a brief rest period which allows the tissue to cool in between laser pulses.

Several studies suggest that micropulse laser system can be used in treatment of specific types of glaucoma patients, especially post-keratoplasty eyes and pediatric patients. However, it has been observed that the IOP reduction effect of micropulse wanes over time. The recent shift in favor of micropulse system over conventional transscleral DLCP system is largely due to the sentiment that it results in fewer postoperative complications while being equally as effective.

37.2.2.1 Procedure (Fig. 37.3, Video 37.2)

- Initial steps are similar to the conventional DLCP.
- The wide curved side of the probe (with notch) is aligned with the surgical limbus (Fig. 37.3b, c). Proper alignment ensures the correct laser delivery position.
- Laser (2000 mW) is delivered for 80–100 seconds in each hemisphere.
- Continuous "to and fro" sweeping motion of the probe over a hemisphere is used (unlike conventional DLCP where the probe is kept stationary).
- Typical time for each sweep over the hemisphere is 10–12 seconds.

Abdelraman et al. compared the safety and efficacy of conventional DLCP with micropulse DLCP in refractory pediatric glaucoma (45 eyes) and reported that both were effective in lowering IOP with micropulse having lesser complications. But Fam et al. reported that conventional DLCP had more significant IOP lowering compared to micropulse DLCP at 1 year in refractory pediatric glaucoma (31 eyes), and retreatment rates were high for micropulse vs DLCP group.

Disadvantage: Micropulse DLCP comes with a single-use, disposable probe costing approximately 250 USD and is active only for 30 min after it is connected. Thus, the cost of the procedure for micropulse DLCP is high compared to conventional DLCP.

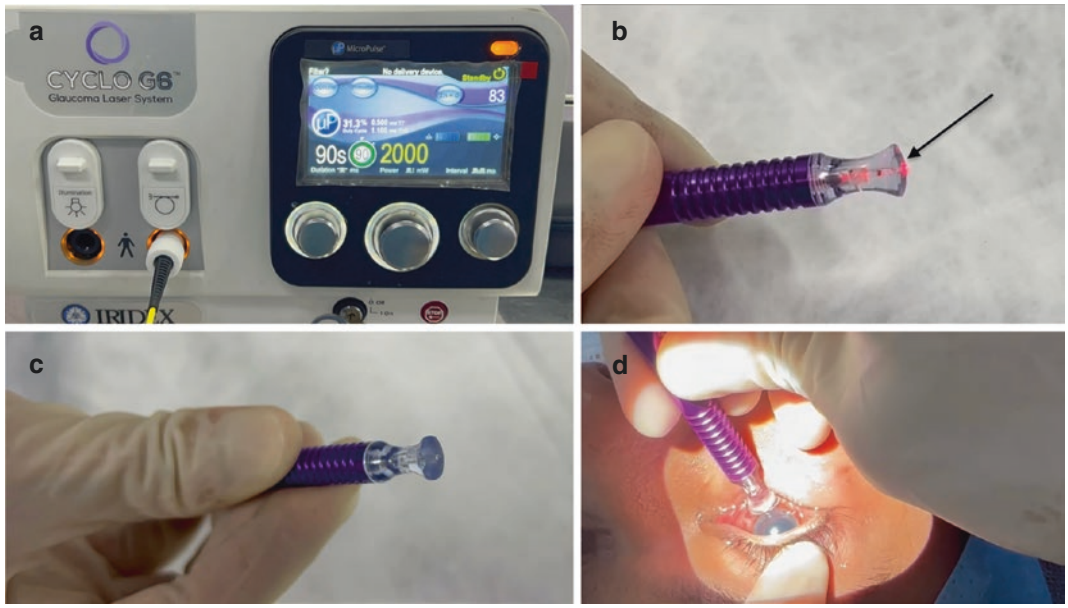

Fig. 37.3 Micropulse diode laser cyclophotocoagulation (CPC) system, CYCLO G6 from IRIDEX: (**a**) Micropulse laser delivery equipment on standby mode. Treat mode is started while delivering the laser. (**b**) Image showing the magnified view of the micropulse probe (arrow pointing towards the notch) and (**c**) shows end-on view of the probe depicting the flat circular surface of the probe. (**d**) Micropulse laser CPC probe applied onto the inferior quadrant with circular surface on the surface just at the margin of the limbus. Micropulse laser is delivered with sweeping movements of the probe

37.2.3 Endoscopic Cyclophotocoagulation

In an attempt to minimize damage to tissue adjacent to ciliary processes, a newer technology called endoscopic cyclophotocoagulation (ECP) has been developed in which ciliary processes are treated with diode laser for its coagulative effect under direct visualization by the endoscope. Currently, ECP is popularly being combined with phacoemulsification and being performed as a combined surgery for better IOP reduction effect even in eyes with good visual potential. It is generally used in adult eyes and less often in pediatric glaucomas and limited litearture is available on its utility in pediatric eyes. It can be used even after failure of other cyclodestructive procedures. It can only be performed in pseudophakic or aphakic eyes.

37.2.3.1 Procedure (Fig. 37.4)

1. Limbal or pars plana approach can be used.
2. In limbal approach, temporal incision of approximately 2 mm is created at the limbus followed by replacing the anterior chamber by a cohesive viscoelastic device. Three endoscopy probes, each with 19, 20, and 23 G are available which provide 70–140° field of view and depth of focus spanning from 1 to 30 mm.
3. Pars plana approach is preferred in patients with anterior chamber intraocular lens, abnormal anterior chamber anatomy, or vitrectomized eyes.
4. ECP probe with correct orientation (to be checked outside the eye) is entered through the corneal/ temporal incision into the posterior chamber of the anterior segment and the ciliary processes are visualized on the monitor. Usually, five to six processes can be seen in one frame and treated by directing aiming beam towards them.
5. The continuous laser energy of 0.2–0.5 W is applied onto the ciliary processes until there is whitening and shrinkage due to photocoagulative effect. In cases when excess energy is delivered, ciliary process explosion can occur which is accompanied by popping sound or bubble formation (Fig. 37.4).

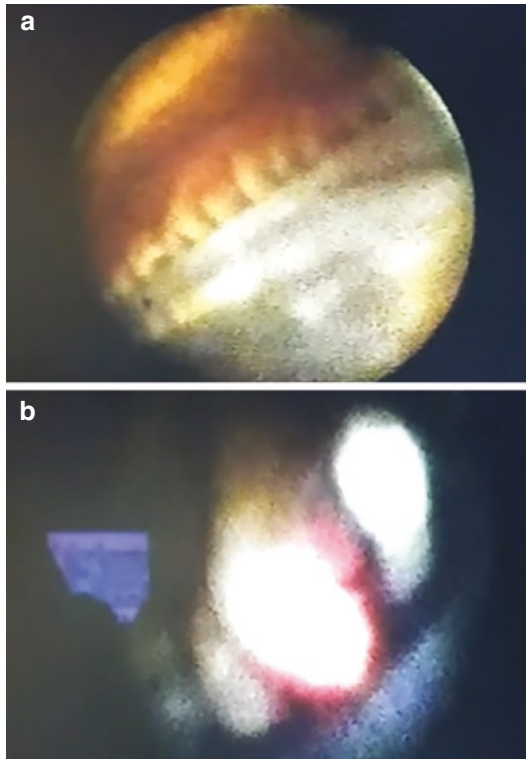

Fig. 37.4 Endocyclophotocoagulation: (**a**) Endoscopic view showing the ciliary processes before laser photocoagulation. (**b**) Endoscopic view showing the bleached ciliary processes after the application of laser

6. According to Chen et al., the treatment of minimum of 180° of ciliary processes is required for significant IOP reduction. However, Schuman et al. recommend treating 270–300° of the tissue.
7. In anticipation of significant postoperative inflammation, the patient can be given subtenon injection of dexamethasone/methylprednisolone/triamcinolone.
8. Topical antibiotics, cycloplegics, and aqueous suppressants are given postoperatively, to be tapered gradually.

A group of eminent vitreoretinal surgeons have also devised the method to perform intraocular CPC under direct visualization in patients with aphakia where through pars plana route, transpupillary visualization of ciliary processes is facilitated by scleral depressor. Fleishmann et al. described it using argon laser.

The efficacy of ECP has been studied in patients with refractory glaucoma, Neovascular glaucoma and pediatric refractory glaucoma as well as standalone procedure and benefit have been reported by multiple authors. In addition to effectively lowering the IOP, ECP can provide significant reductions in patient topical and systemic glaucoma medication burden. As previously mentioned, direct visualization and subsequent treatment of the ciliary processes offer a more focused approach, limiting the tissue injury following ECP to the aqueous humor-producing cells and associated capillary bed. It is believed that minimal collateral damage to the surrounding tissues during ECP contributes to its favorable safety profile.

Neely et al. studied the efficacy of ECP in difficult pediatric glaucoma (36 eyes, minimum 6 months follow-up) and reported a cumulative success rate of 43%. They concluded that ECP is moderately effective and aphakic patients may have increased postoperative complications like retinal detachment.

37.3 Conclusions

Cyclodestructive procedures have found their widespread application in patients with advanced aphakic or pseudophakic glaucoma, inflammatory glaucoma, neovascular glaucoma, traumatic glaucoma, secondary glaucoma post-penetrating keratoplasty or post-vitreoretinal surgery, after any failed filtration/glaucoma drainage devices surgery and any refractory glaucoma with poor visual potential. However, the risk of associated complications like postoperative pain (up to 46%), drop in visual acuity (13–50%), mild to moderate conjunctival fibrosis, conjunctival/scleral burns, inflammation/cystoid macular edema (21%), hypotony (18%), transient rise in IOP (14.5%), hyphema (12%), phthisis bulbi (0–6%), choroidal/retinal detachment (0.2%), and sympathetic ophthalmia (rare) must be considered.

Suggested Reading

Al Faran MF, Tomey KF, Al Mutlag FA. Cyclocryotherapy in selected cases of congenital glaucoma. Ophth Surg. 1990;21:794–8.

Autrata R, Rehurek J. Long-term results of transscleral cyclophotocoagulation in refractory pediatric glaucoma patients. Ophthalmologica. 2003;217(6):393–400.

Basics of Lasers by Daniel Palanker, PhD, AAO.

Bhagat N, Zarbin M, Mansour S, Chong V, and Cardillo JA. Fovea-friendly MicroPulse laser. Supplement to Retina Today, May/June 2012.

Bietti G. Surgical intervention on the ciliary body; new trends for the relief of glaucoma. J Am Med Assoc. 1950;142(12):889–97.

Chen J, Cohn RA, Lin SC, Cortes AE, Alvarado JA. Endoscopic photocoagulation of the ciliary body for treatment of refractory glaucomas. Am J Ophthalmol. 1997;124(6):787–96.

Curran EJ. Subconjunctival cauterization of the sclera over the ciliary body with the Galvano-Cautery to reduce intraocular pressure in advanced glaucoma: preliminary report. Arch Ophthalmol. 1925;54:321–32.

Edward DP, Brown SV, Higginbotham E, Jennings T, Tessler HH, Tso MO. Sympathetic ophthalmia following neodymium:YAG cyclotherapy. Ophthalmic Surg. 1989;20(8):544–6.

Fam A, Vaidya S, Khouri AS. A comparison of micropulse and continuous wave cyclophotocoagulation in the treatment of refractory pediatric glaucoma. Invest Ophthalmol Vis Sci. 2020;61(7):5230.

Fleischman JA, Swartz M, Dixon JA. Argon laser endophotocoagulation. An intraoperative trans-pars plana technique. Arch Ophthalmol. 1981;99(9):1610–2.

Gaasterland DE, Pollack IP. Initial experience with a new method of laser transscleral cyclophotocoagulation for ciliary ablation in severe glaucoma. Trans Am Ophthalmol Soc. 1992;90:225–43; discussion 243–6.

Garcia GA, Nguyen CV, Yelenskiy A, et al. Micropulse transscleral diode laser cyclophotocoagulation in refractory glaucoma. Ophthalmol Glaucoma. 2010;38(3):266–72.

Kirwan JF, Shah P, Khaw PT. Diode laser cyclophotocoagulation: role in the management of refractory pediatric glaucomas. Ophthalmology. 2002;109(2):316–23.

Maus M, Katz LJ. Choroidal detachment, flat anterior chamber, and hypotony as complications of neodymium: YAG laser cyclophotocoagulation. Ophthalmology. 1990;97(1):69–72.

Murphy C, Burnett C, Spry P, Broadway D, Diamond J. A two centre study of the dose-response relation for transscleral diode laser cyclophotocoagulation in refractory glaucoma. Br J Ophthalmol. 2003;87(10):1252–7.

Ndulue J, Rahmatnejad K, Sanvicente C, Wizov S, Moster M. Evolution of Cyclophotocoagulation. J Ophthalmic Vis Res. 2018;13(1):55–61.

Neely DE, Plager DA. Endocyclophotocoagulation for management of difficult pediatric glaucomas. J AAPOS. 2001;5(4):221–9.

Peyman GA, Naguib KS, Gaasterland D. Trans-scleral application of a semiconductor diode laser. Lasers Surg Med. 1990;10(6):569–75.

Schubert HD. The influence of exposure duration in transscleral Nd: YAG laser cyclophotocoagulation. Am J Ophthalmol. 1993;115(5):684–5.

Simmons RB, Prum BE Jr, Shields SR, Echelman DA, Shields MB. Videographic and histologic comparison of Nd:YAG and diode laser contact transscleral cyclophotocoagulation. Am J Ophthalmol. 1994;117(3):337–41.

Shaarawy T, Sherwood M, Hitchings R, Crowston J. Glaucoma. 2nd ed. Amsterdam: Elsevier; 2004.

Walton DS, Grant WM. Penetrating cyclodiathermy for filtration. Arch Ophthalmol. 1970;83(1):47–8.

Weekers R, Lavergne G, Watillon M, Gilson M, Legros AM. Effects of photocoagulation of ciliary body upon ocular tension. Am J Ophthalmol. 1961;52:156–63.

Xenon Arc Photocoagulation. Acta Ophthalmol. 2009;67(194):32–43.

Cataract Surgery in Buphthalmic Eyes

38

Sudarshan Khokhar, Saumya Kumar, and Deeksha Rani

38.1 Introduction

Primary congenital glaucoma (PCG) develops due to anomalous development of the anterior chamber angle which leads to obstruction of aqueous outflow ultimately leading to increased intraocular pressure (IOP) and optic nerve damage. Since the scleral rigidity of an infant's eye is low, the size of the eyeball increases due to excessive stretching from elevated IOP. This leads to increased axial length (axial myopia), stretched limbus, corneal thinning, and visibly enlarged eyeball. The term used for such a large eye is "buphthalmos." Other causes of buphthalmos include infantile-onset glaucoma in cases with Sturge-Weber syndrome, Axenfeld-Rieger syndrome, Peter's anomaly, aniridia etc. Glaucoma surgery increases the risk of cataract formation in adults; however, the exact incidence of cataractogenesis after glaucoma surgery in eyes with congenital glaucoma is not known.

38.1.1 Etiology of Cataract in Buphthalmic Eyes

- Congenital/developmental.
- Secondary glaucoma in eyes with TORCH (toxoplasmosis, others (syphilis, hepatitis B), rubella, cytomegalovirus (CMV), herpes simplex (HSV)) infections. Of these, rubella and cytomegalovirus (CMV), usually have cataracts associated with posterior synechiae (Fig. 38.1).
- Sequelae to filtration or angle surgery.

38.1.2 Morphology of Cataract

- Most common morphology seen: anterior or posterior subcapsular cataract.
- Cataracts can be associated with subcapsular fibrosis if inflammation persists or posterior

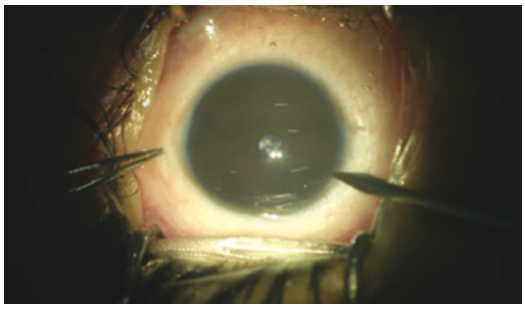

Fig. 38.1 Clinical picture of the eye showing cataract and small pupil due to posterior synechiae, usually seen after intrauterine infection with viruses such as rubella, cytomegalovirus etc.

Supplementary Information The online version contains supplementary material available at https://doi.org/10.1007/978-981-19-7466-3_38.

S. Khokhar · S. Kumar (✉) · D. Rani
Dr. Rajendra Prasad Centre for Ophthalmic Sciences, All India Institute of Medical Sciences, New Delhi, India

S. Gupta et al. (eds.), *Childhood Glaucoma*, https://doi.org/10.1007/978-981-19-7466-3_38

synechiae coexist or if cataract develops as a sequela to filtration surgery.
- Less commonly, zonular cataract can be seen.

38.1.3 Associated Concerns

- High corneal astigmatism due to Haab's striae.
- Hazy cornea due to corneal opacity/Haab's striae or presence of corneal edema if IOP control is suboptimal.
- Post-trabeculectomy eyes: There is a risk of bleb fibrosis, IOP spike, and failure of trabeculectomy following cataract surgery in operated trabeculectomy eyes.
- Low scleral rigidity.
- Intraocular lens (IOL) sizing in highly buphthalmic eyes is an issue.
- Progressive myopia may be seen after IOL implantation, due to IOP and non-IOP related factors.
- High risk of retinal detachment (RD) due to myopia-associated peripheral retinal degenerations predisposing to rhegmatogenous RD following any intraocular surgery.

38.1.4 Role of Ultrasound Biomicroscopy

- This aids in making an appropriate decision during the surgery.
- Measurement of angle-to-angle distance and bag diameter.
- To assess anterior segment anomalies and to detect abnormal iris insertion and anterior chamber depth.
- Can identify preexisting posterior capsule defect and lax zonules.

38.1.5 Challenges During Cataract Surgery in Buphthalmic Eyes

- IOP should be controlled before taking up the child for cataract surgery. If required, IOP-lowering surgery can be performed before that.
- Corneal haze: Hazy cornea leads to poor intraoperative visualization. Retroillumination helps in improving the visualization (Fig. 38.2); however, the anterior capsule should be stained with 0.06% trypan blue for optimal intraoperative visualization. The posterior capsule may also be stained if needed during posterior capsulorhexis.
- Deep anterior chamber: Deep anterior chamber leads to difficult instrumentation. Anterior chamber depth fluctuation can be noted intraoperatively due to low scleral rigidity. Corneal incisions tunnels should be kept short, microincision forceps with longer arm or intravitreal forceps should be preferred to Utrata forceps for anterior and posterior capsulorhexis.
- IOL selection and IOL power calculation: Buphthalmic eyes are myopic and may continue to grow in an unpredictable manner leading to myopic shift. IOL in the bag is often

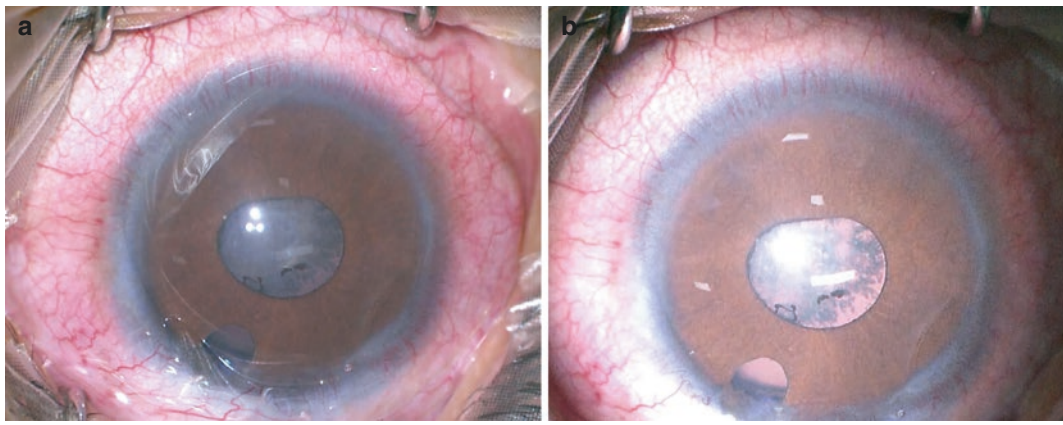

Fig. 38.2 Intraoperative images during cataract surgery (**a**) without retroillumination, and (**b**) improved visualization with retroillumination

associated with an increased risk of decentration due to large bag diameter. Three-piece IOL with haptics in the sulcus and capture of the optic behind the anterior capsule margins is associated with better centration. Appropriate IOL calculation formula should be used based on the axial length. Parents should be counselled for the need of glasses for near and distance and the need for occlusion treatment in unilateral cases. In cases with excessive myopic shift, IOL exchange may be needed after stabilization of refractive error.

- Zonular weakness: There is an increased risk of intraoperative vitreous loss in these patients owing to phacodonesis, lax lens zonules, liquefied vitreous, and a weak posterior capsular support.
- Wound apposition: Due to corneal and scleral thinning in these patients, wound hydration alone may not be sufficient for wound closure. The main wound and if needed, even side ports should be sutured with 10'0 monofilament nylon suture.
- Posterior capsulorhexis should always be done when multipiece IOL is being inserted combined with optic capture.
- Posterior capsulorhexis is preferred till 5 years of age.

38.1.6 Outcomes

Besides controlling the IOP, visual rehabilitation of buphthalmic eyes involves appropriate management for amblyopia, performing timely cataract surgery for visually significant cataracts, and performing keratoplasty for corneal opacity. Our experience with 31 eyes of PCG (post-trabeculectomy) with visually significant cataract undergoing lens aspiration surgery showed a mean best-corrected visual acuity of 6/60 (Snellen) at 1 year postoperatively (Khokhar et al. 2018). Buphthalmic eyes undergoing cataract surgery can achieve successful refractive and visual outcomes if careful preoperative planning is carried out regarding the choice of IOL type and IOL power, taking into consideration achieving the adequacy of IOP control, performing accurate biometry, precise assessment of bag size, and use of appropriate IOL power formulae.

38.2 Case Examples

Case 38.1

A 12-year-old male child with right eye (RE) operated trabeculotomy with trabeculectomy at the age of 9 months for unilateral PCG presented to the outpatient department with progressive diminution of vision in the RE for the past two years. The child also had a history of having undergone bleb revision in the RE for thin cystic bleb with hypotony. Visual acuity in RE was 2/60 with no further improvement on refraction. Visual acuity in the left eye (LE) was 6/6. IOP in the RE was 14 mmHg on three ocular hypotensive medications (brimonidine, timolol, and dorzolamide) while in LE was 16 mmHg on no medications.

Slit-lamp examination in the RE showed a hazy cornea with temporal scarring. There was a superior bleb with conjunctival scarring. The pupil was poorly dilated with anterior capsular fibrosis with posterior subcapsular cataract (Fig. 38.3).

Biometry revealed an axial length of 29.23 mm RE and 22.34 mm LE. The child had a spherical equivalent of -12 D in the RE and was emmetropic in the LE. Intraocular lens (IOL) power calculated for the RE was -2 D.

Diagnosis: RE operated trabeculectomy with cataract with dense amblyopia with unilateral pathological myopia. LE within normal limits.

Treatment: Given visually significant cataract in the RE, the child was planned for RE lens aspiration with posterior chamber IOL under general anesthesia (Video 38.1).

Ultrasound biomicroscopy revealed deep anterior chamber with anterior capsular as well as posterior subcapsular cataract with anterior sub-capsular fibrosis. Bag diameters noted on UBM were 10.51 mm and 9.21 mm in RE and LE, respectively. The incisions were carefully planned to avoid any incisions in the region of bleb. Two side ports were made and pupillary

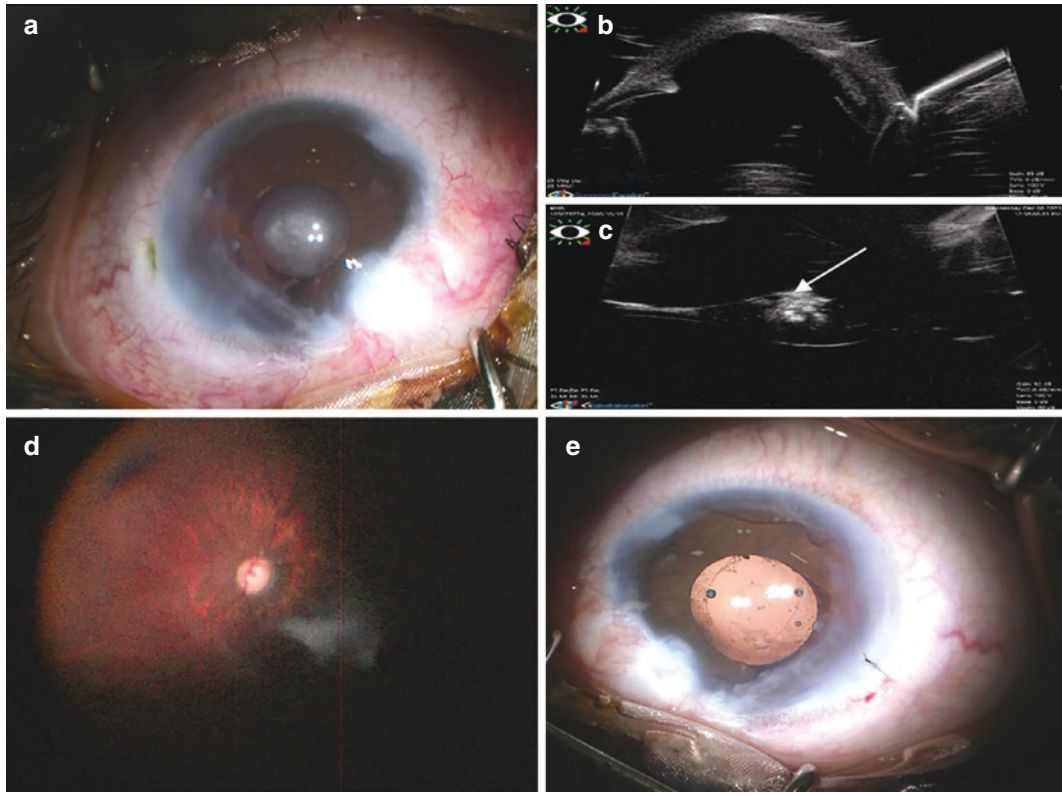

Fig. 38.3 (**a**) Clinical picture showing visually significant cataract. (**b**) UBM showing deep anterior chamber and endothelial scarring. (**c**) UBM showing anterior capsular fibrosis (white arrow). (**d**) Fundus picture showing advanced cupping (0.6:1) during endoilluminator assisted intra-operative fundus viewing and associated chorioretinal degeneration. (**e**) Well-centered IOL with good retro-illumination glow with the main wound sutured at the end of surgery

dilatation was facilitated using intracameral adrenaline. Anterior capsule was stained with 0.06% trypan blue. Anterior capsulorhexis was done followed by gentle hydro dissection. Bimanual lens aspiration was done. Intraoperative fundus evaluation revealed a cup to disc ratio of 0.8:1 and advanced chorioretinal degeneration. Three-piece IOL (Expand series) was inserted into the bag. The wound was sutured with 10-0 monofilament nylon and wounds were hydrated.

Postoperative day 1 vision was 4/60 with no further improvement on refraction. IOP was 7 mmHg on no antiglaucoma medications. There was no wound or bleb leak, frequent topical steroids were instituted, and all glaucoma medications were withheld. IOP normalized at 2-week follow-up. Occlusion treatment in the RE was prescribed.

Learning Points

- Need to appropriately position the incisions in the eyes having undergone trabeculectomy in the past to avoid damaging bleb.
- The anterior chamber is usually deep which may cause difficulty during cataract surgery.
- The hazy cornea may make the surgery even more challenging.
- Post-glaucoma-filtering surgery, recurrent shallowing of the anterior chamber, post-operative inflammation and ocular hypotony can accelerate cataract formation.
- Three-piece IOL can be placed in a bag in cases of normal bag diameter.
- The usual approach in eyes with buphtahlmos is to calculate IOL power using SRK-II formula. For eyes with axial length >24.5 mm, SRK-T is the preferred formula. Undercorrection done is as follows:

Age	Percentage undercorrection (%)
<3 months	20
1 year	10
2 years	5
5 years	2

As buphthalmic eyes tend to grow more, we err towards achieving greater undercorrection in order to attain emmetropisation when the child's eye ceases to grow (Khokhar et al. 2018)

Case 38.2

A 4-year-old child presented to us with complaints of whitish opacity in the LE with diminution of vision noticed by parents 6 months back. The child was a known case of LE congenital glaucoma and a LE trabeculectomy was done at the age of 3 years. On examination, we found that the visual acuity was 6/15 at 50 cm on Cardiff in the RE, whereas in the LE, the child was only able to perceive light. In the LE, bleb was visible in the superonasal quadrant (H2E2V2S0). IOP was 12 and 7 mmHg in RE and LE, respectively. Corneal diameters were increased in LE as compared to the RE. There was a total white cataract in the LE with anterior capsular plaque.

The child underwent an examination under anesthesia. Ocular biometry was done, and axial lengths were 21.88 and 27.59 in RE and LE, respectively.

Diagnosis: RE, fellow eye; LE, buphthalmos with operated trabeculectomy with total white cataract.

Treatment: LE lens aspiration with PCCC + anterior vitrectomy with multipiece IOL with capture was done under general anesthesia (Video 38.2).

Ultrasound biomicroscopy of the LE revealed a deep anterior chamber with an intumescent cataractous lens (Fig. 38.4). Incisions were made carefully avoiding any damage to the bleb. The anterior capsule was stained using 0.06% trypan blue dye, and anterior capsulorhexis was done using intravitreal scissors and forceps due to the presence of anterior capsular plaque. Lens aspiration was done using bimanual irrigation and aspiration. PCCC and anterior vitrectomy were done. The superior incision was enlarged using 3.2 mm keratome, and multipiece IOL was injected in the sulcus, and optic capture was done with the anterior capsule, i.e., optic behind the anterior cap-

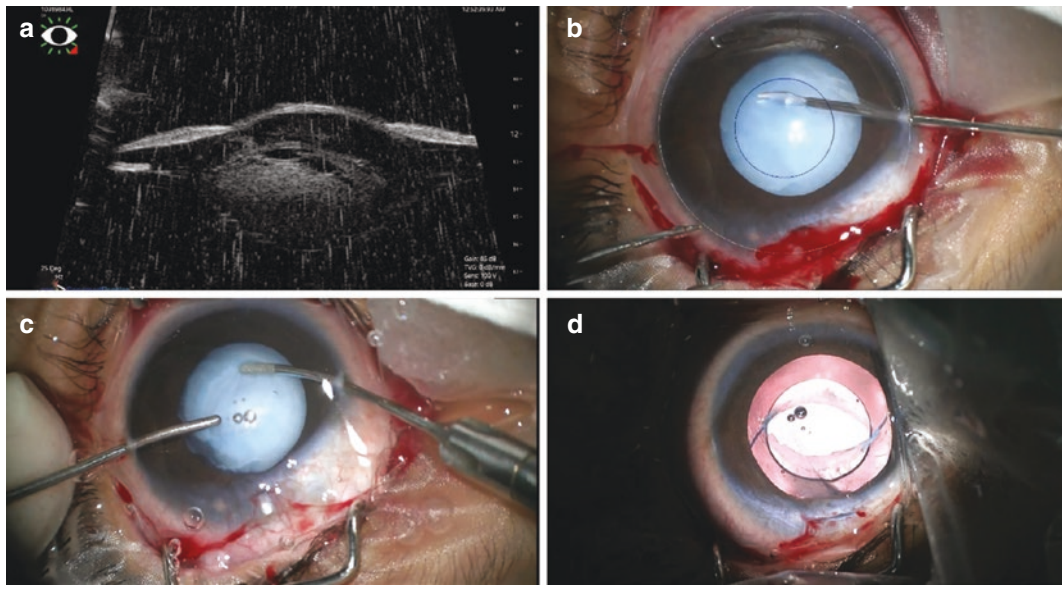

Fig. 38.4 (**a**) UBM of the LE showing deep anterior chamber and intumescent cataractous lens. (**b**) Anterior capsulorhexis being done using long microincision scissors. (**c**) Lens aspiration being done using bimanual irrigation and aspiration. (**d**) Multipiece IOL placed in the sulcus with a capture with anterior capsule

sule and haptics in the sulcus. The main wound was sutured with 10-0 monofilament nylon and sideport wounds were hydrated.

Learning Points

- Buphthalmic eyes have deep anterior chambers leading to difficulty in instrumentation. Microincision forceps and scissors for rhexis and bimanual irrigation and aspiration help in better control of the situation.
- Chances of IOL decentration in the postoperative period are high due to large eye size and bag dimensions. IOL placement in the sulcus with a capture with anterior rhexis or with both anterior and posterior rhexes helps in better centration.

Case 38.3

A 6-year-old case of PCG presented with a complaint of whitish reflex in the LE noticed by parents at the age of 5 years. Visual acuity in the RE was 6/6 and in the LE was counting fingers with accurate projection of rays. IOP in the RE was 12 mmHg (on no medication) and 10 mmHg in the LE on two ocular hypotensive medications (timolol and dorzolamide). Her baseline pressures had been recorded high at 28,30 mmHg two years back.

Slit-lamp examination of the LE revealed a hazy cornea with partial iris defects and total white cataract; RE was within normal limit. Biometry was done and axial length in the RE was 20.34 mm and LE was 21.46 mm.

Diagnosis: RE, fellow eye; LE, congenital glaucoma with partial aniridia with total white cataract.

Treatment: The child was planned for LE lens aspiration + PCCC +AV + PCIOL under general anesthesia. Three MVR incisions were made (temporal, nasal, and superior). Trypan blue dye was injected in the anterior chamber under air to stain the anterior capsule. The anterior chamber was formed with viscoelastic and anterior capsulorhexis was done using long microincision forceps and scissors. Lens aspiration was done using bimanual irrigation and aspiration probe. The bag was formed using viscoelastic and the posterior capsule was stained for better visualization (Fig. 38.5). Posterior capsulorhexis was done. Posterior chamber intraocular lens was implanted in the bag through superior 2.8 mm incision. Superior entry was sutured, viscoelastic removal was done, and wounds were hydrated.

Post-cataract surgery on 1-week follow-up, LE IOP was 20 mm Hg (on timolol and dorzolamide). Oral acetazolamide (dose) was added to tide over the period of high IOP soon after cataract surgery after which it was tapered as IOP normalized.

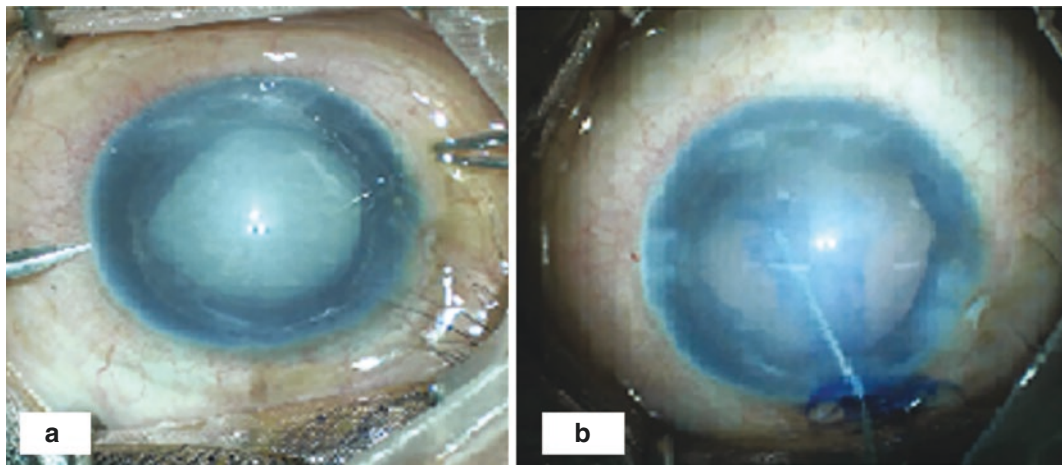

Fig. 38.5 (**a**) Showing a clinical picture of the LE (corneal haze, total white cataract) in an eye with congenital glaucoma operated for trabeculectomy. (**b**) Staining of the posterior capsule with trypan blue dye for better visualization

Learning Points

- Corneal haze causes difficulty in visualization during surgery. Staining of the anterior capsule and posterior capsule is required if the visibility is poor.
- Post-cataract surgery, IOP rise can occur again (due to inflammation, retained viscoelastic, vitreous in anterior chamber, inadequate cortical matter aspiration, inadequately functioning cleb due to fibrosis etc.). Hence, glaucoma medications should be tailored accordingly.

38.3 Conclusions

Cataract surgery in buphthalmic eyes requires special considerations. Besides adequate IOP control that must be achieved intra and post operatively, other factors requiring consideration include, performing appropriate biometry, identifying the IOL (power, type, formula for power calculation), mitigating media haziness intraoperatively identifying status of capsular bag and zonules. Though the eyes are special, they can achieve good visual outcomes with meticulous planning and surgical expertise.

Suggested Reading

Adelman RA, Brauner SC, Afshari NA, Grosskreutz CL. Cataract formation after initial trabeculectomy in young patients. Ophthalmology. 2003;110:625–9.

American Academy of Ophthalmology. Basic and clinical science course. In: Glaucoma. Amsterdam: Elsevier; 2011.

Daugeliene L, Yamamoto T, Kitazawa Y. Cataract development after trabeculectomy with mitomycin C: a 1-year study. Jpn J Ophthalmol. 2000;44:52–7.

Dhull C, Khokhar SK. Congenital glaucoma and anterior segment dysgenesis. In: Khokhar SK, Dhull C, editors. Essentials of pediatric cataract surgery. Singapore: Springer; 2022. p. 175–87. https://doi.org/10.1007/978-981-16-0212-2_15.

Edmunds B, Thompson JR, Salmon J, Wornald RP. The national survey of trabeculectomy III. Early and late complications. Eye. 2002;16:297–303.

Feroze KB, Patel BC. Buphthalmos. In: StatPearls. Treasure Island: StatPearls Publishing; 2018. http://www.ncbi.nlm.nih.gov/books/NBK430887/.

Hugkulstone CE. Changes in keratometry following trabeculectomy. Br J Ophthalmol. 1991;75(4):217–8.

Khokhar S, Yadav D, Gupta S, Chaurasia AK, Gupta A, Gupta V. Refractive outcomes of cataract surgery in PCG. Eye. 2018;33(4):542–8. https://doi.org/10.1038/s41433-018-0253-6.

Khokhar SK, Gupta Y, Surve A, Dhull C. Cataract in childhood glaucoma and anterior segment dysgenesis. In: Khokhar SK, Dhull C, editors. Atlas of pediatric cataract. Singapore: Springer; 2019. p. 103–14. https://doi.org/10.1007/978-981-13-6939-1_11.

Khokhar SK, Pillay G, Agarwal E, Mahabir M. Innovations in pediatric cataract surgery. Indian J Ophthalmol. 2017;65(3):210–6.

Vaz FM, Osher RH. Cataract surgery and anterior megalophthalmos: custom intraocular lens and special considerations. J Cataract Refract Surg. 2007;33(12):2147–50.

Wiggs JL, Damji KF, Haines JL, Pericak-Vance MA, Allingham RR. The distinction between juvenile and adult-onset primary open-angle glaucoma. Am J Hum Genet. 1996;58(1):243–4.

Yanoff M, Duker JS. Ophthalmology. 3rd ed. Philadelphia: Mosby; 2009.

Assistive Devices for Children with Glaucoma

39

Suraj Singh Senjam, Vivek Gupta, Praveen Vashist, and Radhika Tandon

39.1 Introduction

Vision rehabilitation, as defined by the World Health Organization, is a set of measures that assist individuals or children with visual disabilities, to achieve and maintain optimum functioning in interaction with their environments, to remain in or return to their home or community, and to participate in education and civic life. The final goal for vision rehabilitation is to empower every individual or child, to be able to live independently and, thereby, contribute to the community with their full potential. Therefore, vision rehabilitation is an indispensable component to improve independent living skills, daily living activities, and quality of life.

Vision rehabilitation services, ideally, are preceded by an initial couselling and evaluation to determine the level of care and types of intervention or disciplines required based on the complexity of the problems, needs, goals, and mental status, etc.

39.2 Counseling and Education

Rehabilitation services include counseling, a range of functional assessment and support services, including optometry, vision rehabilitation, assistive devices, and advice for welfare benefits, in a "one-stop shop." The following aspects, but not limited, while providing counseling and education can be considered:

- Disease leading to a vision problem, prognosis, treatment, etc.
- Low-vision and rehabilitation assistive devices (as prescribed or reccomended)
- Illumination amplification techniques: glare protection, lighting enhancement with adjustable gooseneck lamp, overhead lighting, wall-mounted lighting, LED lamp, CFL with various brightness capacity, etc.
- Patient safety education: reducing risk of falls or accidental mishaps related to fire, electricity, bathroom tile, sharp objects, cooking cylinder, etc.
- Environmental modification (home safety): arranging furniture, tables, desks, corridors,

Supplementary Information The online version contains supplementary material available at https://doi.org/10.1007/978-981-19-7466-3_39.

S. S. Senjam (✉) · V. Gupta · P. Vashist
Community Ophthalmology, Dr. Rajendra Prasad Centre for Ophthalmic Sciences, All India Institute of Medical Sciences, New Delhi, India
e-mail: drsurajsenjam@aiims.edu

R. Tandon
Cornea, Cataract and Refractive Services, Dr. Rajendra Prasad Centre for Ophthalmic Sciences, All India Institute of Medical Sciences, New Delhi, India

S. Gupta et al. (eds.), *Childhood Glaucoma*, https://doi.org/10.1007/978-981-19-7466-3_39

spacing in the central part of the house, or wall side as per needs
- Daily living activities including personal care, clothing, cleaning, bathing, brushing, eating, home management, financial management, shopping, etc.

39.3 Habilitation

Habilitation: It helps a child with visual impairment to adapt and learn, by skill improvement for everyday activities. For examples, children can be trained in activities like bathing, brushing teeth, eating, food preparation (spreading, peeling a banana, stirring), grooming hair, dressing, organizing (picking up toys), money management, having an understanding of time and related activities (breakfast in the morning, nap in the afternoon, and pajamas in the evening), even indoor mobility, etc. The details of habilitation are beyond the scope of this chapter.

39.3.1 Habilitation Can Be Planned According to the Age of the Child

1. Birth to 3 years, e.g.:
   (a) **E**arly intervention program for habilitation
   (b) Familiarization with regular items, such as household items
   (c) Toys: tactile or learning of sound toys
   (d) Puzzle **blocks**
   (e) Recognition of various **body** parts
2. Preschool child, e.g.:
   (a) Familiarity with various assistive devices for education
   (b) Familiarization with regular home items
   (c) Recommendations for devices for visual impairment such as cane
3. School-age child, e.g.:
   (a) Assessment of visual performance
   (b) Recommendation for devices
   (c) Learning to write
   (d) Braille orientation
   (e) Audio materials
4. Teenagers and younger adults
   (a) Digital assistive technology for visual impairment
   (b) Smartphones, tablets, computers, etc.

39.4 Adaptation and Adjustment

Adaptation is defined as the process of making modifications, whereas adjustment is the process of balancing any conflicting requirements that occur in behavior. Adaptation leads to accepting and trying to adapt to new skills and information, whereas adjustment is clearing the obstacle that occurs in human needs. Adaptive training is tailored to clients' needs or individuals' unique needs, clients' experiences, employment goals, etc.:

- Accessible instructional materials, such as, large print, Braille code, audio, so on.
- Materials should be adapted only to the extent necessary for efficient learning.
- If regular materials can be used in conjunction with environment adaptations or low-vision devices, such an approach is preferable to using specialized materials.

1. **Home adaptation, e.g., home safety, kitchen adaptation, bathroom adaptation**
   (a) Home safety: segregate frequently used items from lesser-used ones, and then keep items together near each other.
   (b) Cover sharp corners.
   (c) Cautious of overhangs.
2. **Kitchen adaptation**
   (a) Tactile markers, bold marker items.
   (b) High-contrast containers.

(c) Use knife holder.
(d) Using tactile markers for oven and microwave.
(e) Always better to use a double spatula.
(f) Cooking practice with a cold pan.

3. **School environment adaptation**

Preschool and kindergarten are the formative years for developing language, social skills, and concepts. School and classroom environmental adaptation can help the student who is blind or visually impaired move safely and efficiently through their school environment. It is important to understand each student's visual diagnosis and the implications concerning functional vision to make the appropriate adaptations to maximize the student's use of vision.

39.4.1 Object Permanence Training

Such training makes the child understand that objects continue to exist even if they are out of reach. These activities motivate a child for playing and learning. The training can be tailored according to the age of the child. It can be carried with the "hands-over-hands" technique to a child with visual loss. Children need to be trained using a specific and unique identification points of each object to recognize it in a correct way. Items can be categorized as follows:

- Kitchen items: household items "clothing items with the help of texture" furniture items

Training settings: Training can be given under various settings, for example:

- Center-based training: hospital, health facilities
- Field-based training: hostels, library, schools

39.5 Individual Visual Rehabilitation Plan

39.5.1 Category I: Children with Binocular Best Correct Vision Acuity (BCVA) Less Than 6/18 to 1/60 in the Better Eye

Children falling into Cat-I vision loss are the potential beneficiaries of visual-based assistive devices, e.g., optical magnifiers (both near and distance) or CCTV (Fig. 39.1). This categorization is particularly useful which media to be chosen for their educational activities. Near-vision assessment using M or N notation will be useful to prescribe large-print books (N 18-20). However, children should not be discouraged in learning other tactile and sound assistive devices.

39.5.2 Category II: Children with Best Correct Visual Acuity Less Than 1/60

Individuals under this Cat-II vision loss are potential beneficiaries of tactile or sound-based assistive devices for visual impairment (Fig. 39.1), for examples, Braille books, digital accessible information system (DAISY) book, embossed print, and digital audio recorder. Nevertheless, children in this category are not to be discouraged from using other visual-based assistive devices, if they still have some usable visual function and are willing the cross use of assistive devices.

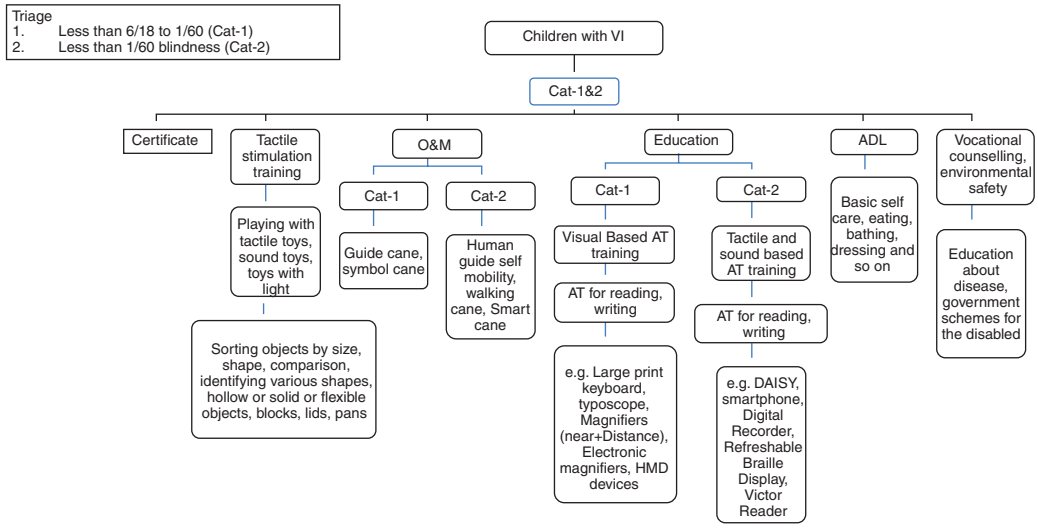

*DAISY: Digital accessible information system, HMD: Head Mounted Display Devices, ADL: Activities of Daily Living, AT: Assistive Technology, Cat: Category, VI: Visual impairment

Fig. 39.1 Recommendation of assistive devices based on BCVA (*O&M* orientation and mobility)

39.6 Assistive Devices for Visual Impairment

Assistive devices for visual impairment are products designed either to improve visual function, such as visual acuity and contrast sensitivity, without affecting ocular diseases or enhance functioning without disturbing physiology or anatomy of visual function, e.g., walking canes, Braille, and accessible apps of the smartphone, in individuals with low vision or blindness. Assistive devices can be divided into optical and nonoptical in ophthalmic practices. Nonoptical devices are primarily used for vision rehabilitation. There are three different types of optical assistive devices:

(a) Distance vision optical assistive devices
(b) Near vision optical assistive devices
(c) Optical field expanders

39.6.1 Distance Vision Optical Assistive Devices

Handheld telescope (Fig. 39.2a, b): A handheld telescope is used with one eye, referred to as monocular which means a single eyepiece. They usually come with cords to allow the scope to be worn around the user's neck. It is used for short viewing purposes, such as reading a bus number, signpost, and street name. They are available in a variety of powers ranging from 2× to 10×. Powers more than 10× are not used for low-vision rehabilitation due to the limited field of view. A more stable view can be achieved by holding the devices in the palm after the user focus the scope to a distance object. The viewing eye should be closer to the ocular lens to achieve a larger field of view.

Spectacle-mounted telescope (Fig. 39.3): Spectacle-mounted telescopes are permanently attached to the lens of eyeglasses. They are avail-

Fig. 39.2 (**a**, **b**) Handheld telescope (uniocular)

Fig. 39.3 Binocular spectacle-mounted telescope

able in a wide variety of powers. They are usually prescribed in very low powers because of their large field of view and ease of use, for example, 3× and 3.5×. For persons with tremors, arthritis, and impaired motor control, such devices are suitable for these types of scope.

Fig. 39.4 See TV glasses for intermediate distance

See TV glasses (Fig. 39.4): It consists of two plastic lenses that are separated in space but not surrounded. See TV glasses are designed to use while watching the television. Focus on objects from 5 feet (1.5 m) to infinity. They are lightweight and have adjustable power manually. Magnification is limited to 2.1×.

Clip-on telescope (Fig. 39.5): Clip-on telescope is to be attached to the spectacles' frame. They can be removed from the spectacle if not in

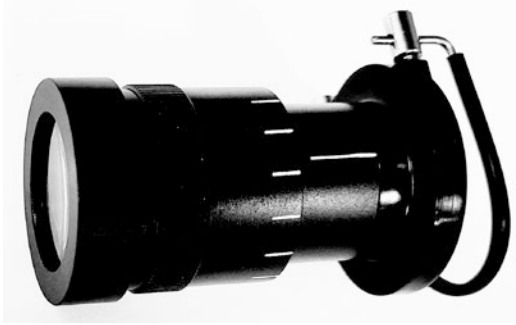

Fig. 39.5 Clip-on telescope

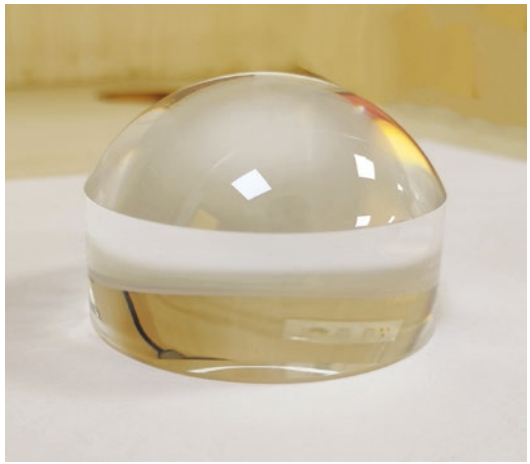

Fig. 39.6 Dome magnifier

use. It is also available with a wide range of powers. It can be used for longer viewing periods, like viewing the television, a program, a ball game, or a movie, as opposed to a handheld telescope.

39.6.2 Near Vision Assistive Devices

Dome magnifier (Fig. 39.6): It is a dome-shaped handheld magnifying device made of glass or acrylic plastic, used to enlarge words on a page. It is usually used for a short period of reading such as spot reading, price tags, and bills. They are suitable for people with tremors or impaired motor skills because they are held in contact directly with the page during the use. It is recommended to use a reading stand while using dome magnifier.

Pocket Magnifiers (Fig. 39.7a, b): Pocket handheld magnifiers are small, compact, lightweight, and functional magnifiers that can be taken with you anywhere. Folding pocket magnifiers are ideal for everyday purposes such as reading the mail, reading menus in restaurants, reading train schedules, or reading the fine print wherever you are. They are available with a wide range of powers from low powered (4×), medium powered (4× to 8×), and high powered (8×) with a multiple

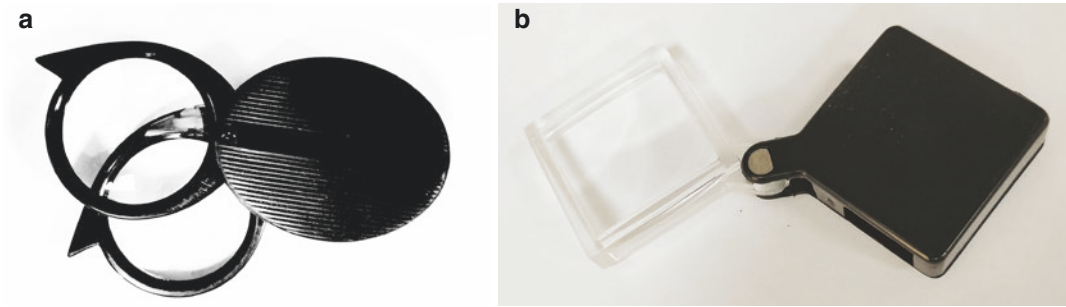

Fig. 39.7 (**a**, **b**) Pocket magnifier

lens system of small diameter. They can be either illuminated or non-illuminated in various designs.

Bar magnifiers (Fig. 39.8): Bar magnifiers, also called 'paperweight' magnifiers, allow sight-impaired and low-vision users the ability to read any kind of printed materials. It is designed to be placed directly onto the object-usually the page of a book. By providing magnifying power up to 3× the size of the original text, bar magnifiers assist individuals with reading or seeing various types of printed pages.

Stand Magnifiers (Fig. 39.9a, b): Stand magnifiers are the convex lens mounted on a stand. The magnification power of stand magnifiers ranges from low-powered 3× to medium or high powered (4× to 20×). The stand magnifiers help to maintain an accurate working distance and are useful when the patient has hand tremors or weakness. There are built-in illumination stand magnifiers that avoid the need to arrange separate lighting systems.

Handheld magnifiers (Fig. 39.10a–c): They are commonly called magnifying glasses. A hand-held magnifier is especially useful for short periods of "spot" reading, such as reading a menu in a restaurant, price tags, bills, labels, checking medication, checking nails or appliance dials at home. The patient can hold it at any distance from the eye, bringing it closer to increase the field of view. Lens-to-object distance needs to be fixed to get clear images. It can be determined if the power of the lens is known, using the formula 100 cm/D. For example, a handheld magnifier labeled as a 20 D lens would have a lens-to-object distance of 100/20 = 5 cm (appro). They require steady hands and good motor control to steady the position of the magnifier. Illuminated hand-held magnifiers are also available.

Fig. 39.8 Bar or flat field magnifier

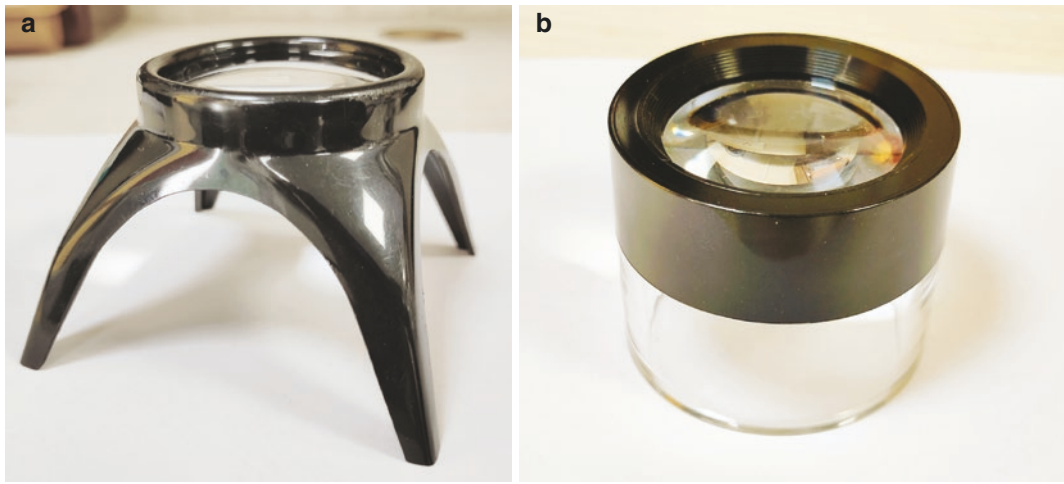

Fig. 39.9 (**a**, **b**) Stand magnifier

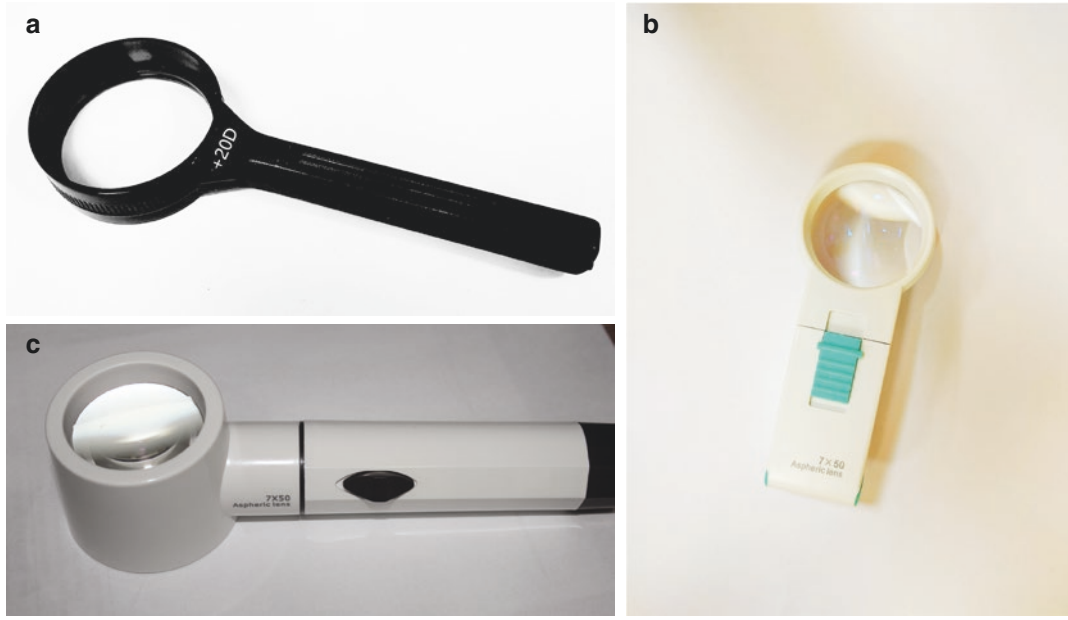

Fig. 39.10 (**a**) Non-illuminated handheld magnifiers. (**b**) Illuminated handheld magnifiers. (**c**) Illuminated handheld stand magnifiers

Fig. 39.11 Fresnel prism

39.6.3 Field Expanders

39.6.3.1 Field Expanders for Low-Vision Patients

Fresnel prism (Fig. 39.11): A Fresnel lens is a type of composite compact lens developed by the French physicist Augustin-Jean Fresnel for use in lighthouses. A flexible Fresnel prism, e.g., 1-mm plastic (polyvinyl chloride) material, can be attached over to the part of the spectacle lens on the side of the field defect, with its prism base toward the non-seeing area. There are a wide range of powers available (from 0.5 prism diopter to 30 prism diopter)

Properties

- Fresnel prisms have been used successfully to treat field defects such as hemianopia and overall field restriction.
- The prisms do not expand the visual field, but they allow the patients to become more aware of objects on the blind side by moving their eyes into the prisms.
- With the prisms in place, small scanning eye movements into the prisms allow the user to see objects located in the blind and peripheral field.
- The prisms act by displacing the apparent position of objects in the blind field toward the primary visual direction.
- The larger the eye movements, the farther away the prisms can be placed from the primary line of sight and the lower the power required.
- Determination of the amount of prism base, the size of the prism, and the position of the prism on the spectacle lens are important factors for the successful treatment of low-vision patients suffering from visual field defects.

Fig. 39.12 Reverse telescope

Fig. 39.13 Spectacle magnifier

Fig. 39.14 Telemicroscope

Reverse telescopes (Fig. 39.12): When the visual field is reduced to less than 20°, the main difficulty for the patient is to gather adequate information from his or her surrounding environment for effective orientation and mobility. To present more information within the limited visual field, the object to be viewed can be minified. This can be achieved by using a conventional telescope as the wrong away around, i.e., the objective lens now is used as eyepieces. The patient views through the objective lens (as opposed to looking through the ocular lens or eyepiece in a conventional telescope), thereby causing minification. There is a loss of resolution proportional to the increase in the field of view.

For example, looking through the objective lens of a 2× telescope will increase the patient's field by approximately two times but will also decrease visual acuity (through minification) by approximately two times, or a 2× minification telescope with a 5° field will compress 10° of the visual field into that 5° image field. The reverse telescope is the best use for patients with severe field restrictions (<5°) but who have near-normal visual acuity.

A patient may use a reverse telescope to spot the number of people in a room, to locate his or her children on a busy playground, to scan an environment for potential obstacles, to find objects on a desk, or even to locate a doorway in a building.

Spectacle magnifiers or microscopic eyeglasses (Fig. 39.13): One method of making print materials larger is to use a plus power lens in the spectacle plane for near work. They are also called "simple microscopes" or near vision only (NVO) because they produce magnified images of small words and objects (relative distance magnification). They require a closer working distance. The main advantage of microscopes is the large field of view that they provide. They allow an individual to read for longer periods.

Telemicroscopes (Fig. 39.14): A telemicroscope is a combined feature of both telescope (distance work) and microscope (near work). It is a telescope that is fitted with an extra removable lens (a lens cap) that fits over the lens farthest from the eye (objective lens), enabling the telescope to focus an arms-length or closer. Telemicroscopes are ideal for the person with low vision wishing to perform tasks at a greater distance than microscopic or hand magnifiers with the same power.

Properties

The individual who needs magnification for near activities sometimes prefers a greater working

distance than microscope lenses can provide. Telemicroscopic glasses, in contrast to strong magnifying reading glasses, allow for a more comfortable working distance when reading, using the computer, doing hand work, cooking, playing cards, and other tasks. These glasses are available for either a single or both eyes.

39.7 Head-Mounted Display (HMD) Devices

Children or patients with Cat-I vision loss (Fig. 39.1) will be beneficial with HMD devices. HMD needs a subjective trial before recommendation.

39.7.1 eSight Eyewear (Fig. 39.15)

eSight is a wearable smart glasses, first developed by a Canadian engineer in 2006, that help people suffering from primarily with peripheral vision loss to see a wider field view but can also be used for a patient having mild central field defect.

1. Glaucoma
2. Retinitis pigmentosa
3. Stargardt disease
4. Optic atrophy
5. Rods and cones dystrophy
6. Albinism
7. Diabetic retinopathy
8. Macular degeneration

Fig. 39.15 eSight

It has adjustable arms that fit over prescription glasses, an adjustable halo band comfortably and securely fits children and adults, two rechargeable lithium-ion batteries, each up to 3 hours of continuous use, 256 GB storage three integrated speakers, and built-in flashlight.

Display specification: System acuity >6/6, two dual independent 1280 × 960 high-resolution OLED color screens, 18 MP camera for stunning clarity paired with best-fit lenses, advanced software autofocus, image stabilization, and personalization options, adjustable inter-pupil distance, and diagonal 37.5° field of view.

Connectivity and controls: Touchpad and menu control, integrated into headset; wireless remote and web account controls; Android and Apple mobile apps; Wi-Fi, Bluetooth, and HDMI connectivity; eCast and eMirror with the eSight mobile apps, eSupport, and shared accounts; and automatic cloud-based software updates.

Properties

- eSight combines bright, clear screens with a high-tech camera to let the patient see text up close or detail in the distance.
- The patient can switch between the two distance objects almost instantly. The visor flips up easily, for face-to-face interaction.
- It helps in walking around in comfort.
- It is expensive (3000 USD).

39.7.2 Acesight S Model (Fig. 39.16a, b)

Acesight S electronic glasses employ augmented reality (AR) technology and feature two full HD displays that float in front of each eye. It has an 8-megapixel camera and a 45° field of view per eye. A tracking autofocus camera between the eyes captures everything the user looks at and presents everything in the magnified form up to 15× normal size. A handheld controller allows the user to adjust magnification, colors and contrast, and enhancement of the edge of the object. It also has a rechargeable Li-ion battery that lasts more than 4 h on a single full charge. Acesight (without s) is useful for a patient with tunnel vision with its narrow mode.

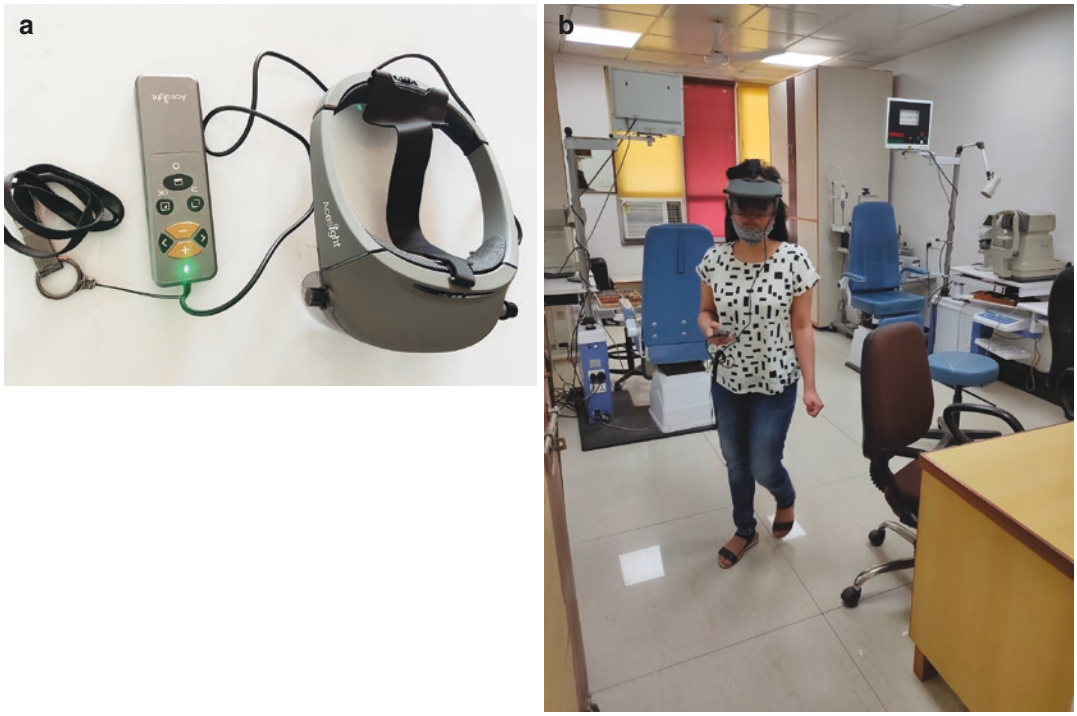

Fig. 39.16 (**a**, **b**) Acesight

Properties

- Acesight is ideally suited to individuals with a visual acuity range from 6/36 to better than 1/60 due to any type of ocular problems.
- Patients whose vision is less than 1/60 cannot get fully benefitted from this device.
- Acesight helps to do routine daily indoor activities**, including watching TV.**
- It is expensive (4295 USA dollars).

39.7.3 OXSIGHT Crystal Glasses

OXSIGHT crystal is a smart glasses and wearable technology designed for people with peripheral vision impairment (PVI), sometimes known as tunnel vision, such as:

1. Glaucoma
2. Retinitis pigmentosa
3. High myopic degeneration

Fig. 39.17 OXSIGHT Onyx

39.7.4 OXSIGHT Onyx (Fig. 39.17)

OXSIGHT Onyx is a wearable HMD device designed for individuals with central vison loss. The device is useful for person suffering the following eye conditions:

1. Age-related macular degeneration
2. Macular hole or edema
3. Stargardt disease
4. Macular dystrophy
5. Leber hereditary optic neuropathy (LHON)

Onyx helps in reading text and recognizing faces or objects, and the users can easily adjust accordingly to enhance vision and change the mode as automatic night mode and a TV mode. The glasses can also increase the users' horizontal field of vision up to 70° and add or remove shade for lower light sensitivity depending on light conditions. It has 8× magnification and adjustable built-in lenses and a rechargeable battery that lasts more than 2 hours.

39.7.5 Vision Jordy (Fig. 39.18)

Jordy is a battery-operated device that can be worn like a pair of glasses to see near, far, and everything in between. It has 720 p HD-60 FPS, autofocus camera for distance, intermediate, and near viewing; 30× max. magnification; color select; locator; freeze and focus lock functions; dual display with a wide field of view; 5-level brightness control; adjustable top strap; and nose piece for optimum comfort, glare reduction eyecup shield, lens holder for your prescription, headset weight (8 oz), and a control unit with a built-in rechargeable battery that lasts more than 4 h on a single full charge. It can also be used as a desktop magnifier.

Jordy enables the person with low vision to read, write, and see in any environment including work, home, and school. It also enables patients to enjoy watching movies and TV and play games. It is not designed for mobility, walking, or running.

Fig. 39.18 Vision Jordy

39.7.6 OrCam (Fig. 39.19)

Children or patients with Cat-II vision loss (Fig. 39.1) will benefit with OrCam devices.

OrCam devices such as OrCam MyEyes are portable, artificial vision devices that allow individuals with visual impairment to understand the text and identify objects through audio feedback, describing what they are unable to see. This device particularly is designed for a person with profound visual impairment or total blindness.

39.7.7 Electronic Magnifiers

Children or patients with Cat-I vision loss (Fig. 39.1) will be benefitted with electronic magnifiers.

39.7.7.1 Desktop CCTV Magnifier (Fig. 39.20)

It is an electronic magnifier ideal for low-vision patients. It uses a camera lens to project the magnified image on the monitor. It uses optical character recognition technology that can read the image captured by the camera. The patient can set the desired magnification accordingly. Color inversion, contrast enhancement, and magnifica-

Fig. 39.19 OrCam

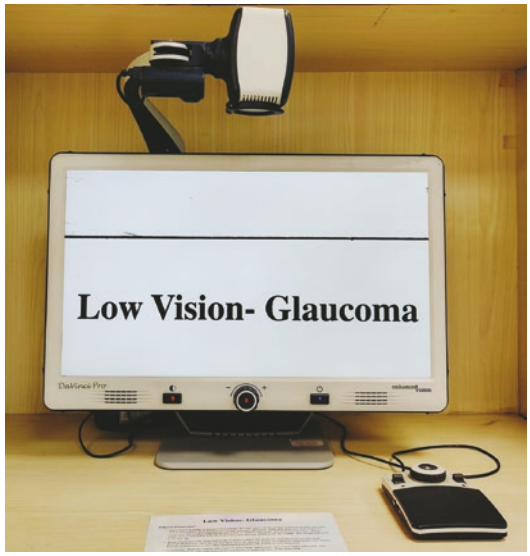

Fig. 39.20 Desktop CCTV magnifier

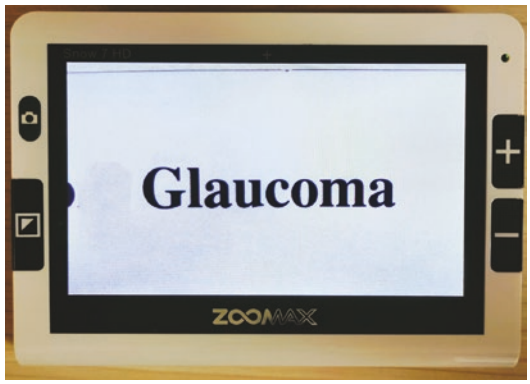

Fig. 39.21 Video magnifier

tion range up to 72× are features of the new-generation CCTV.

39.7.7.2 Video Magnifiers (Fig. 39.21)

It is a simple electronic magnifier, based on projection magnification. They can change the magnification, foreground, and background color according to the patient's preference.

39.8 Nonoptical Devices

Nonoptical aids are visual aids that do not use magnifying lenses to improve visual function. They are a supplement to optical lenses or can be used independently. Children or patients with Cat-I will be benefitted with filters and tinted glasses.

Fig. 39.22 Pink-tint lenses

39.8.1 Glare Control

Absorptive lens: Absorptive lenses are commonly called tinted lenses that improve visual acuity by reducing glare and increasing contrast. The function of these lenses is to filter out excess light before reaching the eye either by absorbing or reflecting radiation. They are different from sunglasses. These lenses are available in varying degree of light transmission strengths. Blue light causes the highest degree of glare, and so it needs to be filtered out.

Pink-tint lenses (Fig. 39.22, Wraparound model):

- Cosmetically more appealing, soothing to the eye
- Reduces eye strain and glare
- Enhances visual depth
- Provides good road visibility

Yellow-tint lenses (Fig. 39.23, Wraparound model):

- Blocks out UV and blue light, but let in other light.
- Can be used both indoors and outdoors.
- Provides greater clarity in fog, haze, and other low-light conditions.
- Not a good choice in any activity that requires accurate color perception.

Fig. 39.23 Yellow-tint lenses

Fig. 39.24 Amber-tinted lenses

- Individual with macular problems like congenital macular dystrophy would benefit the most.

Amber-tinted lenses (Fig. 39.24 fit-over model)

- Gives high contrast in strong sunlight
- Contains a red element to enhance the depth perception
- Almost blocks all the UV rays as well as blocks some blue light
- Suitable for outdoor movement

Gray-tinted lenses (Fig. 39.25)

- Suitable for person whose eye problems does not tolerate the changes in color

Green-tinted lenses

- Gives high contrast for all eye conditions
- Transmits all colors evenly
- Good for general-purpose use

Orange-tinted lenses

- Give higher contrast
- Suitable for retinitis pigmentosa
- Diabetic retinopathy

Fig. 39.25 Green-tinted lenses

39.8.2 Colored Filter Lens (Fig. 39.26)

The prescription of colored filter lens is one of the important features of vision rehabilitation. Eyesight for a few patients with low-vision problems can be improved by using a color filter lens. Such filtering glasses protect the eyes from light and can also enhance brightness. They absorb the short-wavelength, high-energy ultraviolet and blue elements of the incoming light so enhancing contrast and reducing photosensitivity to the users. The color of glasses differs depending on the absorption range and how much ultraviolet is being filtered out. The higher the number, the more UV light is absorbed, so less light is transmitted through to the eyes. The choices depend on each person and the sensitivity of his or her eyes. Subjective trial and error of a variety of colored filter lenses should be done for a prescription rather than the manufacturer's recommendations. For a patient with glaucoma, brown, yellow, orange, and amber are suitable colored filter lens.

39.8.3 Assistive Devices for Vision Rehabilitation

Reading stand (Fig. 39.27): It is a useful nonoptical device for low-vision children. It provides comfortable body posture while reading at distance. The angle of the board can be adjusted according to the need of the patient. It is especially helpful in low-vision children who get tired while standing for a long time.

Mobility canes (Fig. 39.28): A cane is a nonoptical device used by visually impaired or blind people. It allows patients to scan their surroundings for any obstacles. It also helps the onlookers

Fig. 39.26 Various color type of filters

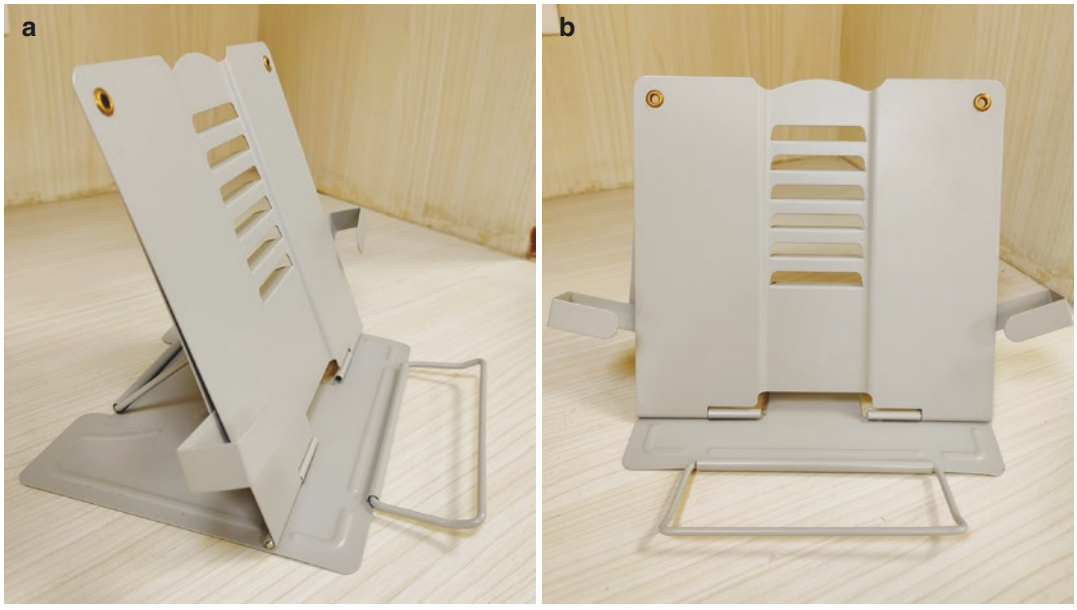

Fig. 39.27 (**a**, **b**) Reading stand

for identifying the patient as visually impaired or blind and take proper care. Children or patients with Cat-II will be beneficial with canes.

Different types of canes are:

- **Long cane:** Designed primarily as a mobility tool used to detect objects in the path of a user. Cane length depends upon the height of a user and traditionally extends from the floor to the user's sternum. It is the most well-known variant, though some organizations favor the use of much longer canes.
- **Guide cane:** A shorter cane, generally extending from the floor to the user's waist, with more limited potential as a mobility device. It is used to scan for curbs and steps. The guide

Fig. 39.28 Mobility canes

cane can also be used diagonally across the body for protection, warning the user of obstacles immediately ahead.

- **Identification cane:** Used primarily to alert others that the user is visually impaired but not to the extent where they require a long cane or another variant. It is often lighter and shorter than the long cane and has no use as a mobility tool.
- **Support cane:** Designed primarily to offer physical stability to a visually impaired user, the cane also works as a means of identification. It has very limited potential as a mobility device.
- **Kiddie cane:** This variant of cane functions the same as an adult's long cane but is designed for use by children and is thus smaller and lighter.

39.8.4 Reading Low Vision Lamp (Fig. 39.29)

In many cases, low-vision patient requires high illumination to see print. A table lamp is a useful nonoptical device for providing high illumination. The light source should be on the side of the better eye. Moving the light closer provides higher illumination.

39.8.5 Typoscope (Fig. 39.30)

It is also known as a reading guide. It is a masking device with a line cut out from an opaque, nonreflecting plastic or thick paper. It reduced glares and increases contrast. It helps in reading text more easily as the cutout line helps the patient to focus on the line he/she wants to read.

Fig. 39.29 Reading lamp

39.8.6 Letter Writing Guide (Fig. 39.31)

A letter writing guide helps visually impaired or blind people to write more easily and accurately. It is a black card with rectangular cutouts horizontally along the card. The patient can feel the

Fig. 39.30 Typoscope-Single window

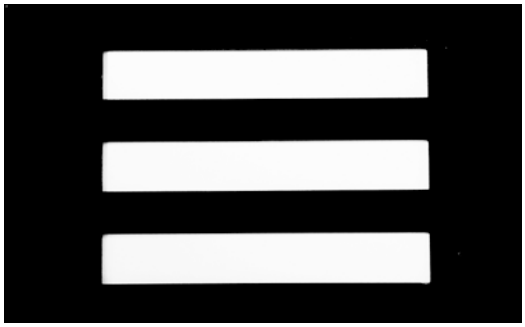

Fig. 39.31 Letter writing guide-multiple window

empty cutout spaces and can write in the space provided.

39.8.7 Signature Guide (Fig. 39.32)

It is a great tool for visually impaired or blind patients. There is a rectangular box cut out from an opaque, nonreflecting plastic or thick paper. It is used to do signatures on cheques, official papers, etc. The patient can feel the empty cut space and can sign in the space provided.

Fig. 39.32 Signature guide

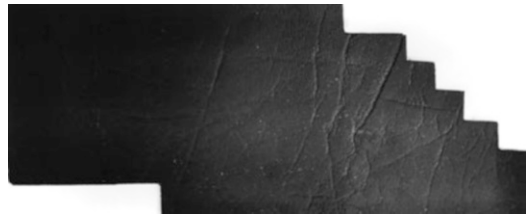

Fig. 39.33 Notex

39.8.8 Notex (Fig. 39.33)

It is a rectangular piece of cardboard with steps on the top right corner which helps in identifying the currency of the note.

39.8.9 Non-disease-Specific Service

This non-disease-specific vision rehabilitation can be offered to a child irrespective of the type of ocular disease. For example, children with vision loss due to glaucoma will need training for mobility and activity of daily living (ADL). However, individual vision rehabilitation plan (IVRP) can be developed for a better outcome such as:

- Adaptive training on utilization of assistive devices: optical low-vision aids if any, e.g., magnifiers, tactile aids, talking devices, etc.
  - How to use at home, about cleaning, maintaining, safe keeping, etc.
- Orientation and learning different body parts: arms, legs, hands, and feet and how they move.
- Encourage purposeful movement, developing the child's gross and fine motor skills.
- Learn concepts about the child's surroundings, beginning with his immediate environment. Recognize what he is seeing, hearing, smelling, and touching.
- Training on activity of daily living: skills assistance, e.g., eating, bathing, clothing, washing, grooming, nail cutting, personal hygiene, etc.
- Finger-over-finger technique. (1) Kitchen items. (2) Household items. (3) Clothing items. (4) Furniture items.
- Texture training: soft, hard, rough, and smooth and sound-based training.
- Sound recognition: using headphones for various sounds, e.g., animals

39.8.10 Orientation and Mobility (Fig. 39.34)

- A child with an acquired visual loss usually feels scared or anxious during mobility.
- The best to start mobility training in children with visual loss is by handing over a sound or light-illuminating toys to a person with sound coordination, straight line walking between two persons. Using a sound toy is always recommended. The training can be started from a few steps and then gradually increases the distance between the persons. For cane learning, someone should not instruct the child on how to hold the cane, to begin with. Let the child hold the cane whatever he or she feels happy. The children should feel that the cane is one of their toys. Gradually, training can be done in the standard manner.
- The sooner the mobility training begins, the better the outcomes are, and the sooner patient learns independent living. (1) Human guide. (2) Self-mobility. (3) Walking cane
- Orientation and mobility—indoors and outdoors (if required):
  - Orientation: awareness about surroundings and environment, position, space, etc.
  - Mobility: meaningful movement through the environment safely, efficiently, and independently

Fig. 39.34 Orientation and mobility

39.9 Conclusions

Assistive devices for individuals with vision impairment are external products, including hardware and software, that can enhance visual functioning and minimize the vision-related activity limitations of daily living skills. For those with total blindness, assistive devices are developed based on body senses other than vision, such as sound, touch, vibration, hearing, and smell. These devices are essential for manag-

ing children with low vision and blindness and improving their essential life skills and academic learning. There is a wide range of assistive technology available, ranging from low-tech devices such as walking canes and Braille to advanced technology based on computer and smartphone technology that incorporates Artificial Intelligence and Augmented Reality or mixed technology. Children with visual impairments can benefit from visual-based assistive devices or visual substitution assistive devices to improve their daily essential skills. Overall, assistive devices play a vital role in enhancing the quality of life among visually challenged individuals.

Suggested Reading

Benjamin WJ. Borish's clinical refraction. 2nd ed. Amsterdam: Elsevier; 2006.

Dickinson C. Low vision principles and practices. Oxford: Butterworth-Heinemann; 2002.

Gopalakrishnan S, Muralidharan A, Susheel SC, Raman R. Improvement in distance and near visual acuities using low vision devices in diabetic retinopathy. Indian J Ophthalmol. 2017;65(10):995–8.

Khanna A, Ichhpujani P. Low vision aids in glaucoma. J Curr Glaucoma Pract. 2012;6(1):20–4.

Lovie-Kitchin JE, Whittaker SG. Prescribing near magnification for low vision patients. Clin Exp Optom. 1999;82(6):214–24.

NFG. Chapter three: enhancing vision through touch. 2021. Available from https://nfb.org/images/nfb/publications/books/integrating-print-braille/integrating-printandbraillechapter3.html.

Persha AJ, Nawvi KR. Visual stimulation activities for infants and toddlers. Secunderabad: National Institute for the Mentally Handicapped; 2004.

RNIB. UK vision strategy: setting the direction for eye health and sight loss services. 2008. p. 1–50.

Scheiman M, Scheiman M, Whittaker S. Low vision rehabilitation: a practical guide for occupational therapists. 2nd ed. Deptford: SLACK; 2016.

Senjam SS, Foster A, Bascaran C, Vashist P, Gupta V. Assistive technology for students with visual disability in schools for the blind in Delhi. Disabil Rehabil Assist Technol. 2020;15(6):663–9. https://doi.org/10.1080/17483107.2019.1604829. Epub 2019 Apr 23. PMID: 31012740.

Senjam SS. Assistive technology for people with visual loss. Off Sci J Delhi Ophthalmol Soc. 2020;30(2):7–12.

Senjam SS. Assistive technology for students with visual disability: classification matters. Kerala J Ophthalmol. 2019;31:86–91.

Senjam SS. Developing a disability inclusive model for low vision service. Indian J Ophthalmol. 2020;69(2):417–22.

Teaching Students with Visual Impairments. Environmental adaptations for students who are blind or visually impaired - teaching students with visual impairments. 2021. Available from https://www.teachingvisuallyimpaired.com/environmental-adaptations.html.

Van Nispen RM, Virgili G, Hoeben M, Langelaan M, Klevering J, Keunen JE, et al. Low vision rehabilitation for better quality of life in visually impaired adults. Cochrane Database Syst Rev. 2020;1:CD006543.